

13  
5-31

2156

GEAP-13787  
AEC RESEARCH AND DEVELOPMENT REPORT  
FEBRUARY 1972

# SEFOR FOLLOW-ON PROGRAM PHASE A FINAL REPORT

JUNE 15, 1971 – DECEMBER 31, 1971

MASTER

U.S. ATOMIC ENERGY COMMISSION  
CONTRACT AT(04-3)-189      PROJECT AGREEMENT 57

GENERAL  ELECTRIC

DISTRIBUTION OF THIS DOCUMENT IS UNLIMITED

## DISCLAIMER

**This report was prepared as an account of work sponsored by an agency of the United States Government. Neither the United States Government nor any agency Thereof, nor any of their employees, makes any warranty, express or implied, or assumes any legal liability or responsibility for the accuracy, completeness, or usefulness of any information, apparatus, product, or process disclosed, or represents that its use would not infringe privately owned rights. Reference herein to any specific commercial product, process, or service by trade name, trademark, manufacturer, or otherwise does not necessarily constitute or imply its endorsement, recommendation, or favoring by the United States Government or any agency thereof. The views and opinions of authors expressed herein do not necessarily state or reflect those of the United States Government or any agency thereof.**

## **DISCLAIMER**

**Portions of this document may be illegible in electronic image products. Images are produced from the best available original document.**

FINAL REPORT  
SEFOR FOLLOW-ON PROGRAM PHASE A  
FOR PERIOD  
JUNE 15, 1971 – DECEMBER 31, 1971

Prepared by:  
J. O. Arterburn

NOTICE

This report was prepared as an account of work sponsored by the United States Government. Neither the United States nor the United States Atomic Energy Commission, nor any of their employees, nor any of their contractors, subcontractors, or their employees, makes any warranty, express or implied, or assumes any legal liability or responsibility for the accuracy, completeness or usefulness of any information, apparatus, product or process disclosed, or represents that its use would not infringe privately owned rights.

Approved:

*L. F. Fidrych*  
L. F. Fidrych, Manager  
Design Engineering

Approved:

*K. M. Horst*  
K. M. Horst, Manager  
Development Engineering

Prepared for the  
United States Atomic Energy Commission  
under  
Contract Number AT(04-3)-189  
Project Agreement No. 57

BREEDER REACTOR DEPARTMENT • GENERAL ELECTRIC COMPANY  
SUNNYVALE, CALIFORNIA 94086

375/180 SEFOR  
MJC 3-31-72

GENERAL  ELECTRIC

THIS PAGE  
WAS INTENTIONALLY  
LEFT BLANK

TABLE OF CONTENTS

		Page
<b>1.0</b>	<b>Task 1—Program Management</b>	1
<b>2.0</b>	<b>Task 2—Option I Plus Selected Plant Tests</b>	1
2.1	Task 2A—Driver Fuel Performance Limits	1
2.2	Task 2B—Transient Experiments on Encapsulated Fuel	43
2.3	Task 2C—Plant Tests	78
<b>3.0</b>	<b>Task 3—Elevated Temperature Operation</b>	82
3.1	Task 3A—Test Program	82
3.1.1	Task 3A1—System Behavior	82
3.1.2	Task 3A2—Vented Fuel	86
3.1.3	Task 3A3—Coolant Chemistry and Impurity Monitoring Equipment	102
3.1.4	Task 3A4—Core Cooling	106
3.1.5	Task 3A5—Core and Fuel Assembly Instrumentation	118
3.1.6	Task 3A6—Boiling Detection	119
3.1.7	Task 3A7—Failed Equipment Detection	120
3.1.8	Task 3A8—Computer Data Acquisition System (DAS)	121
3.1.9	Task 3A9—Pu Capture Ratio (Later)	123
3.1.10	Task 3A10—Level Indicators	124
3.1.11	Task 3A11—Leak Detectors	140
3.1.12	Task 3A12—Cold Trap Performance	141
3.1.13	Task 3A13—Vapor Trap Performance	145
3.1.14	Task 3A14—Refueling Cell Equipment	147
3.1.15	Task 3A15—Refueling Hoist and Grapple	148
3.2	Task 3B—Elevated Temperature Operation Development and Design	149
3.2.1	Task 3B1—Systems	149
3.2.2	Task 3B2—Reactor (Part 1)	171
	(Part 2)	182
	(Part 3)	203
	Appendix A	206
	Appendix B	209
3.2.3	Task 3B3—Elevated Temperature Operation Driver Fuel Analysis	227
3.2.4	Task 3B4—Physics	229
<b>4.0</b>	<b>Task 4—Option IIIA Plus Selected Plant Tests</b>	231
4.1	Task 4A—Test Program	231
4.2	Task 4B—Option IIIA Development Design	241
4.2.1	Task 4B1—Control Drive System	241
4.2.2	Task 4B2—FRED	241
4.2.3	Task 4B3—Fuel and Control Assembly Design	242
4.2.4	Task 4B4—Systems	297
4.2.5	Task 4B5 Physics	304
4.2.6	Task 4B6—Package	337
4.2.7	Task 4B7—Fuel Handling and Shipping	343
<b>5.0</b>	<b>Task 5—Safety and Licensing</b>	345
<b>6.0</b>	<b>Task 6—Quality Assurance Plan</b>	348

LIST OF ILLUSTRATIONS

Figure No.	Title	Page
2A-1	Guinea-Pig Rod Melt Test Schedule . . . . .	6
2A-2	Effect of Irradiation on Ultimate Tensile and Yield Strengths of 316 Stainless Steel . . . . .	7
2A-3	Probability of Fuel Centerline Temperature Being Greater Than Plotted Value . . . . .	8
2A-4	Typical Section of SEFOR Fuel Hexagonal Channel Showing Calculational Flow Cell Model . . . . .	9
2A-5	Clad Circumferential Temperature Distribution at Clad Midwall . . . . .	12
2A-6	Clad Surface Temperature Axial Distribution, SEFOR Guinea-Pig Rod in Nominal Position . . . . .	24
2A-7	Clad Surface Temperature Axial Distribution, SEFOR Guinea-Pig Rod in Central Position . . . . .	25
2A-8	SEFOR Fuel Rod Axial Nodal System Used for BEHAVE-2 Calculations . . . . .	26
2A-9	SEFOR Linear Power Cycle to 24 kW/ft Peak, Time Steps, Power Profile, and Characteristic Temperatures of Guinea-Pig Rod at Core Center . . . . .	29
2A-10	SEFOR Linear Power Cycle to 24 kW/ft Peak, Characteristic Radii of Guinea-Pig Rod at Core Center . . . . .	30
2A-11	SEFOR Linear Power Cycle to 24 kW/ft Peak, Characteristic Volumes of Guinea-Pig Rod at Core Center . . . . .	31
2A-12	Radial Distribution of Post-Irradiation Void Fractions, SEFOR Guinea-Pig Rod in a Peak Flux Position . . . . .	34
2A-13	SEFOR Guinea-Pig Rod Axial Profiles At End of the Four-Hour Linear Startup (Time Step 13) . . . . .	35
2A-14	SEFOR Guinea-Pig Rod Axial Profiles After 30-Minutes Restructuring at 24 kW/ft (Time Step 14) . . . . .	36
2A-15	Calculated SEFOR Fuel Rod 30-Minute Restructured Characteristics and Central Fuel Temperature vs Restructuring Linear Power . . . . .	38
2A-16	SEFOR Linear Peak Power to 10.5 and 21 kW/ft Levels, Time Steps, Peak Power Profile, and Central Temperature of Guinea-Pig Rod AIO . . . . .	39
2A-17	SEFOR Linear Peak Power to 10.5 and 21 kW/ft Levels, Characteristic Radii of Guinea-Pig Rod AIO . . . . .	40
2A-18	SEFOR Linear Peak Power to 10.5 and 21 kW/ft Levels, Characteristic Volumes of Guinea-Pig Rod AIO . . . . .	41
2B-1	Transient T1 Planned Power History . . . . .	50
2B-2	Transient T1 Calculated Fuel Temperatures History . . . . .	51

LIST OF ILLUSTRATIONS (Continued)

Figure No.	Title	Page
2B-3	Transient T1 Calculated Capsule Temperatures History . . . . .	52
2B-4	Transient T1 Predicted Fuel Radial Temperature Profiles . . . . .	53
2B-5	Transient T1 Calculated Melt Fraction History . . . . .	54
2B-6	TREAT C4A TEST Fuel Radial Temperature Profiles . . . . .	55
2B-7	Comparison of TREAT and SEFOR Melt Fractions . . . . .	56
2B-8	STOP Mode Simulation of Normal LMFBR Fuel Radial Temperature Profiles . . . . .	58
2B-9	Comparison of SEFOR Transients to Hypothetical LMFBR Accidents . . . . .	59
2B-10	Transient T2 Planned Power History . . . . .	60
2B-11	Transient T2 Calculated Fuel Temperatures History . . . . .	61
2B-12	Transient T2 Calculated Capsule Temperatures History . . . . .	62
2B-13	Transient T2 Predicted Fuel Radial Temperature Profiles . . . . .	63
2B-14	Transient T2 Calculated Melt Fraction History . . . . .	64
2B-15	Transient T3 Planned Power History . . . . .	65
2B-16	Transient T3 Calculated Fuel Temperatures History . . . . .	66
2B-17	Transient T3 Calculated Capsule Temperatures History . . . . .	67
2B-18	Transient T3 Predicted Fuel Radial Temperature Profiles . . . . .	68
2B-19	Transient T3 Calculated Melt Fraction History . . . . .	69
2B-20	Transient T4 Planned Power History . . . . .	70
2B-21	Transient T4 Calculated Fuel Temperatures History . . . . .	71
2B-22	Transient T4 Calculated Capsule Temperatures History . . . . .	72
2B-23	Transient T4 Predicted Fuel Radial Temperature Profiles . . . . .	73
2B-24	Transient T4 Calculated Melt Fraction History . . . . .	74
2B-25	STOP TEST CONTROLS Block Diagram . . . . .	76
3A2-1	Rod Geometries Analyzed . . . . .	88
3A2-2	Diving Bell Vent Design for Fuel Rods . . . . .	89



LIST OF ILLUSTRATIONS (Continued)

Figure No.	Title	Page
3A2-3	Diving Bell Vent Rod Design, Required Vent Length versus Coolant Pressure at Vent Outlet . . . . .	96
3A2-4	Allowable and Actual Power versus Flow Split . . . . .	97
3A2-5	SEFOR Follow-On Vented Fuel Irradiation Schedule . . . . .	100
3A2-6	SEFOR Follow-On Vented Fuel Test Schedule . . . . .	101
3A3-1	Proposed Location of Cell for Impurity Monitoring Test Loop . . . . .	107
3A3-2a	Conceptual Drawing of Test Cell for Impurity Monitoring Test Loop, Side View . . . . .	109
3A3-2b	Conceptual Drawing of Test Cell, Plan View . . . . .	110
3A3-3	Schematic Diagram of Plugging Indicator . . . . .	111
3A3-4	Schematic Diagram of Overflow Sampling Device . . . . .	112
3A3-5	Diffusion Tube Hydrogen Detector . . . . .	113
3A3-6	Schematic Drawing of Impurity Monitoring Test Loop . . . . .	114
3A10-1	Sodium Level Probe, Indication Type . . . . .	135
3A10-2	Sodium Level Probe, Displacement Type . . . . .	137
3A12-1	Primary Cold Trap, LMFBR-Demonstration Plant . . . . .	144
3B1-1	SEFOR Sodium Systems . . . . .	157
3B1-2	SEFOR Reactor Vessel . . . . .	158
3B1-3	Main Primary Sodium Piping: Reactor to IHX 204 (MPH) . . . . .	159
3B1-4	SEFOR Main Intermediate Heat Exchanger . . . . .	160
3B1-5	Main Sodium Pump . . . . .	161
3B1-6	Main Primary Cold Sodium Piping: IHX-Pump-Reactor (MPC) . . . . .	162
3B1-7	Auxiliary Primary Sodium Piping: IHX 221 . . . . .	163
3B1-8	Helical EM Pump Final Assembly, Inlet/Outlet End . . . . .	164
3B1-9	Auxiliary Primary Cold (APC) Sodium Piping: IHX 221 to Reactor . . . . .	165
3B1-10	Main Secondary Hot Sodium Piping: IHX 204 to Inlet Header . . . . .	166

LIST OF ILLUSTRATIONS (Continued)

Figure No.	Title	Page
3B1-11	SEFOR Main Air Blast Cooler . . . . .	167
3B1-12	Main Secondary Cold Sodium Piping: Outlet Header to IHX . . . . .	168
3B1-13	Auxiliary Secondary Sodium Piping (ASH): IHX to Inlet Header . . . . .	169
3B1-14	Auxiliary Secondary Cold (ASC) Sodium Piping: Outlet Header to IHX . . . . .	170
3B2-1	SEFOR Closure Assembly . . . . .	173
3B2-2	SEFOR Elevated Temperature Operation, 1 November 1973 – December 1974 . . . . .	177
3B2-3	Temperature Distribution, Steady State at 760°F . . . . .	178
3B2-4	CREEP-PLAST Model . . . . .	179
3B2-5	Heatup . . . . .	183
3B2-6	Cooldown . . . . .	184
3B2-7	Normal Scram With Immediate Recovery (7.53 hours) . . . . .	185
3B2-8	Plant Power Failure With Scram (123.03 hours) . . . . .	186
3B2-9	Plant Power Failure With Scram, No Flywheel . . . . .	187
3B2-10	Plant Power Failure Without Scram, No Flywheel . . . . .	188A
3B2-11	Effective Stress Contour Lines, Startup Transient at t = 0 . . . . .	189
3B2-12	Effective Stress Contour Lines, Startup Transient at t = 40 hours . . . . .	190
3B2-13	Effective Stress Contour Lines, Startup Transient at t = 114 hours . . . . .	191
3B2-14	Yield Zones, Startup Transient at t = 0 . . . . .	192
3B2-15	Yield Region, Startup Transient at t = 15 hours . . . . .	193
3B2-16	Yield Regions, Startup Transients at t = 40 hours . . . . .	194
3B2-17	Yielded Zones, Startup Transient at t = 114 hours (Steady-State after Transient) . . . . .	195
3B2-18	Stress-Strain History of Cylinder at Section A-A for Heatup Transient (Axial Components) . . . . .	196
3B2-19	Stress-Strain History of Cylinder at Section A-A for Heatup Transient (Circumferential Component) . . . . .	197
3B2-20	Existing Back-Up Seal . . . . .	198

LIST OF ILLUSTRATIONS (Continued)

Figure No.	Title	Page
3B2-21	Inflatable-Tube Seal . . . . .	200
3B2-22	Metal Bellows Seal . . . . .	201
3B2-23	Belleville Washer Location . . . . .	202
3B2-24	Hole Drilling Assembly . . . . .	204
3B2-25	Hole Drilling Operation . . . . .	205
3B2A-1	Temperature Distribution (1A165) Steady State at 760°F . . . . .	208
3B2A-2	SEFOR Vessel . . . . .	209A
3B2A-3	Effective Heat Transfer Coefficients for the Inner and Outer Heads . . . . .	210
3B2B-1	One-Dimensional Heat Transfer Model of the SEFOR Inner Head . . . . .	212
3B2B-2	Temperature of the SEFOR Head . . . . .	218
4A-1	Comparison of Demo Plant and SEFOR Loop Flow Geometries . . . . .	236
4A-2	Nominal Flow Coastdown Radial Temperature Distribution at 28.5 inches Above the Active Core Bottom . . . . .	237
4A-3	Rapid Flow Coastdown Radial Temperature Distribution at 28.5 inches Above the Active Core Bottom . . . . .	238
4A-4	Effect of Liner Heat Capacity With Bundle Size . . . . .	239
4A-5	Axial Temperature Profiles for Slow and Rapid Flow Transients . . . . .	240
4B3-1	Axial Power Distribution, In Booster . . . . .	249
4B3-2	Relative Power Density versus Axial Peak Location . . . . .	250
4B3-3	Booster Fuel Rod, SEFOR Option III-A . . . . .	254
4B3-4	Circumferential Distribution of the Midwall Cladding Temperature in the Peak Rod at the Core Midplane . . . . .	256
4B3-5	Circumferential Distribution of the Midwall Cladding Temperature in the Peak Rod at the Top of the Core . . . . .	257
4B3-6	Fission Gas Pressure versus Plenum Length, 36-inch SEFOR Booster Fuel Rods . . . . .	260
4B3-7	Plenum Length versus Temperature, 36-inch SEFOR Booster Fuel Rods . . . . .	264
4B3-8	Effect of Irradiation on UTS and YS of 316 Stainless Steel . . . . .	269

LIST OF ILLUSTRATIONS (Continued)

Figure No.	Title	Page
4B3-9	316 SS UTS and YS Unirradiated Properties . . . . .	270
4B3-10	316 SS UTS and YS Irradiated Properties, 0.4 to 0.75 X 10 <sup>22</sup> nvt 7.1 Mev . . . . .	271
4B3-11	Alternate Core Pattern I . . . . .	273
4B3-12	Alternate Core Patterns II and III . . . . .	274
4B3-13	Fuel Loading Sequence . . . . .	275
4B3-14	SEFOR Fuel Assembly Details . . . . .	276
4B3-15	Fuel Assembly Orifice Adapter . . . . .	277
4B3-16	Fuel Assembly Spider, Upper and Lower . . . . .	278
4B3-17	Aligned, Self-Centering Fuel Pin to Spider Connector . . . . .	279
4B3-18	Self-Centering Fuel Pin Upper Spider . . . . .	280
4B3-19	Adaptor for Fuel Assemblies Incorporating Extension Rods . . . . .	281
4B3-20	Fuel Assembly Channel Lock . . . . .	282
4B3-21	Low End of Fuel Assembly Tightening Rod . . . . .	283
4B3-22	Extension Rod Spacer Assembly . . . . .	284
4B3-23	Booster Channel Positioning Collar . . . . .	287
4B3-24	Driver Channel Positioning Collar . . . . .	288
4B3-25	Booster Fuel Assembly Orifice Adaptor . . . . .	289
4B3-26	Driver Fuel Assembly Orifice Adaptor . . . . .	290
4B3-27	Leading Sequence Interlock Provisions, Booster-Driver Assembly . . . . .	291
4B3-28	Locations of Sequence Interlocks . . . . .	292
4B3-29	Core Pattern . . . . .	294
4B3-30	Moveable Control Assembly Cross-Section . . . . .	295
4B4-1	SEFOR Main IHX Required Overall Heat Transfer Coefficient versus Reactor Power . . . . .	299
4B4-2	Main Air Blast Cooler Overall Heat Transfer Coefficient versus Air Flow . . . . .	300
4B4-3	Main Air Blast Cooler Blower Discharge Pressure versus Air Flow . . . . .	301

## LIST OF ILLUSTRATIONS (Continued)

Figure No.	Title	Page
4B4-4	Reactor Inlet Temperature as a Function of Air Blast Cooler Air Flow, Option III-A, 23 MW Operation . . . . .	302
4B4-5	SEFOR Nitrogen Cooling System Load . . . . .	303
4B5-1	61-Rod Subassembly Cross-Section . . . . .	307
4B5-2	Radial Power Distribution in Test Fuel Region . . . . .	310
4B5-3	Absorption Rate in Control Rods ( $\eta$ , $\alpha$ ) versus Boron Enrichment . . . . .	313
4B5-4	Control Rod Worth versus Boron Enrichment . . . . .	314
4B5-5	SEFOR Reference Core Geometry, SEFOR Follow-On, Option III . . . . .	329
4B6-1	Package Loop Outline . . . . .	338
4B6-2	Package Loop Assembly Drawing . . . . .	339
4B6-3	Package Loop Support Tube and Instrumentation Assembly Drawing . . . . .	341A
4B6-4	Package Loop Assembly Sequence Drawing . . . . .	342
4B7-1	SEFOR Fuel Handling and Shipping Equipment Development Plan . . . . .	344
6-1	General Electric Breeder Reactor Department Partial Organization Chart . . . . .	351
6-2	General Electric Breeder Reactor Department Development Program Task Management Relationships . . . . .	352
6-3	BRD Quality Assurance Organization . . . . .	360
6-4	Typical BRD Quality System Documentation . . . . .	362

## LIST OF TABLES

Table No.	Title	Page
2A-1	Core Characteristics—Driver Fuel . . . . .	3
2A-2	SEFOR Uncertainties ( $1\sigma$ ) . . . . .	5
2A-3	SEFOR Flow Model Splits . . . . .	5
2A-4	Expected Pressures (psi) (at 840°F) . . . . .	10
2A-5	Expected Pressure Stresses . . . . .	11
2A-6	Local and Maximum Bending Stresses in the Hot Driver Fuel . . . . .	14
2A-7	Longitudinal Stresses in the Driver Fuel Rod Cladding (20 MW <sub>t</sub> , 840°F) . . . . .	15
2A-8	Radial and Circumferential Stresses in the Fuel Rod Cladding (20 MW <sub>t</sub> , 840°F) . . . . .	16
2A-9	Stress Criteria . . . . .	17
2A-10	Limiting Stress Criteria (psi) . . . . .	18
2A-11	Primary Membrane (Lower Plenum—2 X SEFOR Spec. on Moisture, Temperature — 840°F, Clad I.D.) . . . . .	19
2A-12	Primary Membrane + Primary Bending + Secondary Principal Stresses . . . . .	20
2A-13	Clad Temperature—Linear Power Relationship (20 MW <sub>t</sub> ) . . . . .	22
2A-14	Clad Temperature—Linear Power Relationship (10 MW <sub>t</sub> ) . . . . .	23
2A-15	Guinea Pig Rod Parameters . . . . .	27
2A-16	Relative Power Distribution . . . . .	28
2B-1	Target Fuel Rod Parameters . . . . .	44
2B-2	SEFOR Follow-On Option I Transient Overpower Tests . . . . .	45
2B-3	Candidate Pre-Irradiated Fuel Rods for Transient Overpower Tests . . . . .	48
2C(3)	Sub-Prompt Transient Tests . . . . .	81
3A2-1	Limiting Temperature and Pressure Swings for the Demonstration Plant and SEFOR Reactor . . . . .	87
3A2-2	Rod Vent Lengths, and Maximum Average Volumetric Operating Temperatures in SEFOR at 20 MW <sub>t</sub> . . . . .	90
3A2-3	Gaseous Fission Product Yields . . . . .	92
3A2-4	Fraction of Porosity Available to Gases . . . . .	92

LIST OF TABLES (Continued)

Table No.	Title	Page
3A2-5	Non-Vent Cold Volumes for Gas Expansion . . . . .	94
3A2-6	Hot Blanket ( $V_b$ ) and Core ( $V_c$ ) Volumes for Gas Expansion . . . . .	94
3A10-1	Tabulation of Features of Analogue Level Meter Concepts and Applications . . . . .	126
3A12-1	Data Sheet Primary Cold Traps . . . . .	142
3A13-1	Demo Plant Purge Type Vapor Traps Requirements . . . . .	146
3B1-1	Results of Preliminary Stress Evaluations . . . . .	151
3B2-1	Postulated Operating History of the SEFOR During The Elevated Temperature Phase . . . . .	175
3B2-2	Primary Sodium Outlet Temperature Transients For Evaluation of the SEFOR Reactor Vessel During Elevated Temperature Operation . . . . .	176
3B2B-1	Inner Head Temperature Distribution . . . . .	219
3B3-1	Core Characteristics – Driver Fuel . . . . .	228
4B3-1	Allowable Stress Intensity . . . . .	247
4B3-2	Subassembly Compositions . . . . .	248
4B3-3	Booster Assembly Characteristics SEFOR Follow-On Core Power: 23 MW . . . . .	253
4B3-4	Temperature Effect of Fuel Rod-Channel Clearance . . . . .	255
4B3-5	Peak Cladding Temperatures . . . . .	255
4B3-6	Fission Gas Pressure and Stress vs Plenum Length (50,000 MWd/Te Burnup) . . . . .	261
4B3-7	Local and Self-Equilibrating Thermal Stresses . . . . .	261
4B3-8	Primary Membrane Stresses (Hot Spot Rod at Clad I.D. for 50,000 MWd/Te Burnup) . . . . .	265
4B3-9	Longitudinal Stresses (psi) . . . . .	265
4B3-10	Radial Stresses . . . . .	266
4B3-11	Circumferential Stresses . . . . .	267
4B3-12	Primary Membrane and Primary Bending and Secondary – Principal Stresses . . . . .	268
4B5-1	Reference Scope Design . . . . .	306
4B5-2	Subassembly Options . . . . .	306

LIST OF TABLES (Continued)

Table No.	Title	Page
4B5-3	Pu/U+Pu . . . . .	308
4B5-4	Core Design Parameters . . . . .	309
4B5-5	Reflector Worth For Different B <sub>4</sub> C Thicknesses . . . . .	326
4B5-6	Doppler Coefficient of Booster Region . . . . .	326
4B5-7	Power Generation . . . . .	327
4B5-8	Spectra Comparison . . . . .	328
4B5-9	Materials Available on Mug File . . . . .	331
4B5 10	Materials Available on ENLID File . . . . .	332
4B5-11	Zirconium Cross Sections . . . . .	333
4B5-12	Compositions Used To Obtain Self-Shielded Cross Sections . . . . .	335
6-1A	Typical Activities and Documentation Review and Approval Requirements For Development Programs . . . . .	355
6-1B	Typical Activities and Documentation Review and Approval Requirements For Development Programs . . . . .	356



## 1.0 TASK 1 – PROGRAM MANAGEMENT

### 1.1 OBJECTIVE

The objectives of this task are to coordinate and exercise project control of the work performed within the other five tasks of the Phase A Program, to maintain liaison with all the cognizant parties concerned with the SEFOR Follow-On Program, to prepare and issue the monthly reports and the final report, and to accomplish scheduling and planning activities.

### 1.2 DISCUSSION

Five monthly progress letters were prepared and issued, one for each of the months of July through November, 1971. This document, the Final Report for Phase A, reports on all work accomplished during the period June 15, 1971 through December 31, 1971. Subsequent activities that may occur under an interim extension of Phase A will be reported in monthly progress letters and topical reports as required by the revised scope of work.

Planning and scheduling of activities were accomplished. The engineering software output requirements were identified, scheduled, and monitored by a computer program. Automated planning and scheduling techniques for application on SEFOR Follow-On Phase B were initiated to control and schedule the progress of engineering efforts, to monitor and report status of procurement, fabrication, and delivery of equipment to the SEFOR Site, installation of equipment, performance of the tests, and the reporting of results to assure that commitments were met. A central filing system for the Follow-On Program was established. Completion and thorough implementation of planning, scheduling and control techniques, and procedures were interrupted by the delay in proceeding with Phase B and the uncertainty in scope of work subsequent to Phase A.

Two technical review meetings were held in Sunnyvale between GE personnel and the RDT Task Force for SEFOR Follow-On as follows:

August 19 – 20, 1971

December 1 – 3, 1971

A meeting with DRL occurred on September 29, 1971 which involved initial discussions of the proposed over-all SEFOR Follow-On Program with special emphasis on near-term license requirements.

Progress of work under Phase A was presented, and the proposed scope of work for Phase B generated under Tasks 2 and 3 of a program funded by GE, GfK, and SAEA was discussed with representatives of AEC, SAEA, and GfK during the SEFOR semi-annual Technical Policy Committee Meeting at Karlsruhe, September 17 – 18, 1971.

As a result of conclusions reached in the two technical meetings with the RDT Task Force, some changes in emphasis were made so that work to minimize schedule delays and to more directly address areas of feasibility could proceed as required.

Emphasis was increased on:

FRED relocation

STOP Operation for Option I

Reactor vessel analyses for elevated temperature operation

Development of Option III-A booster fuel

Emphasis was reduced on:

Guinea Pig rod tests

Core clamping tests

Subassembly Instrumentation tests

Failed fuel detection tests

Plant systems analyses for elevated temperature operation

Licensing and safety evaluations for elevated temperature operation

Initial SAR submittal for Option I was limited to transient overpower capsule tests.

## 2.0 TASK 2 – OPTION I PLUS SELECTED PLANT TESTS

### 2.1 TASK 2A – DRIVER FUEL PERFORMANCE LIMITS

#### 2.1.1 Objective

The objective of this task is to complete the preliminary planning of a test program to establish and demonstrate performance limits of SEFOR driver fuel.

### 2.1.2 Discussion

The present SEFOR experimental program uses a sampling of higher enriched fuel rods ("guinea-pig rods") which operate at a linear power rating approximately 15% greater than the peak SEFOR fuel rod. Under present plant operation, power densities are maintained at a level which will prevent these rods from reaching central melting. In the SEFOR Follow-On Program, the SEFOR guinea-pig rods would be operated at steady-state conditions intended to reach power levels approximately 30% greater than the peak SEFOR standard rod to gain early information on operation under conditions with molten fuel.

The objective of this task has been accomplished with the development of an irradiation test plan, and with the performance of preliminary analyses of the driver and guinea-pig fuel rods in support of this plan. These supportive analyses were done using both conventional methods of design analysis and the fuel performance code BEHAVE-2.

The major conclusions of this preliminary study are that present guinea-pig rods may have experienced some melting, that significant melting can be achieved with a guinea-pig rod at core center at reactor full power, and that the cladding will sustain insignificant deformation at that position under the cycle described.

### 2.1.3 Guinea-Pig Rod Melt Test Plan

The proposed irradiations would utilize four of the existing unirradiated SEFOR guinea-pig rods to obtain data on performance when operating under partial fuel melt conditions. All four test rods will initially be non-destructively examined. Figure 2A-1 shows the tentative test schedule. The first test consists of a controlled rise to power using two of the four rods. These rods will be at full-power (partial melt) conditions for a short period of time (few minutes) in order to establish the melted-fuel microstructure and yet keep axial fuel movement at a minimum. A profilometry exam after the power ascent will document any diametral changes. Following this irradiation, one rod will undergo complete non-destructive and destructive examination. These test and exam results will provide the basis for any changes in subsequent test conditions which may be necessary to achieve the desired level of fuel melting.

During the second irradiation test, the remaining partially-melted rod will again be taken to power in a cycle similar to the first and remelted. The destructive examination of this rod will yield information regarding the remelt temperature.

The remaining two unexposed rods will then be tested with the period of operation at steady-state extending to a few weeks. The destructive examination of one of these rods will provide data on axial fuel movement under the partial melt condition. One rod, which can be expected to have fuel geometric features similar to those of the final rod examined, will be held in abeyance in order to provide a specimen for possible further testing.

### 2.1.4 Design Analysis

To assure that the driver fuel would meet design performance criteria during Option I testing, an updated analysis was performed. In this analysis, all calculations, except those dealing with fuel temperatures, were done on a nominal basis without uncertainties. The fuel temperature calculations were undertaken with the object in mind of determining what probability the peak driver fuel (and guinea-pig lead fuel) has of running, at the present SEFOR operating conditions, at a temperature in excess of 5000°F. The object of the fuel-rod stress calculations was a simplified first look at SEFOR fuel-rod stresses on a nominal basis and a comparison to the present MFBR interim stress design criteria. No attempt was made to evaluate the strain fatigue, thermal ratcheting, and buckling portion of the structural criteria.

The fuel temperature hot spot calculations included uncertainty analysis. This work included the present driver fuel, guinea-pig rods in their present core location, and guinea-pig rods hypothetically placed in the center position of the present SEFOR core. The analysis should be considered a preliminary rather than a complete analysis of the present SEFOR core at 20 MWt operation.

Only the hot spot driver fuel was subjected to stress analysis. The analysis was performed at both the core midpoint and core outlet. Changes in the as-designed core versus the present core are shown in Table 2A-1.

The material properties values of yield and ultimate stress have been updated and are shown in Figure 2A-2. This data came from References 2,3,4,5,6,7, and 8. The SEFOR Option I core will have a total rod cumulative peak burnup of 2280 MWd/Te; however, it was also desired to know for what length of time the present driver fuel would stay within criteria limits. Therefore, the fuel was analyzed at two points in time, 2280 MWd/Te burnup and 5000 MWd/Te burnup.

Table 2A-1

## CORE CHARACTERISTICS - DRIVER FUEL

	Original Design Core I and II	Present Fuel Analysis Option I, 2(a)
Power (MWt)	20	20
Heat Flux (Btu/hr-ft <sup>2</sup> )		
Average	152,000	153,000
Maximum	280,000	270,000
Linear Power Generation (kw/ft)		
Average	11.3	10.5
Maximum	20.8	18.4
Specific Power (kw/kg)		
Average	8.89	8.89
Maximum	15.65	15.65
Power Density of Core (kw/liter)		
Average	36.8	36.8
Maximum	64.7	64.7
Coolant Temperatures (°F)		
Inlet	700	700
Outlet - Core Average	820	820
Maximum During Transients	1050	1050
Fuel Temperature (°F)		
Average	1900	~2100
Maximum	<5000	<5100
Coolant Velocity (ft/sec)		
Average	5.4	5.4
Maximum	8.3	8.3
Power Peak-to-Average Factors		
Radial	1.47	1.43
Axial	1.24	1.24
Local	1.01	---
Total	1.84	1.76
Burnup (MWd/Te)		
Peak Local	---	2830
Peak Rod	1500	2280
Peak Internal Gas Pressure (psi)	570	1020
Fluence, Peak Local (nvt)	$2.6 \times 10^{21}$	$4.8 \times 10^{21}$

Table 2A-1 (Cont.)

CORE CHARACTERISTICS - DRIVER FUEL

	Original Design Core I and II	Present Fuel Analysis Option I, 2(a)
Pressure Drop (psi)		
Total Reactor	28.9	28.9
Core	3.8	3.8
Flow Rate (10 <sup>5</sup> lb/hr)		
Core Flow	18.67	18.67
Leakage	2.82	2.82
Total	21.50	21.50

The following conditions were considered for the stress study of the present SEFOR fuel rods:

- Fission gas pressure
- Fuel rod bending
- Radial heat flow
- Circumferential gradients
- Vibration
- Axial gradients
- Fuel-clad mechanical interaction

The following areas were not analyzed due to the preliminary nature of this task:

- Local spacer loads
- Local thermal stress (from spacer perturbation of the coolant flow)
- End and segmenting plug structural and/or thermal discontinuities
- Transient conditions

Because SEFOR fuel clad runs at low temperature and is a low burnup fuel, no allowance has been made for irradiation induced creep (calculated to be  $\leq 0.08\%$  at 5000 MWd/Te) or swelling ( $\leq 0.15\%$  at 5000 MWd/Te). For the same reason (low temperature), no allowance for corrosion and/or fuel-clad chemical attack has been made.

The criteria to which these stresses will be compared are shown in Table 2A-9.

**2.1.5 Results**

**2.1.5.1 Steady-State Temperature Distribution**

- SEFOR fuel centerline temperature

SEFOR fuel steady-state temperatures for a power range from 14 to 25 kW/ft have been calculated using the probabilistic code PEFT (Ref 9). PEFT is a one-dimensional computer code designed to yield probability distributions of fuel, cladding, and coolant temperatures at a single location and time within a reactor for steady-state operation. The principal feature of the program is that 37 of the important design parameters are permitted to be probabilistic (multi-valued), rather than deterministic (single valued). Seven of the most important uncertainties (they account for  $\sim 99\%$  of the total uncertainty effect) were evaluated and input as normal distributions to the PEFT Code. The inputs are shown in Table 2A-2. Figure 2A-3 gives the resultant fuel centerline temperature probabilities for a power range of 14-25 kW/ft. Indicated are the peak powers of the rods of interest at full reactor power.

The above analysis was used to determine the SEFOR design margin. A conservative temperature of 5000° was chosen for the original design limit (page 1 – 117, Ref 13) to insure no melting. With present uncertainties, there is an 88% probability that the peak pellet centerline temperature in the SEFOR driver fuel is less than

Table 2A-2

SEFOR UNCERTAINTIES ( $1\sigma$ )

Parameter	Fractional Uncertainty
Power Measured	$\pm 0.0250$
Local Power Density	$\pm 0.0300$
Fuel Pellet Diameter	$\pm 0.0006$
Fuel Pellet Density	$\pm 0.0108$
Fuel Gap Conductance	$\pm 0.1000$
Fuel Thermal Conductivity	$\pm 0.0913$
Flow Uncertainty	$\pm 0.1000$

5000°F when the reactor is operated at 20 MWt. In relation to nominal values, this is equivalent to a design margin of 11% on temperature and 13% on power. The same analysis has indicated that the highest power guinea-pig rods have a >50% (~53%) probability of exceeding a 5000°F (50%) = 5040°F centerline fuel temperature at a reactor power of 20 MWt in their present position. If these guinea-pig rods were placed in the central location at 20 MWt, approximately 25 to 30% of the peak pellet weight would be expected to be  $\geq$  5000°F and a centerline temperature of 5550°F would be obtained. This analysis does not take into account any effects of Pu migration but assumes sufficient time at steady-state power for complete restructuring of the fuel. Reference 10 is the source of the fuel thermal conductivity used in these calculations.

- Cladding Temperature Distribution

In order to calculate the local and the bending stresses, it is necessary to know the circumferential temperature distribution of the cladding. In order to determine this temperature distribution, a THTD model (Transient Heat Transfer Version D – Reference 11) of a symmetrical section of a SEFOR fuel assembly (see Figure 2A-4) was used.

Figure 2A-4 also shows the model at flow cell divisions used to calculate circumferential temperature effects on the cladding. Table 2A-3 shows the flow division for the model. This flow model neglects the shear forces between adjacent fluid streams resulting in overestimates of the flow and temperature variation around the rod. Since this causes calculated stresses higher than would otherwise be estimated, it produces conservative results.

Table 2A-3

## SEFOR MODEL FLOW SPLITS

Flow Cell Type (Ref. Fig. 2A-4)	Flow in Cell as Fraction of Total Assembly Flow
1	0.0090
2	0.0041
3	0.0090
4	0.0125
5	0.0097
6	0.0063
7	0.0063
8	0.0147
9	0.0073

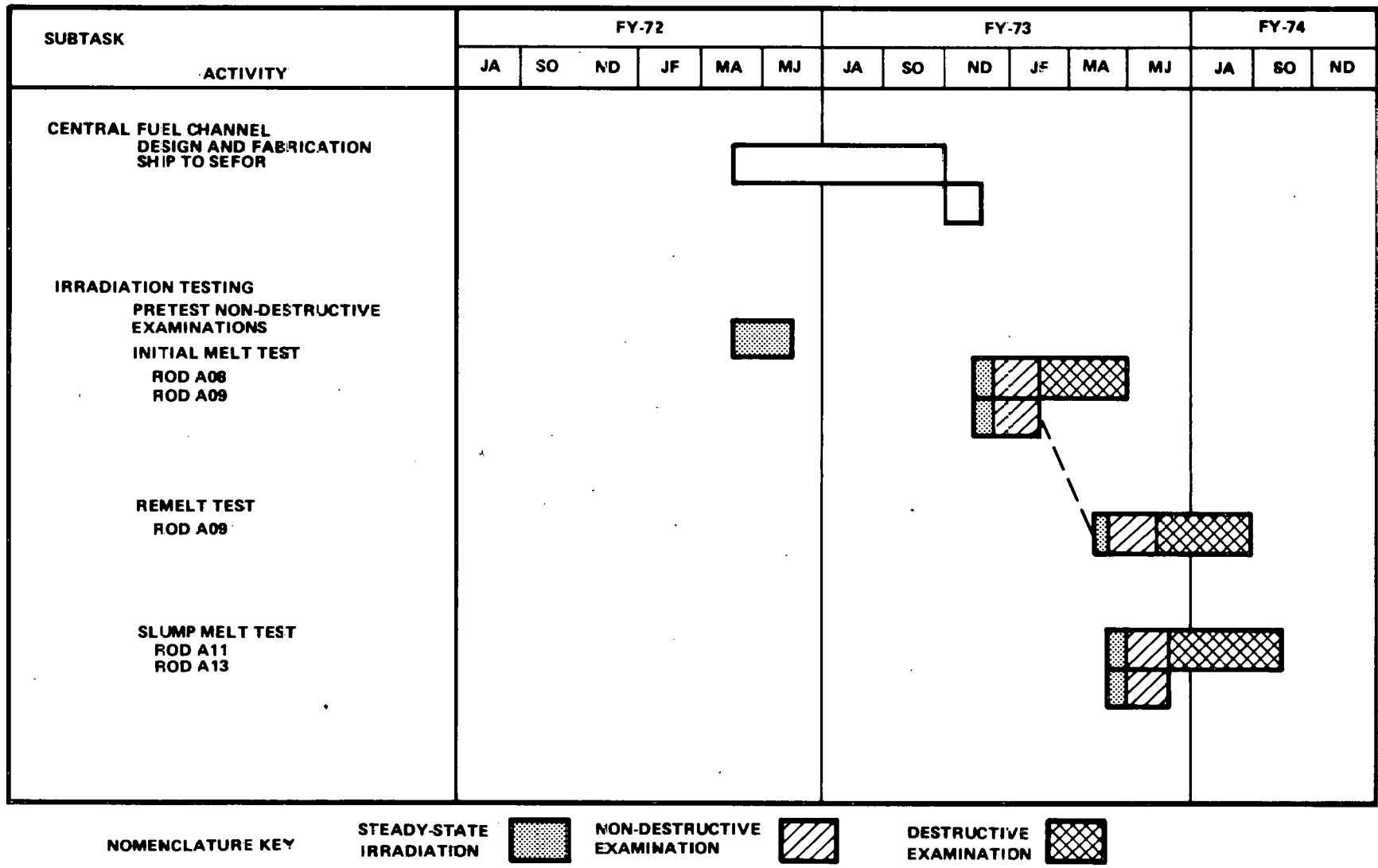


Figure 2A-1. Guinea-Pig Rod Melt Test Schedule

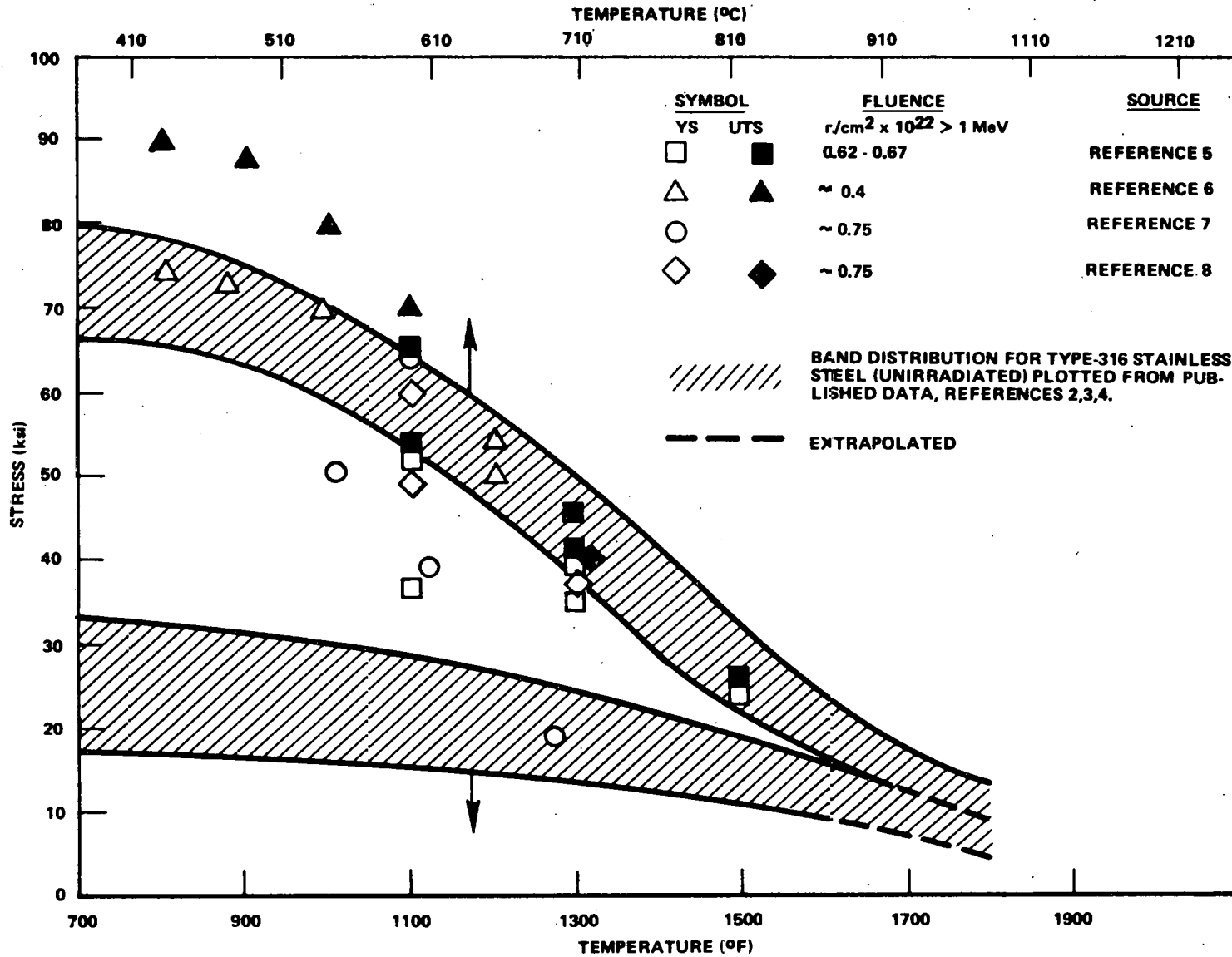


Figure 2A-2. Effect of Irradiation on Ultimate Tensile and Yield Strengths of 316 Stainless Steel

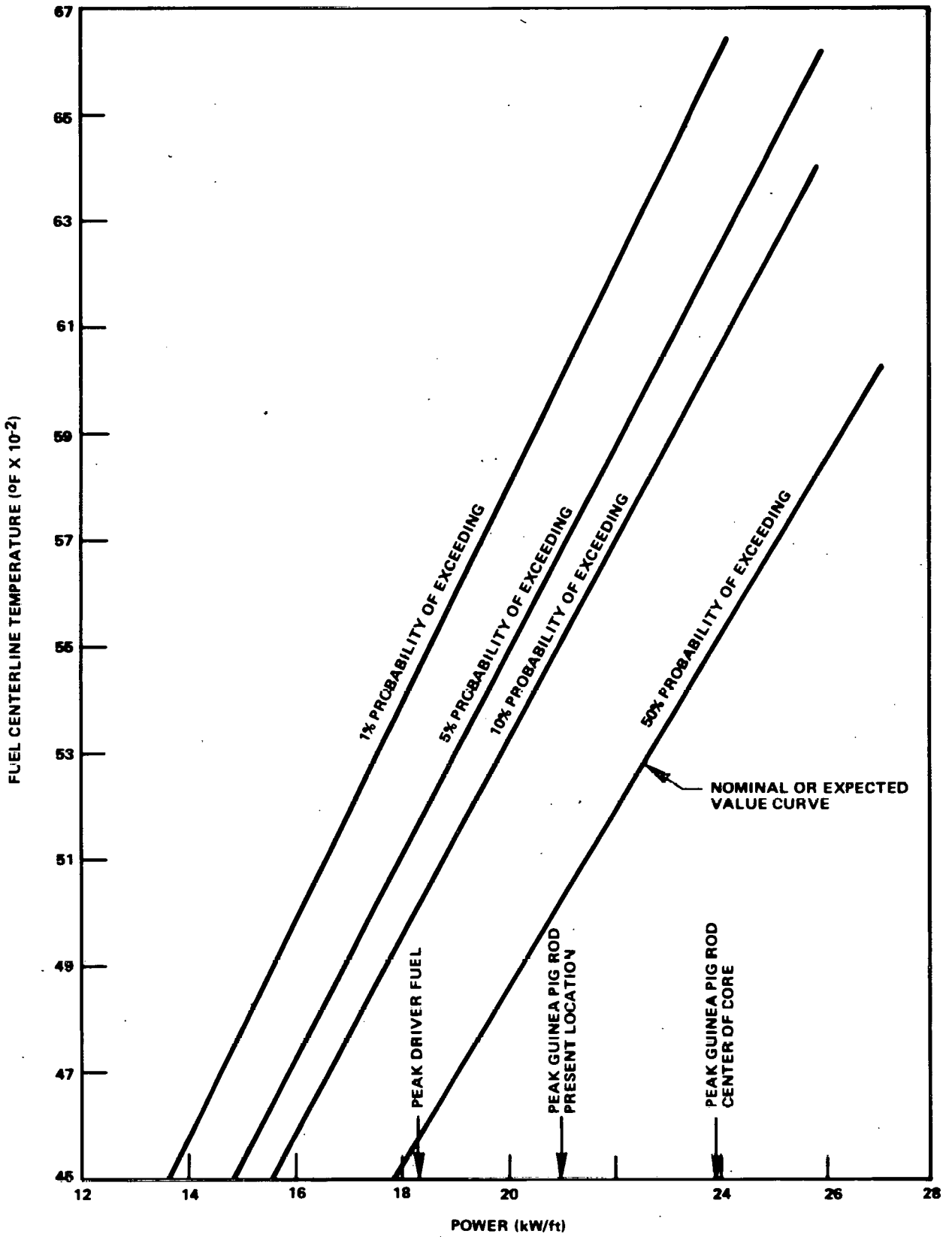


Figure 2A-3. Probability of Fuel Centerline Temperature Being Greater Than Plotted Value



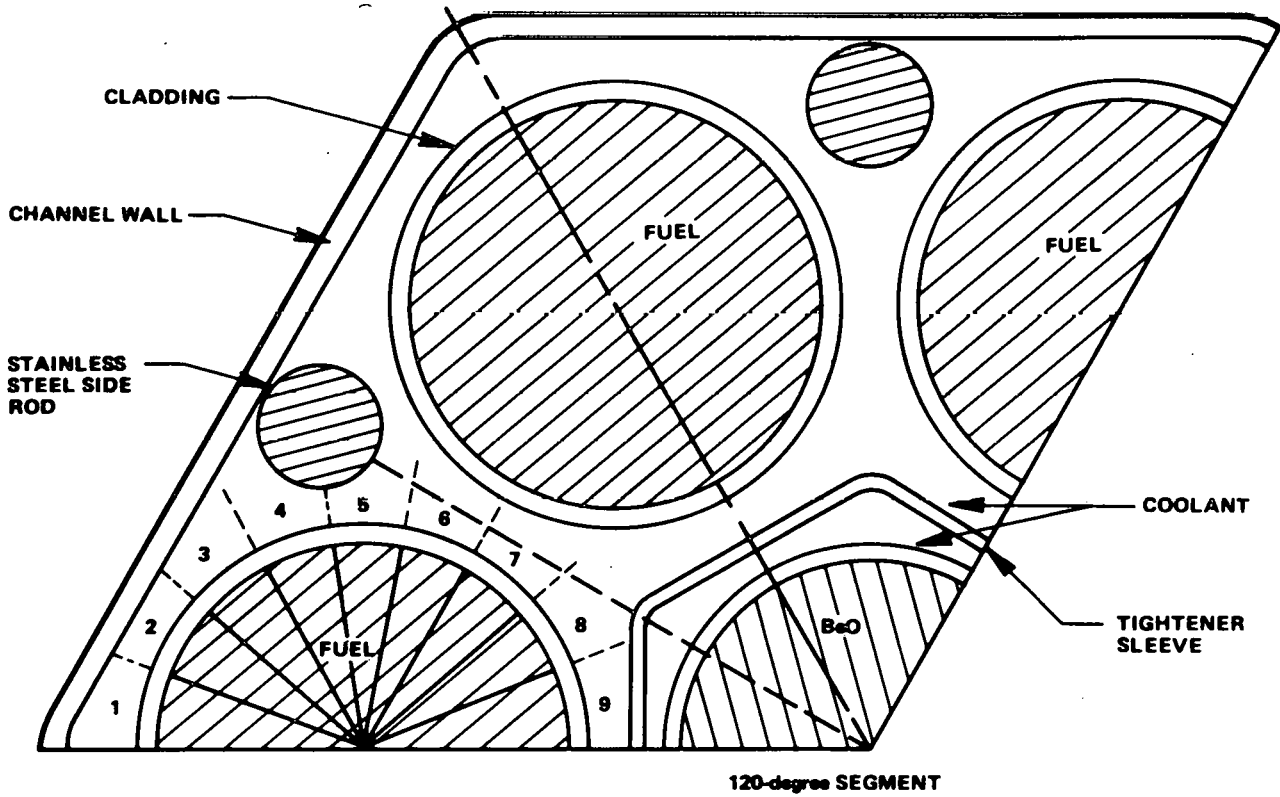


Figure 2A-4. Typical Section of SEFOR Fuel Hexagonal Channel Showing Calculational Flow Cell Model

The clad circumferential temperature distributions for the peak driver fuel rod at 20 MWt operation at the core midplane and outlet are shown in Figure 2A-5.

The SEFOR rod was partitioned to minimize the effects of axial fuel movement on the physics experiments for which the reactor was built. The fuel rod has an upper and lower fuel column with a separate gas plenum for each.

Two axial locations on the SEFOR peak driver fuel rod were considered for structural analysis. These were the core midplane (peak power location) and the core outlet. The average temperatures of the clad midplane and I.D. at these points were calculated using THTD (Ref. 11). They are shown below along with the values for the lower plenum.

	Average Temperature (°F)		
	Core Midplane	Lower Plenum	Core Outlet (Upper Plenum)
Clad I. D.	822	837	844
Midwall	795	812	831
Coolant	760	780	819

**2.1.5.2 Stress Analysis of Peak Driver Fuel**

- Fission gas pressures and stresses

The fission gas pressure and stresses have been calculated for both upper and lower plenums assuming 100% gas release. The effect of 2 times the SEFOR fuel specifications on condensable gases (primarily H<sub>2</sub>O) has also been calculated for the above.\*

If, for present Option I Operation, it is assumed that both the upper and lower plenums operate at 840°F, the pressures and stresses shown in Tables 2A-4 and 2A-5 are predicted. These axial and circumferential stresses occur throughout the clad and are always tensile (positive).

**Table 2A-4**

**EXPECTED PRESSURES (PSI)  
(840°F)**

	0 Burnup	2280 MWd/Te Burnup	5000 MWd/Te Burnup
Upper Plenum			
1x spec. limit moisture	415	615	860
2x spec. limit moisture	565	765	1010
Lower Plenum			
1x spec. limit moisture	560	830	1160
2x spec. limit moisture	750	1020	1350

\*Reference 12 indicates that the SEFOR fuel may be as much as 100% out of specification on condensable gases entrained in the fuel.

Table 2A-5

EXPECTED PRESSURE STRESSES\*  
(PSI)

Circumferential** (Hoop) Stress	0 MWd/Te Burnup	2280 MWd/Te Burnup	5000 MWd/Te Burnup
Upper Plenum			
1x spec. limit moisture	4502	6672	9331
2x spec. limit moisture	6130	8300	10958
Lower Plenum			
1x spec. limit moisture	6076	9005	12586
2x spec. limit moisture	8137	11067	14647
<b>Longitudinal Stress**</b>			
Upper Plenum			
1x spec. limit moisture	2251	3336	4665
2x spec. limit moisture	3065	4150	5479
Lower Plenum			
1x spec. limit moisture	3038	4502	6293
2x spec. limit moisture	4068	5533	7323
<b>Radial Stress*** (Max)</b>			
Upper Plenum			
1x spec. limit moisture	-415	-615	-860
2x spec. limit moisture	-565	-765	-1010
Lower Plenum			
1x spec. limit moisture	-560	-830	-1160
2x spec. limit moisture	-750	-1020	-1350

\* Primary Stress

\*\* Tensile and throughout the clad

\*\*\* Compressive Stress maximum at clad I.D. falling off linearly to 0 at clad O.D.

In addition, a radial stress is present because of the fission gas pressure. It is compressive (negative) and equal to the gas pressure at the clad I.D. and zero at the clad O.D.

• Thermal stresses in clad during normal operation

There are three types of thermal stresses in the clad during normal operation: radial temperature gradient stress, local stresses, (i.e., the self-equilibrating thermal stress due to a harmonic type of circumferential temperature gradient) and the bending stress caused by bowing restraint of the pin.

For center core the peak power is  $150 \text{ w/cm}^3$  or  $18.35 \text{ kW/ft}$  for the innermost driver fuel, (local heat flux =  $270,000 \text{ Btu/hr ft}^2$ ). The clad temperature is  $\sim 825^\circ \text{F}$  at this location, therefore the thermal stress due to the radial temperature gradients was  $\pm 16576 \text{ psi}$ .

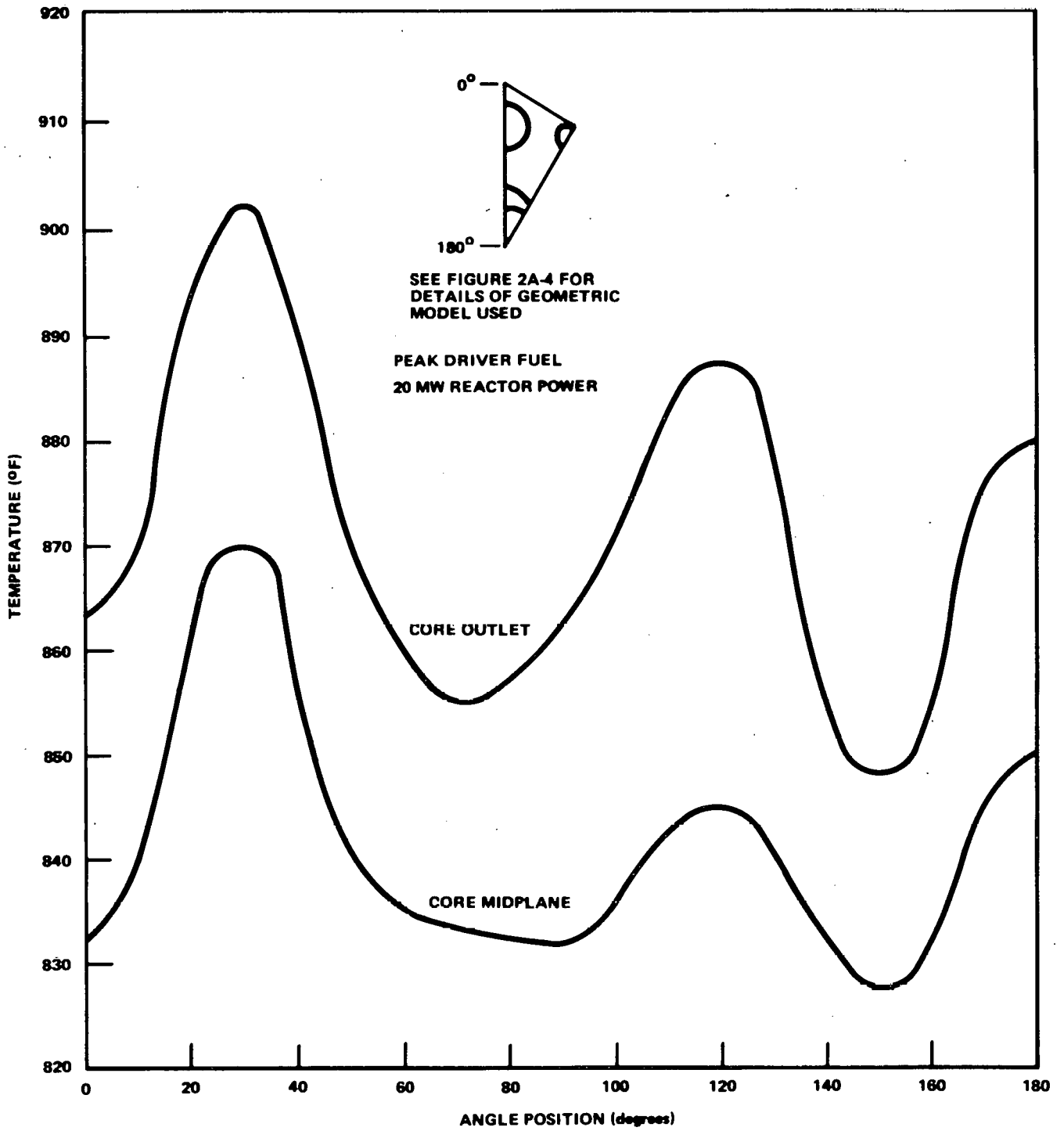


Figure 2A-5. Clad Circumferential Temperature Distribution at Clad Midwall

At the core outlet, the value of heat flux is 0.46 that of the center location (Ref 13) and the clad temperature is  $\sim 900^{\circ}\text{F}$  which produces a stress of  $\pm 7192$  psi.

These stresses are negative on the clad I.D. and positive on the clad O.D. and act in both the longitudinal and circumferential directions. The above calculation also assumes a worse case tolerance effect of the thickness and is thus conservative in this respect.

The local (self-equilibrating thermal stresses) and bending stresses were calculated by the fitting of a Fourier series to the clad mid-thickness temperature distribution (Figure 2A-5) to obtain the zero-th and first harmonic of the distribution. Subtracting the zero-th harmonic (or average temperature) leaves the temperature distribution associated with the thermal stresses when thermal curvature is suppressed along the full length of the rod by a restraining bending moment. Further subtracting the first harmonic temperature component (equivalent to a linear gradient across the diameter) determines the temperature distribution which causes the self-equilibrating thermal stresses. The results of this analysis are shown in Table 2A-6. These stresses occur throughout the clad with the given sign.

- Vibration

Vibration of fuel rods is caused by the turbulent fluid motion as it passes through the fuel assembly. This fluid turbulence tends to be damped as the flow proceeds through the assembly. Vibrational loads and stresses were computed using two different parallel flow induced vibration correlations. The two, that of Chen (Ref 14) and of Reavis (Ref 15), both indicate negligible stresses ( $\leq 10$  psi) due to fuel rod vibration induced by parallel flow.

- Axial gradients

The clad sustains a radial growth due to thermal expansion and irradiation induced swelling, both of which have non-linear axial distributions. At the lower end of the core these expansions tend to reinforce each other while at the upper end of the core the expansions tend to counteract in the axial direction. The result is a non-linear radial deflection of the clad which results in an axial bending stress. Stress resulting from this distortion is essentially a thermal stress. These stresses have been calculated to be  $\leq 10$  psi and are thus negligible.

- Fuel-clad mechanical interaction

During the lifetime of the fuel both the clad and fuel swell. SEFOR fuel is designed with a fuel-clad gap and a fuel density intended to preclude the interference of the fuel with the clad. This has been verified by extensive testing. Thus, stresses and strains from fuel clad mechanical interaction are considered to be zero.

- Combined Stresses

A summary of individual steady-state stresses is tabulated in Tables 2A-7 and 2A-8. These show the longitudinal, radial, and hoop stresses for the peak driver fuel rod in the nominal position at both midcore and core outlet. All fission gas induced stresses (and creep rupture damage fraction) have been calculated using twice the SEFOR specification limit on condensable gases (moisture).

The present design criteria (Ref 16, Table 3-1 and 3-2) has two material categories, ductile and quasi-brittle. A material is assumed to go from ductile to quasi-brittle where the total elongation of the material decreases to 10% (which is mostly due to irradiation effects). Materials irradiated sufficiently to have total elongations below 10% are termed "quasi-brittle", and those with elongations above this, "ductile". For 316 stainless steel annealed Reference 16 (Figure 1-2) shows  $3.5\text{-}4.0 \times 10^{21}$  nvt  $> 0.1$  MeV as the fast fluence needed to reduce the lower limit of total elongation to 10% for temperatures of  $\sim 840^{\circ}\text{F}$ . The SEFOR reactor cumulative peak rod fluence will exceed this amount approximately half way through the Option I operation. Therefore, the peak burnup SEFOR fuel rod (at core midplane) should be considered ductile until the cumulative peak rod burnup surpasses 1750 MWd/Te. The core outlet operates at 0.46 power of the core centerline. Therefore the upper plenum should remain ductile through the Option I operation to approximately 3500 MWd/Te cumulative peak rod burnup. Table 2A-9 summarizes the criteria for these conditions.

Table 2A-6

LOCAL AND MAXIMUM BENDING STRESSES IN THE HOT DRIVER FUEL\*

CORE OUTLET

Circumferential Angle °	Local Stress (psi)	Bending Stress (psi)	Local + Bowing Stress (psi)
0	4858	-2271	2587
15	-234	-2194	-2428
30	-6533	-1967	-8500
45	-822	-1606	-2428
60	4514	-1135	3379
75	5287	-588	4699
90	2587	0	2587
105	-1696	588	-1108
120	-4884	1136	-3748
135	453	1606	2059
150	4580	1967	6547
165	-134	2195	2059
180	-4172	2272	-1900

MIDCORE

0	3573	-1326	2247
15	-920	-1237	-2157
30	-6274	-1148	-7422
45	-216	-905	-1121
60	2387	-663	1724
75	2720	-331	2389
90	2509	0	2509
105	418	331	749
120	-1551	663	-888
135	399	905	1304
150	2406	1148	3554
165	-466	1237	771
180	-3521	1326	-2195

\* These stresses occur throughout the clad with the given sign

Table 2A-7

LONGITUDINAL STRESSES IN THE DRIVER FUEL ROD CLADDING (20 MWt, 840°F)

Location	0 MWd/Te	Pressure Stress* (psi) at		Radial** Gradient Stress	Thermal Stresses (psi)	
		2280 MWd/Te	5000 MWd/Te		Local (Self-Equilibrating) Stress	Bending Stress
<b>Midcore</b>						
(0°)	4068	5533	7324	± 16576	3573	-1326
(30°)	4068	5533	7324	± 16576	-6274	-1148
(150°)	4068	5533	7324	± 16576	2406	1148
(180°)	4068	5533	7324	± 16576	-3521	1326
<b>Core Outlet</b>						
(0°)	3065	4150	5479	± 7192	4858	-2271
(30°)	3065	4150	5479	± 7192	-6533	-1967
(150°)	3065	4150	5479	± 7192	4580	1967
(180°)	3065	4150	5479	± 7192	-4172	2272

\*Using 2 x the SEFOR spec. limit on condensable gases

\*\*It is positive on the clad o.d. and negative on the clad i.d.

Other stresses act throughout the clad.

Table 2A-8

**RADIAL AND CIRCUMFERENTIAL STRESSES IN THE  
FUEL ROD CLADDING (20 MWt, 840°F)**

Circumferential Stresses (psi)

Location  Peak Driver Rod at	Pressure Stress <sup>†</sup>			Radial* <sup>††</sup> Gradient
	0 MWd/Te	2280 MWd/Te	5000 MWd/Te	
Midcore	8137	11067	14647	±16576
Core Outlet	6130	8300	10958	± 7192

Radial Stresses (psi)

	Pressure Stresses <sup>†</sup>		
	0 MWd/Te	2280 MWd/Te	5000 MWd/Te
Midcore	-750	-1020	-1350
Core Outlet	-565	-765	-1010

\*Positive on the clad o.d. and negative on the clad i.d., pressure stress act throughout the clad

<sup>†</sup>Primary Stress

<sup>††</sup>Secondary Stress



Table 2A-9

STRESS CRITERIA

	Rod Cumulative Burnup (MWd/Te)		
	0	2280	5000
<b>Core Midplane</b>			
Category	ductile	quasi-brittle	quasi-brittle
Primary Membrane	$0.9\sigma_y, 0.5\sigma_u$	$0.67\sigma_y, 0.33\sigma_u$	$0.67\sigma_y, 0.33\sigma_u$
Primary Membrane +Primary Bending	$1.35\sigma_y, 0.75\sigma_{II}$	$1.0\sigma_y, 0.5\sigma_{II}$	$1.0\sigma_y, 0.5\sigma_{II}$
Primary Membrane +Primary Bending +Secondary	$1.35\sigma_y, 0.75\sigma_u$	$1.0\sigma_y, 1.5\sigma_u$	$1.0\sigma_y, 0.5\sigma_u$
<b>Core Outlet</b>			
Category	ductile	ductile	quasi-brittle
Primary Membrane	$0.9\sigma_y, 0.5\sigma_u$	$0.9\sigma_y, 0.5\sigma_u$	$0.67\sigma_y, 0.5\sigma_u$
Primary Membrane +Primary Bending	$1.35\sigma_y, 0.75\sigma_u$	$1.35\sigma_y, 0.75\sigma_u$	$1.0\sigma_y, 0.5\sigma_u$
Primary Membrane +Primary Bending +Secondary	$1.35\sigma_y, 0.75\sigma_u$	$1.35\sigma_y, 0.75\sigma_u$	$1.0\sigma_y, 0.5\sigma_u$

Also to be included with the above primary stress is the criterion that the stress intensity must be less than 0.8 of that stress necessary to cause rupture in the given time.

The material properties used with the above criteria come from References 2,3,4,5,6,7, and 8 and are shown in Figure 2A-2. The fact that the criteria are to be applied conservatively, and according to standard ASME practice, the lower band (estimated to be 95% confidence) is used for each material property. For the unirradiated properties it was determined that at 840°F, 0.9 of the yield strength is 15,000 psi and 0.5 the ultimate strength is 32,000 psi. Therefore, for the ductile category the yield strength is limiting (assuming creep rupture is not). For the irradiated properties 0.67 times the yield strength was estimated to be 44,000 psi and 0.33 times the ultimate strength is 28,000 psi which is limiting in the quasi-brittle category (again assuming the creep rupture is not). The 0.8 of the creep rupture stress was calculated for 5000 MWd/Te burnup and found to be 37,000 psi. Therefore, creep rupture is not limiting at this temperature operation out to 5000 MWd/Te. The present limiting stresses which correspond to the criteria of Table 2A-9 are shown in Table 2A-10.

Table 2A-10

LIMITING STRESS CRITERIA (psi)

Stress Intensity	Burnup (MWd/Te)		
	0	2280	5000
<b>Core Midplane (840°F)</b>			
Primary Membrane	14,400	28,000	28,000
Primary Membrane +Primary Bending	21,600	42,000	42,000
Primary Membrane +Primary Bending +Secondary	21,600	42,000	42,000
<b>Core Outlet (840°F)</b>			
Primary Membrane	14,400	14,400	28,000
Primary Membrane +Primary Bending	21,600	21,600	42,000
Primary Membrane +Primary Bending +Secondary	21,600	21,600	42,000

**GEAP-13787**

In this analysis all stresses, other than fission gas pressure induced, were thermal in origin and hence secondary. There were no primary bending stresses considered in this analysis. With the present criteria, principal stresses in each direction are combined using the maximum shear theory of failure. This theory is defined by the ASME Code for Nuclear Vessels (Section III) in terms of principal stresses and states that the maximum algebraic difference between principal stresses is the stress intensity. Part I of the criteria deals with primary stresses. The almost equal temperature and thus equal stress limits, of the upper and lower plenum makes the lower plenum critical since the lower plenum experiences the highest stress. The principal pressure stresses, the combined primary stress intensity, and the criteria limits for primary membrane stresses are shown in Table 2A-11. Note that limits have not been exceeded.

The second part of the criteria deals with primary membrane plus primary bending stresses. In this analysis, it was assumed that no primary bending stress exists. Therefore, since part two limits are less restrictive, part two is automatically satisfied.

Table 2A-11

**PRIMARY MEMBRANE STRESSES (LOWER PLENUM – 2 X SEFOR  
SPEC. ON MOISTURE, TEMPERATURE – 840°F, CLAD I.D.)**

Stress	Burnup (MWd/Te)		
	0	2280	5000
Principal Circumferential (psi)	8137	11067	14647
Principal Longitudinal (psi)	4068	5533	7323
Principal Radial (psi)	-750	-1020	-1350
Maximum Stress* Intensity (psi)	8887	12087	15997
Limiting Criteria (psi)	14400	28000	28000

\*Circumferential minus Radial

Table 2A-12

PRIMARY MEMBRANE + PRIMARY BENDING + SECONDARY PRINCIPAL STRESSES  
(2 x SEFOR Spec. 4.0 temp. = 840° F)

Location Peak Driver Rod At	Burnup (MWd/t)- Clad Location	Principal Longitudinal Stress						Principal Circumferential Stress						Principal Radial Stress						Maximum Stress Intensity*						Criteria Limiting Stress		
		0		2280		5000		0		2280		5000		0		2280		5000		0		2280		5000		0	2280	5000
		ID	OD	ID	OD	ID	OD	ID	OD	ID	OD	ID	OD	ID	OD	ID	OD	ID	OD	ID	OD	ID	OD	ID	OD	ID	OD	
Midcore (0°)		-10261	22891	-8794	24356	-7006	26146	-5439	24713	-5509	27643	-1929	31223	-750	0	-1020	0	-1350	0	9311	24713	7776	27643	5656	31223	21600	42000	42000
	(30°)	-19730	13222	-18445	14678	-16675	16477	-5439	24713	-5509	27643	-1929	31223	-750	0	-1020	0	-1350	0	19120	24713	17625	27643	15325	31223	21600	42000	42000
	(150°)	-8954	25198	-7489	29731	-5699	27453	-5439	24713	-5509	27643	-1929	31223	-750	0	-1020	0	-1350	0	8204	24713	6449	27643	4349	31223	21600	42000	42000
	(180°)	-14703	3449	-13238	19914	-11488	21704	-5439	24713	-5509	27643	-1929	31223	-750	0	-1020	0	-1350	0	12553	24713	12218	27643	10136	31223	21600	42000	42000
Core Outlet (0°)		-1540	2844	-455	13929	870	15256	-1062	13322	1108	15492	3766	17185	-545	0	-755	0	-1010	0	575	13322	1873	15492	4776	17185	21600	21600	42000
	(30°)	-12647	1757	-11542	2842	-10213	4171	-1062	13322	1108	15492	3766	17185	-545	0	-735	0	-1010	0	12062	13322	12650	15492	13979	17185	21600	21600	42000
	(150°)	2420	16804	3505	17889	4834	19218	-1062	13322	1108	15492	3766	17185	-545	0	-755	0	-1010	0	3482	16804	2740	17809	5844	19218	21600	21600	42000
	(180°)	-6027	8357	-4942	9402	-3613	10771	-1062	13322	1108	15492	3766	17185	-545	0	-755	0	-1010	0	5462	13322	6050	15492	7375	17185	21600	21600	42000

\*Using the algebraic difference between principal stresses, Intensity = Max principal - Min principal

Part three is primary membrane plus primary bending plus secondary stresses. The stress intensity of the principal stresses involving these types of stresses must be less than the yield stress and/or one half the ultimate stress. This is designed to preclude thermal ratcheting during thermal cycles. The individual stresses from Tables 2A-7 and 2A-8 are combined into principal stresses in Table 2A-12. Also Table 2A-12 combines the principal stresses into a maximum stress intensity and compares it to the criteria. Note that the stress criteria is exceeded at 0 MWd/Te burnup, at the clad O.D., at midcore. This means the fuel will not have as great a safety factor as the criteria would demand. Stresses less than 2 times yield stress is really all that is required to prevent ratcheting. The criterion is conservative in other respects; the upper limit of a factor of 2 on condensable gases was used along with conservative values of yield and ultimate stress.

The conclusions to be drawn from the above analysis are:

1. The design criteria used were very conservative.
2. The probability of the SEFOR driver fuel undergoing temperatures greater than 5000°F after restructuring during Option I Steady-State Operation is small.
3. The SEFOR fuel will be close to criteria specification limits during the Option I operation.

### 2.1.6 Time Dependent Behavior – BEHAVE-2 Analysis

#### 2.1.6.1 Analytic Tool Description – BEHAVE-2

To provide time dependent predictions of guinea-pig fuel rod behavior under SEFOR reactor conditions, the BEHAVE-2 computer code was used. Developed under AEC sponsorship, this code is designed to model the change in fuel rod geometry (including detailed stress and strain profiles in the fuel and cladding) that results from differential irradiation induced swelling, thermal expansion, and gas and coolant pressures. The code modeling is two dimensional (radial and axial) and accounts for metal swelling, irradiation creep, changes in fuel density, central void radius, and axial fuel transport to mention a few of the salient features.

The thermal analysis requires the input of clad surface temperature and gap conductance for each simulated cycle. Since an equation for gap conductance has been developed experimentally for SEFOR (Ref 17) the BEHAVE-2 temperature calculation routine was modified to include the empirical relation:

$$h = 130 + 1.75 \rho + 0.0277 \rho^2$$

where: h = fuel/clad gap conductance (Btu/ft<sup>2</sup>-hr-°F)  
 ρ = power density (watts/cc)

The values of clad temperature for this evaluation were obtained by thermal hydraulic analyses using the heat transfer code THTD as described earlier. The clad temperature curves, for a 700°F core inlet temperature for 10.5 and 21 kW/ft peak pin power in the third row and 24 kW/ft at core center are shown in Figures 2A-6 and 2A-7.

To make the input with BEHAVE-2 as simple as possible it is not necessary to enter input data for each time step during power level changes. The input consists of the ending power level and the time required to reach it. The code divides the given interval assuming a linear increase such that the size of each linear power increment will not exceed a predetermined input value. Under this arrangement, it is not possible to input the clad temperature or conductance values for each step. For this purpose the clad temperatures are calculated at each time step from the following relation:

where:

$T_{clad}$	=	$T_{inlet} + Q\gamma$
$T_{clad}$	=	clad surface temperature
$T_{inlet}$	=	core inlet coolant temperature
Q	=	rod peak linear power
γ	=	parameter (evaluated at known conditions)

The γ values used for a guinea-pig rod at the core center are shown in Table 2A-13. A single value can be used for all power levels because γ is fairly independent of power level as shown in Table 2A-14 for power levels of 10.5 and 21 kW/ft at the inner port portion. The significant differences in γ values between Tables 2A-13 and 2A-14 is the difference in coolant flow characteristics between the two core locations. The center core position was assumed to have the same hydraulic character as the inner channels (first row).

Table 2A-13

## CLAD TEMPERATURE – LINEAR POWER RELATIONSHIP

Governing Equation: 
$$\Upsilon = \frac{T_{\text{clad}} - T_{\text{inlet}}}{Q}$$

Reactor Power 20 MW

Guinea Pig Rod peak linear power at core center,  $Q = 24 \text{ kW/ft}$

Axial Node	Axial Position from bottom of fuel (in)	Clad temperature $T_{\text{clad}} \text{ } ^\circ\text{F}$	Inlet temperature $T_{\text{inlet}} \text{ } ^\circ\text{F}$	$\Upsilon$
1	3.5	725	700	1.04
2	10.5	763		2.62
3	14.9	787		3.62
4	18.2	804		4.33
5	24.9	823		5.12
6	29.4	838		5.75
7	33.7	850		6.25

Table 2A-14

CLAD TEMPERATURE – LINEAR POWER RELATIONSHIP

Governing Relation: 
$$\Upsilon = \frac{T_{\text{clad}} - T_{\text{inlet}}}{Q}$$

Reactor Power 10 MW

Guinea Pig Rod peak power under innerport, Q = 10.5 kW/ft

Axial Node	Axial Position from bottom of fuel (in)	Clad temperature $T_{\text{clad}}^{\circ}\text{F}$	Inlet temperature $T_{\text{inlet}}^{\circ}\text{F}$	Calculated $\Upsilon$
1	3.5	712	700	1.14
2	10.5	731		2.95
3	14.9	743		4.10
4	18.2	752		4.95
5	24.9	762		5.91
6	29.4	770		6.66
7	33.7	776		7.24

Reactor Power 20 MW

Guinea Pig Rod peak power under innerport, Q = 21 kW/ft

1	3.5	724		1.14
2	10.5	762		2.95
3	14.9	788		4.20
4	18.2	804		4.95
5	24.9	825		5.95
6	29.4	841		6.71
7	33.7	853		7.29

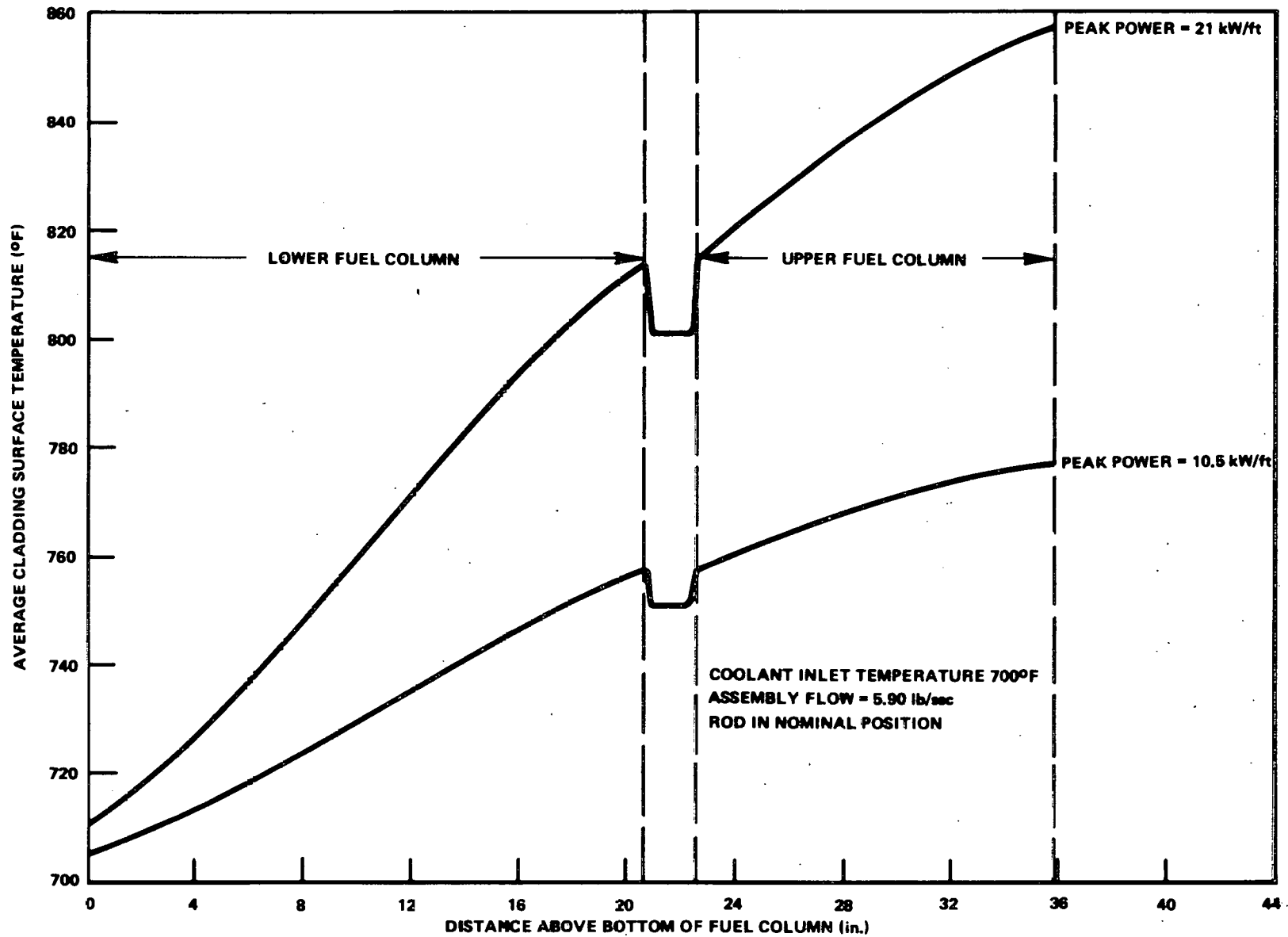


Figure 2A-6. Clad Surface Temperature Axial Distribution, SEFOR Guinea-Pig Rod in Nominal Position



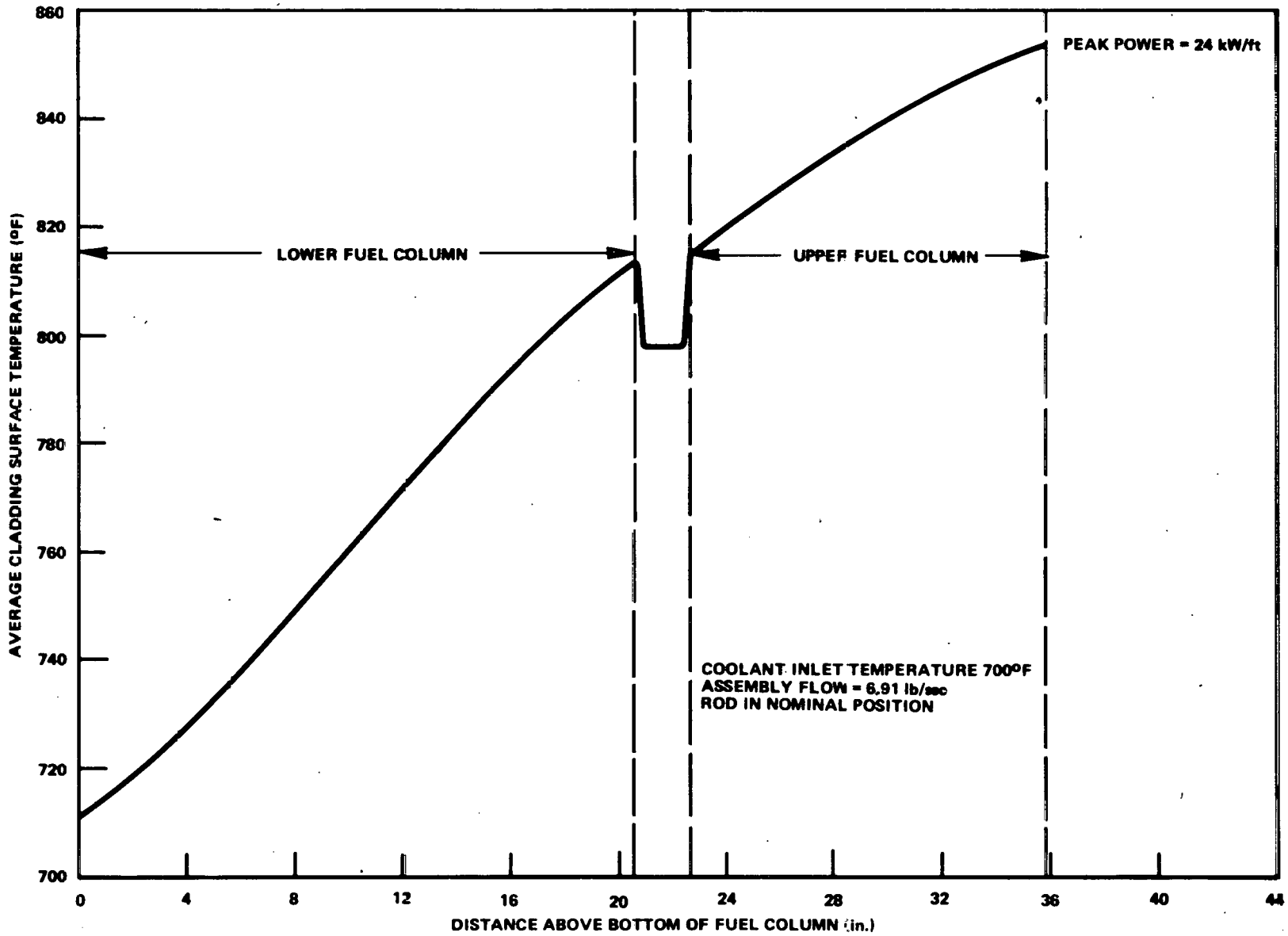


Figure 2A-7. Clad Surface Temperature Axial Distribution, SEFOR Guinea-Pig Rod in Central Position

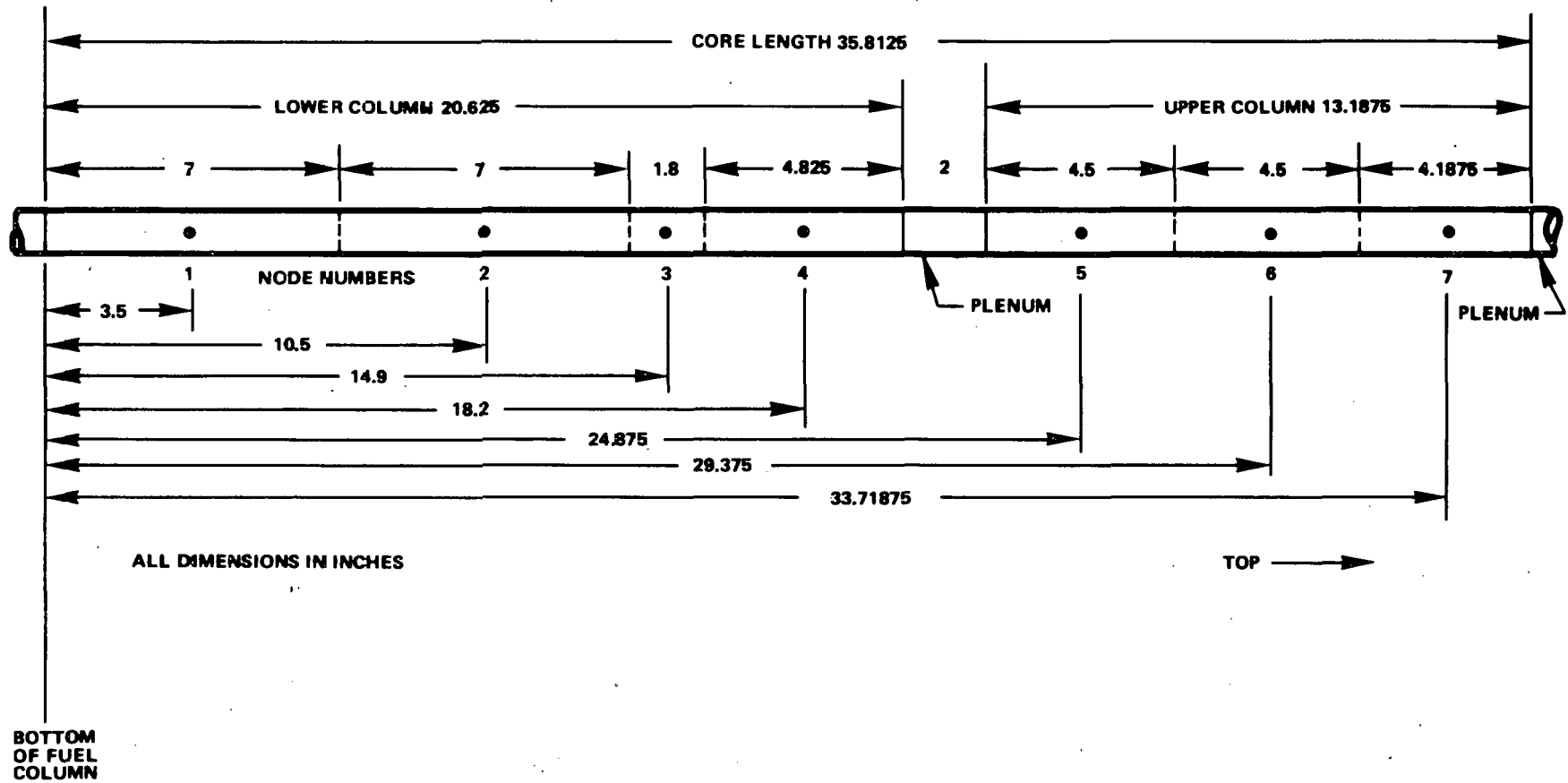


Figure 2A-8. SEFOR Fuel Rod Axial Nodal System Used For BEHAVE-2 Calculations

The BEHAVE-2 radial temperature distribution across the fuel is obtained with limited iteration of the heat conduction equation using between 10 and 30 radial nodes depending on the fuel structural character at the time. The fuel conductivity relation used for this analysis is as follows (Ref 18):

$$K = (3\rho - 1) \left( \frac{1}{5.75 + 0.0503T} + 2.91 \times 10^{-13} T^3 \right) \quad \rho > 0.95$$

$$K = - \left( 1 - 2.1\rho + \rho^2 \frac{1}{0.288 + 0.00252T} + 5.83 \times 10^{12} T^3 \right) \quad 0.85 < \rho \leq 0.95$$

and for densities less than 85% the correlation recommended by Kampf (Ref 19) was used

$$K = \frac{(1 - \rho^{2/3})}{(1 - 0.05^{2/3})} \left( \frac{1}{3.11 + 0.0272T} + 5.39 \times 10^{-13} T^3 \right)$$

- where K = fuel thermal conductivity (w/cm - °C)
- T = temperature (°K)
- ρ = fuel density (fraction of theoretical)
- p = 1 - ρ

Other rod parameters are listed in Table 2A-15 and the axial nodal divisions and general geometry are shown in Figure 2A-8. Table 2A-16 shows the axial relative power distribution.

Some features of the code will become evident in the following discussion. For further details of this code the reader is referred to Reference 20.

Table 2A-15

GUINEA PIG ROD PARAMETERS

Room Temperature Values

Clad O.D.	0.9720 inches
Clad I.D.	0.8900 inches
Upper plenum volume	1.8 cubic inches
Lower plenum volume	2.50 cubic inches
Upper plenum pressure	72.0 psi
Lower plenum pressure	103.0 psi
Fuel O.D.	0.875 inches
Fuel density	92.6%
Energy release	209.0 mev/fission
Fission noble gass production	0.22 atoms/fission
Fuel swelling rate	0.90 $\frac{\text{Fraction Swelling}}{\text{Atom Fraction Burnup}}$
Peak neutron flux (E > 0.1 mev @ 24 kW/ft)	0.332 x 10 <sup>15</sup> n/cm <sup>2</sup> -sec

Table 2A-16

## RELATIVE POWER DISTRIBUTION

Node No.	Axial Position		Axial relative power (Local power/peak power)
	Node	Inches from core bottom	
1		3.5	0.675
2		10.5	0.935
3		14.9	1.000
4		18.2	0.960
5		24.9	0.820
6		29.4	0.685
7		33.7	0.535

## 2.1.6.2 Results

## 2.1.6.2.1 Guinea-Pig Rod in Central Core Position

To determine the behavior of a guinea-pig rod placed at core center the hypothetical operating cycle in Figure 2A-9 was used. A four-hour linear increase in power was assumed to a maximum of 24 kW/ft (20 MW reactor power). This was followed by a steady operating period of one hour at that level, followed by a linear descent to zero power in two hours. During this operation the inlet coolant temperature was assumed to be 700°F. A subsequent step was provided to simulate removal from the reactor which constituted a change in ambient temperature from 371°C (700°F) to 20°C (68°F). The final resulting structure and geometry is assumed to represent that which would be observed during post-irradiation non-destructive and destructive examinations.

- Radial distributions

Figure 2A-9 shows the calculated central temperature while 2A-10 shows the central void radius, the solidus melt radius, and the transport boundary radius for the peak flux position (node 3) as functions of the calculational time steps. It should be noted that, as shown in Figure 2A-9, these time steps are not of equal length. The transport radius defines the outer boundary for densification due to porosity migration toward the center, and should correspond closely with the columnar grain growth radius observed in fuel cross sections on destructive examination.

In Figure 2A-11 some normalized characteristic volumes of interest are plotted as a function of time step. The normalizing value is the cladding inside (I.D.) volume for the computational node of interest. In reality the inside volume changes through the cycle, due to axial and radial expansion and deformation, but in this case deformation is negligible and, since the cladding does not significantly change temperature during operation as shown in Figure 2A-9, the I.D. volume can be thought of as constant for comparative purposes here.

Fuel expansion volume is defined as the volumetric change in the solid matrix fuel due to thermal expansion and the fuel porosity ratio is the normalized porosity within this matrix. The crack volume and central void volume are similarly defined. The sum of these five values at any step will be approximately a constant.

A review of the physical mechanisms at the peak flux position can be obtained from Figures 2A-9, 2A-10, and 2A-11. At the first time step (i.e., increase in linear power), the fuel expands, cracks, and is translated to contact the cladding. This results in the initial central void radius shown on Figure 2A-10, and in the radial crack volume and thermal expansion volume on 2A-11. The transverse crack volume for these SEFOR pins at this point is the result of the initially dished pellet shape, and the fuel porosity is the result of initial fuel pellet density. Through Step 7 as the power level rises, the thermal expansion of the fuel causes the central void to close, the radial and transverse cracks to close, reducing the crack volumes, and the voids within the fuel to expand which increases the fuel porosity volume.

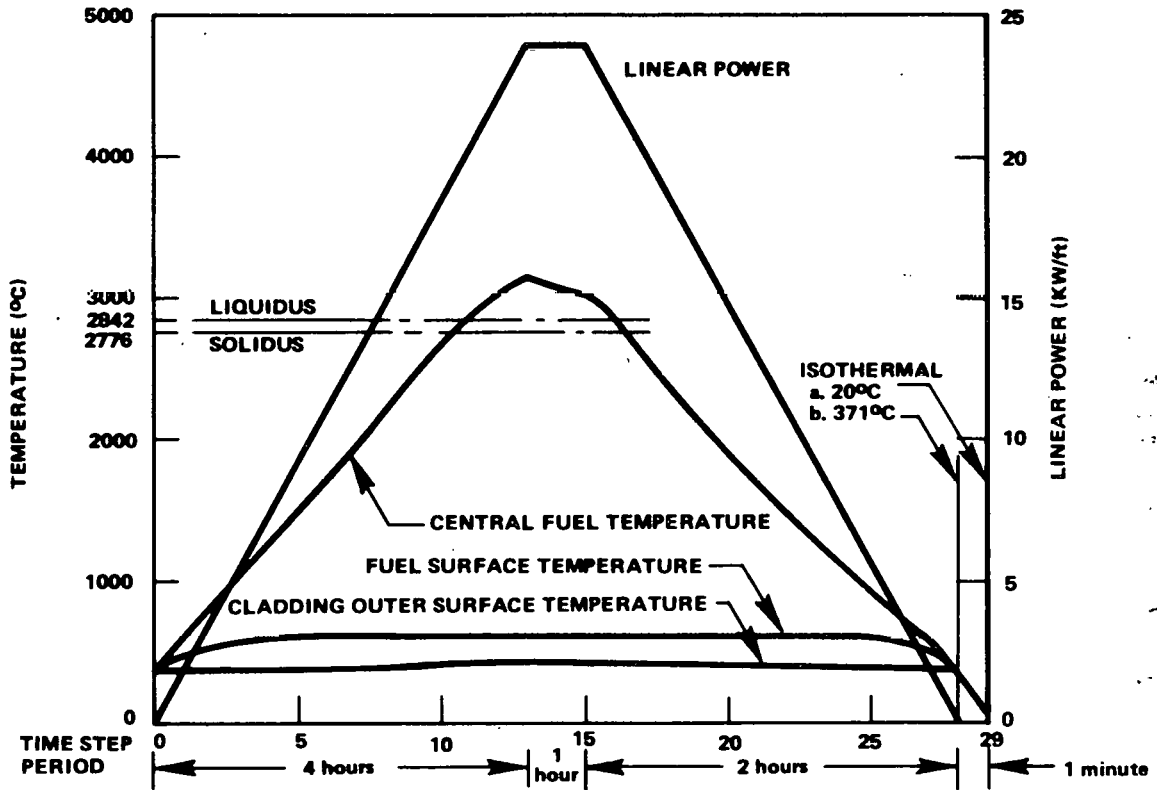


Figure 2A-9. SEFOR Linear Power Cycle to 24 kW/ft Peak, Time Steps, Power Profile, and Characteristic Temperatures of Guinea-Pig Rod at Core Center

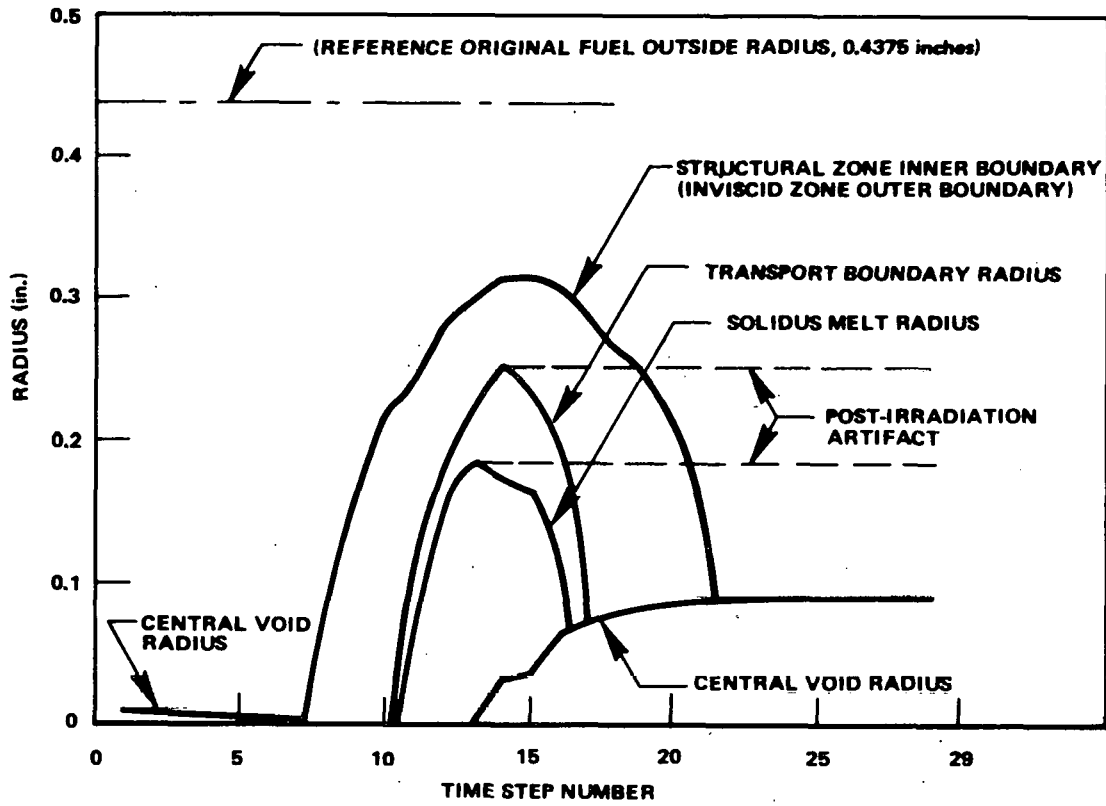


Figure 2A-10. SEFOR Linear Power Cycle to 24 kW/ft Peak, Characteristic Radii of Guinea-Pig Rod at Core Center

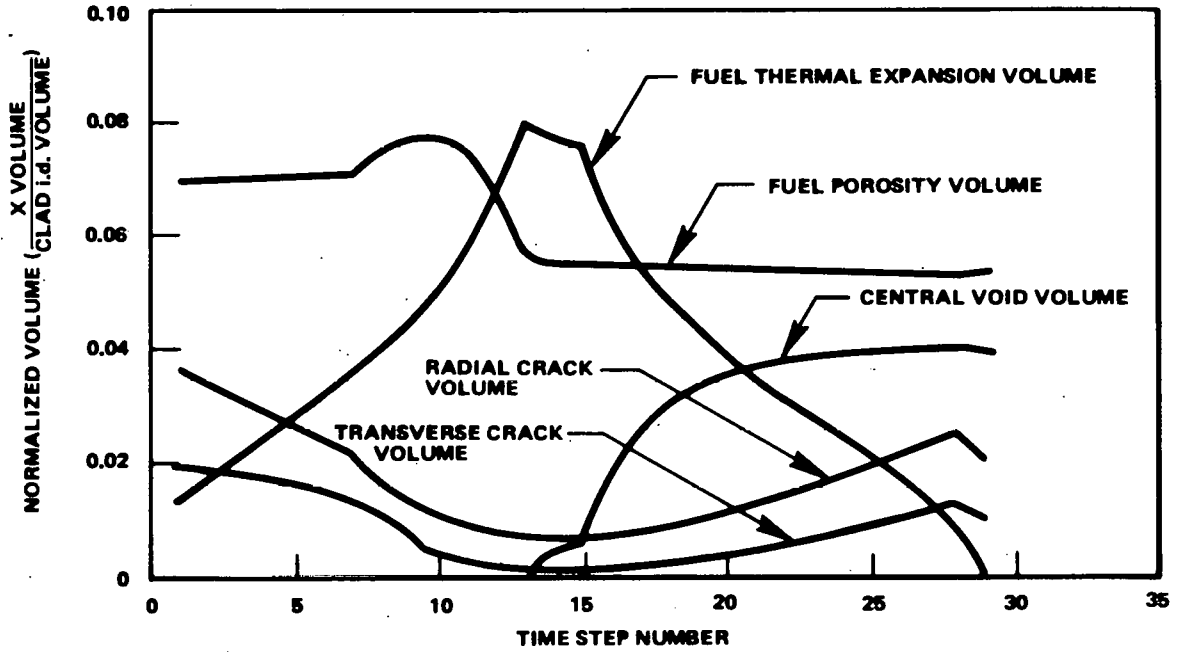


Figure 2A-11. SEFOR Linear Power Cycle to 24 kW/ft Peak, Characteristic Volumes of Guinea-Pig Rod at Core Center

During the eighth time step a different phenomenon begins. As the temperature rises, a region of inviscid fuel develops. This region is relatively easy to deform and is capable of being hot pressed as will be seen later. It is also possible in this region to heal up cracks which is the phenomena observed here. As the inviscid region grows larger the enveloped crack tips are healed and the crack porosity is converted to uniform porosity in the fuel matrix. This is seen as an increase in fuel porosity balanced by a more rapid decrease in crack volume.

During the 11th time step, at about 18.5 kW/ft, melting is initiated and a transport region forms. As densification occurs, the fuel conductivity increases and the central temperature begins to plateau. A central void is not formed during this period because the potential void created by porosity sweeping to the center in the developing transport region is occupied by the increasing fuel thermal expansion volume. The thermal expansion volume starts a more rapid increase because it includes the volumetric change occurring during the melting phase transformation. The thermal expansion volume actually exceeds the rate of center void formation and some of the porosity in the outer inviscid zone is hot pressed to compensate, as shown by the decrease in fuel porosity.

During the first part of the steady power portion of the cycle, the transport radius increases, sweeping more porosity to the center. This causes the formation of the central void which in turn causes a drop in the center fuel temperature. This lowers the thermal expansion volume and decreases the melt radius and transport radius during the 15th time step. The slight increase in central void radius in this step is the result of the thermal contraction exhibited by the decrease in fuel thermal expansion volume. The same mechanism is operative from the 15th step on, as the temperature drops with power decrease. The central void grows, and also seen is the decrease in fuel porosity and increase in crack volumes as the fuel contracts. The sharp readjustment during time step 29 reflects the thermal contraction as the fuel rod is removed from the reactor (isothermal at 700°F) and cooled to room temperature (isothermal at 68°F).

During the cycle negligible strain occurred in the cladding, but some axial fuel flow occurred at the center node to redistribute the inviscid fuel during the final approach to maximum power at the time of hot pressing (step 10-13).

The observable evidence to be seen during destructive examination will be: the maximum transport radius, 0.25 inch, which should correspond closely to the columnar grain growth radius; the maximum melt radius, 0.18 inch, and the final central void radius, 0.09 inch, as indicated in Figure 2A-10; and the porosity distribution as shown in Figure 2A-12. This latter figure indicates the post irradiation radial distribution of void volume in fuel, and in radial ( $r,z$ ) and transverse ( $r,\theta$ ) cracks.

The peak central temperature, 3126°C (5660°F) occurred at the start of the steady-state period. At the end of this steady period restructuring had decreased the temperature to 3029°C (5484°F) which compares to the value of 5550°F obtained earlier with PEFT.

Figure 2A-12 shows the results of mechanisms previously discussed. The outer fuel still maintains the as-fabricated porosity. The increase in porosity closer to the center is the result of transformed crack porosity. The inner fuel has low porosity after voids were swept to the center in the transport region since only a small residual is assumed to remain. The transition region between the inner dense fuel and the outer more porous fuel represents that portion of the previously discussed inviscid zone which was hot pressed during the rise to power.

#### • Axial distributions

The analysis performed during the cycle explained above was two dimensional. Shown was the behavior at the peak flux location identified as node 3 in Figure 2A-8, 14.9 inches above the bottom of the fuel. The results obtained at the other axial nodes defined in this figure at steps 13 and 14 are shown in Figures 2A-13 and 2A-14.



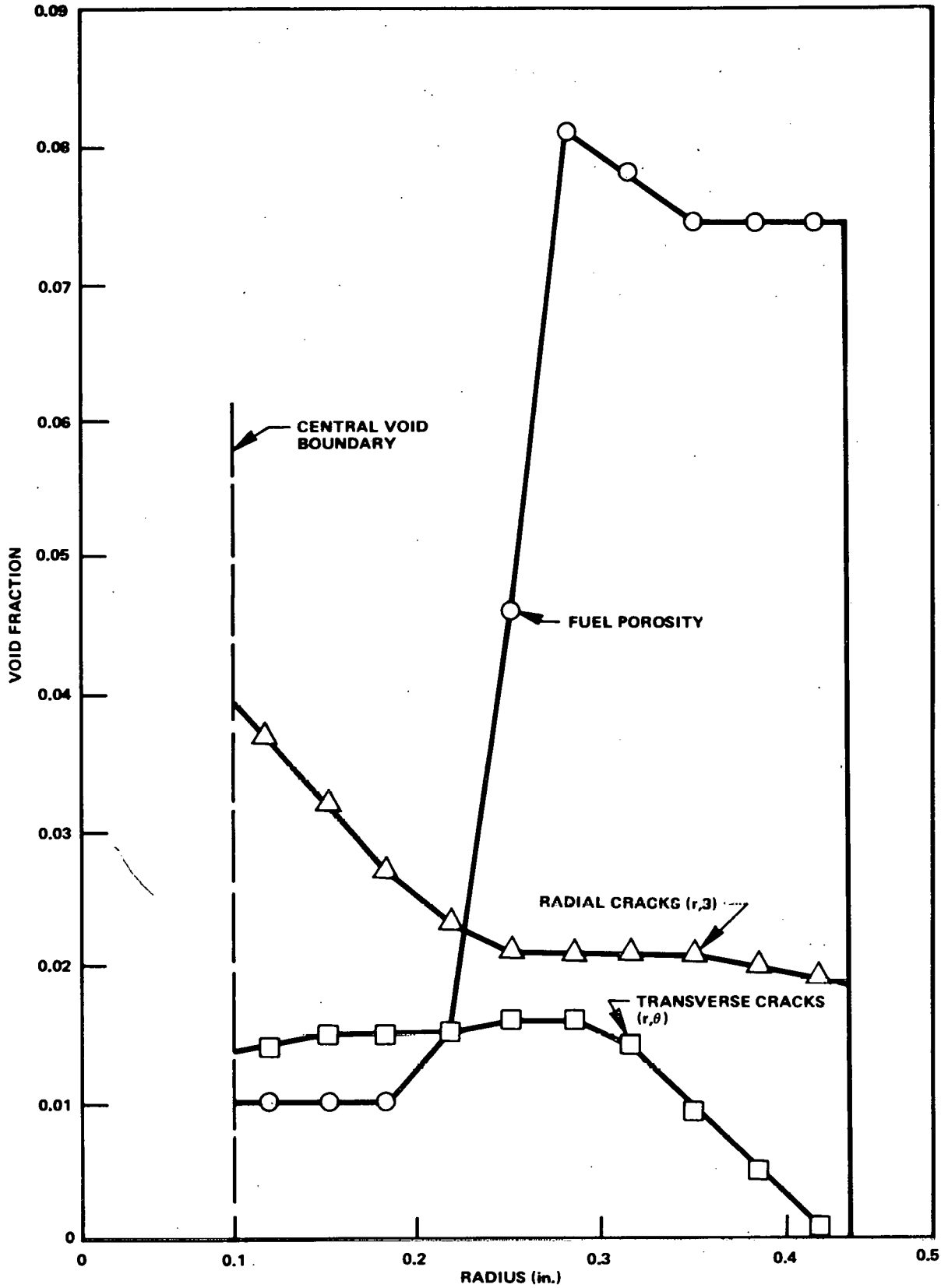


Figure 2A-12. Radial Distribution of Post-Irradiation Void Fractions, SEFOR Guinea-Pig Rod in a Peak Flux Position

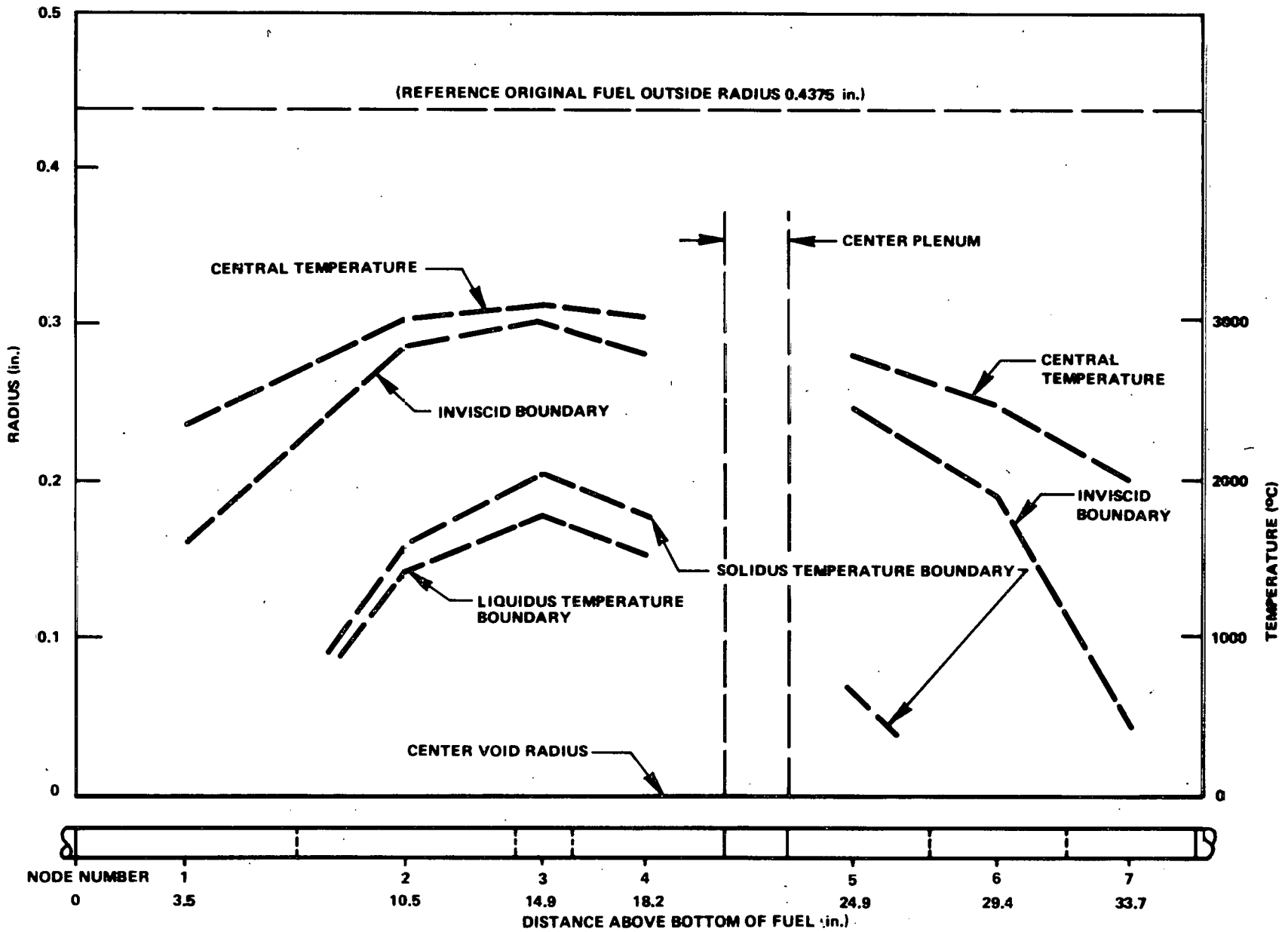


Figure 2A-13. SEFOR Guinea-Pig Rod Axial Profiles At End of the Four-Hour Linear Startup (Time Step 13)

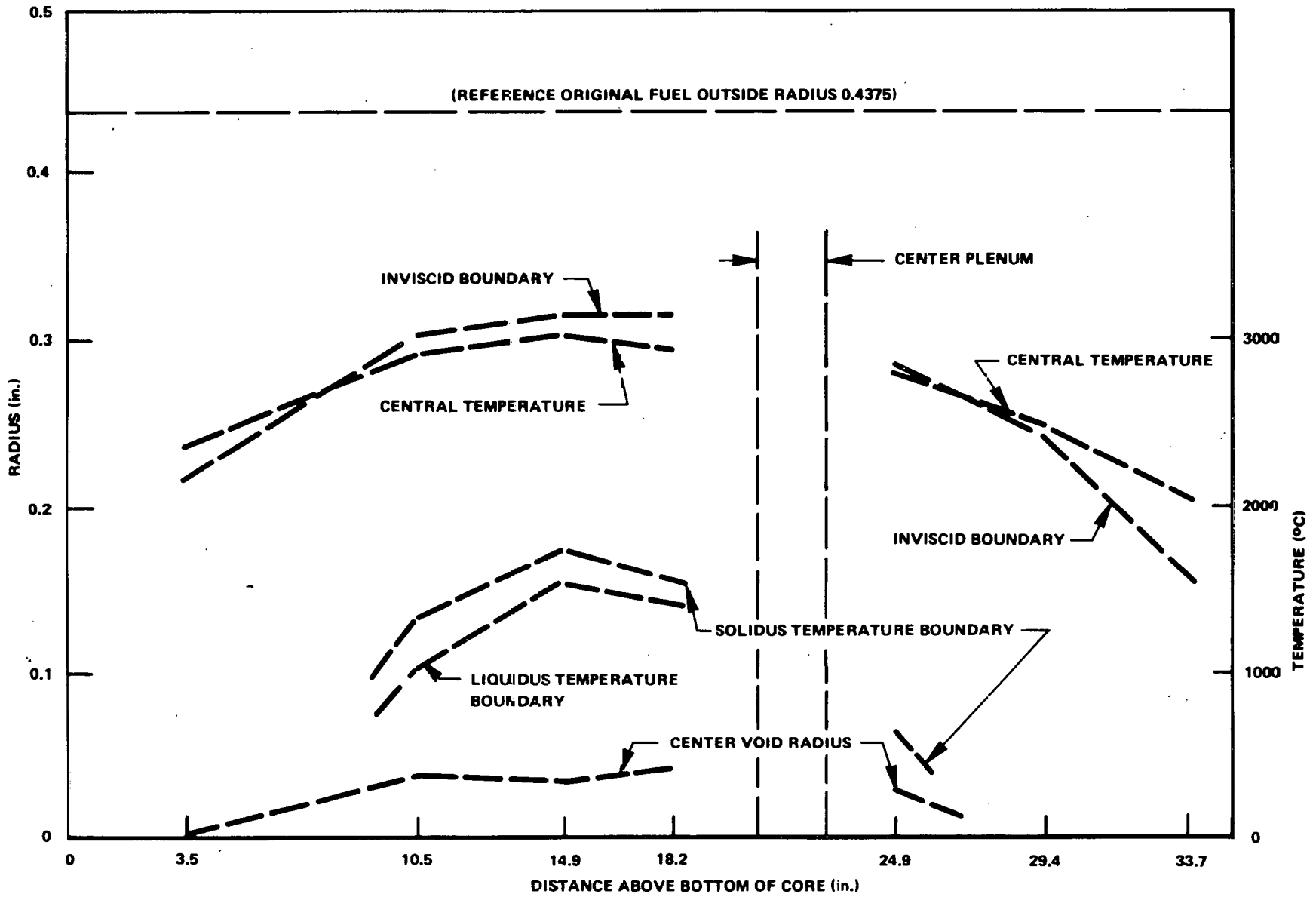


Figure 2A-14. SEFOR Guinea-Pig Rod Axial Profiles After 30-Minutes Restructuring at 24 kW/ft (Time Step 14)

These figures show the axial profile of central temperature, inviscid boundary radius, solidus and liquidus temperature radii, and central void. The effects of restructuring for 30 minutes is evident in the comparison of these figures. At step 13 (Figure 2A-13) a central void does not exist, but has formed after restructuring for 30 minutes as shown in step 14 (Figure 2A-14). The resulting decrease in temperature levels is evident, as shown by the movement of the melt-region radii.

#### 2.1.6.2.2 Parametric Study of Peak Cycle Power

To provide information needed to select the maximum power during the test cycle, the liquidus and solidus radii, the transport radius, the central void radius, the peak central temperature, and the melt fraction have been calculated after a 30 minute restructuring period. This is shown in Figure 2A-15. It is interesting to note that for 30 minutes of restructuring at peak power between 20 and 22 kW/ft the central temperature is relatively constant. The larger central void and greater portion of densified fuel developed at higher maximum power causes better heat transport to the clad surface tending to compensate for larger heat generation. However, cycles to higher power (>22 kW/ft) cause an increase in melt volume fraction with its associated volumetric increase; this reduces the central void radius, and this increase in the heat transport path raises the central temperature.

For maximum powers above 19.5 kW/ft during the described cycle, some material will be above the solidus melting temperature after 30 minutes of restructuring. At a peak power of 24 kW/ft the melt fraction was 0.146 with a central void radius of 0.035 inch.

#### 2.1.6.2.3 Guinea-Pig Rod in Inner Port Position

The reactor power history experienced by a guinea-pig rod under an inner port (such as pin A-10) has been modeled as shown in Figures 2A-16, 2A-17, and 2A-18. An 8-hour linear increase to 10.5 kW/ft (10 MW reactor power) is used to model the actual approach exercised in initially increasing reactor power. A considerable amount of time was spent at approximately 10 MW, and this has been represented as 1000 hours at 10.5 kW/ft. The final stages of power increase were more rapid than the first, which explains the steeper ramp of 4 hours to a full power of 21 kW/ft peak (20 MW reactor). Twenty hours at full power is followed by a decrease in 2 hours to 10.5 kW/ft and a scram from there to zero power in 0.1 second. The last time step represents removal from the reactor to room temperature.

The characteristic details shown in Figures 2A-16, 2A-17, and 2A-18 reflect many of the mechanisms shown in Figures 2A-9, 2A-10, and 2A-11. The restructuring at half power has resulted in a significant inviscid zone which has enveloped a considerable amount of the crack-induced porosity as shown by the increase of fuel porosity volume and decrease in crack volume. The central void radius is kept negligible during this time by the lack of a transport region and by axial fuel movement from adjacent axial nodes. The cladding strain developed during this cycle was negligible. The post-irradiation cross-sectional examination for the assumed power history should indicate at the peak flux position a central void radius of about 0.1 inch, a solidus melt radius of about 0.15 inch, and a columnar grain growth radius of about 0.25 inch. The maximum central temperature was 2904°C (5259°F) which occurred at the beginning of the maximum steady power operating period. The melt volume fraction was 0.09. The temperature value had decreased to 2722°C (4932°F) after 20 hours of restructuring at that power. This is compared to the expected values of 5040°F obtained with the PEFT analysis.

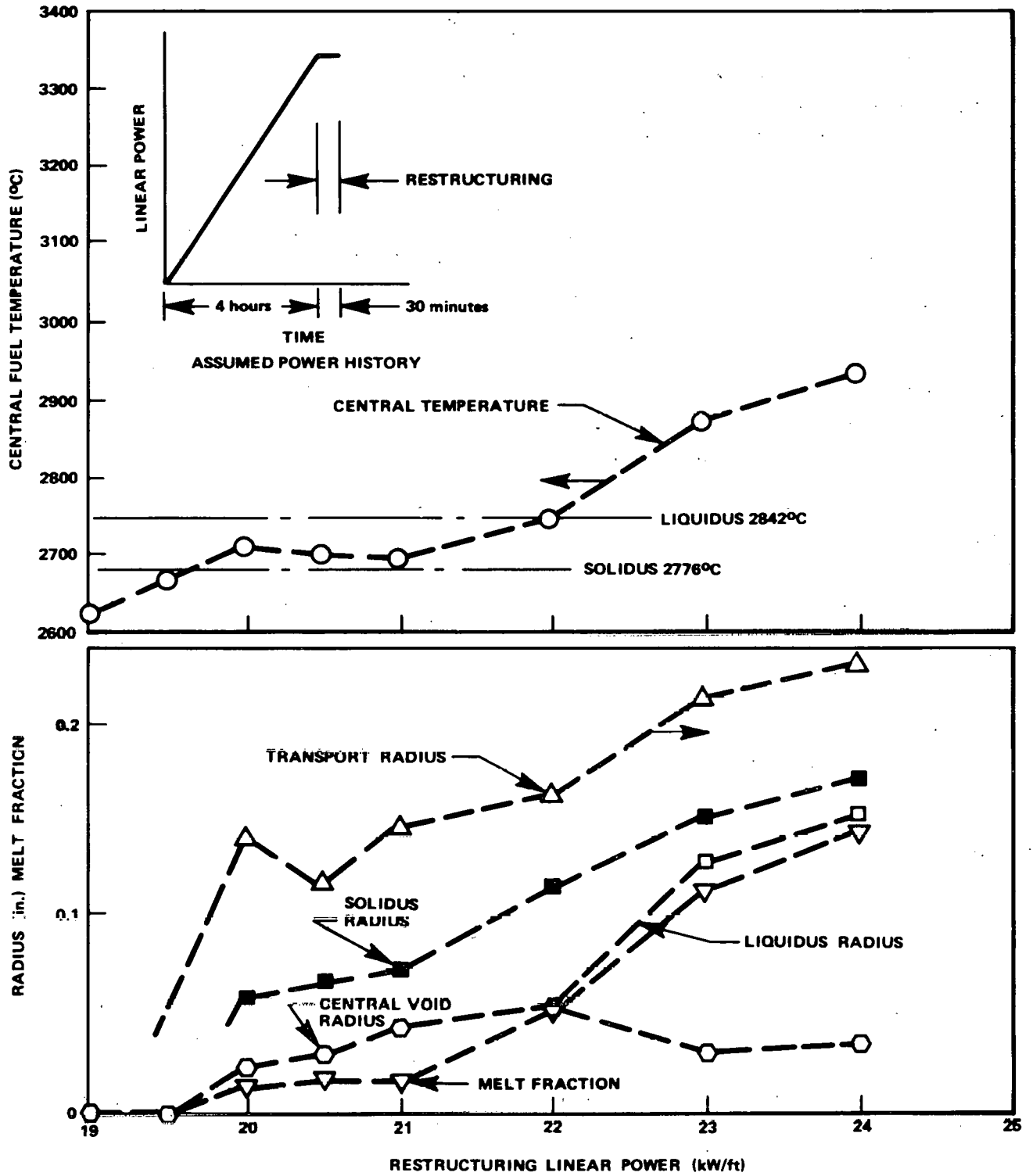


Figure 2A-15. Calculated SEFOR Fuel Rod 30-Minute Restructured Characteristics and Central Fuel Temperature vs Restructuring Linear Power

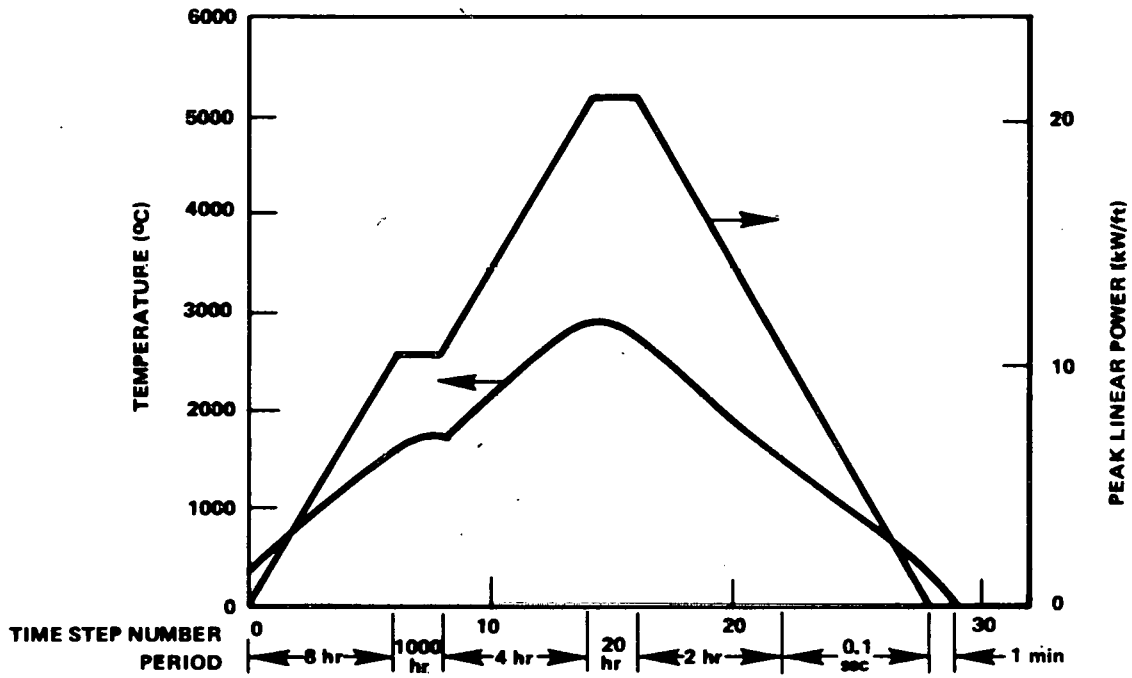


Figure 2A-16. SEFOR Linear Peak Power to 10.5 and 21 kW/ft Levels, Time Steps, Peak Power Profile, and Central Temperature of Guinea-Pig Rod AIO

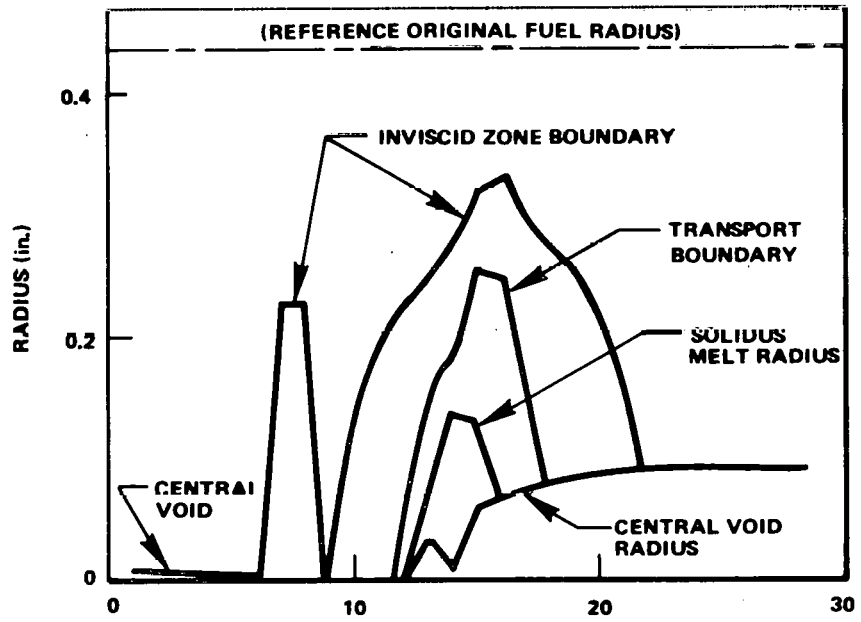


Figure 2A-17. SEFOR Linear Peak Power to 10.5 and 21 kW/ft Levels, Characteristic Radii of Guinea-Pig Rod A10

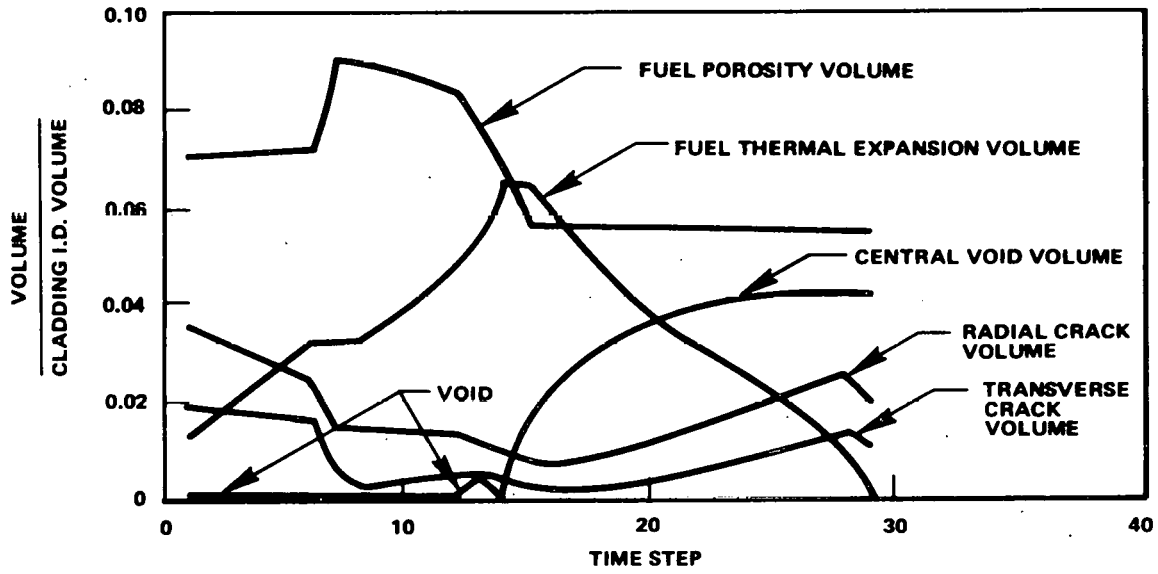


Figure 2A-18. SEFOR Linear Peak Power to 10.5 and 21 kW/ft Levels, Characteristic Volumes of Guinea-Pig Rod A10



## REFERENCES

1. A proposal to the United States Atomic Energy Commission for the SEFOR Follow-On Program, Phase A Preliminary Design and Engineering, General Electric, May 24, 1971.
2. The Elevated Temperature Properties of Stainless Steels, ASTM STP-124, 1952.
3. The Elevated Temperature Properties of Stainless Steels, ASTM DS 5-S1, 1965.
4. A Compendium of Properties and Characteristics for Selected LMFBR Cladding Materials, Battelle Memorial Institute BMI-1900, 1968.
5. GEAP-10066, Mechanical Properties Evaluation of Austenitic Stainless Steels Irradiated in EBR-II, July 1969.
6. 4th Libby-Cockcroft, P.N.L. Presentation, Part II.
7. Mechanical Properties of Irradiated Type 304 and Type 316 Stainless Steel in Fast Reactors, GEAP-10062, June 1969, Ref. 7 data points.
8. Mechanical Properties of Irradiated Type 304 and Type 316 Stainless Steel in Fact Reactors, GEAP-10062, June 1969, Ref. 6 data points.
9. Goldstein, M.B., "PEFT - A Computer Code for the Probabilistic Evaluation of Fuel Temperature", NEDE-13665, March 1971.
10. Asamoto, R.R., et al, "Thermal Conductivity of Uranium-Plutonium Oxide Fuels", proceedings of the 1967 Nuclear Metallurgy Symposium Held in Scottsdale, Arizona, October 1967.
11. Skirvin, S.C., "User's Manual for the Standard THTD Computer Program on GE-600 Series Computers (Transient Heat Transfer - Version D)", Research and Development Center Report No. 69-C-205, May 1965.
12. Southwest Experimental Fast Oxide Reactor Development Program, 21st Quarterly May-July 1969, GEAP-10010-21, August 1969.
13. Meyer, R.A., et al, "Design and Analysis of SEFOR Core I", GEAP-13598, June 1970.
14. Chen, S.S., et al, "Vibration and Stability of Tubes Exposed to Pulsating Parallel Flow", ANS Trans., Biltmore Hotel, Los Angeles, California, June 29-July 2, 1970.
15. Reavis, J.R. "Vibrational Correlation for Maximum Fuel Element Displacement in Parallel Turbulent Flow", Nucl. Sci. Eng., 38, 63 (1969).
16. Tsui, E.Y.W., et al, "Interim Stress Design Criteria for LMFBR Vessel and Core Structures", GEAP-13719, May 1971.
17. Southwest Experimental Fast Oxide Reactor Development Program, 26th Quarterly Report, August-October 1970, GEAP-10010-26, November 1970.
18. "Oxide Fuel Element Development Quarterly Progress Report for Period Ending September 30, 1969", WARD-4135-i.
19. Kampf, H. and G. Karsten, "Effects of Different types of Void Volumes on the Radial Temperature Distribution of Fuel Pins", Nucl. Appl. Technol. 9, 288 (1970).
20. Oldberg, S. Jr., "BEHAVE-2: Oxide Fuel Performance Code in Two Spatial Dimensions and Time", to be issued.

## 2.2 TASK 2B – TRANSIENT EXPERIMENTS ON ENCAPSULATED FUEL

### 2.2.1 Objective

The objectives of this task are to complete the planning of the detailed test sequence of transient overpower tests to be conducted in capsules (test plan) and to prepare the preliminary design specification for the test capsule and test fuel.

### 2.2.2 Discussion

The Option I capsule test plan was completed. Included in the test plan are the design basis SEFOR transients used in determining the test fuel performance and a listing of pre-irradiated fuel pins which will meet the stated test requirements.

The preparation of the preliminary design specification for test capsule and fuel resulted in:

- the first draft of the capsule design specification (BA 2103, dated 11/29/71)
- the conceptual drawing of the test capsule (drawing no. 816E201, dated 11/29/71)
- the fuel pin fabrication specification (BA 2103/22A1858) and (drawing no. 118D9849).

Subsequent efforts on these items were performed under PA-10, Task C-1.

### 2.2.3 Option I Transient Overpower Test Plan

This SEFOR Follow-On Test Program is organized to provide data on the behavior of LMFBR fuel rods under transient overpower accident conditions. The test plan consists of a series of transient tests on single specimen, encapsulated LMFBR type fuel rods which are performed in the SEFOR core.

In most of the tests, SEFOR will be initially operated in a short term overpower (STOP) mode to provide prototypic LMFBR temperature conditions in the fuel and cladding of the test specimens prior to the overpower transient initiated by the fast reactor excursion device (FRED)<sup>1</sup>. This is known as the STOP/FRED mode of operation for SEFOR. The overpower transients and certain fuel parameters will be varied to obtain a broad base of test data responsive to LMFBR safety and design requirements. In addition, certain Option I test conditions are set to establish a correlation between TREAT and SEFOR tests with calculated LMFBR accident conditions.

The overall scope of the Option I test program is designed to provide safety related information for the FFTF and demonstration LMFBR as well as guidance in defining subsequent Option III-A transient overpower tests involving both single rod capsule and multi-rod loop tests in the SEFOR Facility<sup>1</sup>.

The Option I transient overpower tests will be performed with single fuel rods in capsules with a thermal bond of stagnant sodium. All capsules will be instrumented and will have similar heat transfer characteristics for both zero burnup (unirradiated) and pre-irradiated fuel rods. The capsule for the pre-irradiated fuel will provide for remote insertion of the rod as well as the remote connection of the instrument leads within a sodium proof junction.

The tests with pre-irradiated fuel rods will be based on the sibling concept where each capsule containing pre-irradiated fuel will have a companion capsule with zero burnup fuel to be used as a control. The paired capsules will have comparable locations in the core and will be exposed to the overpower transient at the same time. This procedure will permit a direct comparison of the performance of pre-irradiated and zero burnup fuel rods. Should difficulty be encountered in the development of a sodium proof junction for remote operation of the capsules containing pre-irradiated fuel or if the instrumentation of either capsule is impaired during the test, the sibling approach provides a fall back position for evaluating the test results for both capsules.

In the Option I test program, the target fuel rod parameters will attempt to match the demonstration plant fuel. The nominal values for these tests are specified in Table 2B-1.

The fuel rod parameters and expected transient thermal history for the first capsule, TOP-1A, are similar to those for the TREAT test C4A<sup>2</sup>. The purpose of this test is to establish the correspondence between previously completed TREAT tests and the subsequent SEFOR transient overpower test programs. In addition, this is a capsule proof test to confirm the physics and heat transfer characteristics of the system. The smeared density of the fuel rod, 90% T.D. for TOP-1A, probably represents the upper limit of interest in this program.

For the sibling tests, the fabrication parameters and geometries available in the pre-irradiated fuel rods will dictate the design of the zero burnup control fuel. Selection of the pre-irradiated mixed-oxide fuel rods will be limited to those from the FFTF and Task F in PA-10 irradiation testing programs in EBR-II. Fuel rods of interest from these

Table 2B-1

TARGET FUEL ROD PARAMETERS

	Capsule Top-1A Only	Pre-Irradiated and Sibling Fuel
Fuel: Material	20 w/o PuO <sub>2</sub> -UO <sub>2</sub> (U-235/U >93%)	25 w/o PuO <sub>2</sub> -UO <sub>2</sub> (U-235/U >93%)
O/M	1.98	1.98
Manufacturing process	Co-precipitated	Co-precipitated
Fuel Form:		
I. Solid Pellet		
Dimensions	0.216" o.d. ~0.250" long	0.215" o.d. ~0.250" long
Column length	~13.5"	~13.5"
II. Annular Pellet		
Dimensions		0.215" o.d. ~0.050" i.d. ~0.250" long
Density		95% T.D.
Fuel Rod Smear Density:	90% T.D.	~85% T.D.
Blanket-Insulator:		
Material	Natural UO <sub>2</sub>	Natural UO <sub>2</sub>
O/M	2.00	2.00
Form, pellet	0.216" o.d. ~0.250" long	0.215" o.d. ~0.250" long
Pellet, Density	93% T.D.	~93% T.D.
CLADDING MATERIAL:	Type 316 Stainless Steel 0.250" o.d. x 0.015" wall	Type 321 Stainless Steel 0.250" o.d. x 0.015" wall

programs will be selected on the basis of the nominal specifications in Table 2B-1. Other factors such as availability, and possibly the obtaining of destructive examination results on a companion fuel rod for establishing the pre-transient conditions of a candidate test rod, will influence the final selection.

The PA-10 Fast Flux Irradiation Program, Task F<sup>3</sup>, and the HEDL test program<sup>4</sup> have been reviewed and the candidate mixed-oxide fuel rods are tabulated in the next section.

Seventeen capsules (nine tests) are planned for the Option I transient overpower test program. Nominal conditions for the tests are summarized in Table 2B-2. The four transients identified in Table 2B-2 are presented in detail along with the corresponding thermal response of the fuel rods. The test program is organized into four categories with the following general objectives:

Series 1

- Capsule proof test and demonstration of SEFOR potential for transient testing.
- Establish a correlation between TREAT and SEFOR tests with calculated LMFBR accident conditions.
- Evaluate fuel performance when transients are initiated from near normal LMFBR operating temperatures.
- Investigate heating rate effects over a range similar to the accidents considered for LMFBR safety analysis.

In this series of tests, three types of overpower transients will be used and the response of the fuel-cladding system will be evaluated. The experimental conditions are based on simulating such parameters as peak fuel

2

Table 2B-2

SEFOR FOLLOW-ON  
OPTION I - TRANSIENT OVERPOWER TESTS

Date	Test #	Purpose	Special Features	Fuel Column	Burnup MWd/Te	Pre-FRED Power	Transient Mode <sup>(1)</sup>	Expected Results
Apr 72	1A	Capsule proof test to confirm physics and heat transfer characteristics	Demonstrate SEFOR potential, correlate with treat tests	13 1/2"	0	~4 kW/ft	Transient from ~0 power T1	Simulate treat test C-4A with respect to cladding & fuel surface temperatures and fuel melt rate as a function of time
July 72	1B	Slow transient from high power	_____	↓	0	~15 kW/ft	STOP/FRED operation if necessary ↓ T2	Determine the performance of fuel rods in transients initiated from near normal operating conditions with test parameters of burnup and energy in-put rate
	1C		1st pre-irradiated fuel test in SEFOR		~50K			
Sept 72	1D	Vary transient shape from test 1B and 1C ↓	Demonstrate STOP/FRED potential ↓	13 1/2"	0	~15 kW/ft	STOP/FRED ↓ T3	
	1E				~50K			
Nov 72	1F	Backup for previous tests Contingency Tests*	_____	13 1/2"	0	~4 to 15 kW/ft	STOP/FRED ↓	Backup for previous tests if necessary
	1G		_____		~50K			
Mar 73	2A	Simulate large start-up accident with defected fuel rods	Promote sodium logging through clad defect by cyclic power operation prior to transient	13 1/2"	0	~4 kW/ft	FRED from low power ↓ T1	Failure consequences resulting from defected fuel ↓
	2B				50K			
May 73	2C	Slow transient at normal operation with defected fuel		13 1/2"	0	~15 kW/ft	STOP/FRED ↓ T2/T3	
	2D				50K			
Nov 72 Sept 72	3A	Investigate the effect of annular fuel geometry on fuel movement over LMFBR-fuel length	Annular Fuel, Solid Blanket	30"	0	~15 kW/ft	Low energy STOP/FRED T4	Fuel slumping
	3B						STOP/FRED	Significant axial and radial fuel redistribution
	3C						T2/T3	↓

Table 2B-2 (Continued)

Test #	Purpose	Special Features	Fuel Column	Burnup MWd/Te	Pre-FRED Power	Transient Mode <sup>(1)</sup>	Expected Results
May 73 4A 4B 4C	Evaluate the effect of fission gas inventory on fuel rod performance during transient overpower operation	Variation in fission gas inventory	13 1/2"	0	~15 kW/ft	STOP/FRED	Effect of fuel burnup and cladding mechanical properties on failure threshold
			↓	50K	↓	↓	
			↓	100K	↓	T3	
*Contingency Tests	Investigate fuel length effects	LMFBR fuel length and axial power profile	30"	0	~15 kW/ft	STOP/FRED	Effect of fuel length and axial power profile
	Control pin for either contingency test		13 1/2"	0		↓	
	Investigate high fission gas inventory; solid fuel column during start-up accident	Low-Power Pre-radiation	13 1/2"	50-100K	~4 kW/ft	FRED from low power	

(1) Nominal conditions for transients 1 through 4 are presented in Appendix B. The final definition of the proposed transients in series 2, 3, & 4 will be based on the results of series 1 tests.

temperatures, fuel melting rates and melt volume, and the corresponding cladding temperature histories expected in the fuel rod during reactor accident conditions. The SEFOR transients will be defined such that the overpower transient shape and magnitude in conjunction with the capsule thermal characteristics will produce the desired time-temperature relationships in the fuel and cladding. The potential conditions for the three basic transients in this test series are given in the section titled, "Overpower Transients and Thermal Analysis."

#### Series 2

- Determine the failure consequences resulting from an overpower transient on defected fuel rods.

A longitudinal slit  $\sim 1''$  long will be used in this test series for a reasonable representation of a cladding failure during reactor operation<sup>5,6,7</sup>. This defect will be positioned in the peak power region of the fuel rod prior to its insertion into the test capsule. A more prototypic in-reactor environment will be established about the defect by cycling and soaking the fuel rod at reactor operating temperatures to promote sodium penetration and fuel-sodium reaction prior to the overpower transients<sup>8,9,10</sup>.

Two pre-transient conditions will be investigated in this series, each including a zero burnup and a pre-irradiated fuel rod. In one test, the transient will be initiated from low power to simulate a startup accident after the opportunity for sodium entry through the cladding. While in the other test the transient will be initiated after sodium entry but from "normal power" with sufficient pre-transient time allowed for the redistribution of sodium in the fuel rod due to the induced fuel temperature gradients.

#### Series 3

- Determine the effect of molten fuel movement in conjunction with annular fuel and blanket pellets for prototypic LMFBR fuel lengths. This design feature provides a possible way to increase the failure threshold, and investigate the potential for generating negative reactivity feedback due to controlled axial fuel movement<sup>2,11</sup>.

Two levels of fuel movement will be investigated in this test series. The first test will investigate the fuel redistribution within the central void of an annular fuel column resulting from a small overpower transient which produces a low fuel melt volume ( $\sim 10\%$ ). The second test will investigate the effectiveness of a central void in either the fuel column or the blanket to accommodate the fuel volume increase when the fuel is subjected to a large overpower transient sufficient to produce a maximum fuel melt area of  $\sim 70\%$ .

#### Series 4

- Evaluate the effect of burnup (fission gas inventory) on fuel rod performance under transient overpower conditions.

This test will compare the performance of a fuel rod with simulated high burnup effects to the performance of fuel rods pre-irradiated to  $\sim 50,000$  and  $\sim 100,000$  MWd/Te burnup in EBR-II. The transient overpower will be initiated from "normal reactor operation conditions." The transient mode will be determined from the results of the Series 1 tests.

### 2.2.4 Candidate Pre-Irradiated Fuel Rods

The candidate fuel rods from the mixed-oxide irradiation tests in the EBR-II are presented in Table 2B-3. These irradiated rods were selected from the PA-10 and FFTF fuel testing programs and are presented in descending order of preference. The selection was based primarily on the demonstration plant fuel rod parameters summarized in Table 2B-1. In addition, the objective was to pick rods in nearly identical pre-transient condition to aid in the correlation of the post-transient results of the different tests. The factors used to determine the preference were:

- Fuel rods fabricated using the same dimensional tolerance and processes.
- Fuel rods irradiated in the same assembly to have similar irradiation histories.
- Fuel rods operating at 12 to 14 kW/ft to be representative of the fuel condition in the high power zone in an LMFBR core.
- Fission burnups of  $\sim 50,000$  MWd/Tm or greater to be comparable to the target burnup of the early demonstration plant cores.
- Availability of sibling fuel rods for destructive examination to determine the pre-transient condition of the irradiated fuel rods.

To meet the Option 1 test schedule included in Table 2B-2, the first pre-irradiated fuel rod should be available the first part of May 1972 for subsequent insertion in the test capsule for the July 1972 test in SEFOR. A commitment of pre-irradiated fuel rods to this program should be made prior to this time.

Table 2B-3

CANDIDATE PRE-IRRADIATED FUEL RODS FOR TRANSIENT OVERPOWER TESTS

Identification	Cladding	Pu/Pu+U	Smearred Density	O/M	BU	Status*
F-9C 37 Rods	316	25%	~84-88%	1.98	~60K	Out-of-Reactor-assigned to test to failure program
PNL-8 37 Rods	316	25%	~88%	1.97	~40K	In-Reactor for 80K BU
F-9A 37 Rods	304,316,321	25%	~85-88%	1.97	~60K	In-Reactor for 100K BU
PNL-5B 19 Rods	304	25%	~85-88%	1.97	~58K	In-Reactor for 80K BU
F-9B 37 Rods	304,316,321	25%	~85-88%	1.98	~58K	In-Reactor for 100K BU
F-8B Rods 9 & 18	316	25%	83-85%	1.97	~48K	In-Reactor for 50K BU
F-8A Rods B,E,I & L	316	25%	85-87%	1.97	~73K	In-Reactor for 100K BU
F-4 Rods J & G	316	30&20 w/o	87	1.98	~80K	Out-of-Reactor-assigned to molten fuel operation test
F-4 Rods E & A	316 & 304	30&20 w/o	~86%	2.00	~80K	Out-of-Reactor-post exam @ Los Alamos

\*Based on References 3 and 4

### 2.2.5 Overpower Transients and Thermal Analysis

Examples of the capsule thermal response to four SEFOR overpower transients are provided. The basic transients are:

- T1 — fast, high energy transient initiated from low power (maximum planned transient)
- T2 — slow, high energy transient initiated from prototypical LMFBR conditions
- T3 — fast, high energy transient initiated from prototypical LMFBR conditions
- T4 — low energy transient initiated from prototypical LMFBR conditions.

These transients are based upon SEFOR Core II parameters using the FORE code. The capsule thermal response is based upon a radial heat transfer model for the peak flux region using the THTE code.

The four transients are intended to define the nominal conditions that are necessary to achieve the Option I test objectives. The final specification of each test transient will depend upon

- final selection of test fuel parameters
- final capsule design details
- zirc hydride effectiveness tests
- physics calculations of power density distribution
- results of capsule calibration experiments

#### Transient T1

The maximum planned transient, T1, achieves three test objectives:

- this most severe transient is used to proof test the capsule (TOP-1A)
- the thermal response of the test fuel rod (TOP-1A) to T1 simulates the TREAT test C4A
- the thermal response of the test fuel rods (TOP-2A & 2B) to T1 simulate a large start-up accident with defected fuel rods.

The power history for T1 is shown in Figure 2B-1. The transient is initiated from a steady power of 8.5 MWt and attains a peak power of 8900 MWt in 91 msec. Incipient melt occurs in the test fuel on the Doppler tail of the transient at a peak linear power of 105 kW/ft. SCRAM is initiated at 360 msec. The integrated power at 1 second is 175 MW-sec.

The thermal response of the test fuel rod and capsule is indicated in Figures 2B-2 and 2B-3. The peak fuel, cladding, inner and outer sodium annuli and capsule temperatures are 5050 (melt temperature), 1580, 1370, 920, and 850°F, respectively.

Figure 2B-4 shows the radial temperature distribution in the fuel rod at five time periods that correspond to:

- 0.00 steady state at 8.5 MW
- 0.091 peak power at 8900 MW
- 0.140 heating toward fuel melt
- 0.275 incipient fuel melt at a radius of 74 mils
- 0.580 maximum melt fractions.

The radial temperature profiles are rather flat because of the relatively low initial power and the slight flux depression in the fuel.

The fuel melt fraction history is presented in Figure 2B-5. The maximum fuel fraction into melt, ~60%, occurs at 295 milliseconds and the maximum equivalent liquidus fraction is ~40% at 580 milliseconds (mass fraction of fuel that has stored the equivalent heat of fusion).

One of the objectives of the TOP-1A test is to simulate the fuel rod temperatures and melt fractions of TREAT test C4A. Figure 2B-6 shows the development of the radial temperature profiles for the C4A test. A comparison of Figures 2B-6 to 2B-4 indicates the pronounced effect of the thermal flux self-shielding upon the radial temperature profiles in C4A in contrast to that in TOP-1A. However, incipient fuel melt occurs at approximately a 74 mil radius in both cases. Figure 2B-7 shows a comparison of the melt fraction histories for TOP-1A and C4A. The maximum fuel fraction into melt for TOP-1A precedes that for C4A because of the flatter temperature profile at incipient melt for the former. Both achieve ~60% into melt. The equivalent liquidus melt rate for the two tests are similar. The maximum liquidus melt fraction for C4A is higher than that for TOP-1A, reflecting the higher integrated power for the former.

The transients designated T2, T3, and T4 have been selected to investigate accidents on the same time scale as LMFBR accidents occurring at operating power conditions. Each transient utilizes the STOP/FRED excursion mode of SEFOR.



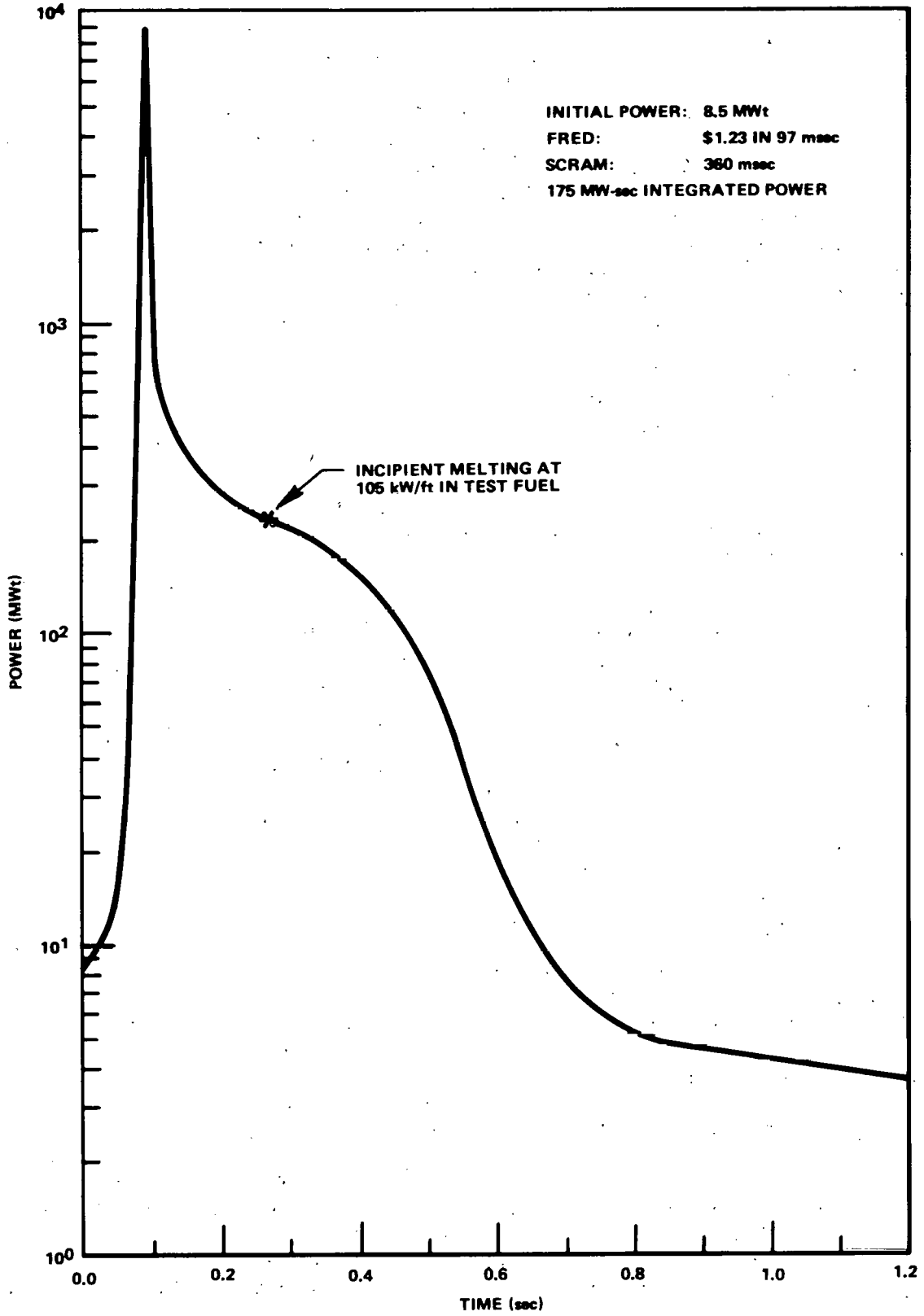


Figure 2B-1. Transient T1 Planned Power History

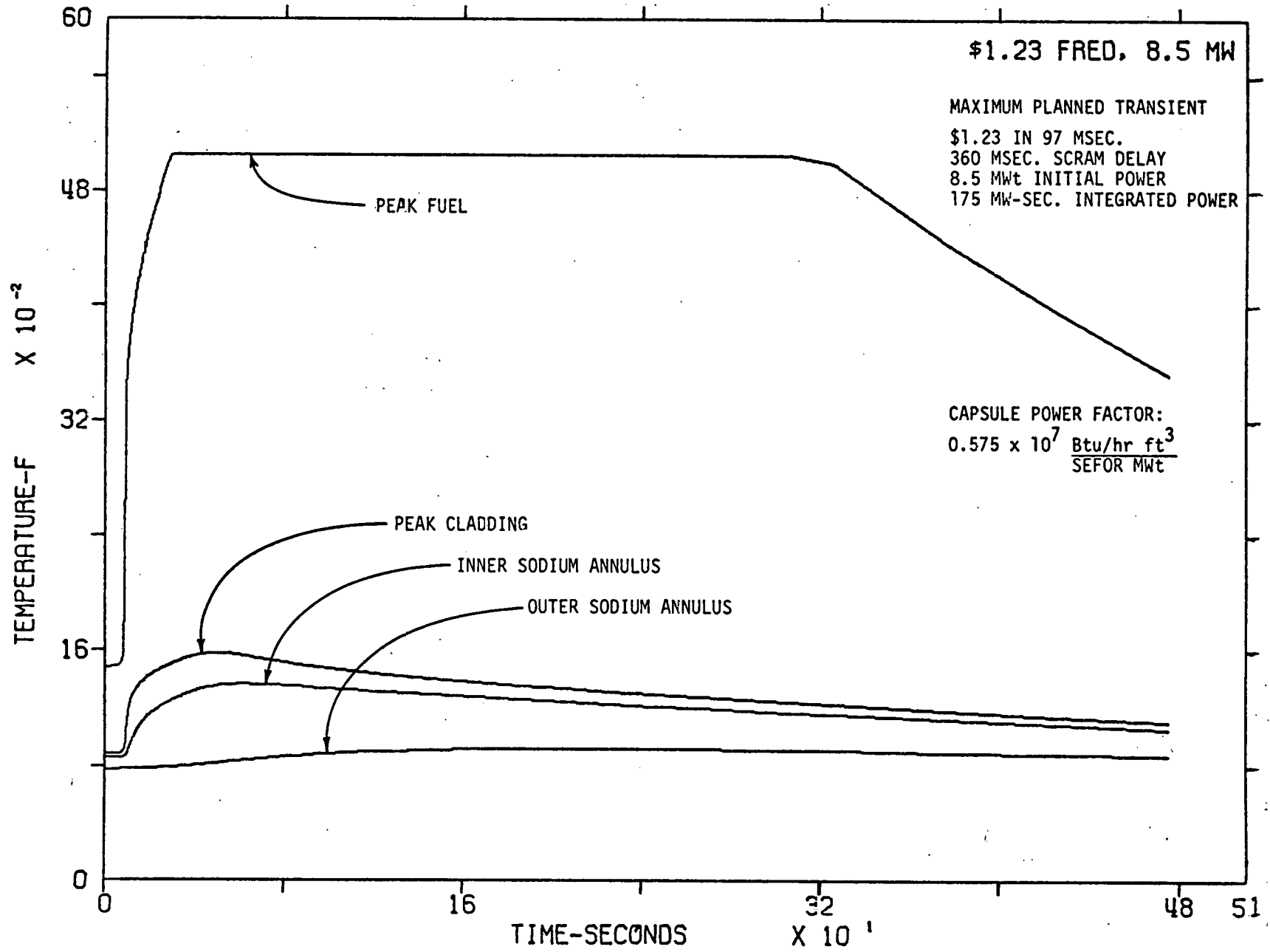
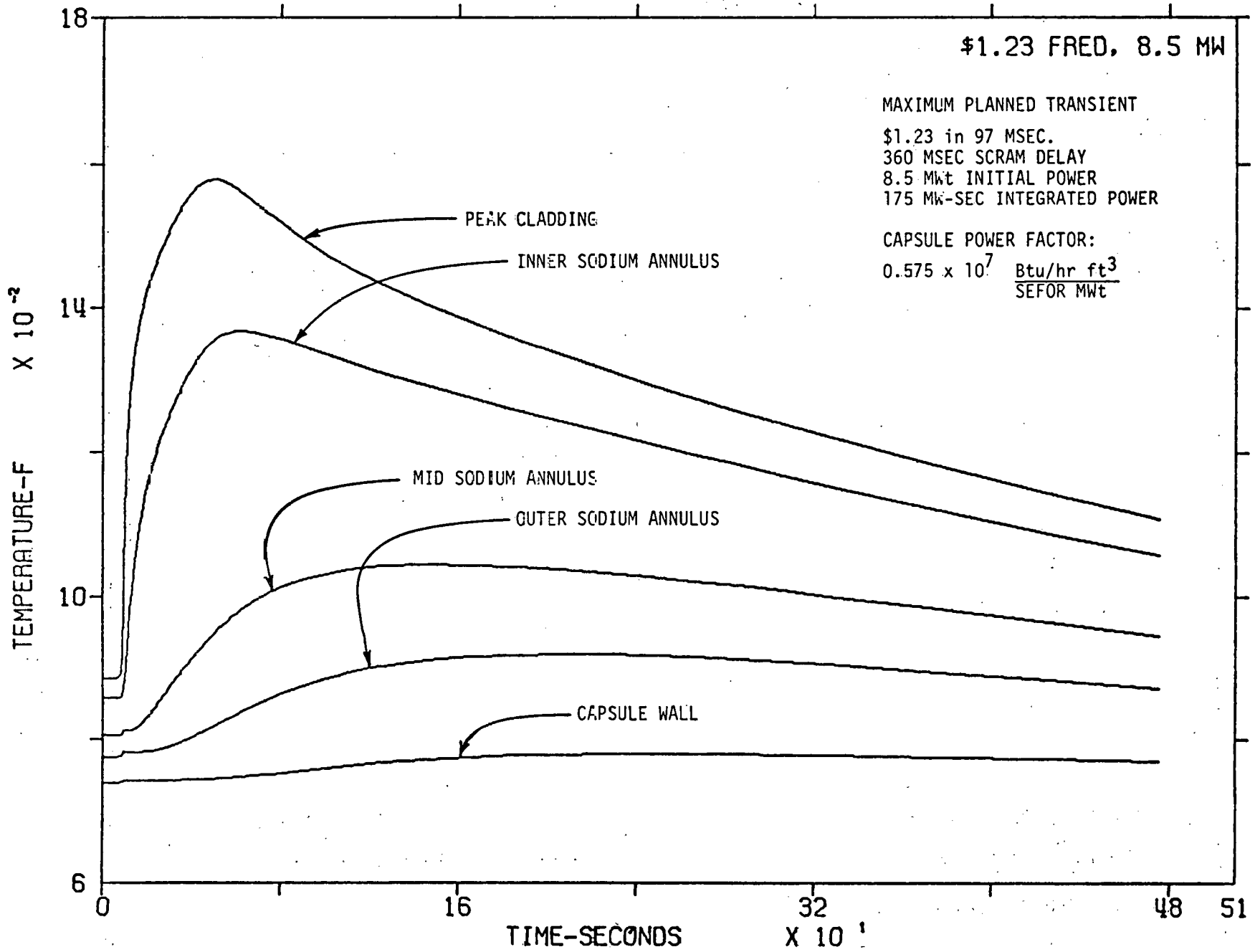


Figure 2B-2. Transient T1 Calculated Fuel Temperatures History



52

GEAP-13787

Figure 2B-3. Transient T1 Calculated Capsule Temperatures History

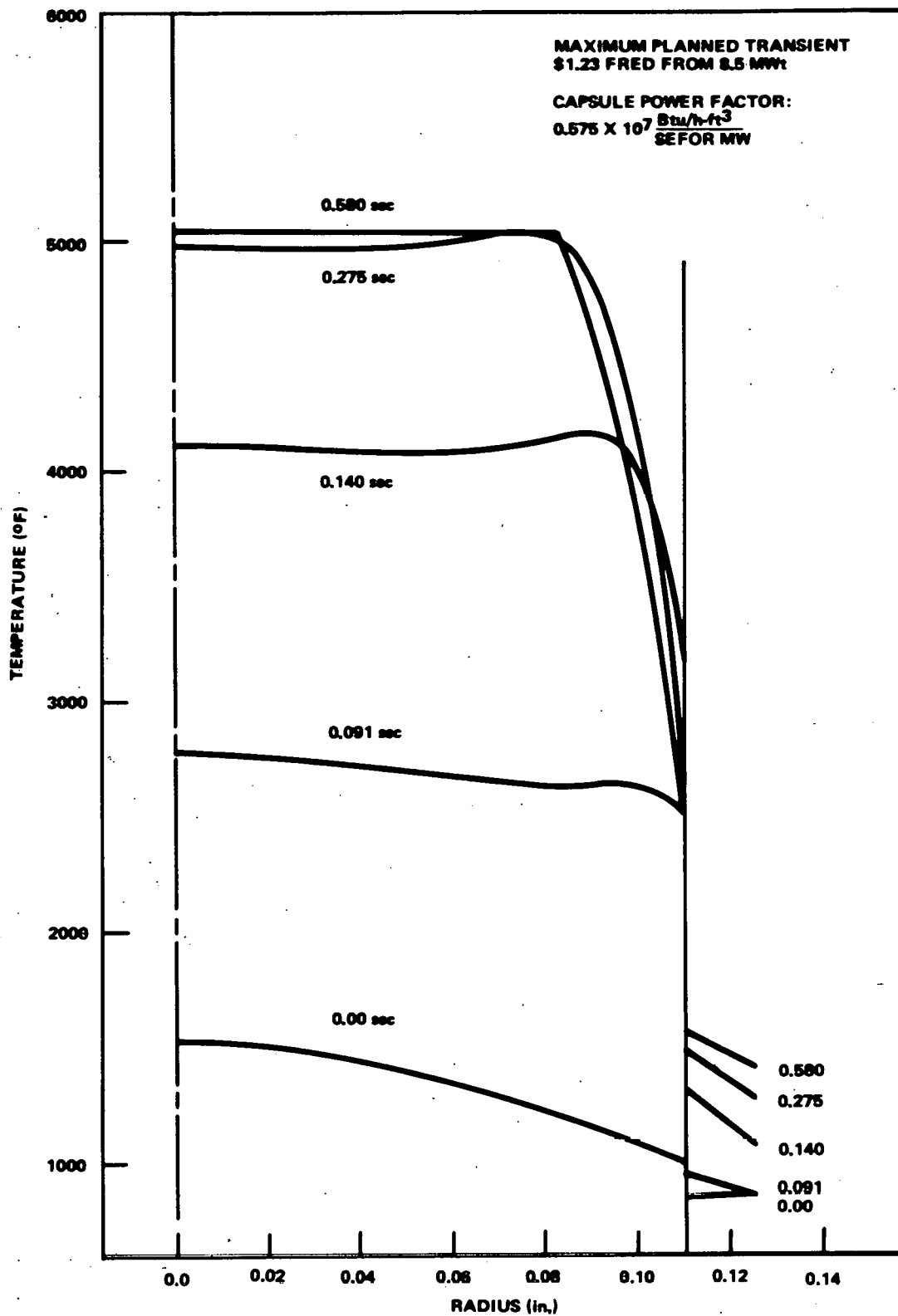


Figure 2B-4. Transient T1 Predicted Fuel Radial Temperature Profiles

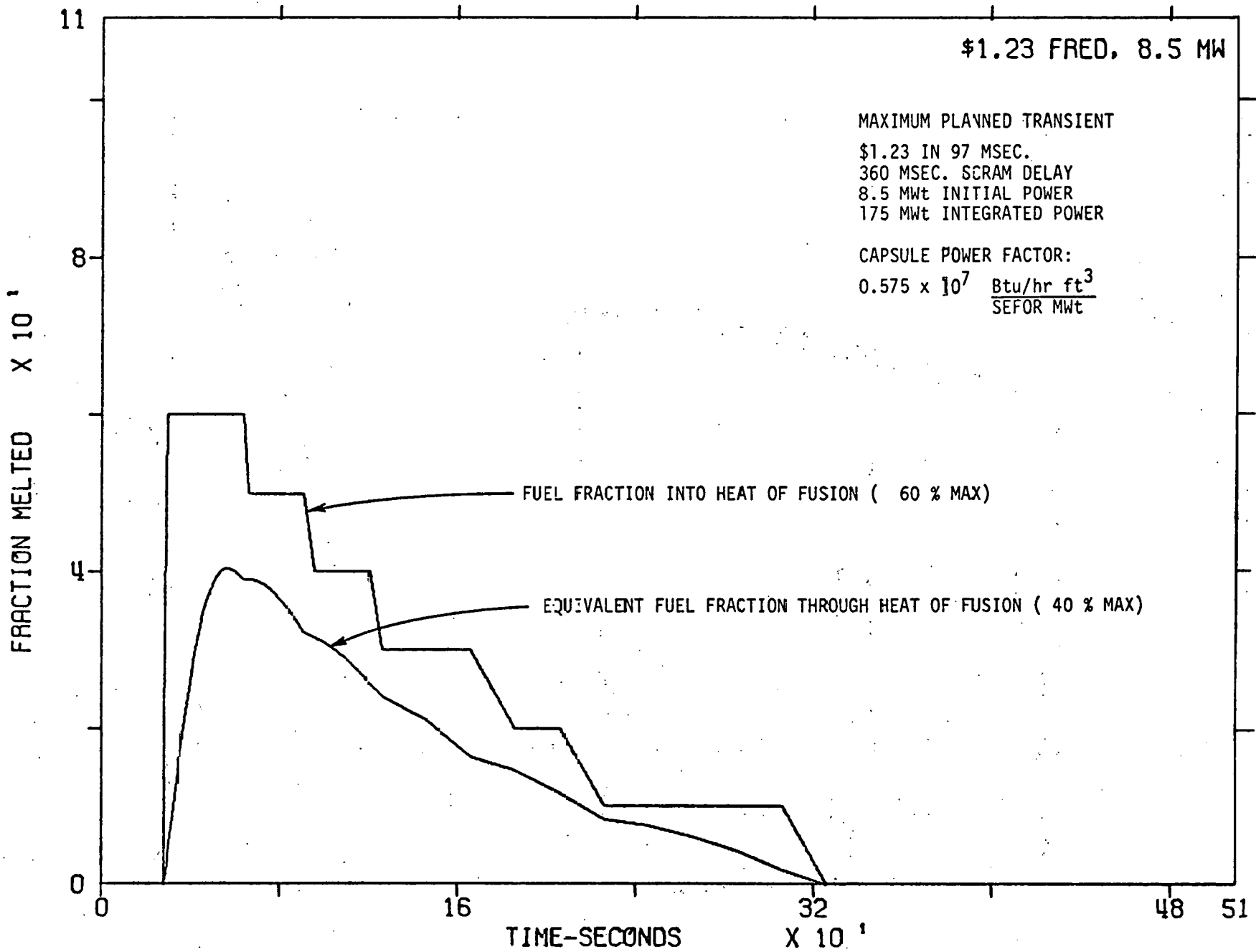


Figure 2B-5. Transient T1 Calculated Melt Fraction History

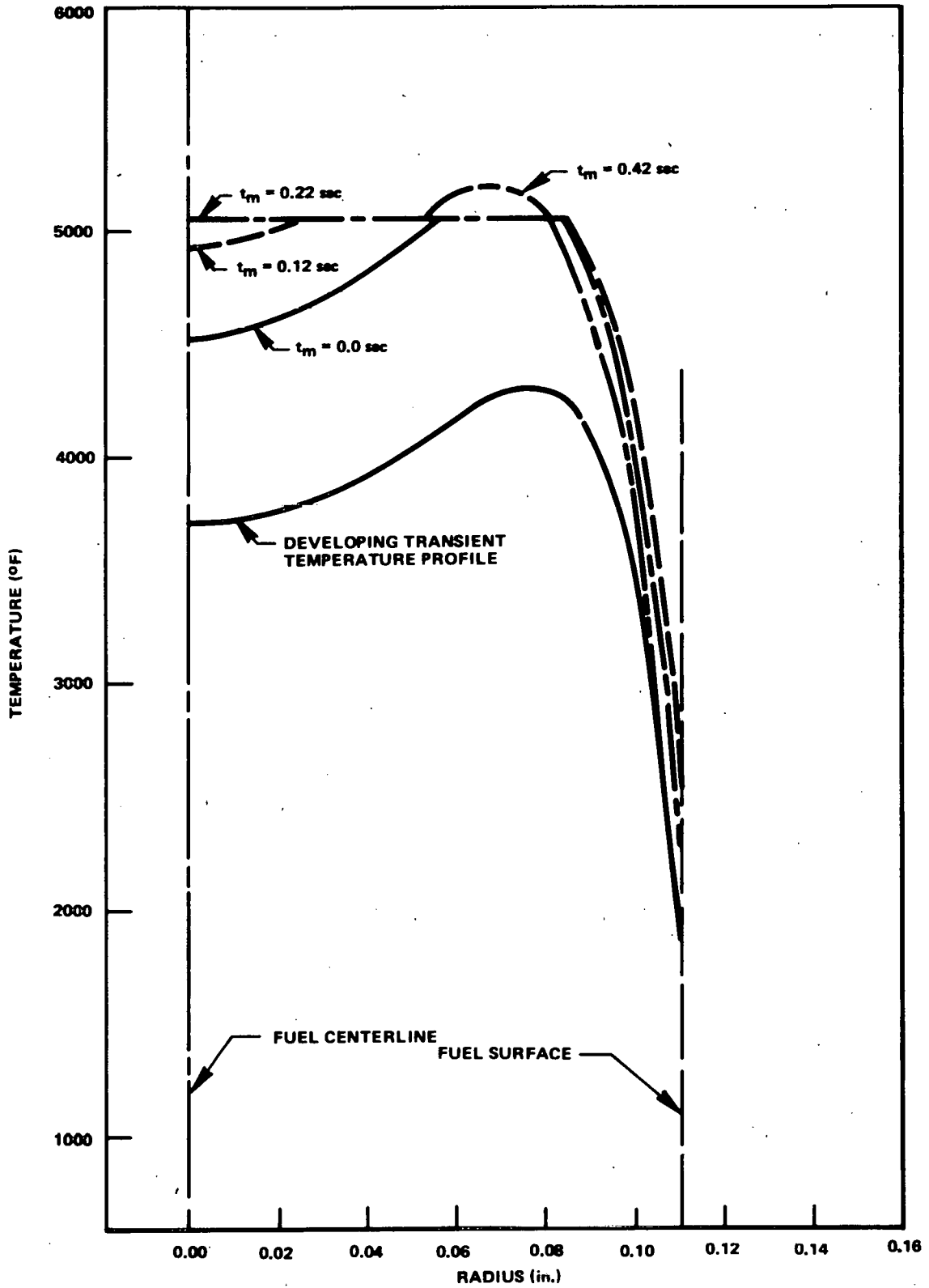


Figure 2B-6. TREAT C4A Test Fuel Radial Temperature Profiles

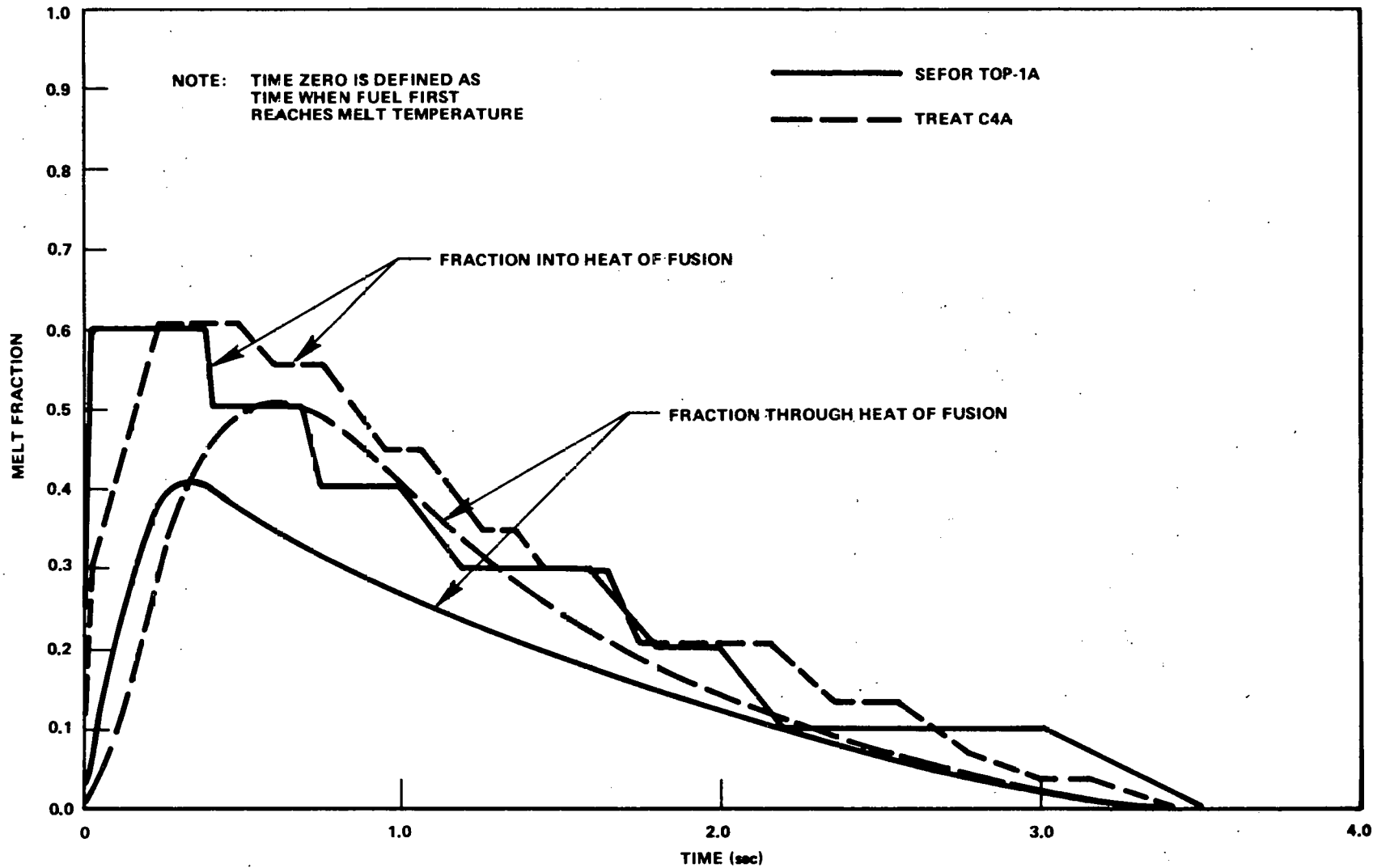


Figure 2B-7. Comparison of TREAT and SEFOR Melt Fractions

The STOP mode ramps the core power from 1 to 30 MWt in 22.8 seconds. However, the initial and final power levels as well as the duration of the STOP mode can be varied as test parameters. Figure 2B-8 shows that the STOP mode can achieve fuel rod temperatures typical of an operating LMFBR fuel rod. The temperature profiles develop in a nearly parabolic manner. At each point in time, the STOP mode temperature profile simulates a steady state LMFBR profile corresponding to a lower linear power rate.

Transients T2 and T3 are designed to investigate the effects upon failure threshold of heating rate and energy density at incipient melt. The range of these two conditions achieved by the T2 and T3 FRED transients is indicated in Figure 2B-9. Also shown is a comparison of their relative power histories to those of three hypothetical LMFBR accidents.

#### Transient T2

The power history for transient T2 is presented in Figure 2B-10. This transient is obtained by ejecting a 74¢ FRED slug from the core in ~400 msec. A peak power of 490 MWt is obtained at 23.2 seconds at which time SCRAM is initiated. Incipient melt in the test fuel occurs at ~55 kW/ft on the power rise of the transient.

The thermal history of the capsule is presented in Figures 2B-11 and 2B-12. The peak fuel, cladding, inner and outer sodium annuli and capsule wall temperatures are 6300, 1760, 1540, 980, and 890°F, respectively. The development of the fuel rod temperature profiles is shown in Figure 2B-13 and the fuel melt history is presented in Figure 2B-14. The maximum fuel fraction into melt is ~70% and begins at 23.34 seconds. The maximum equivalent fuel fraction through melt is ~60% and occurs at 23.46 seconds.

#### Transient T3

The power history for transient T3 is shown in Figure 2B-15. This transient is produced by ejecting the 74¢ slug from the core in 97 msec. A peak power of 670 MWt is attained at 22.91 seconds. SCRAM is initiated at 23.16 seconds. Incipient melt occurs at ~225 kW/ft on the power rise of the transient, a factor of 4 higher than that of T2.

The thermal history of the capsule is presented in Figures 2B-16 and 2B-17. The peak fuel, cladding, inner and outer sodium annuli, and capsule wall temperatures are 6400, 1770, 1550, 980, and 89°F, respectively. The development of the fuel rod temperature profiles is shown in Figure 2B-18 and the fuel melt history is presented in Figure 2B-19. The maximum fuel fraction into melt is ~70% and begins at 23.14 seconds. The maximum equivalent fuel fraction through melt is ~60% and occurs at 23.26 seconds.

#### Transient T4

The smallest overpower transient of interest, T4, is designed to investigate axial fuel movement resulting from slumping. The power history for transient T4 is shown in Figure 2B-20. This transient is produced by ejecting a 60¢ FRED slug from the core in 97 msec. The peak power of 170 MWt occurs at 22.92 seconds. SCRAM is initiated at 23.16 seconds. Incipient melt of test fuel occurs at 93 kW/ft near the peak of the transient.

The thermal response of the capsule is presented in Figures 2B-21 and 2B-22. Peak fuel, cladding, inner and outer sodium annuli, and capsule wall temperatures are 5100, 1540, 1380, 940, and 860°F, respectively. The radial temperature profiles are shown in Figure 2B-23 and the fuel melt history is presented in Figures 2B-24. The maximum fuel fraction into melt is ~30% at 23.18 seconds. The maximum equivalent fuel fraction through melt is ~20% and occurs at 23.44 seconds.

### 2.2.6 Short Term Overpower Test

The object of the short term overpower (STOP) test is to simulate prototypic LMFBR temperatures within a fuel test capsule. The test will be performed within the SEFOR core using encapsulated LMFBR type fuel rods. The STOP operation will establish initial conditions from which the fast reactivity excursion device (FRED) can be fired to approximate the consequences of an overpower transient in the LMFBR plant. Typically, in the STOP mode of operation the reactor power will be increased from 1 to 30 megawatts in 22 seconds by inserting one reflector at a fixed rate. However, the initial and final power levels as well as the duration of the STOP mode can be varied as test parameters.

Computer analyses evaluating the SEFOR response during various STOP tests have been performed. Initial parameter studies have been conducted on effects of reactivity ramp rates, initial power levels, FRED slug worths, and FRED ejection time. These studies while only preliminary have indicated the feasibility of operation of the STOP test and of achieving the prototypic temperatures.



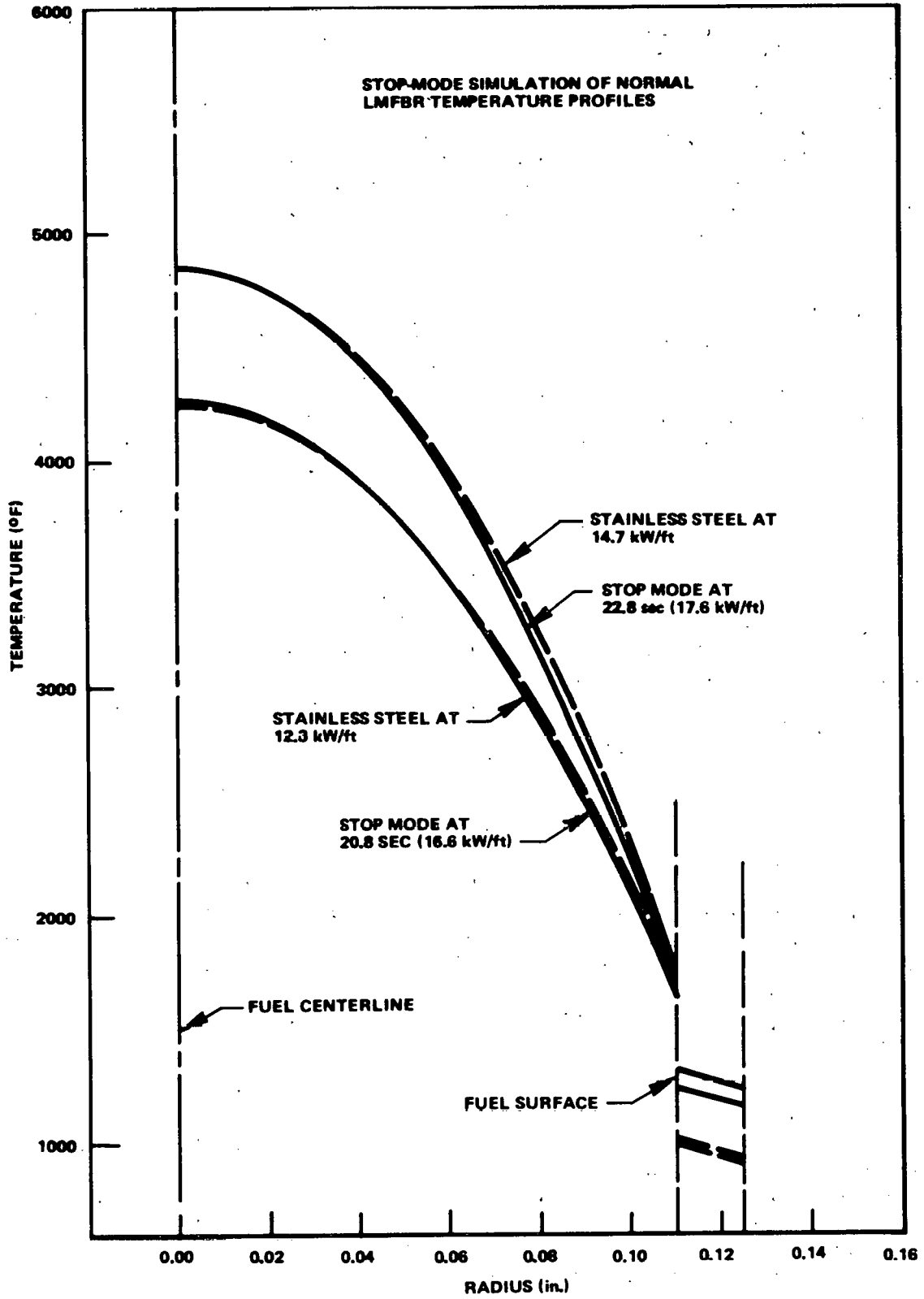


Figure 2B-8. STOP Mode Simulation of Normal LMFBR Fuel Radial Temperature Profiles

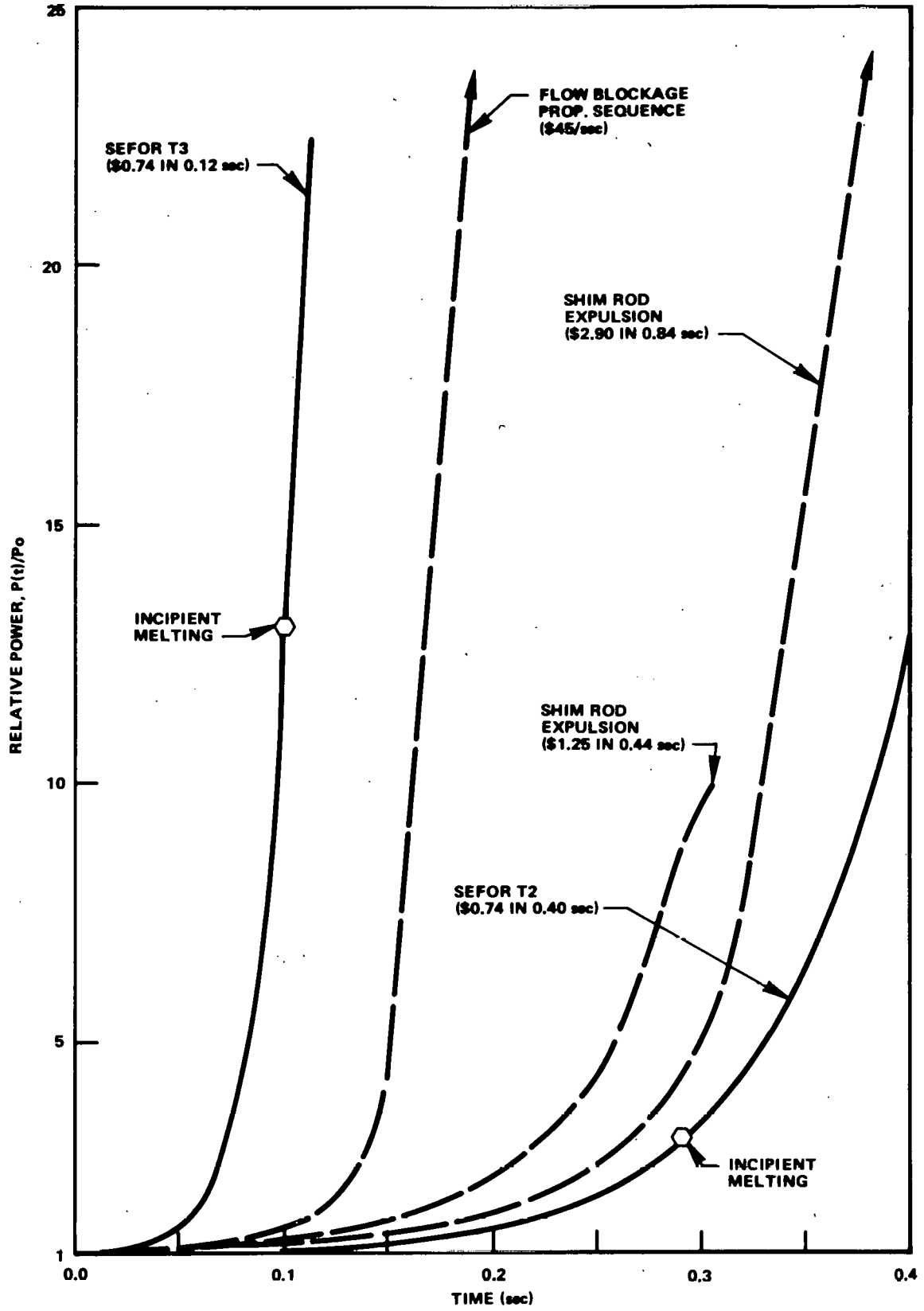


Figure 2B-9. Comparison of SEFOR Transients to Hypothetical LMFBR Accidents

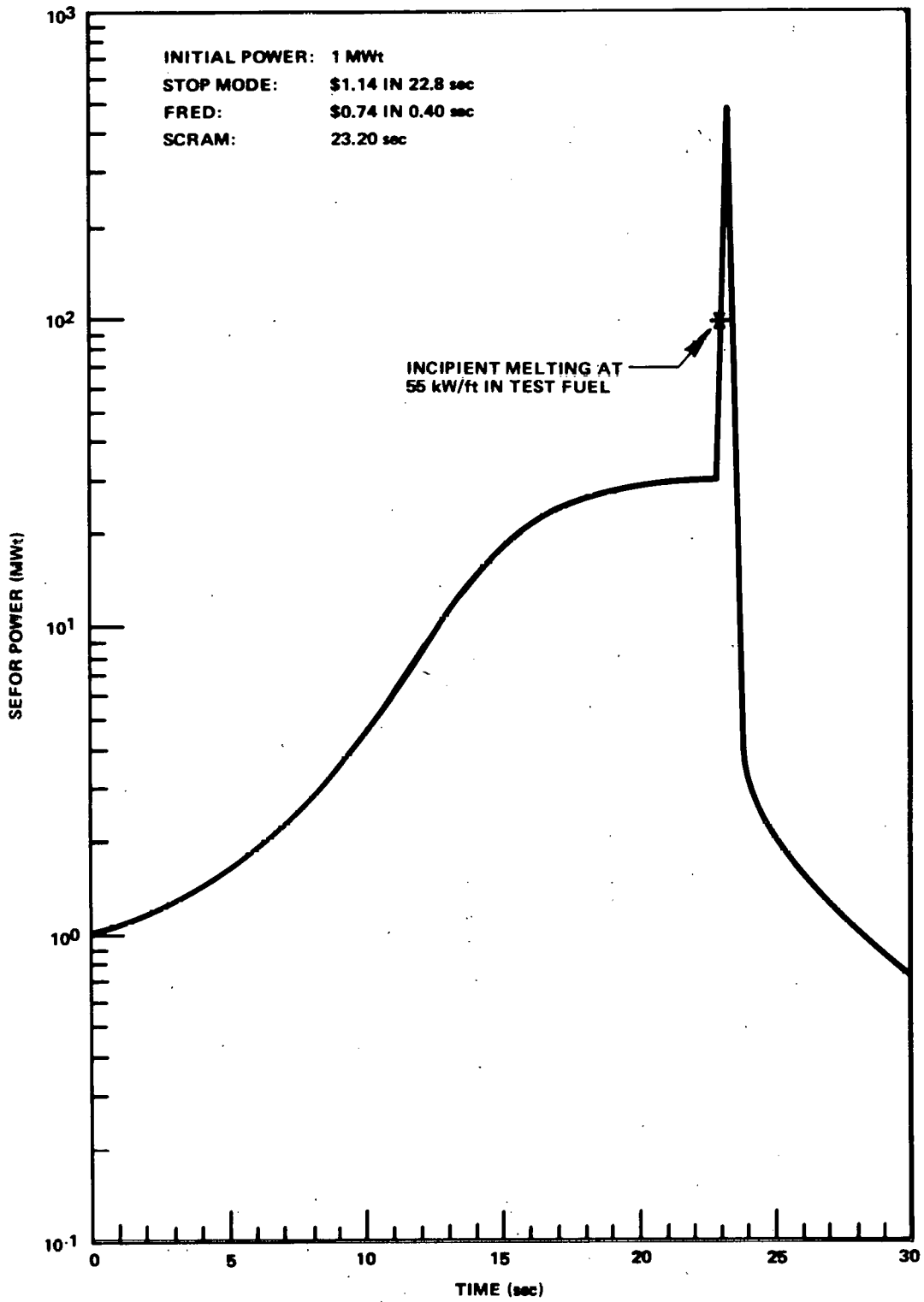


Figure 2B-10. Transient T2 Planned Power History

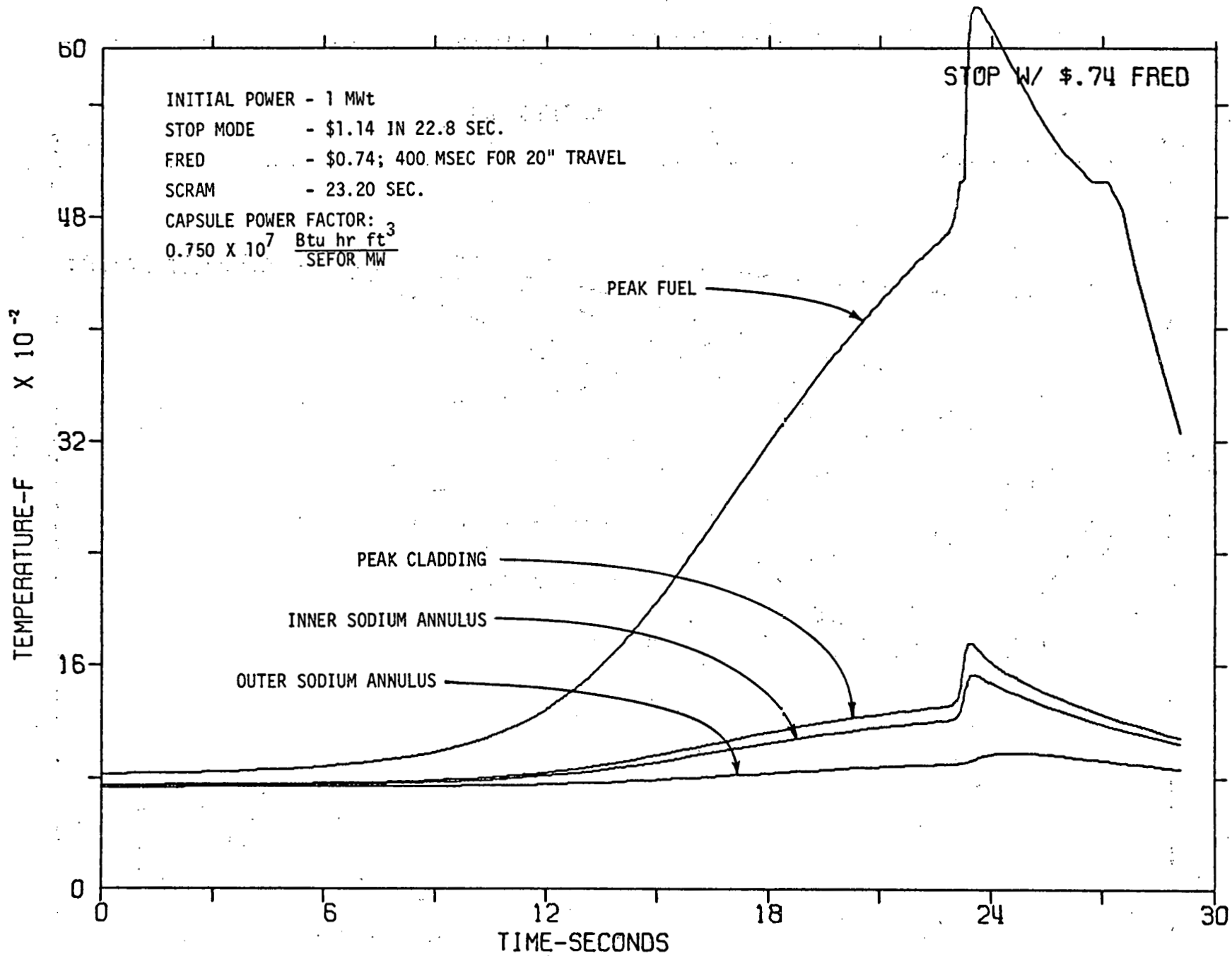


Figure 2B-11. Transient T2 Calculated Fuel Temperatures History

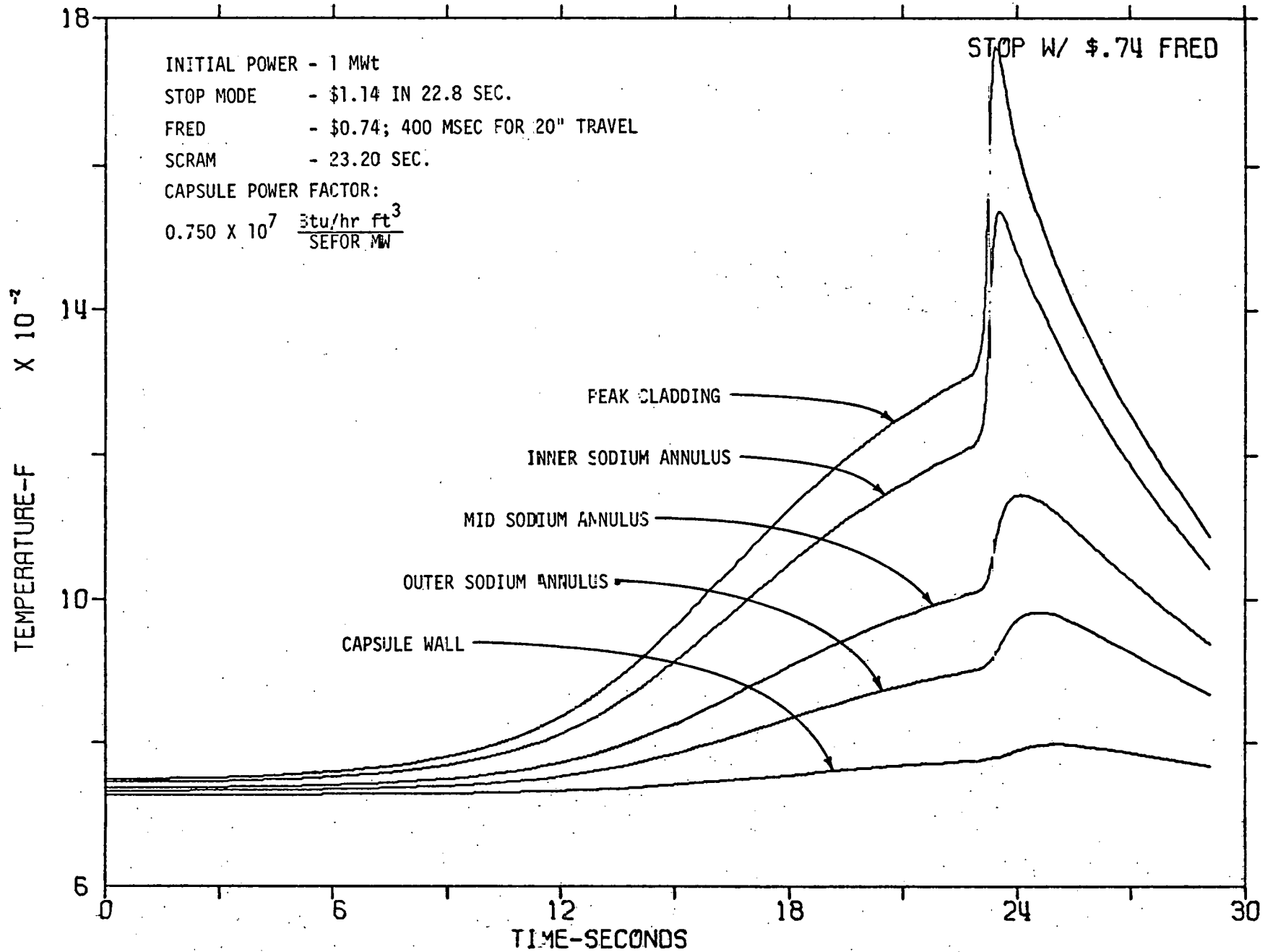


Figure 2B-12. Transient T2 Calculated Capsule Temperatures History

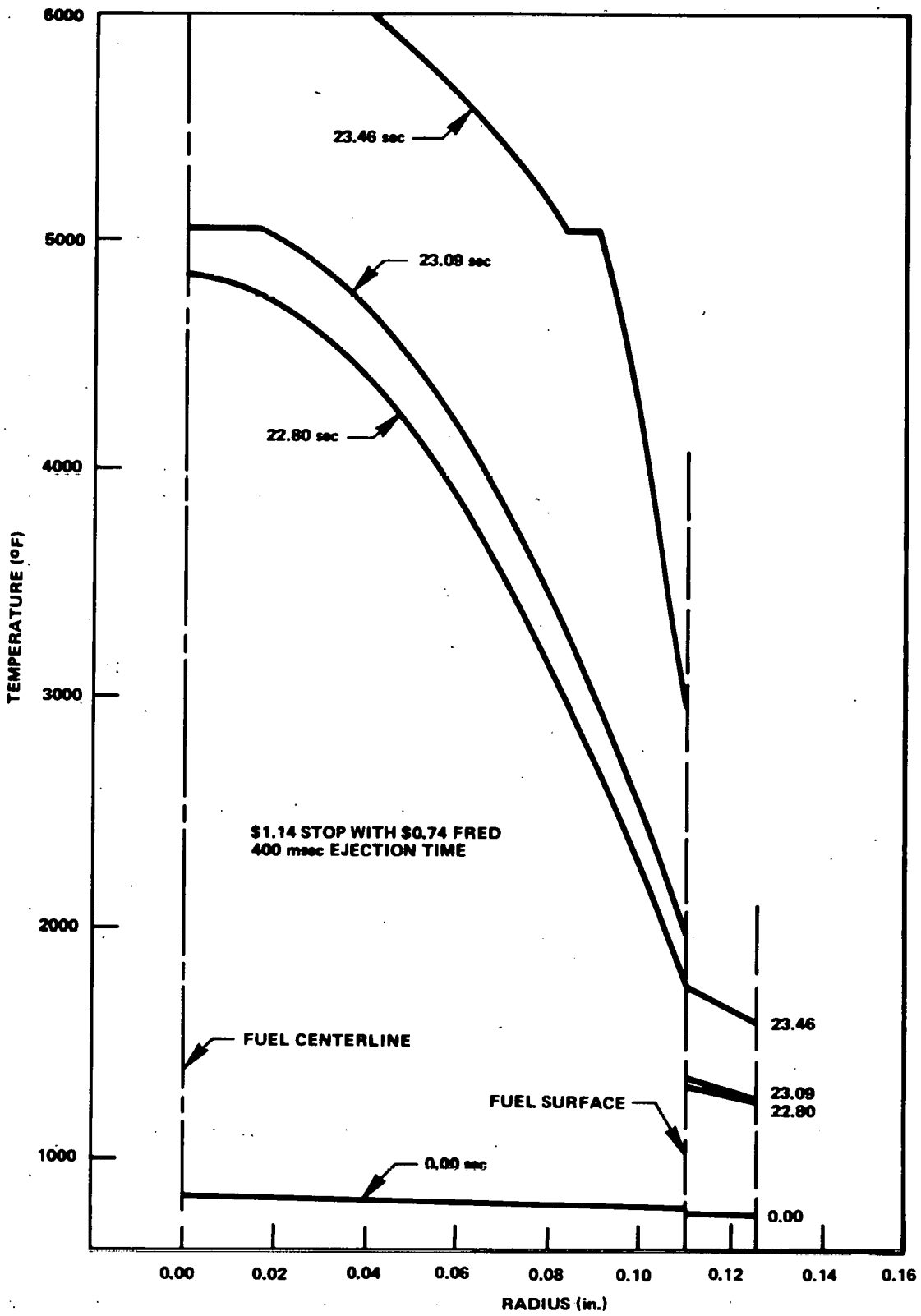


Figure 2B-13. Transient T2 Predicted Fuel Radial Temperature Profiles

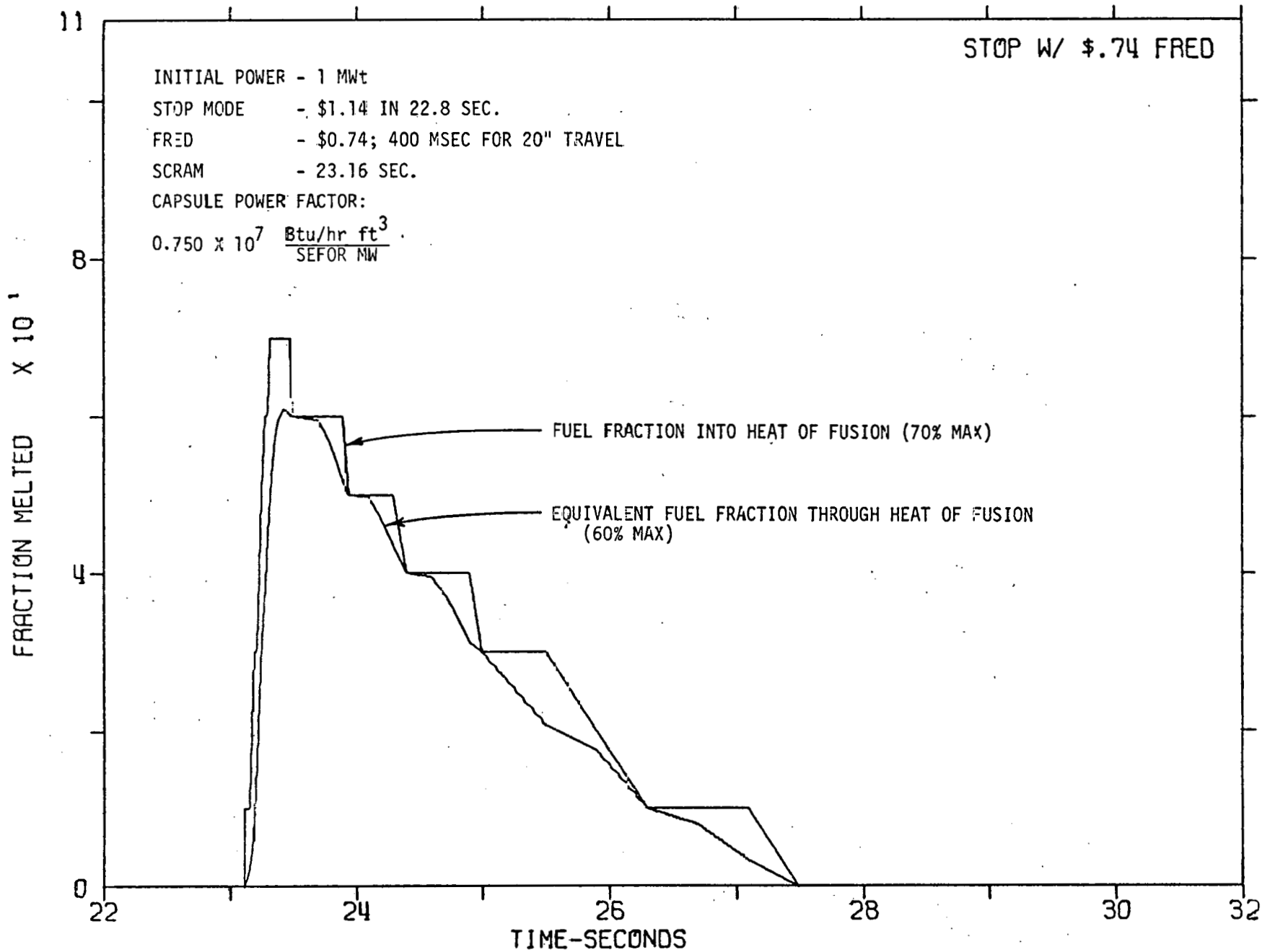


Figure 2B-14. Transient T2 Calculated Melt Fraction History

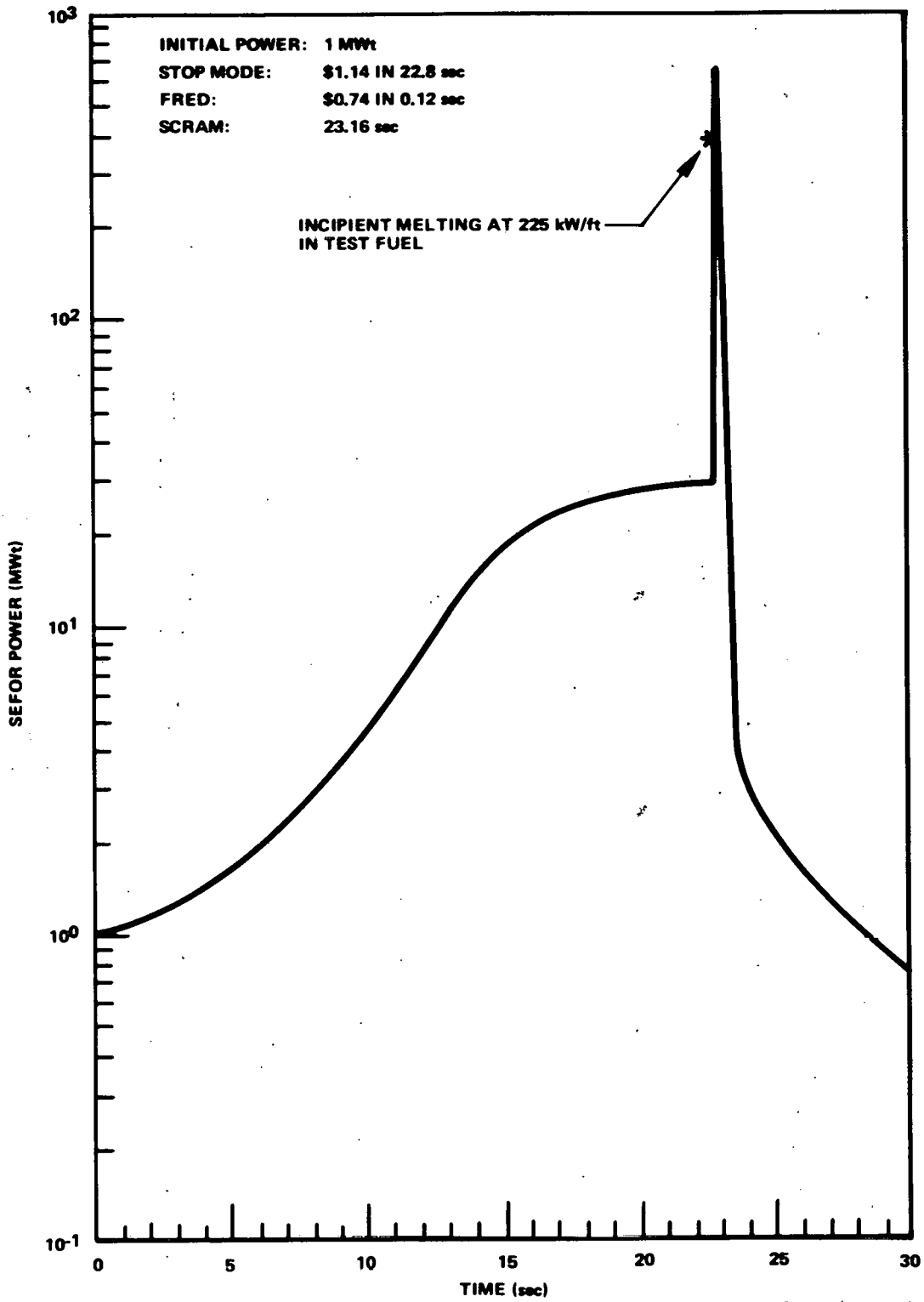


Figure 2B-15. Transient T3 Planned Power History



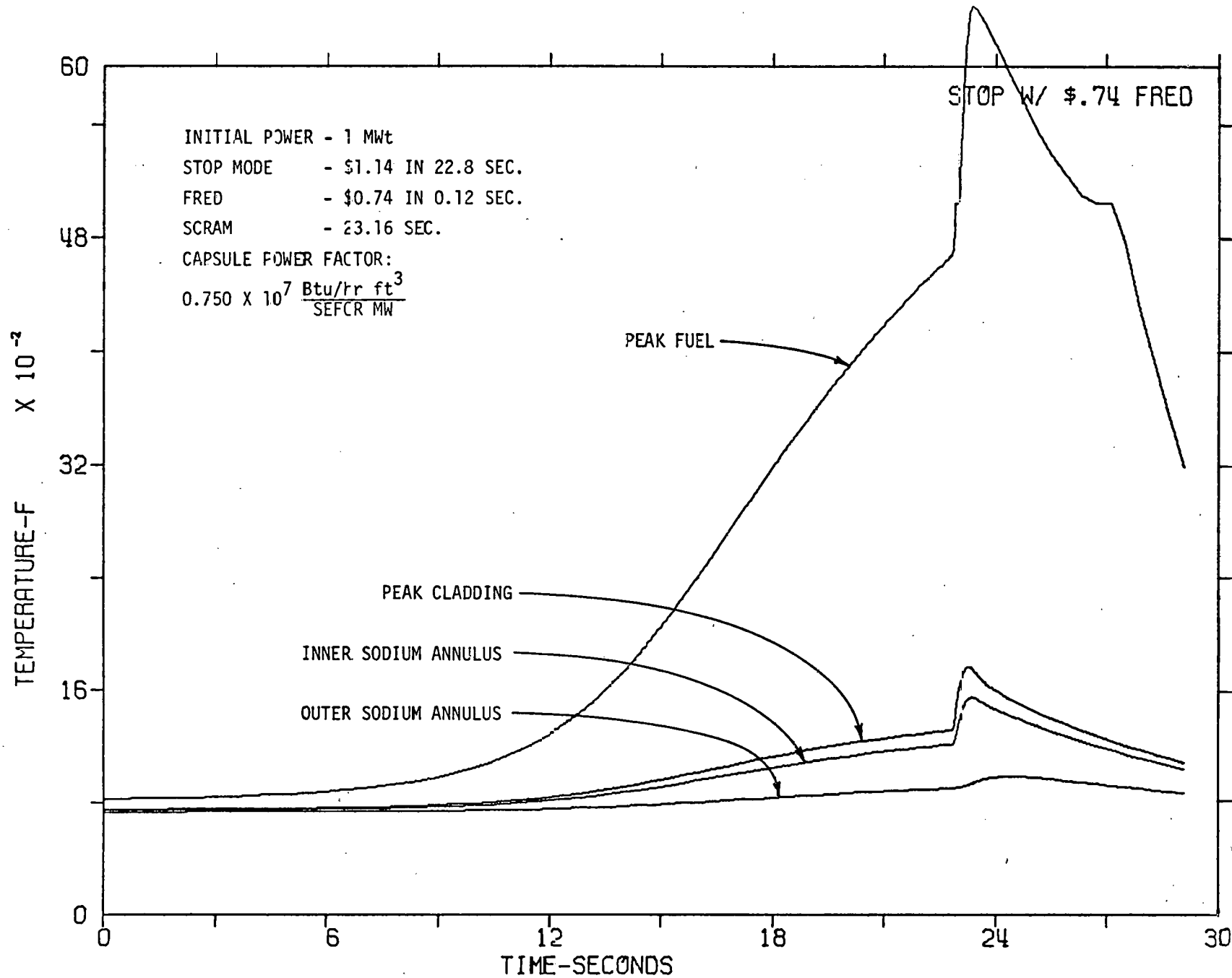


Figure 28-16. Transient T3 Calculated Fuel Temperatures History

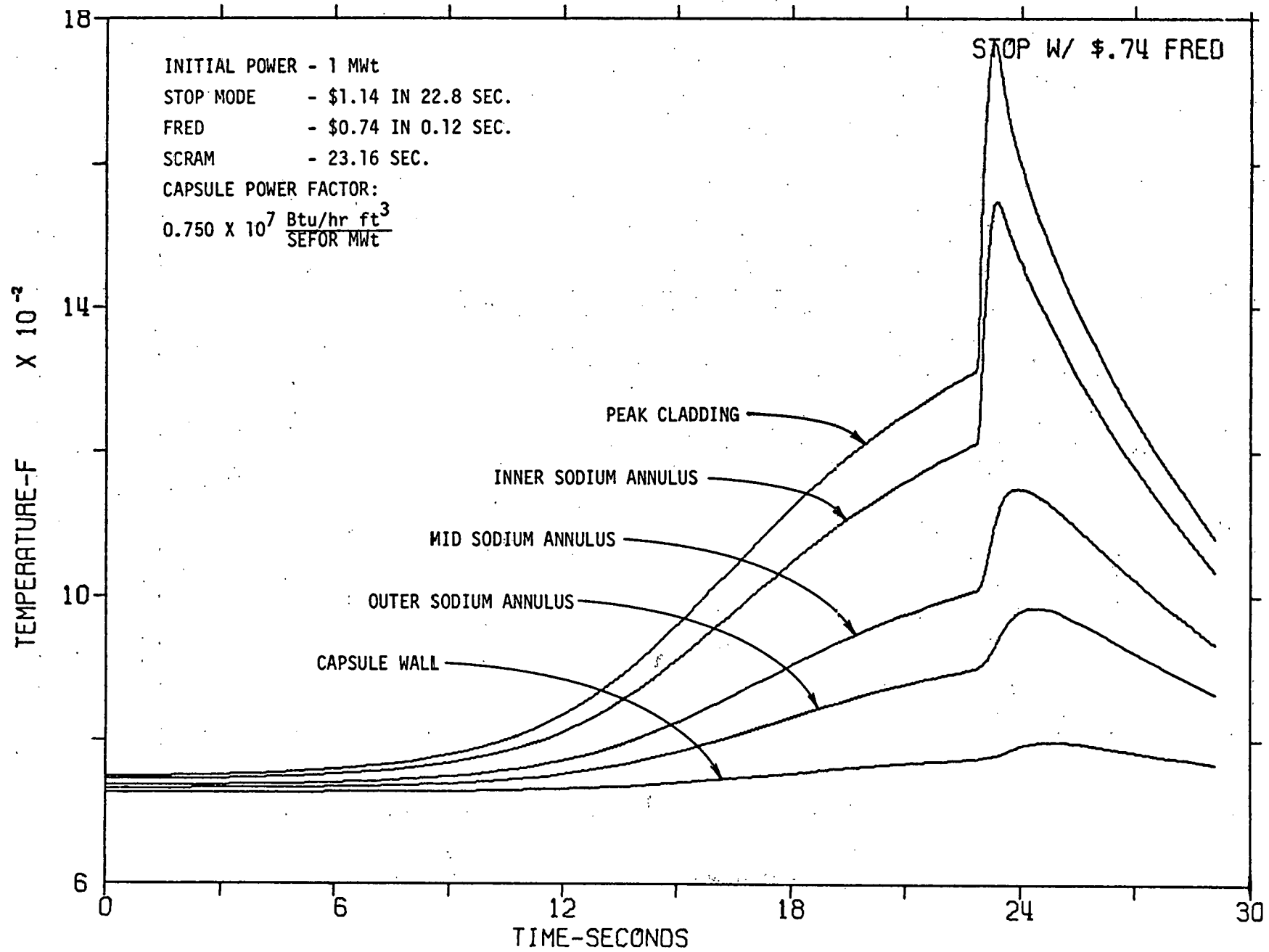


Figure 2B-17. Transient T3 Calculated Capsule Temperatures History

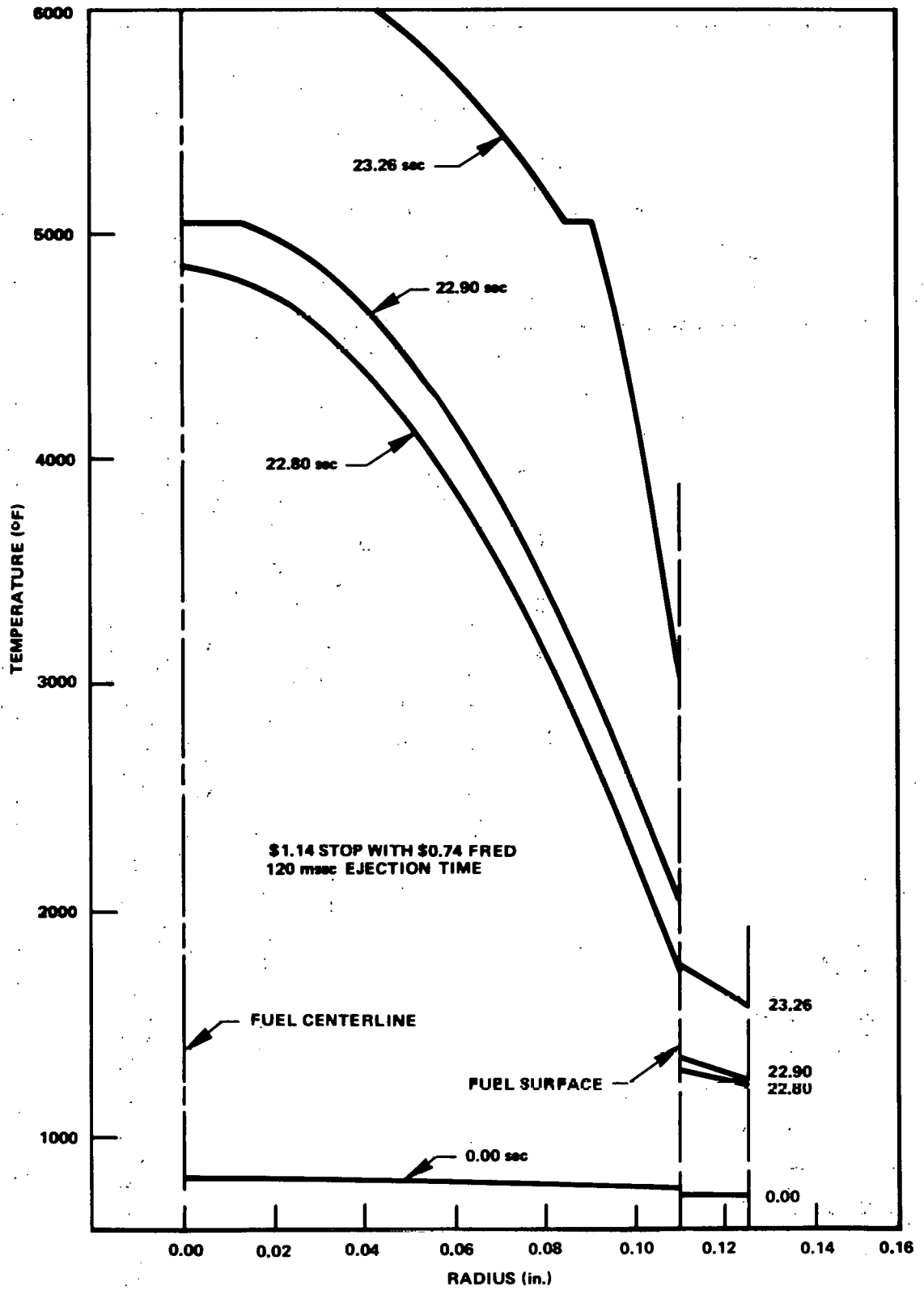


Figure 2B-18. Transient T3 Predicted Fuel Radial Temperature Profiles

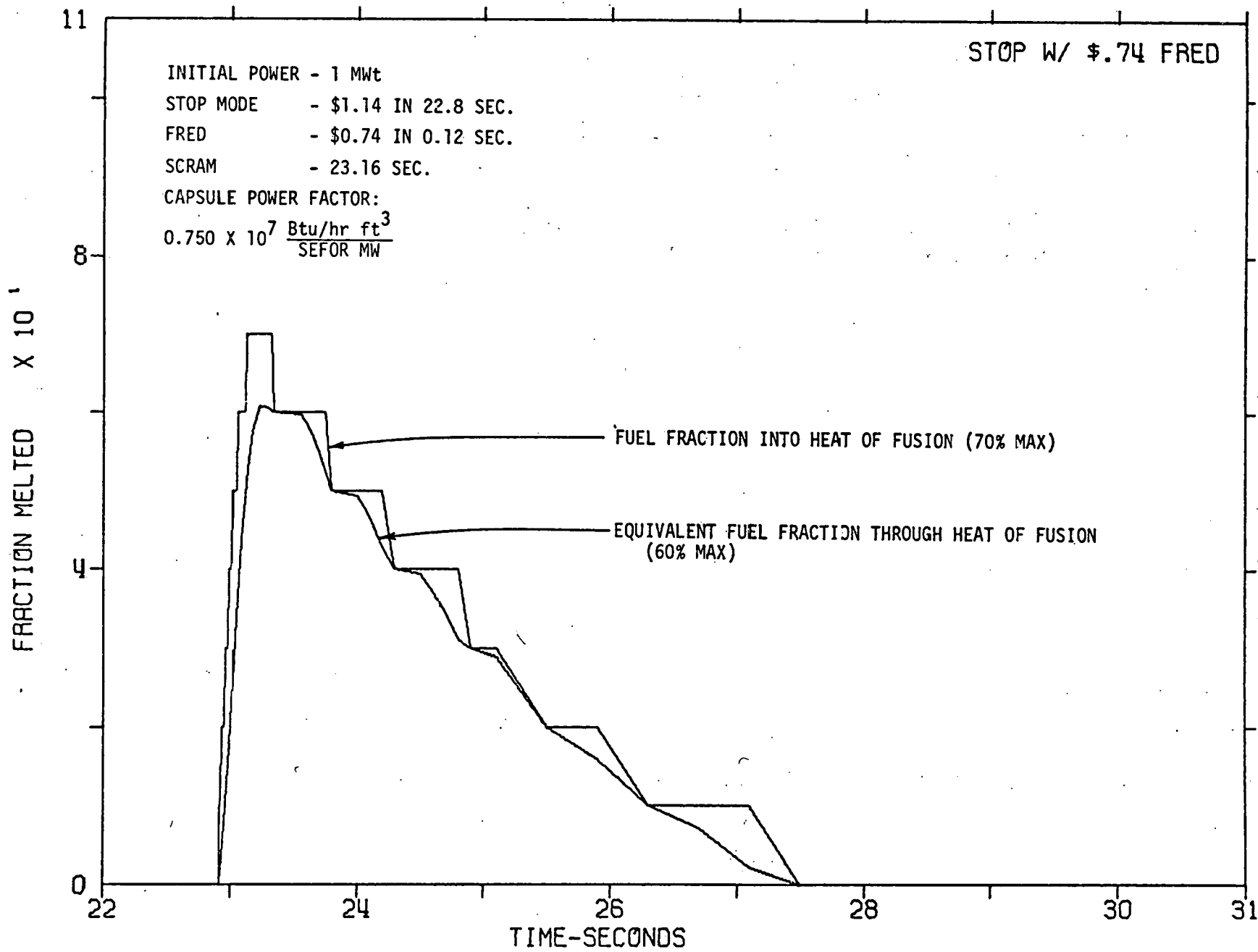


Figure 2B-19 Transient T3 Calculated Melt Fraction History

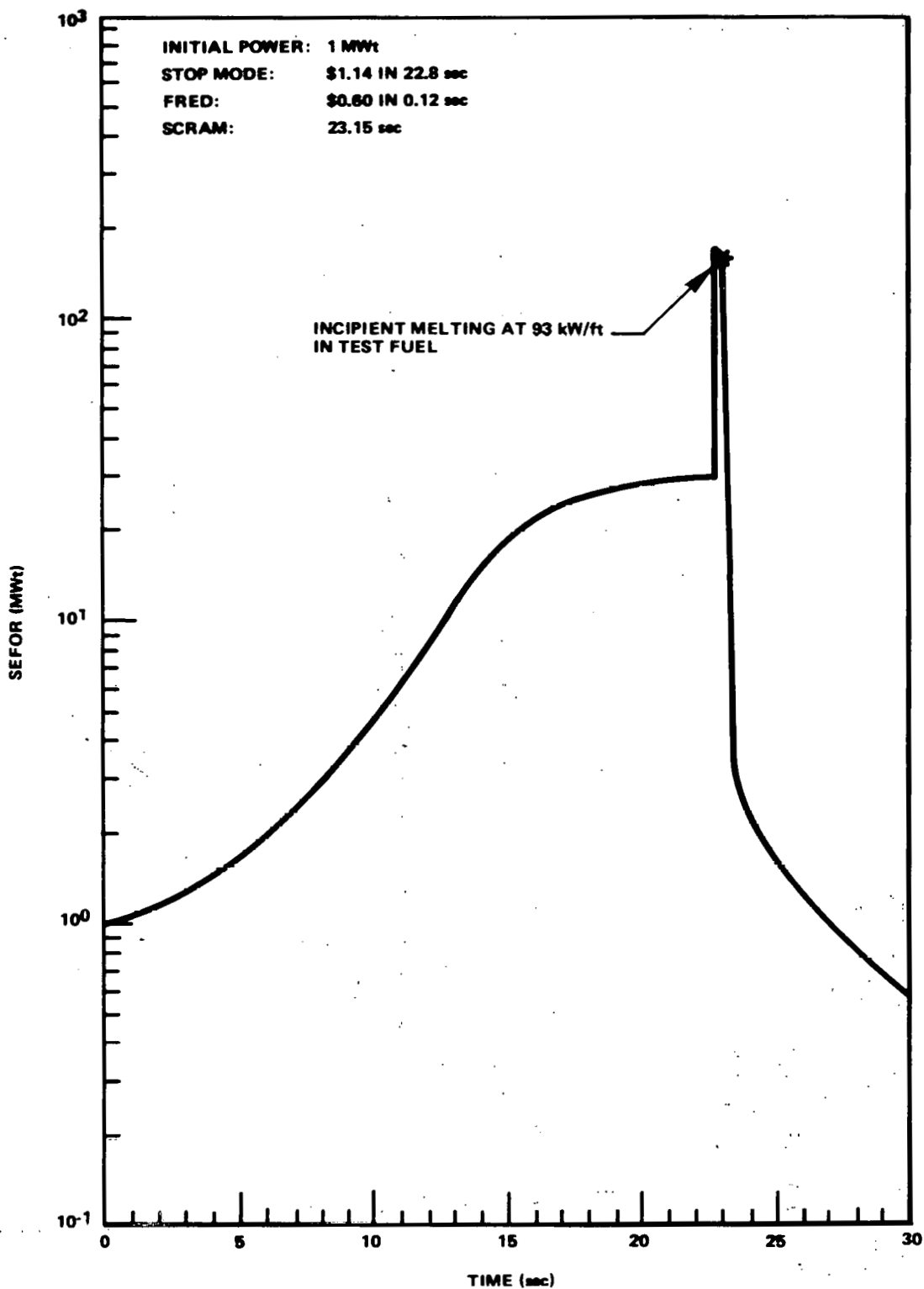


Figure 2B-20. Transient T4 Planned Power History

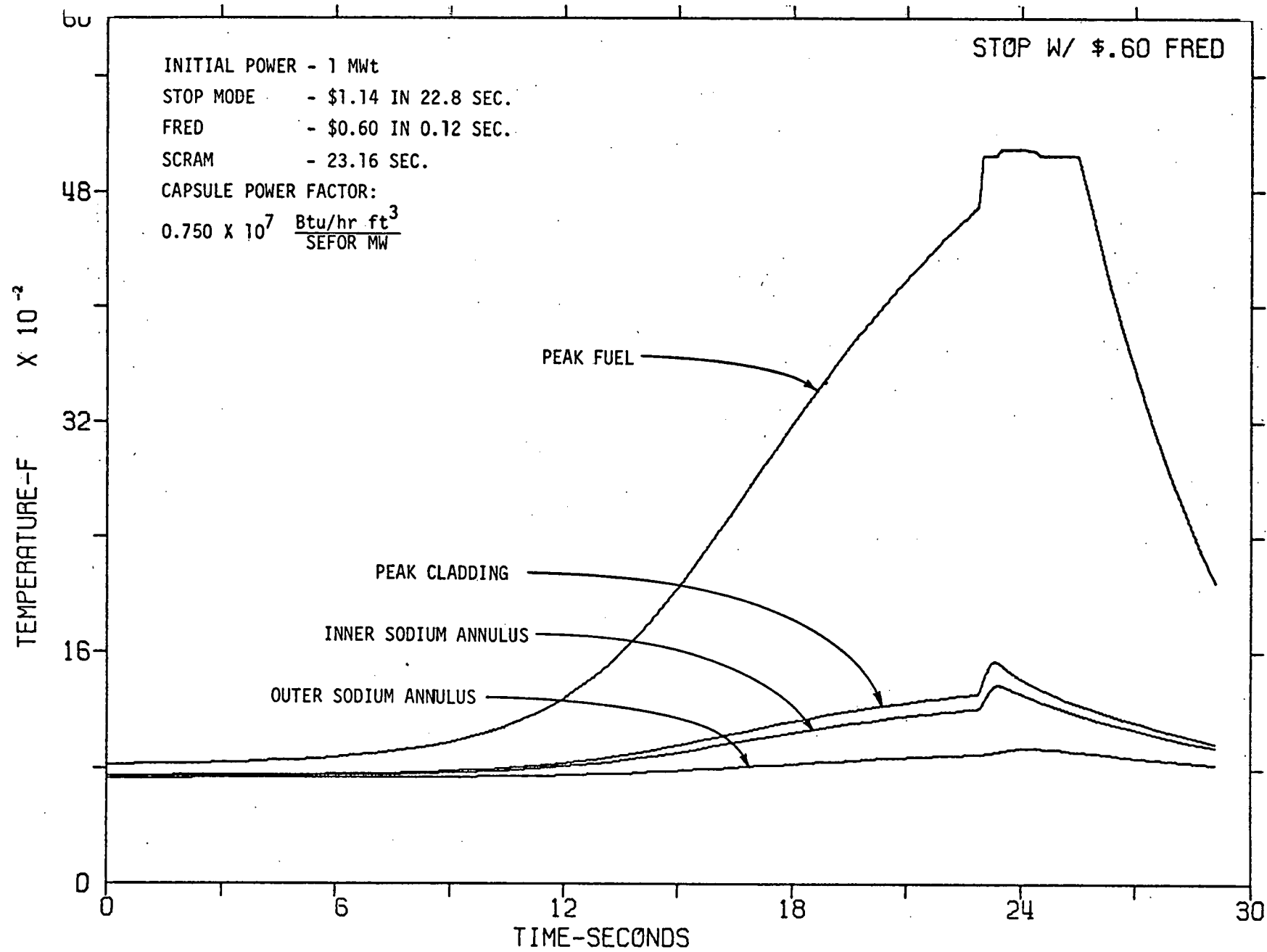


Figure 2B-21. Transient T4 Calculated Fuel Temperatures History

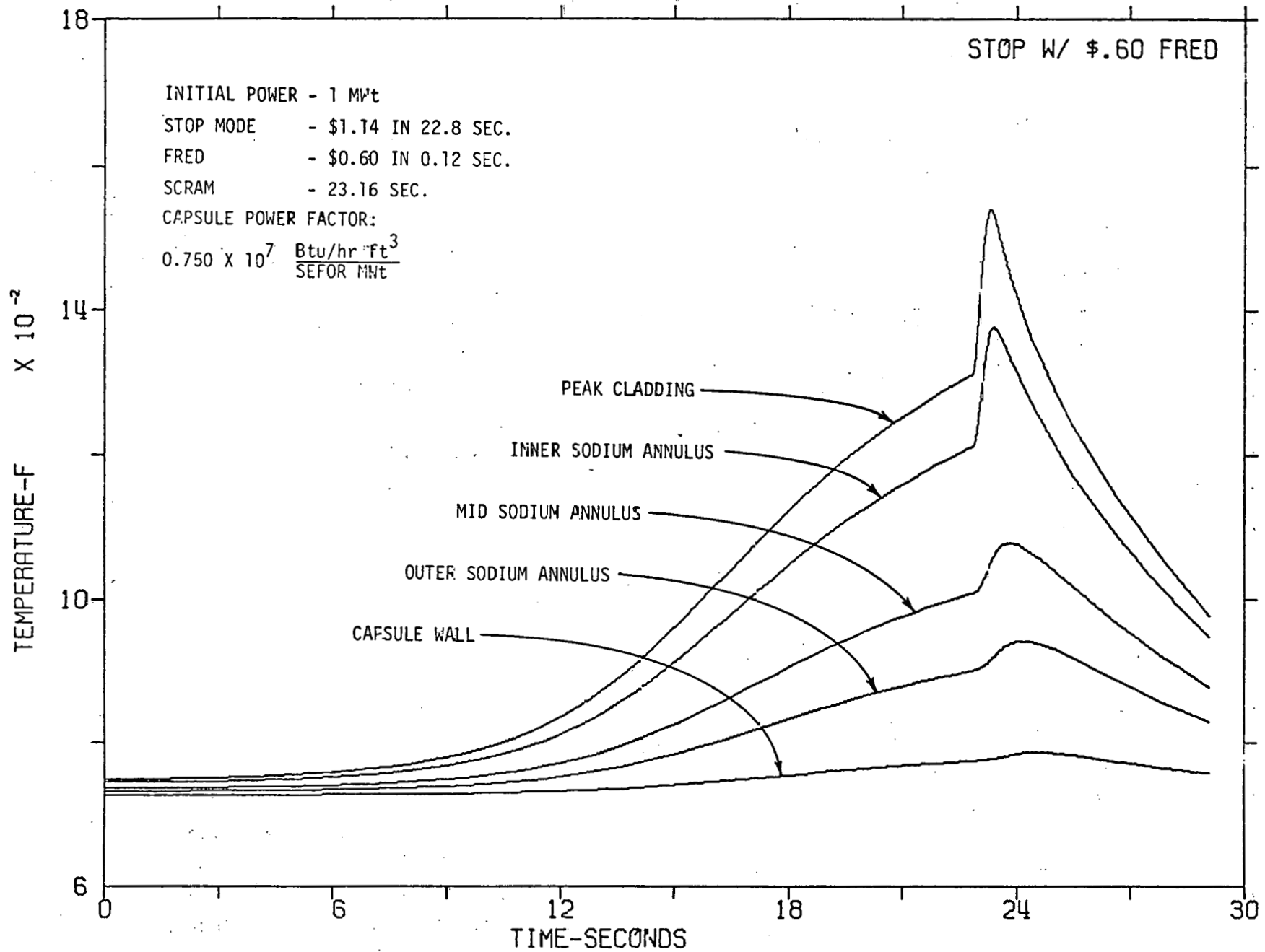


Figure 2B-22. Transient T4 Calculated Capsule Temperatures History

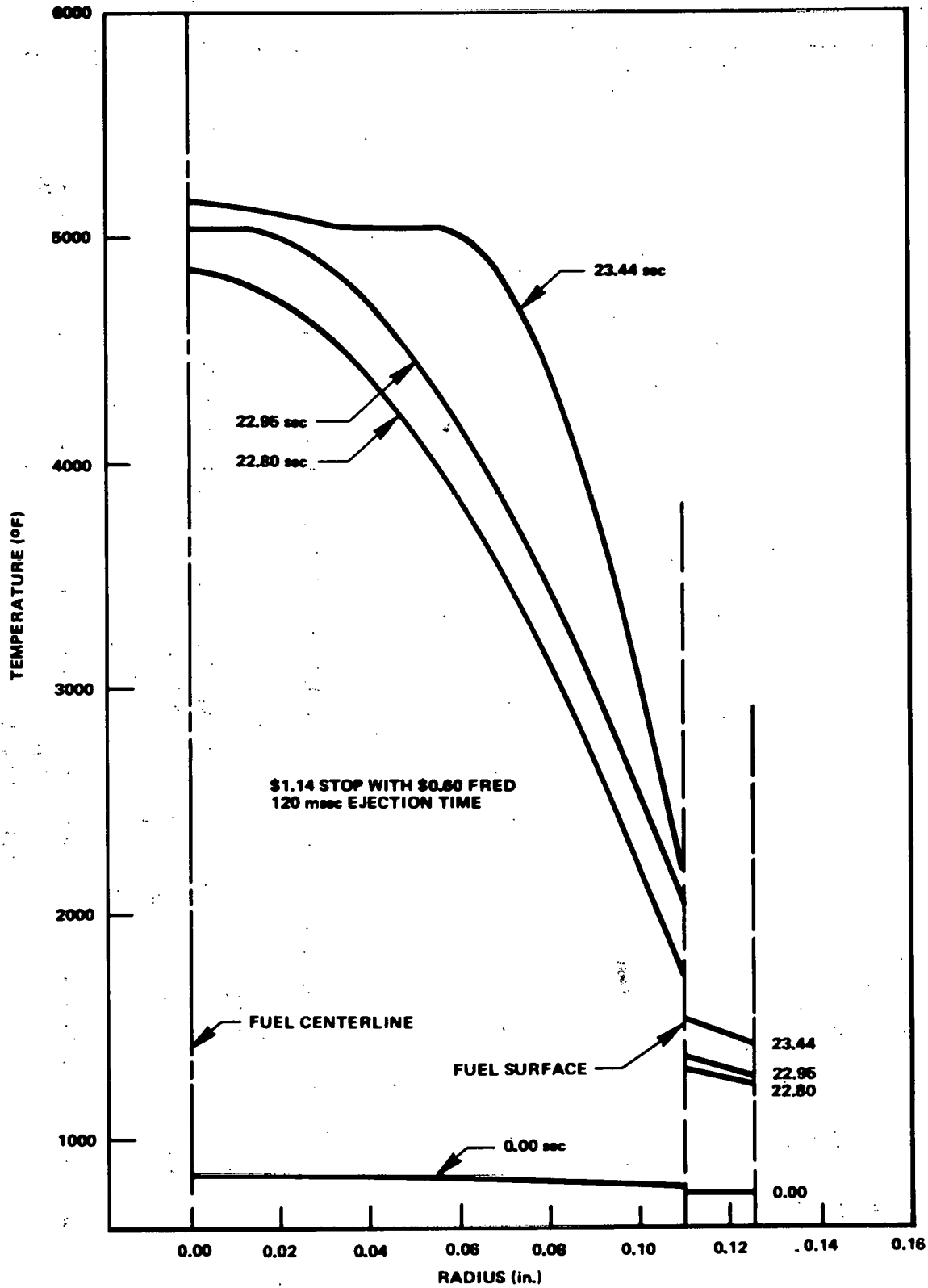


Figure 2B-23. Transient T4 Predicted Fuel Radial Temperature Profiles



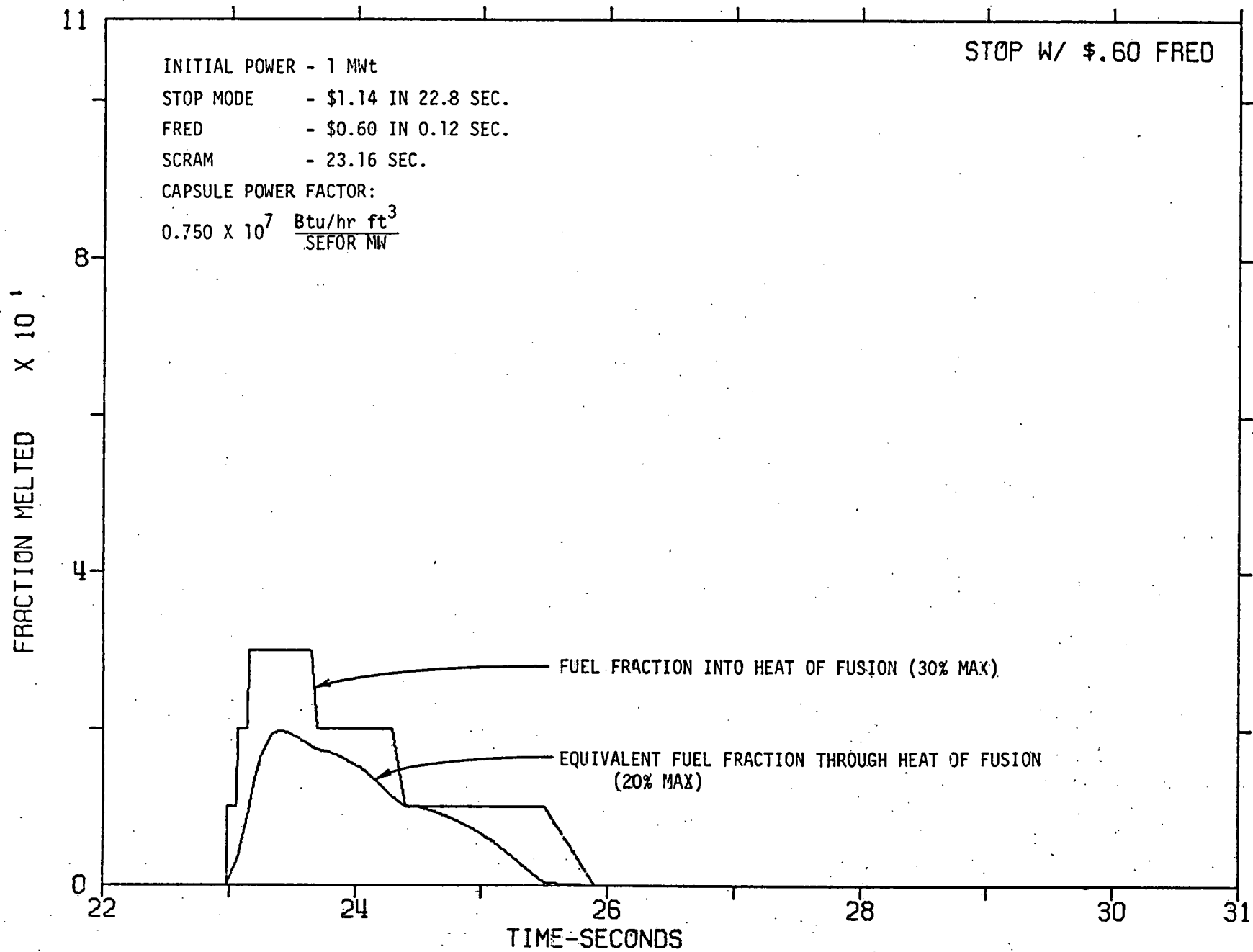


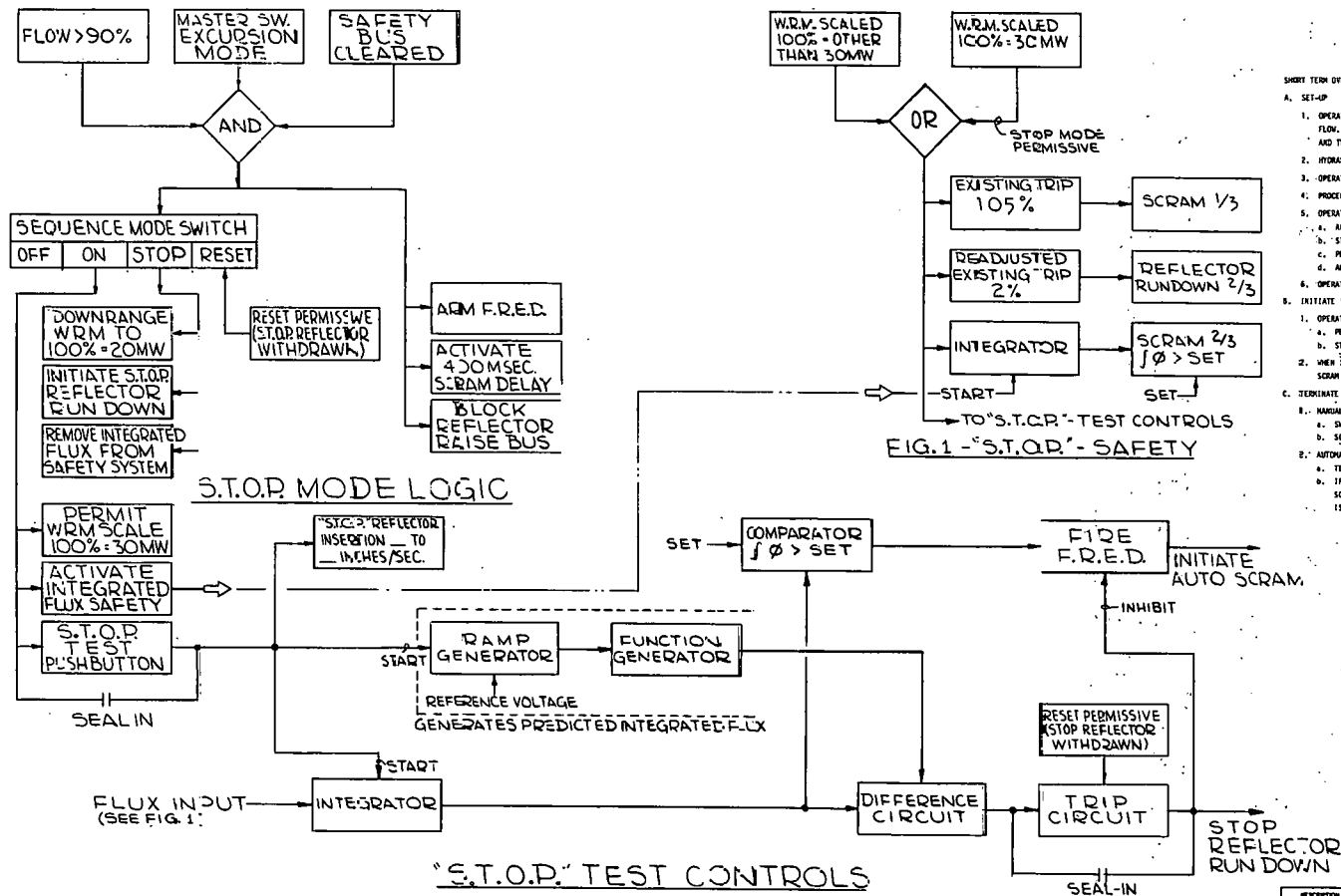
Figure 2B-24. Transient T4 Calculated Melt Fraction History

The design of the controls for the STOP mode provides for automatic test sequencing. After initial set-up, STOP operation will be initiated by turning the mode switch on and depressing the start of test pushbutton. The STOP reflector (modified coarse reflector) will be inserted at a fixed rate calculated to generate the desired power versus time profile. The integrated power during the test is used as an indirect measurement of prototypic temperature conditions in the test fuel. When the specified integrated power has been acquired, FRED will be fired automatically accompanied with a scram delayed by 360 milliseconds. Automatic operation of the test is necessary because of high accuracy requirements on the test sequence.

Figure 2B-25 is a block diagram of the STOP test controls. Important safety and test features inherent in this design are:

- An integrated flux safety circuit will be active when operating in this mode.
- The firing of FRED is inhibited if the test integrated flux profile differs from that predicted.
- If the test is terminated prior to firing of FRED, reset capability by automatically running down the STOP reflector is provided.
- Operation on the WRM scaled 100% = 30 MW is prohibited unless in the STOP mode with the integrated flux safety active.

The hydraulic system to the STOP reflector will be modified to provide the reactivity rate required by the test. The modification consists of adding an additional hydraulic power supply in parallel with the existing hydraulic feed to this reflector. The added supply will be used only during a STOP test and will affect only the one reflector. This modification will not affect the present scram capability.



- SHORT TERM OVER POWER TEST (STOP) TEST
- A. SET-UP
1. OPERATOR ESTABLISHES INITIAL OPERATING CONDITIONS AT 1 MEGAWATT AND FULL SODIUM FLOW. SEVEN COARSE REFLECTORS FULLY INSERTED, STOP REFLECTOR TO DESIRED POSITION AND TWO FINE REFLECTORS USED TO MAINTAIN OPERATING LEVEL.
  2. HYDRAULIC POWER SUPPLY FOR STOP REFLECTOR TURNED ON AND ADJUSTED, ETC.
  3. OPERATOR SETS UP FOR FRED TEST AND SWITCHES TO EXCURSION MODE.
  4. PROCEDURALLY INHIBIT 'FRED' FIRING.
  5. OPERATOR SWITCHES TO 'STOP' MODE WHICH:
    - a. ACTIVATES INTEGRATED FLUX SAFETY.
    - b. STARTS SAFETY INTEGRATORS.
    - c. PERMITS WRM SCALED 100% = 30 MW.
    - d. ACTIVATES 'STOP' TEST PUSHBUTTON.
  6. OPERATOR SELECTS WRM SCALE 100% = 30 MW.
- B. INITIATE 'STOP' TEST
1. OPERATOR DEPRESSES 'STOP' TEST PUSHBUTTON WHICH:
    - a. PERMITS AND INITIATES INSERTION OF 'STOP' REFLECTOR.
    - b. STARTS CONTROL INTEGRATORS.
  2. WHEN INTEGRATED FLUX REACHES A 'RESET LEVEL,' 'FRED' WILL FIRE AUTOMATICALLY AND SCRAM WITH A 400 MILLISECOND DELAY WILL ALSO OCCUR AUTOMATICALLY.
- C. TERMINATE 'STOP' TEST
1. - MANUALLY:
- a. SWITCHING OUT OF 'STOP' MODE WILL CAUSE 'STOP' REFLECTOR TO RUNDOWN.
  - b. SCRAM.
2. - AUTOMATICALLY:
- a. TEST MANUALLY TERMINATES WITH AUTOMATIC SCRAM ON FIRING OF 'FRED'.
  - b. IF INTEGRATED FLUX CURVE DOES NOT MATCH PREDICTED WITHIN A SPECIFIED FULL SCALE TOLERANCE, THE FIRING OF 'FRED' IS PROHIBITED AND THE STOP REFLECTOR IS RUNDOWN.

DESCRIPTION OF GROUP	STATUS
	PRELIMINARY B

Figure 2B-25. STOP Test Controls Block Diagram

REFERENCES

1. "Engineering Study of the Conversion of SEFOR to a Fast Reactor Test Facility," NEDC-13602, April 1970.
2. Thomas, G.R. and Field, J.H., "Transient Overpower Irradiation of Axially-Restrained, Zero-Burnup Fast Reactor Fuel Specimens," GEAP 13562, September 1969.
3. "Sodium-Cooled Reactors, Fast Ceramic Reactor Development Program, Thirty-Ninth Quarterly Report, May-July 1971," GEAP-10028-39, August 1971.
4. "Hanford Engineering Development Laboratory Monthly Technical Progress Report," August 1971, HEDL-TME71-8.
5. Swanson, K.M., Butler, J.K. and Eutwistle, B., "The Post Irradiation Examination of D. F. R. 166, The MkIIA 77 Pin Subassembly with Pin Failures," TRG Memo 4915, May 1969.
6. Kazachkovskii, O.D., et al, "Study of the Operation of an Assembly of Fuel Elements Containing Plutonium Dioxide Fuel in the BR-5 Reactor," Atomnaya Energiya, 24, #2, 136-143, February, 1969, ANL Trans. 609.
7. Leipunskii, A.I., et al, "Experience Gained from the Operation of the BR-5 Reactor 1964-1965," London Conference on Fast Breeder Reactors, May 17-19, 1966.
8. "Sodium-Cooled Reactors, Fast Ceramic Reactor Development Program, Thirty-Fourth Quarterly Report, February-April, 1970," GEAP-10028-34, June 1970, (pp. 18, 19 & 22).
9. "Sodium-Cooled Reactors Fast Ceramic Reactor Development Program, Thirty-Fifth Quarterly Report, May-July, 1970," GEAP-10028-35, September 1970 (pp. 25, 27, 18 & 29).
10. Murata, R.E., Craig, C.N., Pfefferlen, H.C. and Novak, P.E., "Effect of Stoichiometry on the Behavior of Mixed-Oxide Fuel During Extended Operation in Failed Pins," GEAP-13730, July 1971.
11. Hikido, T. and Field, J.H., "Molten Fuel Movement in Transient Overpower Tests of Irradiated Oxide Fuel," GEAP-13543, September 1969.

## 2.3 TASK 2C PLANT TESTS

### 2.3.1 Task 2C1 – Subcriticality Monitor

#### 2.3.1.1 Objective

The long-term objective of this task is to build on the established background and extend the development of the subcriticality monitoring system, for application to the operation of LMFBR's. Experiments will be planned and conducted to provide answers to the major remaining questions relative to this application. These questions involve the following:

- Operation of equipment in a realistic environment with a very subcritical reactor ( $-20$  to  $-35\%$ ).
- Ability to precalculate correction factors to account for changes in neutron source and absorber distributions expected in refueling an LMFBR.
- Demonstration of backup techniques such as movement of a large absorber.
- Ability to perform the subcriticality verification without interference with the refueling schedule.

#### 2.3.1.2 Discussion

These tests are a part of the overall development of a practical and reliable subcriticality monitoring system for LMFBR's, in particular FTR and the Demonstration Plant. The basic theory of possible methods has been developed by several investigators in the United States and abroad. Candidate techniques have been reviewed for application to LMFBR's, in particular the Instrumentation and Control group at ORNL was given a charter to select the most promising technique and develop the basic instrumentation required. The reference approach chosen for FTR and the GE Demonstration Plant Design corresponds to the ORNL selection of a combined neutron noise analysis and source multiplication method. SEFOR provides a uniquely suited facility for answering the remaining questions because of the following features:

- It is an operating sodium-cooled, plutonium-fueled, fast reactor.
- Operation of the reactor produces a shutdown gamma flux level reasonably close to the levels expected in LMFBR's.
- The Pu-240 in the SEFOR fuel provides a low level neutron source. The resulting neutron to gamma flux level is less than expected for LMFBR's.
- BeO rods are available to be loaded into the SEFOR core and produce a large photoneutron source. This allows a greater neutron to gamma ratio than expected for LMFBR's. This source may be distributed to simulate refueling conditions.
- B<sub>4</sub>C rods are available to be loaded into the SEFOR core to simulate an LMFBR control system and replacement of control elements.
- The remote refueling operations required in SEFOR provide a realistic evaluation of the difficulties that will be encountered in LMFBR's.
- Previous ORNL measurements at SEFOR for near critical conditions provide a firm background for subcritical tests.

Requirements for the Subcriticality Monitoring System (SMS) for the Demonstration Plant, FTR, and SEFOR were reviewed to establish the basis for tests in SEFOR. A preliminary test plan was developed and transmitted to SEFOR Operations personnel. Arrangements were made to use ORNL equipment at SEFOR and an orientation session at ORNL was scheduled to precede shipping of the equipment to SEFOR.

Final test specifications are being written and detailed arrangements for data recording and analysis are being finalized. The SMS tests are scheduled to begin as soon after January 3, 1972 as site operations allow. The final report on these tests will be issued during the third quarter 1972.

The approach for the tests in SEFOR is to: provide near core neutron instrumentation typical of that envisioned for LMFBR's (e.g., efficiency,  $\gamma/n$  sensitivity, size, active material;) use electronics, data reduction and recording equipment, and readout equipment that will adequately handle and record data although possibly not as rapidly as the expected Demo Plant SMS. It is expected that much of the data analysis will be done off-site after the measurements are performed, the final method of data analysis will be used to specify the required hardware.

The reactor will be made subcritical from  $\rho_{\infty} - \$1$  to  $\rho_{\infty} - \$20$  by movement of the reflectors, B<sub>4</sub>C rods, and fuel rods. Approximately 6 subcritical states will be used. In several of these states the reactor loading will be changed

to mockup the changes in configuration that will be experienced during refueling of a power reactor. The variations that will be included are: fuel removal and insertion, control insertion and removal, and neutron source insertion (BeO rods).

At each reactor condition measurements will be made of the reactivity by the methods being considered for the SMS and by a standard technique such as the rod drop method. Additional measurements will be made to be used in later data analysis. Examples of these auxiliary measurements are reaction rate distributions in the reactor. These data will be used to evaluate correction factors that must be used for substantially subcritical conditions.

The experimental program may be modified during execution if the on-site data analysis indicate that certain effects should be studied further.

An accurate record will be kept of all of the on-site activities. This record will be used in planning the schedule for LMFBR refueling and for evaluating the candidate methods.

After the measurements are finished, the data analysis will be completed at BRD in Sunnyvale. These results and the other available relevant data may be used to design a reference LMFBR SMS.

The results will be applicable to the FTR RMAS system design and, coupled with the high temperature neutron detector and Data Acquisition System development tasks, to the Demonstration Plant.

#### Preliminary Test Plan

The preliminary test plan is summarized below, the detailed test specification is being prepared:

- Perform a series of rod drop measurements for calibration.
- Measure gamma flux, and gamma spectrum if practical.
- Load BeO tightener rods. About 90 rods will be used.
- Measure neutron source ratio (with BeO)/(without BeO) at a few subcriticality states.
- Set up ORNL equipment, install drywell in core center location, hook up cabling.
- Perform Neutron Noise Analysis and Inverse Kinetic Rod Drop measurements at two outer core locations at near critical condition for one reflector full in and full out.
- Perform inverse kinetics rod drop (IKRD) measurement and take neutron source multiplication (NSM) and neutron noise analysis (NNA) data at near critical, intermediate, and very low subcriticality states. For example, about -0.20\$, -0.40\$, -0.60\$, -0.80\$, -1\$, -2\$, -5\$, -10\$, -15\$, -25\$.
- Map the neutron flux by moving the detectors radially along the midplane to the core boundary for an intermediate and very low subcriticality state.
- With the detectors at the core boundary, install a 7 rod cluster of BeO at a core location near the detectors. Perform IKRD, NNA, and NSM measurements for several subcriticality states while replacing the BeO with fuel. Move the BeO cluster away from the detectors and repeat the measurements.
- Perform inverse kinetics rod drop (IKRD) measurement and take neutron source multiplication (NSM) and neutron noise analysis (NNA) data at near critical, intermediate, and very low subcriticality states with detectors at the core boundary.
- Remove BeO and replace with steel tightener rods. Repeat Steps 7 and 10 above.
- Distribute BeO in core typifying LMFBR source distribution following an operating interval. The BeO will be concentrated at the core center and at an intermediate radius. Map flux distribution.
- Attain a subcriticality state of about -35\$ by replacing fuel with control.
- With the reflectors down and the detectors at the core boundary, take NNA and NSM data while replacing BeO with fuel. Approach about -12\$. Raise the reflectors to attain a critical condition.

Measurements at subcriticality states less than about -10\$ will be performed together because of time requirements involved in moving fuel and poison. However, final sequencing of the entire experiment will be a cooperative effort between SEFOR Operations and the task leader.

Subcriticality states down to about -10\$ will be accomplished with reflector adjustment.

Subcriticality states below -10\$ will be accomplished with reflector adjustment and fuel and poison exchanges. Replacing a fuel rod with a poison rod is worth about -0.68\$. Further activity on this task was deferred pending finalization of test program for SEFOR.

### 2.3.2 TASK 2C2 - SHIELDING TEST

#### 2.3.2.1 Objective

The long-term objective of this task is to further the development of calculational techniques to more accurately predict the shielding requirements for LMFBR's. The objective during Phase A is to identify experiments that could be performed at SEFOR which would provide characteristic data for comparisons with calculations.

### 2.3.2.2 Discussion

Testing recommendations were developed in cooperation with ORNL, after a SEFOR Site inspection by ORNL personnel. Recommended locations for performing flux measurements include the refueling cell above the vessel head, the refueling cell away from the vessel head, and in the radial shield at the core midplane elevation. A testing program was developed to accomplish these measurements and analyze the results. Measurements are to be made using ORNL equipment and personnel. Analysis will be performed on a cooperative basis.

This task supplements the ORNL-LMFBR shielding program - both the experimental and calculational phases. Measured results will be compared to results calculated by methods, cross sections, etc. developed in earlier phases of the ORNL-LMFBR shielding programs. Hence, this benchmark measurement will provide one means of testing current LMFBR shielding methods. This activity also provides the first measurement of a liquid-metal cooled fast oxide reactor which uses  $B_4C$  as its principal neutron shielding material. Since  $B_4C$  may represent the major neutron shielding material inside the reactor tanks and/or vessels of all future LMFBR's, this measurement may be expected to be evaluated many times as a means of testing shielding methods being used to design similar neutron shields.

Further activity on this task was deferred pending finalization of test program for SEFOR.

### 2.3.3 Task 2C3 - Doppler Tests

#### 2.3.3.1 Objective

The objective of this task is to extend the Doppler measurements made in SEFOR Program Core I and Core II tests to the higher fuel temperatures which are of primary interest in LMFBR safety studies.

#### 2.3.3.2 Discussion

The SEFOR Follow-On Program offers a unique opportunity for measuring and demonstrating the inherent Doppler feedback mechanism under transient conditions at those fuel temperatures ( $\sim 5000^\circ F$ ) which are of primary interest in LMFBR safety studies. The initial SEFOR program has provided transient Doppler measurements at peak fuel temperatures to  $3150^\circ F$ . The Follow-On Program could extend these transient measurements to  $5000^\circ F$ .

These tests were scheduled for the later portion of Option I operation, consistent with the schedule for modifying the FRED and relocation of it to an off-center core location. Specific tests proposed include the firing of the  $\$96$  FRED from initial power levels of 15 and 20 MW to demonstrate the Doppler effect at fuel temperature close to melting. Peak fuel temperatures in these tests are summarized in Table 2C(3).

The following points demonstrate the compatibility of these tests with planned modifications and existing specifications.

- The maximum energy release for the proposed transient at 15 MW is less than the limiting value in the present Technical Specifications. In addition, the maximum energy release ( $\sim 90$  MW-sec) for the proposed transient at 20 MW is less than the limiting value ( $\sim 130$  MW-sec, with guinea-pig rods under the ports) obtained by a reasonable projection of the limit curve (Figure 2.1-1) in the Technical Specifications.
- The necessary excess reactivity ( $\sim 1\%$ ) at 20 MW for the proposed transient will be provided when the present license is amended to allow extended operation at elevated sodium temperature.
- Necessary modifications to prevent FRED slug clad damage during 20 MW steady state operation will be required to meet the follow-on over-power test objectives.

Further activity on this task was deferred pending finalization of test program for SEFOR.

### 2.3.4 Task 2C4 - Oscillator Tests

#### 2.3.4.1 Objective

The objective of this task is to obtain system response information for on-line reactivity meter development.

#### 2.3.4.2 Discussion

Balanced oscillator techniques were suggested as a means of obtaining system response information required for on-line reactivity metering. Because of lack of interest by AEC-RDT, these experiments were temporarily deleted from the Option I tests pending possibility of renewed AEC interest resulting from FTR program needs.

Discussions on possible rod "oscillator" tests of the non-sinusoidal or pseudo-random type were held with ORNL (T. Kerlin and N. J. Ackerman) in support of planned FTR tests.

Contacts with FFTF workers indicated a need for both of these types of information for the FTR system.

Table 2C(3)

SUB-PROMPT TRANSIENT TESTS

Initial Power	Peak Fuel Temperature (°F) in Standard Fuel Rods		Test Program
	Initial	Final	
2	1200	1300	Core I & II
5	1850	2050	Core I & II
10	2950	3150*	Core I & II
15	3800	4100	Follow-On (proposed)
20	4600	5000	Follow-On (proposed)

\*For super-prompt transients, the final peak temperature was the same, but the initial value, corresponding to an 8 MW initial power, was 2450° F.



### 3.0 TASK 3 - ELEVATED TEMPERATURE OPERATION

Elevated temperature operation of SEFOR would be devoted primarily to plant tests of equipment and systems at a reactor outlet temperature comparable to LMFBR systems. The reactor would be operated for extended periods of time with an outlet temperature of approximately 1000°F, while selected plant tests are performed.

#### 3.1 TASK 3A TEST PROGRAM

Results of evaluations of selected tests to be performed at elevated temperatures are described in the following section by tasks.

##### 3.1.1 Task 3A1 - System Behavior

###### 3.1.1.1 Objective

The objective of this task is to provide experimental verification of the computational techniques which are used to calculate the energy transport systems (sodium cooling systems) performance for LMFBR's. It is expected that as a result of the improved computational models, it will be possible to design systems and to operate them more reliably.

###### 3.1.1.2 General Approach

Comparisons will be made between measured performance and the corresponding calculated values from the system analytical models. These system models are of three kinds; those which deal with energy being transported by the systems, those which deal with gross mechanical response of the piping system to the imposed condition, and those dealing with local strain in areas of high stress. The three types are considered separately because they require different types of instrumentation and different calculational models.

###### 3.1.1.3 Computational Models

The energy transport analysis code DYNASAR (Ref. 1) has been used as an analytical model of the SEFOR reactor cooling system. Balanced oscillator tests (Ref. 2) were performed with SEFOR Core I which showed some discrepancy between the measured and predicted results. Tests in this task will be used to quantitatively isolate the discrepancies that exist between the system transient analysis and actual plant behavior. In its present state the DYNASAR code is deficient and will require some changes to permit more exact modeling of the heat transport system dynamics. This code will then be used to predict the more severe transients which will be used to complete the re-evaluation of the reactor vessel and heat transport system for elevated temperature operation and to provide input to the associated licensing activities.

A flexibility analysis (Ref. 3) of the main sodium piping loops has been completed using MEL-21P computer code. The reasons for performing this analysis are to provide a working code model for use with this program and as a check on the original calculations. The calculated moments due to weight, cold spring and thermal expansion are combined to obtain the moments at operating conditions. These are then used to calculate stresses in the pipe. To supplement the steady state analysis, a two dimensional (radial and axial) computer code has been developed which will calculate the time dependent wall temperature changes for a given change in sodium temperature entering the pipe. The radial temperature gradients so calculated will be used to calculate the resulting circumferential stress, and the axial temperature distributions at various time increments will be used as input to the flexibility code MEL-21P to calculate the changing stress patterns at various incremental times following the start of a temperature transient. Superposing these solutions will produce a calculated time dependent deflection history.

Input to the computational model consists of a physical description of a loop, the restraints placed upon it, the temperature of the various parts of the loop and the displacement imposed at the anchor points.

Preliminary calculations show high stresses at two positions in the auxiliary primary system hot leg. These involve two vertical elbows located in the primary pipe tunnel external to the reactor vessel cavity liner. If a more detailed study of this loop verifies the high calculated stress then a finite element elastic plastic analysis will be applied to these positions using the procedures currently being used in the vessel flange analysis.

### 3.1.1.4 Preliminary Test Plans

- a) The energy transport tests consist of measuring and recording reactor power, system sodium and air flows and temperatures while the system flow and power are being changed. System variation will consist of ramp increases and decreases in flow, of sinusoidal flow oscillation about the operating point, and of several planned scrams. Preliminary computer runs will be made to permit scaling of the recorder system. A complete simulation of all reactor tests is not planned before obtaining the experimental data because some easily explained experimental finding at SEFOR could invalidate all such computer runs. The transient experiments planned to be performed at SEFOR are as follows:
- Sinusoidal oscillation of the secondary sodium flow rate at six different frequencies in the range between 0.01 and 0.208 radians per second at a specified flow rate and amplitude.
  - Ramp decrease in secondary sodium flow at a specified rate from 5000 gpm to 4000 gpm, stabilize at the lower conditions, then ramp increase back to 5000 gpm.
  - Sinusoidal oscillation of the primary sodium flow rate at six different frequencies in the range between 0.01 and 0.208 radians per second at a specified flow rate and amplitude.
  - Ramp decrease in primary sodium flow at a specified rate from 5000 gpm to 4000 gpm, stabilize at the lower condition, then ramp back to 5000 gpm.
  - Sinusoidal oscillation of the cooling air flow rate at frequencies of 0.01, 0.05 and 0.126 radians per second with a specified amplitude and flow rate.
  - Ramp decrease in cooling air flow rate from 100% to 80% at a specified rate, stabilize at the lower value, then ramp increase at the same rate to 100% of rated flow.
  - Ramp reactor power from 20 MW to 16 MW at a specified rate, stabilize at the lower value, then ramp increase at the same rate back to 19 MW level.
  - Ramp reactor power from 20 MW to 8 MW at a specified rate, stabilize, then ramp back to 20 MW.
  - Perform a normal reactor scram.
  - Perform a reactor scram without tripping the primary and secondary main sodium pumps or the air blast cooler blower drive.
- b) The test plans in this section are designed to evaluate the effect of each of the three factors which contribute to stress and deflection of a loop. These factors are; fabrication induced stress (cold springing), gravity effects (pipe and contents weight), and thermal expansion. Inertia effects and seismic loading will not be considered.
- Fabrication induced stresses were not measured when the loop was fabricated. The loops in SEFOR were cold sprung in fabrication by cutting some of the elements short and cold springing the ends together before welding. The resulting built in stresses may be partially changed by creep when the loop is at operating temperature. The drawing "cut short" dimensions have been used to calculate the initial stress in the loops. Cutting the loops to obtain actual cold spring measurements is not proposed, however, IF FOR ANY REASON EITHER OF THE MAIN LOOPS IS CUT, THE RESULTING END DEFLECTIONS SHOULD BE ACCURATELY MEASURED AND RECORDED.
  - The gravity effects of pipe, insulation and sodium weight can be evaluated by measuring pipe deflection as the loop weight is changed by either filling with sodium or dumping. It has been estimated that the contained sodium represents about 40% of the total weight of a section of pipe. To minimize the contributions of temperature to the displacement being measured, it is suggested that the test be conducted with an isothermal loop at a temperature as close to the melting point of sodium as possible. The range from 300 to 350°F appears practical. Starting with a full loop and dumping followed by a refill avoids the difficulty of achieving isothermal conditions while preheating an empty loop.
  - Thermal expansion causes deflection and stresses in a loop when the loop material expands with temperature while the support structure and anchors remain relatively fixed. There are two parts to the thermal stress problem. The first is the steady state condition in which the section of the loop being analyzed is at a uniform elevated temperature. The second condition is during a power change in which the loop temperature is changing with time. The magnitude of the transient thermal stresses are dependent on the rate of change of temperature with time, and on the fluid flow rate through the pipe. The steady state component of the thermal expansion effect will be obtained by measuring loop displacement during steady state operation. Repeated measurements will be obtained at each increment of 50°F between the reactor shutdown operating temperature of 400°F and the maximum system operating temperature. To measure the transient component of loop displacement, it will be

necessary to measure displacement changes, loop temperature and sodium temperature as a function of time while the reactor power level is being varied. The transient listed in section a) will be used to obtain these data. The instrumentation will be installed as early as possible in the program and will remain in place during the remainder of SEFOR operation for the purpose of measuring long term changes in loop deflections.

A temperature time history will be kept for each of the locations on the loops which are instrumented to measure plastic deformation. This information will be used in the calculations which will be performed to predict the amount of plastic deformation which is expected to occur.

### 3.1.1.5 Instrumentation

The energy transport tests will require recordings of the following signals from plant instrumentation:

#### *Reactor*

Reactor Flux, Channel 1  
 Reactor Flux, Channel 2  
 Reflector Rod on-off Signal

#### *Primary Sodium System*

Main IHX Primary Sodium Flow  
 Auxiliary IHX Primary Sodium Flow  
 Vessel inlet sodium temperature (from main IHX)  
 Vessel inlet sodium temperature (from auxiliary IHX)  
 Core Exit Sodium Temperature, Channel 1  
 Core Exit Sodium Temperature, Channel 2  
 Vessel Exit Sodium Temperature (to main IHX)  
 Vessel Exit Sodium Temperature (to auxiliary IHX)  
 Main IHX primary inlet sodium temperature  
 Auxiliary IHX primary inlet sodium temperature  
 Main IHX primary exit sodium temperature  
 Auxiliary IHX primary exit sodium temperature  
 Reflector Position  
 Primary sodium flow demand signal

#### *Secondary Sodium System*

Main IHX Secondary Sodium Outlet Temperature  
 Main IHX Secondary Sodium Inlet Temperature  
 Main ABC Secondary Sodium Inlet Temperature  
 Main ABC Secondary Sodium Outlet Temperature  
 Main Secondary Sodium Loop Flow  
 Secondary Sodium Flow Demand Signal

#### *Cooling Air System*

Main ABC air exit temperature  
 Main ABC air flow (Blower RPM or  $\Delta P$  Signal)  
 Air flow demand signal

- The hot leg of the secondary main coolant system has been chosen for the structural experiments because it is the highest temperature section where access is available to all parts of the loop. This is necessary because the two end points of the loop act as anchors but their relative positions change as a function of loop temperature

because of thermal expansion of the equipment to which they are connected. The motion of these anchor points is required input for the analytical model used to predict loop displacements. A second major advantage of this selection is that a majority of the instrumentation will be in an air atmosphere where the radiation field is low enough to permit frequent calibration. Displacement measurements will be made at a minimum of five locations on this segment of the secondary loop.

Linear displacement will be measured with reference to the building foundations in three mutually perpendicular directions, x, y and z, at both end anchors, one on the IHX and the other on the air blast cooler inlet; additionally the angular displacements Mx, My and Mz, about these three axes will be measured. This loop segment is guided in the neighborhood of containment vessel bellows seal to permit free axial motion while preventing transverse motion. Instrumentation will be placed at this location to verify that the design restraint conditions are in fact achieved.

Hanger MCS-296-28 in the operations building has been tentatively selected as the principal measuring location to test the effectiveness of the calculation system. This hanger is located in building area 2, and the corresponding point in the pipe flexibility analysis (Ref. 3) is number 50 of the main IHX to cooler branch. At design conditions, the linear displacements from the cold condition are expected to be  $x = 2.97$  in.,  $y = 0.16$  in. and  $z = 5.16$  in. The measurements to be taken at this station are the three linear displacements, x, y and z and the three rotational displacements Mx, My and Mz.

It is planned to record two temperatures from each loop section using the existing immersion thermocouples as follows:

Primary System	Inlet	Outlet
Hot Leg	TX 269-3 or -4	TX 271-2 or -3
Cold Leg	TX 271-1	TX 269-1 or -2
Secondary System	Inlet	Outlet
Hot Leg	TX 271-7	TX 271-9
Cold Leg	TX 271-10 or -4	TX 271-6

The output signal from the primary and secondary electromagnetic flowmeters will be recorded.

- Linear variable differential transformers have been selected as the dynamic displacement measuring devices. Permanently installed calibrating devices will be used as a means of frequent calibration.
- A reed type scanning data acquisition system (DAS) recording on magnetic tape has been tentatively selected as the data recording system. Present plans require a minimum of 53 data channels and the system to be procured should provide at least 25 additional channels for possible expansion of the measuring system. This recording system will be supplemented by the analogue recording equipment currently available at the plant.
- After additional study of possible options, some very stable system will be selected for measuring long term strain in the high stress areas. Several optical systems appear to offer adequate long term stability.

### 3.1.1.6 SEFOR Modifications

Planning in this area is just being started. The major change identified, to date, is the need for equipment to allow oscillation and ramp changes of the main air blast cooler air flow rate.

During shutdown between test phases, a series of radiographs will be obtained of critical areas such as the Auxiliary E.M. Pump ducts and other areas which have a high sodium velocity. At the end of SEFOR operation when the plant is being decommissioned, these same areas may be removed for detailed metallographic examination.

## REFERENCES

1. Engineers Manual for GE 625/635 DYNASAR V.
2. Results of the Balanced Oscillator Experiments for Core I. GE Company, Breeder Reactor Department, July 14, 1971.
3. Letter J.C.H. Lee to J.C. Whipple, 9/28/71, "Flexibility Analyses of the SEFOR Sodium Piping Systems."

### 3.1.2 Task 3A2, Vented Fuel

#### 3.1.2.1 Objectives

The long-term objective of this endeavor is to establish vent feasibility to the extent needed for adoption as viable core designs. This objective will be attained by demonstrating successful performance of a reference and alternate fuel rod vent capable of reliable operation under conditions typical of those expected in an oxide fueled LMFBR. The objective of this task during Phase A are to identify test objectives and parameters and to prepare a preliminary test plan.

#### 3.1.2.2 Discussion

Work performed during Phase A consisted of; (1) formulating a preliminary test plan for vented fuel, (2) establishing the relevance of performing such tests in SEFOR with respect to fuel pin design, and (3) determining the amount of  $B_4C$  which must be incorporated in each test rod to provide neutron shielding to meet safety requirements.

Preliminary evaluations were made concerning the vented fuel to be tested in the SEFOR reactor. The evaluations included:

The determination of the most significant vent performance characteristics requiring in-pile testing.  
Proposed conceptual vented fuel rod design which can be tested within the SEFOR fuel rod envelope.  
Prototypicality of the recommended fuel rod design.

#### 3.1.2.3 Significant Vent Performance Characteristics

Vent characteristics and consequences of vented fuel operation to be investigated include:

- Hold Time for simulated fission gases (in restricted flow vents).
- Limiting operating conditions of pressure and temperature for satisfactory vent performance.
- Gas release characteristics during steady state operation.
- Fission product release from the fuel during steady state operation and the movement of fission products within the primary system.
- Extent and consequences of sodium vapor ingress into an operating fuel pin.
- Plugging tendencies exhibited by vents due to condensable fission products.
- Relative performance characteristics of alternate vent design.
- \* Comparison of performance of vented fuel pins with sealed plenum fuel pins during transient irradiation.
- \* Measurements of tendency for liquid sodium ingress during transient overpower irradiations.

The most significant vent testing parameters are the operational pressures and temperatures at the vent outlet to be experienced by Demonstration Plant fuel. The values for these parameters appear as in Table 3A2-1.

Prototypicality is of the utmost importance in these experiments. The operational behavior of the vented element in the reactor with regard to such areas as liquid sodium ingress into the fuel region, and plugging in the presence of fuel, fission products and sodium is directly dependent on the operating temperatures and pressures. Only by operation at or near prototypical conditions can useful information be gained from the SEFOR vent tests.

#### 3.1.2.4 Conceptual Vented Fuel Rod Design

The limiting vented fuel rod design to be tested in the SEFOR core is defined by the diving bell vent concept. The restricted flow vent design can be incorporated within this envelope.

\*These items represent one program goal from the transient test program to be conducted during Option IIA under Task 4A2 - Transient Overpower Tests. Output from the vented fuel program will be utilized in the design of these transient experiments.

Table 3A2-1

**LIMITING TEMPERATURE AND PRESSURE SWINGS FOR THE DEMONSTRATION PLANT AND SEFOR REACTOR**

	Hot Conditions		Cold Conditions	
	DEMO	SEFOR	DEMO	SEFOR
Vent Temperature, °F	1200	1000	350	350
Axial Blanket Temperature, °F (Volumetric Average of Top and Bottom Blanket)	1150	1150 (assumed)	350	350
Core Temperature, °F (Volumetric Average)	2850	*	350	350
Vent Pressure, psia	19	16	30-55	36

\*Depends on test rod design -- see Table 3A2-2

**3.1.2.4.1 Geometries Analyzed**

The two rod geometries analyzed are shown in Figure 3A2-1. One was of a basic SEFOR rod size: I.D. = 0.890 inch and O.D. = 0.972 inch. The other was a 0.250-inch O.D., 0.220-inch I.D. rod that was assumed to be surrounded by an annulus of ZrH<sub>1.6</sub> 0.2-inch thick to maximize its linear power. The vent section was assumed to have the basic bell vent configuration seen in Figure 3A2-2.

These two rods span the practical range of outside diameters to be evaluated for the testing series. The resulting vent lengths and maximum bulk fuel temperatures for SEFOR operation are given in Table 3A2-2. The vent lengths are based upon a limiting transient mode (a loss of pump power resulting in a pump coastdown and subsequent reactor scram from full power to refueling conditions). It should be noted that a decrease in vent length would occur if the fuel column length were decreased; however, any decrease in fuel length from the assumed SEFOR fuel length could lead to a nonprototypical axial power and temperature distribution.

The 0.250-inch O.D. rod is limited to a volumetric operating temperature of 2410°F. This presumes that the rod envelope is placed within a SEFOR bundle (7 total SEFOR sized rods/bundle). The flow passing through the bundle can split between the 6 standard SEFOR rods and the 0.250-inch O.D. rod-ZrH<sub>1.6</sub> annulus. A large annulus is required to cool the small rod; however, the larger the annulus the smaller the thickness of ZrH<sub>1.6</sub>, which results in lower power operation. The optimized power is 10.4 kW/ft requiring 0.084 inch of ZrH<sub>1.6</sub> thickness and resulting in a volumetric operating temperature of 2410°F.

The 0.972-inch O.D. vented rod within a regular SEFOR bundle is predicted to have a 2837°F volumetric average temperature. This is based upon calculations of the present guinea-pig rod (25% Pu enriched) which is predicted to reach near-melt conditions (>5100°F) with a larger than 50% confidence.

The prototypicality of using either size of rod analyzed, or a rod of intermediate geometry is difficult to assess. The 0.250-inch O.D. rod is the same geometry as the Demonstration Plant fuel rod. The use of any "device" to vent the gas thus would result in near prototypical operation with regard to plugging, etc. for all devices to be tested. The volumetric temperature is, however, 440°F lower than that for the limiting Demonstration Plant rod. This temperature is probably the most important characteristic with regard to fission product mobility. The 0.972-inch O.D. SEFOR size rod, however, has approximately the same volumetric temperature as the Demonstration Plant rod, but does not have a prototypical geometric size. This latter factor, however, can be modified to approach prototypicality. A section of the vent may be fabricated with a 0.250-inch envelope to incorporate a flow restrictor type vent or even a porous plug type vent. The tubes of a diving bell vent can be made the same internal diameter as the reference vent selection (presently 0.020 inch) and, thus, results in a similar flow restricted path, being somewhat prototypical to plugging. The remaining section of the diving bell vent must be made with the same diameter as the present SEFOR rod. This latter factor may effect fission gas movement and thus be atypical. The large fuel diameter causes a different radial temperature gradient per inch than that of the Demonstration Plant rod (3470°F/in for the SEFOR rod at 24300°F/in for the Demonstration Plant rod). The 0.250-inch O.D. rod, however, has a radial temperature gradient (°F/in) of 19,400 which is considerably more prototypical.

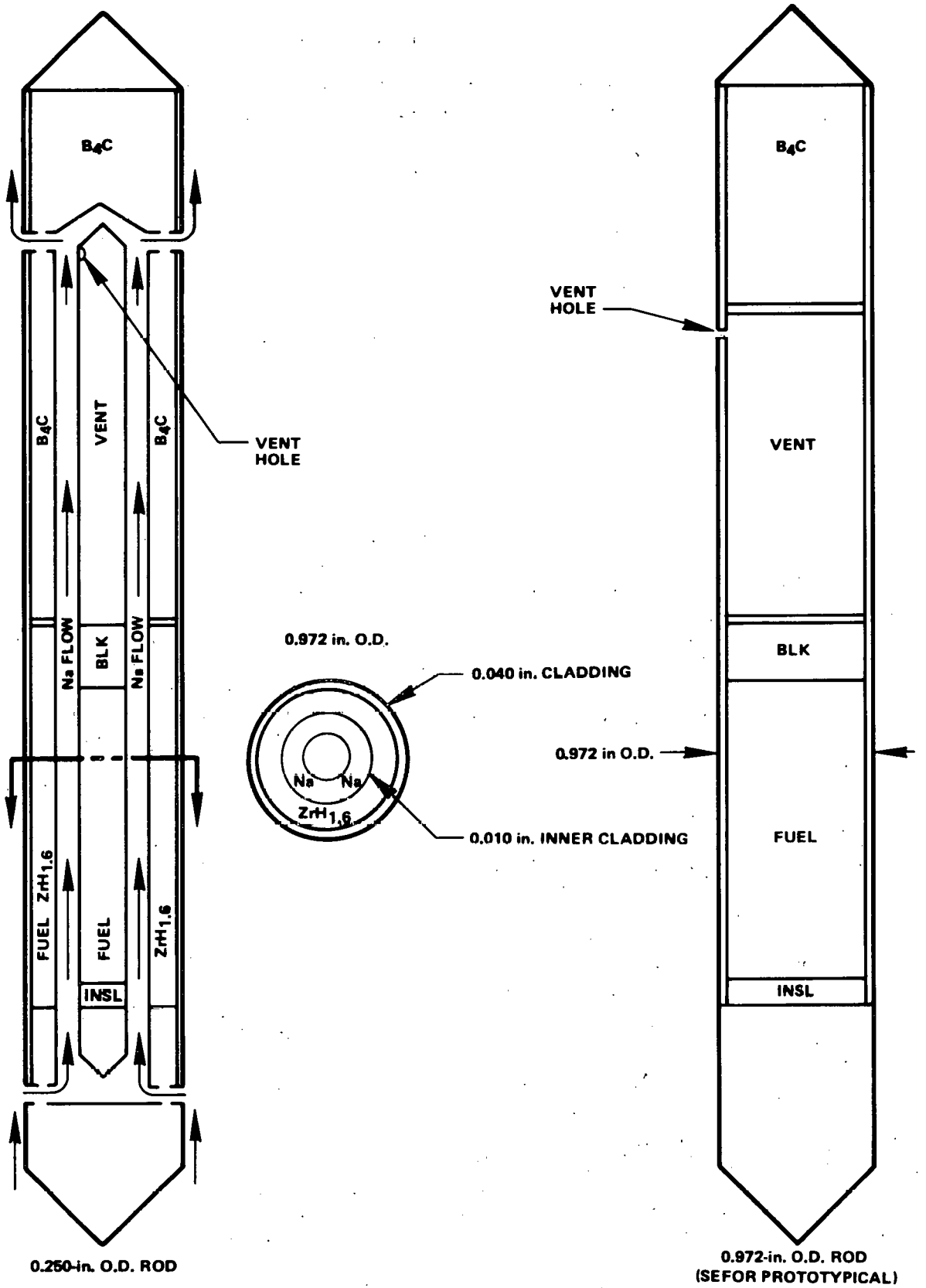


Figure 3A2-1. Rod Geometries Analyzed

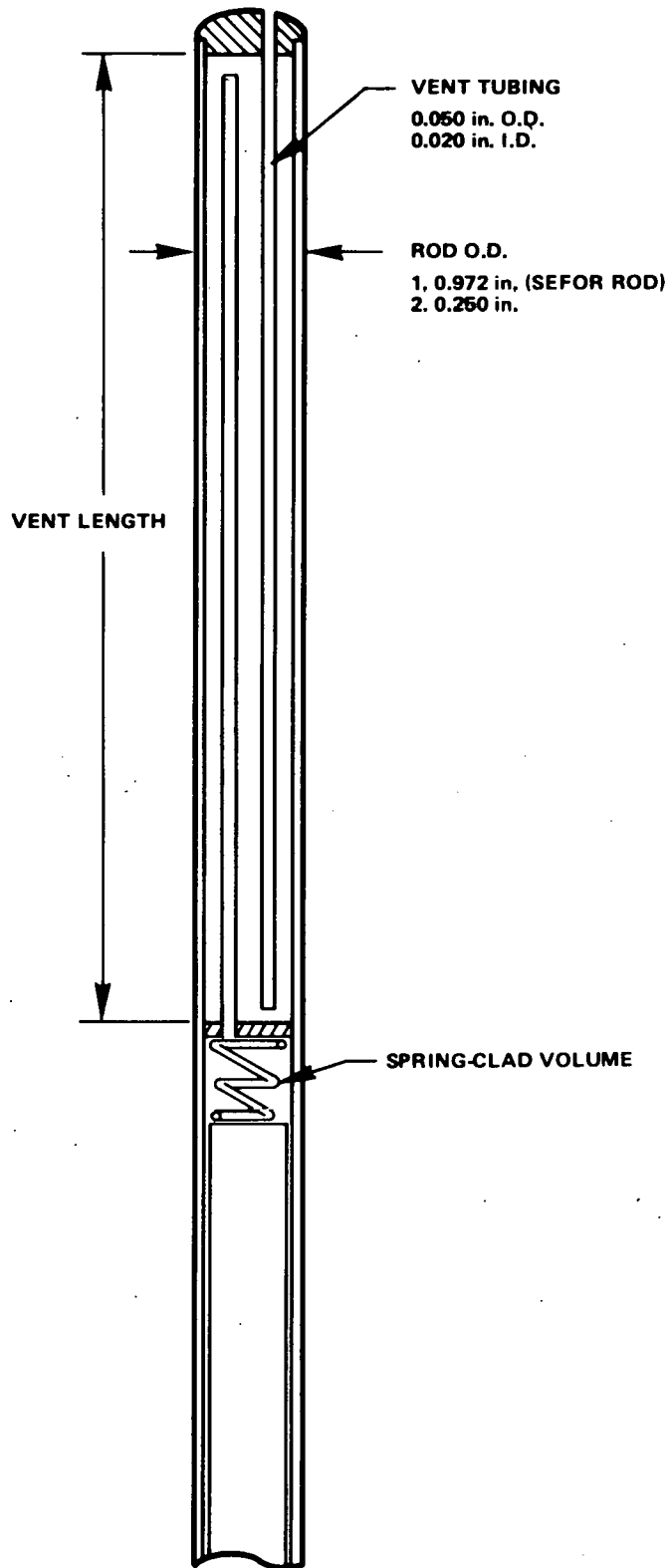


Figure 3A2-2. Diving Bell Vent Design for Fuel Rods



Table 3A2-2

**ROD VENT LENGTHS, AND MAXIMUM AVERAGE VOLUMETRIC OPERATING TEMPERATURES IN SEFOR AT 20 MWt**

Rod Type	Required Vent Length*	Volumetric Operating Temperatures**
0.250" o.d.	49.3"	2410°F
0.972" o.d.	44.4"	2837°F

\*Vent length to prevent liquid sodium ingress

\*\*Both temperatures assume a reactor inlet of 900°F and a 1000°F outlet

The 0.250-inch O.D. rod with the  $ZrH_{1.6}$  flux booster jacket is recommended as the reference vented fuel test for SEFOR, with the larger diameter rod as backup in the event of unforeseen mechanical design complications with the  $ZrH_{1.6}$ .

The adequacy of the proposed upper axial shielding design of vented fuel rods to be tested in SEFOR was evaluated using the two-dimensional computer code, SN2D. The results of these calculations indicate that the proposed shielding for the vented fuel rods provides neutron attenuation equivalent to the existing extension rod ( $B_4C$ ) shielding. However, a close evaluation of the total flux distribution for the 3 cases analyzed indicates further evaluations will be required to verify the accuracy of these results.

Since the proposed task for testing vented fuel in SEFOR was cancelled and no funds exist for further analysis of these results, the additional effort required to provide reliable and consistent analysis of the proposed shielding for the vented fuel rods has been deferred.

#### 3.1.2.4.2 Limiting Operational Case (Largest Swings in Pressure and Temperature)

Temperature and pressure swings are the main driving forces which cause sodium to enter the fuel rod vent. These swings can be expected to occur at regular intervals such as during refueling. The entire spectrum of possible swings need to be studied to identify those conditions which are most limiting to the design. Due to limiting time and available funds, a detailed evaluation of various cases could not be undertaken; however, the most pessimistic and conservative of three cases defined for the Demonstration Plant fuel (Reference 1) assumed a pump trip followed by a reactor scram together with the adverse effects of steel swelling. The relative swelling of a rod placed in the SEFOR core at its peak flux for approximately 11 months (length of total testing sequence) is insignificant ( $\sim 0.1\% \Delta V/V$ ) when compared to the peak Demonstration Plant rod (2 years  $-0.8$  L.F.,  $\sim 9.5\% \Delta V/V$ ).

The second limiting case involved only the pump trip followed by the reactor scrambling. Transient operation of SEFOR, particularly power failure resulting in pump coastdown, has occurred a number of times during the reactor's past operation. Thus, the most conservative operation that can be tested in the SEFOR reactor involves a pump trip followed by a reactor scram. The sequence of events that define this limiting situation for the diving vent length is as follows:

The fuel is assumed to be operating at normal conditions when a pump outage occurs. This reduces the vent pressure and allows some of the gas to rapidly escape. Depending on how fast the reactor can be scrammed following this loss of flow incident, the temperatures which the gas in the rods see may rise above normal operational levels. In this case, even more gas will escape from the vent.

Following the pump trip the reactor is scrammed. This rapid shutdown causes the fuel to crack and to release a substantial quantity of the fission gases which had been trapped in the fuel matrix. These escaping gases, still at high temperatures, will force much of the gas which was initially in the vent out of the rod. The gas which remains in the vent will contain substantial quantities of isotopes which may either condense out or decay to non-gaseous forms. Subsequent to this burst release, the reactor temperatures are brought down to at least the normal inlet temperature of the reactor. The volatile constituents will condense out at these lower temperatures.

3.1.2.4.3 Basic Equation and Input

The basic equation that was used to evaluate the limiting bell vent length is:

$$L_v = \frac{T_{v,h}}{A_v} \left[ \frac{V_r P_c}{T_c P_h (1-C_1-C_2)} - \frac{V_b}{T_{b,h}} - \frac{V_c}{T_{c,h}} \right] \quad (\text{Ref. 1})$$

where

- $T_{v,h}$  = Temperature of vent gases, hot conditions
- $V_r$  = The non-vent volume available to the spaces in the cold condition
- $P_c$  = The pressure in the cold condition
- $V_b$  = Gas volume in axial blanket portions of the rod
- $V_c$  = Gas volume in core portions of the rod
- $A_v$  = The vent area available for gas expansion
- $T_c$  = Cold condition temperature (all regions at the same temperature)
- $P_h$  = Pressure at the vent outlet under hot conditions
- $C_1$  = Fraction of rod gases which will condense out when the temperature is lowered.
- $C_2$  = Fraction of rod gases which are active and which will decay to non-gaseous daughter products during a zero power period.
- $T_{b,h}$  = Temperature (average) of axial blanket portion of rod, hot conditions
- $T_{c,h}$  = Temperature (average) of core portions of rod, hot conditions.

- *Pressure and Temperature Swing*

As mentioned previously, the main forces driving sodium into the vent are the temperature and pressure swings. For the postulated, limiting case (Section b) in SEFOR, the following temperatures and pressures will occur:

- $T_{v,h}$  = 1000°F
- $P_c$  = 36 psia (20 psig at full power + 1.3 psig (Na head) + 14.7 psi (ATM))
- $T_c$  = 350°F (Minimum refueling temperature)
- $P_h$  = 16 psia (0 psig (loss of pump pressure) + 1.3 psig (Na head) + 14.7 psi (ATM))

- *Fraction of Condensable Gases ( $C_1$ ) (Taken from Reference 1)*

Under the assumed case, a considerable quantity of fission gas is released from the fuel matrix in a short time period. The condensable species will not have time to diffuse out. In this case, a much greater fraction of the total gases present will be of a volatile nature.

The conservative assumption can be made that the gases released from the fuel in a burst will push out most of the gases which were in the vent prior to the burst. The gases which remain in the vent following the burst release will have a composition similar to that of the gases rapidly released from the fuel during transient. Thus, it can be assumed that this composition will be defined by the fission yields of each of these gaseous and volatile species.

Table 3A2-3 quotes the fission yields of the potentially gaseous fission products. At temperatures of 1000°F or higher, each of these products have substantial vapor pressures. Thus, it can be assumed that each of the species will be in a gaseous or vapor form under the temperature and pressure conditions which are likely to exist within a fuel rod. If this is the case, then the yields quoted in Table 3A2-4 also indicate the relative composition of the fission gases leaving the fuel and entering the vent.

Table 3A2-3  
(Reference 1)

GASEOUS FISSION PRODUCT YIELDS

Element or Isotope	Yield, %	Atoms Produced Per 100 Fissions
Selenium	0.106	*
Bromine	0.178	*
Rubidium	1.47	*
Cadmium	0.514	*
Iodine	2.16	*
Xenon (stable)	24.57	
Krypton (stable + Kr <sup>85</sup> )	1.83	
Xenon <sup>133</sup>	6.60	*
Xenon <sup>135</sup>	6.80	*
Cesium	6.56	*
Total	50.788	

\*Potentially condensable species. Xe<sup>133</sup> and Xe<sup>135</sup> eventually decay to Cs, which can condense.

Table 3A2-4  
(Reference 1)

FRACTION OF POROSITY AVAILABLE TO GASES

	Fuel		Blanket	
	Hot	Cold	Hot	Cold
Pessimistic Estimate	0.0	1.0	0.0	1.0
Conservative (Reference 1)	0.25	0.75	0.25	0.75
Optimistic Estimate	0.2	0.5	0.2	0.5

Xenon-133 and Xe-135 eventually decay to cesium. They can be considered as essentially condensable gases at 350° F. If this is assumed to be the case, then approximately 49% of the gaseous species generated during the fission process may condense out if the temperatures drop significantly below 1000° F.

When the fission gases which were retained in the fuel are rapidly released into the vent, it can reasonably be assumed that most of the vent gases which were previously present will be swept out of the rod. The gases remaining in the vent will be low in Na vapor following the transient. For the purposes of the present calculations, it was assumed that the sodium vapor concentration in the vent gases was negligible. Thus, the only volatile species accounted for in the analysis were those which originated as fission products. These are listed in Table 3A2-3. The net fraction of the gases which can potentially condense out at low temperatures becomes:

$$C_1 = \frac{24.39}{50.79} = 0.48.$$

The above analysis was performed in the Demonstration Plant fuel (Reference 1). Assuming that the fission product yields for the SEFOR reactor were approximately the same as those for the Demonstration Plant, an evaluation was made to determine  $C_1$  for the operating conditions in SEFOR. The total moles of condensable gases produced was divided by the total gas moles produced (during a maximum reactor operation of 11 months – 0.8 load factor). The resulting fraction,  $C_1$  was found to be approximately 0.48.

- *Active Gas Fraction Which May Decay to Non-Gaseous Daughter Products ( $C_2$ )*

The design limiting conditions basically assume that all fission gases which can decay to non-gaseous daughter products do so during the outage interval. These active gases are thus treated directly as being condensable gases.

The remaining input parameters  $A_v$ ,  $V_r$ ,  $T_{b,h}$ ,  $T_{c,h}$ ,  $V_b$  and  $V_c$  depend on the analyzed fuel rod diameters and operating power.

#### 3.1.2.4.4 Fuel Rod Designs

- *Rod Diameters*

As mentioned in Section (a), two rod diameters were evaluated in this study; (1) a 0.250-inch O.D. with 0.015-inch walls surrounded by a 0.2-inch thick ZrH<sub>1.6</sub> annulus prototype Demonstration Plant rod; and (2) a 0.972-inch O.D. rod with 0.041-inch walls (present SEFOR rod envelope).

- *Core and Blanket Lengths*

Since the vent length is directly proportional to the non-vent volume and a short vent would be beneficial (shielding requirements), the core and blanket lengths for both rod diameters were minimized. The axial geometry for both rods was made the same. Since the relative importance of the lower blanket was thought small when compared to the upper blanket and core (i.e., in such cases as Na-fuel reaction), no lower blanket was designed in the rods. The present SEFOR reflector section was used in its place.

The core length was selected as 35 13/16-inch since (1) a resulting prototypical axial power distribution (present SEFOR core length), and (2) a shorter length (such as 30 inches prototypical) would result in non-prototypical hot upper blanket operation due to adjacent SEFOR rods.

The length of the upper axial blanket was based upon the criteria of limiting rod height and yet incorporating enough blanket so that such factors as sodium vapor diffusion and interaction with the blanket would be prototypical. A preliminary height of 4 inches was selected (approximately equal to the upper reflector length on the SEFOR rod).

- *Core and Blanket Densities*

The smeared densities for the test rods were selected based upon the references for the Demonstration Plant rods. The fuel smeared density is 85% while the blanket smeared density is 89.7%.

**3.1.2.4.5 Vent Length Calculations**

With the fuel rod designs selected the input parameters  $T_{b,h}$ ,  $T_{c,h}$ ,  $V_r$ ,  $V_b$ ,  $V_c$  and  $A_v$  can be evaluated.

The hot blanket and core volumetric temperatures depend upon the rod diameter as well as its enrichment and location within the core. For prototypicality, the temperature should be approximately the temperatures to be experienced in the Demonstration Plant for the peak rod. The axial blanket has a volumetric temperature of 1150°F while that for the core is 2850°F (Table 3A2-1).

Combinations of enrichment together with core position will be made so as to approach as near as possible these volumetric temperatures for the selected design.

The non-vent volumes can be determined only after the selection of open porosity for gas expansion is made. Considerable uncertainty exists in this parameter and thus a range of values must be studied. Table 3A2-4 lists the current assumption on fuel and blanket porosity.

Assuming the porosity values in Table 3A2-4, the non-vent volumes determined for each rod design are as in Table 3A2-5. The calculated values of  $V_b$  and  $V_c$  are given in Table 3A2-6.

Table 3A2-5

**NON-VENT COLD VOLUMES FOR GAS EXPANSION**

Rod Outside Diameter	$V_c$ (in <sup>3</sup> )		
	Pessimistic	Conservative	Optimistic
0.972	4.03	3.14	2.24
0.250	0.246	0.191	0.135

Table 3A2-6

**HOT BLANKET ( $V_h$ ) AND CORE ( $V_c$ ) VOLUMES FOR GAS EXPANSION**

(Volumes -- in<sup>3</sup>)

**Blanket Volumes ( $V_{b,h}$ )**

Rod Outside Diameter	Pessimistic	Conservative (Reference 1)	Optimistic
0.972	0	0.064	0.0512
0.250	0	0.0039	0.0031

**Core Volumes ( $V_{c,h}$ )**

Rod Outside Diameter	Pessimistic	Conservative (Reference 1)	Optimistic
0.972	0	0.835	0.667
0.250	0	0.051	0.0408

Substituting the values listed in Tables 3A2-1, 3A2-3, and 3A2-4 into the basic equation, the relationship between the diving bell vent length and the maximum pressure during shutdown can be obtained. The resulting curves generated from these equations are seen in Figure 3A2-3.

#### 3.1.2.4.6 Cooling of Fuel Rod Designs

- *0.250-Inch O.D. Rod*

An evaluation was made to determine the amount of flow that would occur through a SEFOR rod envelope which contained a 0.250-inch diameter rod surrounded by a  $ZrH_{1.6}$  annulus. The rod was assumed to operate at the prototypical Demonstration Plant nominal peak average power of 13.85 kW/ft so as to result in the same temperature (2850°F). The required  $ZrH_{1.6}$  thickness to obtain the desired power was 0.175-inch (assuming a Pu enrichment limit of 40% due to sinterability). This resulted in a fuel rod- $ZrH_{1.6}$  radial gap of 0.175 inch. Utilizing this gap, a ratio of flow through the gap versus total flow through a peak bundle was determined. The results showed that the flow through the annulus was 0.284 lb/sec. The required flow (assuming a 100°F entrance to exit sodium temperature rise) is 1.305 lb/sec. Operating the rod within a SEFOR bundle would thus result in an  $\sim 460^\circ\text{F}$  temperature rise or 1360°F exit sodium temperature, which, of course, cannot be tolerated. If the power of the fuel rod were reduced so as to result in a 100°F sodium temperature rise, the resulting power would be 3.01 kW/ft. This would have a volumetric temperature considerably below prototypical.

Because of the aforementioned conditions, a conceptual optimization study was undertaken to determine the maximum power that could be utilized and still meet cooling requirements. This was done by first determining the power allowable (limited by  $\Delta T = 100^\circ\text{F}$ ) as a function of the flow split to the rod annulus. Then a determination was made of the actual power for a given flow split (larger flow split has less  $ZrH_{1.6}$  and thus lower power for a limit in Pu enrichment). The resulting two curves were then plotted (Figure 3A2-4). The optimum power determined was 10.4 kW/ft with a 0.13 flow split and a 0.084-inch  $ZrH_{1.6}$  thickness. The resulting volumetric temperature is 2410°F. Placement of this rod within a SEFOR bundle requires that bundle flow be increased 15%. Additional work is required to establish the actual geometry, power and practicability of this scheme.

- *0.972-inch O.D. Rod (Reference SEFOR Rod)*

The full sized SEFOR rod does not require consideration of flow splitting since the flow path for this rod is similar to adjacent SEFOR rods (assuming all rods are guinea-pig rods).

## REFERENCE

1. Meinhardt, W. G., "Vented Fuel Rod Design Study Demonstration Plant," BC0004, February 15, 1970.

#### 3.1.2.5 Preliminary Test Plan

The scope of tests to be conducted will include out-of-pile vent development and testing followed by in-pile integral performance tests.

Out-of-pile tests will be conducted to evaluate vent characteristics and to aid in the selection of one reference vent and one alternate vent design for in-pile testing.

Vent candidates to be tested will be consistent with current design thinking at that time. Specimens to be tested will be prototypical to those used for irradiation testing.  $UO_2$  will be used to simulate mixed oxide fuel. Each specimen will have a gas pressure line attached to the bottom end plug through which a tag gas may be injected.

Vents will be tested in a sodium environment so as to determine environmental performance limits (i.e. pressure and temperature), fission gas holdup time, (for flow restricted vents) and to evaluate vent potential for sodium ingress (either liquid sodium or sodium vapor).

Testing will be conducted in a sodium facility having a variable pressure and temperature capabilities. Fission gas hold time will be determined for restricted flow type vents by injecting a radioactive tag gas into the test specimens through the bottom end plugs. Hold time will be determined by measuring the gas pressure at which the tag gas is released by the vent. The time of release will be measured utilizing gamma ray spectroscopy. Limiting conditions for vent operation as determined by liquid sodium ingress will be defined by determining the sodium pressure-temperature swing necessary to cause sodium ingress. Permissible vent operating temperatures will be determined on a go-no-go basis between 400 and 1300°F.

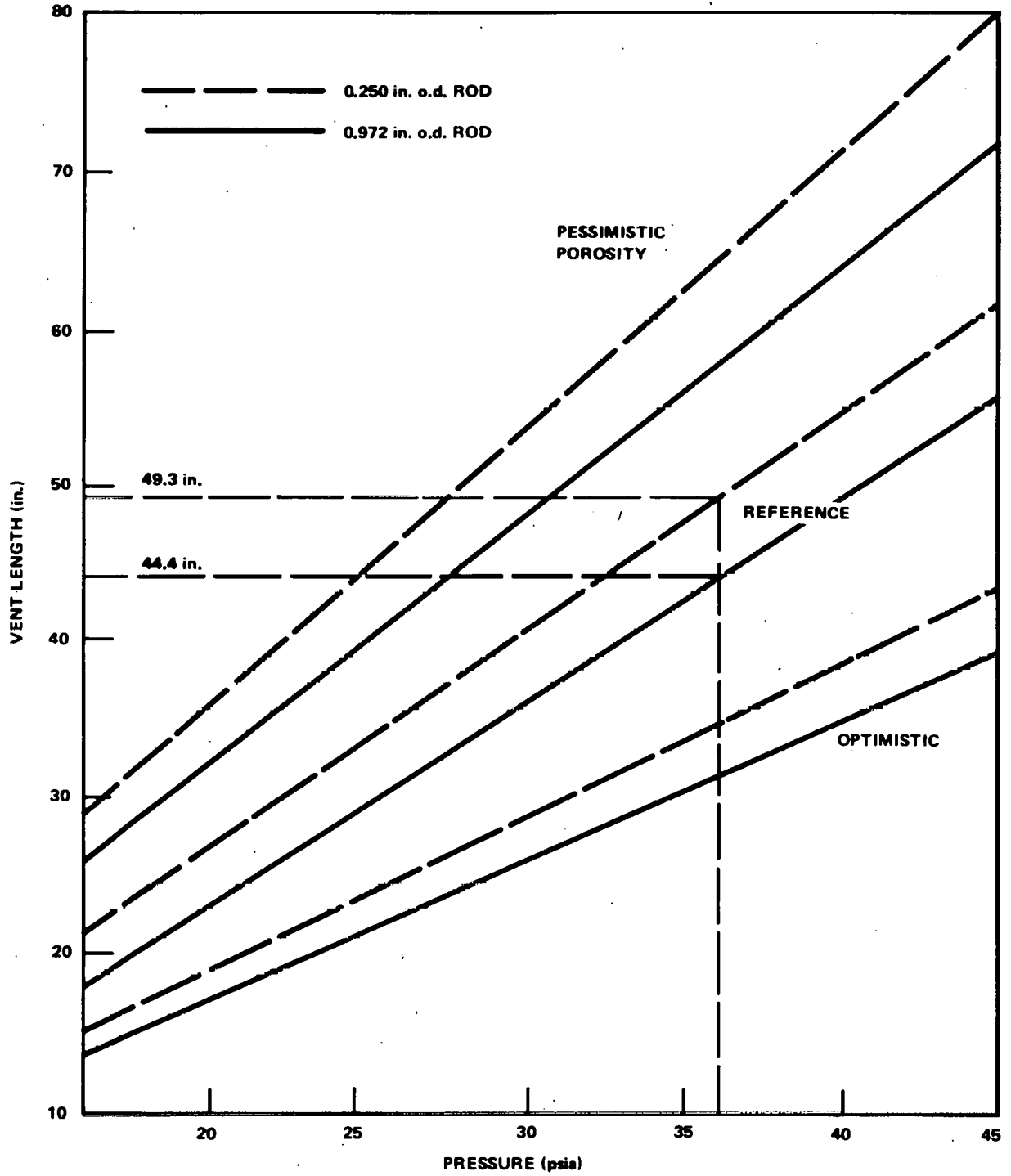


Figure 3A2-3. Diving Bell Vent Rod Design, Required Vent Length versus Coolant Pressure at Vent Outlet

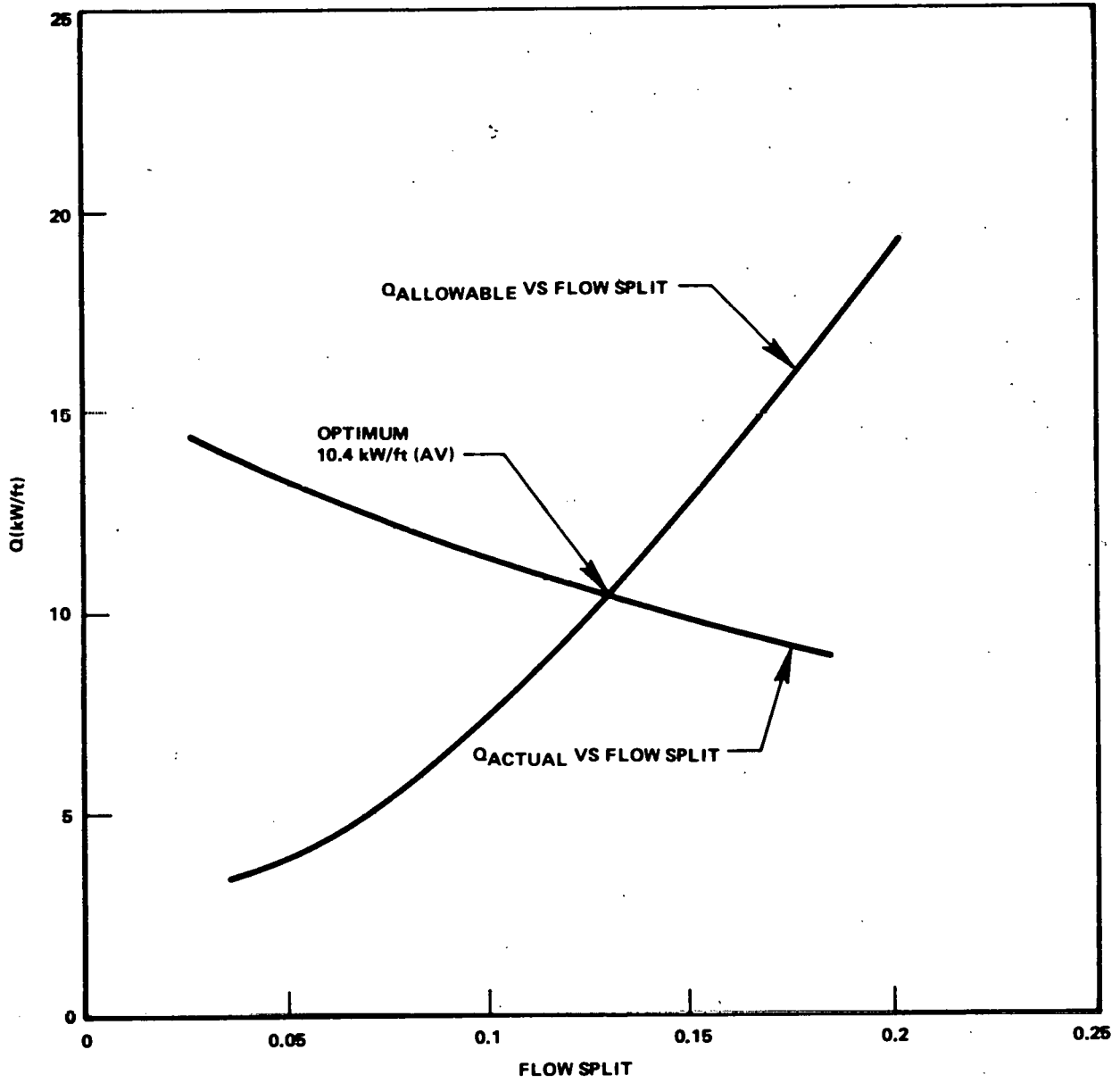


Figure 3A2-4. Allowable and Actual Power versus Flow Split



The purpose of these tests will be to screen vent candidates and compare various restricted flow vents with the low pressure diving bell vent. Tests will be of short duration, up to ~1 week. Approximately 15 tests will be conducted.

In-pile experiments will be conducted in two phases. The first phase will demonstrate vent performance under steady state operating conditions. The second phase will investigate vented fuel pin performance under transient overpower conditions. Transient tests will be conducted during Option IIIA Transient Overpower Tests. Details of this phase of the testing program are described in that task.

Steady state irradiation tests will be single pin tests, with up to six (6) vented fuel pins being simultaneously tested in various reactor positions. A total of eight (8) vented fuel pins will be irradiated to investigate the performance of one reference vent design and one alternate. For comparison purposes vent tests will be run in pairs. Each pair will be irradiated with a sealed plenum fuel pin of identical fuel geometry and will serve as a standard for evaluation of fuel pin performance. Fuel pins will be irradiated for periods of 2, 5, 8, and 11 months.

In-pile tests under steady state operating conditions will be integral performance tests conducted to establish vent reliability and investigate system behavior. Test specimens will be vented directly to the primary sodium coolant system. Vent action will be monitored at all times by sampling the reactor cover gas to determine the fraction of volatile fission products being released. Samples of sodium coolant will be routinely taken and analyzed for condensible fission products to investigate the movement of fission products within the primary system. Fuel pins will undergo destructive examination after irradiation with special emphasis on the extent and consequences of sodium ingress and vent plugging tendencies.

Six (6) additional sealed plenum fuel pins containing limited amounts of liquid sodium will be irradiated to determine the consequences of liquid sodium ingress and to establish permissible limits of sodium ingress. Fuel pins will be irradiated for 3 and 11 month periods. At the end of each period three fuel pins, each containing a different quantity of sodium, will be removed and destructively examined.

- Prior to destructive examination each fuel pin will undergo the following non-destructive examination:

- Fuel pin weight measurement
- Balance point determination
- Profilometry
- Gamma scanning
- Neutron radiography
- X-radiography
- Determination of amount of open fuel porosity at temperatures between 350 and 720° F.

- Destructive examination will consist of the following:

- Fuel Pin Metallography
- Burnup analysis
- Flow versus  $\Delta P$  through the vent at temperatures up to 1200° F
- Vent metallography
- Electron microprobe of fuel/sodium/clad reactions.

During all aspects of the examination particular attention will be given to vent performance and implications of vented pin operation on overall performance of the test specimens. Vented pins will be examined in conjunction with a sealed plenum pin so as to allow direct comparison of behavior and determine consequences and extent of sodium vapor ingress.

#### 3.1.2.5.1 Expected Results

Results from these tests will establish vent feasibility to the extent needed for adoption as viable core designs. Tests will serve as a basis for further testing of vented fuel in either EBR-II, FFTF or Demonstration Plant bundle experiments. (Bundles containing large numbers of fuel rods featuring vents.)

#### 3.1.2.5.2 Reactor Modifications Needed to Accommodate this Experiment

No reactor modifications are required for this experiment. However, hot cell space will be required to accommodate weighing scales and equipment for determining the balance point of fuel pins.

#### 3.1.2.5.3 Equipment Required to Perform Test Program

- Sodium pot or loop with sodium environment and variable pressure capabilities
- Location – San Jose or Vallecitos.

Gamma ray spectroscopy unit for counting tag gas.

Location — adjacent to autoclave.

Gas chromatography unit.

Location — San Jose or Vallecitos

Weighing scales accurate to  $\pm 0.1$  gms.

Location: SEFOR refueling cell and Vallecitos or San Jose.

Balance point scales.

Location: SEFOR refueling cell and Vallecitos.

Pressure regulation unit with gas flow meter.

Location: Adjacent to autoclave.

Pressure transducers.

Location: Adjacent to autoclave.

Strip chart millivolt recorders.

Location: Adjacent to autoclave.

Fuel cask for transferring irradiated fuel elements to a post-irradiation examination facility. Common with other irradiated fuel transport which must accommodate failed fuel elements.\*

#### 3.1.2.5.4 Prior Development Work

##### Development of Vent

Four vented fuel experiments were done at GETR in the period of 1965-1967. These tests were successful but accurate measurement of hold times for fission products was not possible in the design used. Also, post-irradiation examination was not conclusive enough to establish a reliable vent design. The specific design used was the diving bell type. It is necessary to consider this design type again, as well as several modifications which have been suggested to improve its operating characteristics and reliability.

Vent design candidates which may be tested are:

- Diving bell
- Modified diving bell with a porous plug
- Selective series of porous plugs
- Restricted flow vent

#### 3.1.2.5.5 Vented Fuel SEFOR Follow-On Justification

The testing of vents in the reactor environment is necessary in order to establish functional reliability of vent design. The vent properties which need to be investigated have been listed under the objectives. These properties can be best demonstrated in a system such as SEFOR because of the following advantages:

Sodium temperature (coolant) will be 1000°F which is the reference outlet temperature for the demonstration reactor. Because of power cycling which includes shutdowns and startups it will be possible to test the functioning of the vent under pressure gradients.

Access to the reactor cover gas will permit continuous monitoring of the fission gases vented to the coolant. Single fuel tests will permit evaluation of a given vent design plus one back-up concept. The information from this experiment is essential to the strategy for developing vented fuel. The results obtained will form the basis and justification for including vented fuel concepts in operating reactor cores such as EBR-II, FFTF and the demonstration reactor.

Aside from the operating data regarding reproducibility and reliability of these vents, the SEFOR follow-on experiments will also provide a licensing basis for permitting testing of vented fuel in the demonstration plant.

Alternates for testing fuel vents in reactors have been considered; but this suffers from serious technical, schedule or economic drawbacks. These are briefly stated as follows:

Thermal test reactor loops in the campaign for testing vented fuel will be severely complicated by auxiliary systems that do not contribute to the desired objectives of the experiment. System complications analogous to those encountered with the FCC will be common. The expense for designing, developing and fabricating such systems are greater than \$2 million.

\*Existing SEFOR cask can be modified to transport irradiated vented fuel elements, Drawing #277R293.

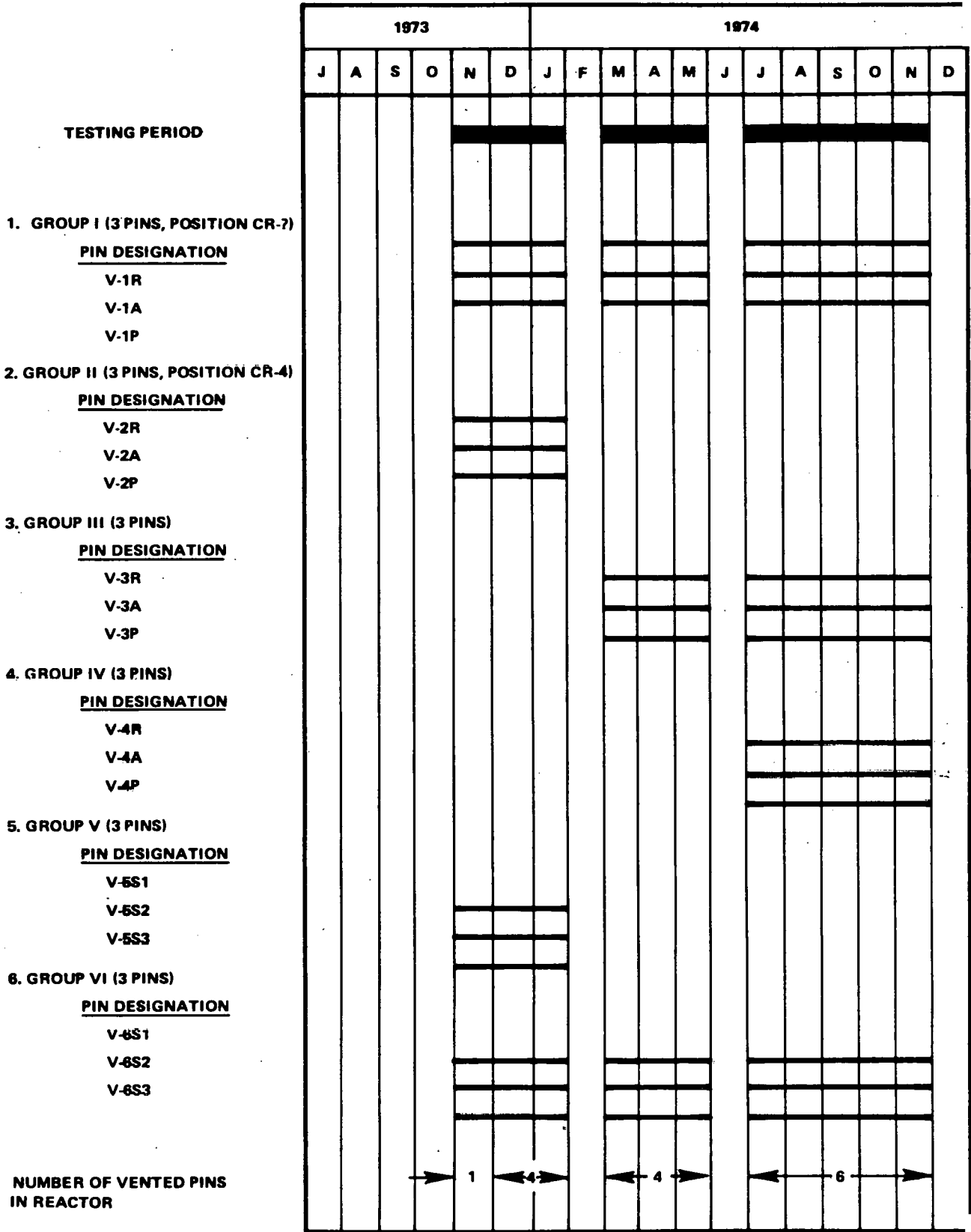


Figure 3A2-5. SEFOR Follow-On Vented Fuel Irradiation Schedule

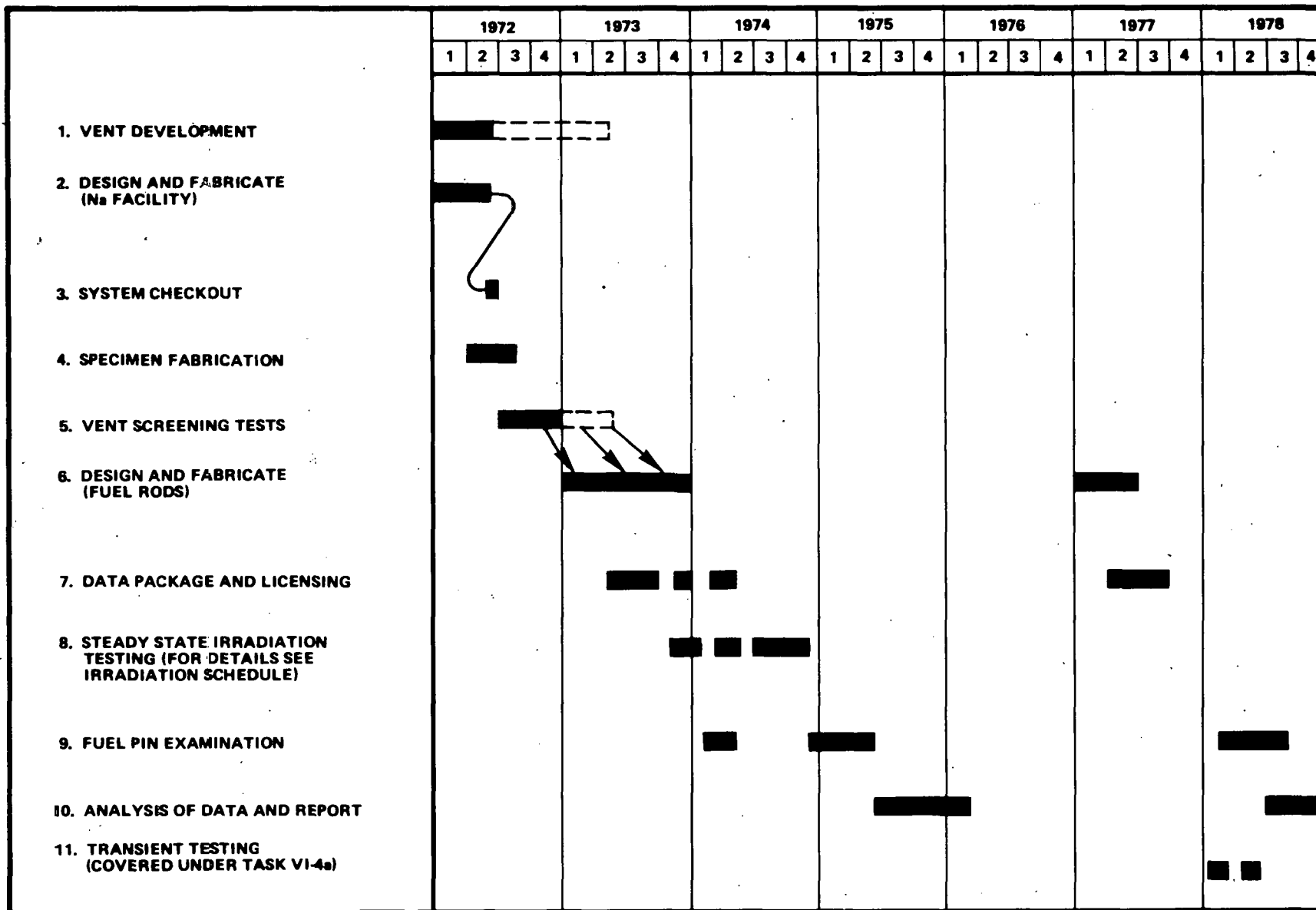


Figure 3A2-6. SEFOR Follow-On Vented Fuel Test Schedule

Reactor space in EBR-II is estimated to be available during the latter part of 1973 provided that the test does not interfere with priority number one — fuel testing of the FFTF driver core or demonstration initial core plenum designs. Instrumented fuel assemblies in EBR-II are cumbersome and materials tests and other instrumentation testing programs have high priority in EBR-II for the next two years.

Closed test loops in FFTF will provide the first opportunity for vent testing and may be available in 1975 or 1976. Thus, the SEFOR tests will have a two to three year advantage over the other available options at this time.

### 3.1.3 Task 3A3 – Coolant Chemistry and Impurity Monitoring Equipment

#### 3.1.3.1 Objective

The objective of this task is to investigate the feasibility of using modern analytical instrumentation for continuous measurement of impurity concentrations and radioactive buildup in an operating LMFBR at 1000°F.<sup>1</sup>

#### 3.1.3.2 Introduction

It was envisioned that sampling stations could be installed in critical locations in SEFOR to monitor transport and buildup of radioactivity, and that continuous surveillance for hydrogen, carbon and oxygen could be accomplished by means of on-line instrumentation developed in the National Meter Program.

As the result of this study it was concluded that such tests were feasible and that they would provide:

- the first opportunity to test the validity and define the limits of the by-pass concept to monitor impurities in reactor sodium at 1000°F,
- the first data on carbon, oxygen and hydrogen activity in reactor at 1000°F,
- the first U.S. data on rates of deposition of radioactive corrosion and fission products in reactor at 1000°F,
- the first opportunity to evaluate the performance (contamination during refueling, cleanup after refueling, and system response to cold trap temperature) of a reactor cold trap with modern instrumentation.

The main technical areas investigated during this work were the selection of a suitable location for test equipment at SEFOR, the conceptual design of a test cell and test loop, a review and preliminary selection of analytical instrumentation, and a preliminary definition of specific tests to be performed. The results of these studies are discussed in the following section.

#### 3.1.3.3 Results and Discussion

The technical tasks completed during this program were:

- Selection of a suitable location for test equipment in SEFOR.
- Conceptual design of the test cell and the test loop. Review and preliminary selection of the impurity monitoring instruments to be installed in SEFOR.
- Preliminary definition of the specific tests to be performed in SEFOR during high temperature operation.
- Definition of the relationship of the proposed follow-on (Phase B) tests with other RDT sodium technology programs at EBR-II, FFTF and the Demonstration Plant.

##### 3.1.3.3.1 Test Cell Location

Several locations for the test cell were examined. These were:

1. East Side of Refueling Cell (Area 14 of Figure 3A3-1)

This region is used infrequently, but it is complicated by the nearness of the equipment transfer lock and the refueling cell crane bay overhang which prevents use of a removable top shield plug for the cell. However, the east wall of the refueling cell could serve as the west wall and the crane bay overhang as a portion of the roof of the cell. Additional shielding would be required for the south, east and north walls. The south wall could be provided with a window and two through-wall manipulators. The north wall could be a removable plug into the spent fuel cask cart area, similar to the removable shield plug for the refueling cell man access panel. Based on dimensions taken at this location and estimating ~24-inch thick shield walls, there would be available space within the shielded area approximately 5 ft. wide x 6 ft. deep x 15 ft. high (referenced from the pit floor). By suitable choice of shielding material (e.g., lead or uranium) it may

<sup>1</sup>SEFOR Follow-ON Program — Phase A — Preliminary Design and Engineering — Proposal to USAEC, May 24, 1971

be possible to increase the area of the cell. The operating deck would be just to the right of the personnel air lock with is ~8 feet above the pit floor. An existing concrete block (3'-9" wide x 7'0" deep by 3'8" high) in this area would require removal.

Penetrations through the pit floor would be necessary to gain access to the 10-inch primary sodium line from the reactor outlet to the main IHX. The inner containment penetrations for the cell would need to be sealed to allow air purging during maintenance of monitoring equipment without the necessity of purging the entire primary N<sub>2</sub> zone. The impurity monitors would have to be located along the walls with the sensors, isolation valves, couplings or flanges located at the elevation convenient for the operator to view and manipulate remotely. (This would be at a level approximately 13 ft. from the pit floor, assuming the window centerline to be at this level. This corresponds to 5 ft. from the operating deck floor on the south side.) The removable north wall could be arranged to admit the loop essentially in large section and could contain a submarine hatch similar to that of the refueling cell man entry panel for entry to effect occasional equipment repairs or modifications. It is likely that the pump, cold trap and plugging indicator could be located in the lower regions of the cell.

Conclusion: This location is feasible for the cell and does not appear to conflict with other vital operations. This area has been recommended as the prime location for the test cell. A conceptual drawing of a 750 cubic foot test cell which could be constructed in this area is shown in Figure 3A3-2.

2. Above Cold Trap Vault (Area 14 of Figure 3A3-1)

This area is located along the north wall of the refueling cell and is a very busy area. The space which the cell would require is partially preempted by that required to remove the shield plug for the man entry panel. In addition, there is considerable equipment which would have to be removed and relocated.

Conclusion: This location is not practicable for the test cell.

3. In the Hot Trap Vault

There is considerable space for monitoring equipment in the unused region reserved for the hot trap. However, the operating deck for this equipment would either have to be from the refueling cell deck above, or a portion of the hot trap vault would have to be separated and made into an air zone accessible through the hot trap shield plug. Although the vault is not overly crowded, considerable layout work would be required to establish monitoring equipment locations accessible to an operator. Connections to the 12-inch line between reactor outlet and main IHX inlet would be 40 ft. away, on the opposite side of the reactor. The test loop would have to be installed in pieces instead of as a pre-tested integral unit in order to gain entry to this zone.

Conclusion: This location is feasible but has serious drawbacks, namely: poor operator accessibility, long connections to reactor outlet sodium, piecemeal installation of modules.

4. Area Occupied by Primary Pump and Main Flowmeter

This area, normally under a N<sub>2</sub> atmosphere, is opposite an air zone accessible by stairways from the main refueling cell deck. A concrete wall 5-6 ft. thick separates these areas. There are two existing 3-inch diameter penetrations for pressure sensor lines. There is adequate room to locate impurity monitoring equipment without crowding, and primary sodium is available from the main or auxiliary IHX's overhead. The operating area for the loop would have to be in the region now occupied by the monorail beam structure intended to aid in installing and removing the reflector drives.

In lieu of a window, closed circuit TV and/or periscope viewing could be employed here. However, penetrations for manipulator(s), periscope and hot equipment for sample transfers would have to be made through thick concrete walls and maintenance of equipment would require purging of the entire N<sub>2</sub> zone and radioactive decay of adjacent main primary components. The monitoring equipment would require installation in small sections due to access limitations.

Conclusion: This location is feasible but has serious disadvantages in initially locating equipment and in gaining access for maintenance. Viewing equipment would be expensive to install.

In addition to the selection of the prime location of the test cell, the following major facility modifications were identified:

- Construct test cell by removing small block of existing shielding, installing cell shielding and ancillaries and providing air-to-nitrogen zone penetrations.
- Install piping between SEFOR primary piping and test loop connections.
- Install modifications to the nitrogen zone cooling system for cell cooling, for isolation of the nitrogen zone and for periodic introduction of air atmosphere and purging.
- Install C&I leads through sealed penetrations in the nitrogen to air zones and the station to air zone.
- Install C&I panels in control room and reactor building.
- Perform installation tests including main sodium system integrity, nitrogen system integrity containment penetrations and power, control and instrumentation leads.

### 3.1.3.3.2 Review and Preliminary Selection of Monitoring Instruments

A detailed review was made of the monitoring instruments which potentially could be used in the impurity monitoring test loop. For each instrument, the principles of operation, laboratory experience, operational requirements, advantages and disadvantages for the particular application were evaluated. Based on these evaluations, the following preliminary selections of impurity monitoring instruments were made for the SEFOR impurity monitoring test loop:

#### Oxygen Monitoring:

1. Oscillating plugging indicator
2. Electrochemical oxygen cells
3. Remote controlled rapid sampler
4. Vanadium wire equilibration module
5. Remote controlled on-line distillation device

#### Hydrogen Monitoring:

1. Diffusion tube with dynamic and static pressure measuring devices
2. Cover gas chromatography

#### Carbon Monitoring:

1. Alloy tabs/Vanadium wire equilibration
2. Fused salt electrochemical cell

#### Radioactive Materials Deposition:

1. Isothermal and non-isothermal deposition samples (impingement and non-impingement specimens)
2. Specimens to be located in test loop and, if feasible, in critical locations in the main sodium stream.

Since most of the monitoring instruments are at various stages of development, the final selections of the types of instruments to be installed in SEFOR will be based on the performance and reliability of these instruments as the development and testing program progresses at various laboratories. It is anticipated that space limitations in the test cell may prevent the inclusion of some of the above instruments or methods. Therefore, the final decision on instrumentation will be deferred to the detail design phase of the follow-on program.

### 3.1.3.3.3 Preliminary Selection of Specific Tests

The specific tests which would be performed in SEFOR during the 1000°F operation phase are summarized below:

#### a. By-Pass Loop

This test is designed to determine whether the monitoring instruments installed in by-pass loops which draw only a very small fraction of reactor sodium are adequate to monitor impurities in reactor sodium.

*Justification:* In general the concept of the by-pass loop to monitor impurities has been accepted by the designers. Furthermore, one loop somewhat different than the present design will be installed in EBR-II in the near future. This experiment, in conjunction with the experiments in EBR-II, will establish the design criteria for monitoring impurities in reactors.

*Required Facility:* Instrumented by-pass loop in SEFOR with capability of internal calibration of the instruments.

b. Characterization of a Large Reactor Cold Trap

An attempt will be made to characterize the performance of a large reactor cold trap, provided some variations of the SEFOR cold trap operations (e.g., flow, temperature) are permitted during the reactor operations.

*Justification:* To date very little information on the performance characteristics of a large cold trap is available. Installation of the instrument package will give us for the first time an opportunity to study the performance of a large cold trap.

*Required Facility:* Instrumented loop. For short periods, some flexibility in SEFOR cold trap operation, e.g., flow and temperature variations, without disturbing the normal SEFOR operations.

c. Deposition of Radioactive Materials

This test is designed to measure and characterize the deposition of radioactive corrosion products during normal operation and fission products during the failed fuel test operation.

*Justification:* The location and magnitude of the deposition of radioactive corrosion products and fission products in reactors is one of the main concerns for reactor designers. For example, a high activity buildup in high maintenance areas will require sophisticated shielding. Unless the locations of high activity buildup areas are identified and proper shieldings are designed, it will create severe maintenance problems during reactor operation.

*Required Facilities:* A sample station with about 300°F  $\Delta T$ , with high velocity channels for specimens, will be required. The sample station must be accessible even when SEFOR is in operation for periodic removal of the specimens. If feasible, sample stations in the main sodium stream (inlet and outlet of IHX) would be highly desirable for comparison and verification of radioactive deposition data from the test loop.

d. Interstitial Movement

This test is directed toward the measurement of magnitude of the interstitial (carbon, boron, nitrogen) gains or losses in Demonstration Plant materials.

*Justification:* The degradation of mechanical properties of structural materials due to gains or losses of interstitials has been observed in tests carried out in small loops. This test will be the first opportunity to study interstitial movement in a large reactor operating at prototypic temperatures of the Demonstration Plant and FFTF.

*Required Facilities:* A sample station with about 300°F  $\Delta T$ , with high velocity channels for specimens, will be required. The sample station must be accessible even when SEFOR is in operation for periodic removal of the specimens. If feasible, sample stations in the main sodium stream (inlet and outlet of IHX) would be highly desirable for comparison and verification of radioactive deposition data from the test loop.

e. On-Line Instrument Performance

This test is designed to evaluate the performance of advanced on-line instruments in reactor radiation conditions. The long term operations of the instruments will also establish the problems associated with removal, installation and calibration of the instruments during reactor operation.



**Justification:** Use of the monitoring instruments in primary system of the reactor requires the knowledge of their performance in radiation field.

**Required Facility:** Based on the present state of the art on monitoring instruments, the following instruments are to be considered:

- O<sub>2</sub> monitoring (in order of priority)
  1. Plugging indicator (See Figure 3A3-3.)
  2. Electrochemical oxygen meter
  3. Flow through rapid sampler (See Figure 3A3-4.)
  4. Vanadium wire equilibration module
  5. On line vacuum distillation
- H<sub>2</sub> monitoring
  1. Diffusion tube type hydrogen detector with static and dynamic pressure measuring device. (See Figure 3A3-5.)
  2. Cover gas chromatography.
- C monitoring (in order of priority)
  1. Alloy tabs in specific locations in the loop with the capability of intermittent removal.
  2. Electrochemical carbon meter.

#### 3.1.3.3.4 Preliminary Design of Impurity Monitoring Test Loop

A schematic representation of the impurity monitoring test loop is shown in Figure 3A3-6. Although the detailed design of the loop will be done during the follow-on program, the essential elements of the loop are shown in Figure 3A3-6. As shown, the loop is located in a heavily-shielded cell with capability for operation under inert or air atmosphere. Hot cell facilities including a lead-glass window and master-slave manipulators are included. Wherever possible, auxiliary equipment (cold traps, pumps, blowers, valves) is located outside the test cell in order to provide maximum space for analytical instrumentation. The loop itself can be rapidly isolated from the main sodium stream by a double set of remote operating isolation valves. The loop will be capable of being run in the isolated mode and will utilize this capability during on-line calibration of instruments. In addition to these major features, the following criteria to be used in the detail design of the test loop have been selected:

- Loop must conform to space and weight restrictions in SEFOR.
- Loop must have remote operation capabilities – minimum capability to consist of remote filling and dumping.
- Loop must be enclosed in cell with adequate radiological shielding.
- Major analytical elements (hydrogen meters, oxygen meters, etc.) must be readily removable for repair outside of the loop containment.
- Analytical methods and instrumentation must provide facilities for on-line calibration.
- Entire loop and associated equipment must be transportable, either as a unit or in sections.
- Loop must be designed for 10 gpm flow at 1000°F with a 300°F  $\Delta T$  through the sample holders. The loop must have the capability of reheating the sodium to 1000°F, prior to re-entry to the primary sodium system.
- Loop and auxiliary equipment must be designed and built with highly reliable components. Sufficient redundancy of critical or inaccessible components must be utilized to prevent forced shutdown of the entire test loop.

#### 3.1.4 Task 3A4 – Core Clamping

##### 3.1.4.1 Objective

The long-term objective of this task is to confirm the ability of the internal core clamping mechanism to function properly in a fast reactor environment, including the effects of temperature, liquid sodium, and fast neutron fluence in the range which causes metal swelling and irradiation induced creep. The objectives during Phase A are to specify test requirements, to evaluate the suitability of SEFOR for performance of the tests, and to prepare a preliminary test plan.

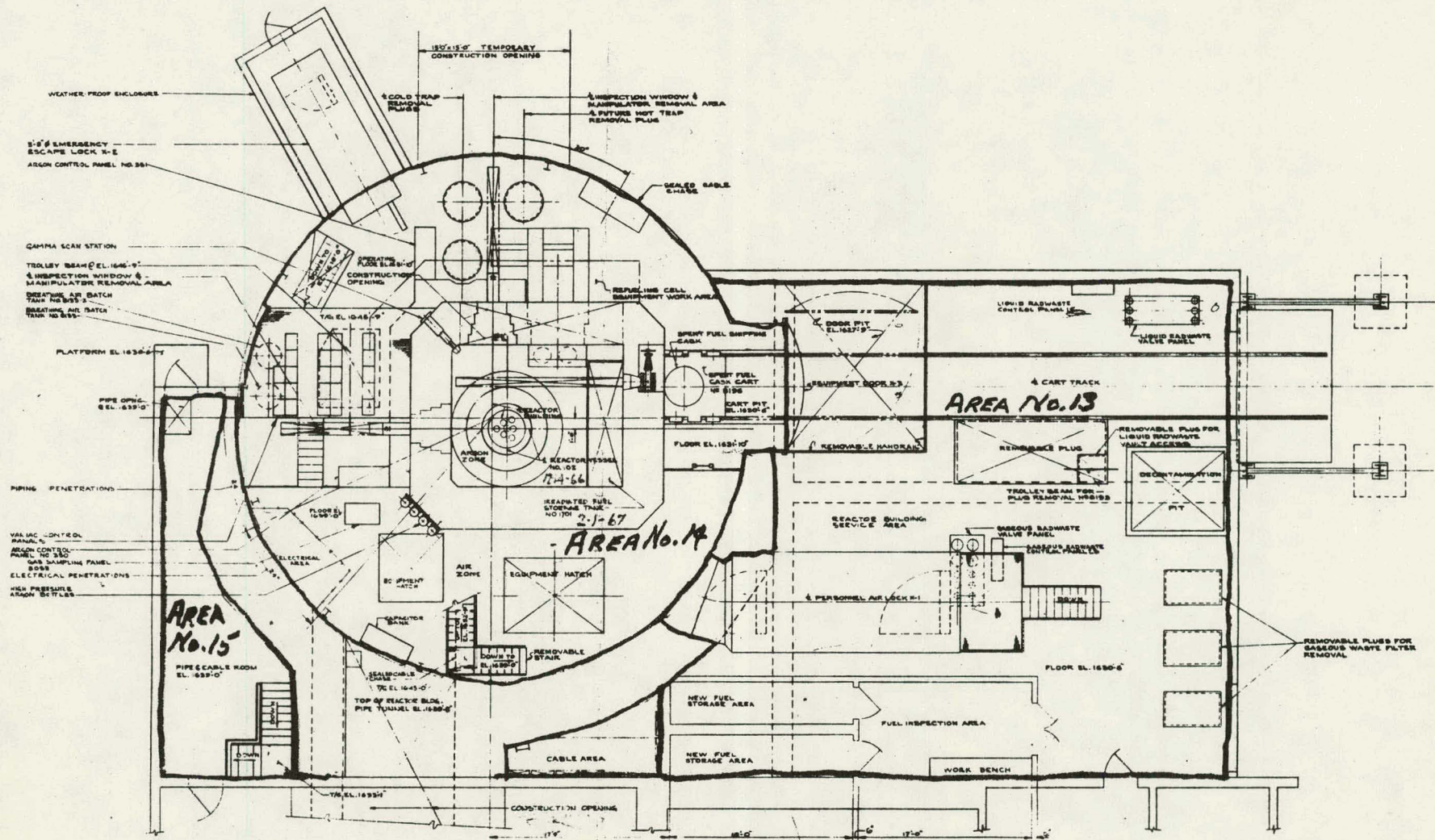


Figure 3A3-1. Proposed Location of Cell for Impurity Monitoring Test Loop

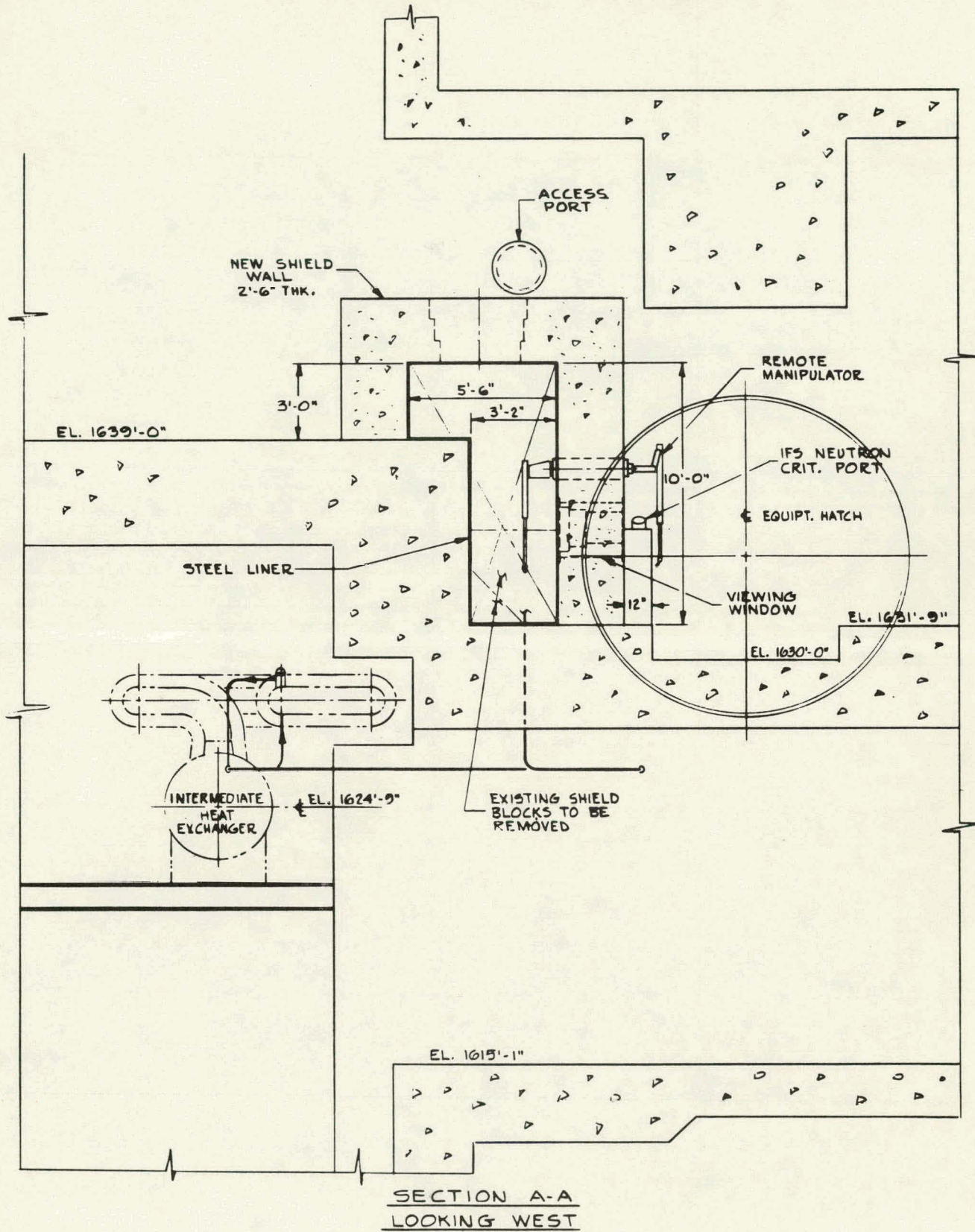
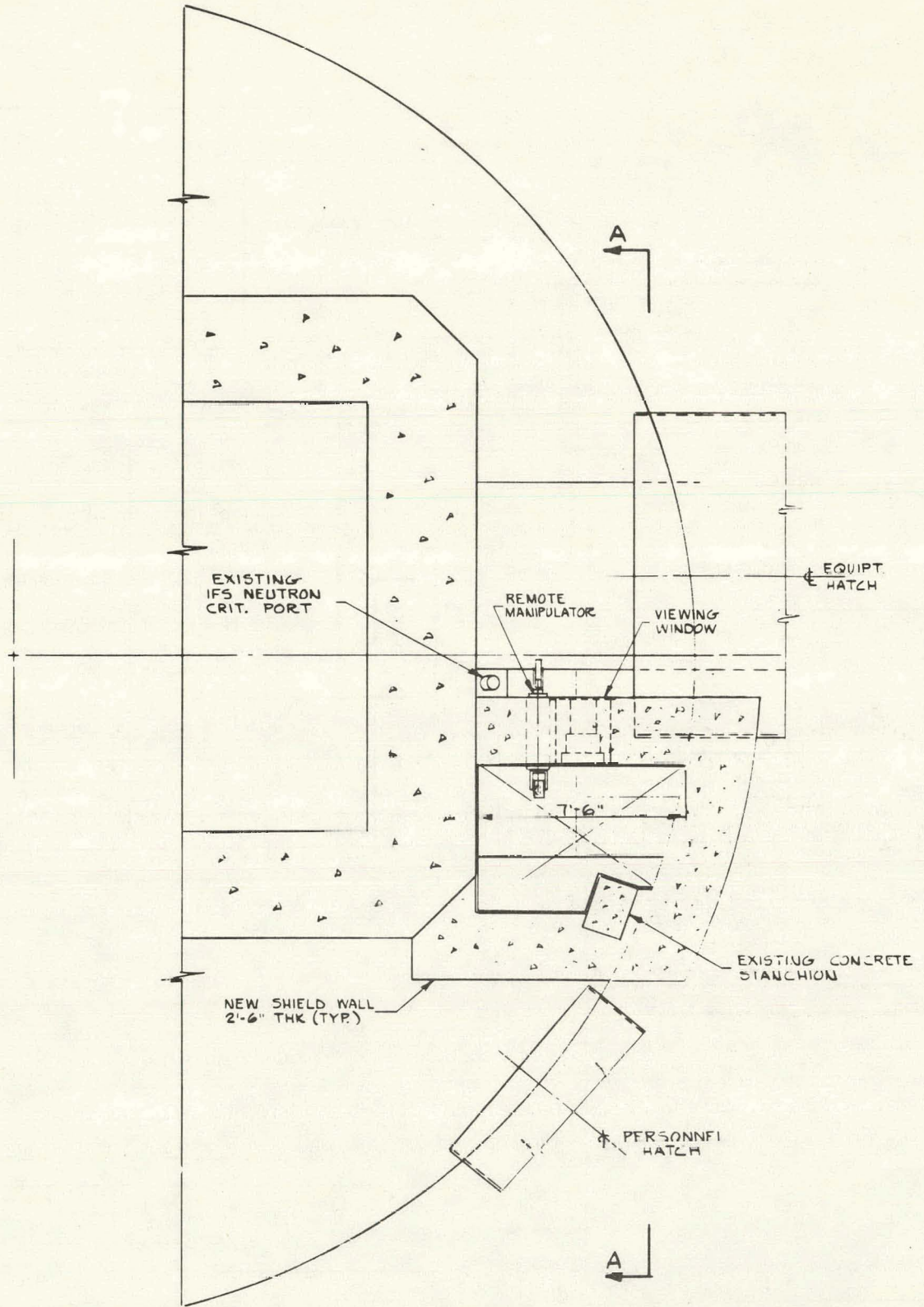


Figure 3A3-2a. Conceptual Drawing of Test Cell for Impurity Monitoring Test Loop, Side View



PLAN EL. 1630'-0"

Figure 3A3-2b. Conceptual Drawing of Test Cell, Plan View

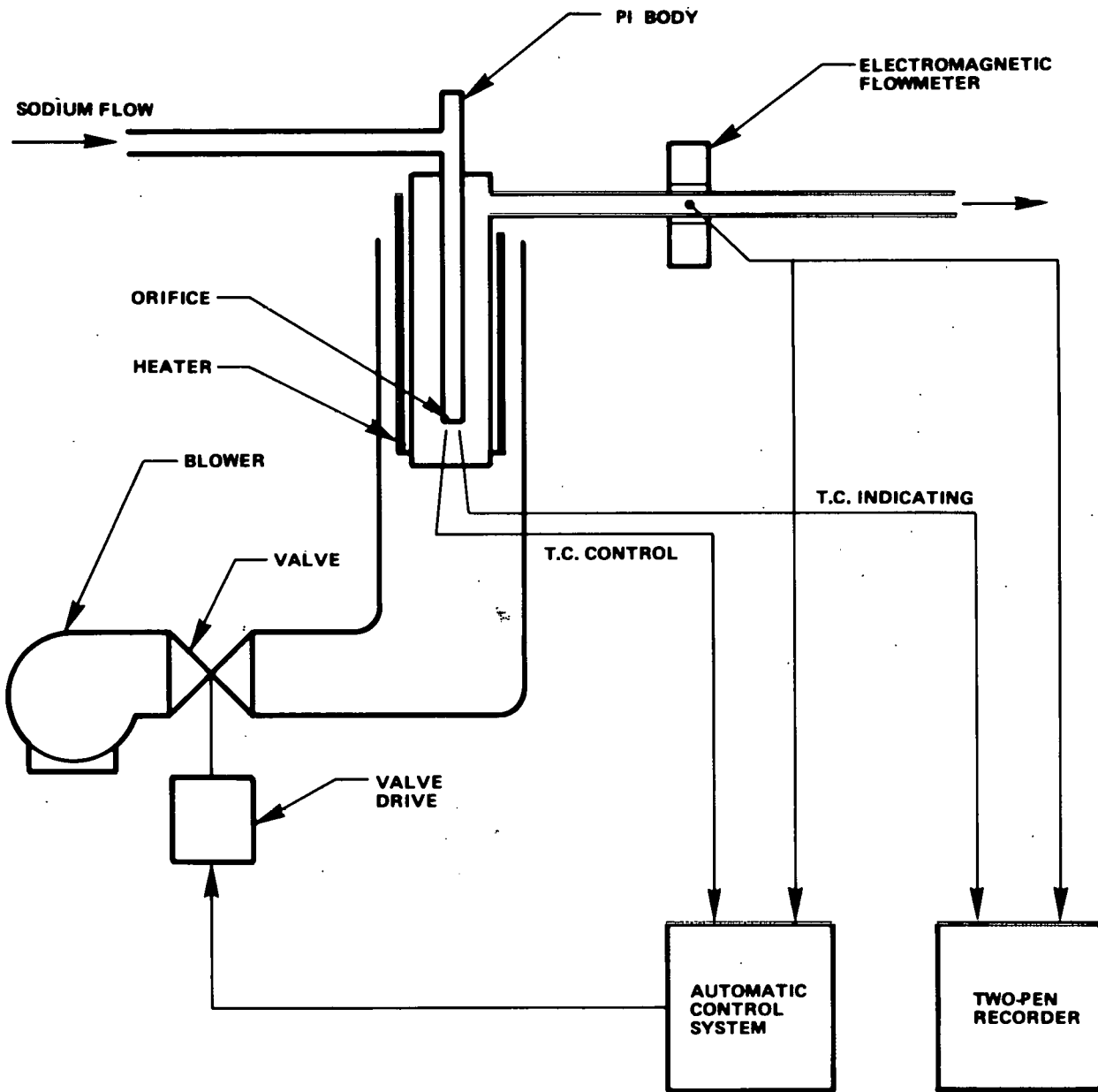


Figure 3A3-3. Schematic Diagram of Plugging Indicator

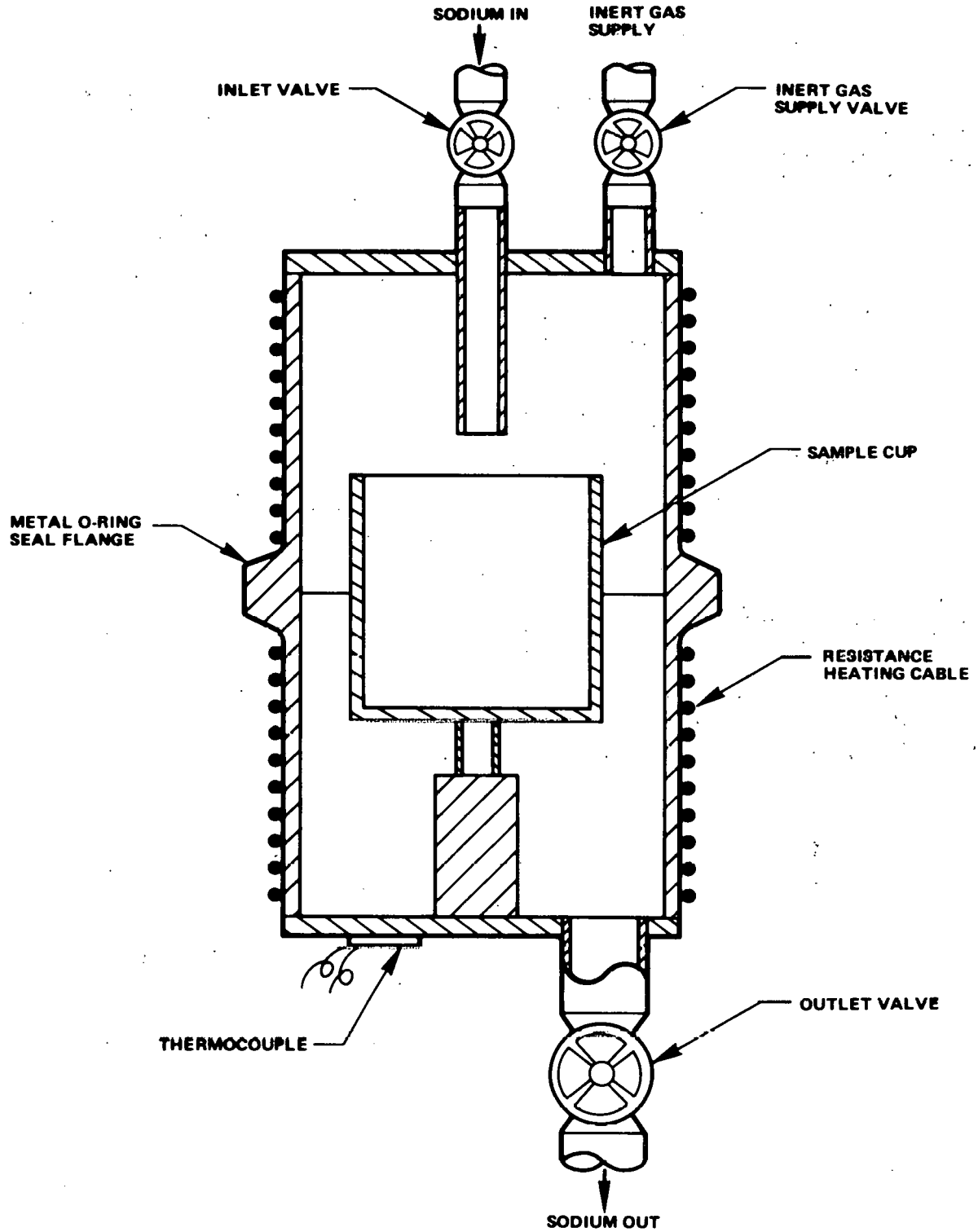


Figure 3A3-4. Schematic Diagram of Overflow Sampling Device

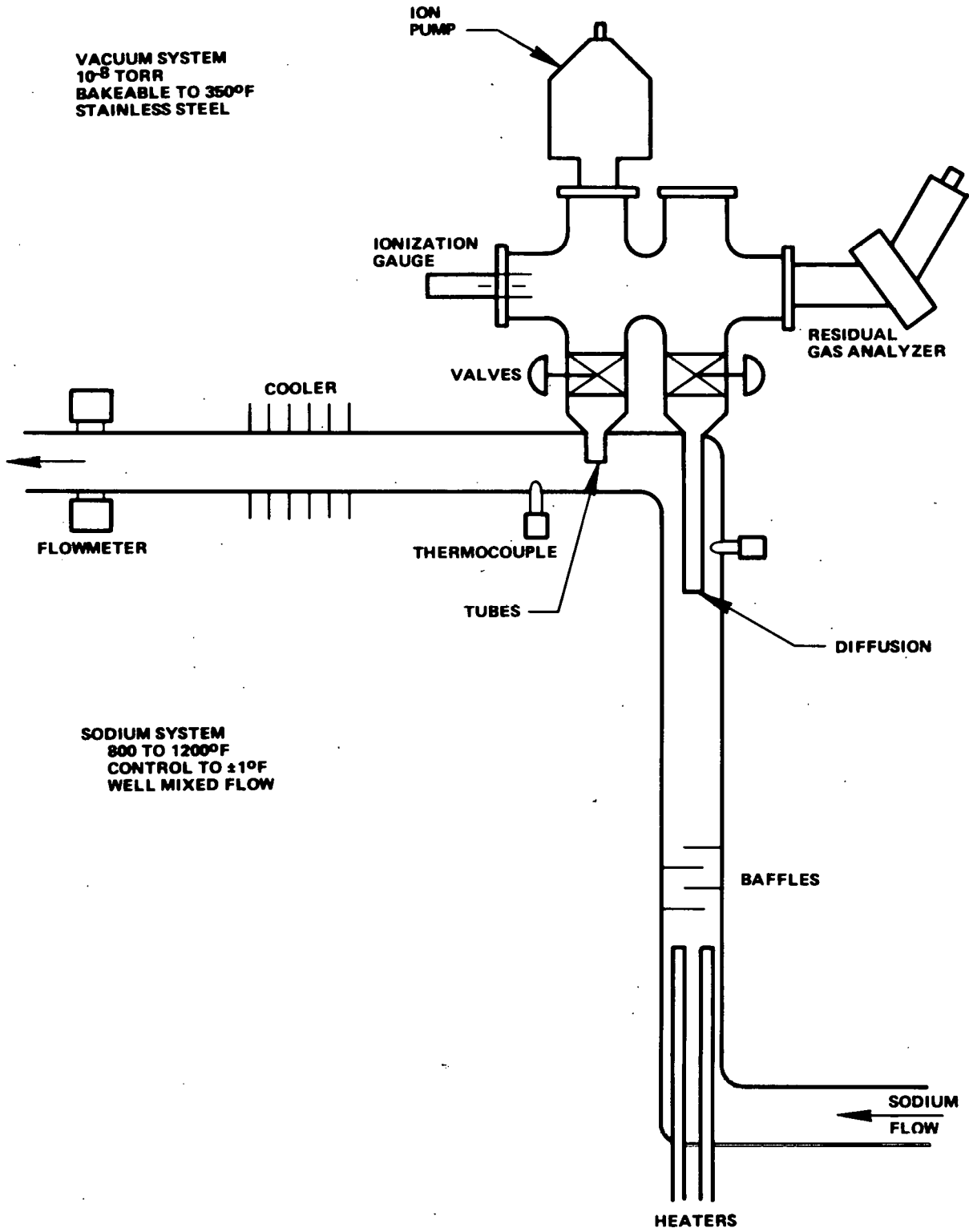


Figure 3A3-5. Diffusion Tube Hydrogen Detector

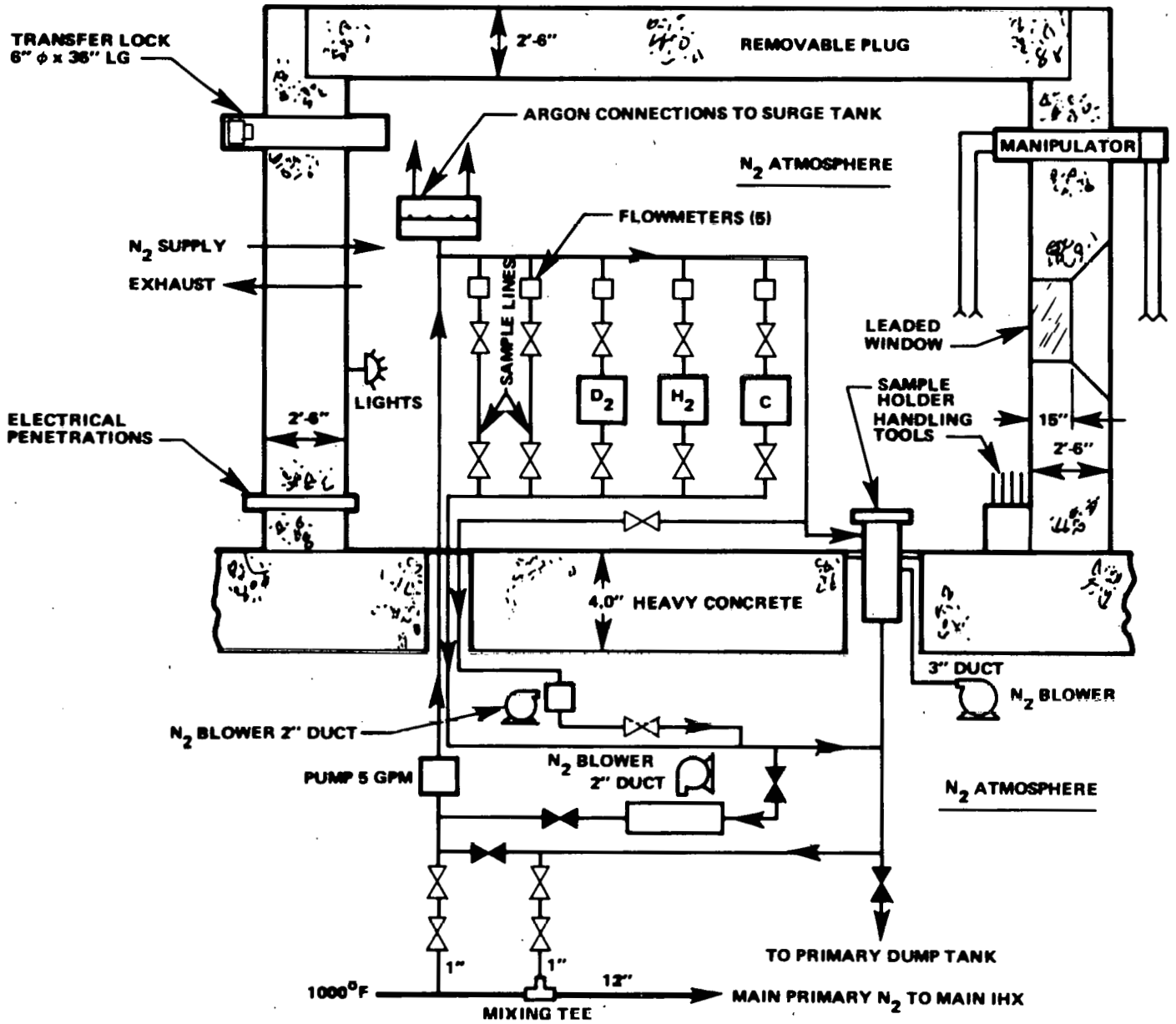


Figure 3A3-6. Schematic Drawing of Impurity Monitoring Test Loop

3



**3.1.4.2 Discussion**

The internal core clamping mechanisms, which are employed to take up the clearances between fuel channels of the Demonstration Plant, must be readily actuated during core refueling operations. This actuation must follow periods of six months to one year of relatively steady reactor operation during which the mechanisms are under significant loads and are submersed in sodium at temperatures in the 1000°F range. Further, the mechanisms will be subjected to some irradiation induced effects, such as swelling and creep, and must be capable of actuation by remote handling means in a refueling cell.

The scope of this task includes the design, related analyses, fabrication, reactor installation, and irradiation testing in reactor of a mockup of the reference internal core clamping mechanism. The mockup, which will be a partial scale model of the actual mechanism, will include proper consideration of loads and stresses, bearing types, spring devices and actuating mechanisms. Testing will include operation of the clamping mechanism to determine required actuation forces initially and following periods of extended reactor operation.

**3.1.4.3 Description of Reference Design Core Clamping System**

The core clamping system is an integral part of the reactor design for the 350 MWe Demonstration Plant. The purpose of the clamping system is to provide alignment and constraint for core fuel, blanket and control channels during reactor operation and to provide for removal of this constraint to accommodate refueling during reactor shutdown.

The core clamping system reference design consists of three types of components:

1. Banding ring segments
2. Spring banding rods
3. Internal tighteners

The purpose of the banding ring segments is to provide a fixed boundary for the core. The spring banding rods are located between the blanket channels and the shield rods. The spring action in these units (provided by a torsion bar) provides the compliance necessary to accommodate thermal expansion and irradiation induced swelling in the core.

The internal tighteners are devices which remove clearance within the core and blanket. They are located on each of the control rod channels and on blanket assemblies that form a continuation of the control channel pattern in the core. During operation of the core, the internal core tightener clamping pads are located in an extended position taking up the clearance between channels. During the refueling process the clamping pads are retracted in order to provide the clearance necessary to remove the fuel channels.

The design requirements for the Demonstration Plant core clamping system are given in Design Specification 22A3276. Those items which are pertinent to defining the internal tightener mockup test in SEFOR are repeated below.

1. Design life – Individual component design life is dependent on the location of the component in the reactor container and the local values of fluence (>0.1 MeV) and irradiation induced swelling. Internal tightener lifetime shall match the control channel or blanket assembly lifetime on which the tightener is mounted. The following life shall be required based on an 0.8 capacity factor.

Design Life (Years)

Internal tighteners –	
core region	2
blanket region	6

2. Neutron fluence – Components shall be changed out so that the fluence for neutron energies greater than 0.1 MeV shall not exceed  $4.0 \times 10^{22}$  nvt on any core clamping system component. This fluence limit is selected so as to restrict the clamp swelling to less than 10% of the clamp travel. The actual peak fluence at the lower clamping plane (64 cm above core midplane) is  $2.5 \times 10^{22}$  nvt (>0.1 MeV) based on the two year design life.
3. Steady state coolant temperatures – Steady state coolant temperatures will be based on a mixed mean reactor outlet temperature of 1050°F and shall be limited to:

Internal tighteners	
Inner coolant	1110°F
Outer coolant	750°F to 1000°F

Actuation of the clamping mechanism will be done at the refueling temperature of 400°F.

4. Interface dimensions — Nominal reference design dimensions at interfacing locations at 72°F should be as follows:

Assembly pitch	4.009 in
Assembly clamping pad flat-to-flat	3.959
Enlarged clamp pad flat-to-flat	4.134

5. Lateral clamping loads — The internal tightener shall be designed to accommodate a loading normal to each of the six clamping pad faces of 1500 lbs (1000 lbs design, 500 lbs margin) and a shear load in any direction on each of the six clamping pad faces of 1500 lbs (1000 lbs design, 500 lbs margin).

#### 3.1.4.4 Test Requirements

The following test requirements for the SEFOR internal tightener mockup test have been generated based on the reference tightener design requirements:

1. Dimensions — as near prototypic as possible
2. Pad forces — scaled to size
3. Fluence — as near actual peak fluence of  $2.5 \times 10^{22}$  nvt ( $>0.1$  MeV) as possible
4. Clearances — radial clearance to be prototypic
5. Operating temperatures — as near prototypic as possible
6. Frequency of actuation — approximately once every 6 months during irradiation
7. Materials — prototypic
8. Interaction with SEFOR operation —
  - a. Inclusion of test mockup in SEFOR core must not interfere with other reactor tests
  - b. Test mockup must not cause deformation of SEFOR hex channels

#### 3.1.4.5 Evaluation of SEFOR as Test Bed

The suitability of SEFOR as a test bed for a mockup of the internal tightener can be evaluated on the basis of how well the proposed test meets the specifications.

#### 3.1.4.6 Dimensions

The SEFOR hex channels are nominally 2.58 inches across inside spacer flats. A second hex channel of 0.10 to 0.14 inch wall thickness will be placed inside the SEFOR channel as a loading surface for the tightener clamping pads. Consequently, the tightener mockup will be 2.300 to 2.35 inches across pads (expanded). This is 0.55 the size of the reference design tightener.

#### 3.1.4.7 Pad Forces

The clamping spring forces will be scaled with the pad size so as to result in pressure loadings identical to those of the reference design tightener.

#### 3.1.4.8 Fluence

The tightener mockup will be in the SEFOR core during two operational periods: elevated temperature tests and Option III tests. Each testing period will be discussed separately.

During the eleven months of elevated temperature operation, the mockup will be inserted in a Row 2 channel next to the core centerline. The total accumulated fluence over 11 months at this maximum flow location will be  $1.1 \times 10^{22}$  nvt ( $>0.1$  MeV). An 0.8 load factor is assumed for this calculation.  $1.1 \times 10^{22}$  nvt is 44% of the peak fluence and 28% of the anticipated peak swelling.

Prior to Option III testing, the mockup must be moved from the Row 2 channel. It will be relocated to the first row of outer driver elements, the fifth row overall. With the mockup in this position, the perturbation of flux in the SEFOR central region is negligible.

The tightener mockup will be exposed to a significantly lower flux in a Row 5 channel during Option III than it will be in a Row 2 channel during the elevated temperature tests. At full power, the flux at Row 5 is  $1.95 \times 10^{19}$  n/cm<sup>2</sup> day ( $>0.1$  MeV) or  $0.76 \times 10^{21}$  nvt/mo. During the four years of Option III testing, SEFOR will be down a large percentage of the time for test insertion and removal. It is estimated that there will be 175 days or approximately 6 months of equivalent full-power operation. Thus, the fluence accumulated on the tightener mockup during Option III

will be  $0.45 \times 10^{22}$  nvt ( $>0.1$  MeV), 18% of the peak fluence. Summed over the two periods of operation, the total fluence is  $1.56 \times 10^{22}$  nvt, 62% of peak; the diametral swelling is 47% of the anticipated peak swelling.

#### 3.1.4.9 Clearances

Although the linear dimensions of the SEFOR mockup tightener will be reduced to approximately one-half those of the Demonstration Plant tightener, the clamp travel will be made prototypic. All radial clearances and associated tolerances will also be prototypic. This will permit the effects of swelling on the clamping mechanisms to be most easily evaluated.

#### 3.1.4.10 Operating Temperatures

During the eleven months of elevated temperature testing, the tightener mockup will be submerged in sodium at temperatures in the 1000°F design range. This time period appears adequate (as compared to the two year design life of core tighteners) to study time-at-temperature effects such as galling, self-welding and crud accumulations. Actuation of the clamping mechanism will be done at a refueling temperature of 400°F as in the demonstration plant. Following the high temperature tests, irradiation will continue at a reduced temperature of 900°F.

#### 3.1.4.11 Actuation

The clamping mechanism will be actuated at least twice during the elevated temperature tests. The actuations will be done remotely through the top head.

No special provisions will be made to permit remote actuation during the Option III transient tests. Rather, actuation will be done when the reactor head is pulled off to inspect the booster fuel. This will occur at least annually, and probably every six months.

The total number of mockup actuations will vary from 8 to 10. This is significantly greater than the 4 or 5 actuations anticipated during the two year lifetime of core tighteners (assuming a six months refueling cycle) and only slightly less than the 12 to 14 actuations anticipated for the blanket tighteners.

#### 3.1.4.12 Interaction with SEFOR Operation

Inclusion of a mockup test of the core clamping tightener mockup will not interfere with any other SEFOR tests nor with the future operation of the SEFOR reactor. A Row 2 channel is open and available for mockup testing during the elevated temperature tests. A Row 5 channel location during the Option III tests is available; the mockup will not interfere in any way with the transient tests which are the primary thrust of the Option III test period.

To avoid possible deformation of the SEFOR hex channels, a smaller hex channel will be inserted in the SEFOR channel. The tightener mockup will then load this secondary channel. The insert will be sized so that, after the irradiation, it can be removed without damaging the permanent channel.

#### 3.1.4.13 Conclusion

The installation and operation of a mockup of the reference internal core clamping tightener in the SEFOR reactor meets the stated test objective: to confirm the ability of the clamping mechanism to function properly in a fast reactor environment, including the effects of temperature, liquid sodium and neutron fluence. The test will verify that an unsuspected failure mode does not occur, or if it does, the test will identify the problem thus permitting modification of the tightener design.

The use of SEFOR as a test bed for a core clamping "proof-of principle" test is justified. The mockup must be about one-half scale but the materials, mechanical design, loads, radial travel and clearance can all be prototypic. The design temperature range of 1000°F is maintained during one year of operation. The total fast fluence, while not equal to the peak fluence in the Demonstration Plant, is reasonably high (62% of peak). The calculated swelling is almost one-half the maximum swelling anticipated on the tightener in the Demonstration Plant reactor.

#### 3.1.4.14 Required Facility Modifications

No facility modifications are foreseen. One (of six) Row 2 core channels will be occupied during the elevated temperature tests; a Row 5 channel will be occupied during the Option III transient tests. Insert channels will be used to remove any possibility of deforming the permanent SEFOR channels. The mockup can be remotely actuated through the top head when it is located in Row 2. The top head must be removed to permit actuation in the Row 5 position.

### 3.1.4.15 Preliminary Test Plan

During development of the internal tightening clamping mechanisms, numerous selected tests will be performed on the devices (such as component tests in air and in sodium), followed by in-reactor proof tests of the entire mechanism in as prototypical an environment as possible. The internal tightener clamping mockup test in SEFOR is intended to provide basic design information on the effects of irradiation-induced swelling and creep, self-welding, galling, and thermal-induced creep. Prior to insertion in the reactor, a complete set of as-fabricated measurements will be made on the clamping mechanism. These will be repeated after irradiation and removal from the reactor.

The clamping mechanism will be installed within an existing fuel channel near the core center. The force required to actuate the clamping mechanism will be measured before irradiation, at each unclamping and clamping operation (at approximately 6 months intervals) and after removal from the reactor. The mechanism will be actuated to simulate the proper mechanism loads, and will be subjected to steady state operation to study temperature-sodium-stress effects and to accumulate fast neutron fluence. Periodically, when the reactor is shut down, the mechanism will be actuated remotely to study possible changes in actuation forces. The high temperature testing period will allow an operating period of approximately one year at temperature on the mechanism, which should be adequate to study effects such as galling, self-welding, or crud accumulation on mechanism operation. Following the high temperature tests, irradiation of the device will be continued principally to study the effects of metal swelling and creep. Following irradiation, the mechanism will be subjected to an extensive post-test examination to determine wear characteristics and possible incipient failure modes. If failure occurs, the mode of failure will be determined. At the conclusion of the tests, the mockup will be examined for evidence of incipient failure modes. Material samples will be taken and tested to determine property changes.

### 3.1.5 Task 3A5 — Core and Fuel Assembly Instrumentation

#### 3.1.5.1 Objective

The long-term objective of this task is to conduct proof testing of prototype fuel assembly instrumentation probes, including transient behavior as well as long-term stability. The objectives for Phase A are the preparation of a preliminary Test Scope including specification of test objectives and the identification of major SEFOR plant modifications.

#### 3.1.5.2 Discussion

Environmental and final proof tests are required to demonstrate that the probe and sensor mechanical and electrical performance will be maintained during design thermal and sodium flow conditions. Discovering an inadequacy or common type failure mode after the Demonstration Plant begins operation would mean that the probes would have to be redesigned and the ones in the reactor replaced at a considerable expense.

Elevated temperature operation of the SEFOR reactor provides a realistic environment for final instrument probe qualification tests with respect to the most relevant factors. These factors include proper temperature and flow conditions, true, known reactor transients, and remote handling environment. Proof testing of the probes does not preempt other tests because of the fact that the required transient testing and cycling can be performed during reactor startup and shutdown.

One limitation on the performance of the tests in SEFOR is that due to the limited height of the reactor head above the core, and the fact that the caps on the through-head ports must be in place during reactor operation, the lead-out length and guide tube mockup is limited to only a few feet (instead of ~20'). For this reason, insertion and withdrawal techniques and conditions cannot be mocked up adequately. It is felt that some measure of the "sodium frost" buildup problem will be obtained, however, in spite of this limitation.

Another possible limitation is that since one through-head port is required for each instrument probe tested, that the maximum number of probes that can be included in the testing program without interfering with other programs is three.

#### 3.1.5.3 Required Facility Modifications

Two possible methods are available for accommodating a fuel assembly instrument probe below a through-head port. The first, and most desirable is to shorten the fuel extension rods so that the instrument probe can fit down into the fuel channel assembly. This is made possible by the fact that the fuel grapple can reach down into the channel approximately ten inches. A dummy mockup of the reference fuel handle could then be inserted into the top of the

channel. A possible problem with this approach is that since the extensions contain  $B_4C$ , shortening them may remove required shielding.

A second possibility is to build a dummy fuel handle area into a one-two foot tall shroud which fits over a fuel assembly and extends up above the fuel extension rods. The guide tube mockup would then extend down from the through-head port and match up with the channel handle mockup. A disadvantage with this approach is that it further shortens the available guide tube length. Both approaches require additional investigation.

Another plant modification required is a feed-through collar for each instrument probe which would fit above a through-head port and allow bringing out the sensors signals during reactor operation when the cap is in place over the port. These collars would be similar to the ones presently being used on the Instrumented Fuel Rods (IFR's). Adequate penetrations already exist for bringing the signals out of the refueling cell.

#### 3.1.5.4 Conclusions

The SEFOR reactor provides a realistic environment for conducting final proof tests of the fuel assembly instrumentation probes. Only minor facility modifications are required to provide a reactor environment encompassing the most relevant factors required for qualification testing.

#### 3.1.5.5 Preliminary Test Scope

Upon completion of the reference design of the fuel assembly instrumentation probe and related component development activities, final environmental tests of the probe and lead-out system will be conducted. These tests will be designed to uncover any design or fabrication inadequacies and will consist of:

1. Thermal transient tests to study thermocouple response and to assure that mechanical integrity is maintained.
2. Time-at-temperature tests to insure that the probes and sensors maintain mechanical and electrical stability.
3. Vibration tests of mechanical integrity.
4. Tests of an instrument probe installed in a sodium loop to assure materials compatibility and to measure transient and steady state behavior. These tests will also allow a careful calibration of the probe sensors.

Following the environmental tests, three probe assemblies which closely mockup the reference design will be installed in the SEFOR reactor for final proof testing. One probe will be used to monitor the exit flow from a normal SEFOR channel during the elevated temperature operation tests. A second probe will be used to monitor a channel which has had its exit sodium temperature increased to a value representative of the maximum expected in the reference Demonstration Plant design (either by proper flow orificing or by auxiliary heaters). The third probe will monitor a channel which either incorporates a flow mixer or which has been altered to mockup non-uniform or off-standard flow conditions in the core.

During periods of reactor startup and shutdown, an evaluation of the probes' ability to monitor specific flow and temperature transients will be ascertained. During steady-state periods of at-power operation (in the elevated temperature testing period) the stability behavior of the sensors will be evaluated, and some measure of probe reliability ascertained.

At the conclusion of the elevated temperature testing period, the probes will be removed from the reactor. During this operation some measure of the possible "sodium frost" problem will be obtained. First, a reasonable removal force will be applied to the probes in an attempt to remove them from their guide-tube mockups. If this is unsuccessful, various amounts of heater power will be applied to the lead-out heaters to determine the requirements for removing the frost buildup.

Following removal of the probes, a careful post-test inspection will be conducted to determine wear patterns, uncover any possible incipient failure patterns, and, in general, evaluate mechanical integrity. A re-check of the sensor calibrations will also be performed to uncover any changes during the final proof test period.

#### 3.1.6 Task 3A6 - Boiling Detection

##### 3.1.6.1 Objective

The long-term objective of this task is to experimentally determine the boiling detection sensitivity of an acoustic emission monitoring system with typical reactor background noise and reactor geometry. The objective during Phase A is to prepare a preliminary test scope.

### 3.1.6.2 Discussion

A high performance sodium boiling detection system would be an attractive supplement or an alternate to the reference subassembly instrumentation system. Potential advantages of a boiling detection system are that the entire core might be monitored by a limited number of in-vessel probes and that these probes might be stainless steel rods serving as mechanical wave guides. A boiling detection system could, therefore, be economical as well as very reliable. Further, a great deal of protection is afforded by a boiling detection system since boiling occurs before an over-temperature condition reaches the point of clad melting.

### 3.1.6.3 Suitability of SEFOR as Test Bed

The ease of installing an electrical boiling source in the core of the SEFOR reactor is a strong recommendation for its use. Additionally, the absence of the need to maximize the operating time at maximum power allows scheduling flexibility required by this test.

### 3.1.6.4 Conclusions

It appears that performing this test will not present any insurmountable problems; however, there is no assurance that results will be positive. The noise background in an operating reactor might be so large that the detection sensitivity would not be adequate.

The maximum flow rate in a channel that would result in boiling in an array of 15 kW/ft heaters was calculated. It is concluded that channel plugging along a considerable length would be the most likely cause of boiling. Fuel pin bowing of itself would not cause boiling.

Procurement of electrical heaters should not pose a problem. Heaters can be purchased from Watlow Co. Similar heater arrays have been used in the forced circulation capsules tests at GTR.

There is a need for loop testing prior to reactor testing. It would be desirable, if possible, to relate the void volume to the thermal-hydraulic conditions by the use of a fluoroscope.

### 3.1.6.5 Preliminary Test Scope

Current technology will be reviewed and detection techniques will be chosen for further development which are compatible with commercial LMFBR's. Test equipment will be designed and built. This test equipment will consist of an electrical heater to produce boiling in the sodium, an orifice to cause cavitation at high flow rates, and, if possible, a frequency and amplitude controllable acoustic source. Out-of-vessel transducers in conjunction with wave guides, as well as in-vessel transducers, if available, will be used. Operational tests will be performed in water and sodium loops where appropriate.

After operational tests in-loop, the monitoring equipment will be installed in the reactor. Appropriate modifications will be made to the fuel pin extension rods to provide space for wave guides. Acoustic emission data will be taken under a variety of conditions. Initially background data will be recorded over the full range of sodium flow through the core.

Subsequently, the acoustic properties of the reactor system will be investigated by use of the controllable source, if available. In turn, the electrical boiling source will be monitored with and without a background cavitation noise.

On the basis of reactor test data, the capabilities of a boiling detection system will be defined.

## 3.1.7 Task 3A7 - Failed Element Detection and Location

### 3.1.7.1 Objective

The long-term objective of the Failed Element Detection and Location (FEDAL) task is to provide the bases for the definition of the design and operation of the Demo Plant FEDAL system. This definition includes the following:

1. Determine detection sensitivity limits and calibrate detectors for both concentrated and distributed fuel sources.
2. Determine optimum detection method.
3. Establish optimum location method.
4. Establish criteria for taking control actions.
5. Determine required system configuration.
6. Provide proof testing of major system components.

The objective during Phase A is to identify possible plant modifications and to prepare a preliminary test scope.

**3.1.7.2 Suitability of SEFOR for Tests**

SEFOR has several advantages as a testing site for FEDAL tests. The primary system has a low contamination level which will result in low background radiation levels. The constraints on location of equipment in the primary system is not as great as might be the case in other reactors. Finally power maneuvers can be conveniently performed and shutdowns can be scheduled frequently.

**3.1.7.3 Plant Modification**

The sodium sampling system requires a number of plant modification. Extension rods on one or more fuel pins need to be shortened to permit sodium sampling below the elevation at which intersubassembly coolant mixing occurs. Means of assuring a representative sample of the subassembly flow might also be required. The sodium line in the refueling cell and its associated equipment must be mounted and radiation shielded to prevent the sample line sodium radiation causing refueling cell radiation limits to be exceeded. Additionally, the sample line must be thermally insulated and heated to prevent sodium freezing. Two special penetrations in the refueling cell wall are needed for the sodium lines as it leads to and from the delayed neutron and rare gas monitoring stations located in the enclosure external to the refueling cell wall. In the latter area, an above-floor level scaffold is needed on which to locate the monitoring stations. The scaffold is needed because of the lack of ground level space. The sample line external to the refueling cell must be radiation shielded to observe the proper radiation limits. The sodium line must also be enclosed so that it is exposed to the same gas atmosphere as that in the refueling cell proper.

For the sipper tests, means to restrict the flow through the subassembly being probed and a gas bomb sampling system must be provided.

**3.1.7.4 Conclusions**

The SEFOR reactor represents an ideal test facility for performing FEDAL development. Only modest modifications are required to allow conduct of the tests and gain significant knowledge regarding detection sensitivities for exposed fuel.

**3.1.7.5 Preliminary Test Scope**

In support of this task and others in which fuel is exposed to and possibly released into the primary coolant, the SEFOR plant system will be modified and calibrated by the use of in-core fission product sources. This calibration will assure adequate plant protection during the course of the program and assists in licensing activities.

A series of tests are planned to obtain data which measures the sensitivity of various monitoring techniques to know amounts of exposed fuel in the reactor core. In particular, the following will be determined:

1. Sensitivity of a delayed neutron monitoring system and a rare gas monitoring system to an exposed fuel surface in the core by monitoring the sodium exiting from a core subassembly containing a fission product source of known strength.
2. Sensitivity of a delayed neutron monitoring system and a rare gas monitoring system to distributed fuel in the primary coolant system by injection of a predetermined amount of particulate fuel into the primary sodium system.
3. Concentration of rare gas in the cover gas and in the sodium exiting from a subassembly containing a vented fuel element.

These exposed fuel sensitivity calibration data, in conjunction with data from upper plenum flow distribution which will be obtained in the course of Demo Plant development tests, will permit the design of an efficient sodium sampling system for the Demo Plant. Both the tests with fixed source and the distributed fission product sources will aid in establishing the Demo Plant's operating limits with failed fuel elements.

Finally, the evaluation of a dry sipping technique as an off-line means of locating a failed fuel element will be performed. This dry sipper capability will improve the Demo Plant system by providing means of precisely locating failed fuel elements in conjunction with an on-line system and/or locating a failed fuel element in the event of a shutdown prior to location by the on-line system.

**3.1.8 Task 3A8 - Computer Data Acquisition System (DAS)**

**3.1.8.1 Objective**

The long-term objective of this task is to demonstrate the feasibility of control of a fast reactor by computer DAS system. The objective during Phase A is to prepare a preliminary test scope.

### 3.1.8.2 Discussion

The anticipated complexity of the LMFBR control and instrumentation systems in conjunction with the emphasis on reactor safety strongly recommends an advanced plant monitoring system. It is doubtful if a conventional system can provide the required degree of plant control. The Fermi accident illustrated the inadequacy of a conventional system in that the operators improperly evaluated the data allowing fuel damage to occur.

The original scope of the test was expanded from evaluation of an in-refueling cell multiplexer and A to D converter to a computer DAS control channel. The expanded test is more meaningful and will have more far reaching results.

The vendor of the present SEFOR system has indicated that practically all of the present system could be used in the expanded system. The vendor is now preparing a description of the expanded system.

### 3.1.8.3 Suitability of SEFOR as a Test Bed

The SEFOR plant will provide a realistic environment for a computer DAS system. Typical atmosphere, temperatures, and interactions with other systems will exist. The normal outputs from the plant in addition to the outputs from experimental setups will provide a reasonable load for the system. Reactor operational maneuvers to test the transient response of the system will present no problems. The use of the current SEFOR computer DAS system as the base of the expanded system will significantly reduce the costs for the tests.

### 3.1.8.4 Preliminary Test Scope

A computer control channel with reactor control capabilities will be designed and procured for the SEFOR plant. It will be installed in parallel to the manual control system. Both reactor control signals and experimental signals will be fed into this computer control channel. Control indications will be printed out and compared with the actual manual control actions.

The computer control system will be built around the present SEFOR computer DAS system. The expansion of the present system will require in the main, the addition of a disc storage unit, a graphic display unit, and interface modification. The existing computer, multiplexers, A to D converters, paper and magnetic I/O capabilities will be utilized in the expanded system. The expanded system will utilize an in-refueling cell multiplexer and an A to D converter which is made highly desirable by the extensive in-vessel instrumentation anticipated in commercial LMFBR's. In addition to the hardware, a considerable amount of software in the form of programming will be needed.



**3.1.9 Task 3A9 – Pu Capture Ratio**  
No work was performed on this task.

**3.1.10 Task 3A10 - Level Indicators**

**3.1.10.1 Objective**

The objective of this task is to evaluate sodium level indicators and concepts to arrive at one or more systems which have higher reliability, fewer maintenance requirements, and a greater degree of surveillance capability than present systems.

**3.1.10.2 Discussion**

After an introductory evaluation of level probe concepts was made, a small task force, formed to examine level probe technology reached the following consensus:

1. Operating experience in SEFOR, SCTI, EBR II, FERMI, UKAEA, tend to confirm the following observations:
  - a. All level probes concepts can be made to work after a fashion.
  - b. Mechanical design of the probe is not always satisfactory, often because the instrument is not integrated into the plant design at an early stage and compromises in probe design lead to poor reliability.
  - c. Reliability and performance characteristics of a system, mechanical and electronic, can only be determined by testing the system under prototypical operating conditions. A feasibility experiment with an Engineer operating and interpreting the electronic equipment does not necessarily lead to a "commercial" design.
2. An examination of level probe technology shows this to be an area which requires a definitive commitment to designing and testing one or more level probe systems. Many techniques exist for monitoring liquid metal levels and feasibility studies have been performed on many of the concepts. BRD has improved the resistance probe until the design has been almost optimized, UKAEA has developed an inductance probe to the same stage, EBR II is using the buoyancy cylinder probe.
3. The trend at BRD in the past was to use resistance probes to monitor sodium level. For many applications they have been successful, especially as a trip-level indicator where the change in resistance is relatively large when the probe is covered by sodium. Resistance probes have several fundamental defects:
  - a. Contact resistance between probe and liquid can form an appreciable part of total resistance, errors in analogue measurement of level indication can be severe.
  - b. Condensed sodium on the probe changes resistance and gives erroneous level indication.
  - c. Sensitive to surface scum/oxides. Especially if they remain attached to probe as the sodium level falls.

Like all known techniques for measuring level, the resistance probe requires compensation or correction for temperature changes. For some applications in the demonstration plant, this relatively inexpensive, simple level probe may be satisfactory. For this reason it is recommended that operating experience be collected and any design defects noted. Suggestions for improving the design should be incorporated in a state-of-the-art reference design which represents the best resistance probe design available.

**3.1.10.3 Concepts Chosen for SEFOR Reactor**

A need exists in the SEFOR reactor vessel for a reliable level probe as alternate to the existing resistance type. This need may become more severe if level measurement becomes critical parameter during high temperature operation. After examination of level measuring concepts, the task force recommend that two level probe instrumentation systems be designed and operated in SEFOR, and these systems be based on the inductance probe and the buoyancy cylinder. The inductance probe was chosen because of the extensive development of a commercial design by the UKAEA and other suppliers. During a visit to UKAEA Laboratories at Risley, (by D. A. Greene) rig operators reported excellent reliability of these level probes. Commercial designs are available to measure level changes in the range 1 foot to 6 feet, and UKAEA report designs are available with an active length of 40 ft. The Buoyancy Cylinder/Load Cell design was chosen because of the good reliability and operating experience with this instrument system in EBR II. They report that this design will replace other concepts throughout the reactor system.

It is essential that long term operating experience is obtained with an instrumentation system under typical reactor conditions to provide the knowledge for reliable Demonstration Plant level measurements. The task force believes both of these systems have the potential to fulfill many of the level probe requirements. Both systems have had

extensive operating experience with good reliability. Conceptual designs for an inductance probe (Figure 3A10-1) and a buoyancy cylinder probe (Figure 3A10-2) were reviewed by the task force, and altered to reflect the ideas of the members. A specification for a level measuring system for SEFOR was prepared and reviewed.

#### 3.1.10.4 Development of Level Probe Concepts

The task force also recognized that the concepts chosen above may not fulfill all demonstration plant requirements. Table 3A10-1 was generated to attempt to match demonstration plant requirements with level measuring concepts. Initial attempts to complete the table confirmed that specific applications in the reference plant design could not be easily met by the concepts described above. For example:

- a. Level measurement in the steam generator central relief duct.
- b. Wet well level measurement on reactor vessel.
- c. Measurement of level in IHX.

For some applications, iteration between design, development and instrument engineers might produce system changes which would allow the use of above concepts.

Until further iteration and examination of plant requirements is completed, the task force cannot recommend that any specific level measuring concept undergo feasibility testing and development. A description of level measuring techniques and concepts follows.

#### 3.1.10.5 Description of Level Measuring Techniques and Concepts

##### Resistance "J" Level Probe

#### SEFOR

##### Design

- Restricted and angled opening provided through head.
- Initial probe could not be removed without partial removal of core or destruction of the probe.
- Range of probe, and hence, probe length to diameter ratio produced a poor transducer design. Distortion and broken leads due to thermal effects.
- Initial probe forcibly removed from head, replaced with narrower diameter, curved probe. Only real change from initial probe is the new design is removable.

##### Environment

- Surface scum on sodium causes erroneous reading, can remain on probe even when level falls.
- Sodium vapor film creates a short circuit across measuring element tube.
- Probe is inaccurate unless wetted by sodium. Contact resistance can be an appreciable part of the probe resistance, because of inherent low resistance of thin wall tube.
- Activation of probe can cause handling problems at later stages of life.
- Because of relatively fragile design, the probe may be damaged by a reactor explosion, leaving no level measurement when most needed.

##### Data Acquisition

- The probe has an inherently low resistance, care required in making electrical contacts.
- Initially problems were found in using commercial instrument to monitor resistance changes. These included:
  - Overheating of auto-transformer
  - Interaction between probes in the vessel
  - Method of measuring resistance
 These problems have been overcome by using different power supply and constant voltage regulation at probe terminals.

Table 3A10-1

TABULATION OF FEATURES OF ANALOGUE LEVEL METEE CONCEPTS AND APPLICATIONS

Descriptive Features												Design Application
Dimensional Requirements												Dimensional Restraints
Penetration Dia.	6"	6"	3"	3"	3"	3"	3"	2"	10"	3"	3"	
Above Head Dia.	2"	2"	2"	2"	6"	12"	12"	6"	6"	12"	2"	
Above Head Length	NA	NA	NA	NA	12"	12"	12"	12"	6"	12"	60"	
Skew Angle of Insertion Path	5-10°	5-10°	0	0	5-10°	0°	5-10°	10-15°	NA	5-10°	0°	
Functional Capabilities												Functional Reqmts.
Range	5'	5'	20'	20'	20'	40'	40'	40'	40'	40'	40'	
Accuracy	±5%	±5%	±5%	±5%	±5%	±2%	±2%	2-5%	2-5%	2-5%	±5%	
Resolution	1%	1%	1%	1%	1%	0.1%	0.1%	1%	1%	0.1%	1%	
Time Constant (sec)	4.0	4.0	0.1	0.1	—	0.01	0.1	10	1.0	0.1	0.1	
Reactor Downtime for Probe Maintenance	8 hrs	8 hrs	0	0	8 hrs	8 hrs	8 hrs	8 hrs	20 hrs	8 hrs	0	
Concept Tolerance												System Environment
Temp. Change	low	med	low	med	high	high	low	low	med	med	high	
Mechanical Motion	high	high	low	low	low	high	high	high	med	high	high	
Adjacent Flow	high	high	high	high	low	high	high	low	low	high	high	
Sodium Impurity	low	low	low	low	high	high	high	high	med	high	high	
Pressure Change Rate	high	high	high	high	med	high	low	low	high	med	high	
Sodium Frosting	low	low	med	med	low	low	med	med	?	med	high	

Estimated Values Only

\*TDR Time Domain Reflectometer

Calibration

- Calibrated probes using a dip-stick technique.
- Temperature calibration included, to some extent, by using compensating resistance.
- Calculation and preliminary resistance measurement did not match exactly. Further resistance change after short-term operation in sodium.

SGTR

Design

- Probe used in evaporator and superheater units was scaled electrically from SEFOR design, mechanical design not improved.
- No provision was made in superheater design to insert a level probe. Probe added by difficult field modification.
- Mechanical design resulted in broken leads, etc., requiring field changes in design.
- Evaporator unit has side-arm to use in level measurement. A similar feature is planned for demonstration plant unit.

Environment

- The side-arm on the evaporator has insufficient heating capacity. Potentially, this could cause a problem with the side arm becoming a cold leg and trapping impurities.
- The SGTR sodium system operates with continuous cold trapping of impurities resulting in extremely clean sodium circuits.

Data Acquisition

- No problems experienced in power supply or normal operation
- Drift in calibration of GEMAC transmitters and recorders during operation. Can be recalibrated without removing probe.
- When level probe developed fault and went open circuit, an attempt was made to operate the superheater unit without a level indicator, by reading two thermocouples close to surface. Level increased resulting in leakage of sodium from flange.

Calibration

- The "empty" resistance was measured with the side-arm heated by trace heaters. Knowing the active length of the probe, the change in resistance per unit length was calculated.

**Building "D" Loops (San Jose)**

Design

- Most of the probes are very short in active length, approximately 12" to 15" long. Inherently, strong mechanical design resulted.
- Level probe is not in a complex geometry, usually in a simple sodium pot.

Environment

- Most of loops contain relatively clean sodium with less chance of surface scum forming.
- Vapor bridging in high temperature sodium has been observed.

Data and Calibration

- Similar technique to that used on SGTR. In some cases, the calibration is checked against a dip-stick level probe.

**Inductance Probe**

Several different techniques of using changes in the inductance of coils to measure sodium level are used. From a practical viewpoint, the two main divisions are:  
Analogue measurement  
Digital measurement

For the first class of probe, commercial designs are available to measure in the range of 1 ft. to 6 ft. The UKAEA Reactor Engineering and Materials Laboratory claim the technique can be used for 40 ft. measuring range with good accuracy. The coil contained in a thimble, is typically 1.5-inch diameter. Basic problems in using this technique are:

**Coil Fabrication:** UKAEA claim the problem of making a mechanically robust sensor with windings capable of resisting high levels of temperature and radiation has been virtually eliminated. They have developed bifilar windings of mineral insulated, stainless steel sheathed nichrome brazed to a robust central support tube. The braze material diffuses through the S/S sheath at high temperatures limiting the life at 900°C. At 700°C, excellent stability is claimed.

**Effect of baffles, etc.:** The inductance of the coil is affected by massive metal structures in the vessel causing non-linearity, and spurious level indications. This problem is overcome by defining the electrical boundary seen by the coil. A 4-inch diameter sheath, concentric with the thimble, gives the same electrical fields associated with the coil as an infinite sea of sodium.

**Electronic Equipment:** The mutual inductance of the sensors is low, with a change of ~25% between "empty" and "full" values. This requires specially designed electronic equipment to avoid earth loops and inductive pick-up. The UKAEA have designed such equipment and it is available commercially through English Electric. At least one other supplier of induction probe meters is available, Mines Safety Appliances Research Corporation.

**Vapor Film and Surface Scum:** The manufacturers claim that the operation of the level probe is virtually unaffected by these problems because the change in inductance is a bulk sodium effect. The sodium effectively forms a single short circuiting turn. A thin film of vapor on the thimble will be seen as a thin film, not as a bulk fluid effect; since its depth is a small portion of the depth of field of the coil. In a similar manner, a local buildup of impurities will only have a local effect on a portion of the coil.

**Calibration:** (ANL 7153, UKAEA & English Electric Data sheets) The level sensor is temperature dependent and corrections are required to compensate for variations. Most of the published reports used an isothermal sodium pool in investigating the level probe performance, no information on correcting for temperature gradients along the coil has been found. The temperature correction has three components:

- Temperature coefficient of resistivity of sodium
- Temperature coefficient of resistivity of thimble
- Temperature coefficient of coil.

All reports indicate temperature correction is fairly simple and straightforward.

For all induction probes, the calibration is non-linear close to the ends. The effective working length is approximately  $L-2d$  where  $d$  is the coil diameter. For accurate results, some form of "dry" measurement is required to set the zero value. This requires the probe to be at normal operating temperature without sodium surrounding the pocket. However, since the electrical boundary is defined by a shroud, this calibration check can be made in a separate rig. Some form of on-site calibration might be required during plant commissioning tests.

### Ultrasonic Level Transducer

#### Basic Concept

A series of pressure pulses are reflected from the sodium/argon interface. The time of transit for the reflected pulse to return to a detector is a measure of the path length, and hence, the sodium surface position. High frequency pressure pulses, often called ultrasonic sound, are generated by typically a piezo-electric crystal. The same crystal may also become the detection element.

#### Source

- A potential high temperature source is piezo-electric crystal. This material is under active development throughout the world. A local firm is willing to cooperate with GE in providing a crystal transducer suitable for mounting in sodium.
- If the passage of a sound pulse along a gas column proves to be a practical possibility, a loudspeaker source would need to be developed.

#### Feasibility Studies

Dorfman & Boyd (DCM 150-18) Gas Column: A loudspeaker/microphone transducer emitted sound which travelled through an air space in a tube to a water/air interface. Here the pulse was reflected back along the gas column

in the tube to the microphone/loudspeaker. The time between emitting the pulse and detecting the reflected pulse was as predicted for the experimental set-up. The basic equations are:

$$C_m = \text{speed of sound in medium} = \frac{1}{m K}$$

where  $m$  = density of medium

$K$  = compressibility of medium

$$\text{Length of gas column} = L = \frac{C_m * t}{2}$$

where  $t$  = time between emission and detection

#### Source

The noise source was a electro-mechanical device which "rings" when pulsed by a step change in voltage. As a result, the pressure pulse is a damped oscillation at a frequency governed by the resonant frequency of the coil and mounting. Similarly, the detector responds with a damped oscillation to the reflected pulse.

#### Questions:

- Can a noise source of sufficient power be accommodated into the reactor system?
- Can the mechanical stiffness be increased until the damped oscillations have a total period which is small compared to expected transit times?
- If the sound frequency is increased towards very high frequencies, to move away from random noise source frequencies present normally in the plant (ranging up to 15 kHz), will the dispersion and attenuation increase reducing the effectiveness of detection?

#### Multiple Reflections

The transit time depends upon the speed of sound which is a function of gas composition, pressure and temperature. It is suggested that errors associated with changes in density can be reduced to a practical level by using a "reflection datum ring"

#### Question:

- Will a datum point reflector work?
- Will the reflector increase the attenuation and dispersion to such an extent that the signal to noise ratio causes detection problems?
- Will multiple reflections from the ring and sodium surface give a confusing signal by overlapping because of "ringing" of transmitter/detector?
- If a high frequency source is used, multiple reflections may be produced by holes in the carrier tube. These holes are required to allow the sodium and cover gas to move into or out of the carrier tube. Will these multiple reflections further degrade the signal.

#### Signal Interpretation

After the reflected pressure pulse is detected, the electronic signal must be transposed into a level measurement.

#### Questions:

- Will random loud noises produced during plant operation, such as remote closing of a valve using hydraulic piston, cause the detection system to overload or saturate and cause a reactor scram?
- During a reactor scram, the background noise level increases several orders of magnitude as valves close, pumps stop and start, etc. Will this cause faulty readings during a period when the level controller may be a critical component?

Expense

- Since a fairly sophisticated electronic emission/detection system is required, will the expense prove prohibitive?

NOTE: It is extremely unlikely that a piezo-electric transducer can supply sufficient power transfer into the gas column because of the impedance mismatch as the transducer/gas interface. An electro-mechanical speaker/microphone system is possible choice.

If the emitter/receiver can be mounted within a liquid the time taken for the pulse to transverse, a liquid column can be used to measure level.

Two methods have been suggested:

Direct measurement

- The emitter/detector is within the high temperature sodium. This requires a high temperature, sodium compatible transducer. No such transducer exists at present, but they are under active development, including:
  - Bentley, UKAEA and Argonne National Laboratories (barium niobate piezo-electric crystals)
  - Saratoga Systems: uses (commercial) crystal mounted on a MONEL 400 metal diaphragm suitable for operation up to possibly 900°C.

Waveguide measurement

- A liquid filled tube is used as a waveguide to transmit the pressure pulses to a low temperature region. The transducer is coupled directly to the fluid. A low temperature transducer can be used with NaK as the intermediate fluid. The NaK is separated from the sodium by a diaphragm.

Feasibility Studies Atcheson & Boyd ACSA 144

- All of the tests to date have been performed at ambient temperature using water to simulate sodium. Dorfman & Boyd (CDM 150-18)
- Attenuation and dispersion produced in a solid waveguide makes it unsuitable for operation.
- Coupling the pressure source to the fluid column is quite difficult, care must be taken in alignment of the crystal and tube axis as an example.

Alignment of probe

- With temperature gradients and possibly vibration of the long, thin tube, will alignment become a problem?
- At any liquid/solid interface, such as the diaphragm separating the waveguide, fluid from the tank fluid; the signal is attenuated strongly (40dB)

Sonic power generation

- Can sufficient power be transferred into the NaK column to give a strong reflected pulse at the detector.

Operating frequency

- The attenuation of the signal is also a function of frequency of pulse.
- What is optimum frequency, and frequency limits for level prove?

Multiple reflections

- The same questions on multiple reflections arise as in the gas column technique

Detector

- The same questions on the performance of the detector circuit under plant generated noises apply here as for the gas column technique  
Other questions which arise in using a liquid path length include:



**Bends**

- For one suggested design, a J type of waveguide would be used so that the pulse can be reflected from the underside of the sodium/covergas interface. The transducer would be either in the cover gas or outside the vessel, the pulse would travel along the waveguide.
- Would the dispersion and attenuation produced by the bend prevent detection of the reflected pulse?

**Bubbles**

- One of the most serious defects in the design is the tremendous attenuation produced by even a few gas bubbles in the liquid path. The compressibility of the medium changes, altering the character of the signal.
- Is it feasible to design a level probe and guarantee no serious effects due to entrained gases?

**Economics**

- High temperature transducer: the cost of a flowmeter based on transducers similar to a level meter would be a minimum of \$3,500 with a more probable cost in the range \$20,000 to \$46,000. This system uses a 1/2-inch diameter emitter, has a path length of 24 inches maximum, and operates at 1.5 MHz. The cost of the high temperature crystal to the manufacturer is ~\$200. For a level probe to operate over 20 ft., the probe size would increase to 2 inches diameter, operate at 300 kHz. Assuming the size of the crystal is proportional to the diameter squared, the cost of high temperature crystal to the manufacturer would be of the order of \$2000. To treat the crystal and mount into a suitable probe suggests that the minimum cost of the emitter/detector might be \$4000. To this must be added the cost of electronics to convert the pulses into an analogue of sodium height.

**Force Displacement Level Probe**

**Concept**

When a body is immersed in a fluid, the fluid exerts an upthrust which is equal to the weight of the fluid displaced. (Archimede's Principle).

**Feasibility ANL-7623, EBR-II (Moriarty)**

The buoyance forces on a 4-inch diameter 20-inch long stainless steel cylinder varied from 45 lb in air to 37 lb when approximately 15 inches of the cylinder is submerged. Approximately 0.4 lb change in force per one inch change in sodium level. A level probe based on this principle has been in use on the EBR II primary tank for a couple of years. Operating experience is entirely satisfactory, and, in fact, five more units have been ordered to replace resistance probes in various parts of the plant. No effects due to fluid turbulence or resonance of the cylinder have been noticed.

The Datronics electronic system used in conjunction with the load cell is sensitive to voltage variations and harmonics. A small modification to system has improved stability. The EBR II primary sodium system is very clean and expected problems in oxidizing of bellow did not arise. During maintenance shutdown of reactor temperature is allowed to fall from normal 700°F to 580°F, this changes the level of the sodium by ~6 inches. The level probe indication is within 1/8 inch of calculated level.

The unit is sensitive to changes in density of sodium produced by changes in temperature. A correction can be made to improve accuracy, in general, for EBR II the sodium is considered isothermal along the length of the cylinder.

**Comments and Length**

The basic concept is very simple leading to a robust mechanical design. With correct design, the unit could be used for measuring quite long lengths, however, the sensitivity to small changes in level would be reduced because of the sensitivity, or deadband of the force measuring transducer. As the cylinder increases in length, it may become more flexible and require support spiders. This could lead to jamming of the buoyancy cylinder.

**Bellows**

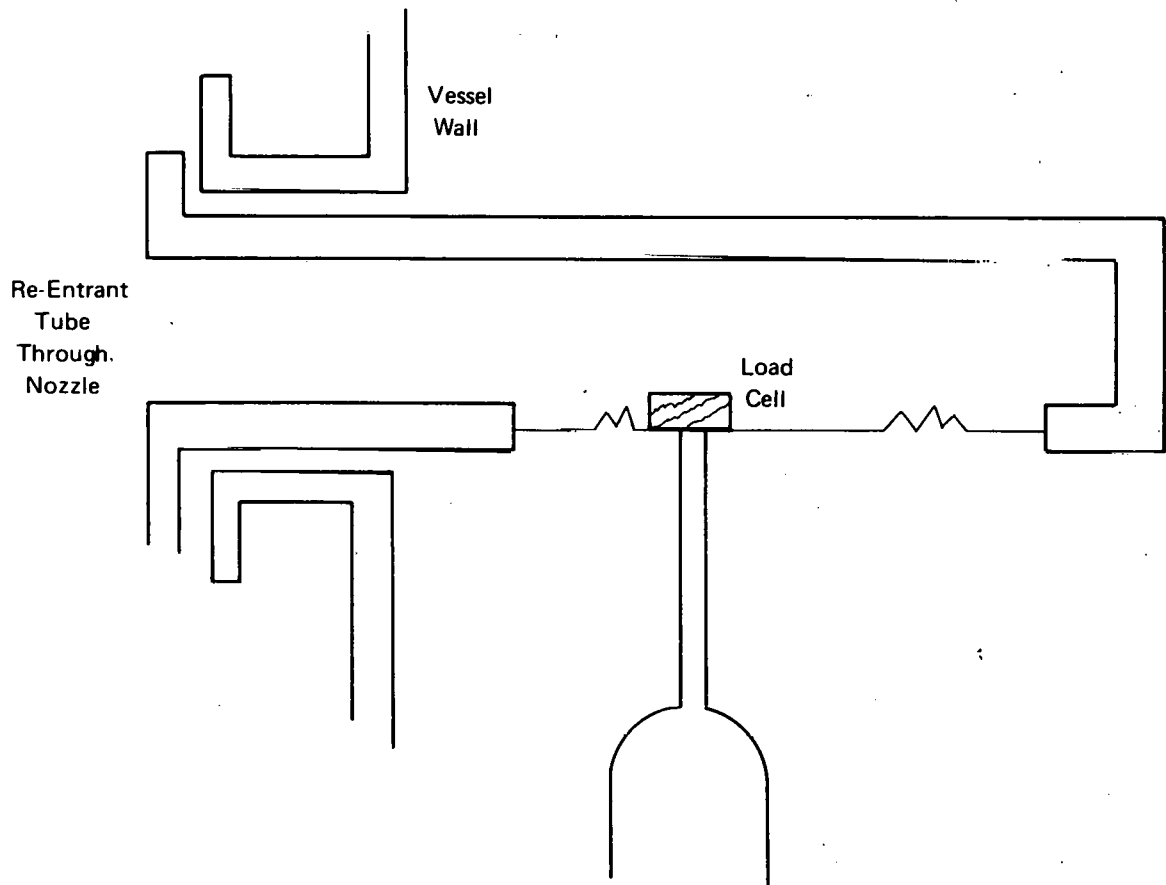
In the EBR II design, the support rod from the load cell to the cylinder uses a stainless steel bellows to give a gas tight seal. This should be changed to a flexible diaphragm.

Force Balancing

A technique for increasing the sensitivity of a long buoyancy cylinder would be to balance the upthrust force outside the reactor head. Differential change in force would then be measured, in effect the externally applied force becomes a range switch.

Steam Generator Design

In the steam generator units it is difficult to provide access through the tubesheets. To overcome this problem, side arm "sight-glass" tubes are provided. The force transducer does not need to have access through the top of the vessel, for example a design such as the following becomes feasible since the active element (buoyancy cylinder) should not need replacing. The movement of the support rod is typically less than 0.050 inch. The buoyancy cylinder can also be used in the "sight-glass" of course.



#### Load Cell

This is a commercial well tested component which is easily maintained and replaced since it is external to the vessel, and in a low temperature and radiation environment.

#### Heat Transfer Level Probes

##### Concept

A heated rod is monitored with thermocouples. As the sodium moves along the rod, the heat transfer coefficient changes reducing the local temperature. The thermocouple responds to the large ( $\sim 100^\circ\text{F}$ ) change in temperature. Although not strictly an analogue level probe, a large number of thermocouples can give fairly small step changes.

##### Feasibility

A level probe of this type was used on the Control Rod rig in BTF, San Jose. It performed well and became the primary level indicator when the gas bubbler tube blocked.

##### Comments

The main disadvantage of this technique is the use of two active components, the heater and the thermocouple. For analogue indication of height, a large number of thermocouples are required. Reliability of thermocouples should be good, even though they are in contact with sodium. Should either the heater or thermocouples fail, the probe must be removed and replaced after repair. Erroneous readings could result from vapor convection cooling, but with sufficiently high  $\Delta T$  this can be avoided. A large number of electrical penetrations through the vessel are required for heater and thermocouples.

An alternative approach is to place the heated rod and thermocouples in a thimble. This allows replacement of the active elements without opening the vessel. Reduced definition in the height measurement is the penalty paid since the heat transfer is not as well defined. One suggested design used hot gas flowing through the thimble, the sodium modifying the temperature gradient along the thimble by improving heat transfer from the hot gas.

#### Differential Pressure Level Gauges

##### Concept

The pressure at a given location in the sodium is a function of the sodium level. Two techniques have been tried:

##### Bubbler

The pressure at the location is defined by the gas pressure required to just inject gas bubbles.

##### Pressure

$\Delta P$ : a NaK filled diaphragm pressure gauge is used to obtain the pressure differential between the cover gas and the datum point.

##### Feasibility

These techniques have been tried at EBR II without success. Low reliability of the pressure gauge and blocking of the bubbler tube were the main problems. A bubbler tube was used on the Control Rod Drive Rig with similar problems.

#### Float Mechanism

The movement of a float on the liquid surface is an indication of level. Moving parts became jammed. Not considered satisfactory.

GENERAL ELECTRIC		816E227
SODIUM LEVEL PROBE		
INDUCTION TYPE		

\*BASIC PROBE REFERRED TO IS THE INDUCTIVE SODIUM LEVEL PROBE AS MADE BY REACTOR EQUIP DIV. OF ENGLISH ELECTRIC.

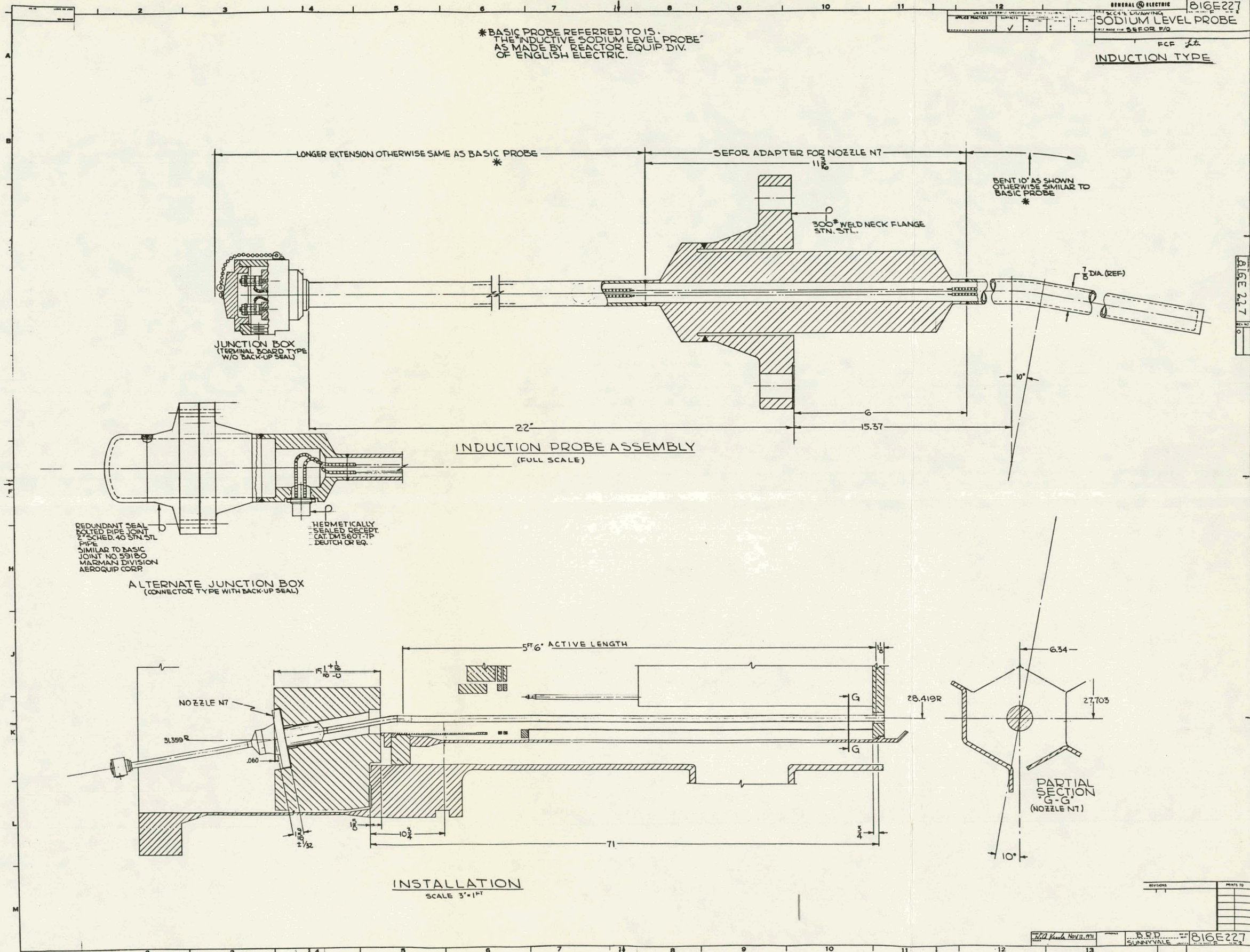
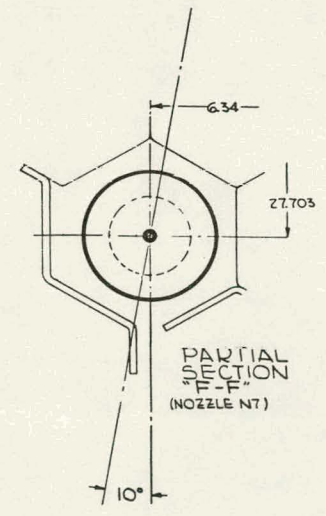
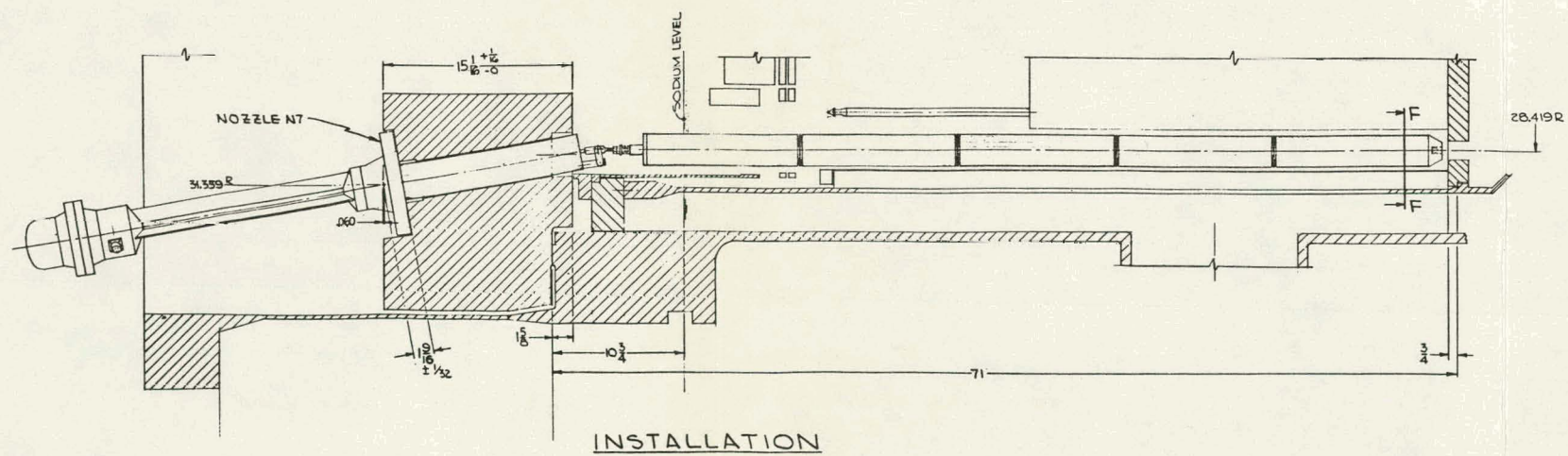
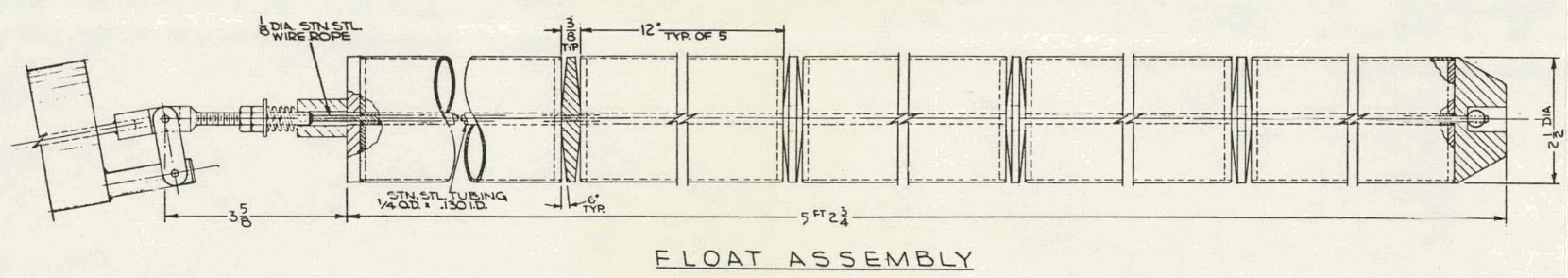
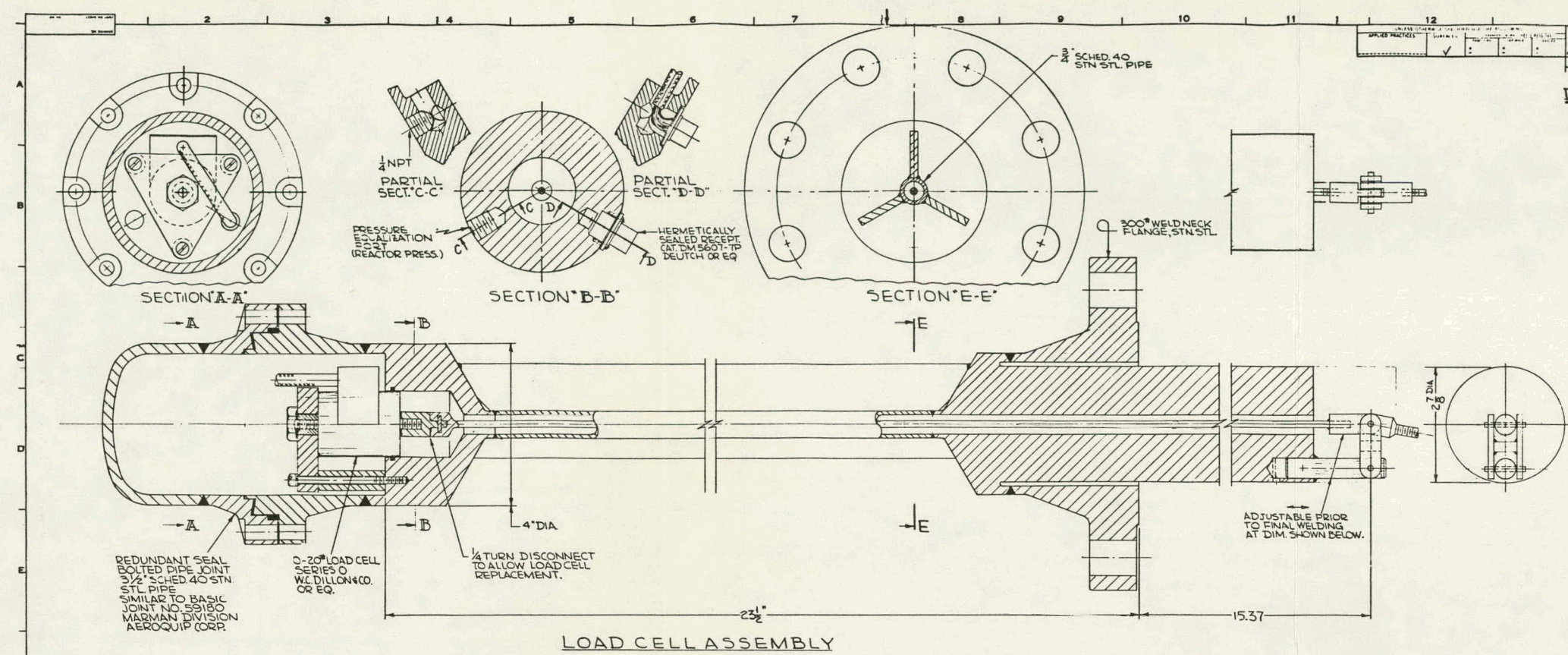


Figure 3A10-1. Sodium Level Probe, Induction Type

GENERAL ELECTRIC 816E227  
SODIUM LEVEL PROBE  
DISPLACEMENT TYPE  
FCF J.6.



INSTALLATION

REV	BY	DATE	DESCRIPTION

Figure 3A10-2. Sodium Level Probe, Displacement Type

REFERENCES

1. Waldo and Christensen, "System for Measuring Sodium Level in EBR II," ANL-7623.
2. Costello, et al, "ADPA Reactor Components Test," APDA-146, November 1962.
3. H. W. Slocumb, "Liquid Level Measurement (Sodium), State-of-the-Art Study," NAA-SR-MEMO 12582, November 15, 1967.
4. "Sodium Level Measurement in PFR," UKAEA REML (Leaflet).
5. McGonegal, Dean and Ferguson, "Measurement of Sodium Level in PFR," Nuclear Engineering International, Vol. 16, No. 175/6 pp 62-65, January/February 1971.
6. G. E. Turner, "Continuous Sodium Level Instruments," Technical Data Record. NAA-SR-MEMO 2825.
7. "Liquid Metal Level Detectors," ORNL-4091, September 1, 1966.
8. John Teats and Pierce, "An Induction Probe for Measuring Liquid Levels in Liquid Metals," ANL 7153, February 1966.
9. Lynch, Personal Communication - Saratoga Systems.
10. Moriarty, Personal Communication - EBR II.
11. Greene, Trip Report UKAEA, Risley, July 1971.
12. Dorfman and Boyd, "Investigation of Two Methods to Measure Sodium Levels," Core Development Memo 150-18, April 1971.
13. Atcheson and Boyd, "Ultrasonic Position Indicator System for a Hydraulically Drive Control Rod. Test Program results," ACSA 144.
14. Hines, Boyd, Marian, "In Core Boiling or Overtemperature Detector Development," NEDC 13650, April 1971.
15. Personal Communication with Schwarz, Schad, Cochran, Kruger, Muir, SEFOR, August 1971.
16. Personal Communication with Scott, Damon, SGTR

### 3.1.11 Task 3A11 – Leak Detectors

#### 3.1.11.1 Objective

The objective of this task was to evaluate and proof test sodium leak detectors which have a greater reliability, fewer maintenance requirements and a greater degree of surveillance capability than are available from present systems.

#### 3.1.11.2 Discussion

The same task force examining level probe technology examined leak detection techniques. A similar approach was being used, of a search of present technology to be followed by a recommendation for installing prototype systems in SEFOR. Two recent reports on sodium leak detection (ANL 7691 "Guidelines for Sodium Fire Prevention, Detection and Control," and HEDL-TME-71-129 "FFTF/LMFBR Methods for Sodium Leak Detection, Fire Prevention and Fire Control," August 1971) were studied in depth. It became obvious from these studies and subsequent discussion within the task force that no single concept was likely to fulfill all demonstration plant requirements. A table was generated to match sodium leak detection concepts against future plant requirements.

One of the most important conclusions reached by the task force was recognizing the importance of early sodium leak detection in the safe and reliable operation of a LMFBR. It is essential that very small sodium leaks be detected and responsive action taken before a major incident is caused by the corrosive reaction products. Since the task force strongly recommends that further work in this area be performed, reliable systems to detect leaks have not been proven, and systems to detect large leaks are questionable, present techniques of leak detection have not yet been proven to have reliable surveillance capability. This is due, in part, to the low incidence of leaks in existing systems. The task force further recommends that the matching of concepts and applications be continued in order to define those techniques which should be developed into operating systems.

Finally the task force recommends that the SEFOR reactor system be examined to match typical application areas to those expected in the demonstration plant. These areas should be fitted with the appropriate leak detection systems and operating experience, and possibly controlled sodium leak experiments be used to refine the systems for the demonstration plant (The sodium leak experiments would be the injection of a few mg of Na into a monitor gas stream, as an example).

**3.1.12 Task 3A-12 – Cold Trap Performance**

**3.1.12.1 Objective**

The objective of this task is to determine the effects of scale up, from small sizes, and performance of a cold trap sized for demonstration plant service.

**3.1.12.2 Discussion**

Reviews of state-of-the-art of sodium cold traps produced two memoranda on the subject:  
D.A. Greene, "SEFOR Follow-On; Cold Trap Performance," September 14, 1971.

L. E. Pohl, "Proposal for New Cold Trap Concept to be Evaluated Under SEFOR Follow-On or Other Sponsorship," December 2, 1971.

The evaluation effort carried out under this task established the following bases for arriving at a concept for testing at SEFOR:

- The cold trap to be tested should be a prototype of the Demo Plant Primary Cold Trap (presently requirements for this 100 gpm unit are as shown in Table 3A12-1 and Figure 3A12-1).
- The design of this cold trap (Demo Plant Cold Trap Reference Design) should embody improvement features to overcome deficiencies of the current state-of-the-art designs.
- Studies of operational experiences with conventional cold traps support the need for significant improvements in design, backed up by appropriate laboratory development testing and evaluation, in order to accomplish the following:
  - Prevent premature plugging in any part of the cold trap circuit or its associated circulation system.
  - Increase capacity for storage and retention of precipitated impurities.
  - Increase cleanup effectiveness to enhance impurity removal.
  - Improve control of cold trap operation to make it less prone to mal-operation and to permit rapid response to transient impurity removal requirements.
- Candidate ideas for improving the conventional cold trap include use of a single zone cooler-crystallizer to prevent premature deposition, use of devices or techniques to induce progressive loading of the cold trap volume in order to optimize its utilization, employment of forced turbulence to increase impurity removal rates, use of NaK cooling (instead of gas) for more flexible heat transfer and temperature control, and modularization of the cold trap crystallizer to aid in controlling deposition and to facilitate disposition of spent traps.

**3.1.12.3 Prototype Tests at SEFOR**

*Plant Modification Requirements*

- Space and facilities are required at SEFOR to install the trap, economizer, recirculation loop, impurity injection station and valved connections to and from the main secondary system.
- During a visit to the site, it was established that space for such equipment is available within the secondary sodium building, if some of the sodium receiving equipment were removed, or outside of the building south of the main air blast cooler. Piping connections to the secondary system could be readily added for either location. The inside location is favorable from the standpoint of economy, weather protection, operator convenience and availability of utilities. The outside location is advantageous for heat and noise dissipation and more favorable location of the impurity addition system (possible Na-H<sub>2</sub>O reaction). In either case, there is room in the secondary sodium building for associated control and instrumentation racks.

*Tests*

The cold trap to be tested would be well instrumented for measurements of sodium temperature and flow rates, heat rejection fluid temperatures and flow rates, and heat transfer surface temperatures. Measurements of the



Table 3A12-1

**DATA SHEET  
PRIMARY COLD TRAPS**

Service	Primary Sodium System
Type	Forced Circulation
Number	2 CT-102A, CT-102B
Capacity, lb Na <sub>2</sub> O	2000
<b>Normal Operating Conditions:</b>	
Sodium Flow Rate, lb/Hr	42,500
Sodium Flow Rate, gpm	100 at 720°F
Sodium Temperature, °F	230 - 720°F
Sodium ΔP, psi max.	15
Sodium pressure, psig	—
Sodium retention time, min.	5 min.
Coolant	Nitrogen*
Coolant Duty, Btu/Hr	1,725,000
NaK Temp. °F, in/out	100/300
NaK Flow Rate, lb/Hr	1 x 10 <sup>5</sup>
NaK Flow Rate, gpm	
NaK ΔP, psi	
NaK pressure, psig	—
<b>Nozzles:</b>	
Sodium	2" - Sch. 40
NaK	2" - Sch. 40
<b>Material:</b>	
	Carbon Steel - Sodium
	Nozzle w/transition to 304 SS
<b>Design Conditions:</b>	
Temperature, °F	800°F
Pressure, psig	100/Vac
Code:	ASME - Section III, Class C

\*If feasible; otherwise NaK to N<sub>2</sub>

Table 3A12-1 (Continued)

DATA SHEET  
PRIMARY COLD TRAP ECONOMIZER

Service	Primary Cold Trap	
Type	Counter flow - tube in shell	
Number	2 E-106A, E-106B	
Surface, ft <sup>2</sup>	61	
Heat Exchanger, Btu/hr	5,900,000	
MTD °F	97	
Transfer Rate, Btu/hr °F ft <sup>2</sup>	1000	
Performance:	Shell	Tube
Fluid	Sodium	Sodium
Rate, lb/hr	42,500	42,500
GPM	100	96
Temp., °F, in/out	720/355	200/600
Pressure Drop, psi	10	10
Construction:		
Design Pressure, psig	100-Vac	100-Vac
Design Temp., °F	1200	1200
Nozzles,	2"-Sch. 40	2"-Sch. 40
Tubes, OD/No./BWG	1 inch/78"/18	
Shell, OD/Length	40"/9'-0"	
Code	ASME-Section III, Class C	
Material	304 SS	

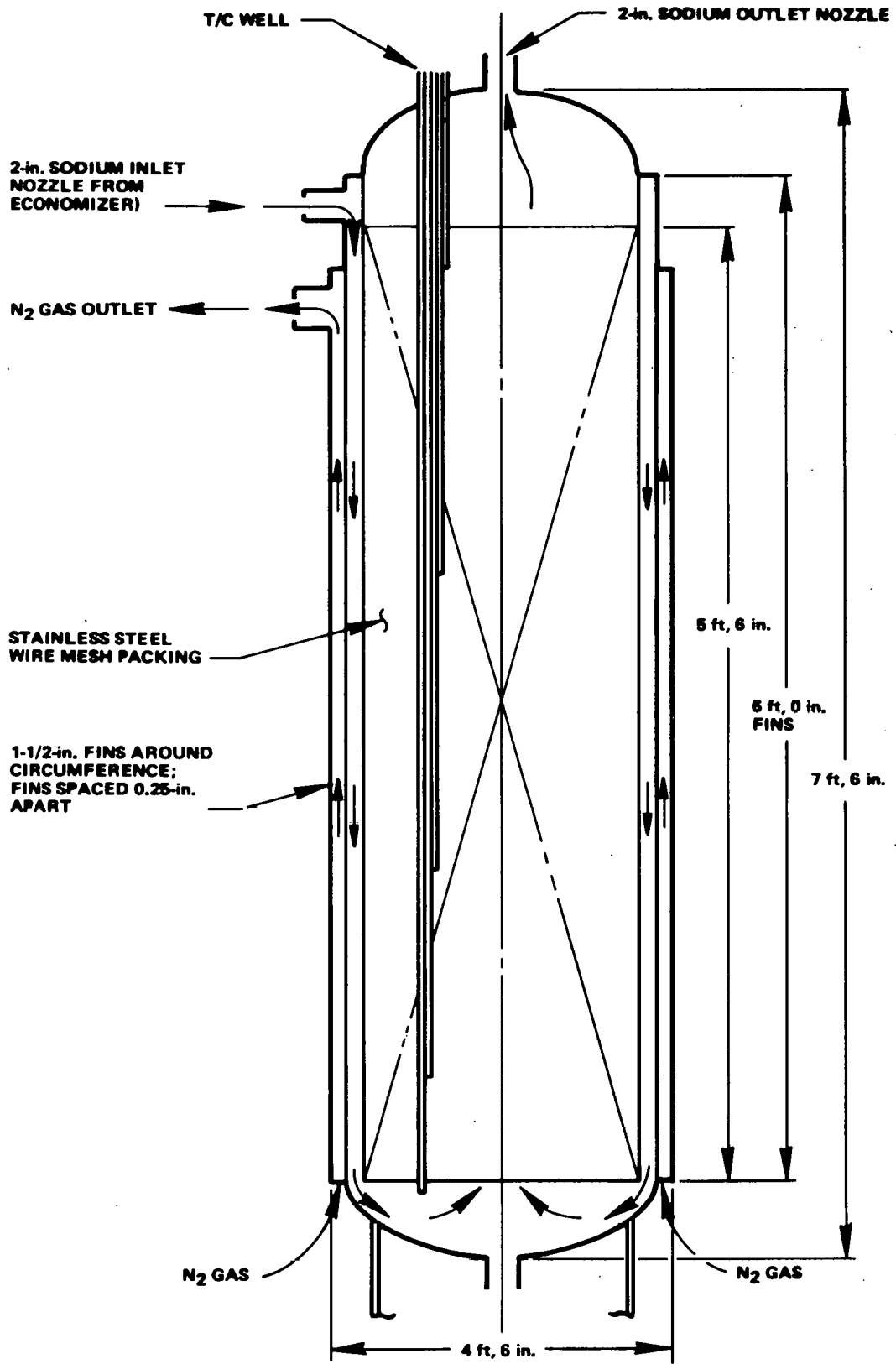


Figure 3A12-1. Primary Cold Trap, LMFBR-Demonstration Plant

Effectiveness of the trap for removal of impurities would be made by controlled injections of moisture with monitoring of the inlet and outlet sodium purity. The same injection technique would establish any tendency toward premature plugging and increase utilization of the crystallizer, and establish the changes in thermal-hydraulic performance, if any, due to buildup of impurities.

### 3.1.13 Task 3A-13 – Vapor Trap Performance

#### 3.1.13.1 Objective

The objective of this task is to determine the performance of sodium vapor traps sized for Demo Plant requirements.

#### 3.1.13.2 Background

Studies of the state-of-the-art of sodium vapor traps consisted of reviews of the following pertinent references:

D.H. Thompson, "Vapor Traps Protect Liquid-Metal Systems," *Power Reactor Technology* 8:4 (Fall 1965), pp. 259-270.

RDT Standard RDT E4-14: Vapor Trap Assembly for Sodium Service (October 1971).

E.L. Kimont, "Engineering Development of a Practical 1200°F Sodium Vapor Trap," *Trans. Am. Nucl. Soc.*, 8(1): 147 (1965).

Based on current requirements for vapor traps on the Demo Plant, it is recommended that the following types be evaluated at SEFOR:

- A dynamic, purge type trap prototypical of that required on the reactor vessel cover gas outlet line for 4-5 SCFM throughput. This trap consists of a 2-inch I.D. tube approximately 10 ft. long. It is surrounded by a heater unit, a guide tube and guide tube insulation. The lower (inlet) end of this tube is in the 1000°F pool region. The upper end is in a 150°F ambient. Because of the unusual configuration of this line (large L/D) and complex heat transfer, there is considerable uncertainty in its vapor trapping capabilities. It appears to be an excellent candidate for performance testing at SEFOR.
- A dynamic, purge type trap prototypical of that required on the primary overflow tank cover gas outlet line. This trap must be capable of accommodating up to 20 SCFM throughput while going from 20 psig to 0 psig as a result of a plant load change. The sodium pool temperature is normally 1000°F.
- A static trap prototypical of that required for cover gas inlet lines. Demo Plant requirements for this type trap have not been defined as yet. It is believed that this type trap will generally be smaller and simpler than the dynamic purge type, although it is possible that it could be the same.

#### 3.1.13.3 Prototype Tests at SEFOR

##### *Plant Modification Requirements*

- Space and facilities are required at SEFOR to install the prototype traps and auxiliary equipment to circulate the vapor and cool the trap.
- During a visit to the site, it was established that some space is available around the SEFOR primary drain tank to install the test equipment. This tank provides a source of high temperature (1000°F) vapor under nearly prototypical conditions due to the pump around reactor overflow system. Space for controls and instrumentation exist in the air zone stairwell above the control drive room.
- An alternative or additional test location is the secondary drain tank. Although it is a stagnant system at present, with lower sodium pool temperatures than the primary drain tank, addition of a suitable pump around circuit could increase the sodium temperature. This would provide a good location for vapor trap testing, with the advantage of full time accessibility.

##### *Tests*

Vapor traps to be tested would be instrumented to measure vapor carryover, cooling and heating requirements, temperature distributions, and effective trapping capacity. Other factors to be evaluated include draining and/or renewal requirements and effects of position or orientation on operation and life.

Table 3A13-1

## DEMO PLANT PURGE TYPE VAPOR TRAPS REQUIREMENTS

Location	Thru-Put SCFM	Condition	Na Pool Temp-°F	Operating Pressure psig	Trap Location
Primary Systems					
Main Loop	4-5	Fission Gas* Sweep	1000	1	Reactor Vessel Closure and Primary Pumps
Over Flow	20	Load Change* (Increase)	1000	20-0	Overflow Tank
FEDAL	0.5	Vent During* System Fill	1000	1	Vent at high point of system
Backup Control	1.0	Vent During* System Fill	720	60	Vent at high point of system
Fuel Storage	0.25-0.5	Vent During* System Fill	800MAX	20	Fuel Storage Tank
Service (Purif.)	10	Blowdown or System Drain	720	50-10	Drain Tank/Exp. Tank in Purif. System
Secondary Systems**					
Main Loop	~10	Load Change	935	175(S.H.)	Pump/Evap/S.H.
Service (Purif.)	10	Blowdown or System Drain	600	75	Sec. Drain Tanks
RACS	0.5	Load Change	1000	175	High Point Exp. Tank
RSCS	0.25	Load Change	600	20	High Point Exp. Tank

\*All part of Gas Rad-Waste System

\*\*Not including Strn. Con. Protection System

**3.1.14 Task 3A-14 – Refueling Cell Equipment**

**3.1.14.1 Objective**

The long-term objective of this task is to obtain experimental verification that critical active components of the equipment will deliver long trouble-free operation in the cell environment.

**3.1.14.2 Preliminary Test Plan**

A test plan was prepared which identified lubrication systems and materials as well as some electrical components as key elements in any system whose longevity would have a direct bearing on the life of the equipment. A test module is proposed to develop reliability data on such components operating continuously in the SEFOR refueling cell.

- A test module will be designed to include a variety of components which are expected to have a critical bearing on the reliability and life expectancy of the major equipment items operating in the refueling cell. These will include bearings, gears, clutches, brakes, seals, switches, and electric motors. The test module will make use of the size and type components which are planned for use in the Demonstration Plant equipment.
- The cell environment of very dry argon differs from a normal air ambient in three significant areas; cooling is impaired because of the lower thermal conductivity of argon; electrical insulation is impaired because of the lower dielectric strength of argon gas as compared to nitrogen or oxygen, and there exists the possibility that sodium evaporating from the pools will deposit on the equipment.
- Because the equipment must be capable of working in a relatively inaccessible space and at times over the open reactor it is highly desirable that lubricating material be kept to a minimum and that its dispersal in the cell be strictly controlled. Part of this task will be devoted to minimum lubrication requirements and to long lived seals.
- Bearings have been developed for space applications which are capable of operating without oil or grease for extended periods of time. Bearings of this type were used in the cover gas of a sodium system of PA-15 loop 3-R with encouraging results. The bearings are made up from a standard chassis (inner and outer races and balls) and a self-lubricating retainer. As the ball rotates in the retainer pocket, minute quantities of the self-lubricating container are transferred to the balls and to the raceway. Bearings of this type will be used in the test module where they will be given accelerated life tests under typical loads in a typical cell environment.
- The retainer material is one of a group of high temperature, rigid self-lubricating materials based on solid lubricant fillers and low shear thermally conductive metal fillers dispersed in a polyimide matrix. This material can be used to make gears and cams in addition to its use as a ball bearing retainer. Its use in these capacities will be considered as a means of reducing lubrication requirements in the cell equipment and suitable components will be incorporated into the test module for accelerated life testing in the cell environment.
- It is expected that the development of the self-lubricating materials will reduce the need for high performance oil and grease seals, however, such devices will still be required in certain areas. The majority of available shaft seals of the type used for in-cell equipment have been developed for automotive use and are relatively inexpensive. Because of the high cost of failure or repair of in-cell equipment, it is expedient to consider alternate designs and materials which will give longer life and then to perform accelerated tests on these devices under realistic environmental conditions.
- Electromechanical clutches and brakes are generally used in the hoisting equipment in the refueling cell. Two types of problems can be anticipated; one with high temperature because of poorer cooling in the argon atmosphere and the second with wear on the friction surfaces in the dry argon atmosphere. The first of these can be solved by using conservative electrical design, but the second can best be answered by an accelerated life test of a typical element in the SEFOR refueling cell.
- One of the operator comments from SEFOR concerning cell equipment was the desirability of hard wiring inside the cell instead of using pin connectors. One of the considerations in the test module design will be to resolve the relative advantages of these two arrangements for making electrical connections both in the power wiring and in the instrumentation signal wiring.

- In the SEFOR plant it has occasionally been expedient to admit an air atmosphere to the refueling cell when special repair procedures were being undertaken. When this is done, there will be reaction between oxygen and water vapor in the atmosphere and sodium deposits on equipment in the cell. In SEFOR, as in older sodium cooled reactors, carbon dioxide has been used as a dry cleaning agent to convert the sodium hydroxide to sodium carbonate so that it can be picked up with a vacuum cleaner. This task will test the effectiveness of this and other cleaning procedures on equipment which is removed from the cell for service or inspection and which is then returned for further use.

### 3.1.14.3 Alternate Concepts.

- The alternate concept of testing whole grapples or cranes in the cell has been rejected because of the space required and because of the difficulty of applying a realistic load under accelerated test conditions. Also, it is difficult to test a number of machine elements in one component.
- The alternate concept of providing a separate test facility has been rejected because it was thought to be a more expensive means of providing the environment. It may be possible to make this alternate more attractive by combining several tests so that each one only bears a portion of the total facilities cost.

### 3.1.15 Task 3A15 – Refueling Hoist and Grapple

#### 3.1.15.1 Objective

The long-term objective of this task is to obtain assurance that the plant equipment will perform reliably following extended storage in the cell argon after having been wet by sodium during operation. The objective during Phase A is to prepare a preliminary test plan.

#### 3.1.15.2 Preliminary Test Plan

A test concept has been selected which will combine two test hoists and grapples with one test tank in such a way as to permit inserting either of the hoists into the tank when the other is moved to one side. One grapple will be exposed to sodium and then stored in argon for an extended period of time before being returned to the tank to determine if there has been a deterioration in performance. During this hold period, it is planned to perform accelerated life tests in sodium of the other grapple.

- The test will be designed to make use of the dry argon atmosphere in the SEFOR refueling cell, but it is to be self-contained and independent of the reactor system insofar as the test sodium system is concerned.
- Two test hoists and grapples will be combined with one test tank in such a way as to permit inserting either of the hoists into the test tank. A dead weight will be provided in the test tank with a grapple attachment so that it can be used to apply a load on the hoist and grapple. The hoist and grapple which is not in the test tank, will be located to one side adjacent to the tank.
- The sodium system will be an integral unit consisting of a dump tank, a test tank, and a purification system. The purification system will consist of a convection cooled cold trap and a D.C. conduction pump. Filling of the test tank will be accomplished by pressurizing the dump tank which will cause sodium to flow up into the test vessel through a metal filter. Sodium will be returned to the reservoir by releasing the gas pressure in the dump tank and allowing a gravity drain from the test tank back to the dump tank.
- Part of the test sequence will be designed to show the effect of long term storage in the cell argon following operations in sodium which have caused wetting of the moving parts. After initial checkout in the cell gas, one of the grapples will be exercised in sodium sufficiently to insure that the working parts are wet with sodium. The operating parameters of the drive such as travel time, equilibrium temperature, motor current and lifting capability will be measured and recorded during the sodium operation. This drive will then be moved to one side and exposed to the cell ambient gas for a period of eight months. Following this prolonged exposure, the hoist and grapple will be returned to the test tank where its performance will be compared with the pre-exposure values. If the schedule permits, a second cycle will be performed.
- The second grapple will be subjected to an accelerated life test in sodium. The cycle will start and end in the full-up position with the following intermediate steps:
  - Drive down and engage the dead weight.
  - Actuate grapple to lock onto the weight.
  - Lift the weight to full-up position then return to full-down position.

Unlock the grapple.

Raise the unloaded grapple to the full-up position.

Cycle testing will be carried out continuously while the cell argon atmosphere is maintained until the equipment fails or until 125% of the demonstration plant design cycles have been accumulated. In the event of failure or when the specified number of cycles have been accumulated, the equipment is to be removed from the cell and cleaned in preparation for detailed inspection.

- To permit major cell maintenance while this test is installed, it may be desirable to return the SEFOR cell to an air atmosphere. To permit this, sodium will be drained from the test vessel into the drain tank where it will be maintained at a low temperature or frozen. A temporary cover will be placed on the tank and sealed with RTV Silicone rubber. The test hoist and grapples which have been wet with sodium will be extended into plastic bags which will be fastened near the upper ends of the tubes just below their support. Argon gas will be bled into the lower end of bags and allowed to leak out near the upper end. Equipment will be used to dry the cell air to a low dew point so as to minimize the sodium hydroxide contamination of the exposed sodium in the cell. Testing of the hoists and grapples should include at least one cycle of returning the refueling cell to an air atmosphere followed by renewed operation of the equipment.

### 3.1.15.3 Alternate Concepts

- The alternate concept of using the SEFOR vessel to expose the grapples to sodium was rejected because it could only be used when the head was off for refueling which limited the test time available, and because it would have been necessary to leave an open channel so as to get enough submersion for the test grapple. This alternate might be satisfactory for the test of exposing a wet grapple to the cell environment, but it would not permit the accelerated life test.
- The alternate concept of devising a system which connected the test tank to the primary sodium system was rejected because it would have increased the radiation level in the reactor cell and would have imposed a number of safety restrictions on operation of the system.
- The alternate concept of providing a separate test facility was rejected because it was thought to be a more expensive means of providing the environment. It may be possible to make this alternative more attractive by combining several tests so that each of them bears only a portion of the total facility cost.

## 3.2 TASK 3B ELEVATED TEMPERATURE OPERATION DEVELOPMENT AND DESIGN

### 3.2.1 Task 3B1 -- Systems

#### 3.2.1.1 Objective

The long-term objective of this task (together with other tasks in 3B) is to determine that SEFOR can operate at an elevated temperature ( $\sim 1000^{\circ}\text{F}$ ). The objectives during Phase A are to perform preliminary stress and thermal analyses for steady-state operation at elevated temperatures and for thermal transients in the sodium system components, and preliminary assessment of nitrogen cooling system changes required for steady-state elevated temperature operation.

#### 3.2.1.2 Plant Tests

In support of the systems work tests were run at SEFOR on the nitrogen cooling system and sodium pumps. Nitrogen cooling system heat balance tests were conducted in September at reactor power levels of 5, 10 and 15 MW. Additional heat balances were run in December at 15 and 20 MW.

Also in September performance tests were run on the main primary and secondary and auxiliary primary and secondary electromagnetic sodium pumps. The test data were reduced to plots of various performance parameters and transmitted to GE-LMGD for their evaluation of the EM pumps capability for high temperature operations. Comparison of the test data with pre-operational test data showed no discernible degradation of performance. Higher efficiencies and lower current and power requirements for the main secondary pumps were realized as the result of the installation of additional capacitors after the pre-operational tests.

#### 3.2.1.3 Sodium System Components Structural Evaluation

As a part of the overall requirement to demonstrate the SEFOR Follow-On Program elevated temperature adequacy, it was necessary to obtain a preliminary determination of stresses in critical regions of components comprising the primary and secondary cooling system.



The basis for demonstrating the elevated temperature feasibility was to determine the highest stressed region during elevated temperature operation and then to initiate a detailed elastic-plastic, creep, analysis on this component to demonstrate the component meets the stress requirement of the new ASME Section III Elevated Temperature Code Case 1331-5 (described in Task 3B2).

A matrix summarizing the results of a preliminary stress evaluation of the SEFOR primary and secondary structural components is presented in Table 3B1-1. Included in the structural evaluation were the reactor vessel, intermediate heat exchangers, pumps, air blast coolers, and all associated piping. In order to establish a better picture for the reader, sketches of the various components analyzed are also included along with the regions of critical stresses.

This evaluation has established the reactor vessel flange as being the most highly stressed region under the operating conditions assumed for the SEFOR Follow-On Program.

The highest stressed regions of the components listed in the matrix exclusive of the sodium piping were identified from a review of the original vendor analysis. A reassessment of the vendor's stress analysis was made using conservative estimates of the thermal gradients expected during elevated temperature operation. Using the thermal gradients as input, the resulting primary plus secondary stress ranges were obtained. In many cases, G.E. performed new structural analysis to obtain the tabulated values in the matrix.

For the main and auxiliary piping systems, flexibility analyses were conducted to determine reactions and highest resultant moments. Stresses were then determined for regions of highest moments using elastic analysis techniques.

Although primary stresses are not significant components of the overall stress range, it was believed that they should be included wherever possible for the sake of completeness. In many instances, the primary membrane plus bending, or local primary membrane stresses were not evaluated because they were relatively small and did not contribute to the overall purpose of this study. Their computation would detract from the effort to obtain the most limiting stress component, namely the secondary stress range.

In addition to establishing the most critically stressed component, the tabulation gives preliminary indication of the differences in applied stresses among various components. This purpose of the tabulation is to pinpoint the highest stressed regions and the numbers should be used to make this assessment. *Because of the conservatism in the analysis no effort should be made to use the numbers for a quantitative indication of feasibility.*

The next highest stressed region is the reactor vessel outlet nozzle which sustains a stress of sixty percent that of the reactor flange to vessel junction.

The fatigue life of each component was not evaluated, primarily because in the new code case the most limiting criteria are the strain limits. Various FFTF vendors have already found this to be so. Furthermore, the extent of the elevated temperature operation for the SEFOR Follow-On Program is only for approximately 10 months. In this time only a limited number of cycles will be applied. A final reason for not conducting a fatigue analysis is that the new ASME elevated temperature code case requires a creep fatigue interaction evaluation. Creep strains must include primary creep, which is non-linear; therefore, within the linear assumptions utilized in this analysis, it was not possible to obtain meaningful results.

In determining the stress range for all the components, only the normal transients such as startup, shut-down, and normal scrams were considered. One additional transient that is now being included in the Phase A extension in the inelastic stress evaluation of the reactor flange is the sodium temperature changes resulting from a loss of on-site power. This omission does not detract from the overall evaluation because the components within the reactor vessel will experience the largest temperature drops as a result of this transient. Temperature drops of other components within the system are attenuated. If the loss of power transient was included in the overall evaluation, the resulting stress range of those components within the reactor vessel will be higher than for other structural components within the system.

Many of the statements made in the remarks column of Table 3B1-1 include the term "scoping calculations". In these instances, it was necessary to re-evaluate the vendor analysis for the thermal transients that are expected on the SEFOR Follow-On Program. When this evaluation was conducted, temperature profiles were established by the use of temperature response charts. Conservative estimates were made of the thermal gradients, and these thermal boundary conditions were utilized in an elastic shell analysis computer program called "SNAP". The SNAP program was used to obtain a more precise assessment of the overall stress picture in the complex geometry of the various components involved in the analysis.

The stress range was the basis for stress comparison because its limitation is utilized in the new code to prevent excessive deformation (strain limits) and the stress range magnitude is used on the new code case to establish whether or not an elastic analysis may be applied.

Table 3B1-1

## RESULTS OF PRELIMINARY STRESS EVALUATIONS

	INTERIM ELASTIC STRESS EVALUATION			EST. MARGINS*		Remarks	Operating Temp. °F
	Est. Primary Stress			Based on Primary Stress	Based on Secondary Stress		
	psi	Membrane + Bending	Est. Secondary Stress Range (for Fatigue Evaluation)				
I. MAIN PRIMARY SYSTEM See Figure 1 for location of regions tabulated							
A. Reactor Vessel (Figure 2)							
1. Flange Shell Junction	1,400	1,400 +	70,000	0.90	-.30	Extrapolated from flange rotations predicted and verified by measurements at 800°F operation.	1,000
2. Outer Head Bolts	500	500 +	8,400 Membrane <12,500 Membrane + Bending	.91 .91	.28 .28	Stresses may be lowered by reducing bolt preload; any seal leakage will be restrained by the installation of a new seal	< 800
3. Outlet Nozzle	1,000	9,500	42,000	.93	.21	Based on Vendor Calculations (United Nuclear Corp.)	1,000
4. Outer Head	Small	Small	3,000	<1.0	.94	Estimate from G.E. calculations conducted at 800°F	<700
5. Inner Head	Small	Small		<1.0		Based on Vendor Calculations (United Nuclear Corp.)	600
6. Seal Ring	4,600	~4,600	15,000	.68	.73	Based on Vendor Calculations (United Nuclear Corp.)	900 +

\*Margin is defined as  $\frac{\sigma_{allow.} - \sigma_{applied}}{\sigma_{allow.}}$

Table 3B1-1 (Continued)

RESULTS OF PRELIMINARY STRESS EVALUATIONS

	INTERIM ELASTIC STRESS EVALUATION			EST. MARTINS		Remarks	Operating Temp. °F
	Est. Primary Stress		Est. Secondary Stress Range (for Fatigue Evaluation)	Based on Primary Stress	Based on Secondary Stress		
	psi Membrane	psi Membrane + Bending					
B. Hot Leg Piping See Figure 3 for location of highest stressed pipe	<<2,300	2,300	3,300	.83	.93	Expansion stress based on G.E. calculation for 1000°F operation; highest stressed point at a constant support hanger	1,000
C. IHX (See Figure 4)							
1. Shell-Adjacent to Primary Nozzle	<<1,700	1,700	~6,000	.89	.89	Based on G.E. scoping calculations for 1000°F operation. Caused by difference in film coefficient between nozzle I.D. and shell I.D.	1,000
2. Primary Nozzle	1,000		22,000	.93	.60	Based on G.E. scoping calculation for 1000°F operation	1,000
3. Secondary Nozzle	2,400		20,100	.82	.63	Based on G.E. scoping calculations for 1000°F operation	1,000
4. Tube at Tube Sheet Junction	2,500		15,000	.82	.73	Based on G.E. scoping calculations for 1000°F operation	1,000
5. Tube at the Last Tube Support	1,000		27,000	.93	.51	Based on G.E. scoping calculations for 1000°F operation (caused by thermal expansion of tubes)	1,000
D. Pump (See Figure 5)							
1. Rigid Connection of Suction to Discharge Line (See Figure 4)	1,300		13,000	.91	.76	Based on Pump Vendor calculation modified for 1000°F	900

Table 3B1-1 (Continued)

RESULTS OF PRELIMINARY STRESS EVALUATIONS

	INTERIM ELASTIC STRESS EVALUATION			EST. MARGINS		Remarks	Operating Temp. °F
	Est. Primary Stress		Est. Secondary Stress Range (for Fatigue Evaluation)	Based on Primary Stress	Based on Secondary Stress		
	psi Membrane	psi Membrane + Bending					
E. Cold Leg Pipe (See Figure 6)	1,800	2,400	9,000	.87	.83	Expansion stress based on G.E. calculation for 1000°F operation; complete stress evaluation made; highest stress point is at an elbow	900
F. Drain Tank	2,000	+2,000	2,000	.85	.96	Maximum membrane stress. Local primary membrane plus bending is slightly larger but not significant enough to calculate (Pressure 20 psi; diameter 114"; thickness .565") No significant thermal stresses. Max sodium injection rate of 25 gpm into a minimum 1300 gal. storage	<1,000
G. Pump Around Pump	2,000	2,000	2,000	.85	.96	From G.E. calculations (No significant secondary stresses)	<1,000
<b>II. AUX. PRIMARY SYSTEM</b>							
A. Hot Leg Piping (See Figure 7 for Highest Stressed Pipe)	450	700	32,000	.97	.41	G.E. estimate for 1000°F from original vendor (Sargent Lundy) analysis. Stresses are given for the highest stressed pipe section	1,000
B. IXH (Similar to Main IHX, Figure 4)							
1. Shell-Adjacent to Primary Nozzle	350	Small	~6,000	.98	.89	Based on G.E. scoping calculations for 1000°F operation. Caused by the difference in heat transfer film coefficient between the nozzle and shell.	1,000

Table 3B1-1 (Continued)

## RESULTS OF PRELIMINARY STRESS EVALUATIONS

	INTERIM ELASTIC STRESS EVALUATION			EST. MARGINS		Remarks	Operating Temp. °F
	Est. Primary Stress psi		Est. Secondary Stress Range (for Fatigue Evaluation)	Based on Primary Stress	Based on Secondary Stress		
	Membrane	Membrane + Bending					
2. Primary Nozzle	165	Small	22,000	.99	.60	Based on G.E. scoping calculations for 1000°F operation	1,000
3. Secondary Nozzle	300		19,900	.98	.64	Based on G.E. scoping calculations for 1000°F operation. Caused by sodium temperature difference between the nozzle interim and heat exchanger shell	1,000
4. Tube at Tube Sheet Junction	2,500		15,000	.73	.72	Based on G.E. scoping calculations for 1000°F operation	1,000
5. Tube in the Bend	630		26,000	.96	.52	Based on Vendor calculations (Caused by thermal expansion of tubes)	1,000
C. Pump (Figure 8)							
1. Outer Wrapper	3,000		3,500	.78	.94	Based on original calculation from G.E. Large Motor Gen. Dept.	900
D. Cold Leg Piping (Figure 9)							
	1,500	2,500	27,000	.88	.50	Based on G.E. estimates from 1000°F operation from original Vendor calculation (Sargent Lundy)	900
III. MAIN SECONDARY							
A. Hot Leg Piping (Figure 10)	1,800	3,000	19,000	.86	.51	Based on G.E. estimates for 1000°F operation from original Vendor calculation (Sargent Lundy)	900

Table 3B1-1 (Continued)

RESULTS OF PRELIMINARY STRESS EVALUATIONS

	INTERIM ELASTIC STRESS EVALUATION			EST MARGINS		Remarks	Operating Temp °F
	Est. Primary Stress psi Membrane Membrane + Bending	Est. Secondary Stress Range (for Fatigue Evaluation)	Based on Primary Stress	Based on Secondary Stress			
B. Air Blast Cooler (See Figure 11)							
1. Manifold cap junction with tube sheet	5,400	5,400 +	30,000	.64	.45	G.E. estimates for 1000°F operation from vendor analysis	800
2. Tube at tube sheet junction	1,500	1,500 +	32,600	.90	.40	Obtained from G.E. scoping calculations	800
3. Tube at last tube support	600	Small	14,400	.96	.73	G.E. estimate for 1000°F normal calculation from vendor analysis	<800
C. Main Secondary Cold Sodium Piping (See Figure 12)	1,800	Small	33,700	.87	.38	Based on G.E. estimate for 1000°F operation from original vendor calculation	800
D. Pump (Similar Configuration to Figure 5) Rigid Connection of Suction to Discharge Line	2,000	2,000 +	29,000	.85	.47	Obtained from G.E. scoping calculation	800 +
E. Drain Tank	5,200	5,200	5,200	.62	.91	Small temperature changes	800
F. Expansion Tank	2,100	2,100	2,100	.85	.96	Small temperature changes	800
IV. AUX. SECONDARY SYSTEM							
A. Hot Leg Piping (See Figure 13)	1,500	1,750	8,000	.89	.85	G.E. extrapolation of Sargent Lundy's results	900

Table 3B1-1 (Continued)

RESULTS OF PRELIMINARY STRESS EVALUATIONS

	INTERIM ELASTIC STRESS EVALUATION			EST. MARGINS		Remarks	Operating Temp. °F
	Est. Primary Stress		Est. Secondary Stress Range (for Fatigue Evaluation)	Based on Primary Stress	Based on Secondary Stress		
	psi	psi					
	Membrane	Membrane + Bending					
B. Air Blast Cooler							
1. Manifold Cap Junction With Tube Sheet	5,000	—	24,000	.63	.56	G.E. extrapolation of vendor analysis	800
2. Tube at Tube Sheet Junction	1,500	1,500	32,600	.90	.40	Obtained from G.E. scoping calculation	<800
C. Cold Leg Piping (See Figure 14)	1,500	2,100	14,000	.89	.74	Based on extrapolation of vendor analysis	800
D. Pump (Similar to Figure 8) Outer Wrapper	3,000	—	20,000	.78	.63	Based on extrapolation of vendor analysis	800
E. Expansion Tank	1,600	—	Small	.88	<1.0	Based on extrapolation of vendor analysis	900

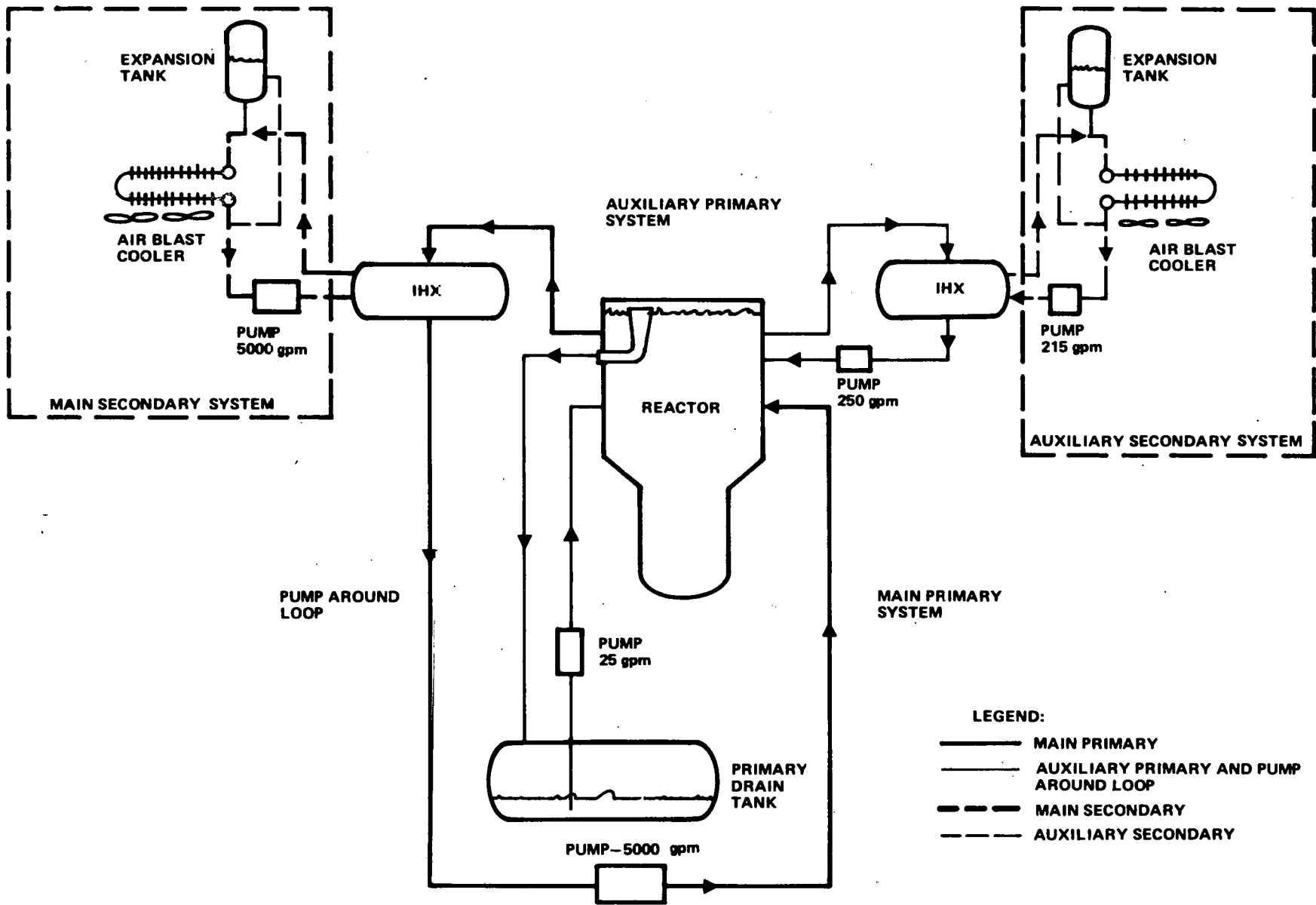


Figure 3B1-1. SEFOR Sodium Systems



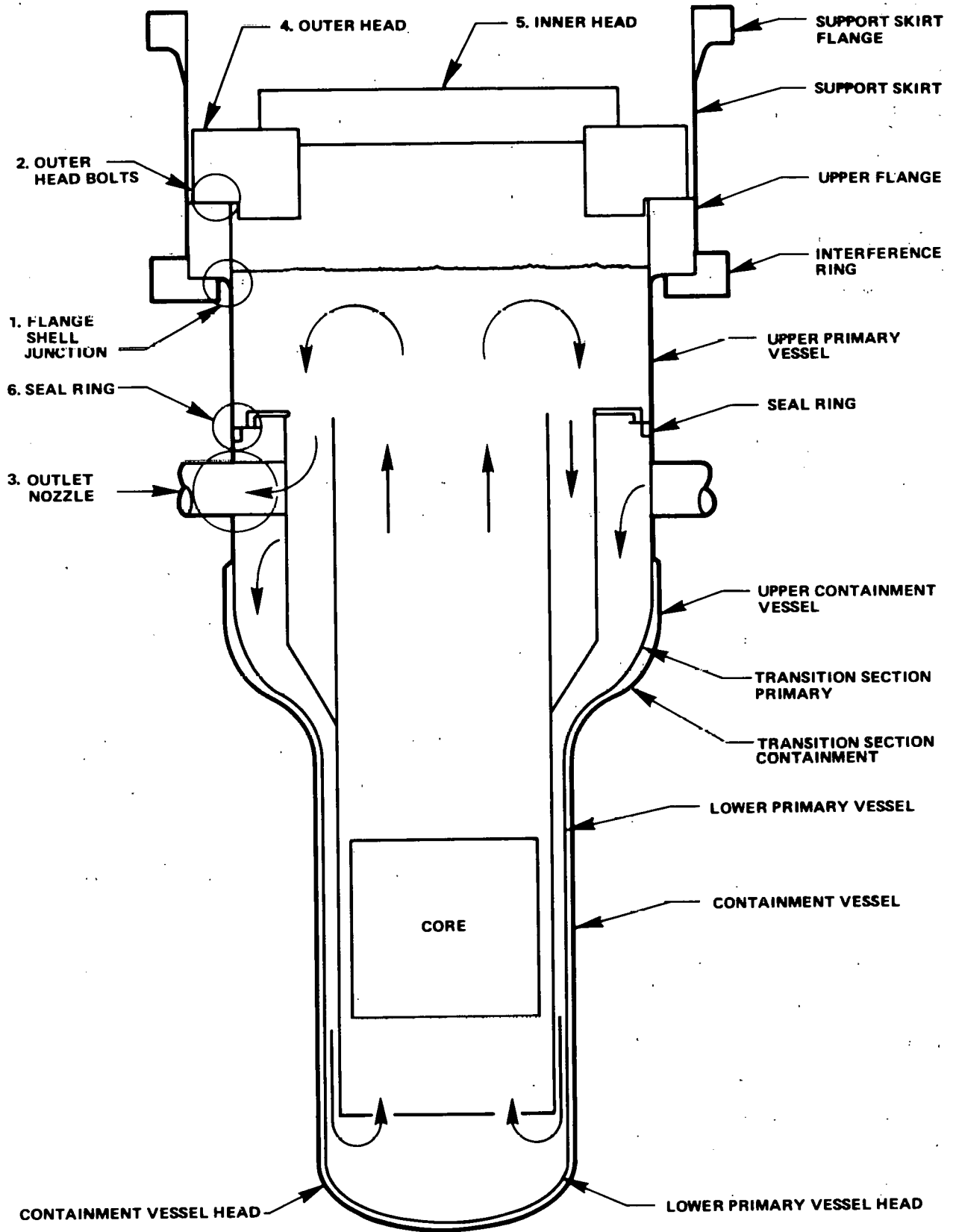
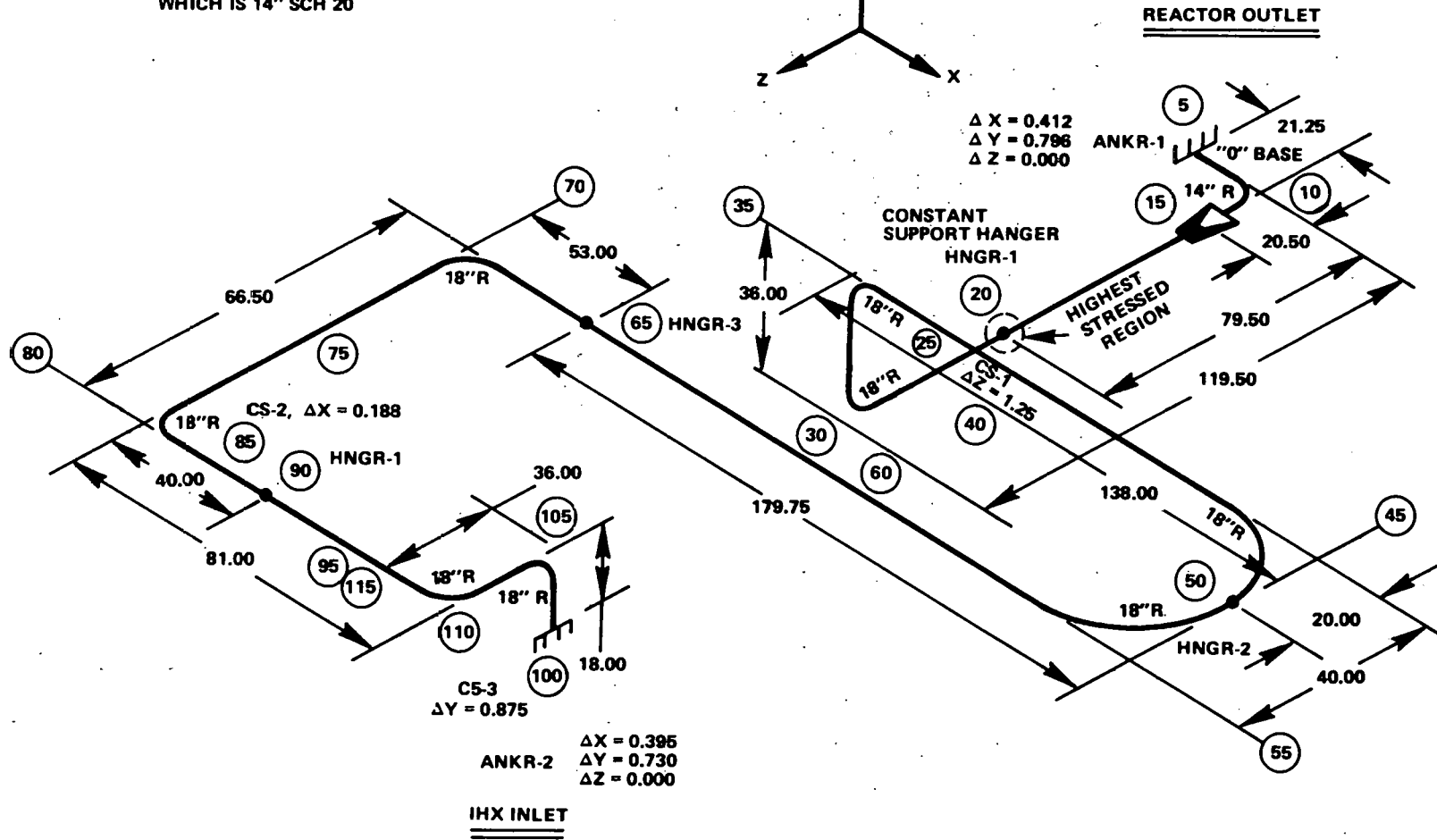
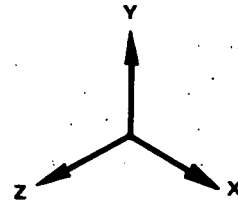


Figure 3B1-2. SEFOR Reactor Vessel

ALL 12" SCH 20 EXCEPT BETWEEN 5 AND 10 WHICH IS 14" SCH 20



159

GEAP-13787

Figure 3B1-3. Main Primary Sodium Piping: Reactor to IHX 204 (MPH)

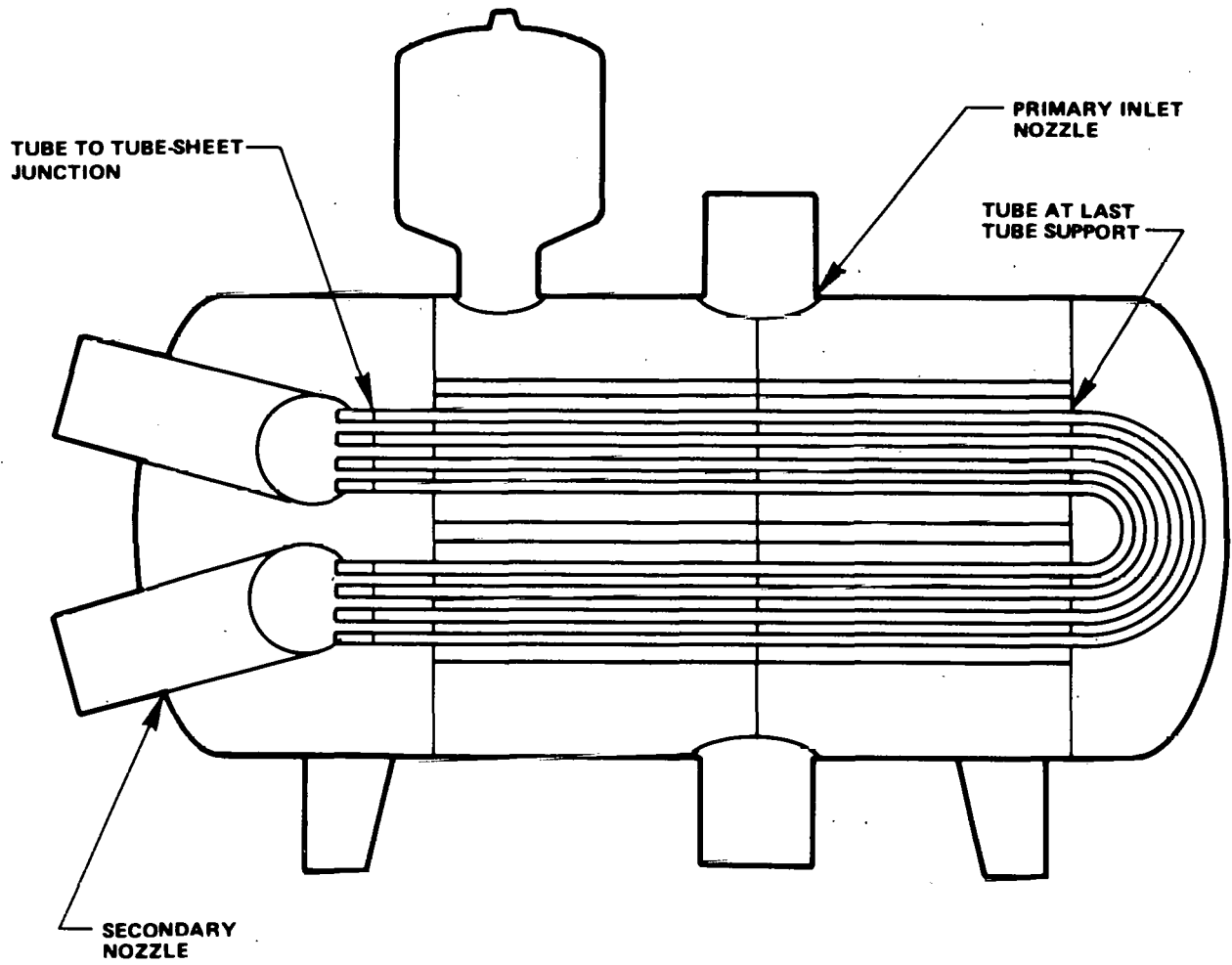


Figure 3B1-4. SEFOR Main Intermediate Heat Exchanger

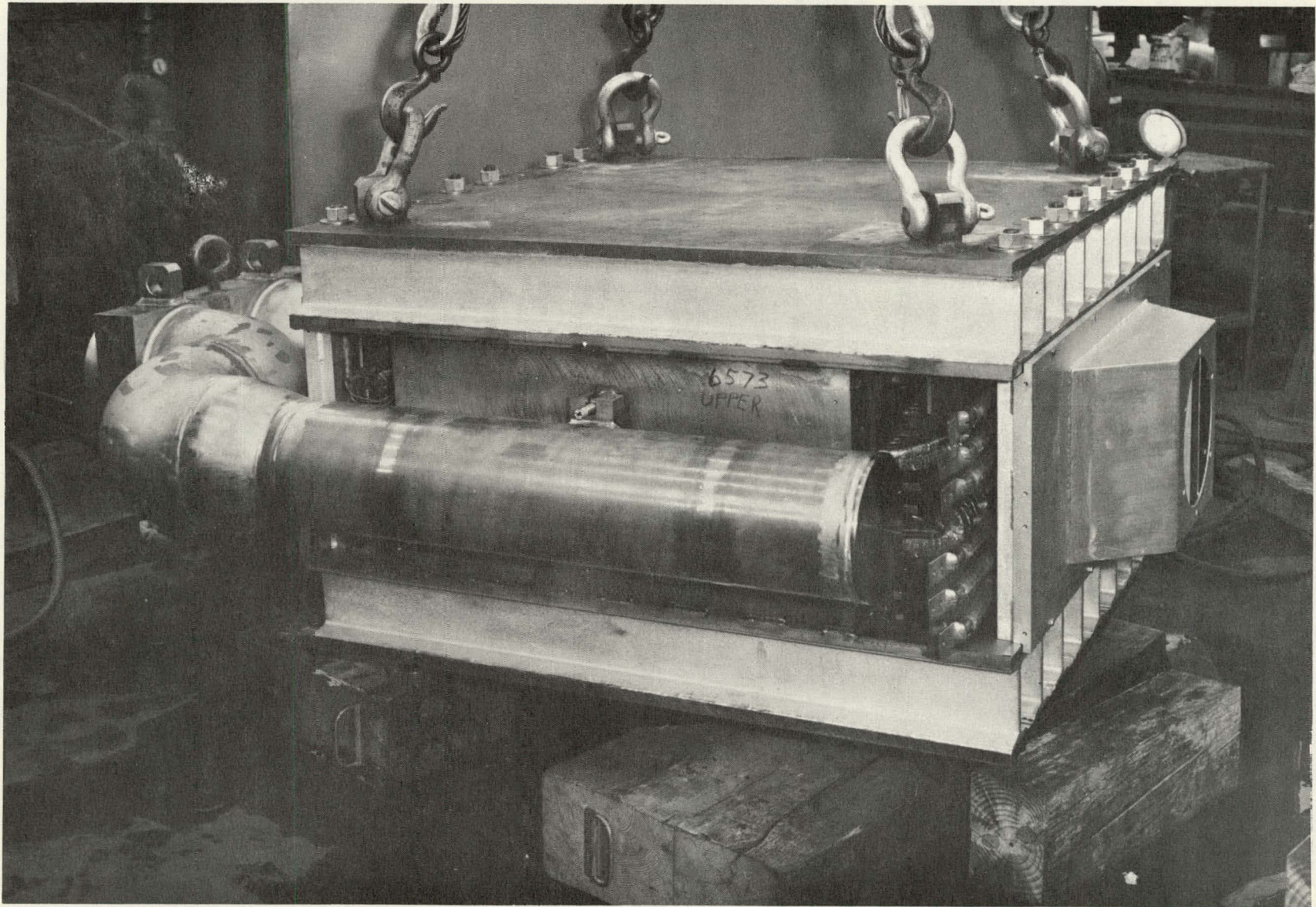


Figure 3B1-5. Main Sodium Pump

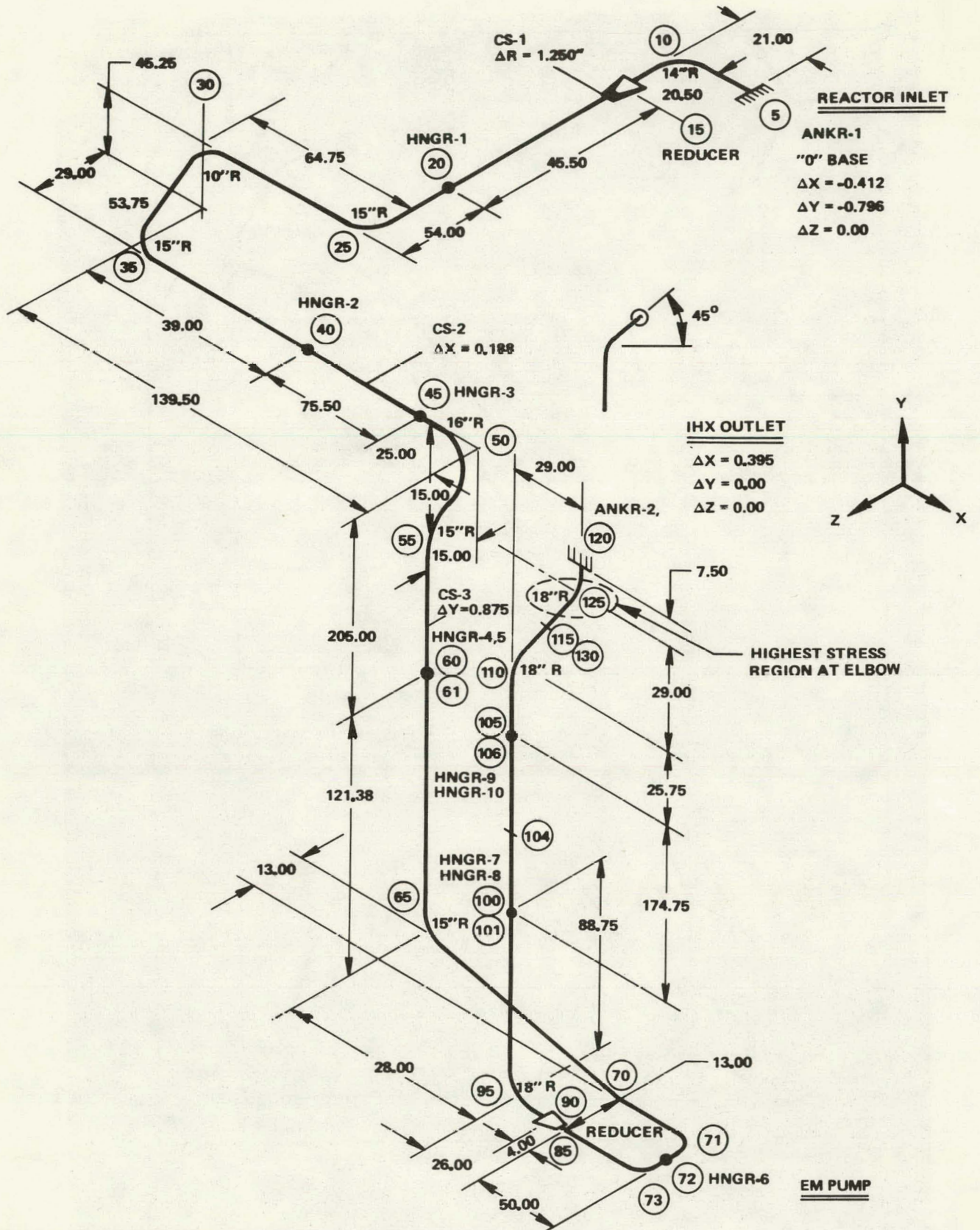


Figure 3B1-6. Main Primary Cold Sodium Piping: IHX-Pump-Reactor (MPC)

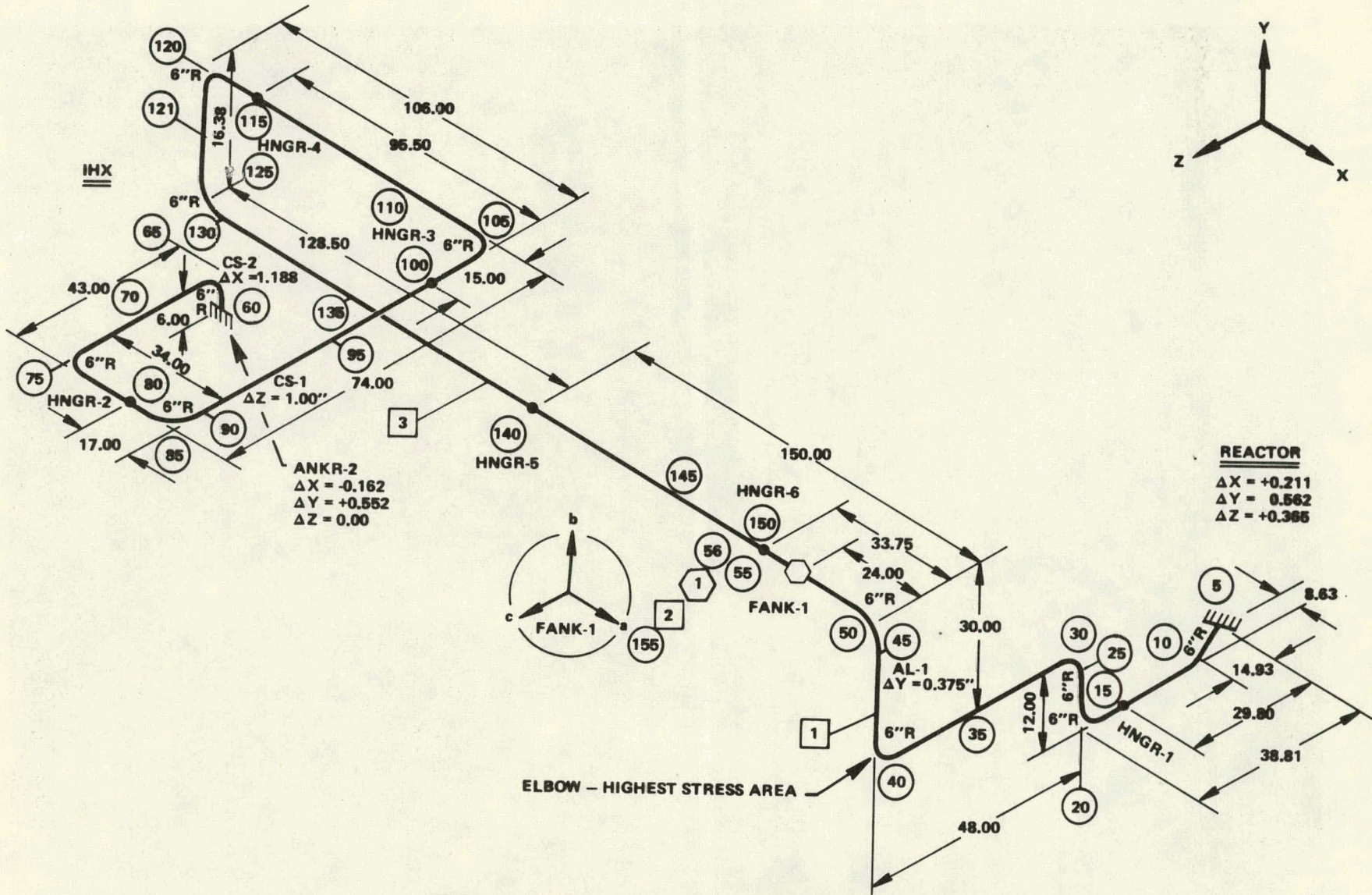


Figure 3B1-7. Auxiliary Primary Sodium Piping: IHX 221

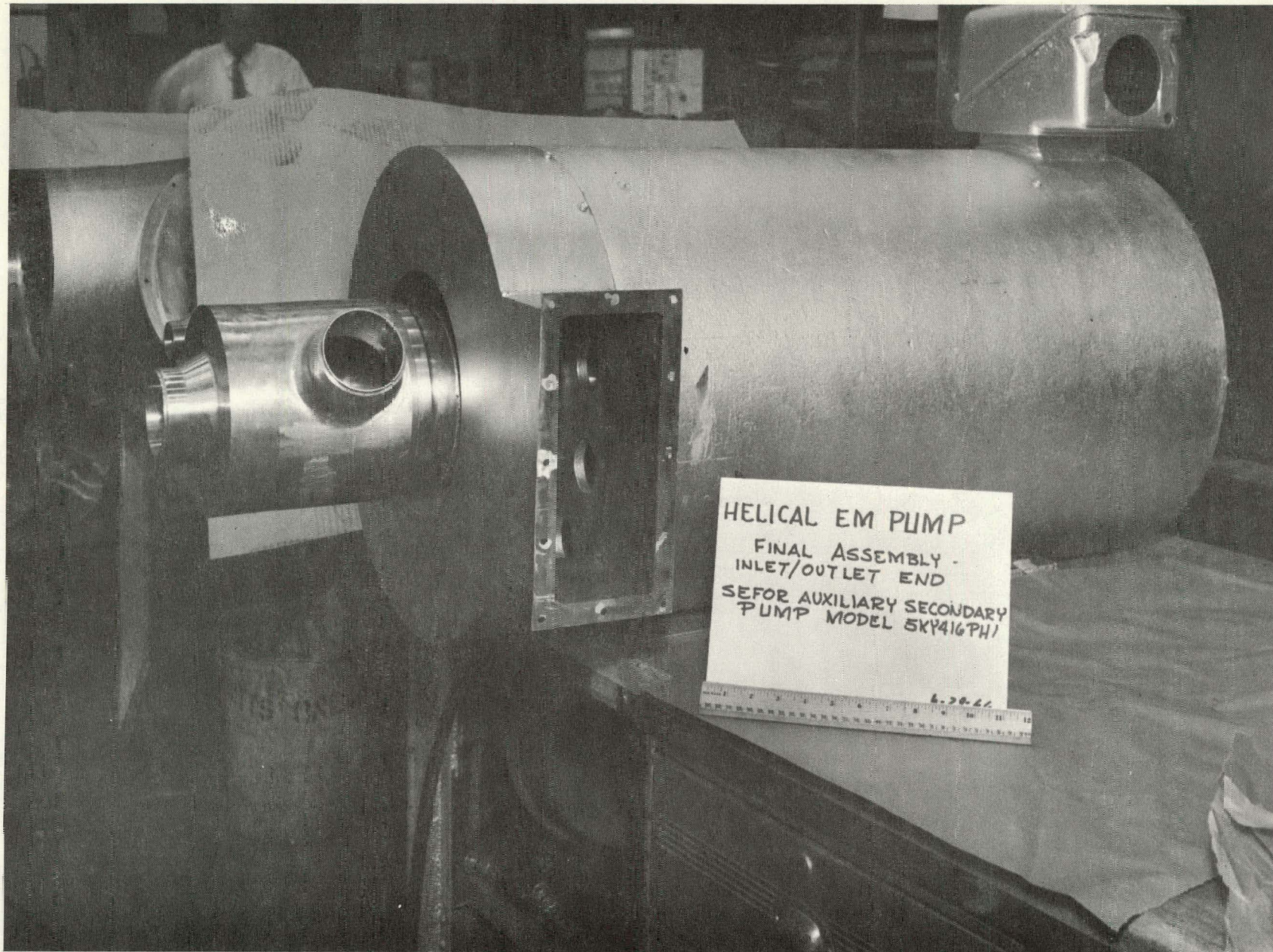
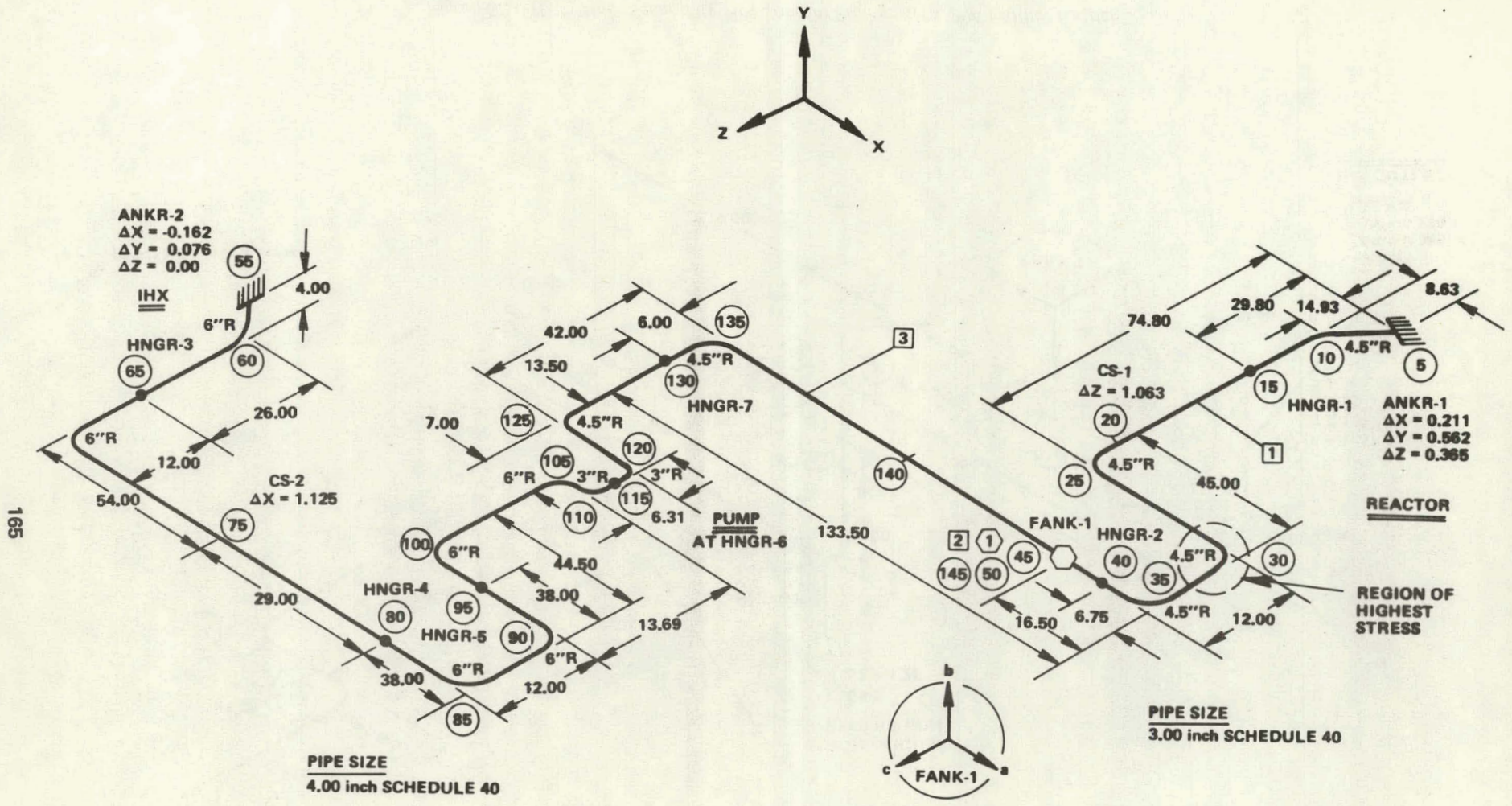


Figure 3B1-8. Helical EM Pump Final Assembly, Inlet/Outlet End



165

GEAP-13787

Figure 3B1-9. Auxiliary Primary Cold (APC) Sodium Piping: IHX 221 to Reactor



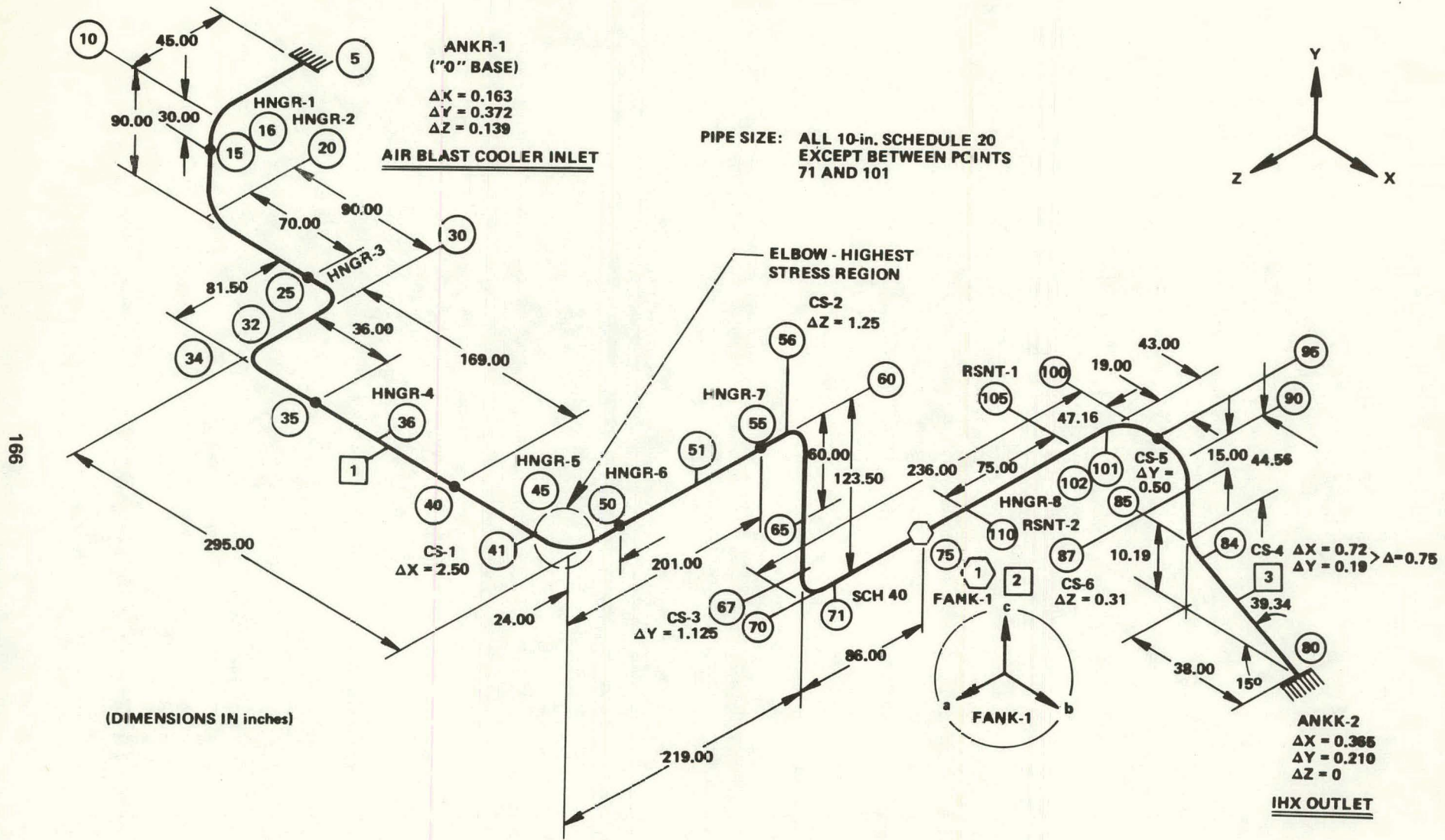
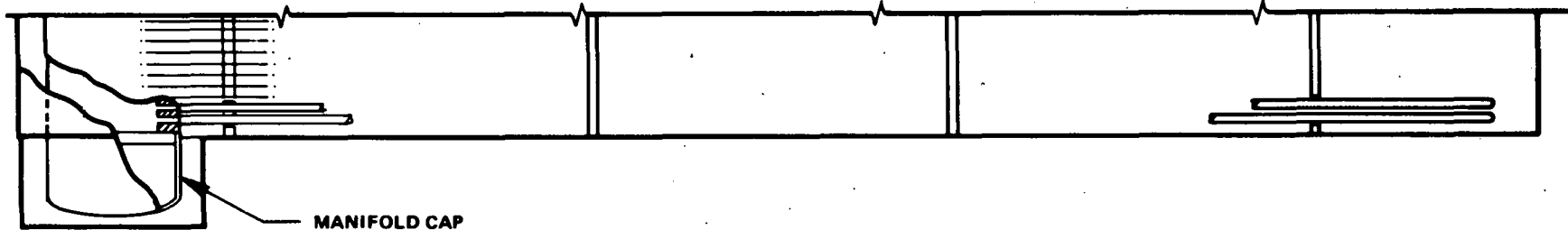
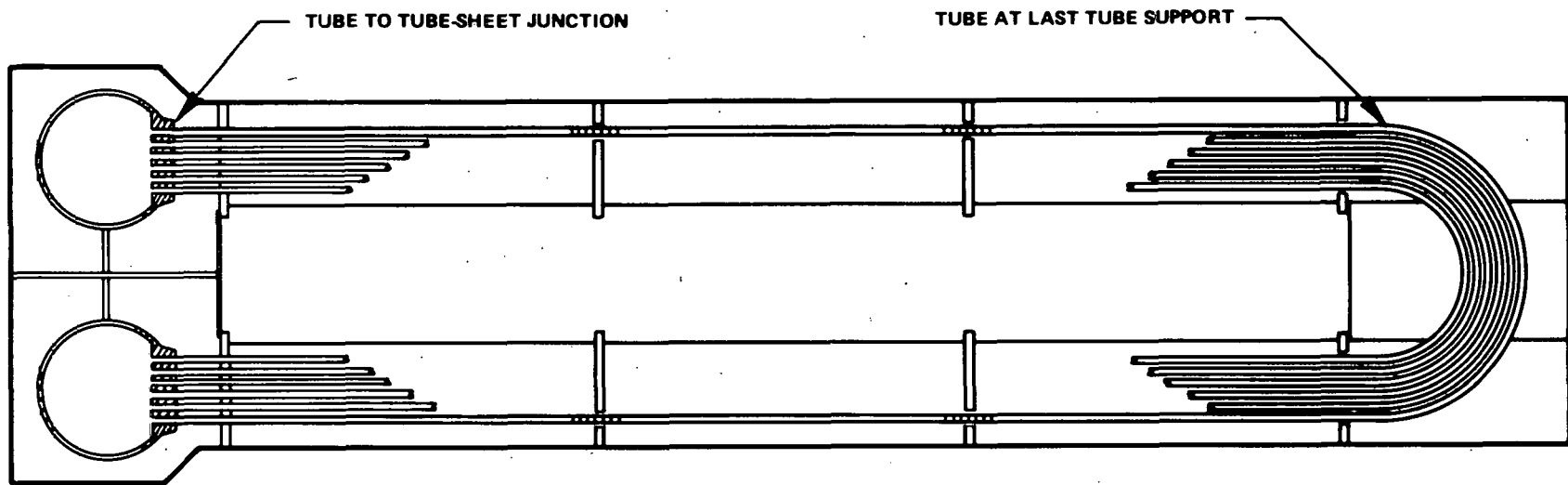


Figure 3B1-10. Main Secondary Hot Sodium Piping: IHX 204 to Inlet Header



MANIFOLD CAP



TUBE TO TUBE-SHEET JUNCTION

TUBE AT LAST TUBE SUPPORT

Figure 3B1-11. SEFOR Main Air Blast Cooler

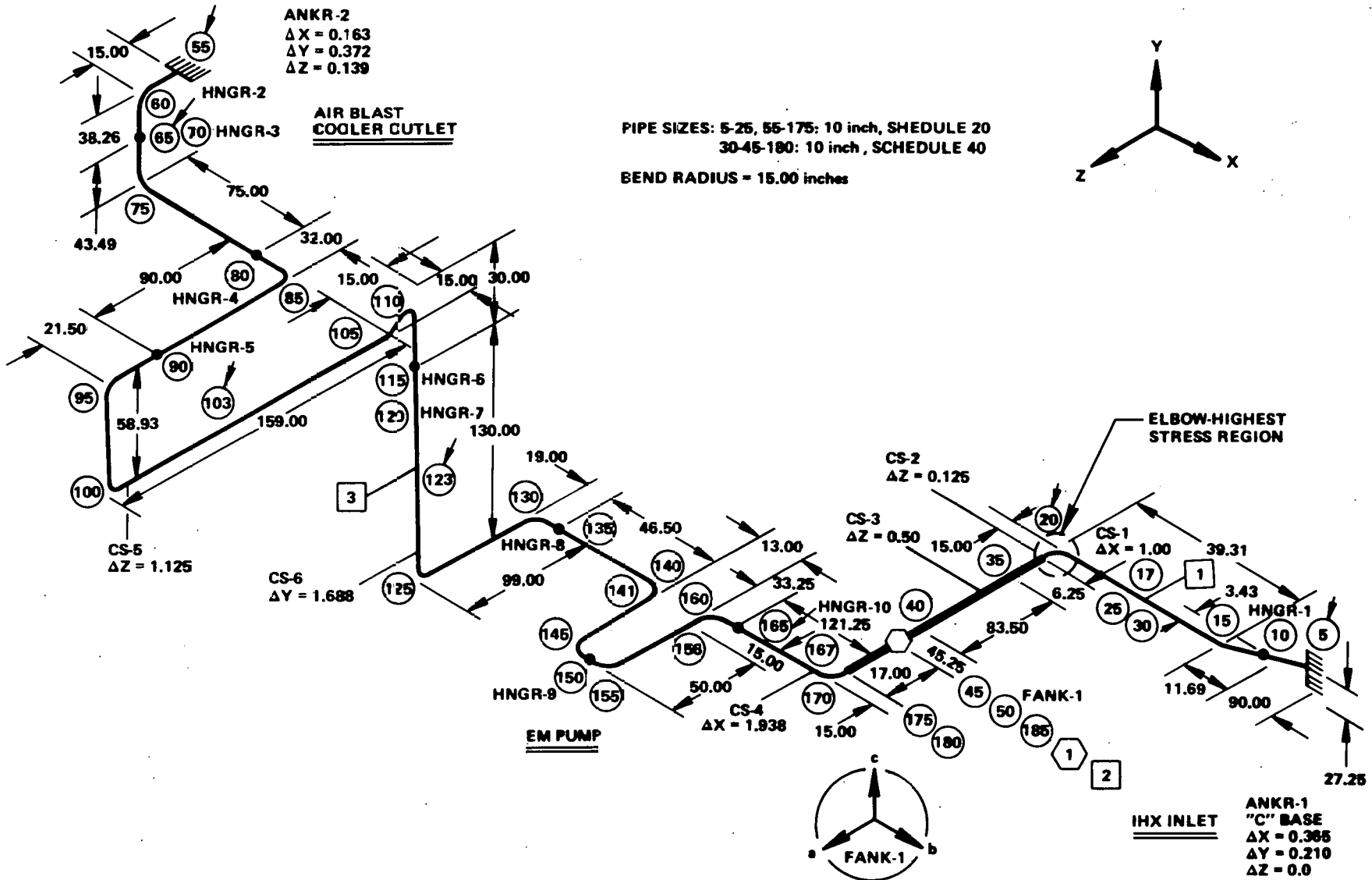


Figure 3B1-12. Main Secondary Cold Sodium Piping: Outlet Header to IHX

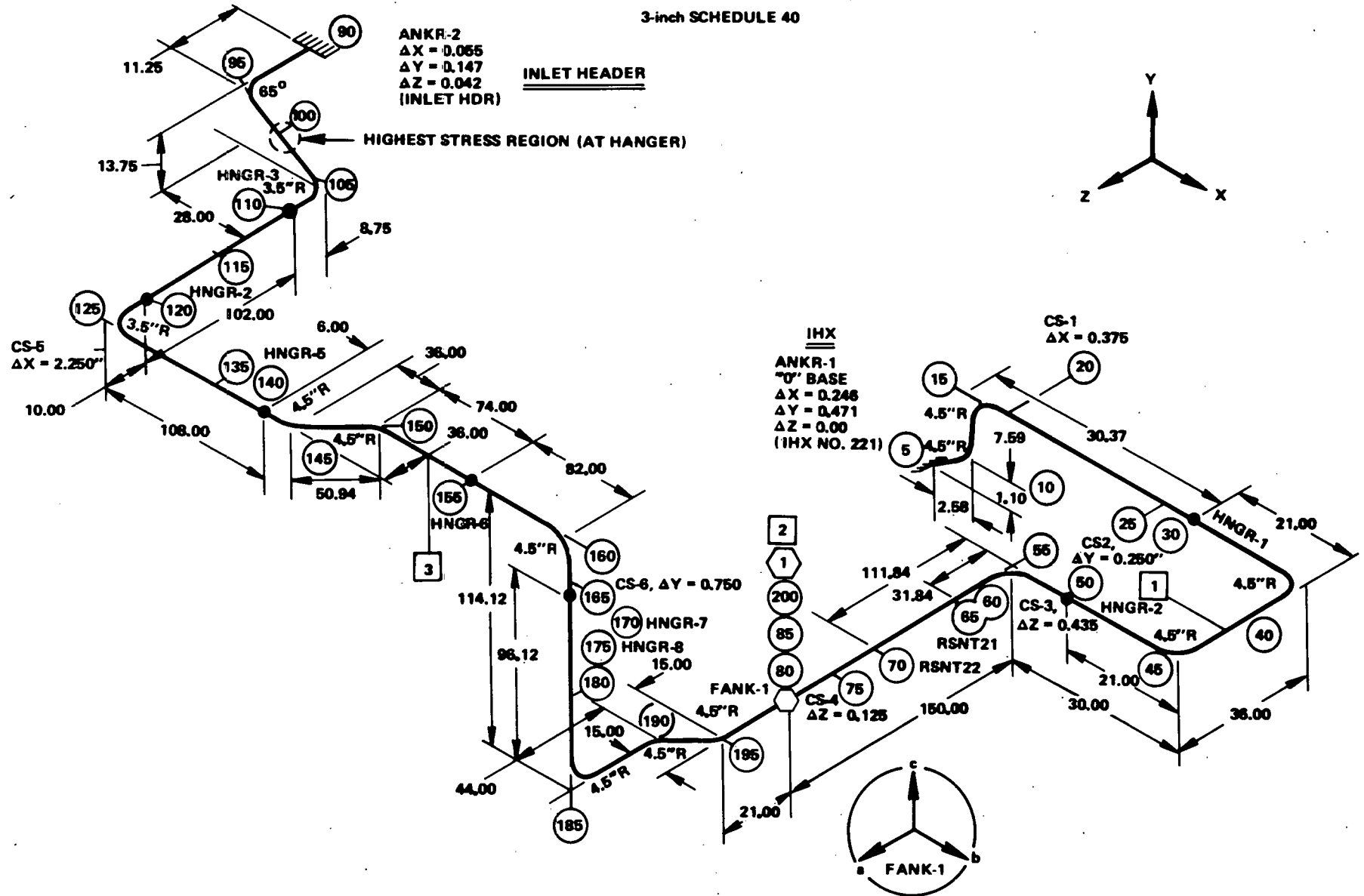


Figure 3B1-13. Auxiliary Secondary Sodium Piping (ASH): IHX to Inlet Header

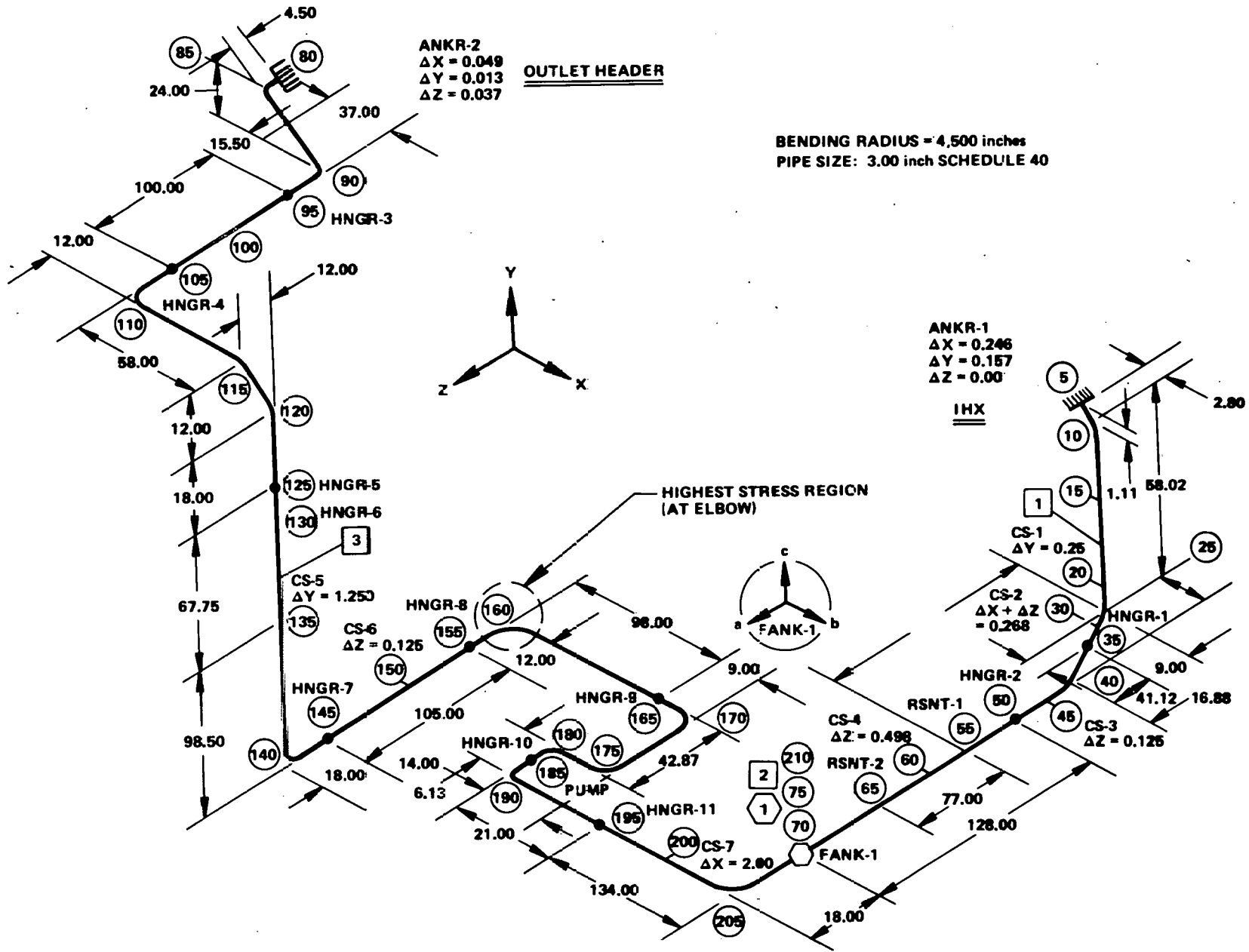


Figure 3B1-14. Auxiliary Secondary Cold (ASC) Sodium Piping: Outlet Header to IHX

The values of stresses computed were obtained with conservative assumptions of thermal gradients; therefore, the stress resultants should not categorize whether or not a plastic analysis should be conducted nor should any conclusions be made other than to pinpoint the critical areas. In other words, the stress value for the reactor flange vessel junction should not determine whether or not the criteria of the new code case can be met.

The margins were conservatively computed using the stress requirements of the elevated temperature code case 1331-4. Margins were defined as the ratio of the difference between the ASME code allowable and the actual applied stress over the ASME code allowable. A negative margin implies stresses in excess of code.

### *Conclusions*

The reactor flange to vessel junction was established as the highest stressed region by a large margin over the second highest stressed region (reactor outlet nozzle). However, if the flange vessel junction meets the requirements of the new ASME code case 1331-5, it can reasonably be assured that the SEFOR plant is feasible to be operated at elevated temperatures for the design conditions of the SEFOR Follow-On Program.

The stresses in the nozzle need to be further evaluated since the nozzle is particularly sensitive to thermal transients; consequently, a more elaborate thermal analysis is needed to obtain more precise numbers. Because the calculations were in many cases formulated using conservative predictions of thermal gradients, the results cannot necessarily be utilized to establish whether or not a given component meets the stress requirements of the new ASME elevated temperature code case 1331-5. In some cases, the numbers are preliminary in that a more extensive evaluation is needed to confirm the result (reactor outlet nozzle for example).

It will be necessary to conduct creep and plastic analyses in other component stressed regions to offer documentary proof that all stresses and stains are within ASME code requirements; however, the results of this study coupled with one or two plastic creep analyses can be utilized to demonstrate elevated temperature operational feasibility at an early stage in the overall program.

#### **3.2.1.4 Sodium Pump Electromagnetic/Thermal Analysis**

The GE-Large Motor Generator Department (GMGD) analyzed the electrical performance, stator winding temperature rise, and ventilation requirements. Results to date are:

1. The electromagnetic design of the main primary and auxiliary primary EM pumps is capable of producing the required flow/head at temperatures up to 900°F.
2. A satisfactory winding temperature of 350°F is predicted for the main primary pump producing 5400 gpm and 29 psi developed pressure at 900°F sodium temperature.

#### **3.2.1.5 Nitrogen Cooling System Evaluation**

Results from nitrogen cooling system test data were used to estimate the nitrogen cooling requirements during elevated temperature operation. Operation under this condition will require about 15% more nitrogen cooling capacity than is presently required for 20 MW operation at normal temperatures. It appears that the freon evaporator coils capacity is adequate, but that additional compressor/condenser capacity will be required. In order to assure availability during the hot summer months, the design ambient temperature should be increased from the present 88°F to a more typical summer temperature of 95°F. Various modifications to increase the capacity will be discussed with vendors.

#### **3.2.2(1) Task 3B2 – Reactor Part I**

##### **3.2.2(1).1 Objective**

The long-term objective of this task (together with other tasks in 3B) is to determine that SEFOR can operate at an elevated temperature (~1000°F). The objectives during Phase A are to perform preliminary stress analyses for the reactor flange-vessel juncture and to develop a backup seal for the reactor vessel outer head. (With the utilization of a back-up seal, the bolt preload can be reduced so that the stress components of the ASME code can be satisfied.

##### **3.2.2(1).2 Discussion**

The reactor flange-vessel junction has been preliminarily determined to be the highest stressed component of the SEFOR primary and secondary systems. The bases for this conclusion were the results of a stress matrix, which

was submitted to RDT in an informal form. With the stress matrix outlining the relative ranking of the critical structural components studied, a preliminary basis for elevated temperature operation feasibility could be obtained by the detailed evaluation of the highest strained component using the ASME Code Case 1331-5 as the base criteria. The matrix did indicate the reactor flange-to-vessel junction as the highest stressed component; thus, the objective of the analysis required herein, to preliminarily assess the structural capability of SEFOR operating at elevated temperature, could be realized.

The results of a high temperature stress analysis conducted on the SEFOR reactor vessel are presented. The purpose of this analysis is to determine the maximum stress-strain levels incurred by operating the SEFOR reactor at a maximum normal operating sodium temperature of 1000°F. Previous studies (References 1 and 2) have established the reactor vessel-flange junction as a region of high stress. Increasing the vessel material temperature above 800°F necessitates the inclusion of creep and plasticity effects in performing stress calculations.

The mathematical model formulated consists of an axisymmetric flange having a thin cylinder attachment. Heat transfer analyses were conducted using the TIGER V computer code to determine temperature distribution as a function of time for the various operating transients examined. This temperature distribution data was used as input to the newly developed CREEP-PLAST finite element stress analysis computer code.

The computer program CREEP-PLAST (Reference 3), developed by Dr. Y. Rashid, provides a tool to conduct high temperature stress analyses. This two-dimensional, finite element stress analysis code includes creep and plasticity effects utilizing "memory" theory to account for creep. Preliminary correlations of the CREEP-PLAST code with experiment and other theories indicate excellent results are obtainable. However, it should be emphasized that any creep and analysis program is limited by the availability of the experimental data required to formulate the empirical creep laws contained therein. Particularly lacking is the low stress-low temperature regime. Several years will probably pass before a complete set of data becomes available.

Temperature distributions were obtained as a function of time for startup, normal scram, scram with plant power failure, and shutdown. Stresses and strains were calculated as a function of time for the startup transient. The maximum effective strain resulting from startup was calculated to be approximately 0.2% and a maximum effective stress was predicted of approximately 17,000 psi. Future analyses are planned to examine the other operating conditions with their accumulated effect as a function of the application order.

The results obtained for the startup transient provide only a portion of the information needed to make a final assessment on the practicality of using the SEFOR plant for high temperature operation of 1000°F. However, based on the partial analysis results obtained, the SEFOR reactor should meet ASME Section III Code allowing for all loadings in the vessel-flange region.

In the remote event the flange to vessel junction is overstressed, it is possible to substantially reduce the stress dependent flange rotations and displacements by reducing the flange thermal gradients. The flange thermal gradients can be substantially reduced by lowering the sodium level in the reactor approximately six to eight inches.

Two feasibility questions concerning lowering the sodium level must be answered: one concerns making the modifications to the reactor so that operation at a lower sodium level is possible; a second question concerns the remote possibility of gas entrapment in the system as a consequence of the sodium level decrease.

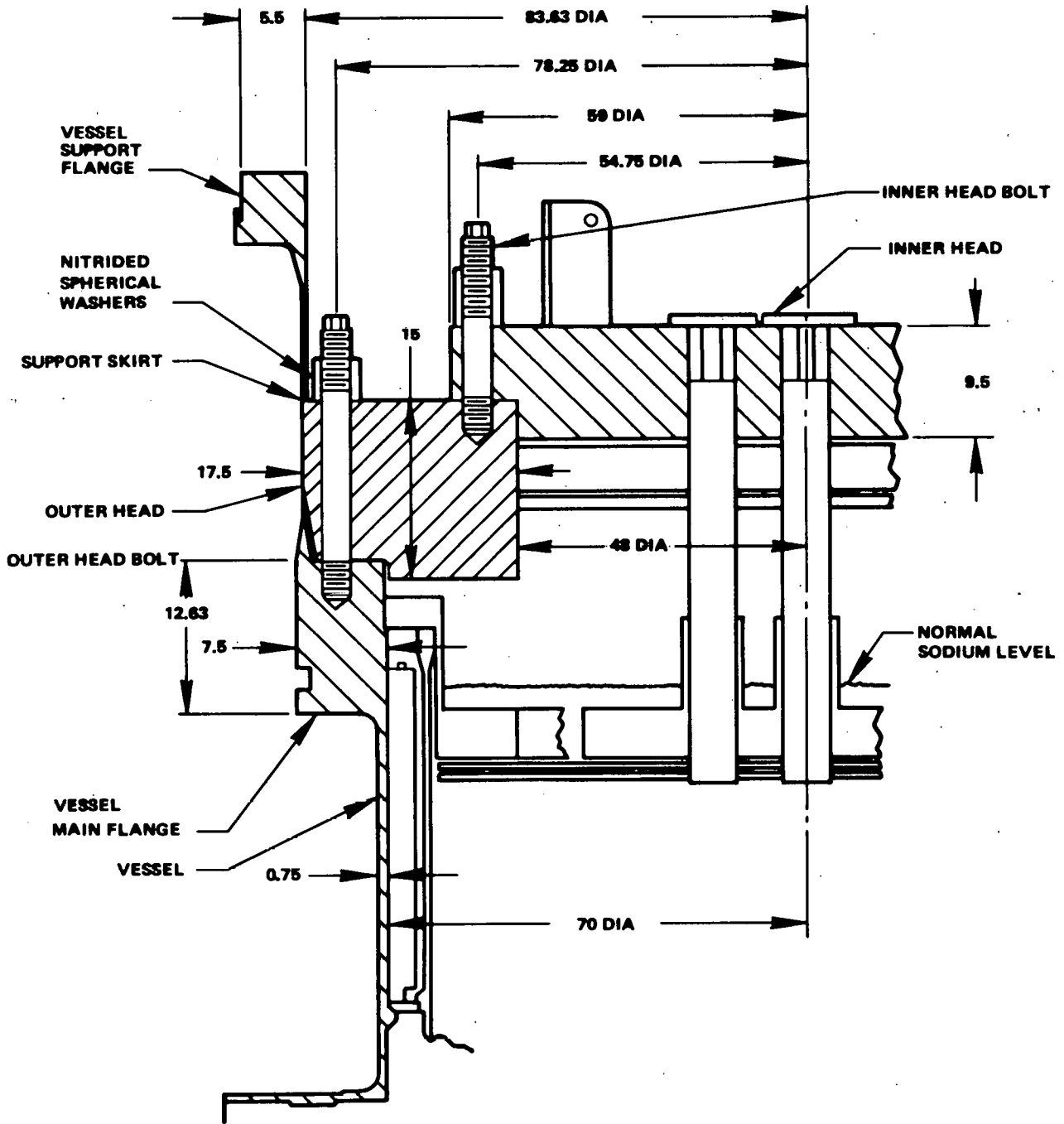
Part 3 of this memo describes the techniques by which the necessary simple modification to the reactor can be made so that operation at a lower level is possible. The remote possibility of gas entrapment study must be extended into next year.

### 3.2.2(1).3 Analysis

#### *Description of the Problem*

Figure 3B2-1 shows the arrangement of the SEFOR reactor vessel at the main flange. The lower end of the flange is in contact with the sodium, and the upper portion is in contact with the cover gas. The top of the flange contacts the massive outer head and the outside is insulated. In addition, a group of B<sub>4</sub>C shielding rods and a steel cylinder are interposed between the flange and the bulk of the sodium.

The first portion of this analysis is concerned with determining the temperature distribution in the flange-vessel region during and following rapid changes of the bulk sodium temperature. This temperature distribution data will be utilized as input for the final portion of the analysis: determination of the stresses and strains via the CREEP-PLAST computer code.



ALL DIMENSIONS IN INCHES

Figure 3B2-1. SEFOR Closure Assembly



*Description of the Expected Operating History*

Between November 1973 and December 1974, it is planned to operate the SEFOR with a reactor outlet temperature of about 1000°F. During that period, it is expected that several transients will occur in the reactor outlet temperature. It is necessary to determine whether the flange and vessel can absorb the creep and plastic strain resulting from steady operation at high temperature and from the transients. Therefore, the postulation of an operating histogram is required for the reactor during the elevated temperature operation phase. Table 3B2-1 presents the postulated history of the reactor outlet temperature during the elevated temperature operation phase. This is also shown schematically on Figure 3B2-2.

During the second week it is presumed that the reactor will experience a scram due to loss of off-site power. During the 29th and last week, the reactor is presumed to experience this condition again. These events are unlikely but not improbable.

The four transients mentioned in the postulated histogram are described in detail in Table 3B2-2. In addition, two other emergency condition transients are listed. The occurrence of these two transients are considered to be too improbable to allow their inclusion in the histogram.

*Thermal Model*

Thermal model used in the transient analysis is shown on Figure 3B2-3. This figure shows the steady state temperature distribution of the vessel wall, the flange, the support ring, the outer head, and the inner head. The temperatures correspond to a sodium temperature of 760°F. The numbers shown in parentheses are measurements taken after the reactor had been held at steady-state for an extended period.

An equivalent heat transfer coefficient at each surface is shown on the figure. A detailed discussion of these coefficients is presented in Appendices A and B. The computer model actually used on the transient analysis differs somewhat from the one discussed in Appendix A. First, the support skirt was eliminated to reduce computation costs, after it was determined that its inclusion would not significantly affect the flange to vessel junction results. Secondly, the heat capacitance of the B<sub>4</sub>C rods and the steel skirt on the inside of the vessel wall is included.

*Stress Model*

The theoretical model formulated for the stress analysis is shown in Figure 3B2-4. It is seen that this axisymmetric structure consists of 903 triangular elements having a total of 532 nodal points. Each control point has radial and axial degrees of freedom resulting in a 1064 degree-of-freedom model. Radial and axial coordinates are scaled along the margin of the figure. Appropriate boundary condition loadings such as surrounding structural dead weight and a 30 psi cover gas pressure were applied to the model in the stress analysis.

**3.2.2(1).4 Creep Theory Formulation**

The analysis is based on the memory theory of creep which postulates that the strain state at the current time is a functional of all previous stress rates. Symbolically this is written as follows for the strain-stress relation:

$$\epsilon(t) = F \left[ \sigma(\tau) \right]_{\tau = \infty}^{\tau = t} \tag{1}$$

This equation can be approximated arbitrarily closely by the following series:

$$\begin{aligned} \epsilon(t) = & \int_{-\infty}^t J_1(t-\tau_1) \frac{d\sigma(\tau_1)}{d\tau_1} d\tau_1 \\ & + \int_{-\infty}^t \int_{-\infty}^t (J_2(t-\tau_1; t-\tau_2)) \frac{d\sigma(\tau_1)}{d\tau_1} \frac{d\sigma(\tau_2)}{d\tau_2} d\tau_1 d\tau_2 \\ & + \int_{-\infty}^t \int_{-\infty}^t \int_{-\infty}^t J_3(t-\tau_1; t-\tau_2; t-\tau_3) \frac{d\sigma(\tau_1)}{d\tau_1} \frac{d\sigma(\tau_2)}{d\tau_2} \frac{d\sigma(\tau_3)}{d\tau_3} d\tau_1 d\tau_2 d\tau_3 \\ & + \dots \end{aligned} \tag{2}$$

Table 3B2-1

POSTULATED OPERATING HISTORY OF THE SEFOR  
DURING THE ELEVATED TEMPERATURE PHASE

Week Number 1: (1Nov. 73)	
Heatup	80.00 hours
Steady at 1000°F	88.00 hours
Week Number 2:	
Plant Power Failure with Scram	123.03 hours
Steady at 1000°F	44.97 hours
Week Number 3:	
Normal Scram with Immediate Recovery	7.53 hours
Steady at 1000°F	106.47 hours
Week Numbers 4 through 12: (same as No. 4)	
Week Number 13:	
Normal Scram with Immediate Recovery	7.53 hours
Steady at 1000°F	80.47 hours
Cooldown	80.00 hours
Week Numbers 14 through 16: (Feb. '74)	
Steady at 400°F	168.00 hours
Week Number 17: (same as No. 1)	
Week Numbers 18 through 28: (same as No. 3)	
Week Number 29: (same as No. 2)	
Week Number 30: (same as No. 13)	
Week Numbers 31 through 35: (June '74)	
Steady at 400°F	168.00 hours
Week Number 36: (same as No. 1)	
Week Numbers 37 through 55: (same as No. 3)	
Week Numbers 56 and 57 (inclusive):	
Plant Power Failure with Scram	123.03 hours
Steady at 1000°F	132.97 hours
Cooldown	80.00 hours

Table 3B2-2

**PRIMARY SODIUM OUTLET TEMPERATURE TRANSIENTS FOR  
EVALUATION OF THE SEFOR REACTOR VESSEL  
DURING ELEVATED TEMPERATURE OPERATION**

1.	Heatup (80 hours)	From 400°F To 800°F At 10°F/hr	
		From 800°F To 1000°F At 5°F/hr	
2.	Cooldown (80 hours)	From 1000°F To 800°F At 5°F/hr	
		From 800°F To 400°F At 10°F/hr	
3.	Normal Scram with Immediate Recovery (7.53 hours)	From 1000°F To 850°F At 100°F/min	
		From 850°F To 1000°F At 20°F/hr	
4.	Plant Power Failure with Scram (123.03 hours)	From 1000°F To 850°F At 100°F/min	
		From 850°F To 550°F At 10°F/hr	
		From 550°F To 700°F At 10°F/hr	
<b>Stabilize at 700°F for 48 hours</b>			
5.	Plant Power Failure with Scram, No Flywheel (128.04 hours)	From 700°F To 1000°F At 10°F/hr	
		From 1000°F To 1500°F At 20°F/sec	
		From 1500°F To 900°F At 5°F/sec	
		From 900°F To 550°F At 10°F/hr	
6.	Plant Power Failure Without Scram, No Flywheel (230.05 hours)	From 550°F To 700°F At 10°F/hr	
		<b>Stabilize at 700°F for 48 hours</b>	
		From 700°F To 1000°F At 10°F/hr	
		From 1000°F To 1600°F At 40°F/hr	
		From 1600°F To 1250°F At 2°F/sec	
<b>Stabilize at 1250°F for 100 hours</b>			
		From 1250°F To 800°F At 5°F/hr	
		From 800°F To 400°F At 10°F/hr	

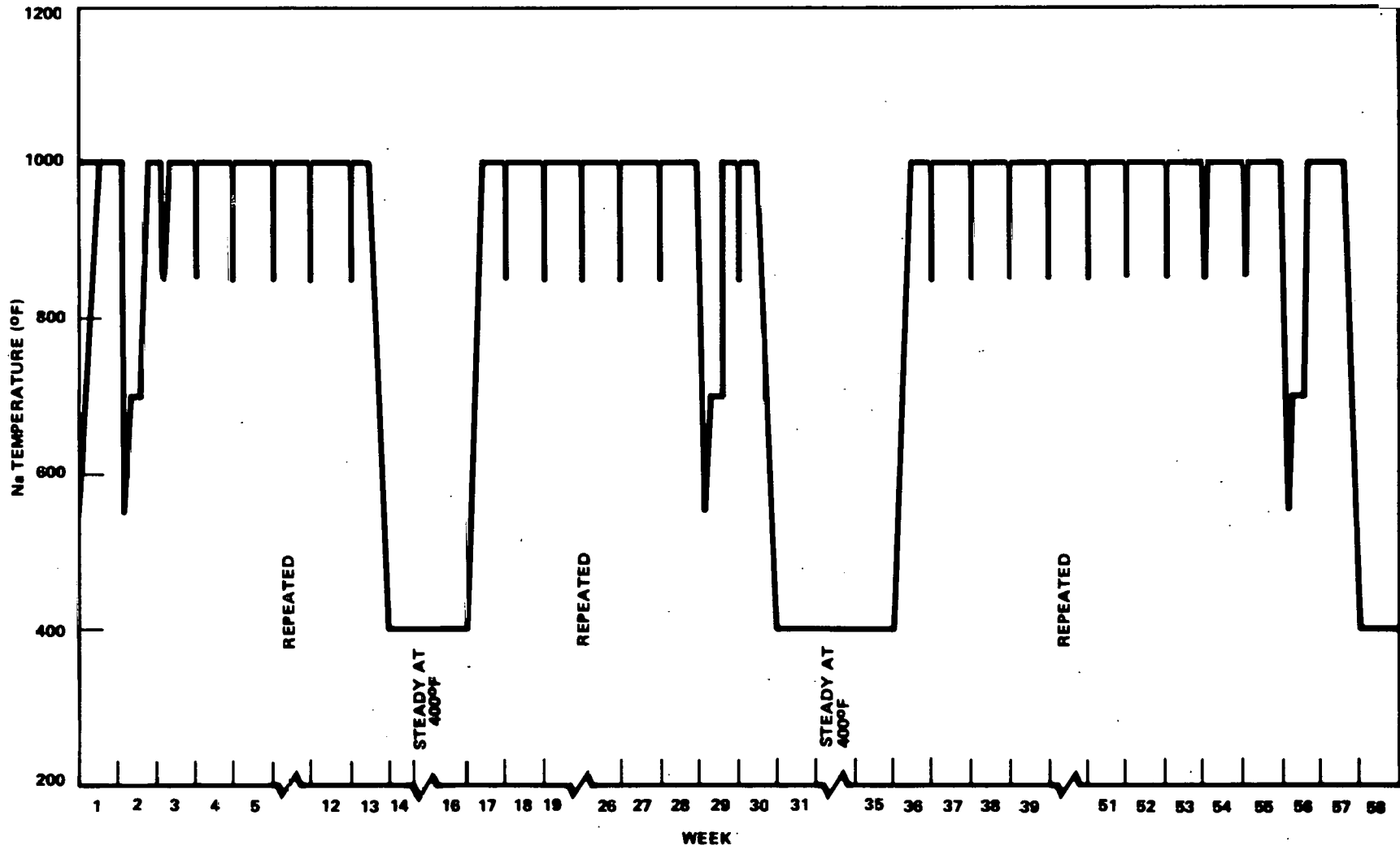


Figure 3B2-2. SEFOR Elevated Temperature Operation, 1 November 1973–December 1974

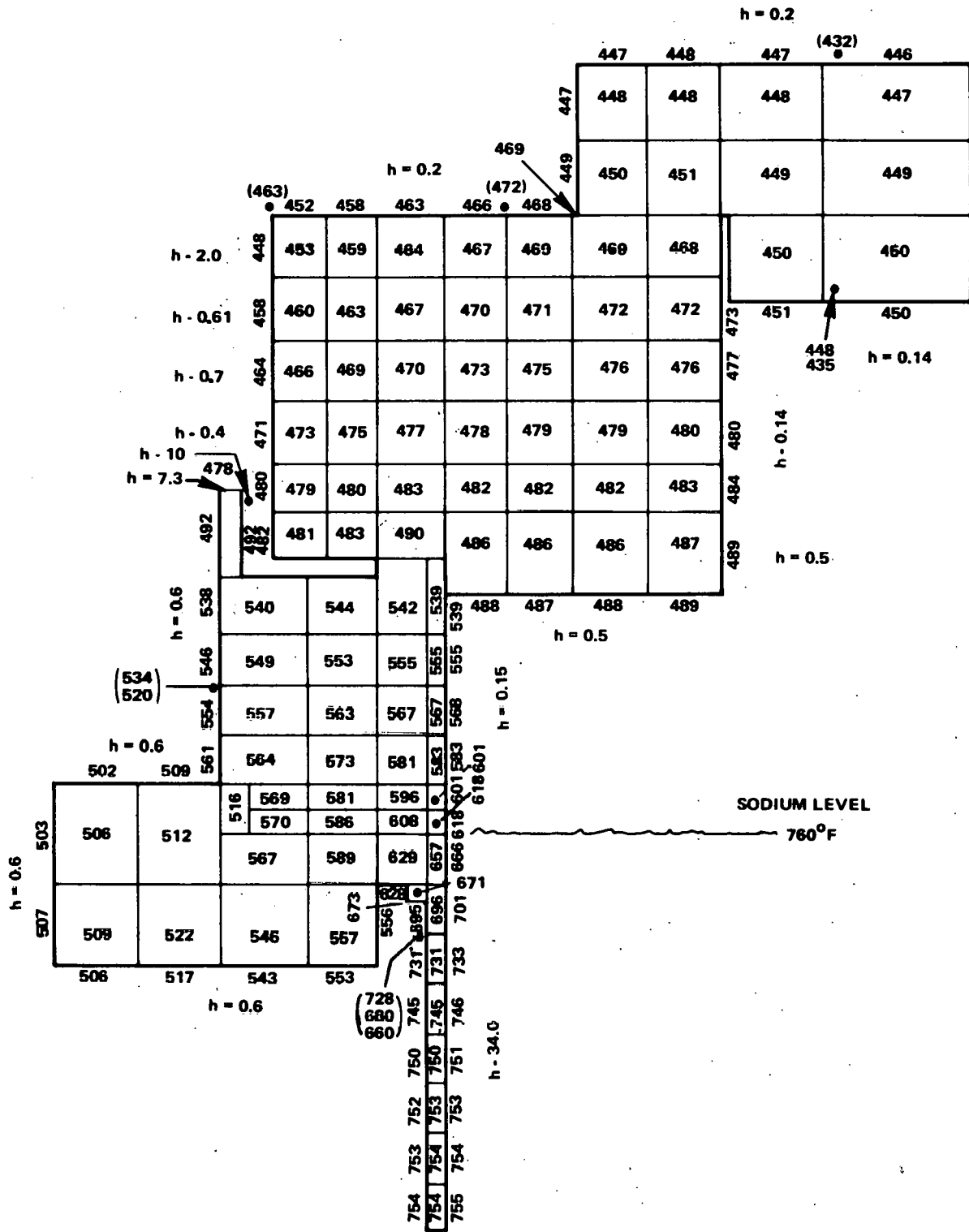


Figure 3B2-3. Temperature Distribution, Steady State at  $760^{\circ}\text{F}$

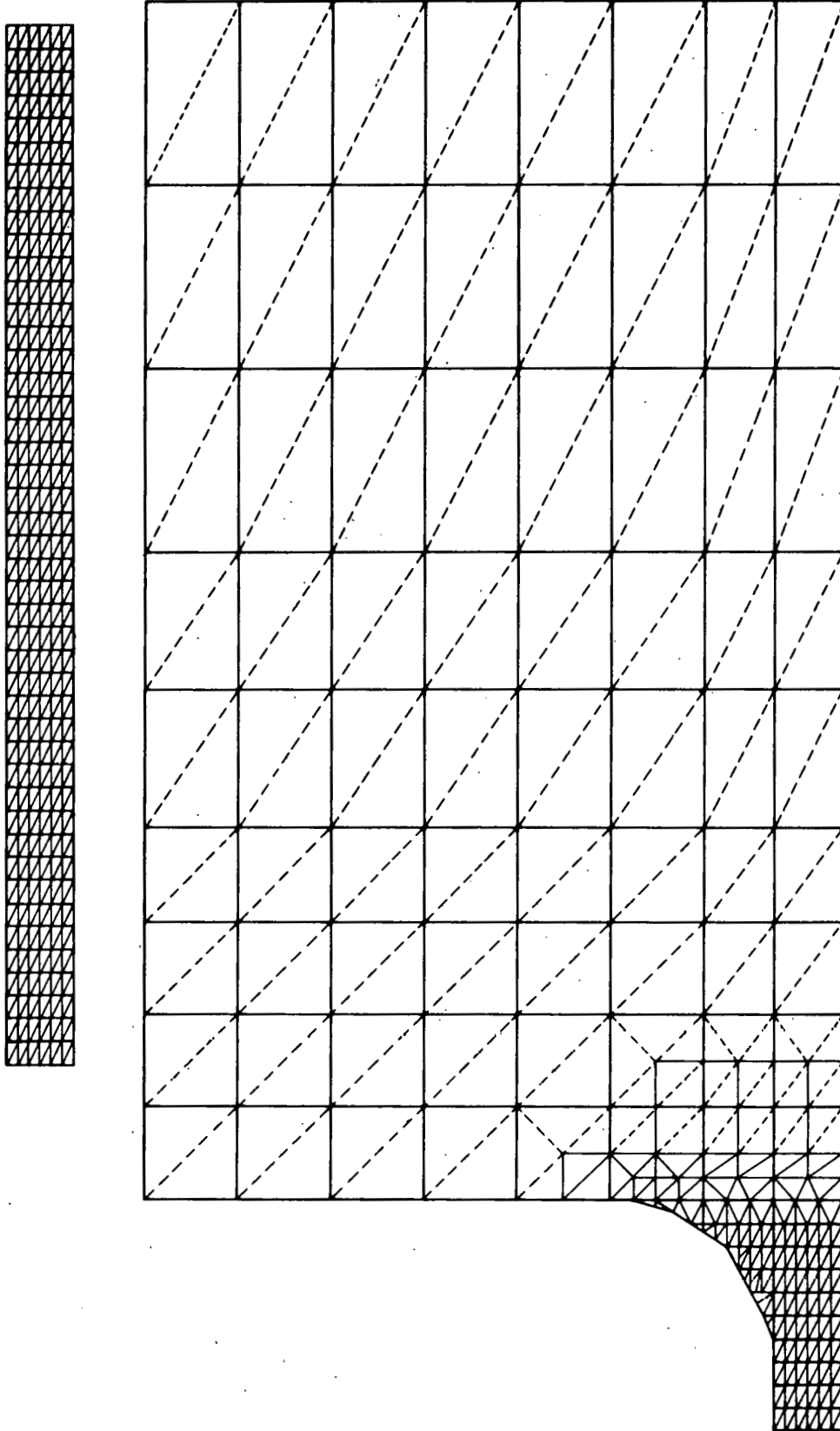


Figure 3B2-4. CREEP-PLAST Model

Equation (1) is the counterpart of the time-hardening (or strain-hardening) equation in the well known equation-of-state creep theory. In a creep experiment where the stress  $\sigma$  does not vary with time, equation (2) reduces to

$$\epsilon(t) = \sigma J_1(t) + \sigma^2 J_2(t,t) + \sigma^3 J_3(t,t,t) + \dots \quad (3)$$

which is a polynomial representation of a single-step creep test.

The use of equation(2) in its generality is not within our experimental and computational means at this time since it requires several multi-step creep tests for the determination of the creep kernel functions  $J_1, J_2, \dots$ , which are not presently available. In order to make use of this general concept within the limitation of single-step creep data, equation (2) is replaced by the following non-linear superposition equation:

$$\epsilon(t) = \int_{-\infty}^t \frac{\partial C(\sigma, t-\tau)}{\partial \sigma} \frac{d\sigma(\tau)}{d\tau} d\tau \quad (4)$$

where  $C(\sigma, t)$  is the usual single-step creep curve. Equation (4) can be rewritten as

$$\epsilon(t) = \int_{-\infty}^t J(\sigma; t-\tau) \frac{d\sigma(\tau)}{d\tau} d\tau \quad (5)$$

where  $J$  is the creep compliance at stress level  $\sigma$ . Equation (5) predicts the strain due to time-varying  $\sigma$  by superposing single-step creep data. This equation is exact only for linear materials and it serves as a first approximation to equation (2). It has the advantage that it requires the same creep test as the equation of state theory.

Instead of generalizing the single-step creep data to time-varying stresses by direct superposition, as indicated by Equation (5), use is made of the time-temperature-stress shift hypothesis, namely,

$$\epsilon(t) = \int_{-\infty}^t J[\xi(t) - \xi(\tau)] \frac{d\sigma(\tau)}{d\tau} d\tau \quad (6)$$

where

$$\xi(t) = \int_{-\infty}^t \phi[\sigma(\tau); t(\tau)] d\tau \quad (7)$$

In equation (6) the physical time  $t$  is replaced by the equivalent time  $\xi(t)$  defined in equation (7) where  $\phi(\sigma)$  is called the shift factor which depends on the stress  $\sigma$  and temperature  $T$ . The basis for this formulation is the following: If one plots specific creep curves for various  $\sigma$ 's and/or  $T$ 's on a semi-log plot where  $J$  is plotted against  $\log t$  one observes that all the curves can be obtained by simply displacing a suitable base  $e$  curve rigidly parallel to the  $\log t$  axis. For example, if the base curve  $J_0$  corresponds to  $\sigma_0$  then curves for stress less than  $\sigma_0$  are obtained by displacing  $J_0$  to the right and those higher than  $\sigma_0$  are obtained by displacing  $J_0$  to the left. This process of course is not exact; i.e., it does not always result in congruent curves but it is possible to generalize this method to permit piece-wise shift of the base curve to obtain satisfactory accuracy.

**3.2.2(1).5 Elastic-Plastic-Creep Interaction**

The problem of combined creep and plasticity has been treated on the basis that the total strain at any instant of time  $t$  consists of three parts: elastic, plastic, and creep, namely

$$\Delta\epsilon(t) = \Delta\epsilon^E(t) + \Delta\epsilon^P(t) + \Delta\epsilon^C(t) \quad (8)$$

in which  $\Delta\epsilon^E(t)$  is the elastic strain increment,  $\Delta\epsilon^C(t)$  is the creep strain increment, the treatment of which is discussed above, and  $\Delta\epsilon^P(t)$  is the plastic strain increment yet to be determined.

The elastic-plastic problem is well developed and need not be discussed in detail here. Briefly, however, there are two possible techniques which have been used in the past: The first is to treat the plastic strains as initial strains in an incremental procedure. The second is to derive the non-linear stress strain relations which satisfy the appropriate yield condition and a corresponding flow rule. The first approach is referred to as the initial stress approach and the second as the tangent modulus approach.

The tangent modulus approach is used here as a more reliable procedure. The elastic-plastic incremental stress-strain relations are given by

$$\Delta\sigma = (H_e - \eta H_p) \Delta\epsilon \quad (9)$$

where  $\Delta\sigma$  and  $\Delta\epsilon$  are the incremental stress and strain vectors respectively,  $H_e$  is the elasticity matrix,  $\eta = 0$  or 1 for elastic or plastic states respectively, and  $H_p$  is the plasticity matrix where elements  $(h_{ij})_p$  are given by

$$(h_{ij})_p = \frac{2\mu}{2k^2(1+c/2\mu)} S_{ij} S_{jj}, \text{ no sum implied} \quad (10)$$

where  $\mu$  is the shear modulus,  $c$  is the hardening modulus,  $k$  is the uniaxial yield stress divided by  $\sqrt{3}$  and  $S_{ij}$  are the deviatoric stresses given by

$$S_{ij} = (\sigma_{ij} - \alpha_{ij}) - \frac{1}{3} (\sigma_{kk} - \alpha_{kk}) \delta_{ij} \quad (11)$$

In this equation  $\sigma_{ij}$  are the stress components,  $\delta_{ij} = 1$  for  $i=j$  and zero otherwise, and  $\alpha_{kk}$  are the stress coordinates of the translation of the yield surface. The above derivation is based on von Mises yield condition:

$$\frac{1}{2} S_{ij} S_{ij} - k^2 = 0 \quad (12)$$

#### Material Data

The creep equation supplied by L. D. Blackburn, of WADCO/HEDL, for annealed 304 stainless steel is used in the computer program. This equation has the following form:

$$\epsilon_c = A (1 - e^{-rt}) + Bt, \quad (13)$$

where  $A$  and  $B$  are functions stress and temperature and  $r$  is function of stress given below:

$$A = 2.74 \left[ \frac{\sinh\left(\frac{\beta e \sigma}{6}\right)}{\sinh\left(\frac{\beta r}{3.5\sigma}\right)} \right]^6 \cdot 3.5, \% \quad (14)$$

$$B = (1.382 \times 10^{13}) \left[ \sinh\left(\frac{\beta e \sigma}{n_e}\right) \right] n_e \exp\left(\frac{-67000}{1.987T}\right), \% \text{ per hour} \quad (15)$$

$$r = (2.518 \times 10^{13}) \left[ \sinh\left(\frac{\beta r \sigma}{n_r}\right) \right] n_r \exp\left(\frac{-67000}{1.987T}\right), \text{ hours}^{-1} \quad (16)$$

where  $n_e = 6$

$$n_r = 3.5$$

$$\beta e = -3.652 \times 10^{-4} + 7.518 \times 10^{-7} T$$

$$\beta r = -2.252 \times 10^{-4} + 5.401 \times 10^{-7} T \quad (17)$$

$\sigma$  is in psi, and  $T$  is in  $^{\circ}K$

The stress-strain relations for the same material are given below:

$$\begin{aligned} \epsilon_t &= \sigma_t/E & \sigma_t &\leq PEL_a \text{ Ksi} & (18) \\ \epsilon_t^{1/2} &= 0.003\sigma_t + 5.03 \times 10^{-6} T - 0.0143 & PEL_a &< \text{Ksi} & \sigma_t \leq B_a \text{ Ksi} \\ \epsilon_t^{1/2} &= 0.0093\sigma_t + 7.23 \times 10^{-5} T - 0.1877 & \sigma_t &> B_a \text{ Ksi} \end{aligned}$$



where

$$PEL_a = 11.29 - 1.23 \times 10^{-3} T$$

$$Ba = 27.5 - 1.07 \times 10^{-2} T$$

### 3.2.2(1).6 Results

#### *Temperature History of Selected Points*

For each of six transients, the resulting temperature history was calculated for the 903 stress model element centroids in the reactor main flange and adjacent vessel wall. This information was sorted on punched computer cards for the use in the CREEP-PLAST computer code. The results are summarized on Figures 3B2-5 through 3B2-10. These figures show the sodium temperature and the temperatures of four arbitrarily selected points on the flange. Some of the curves show a slight jog (e.g. 40 hours, Figure 3B2-3). This is due to the calculational procedure. Running the entire transient on the TIGER V<sup>(4)</sup> computer code is expensive. Consequently, a short computer routine was written to linearly extrapolate the temperature of each node, after TIGER V indicated that the temperatures were changing approximately linearly.

In addition, the heat transfer coefficients, which vary with temperature, were adjusted only at the points where changes of slope occur in the sodium temperature trace (e.g. 40 hours, Figure 3B2-3). The end of the transient was arbitrarily selected.

#### *Stress Analysis for Startup Transient*

Figures 3B2-11 through 3B2-13 present contour plots of the effective stresses incurred during the startup transient (Figure 3B2-5). Figure 3B2-11 is at time zero corresponding to a sodium temperature of 400°F. Figures 3B2-12 and 3B2-13 correspond to sodium temperatures of 800°F and 1000°F respectively at times of 40 hours and 114 hours after the initiation of the startup transient. It is seen that the peak effective stresses occur at 40 hours after startup, which is the end of the 10°F/hour portion of the startup transient. The peak effective stress of approximately 17,000 psi occurs at the base of the fillet which joins the main flange and lower vessel. Figures 3B2-14 through 3B2-17 show the propagation of plasticity zones on the structure as the startup transient progresses. Plasticity is assumed to occur at the point where the stress-strain curve deviates from a straight line, which is about 11,000 psi. Significant yield (0.2% offset) will occur at a somewhat higher stress; however, the information presented is consistent with the yield point used by the CREEP-PLAST Program.

Figures 3B2-18 and 3B2-19 present through-the-thickness stress and strain components located just below the flange where the attaching fillet meets the vessel cylinder. On Figure 3B2-18 the axial stress and strain components are seen to be linear at time zero with a classical bending stress yield pattern developing as the reactor progresses through the heatup transient. The circumferential (hoop) stress pattern seen on Figure 3B2-19 begins with a linear pattern at time zero and appears to undergo some relaxation as the bulk sodium temperature approaches 1000°F.

### 3.2.2(1).7 Conclusions

Based on the results of this analysis, it is concluded that the SEFOR vessel-flange region will not experience stresses and strains in excess of ASME Code allowables for the startup transient. Future analyses will have to be concluded to determine the stresses and total strains accumulated from repeated transient applications. However, there is no reason to expect that code allowables will be exceeded for the projected plant operating histogram. Although the results to date show no elevated temperature problem, the effort has not progressed to an extent that a clear feasibility judgment can be made.

### 3.2.2(1).7 Task 3B2 - Reactor - Part 2

#### **Discussion**

At present an elastomer (silicone rubber) "O" ring is used as a backup seal for the two metal "O" rings between the outer head and the reactor vessel (Figure 3B2-20). This backup seal is necessary to minimize any leakage of the argon cover gas (25 psig) into the refueling cell because of the inability of the present melted "O" ring seals to completely seal due to flange rotations. With the existing design the seal experiences temperatures of 450°F. If the

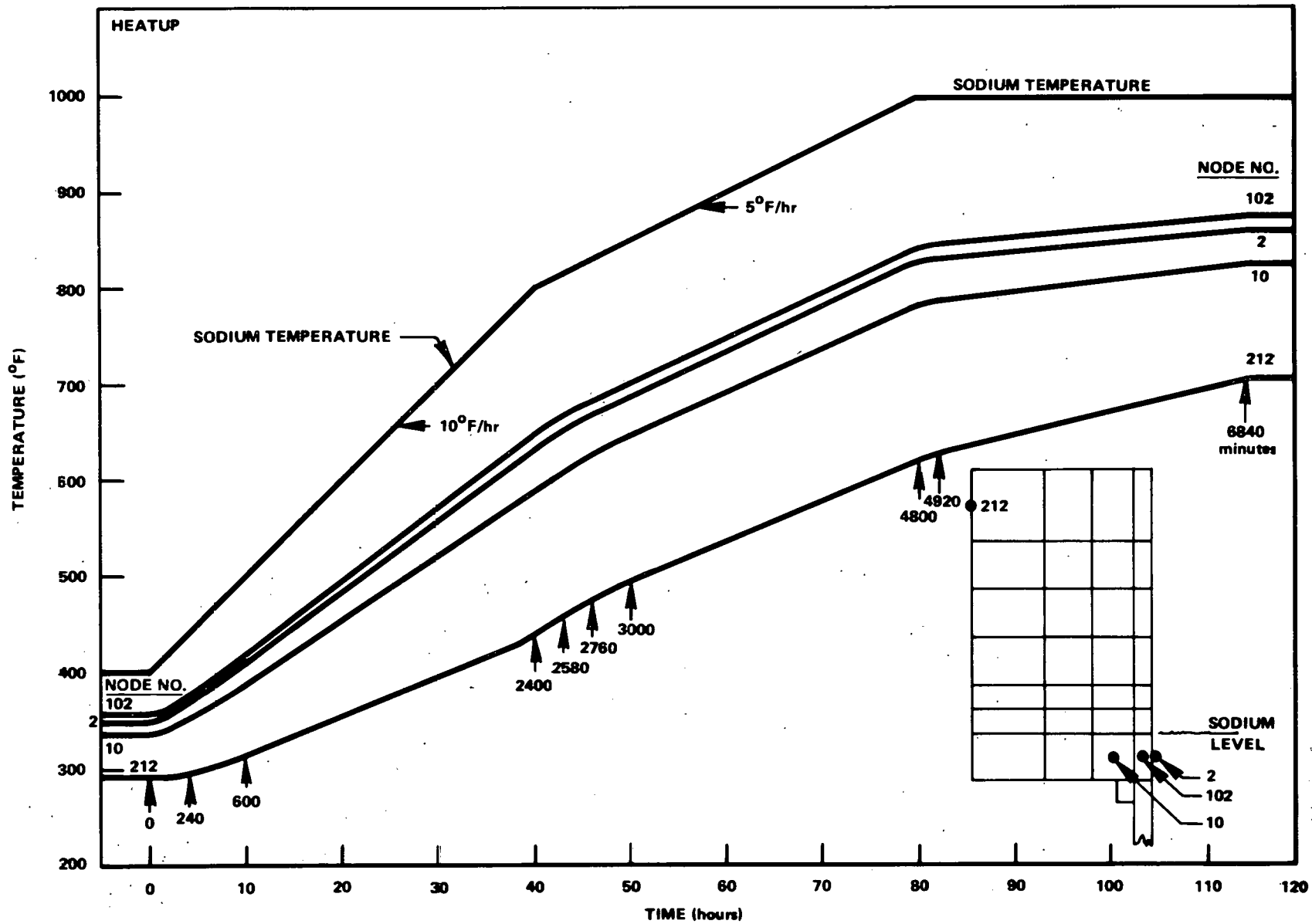


Figure 3B2-5. Heatup

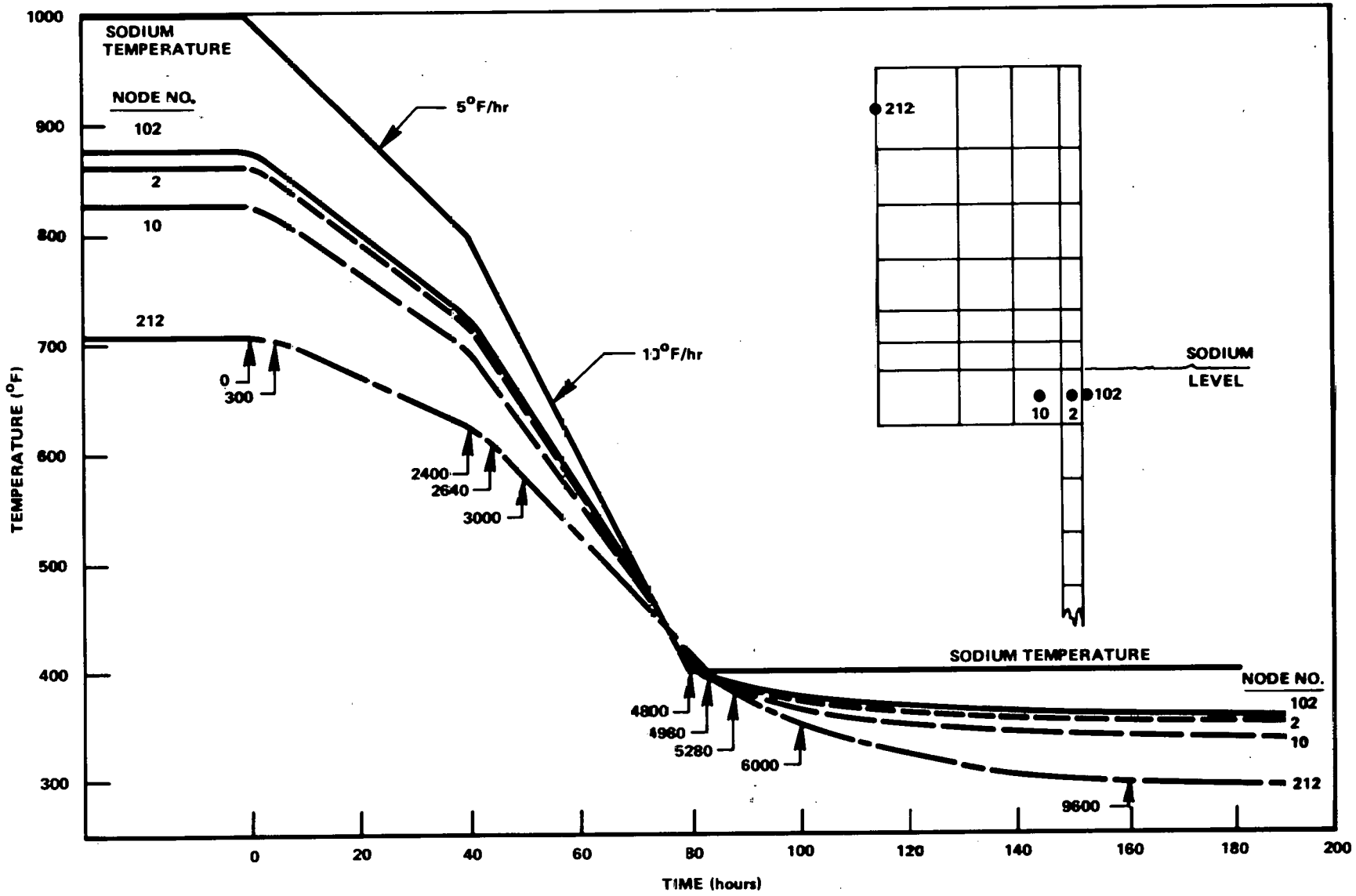


Figure 3B2-6. Cooldown

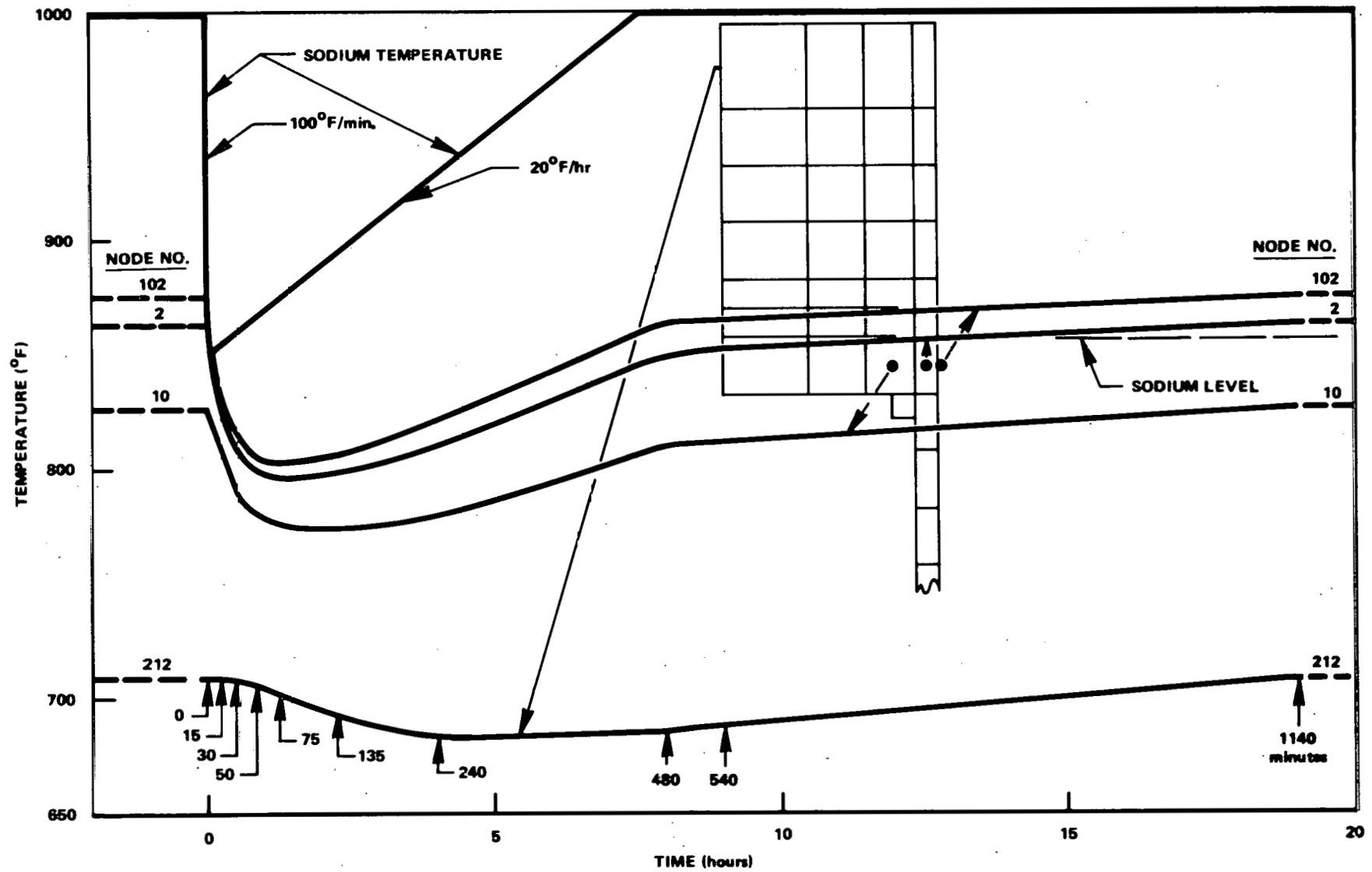


Figure 3B2-7. Normal Scram with Immediate Recovery (7.53 hours)

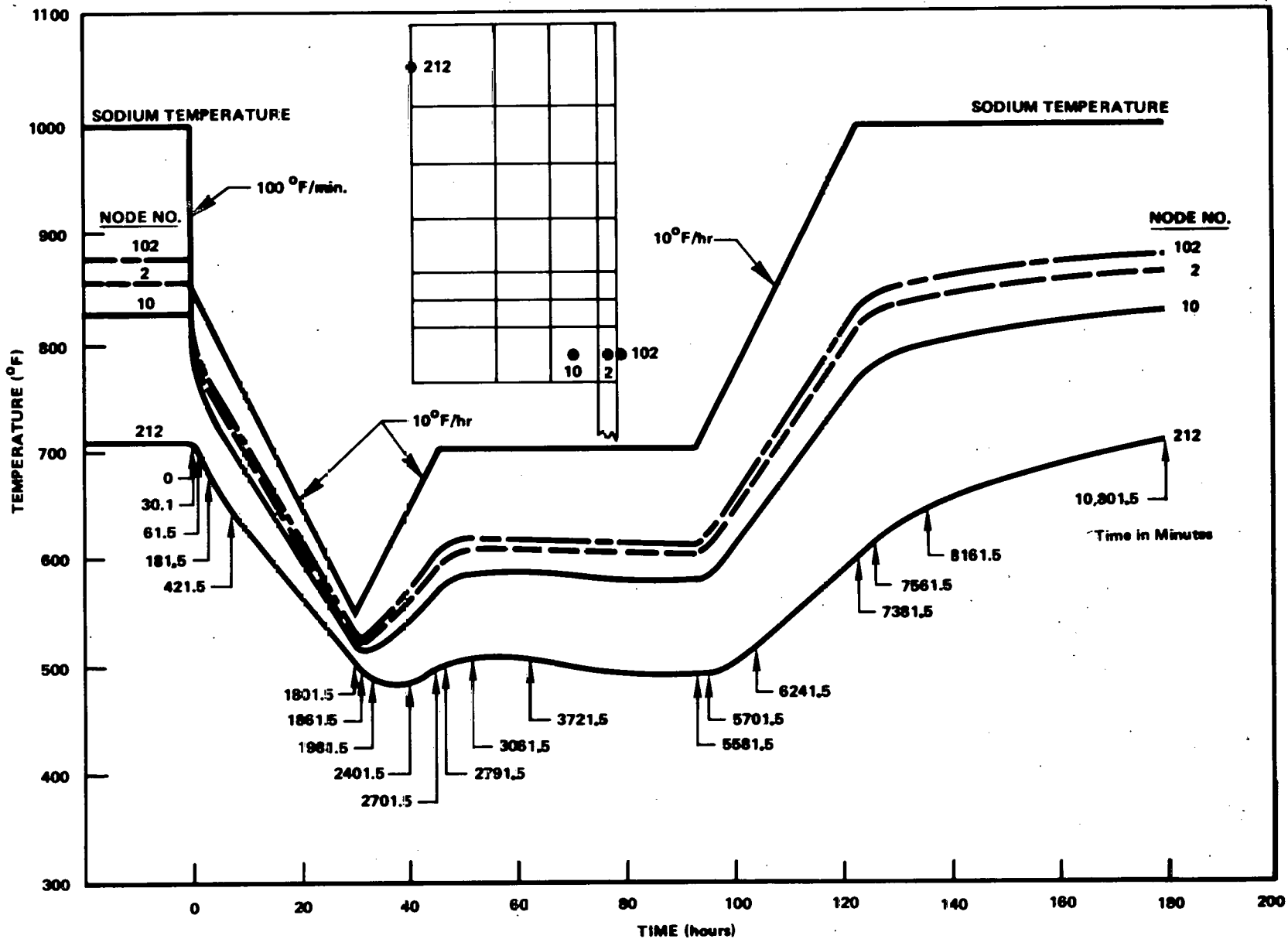


Figure 3B2-8. Plant Power Failure with Scram (123.03 hours)

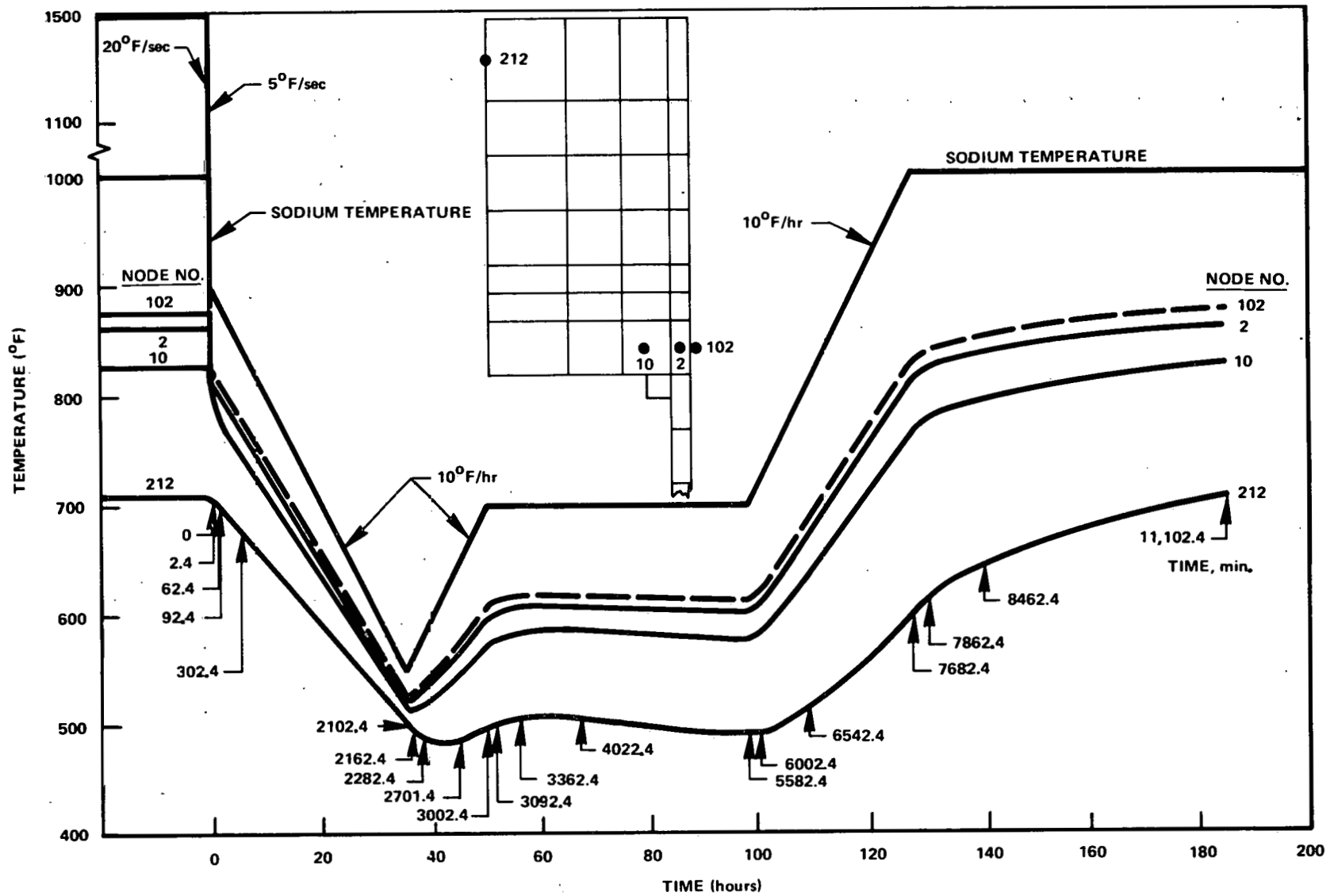


Figure 3B2-9. Plant Power Failure with Scram, No Flywheel

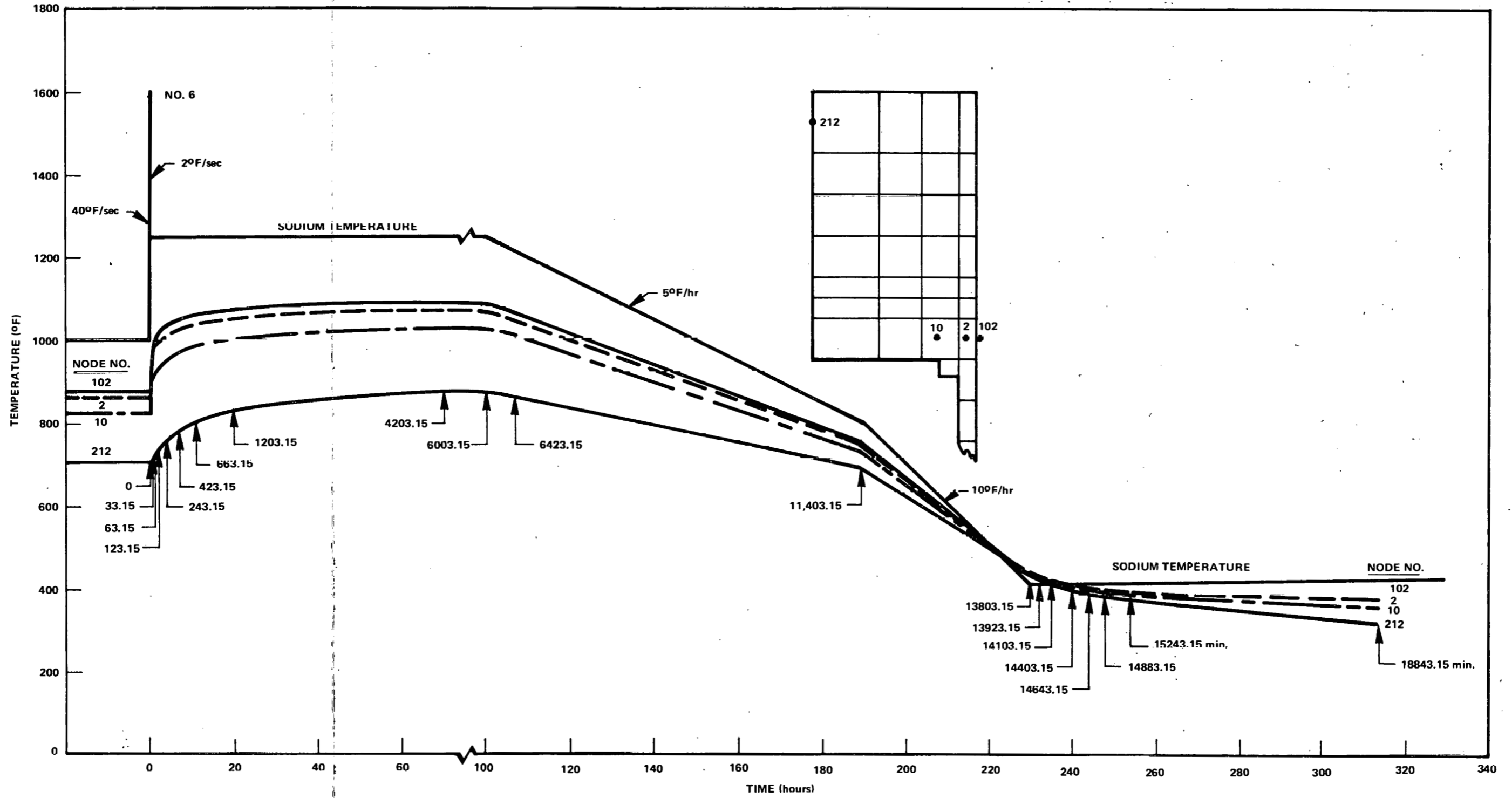


Figure 3B2-10. Plant Power Failure without Scram, No Flywheel

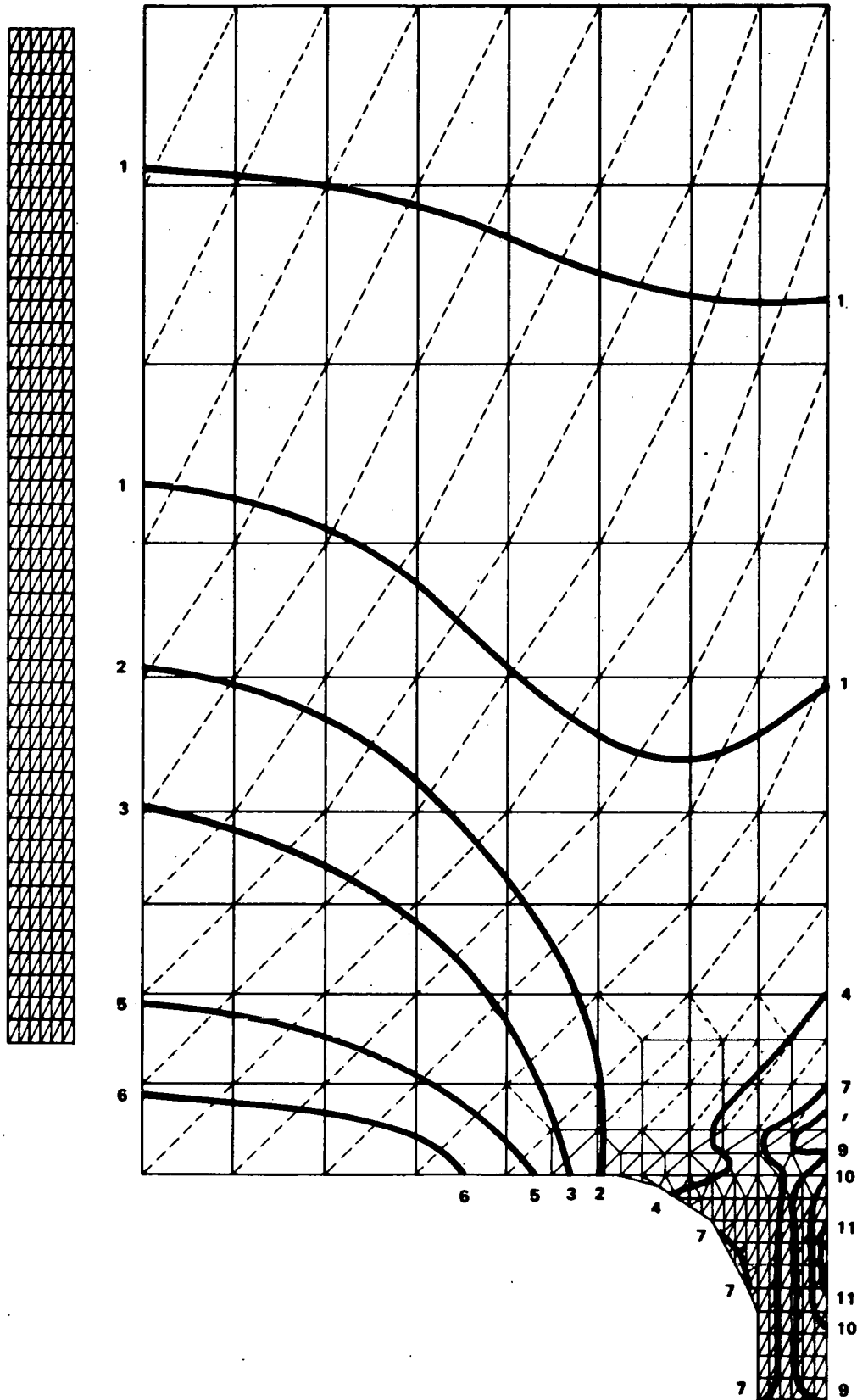


Figure 3B2-11. Effective Stress Contour Lines, Startup Transient at  $t=0$



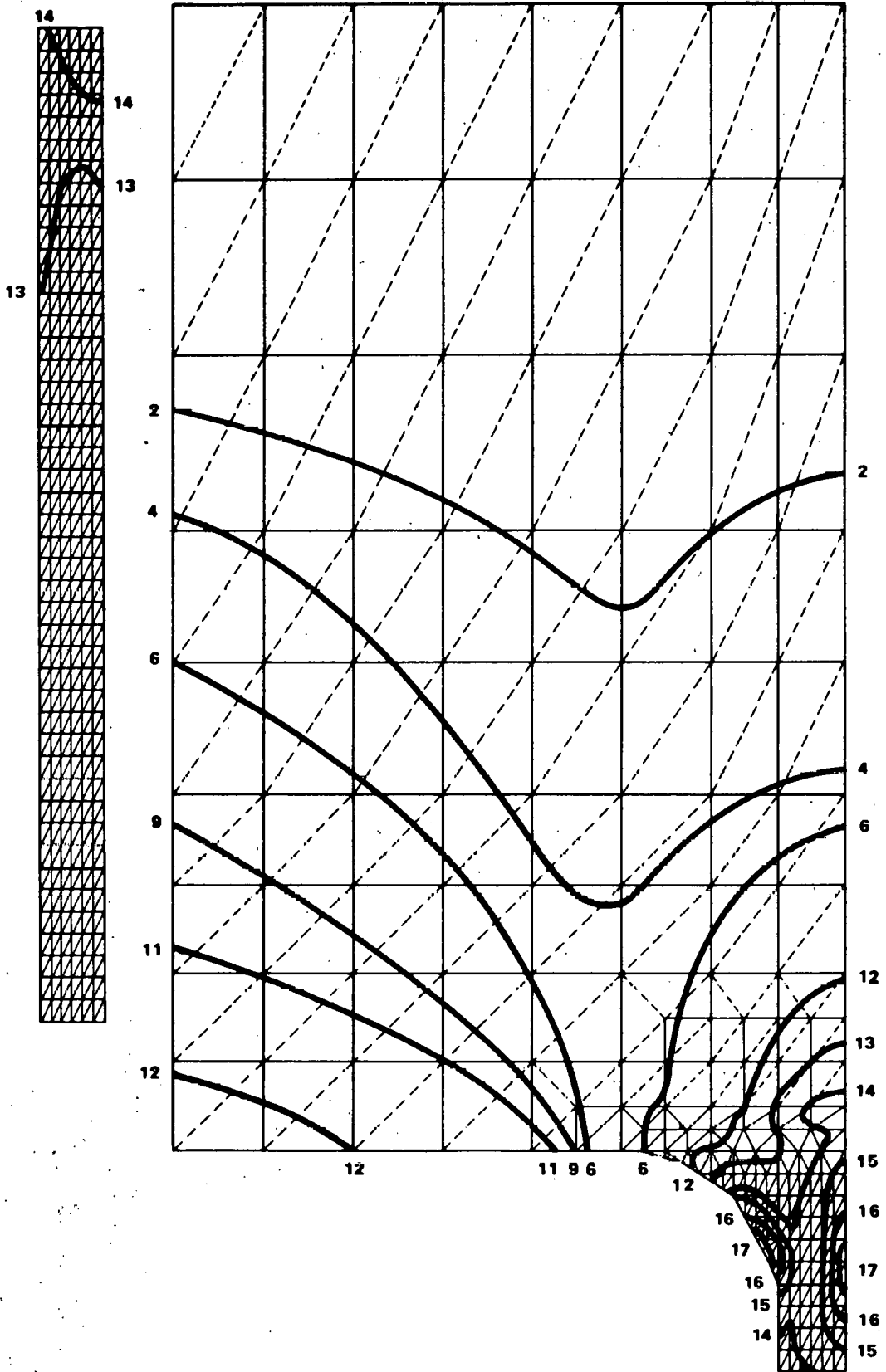


Figure 3B2-12. Effective Stress Contour Lines, Startup Transient at  $t = 40$  hours

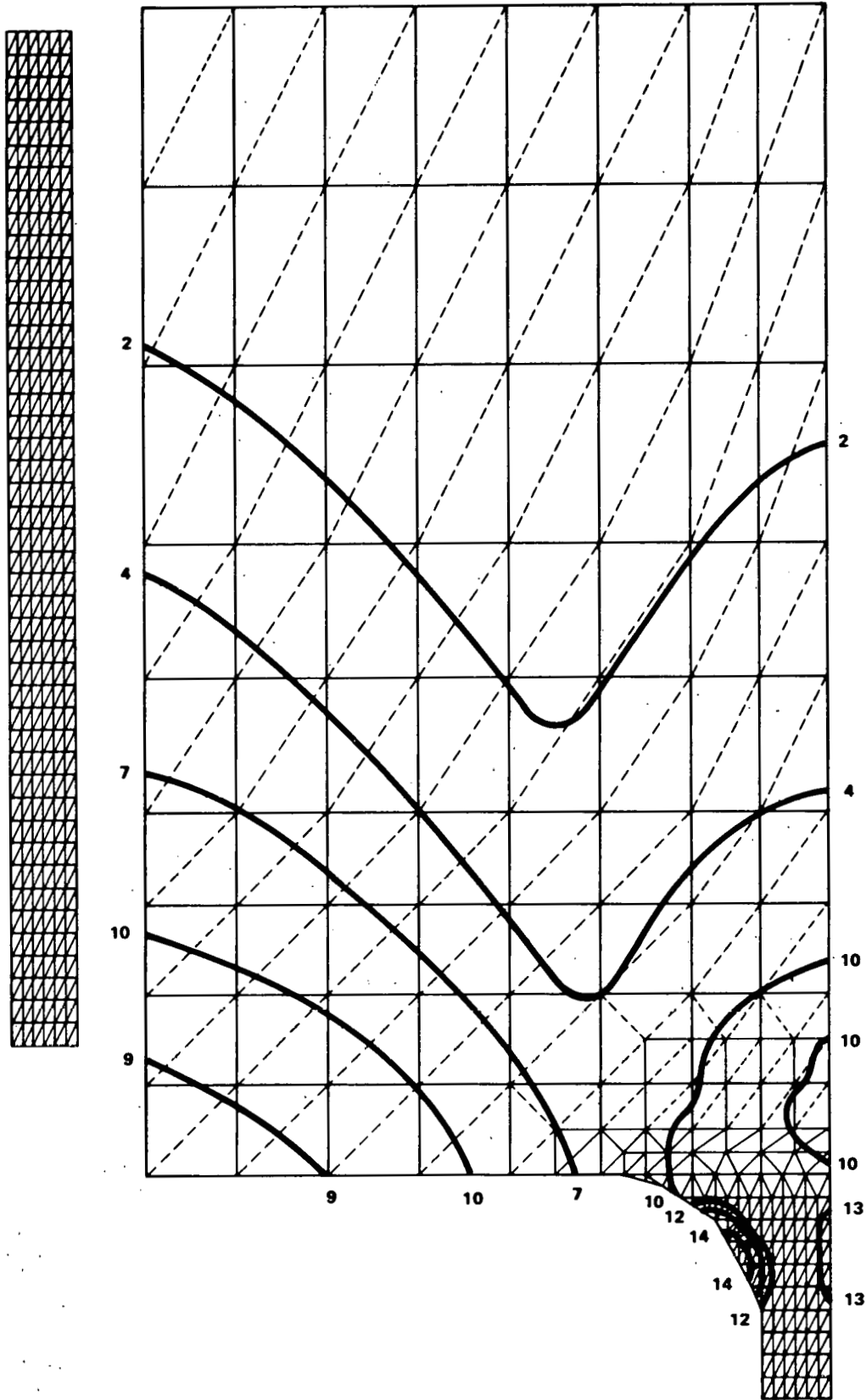


Figure 3B2-13. Effective Stress Contour Lines, Startup Transient at  $t = 114$  hours

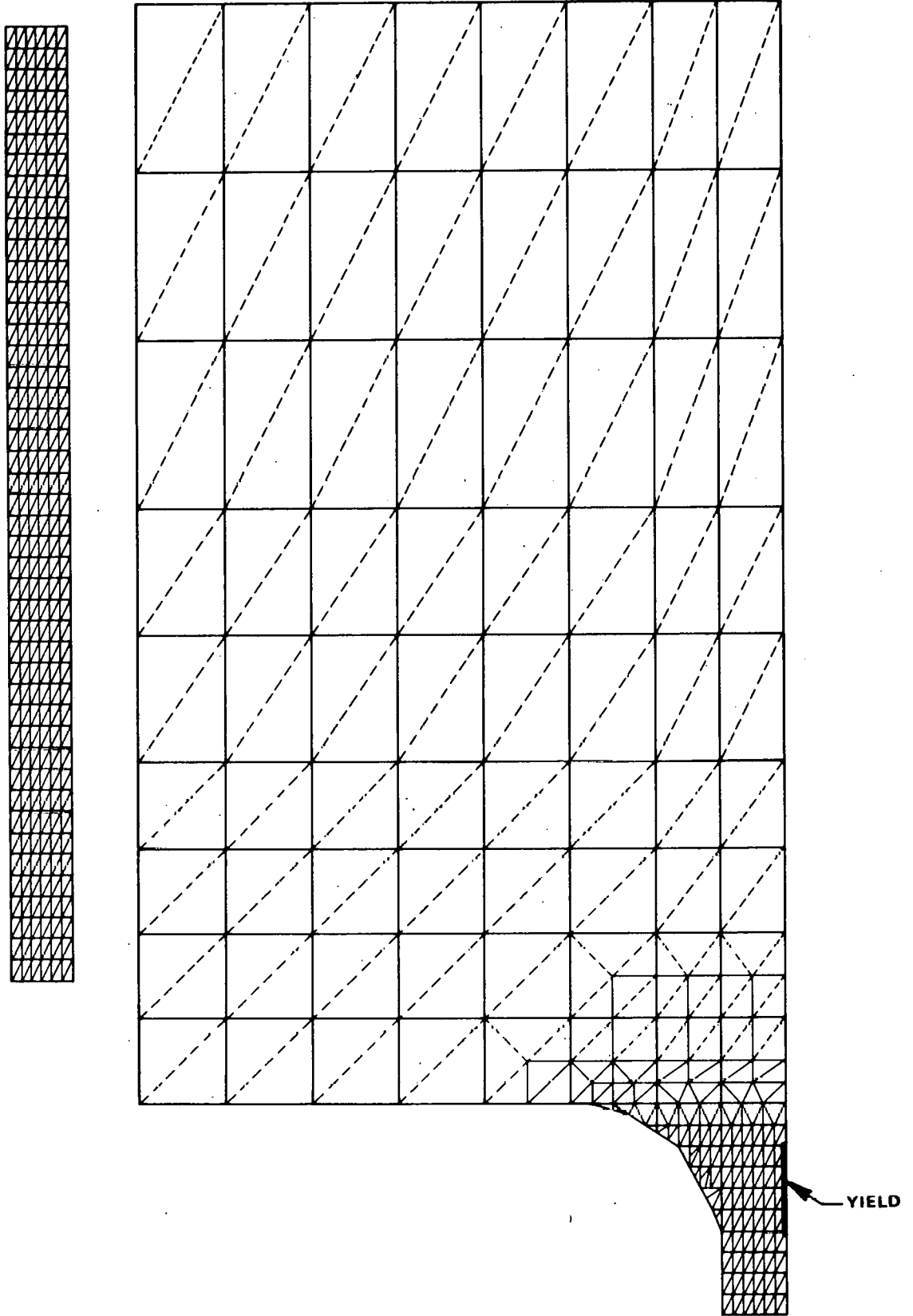


Figure 3B2-14. Yield Zones, Startup Transient at  $t = 0$

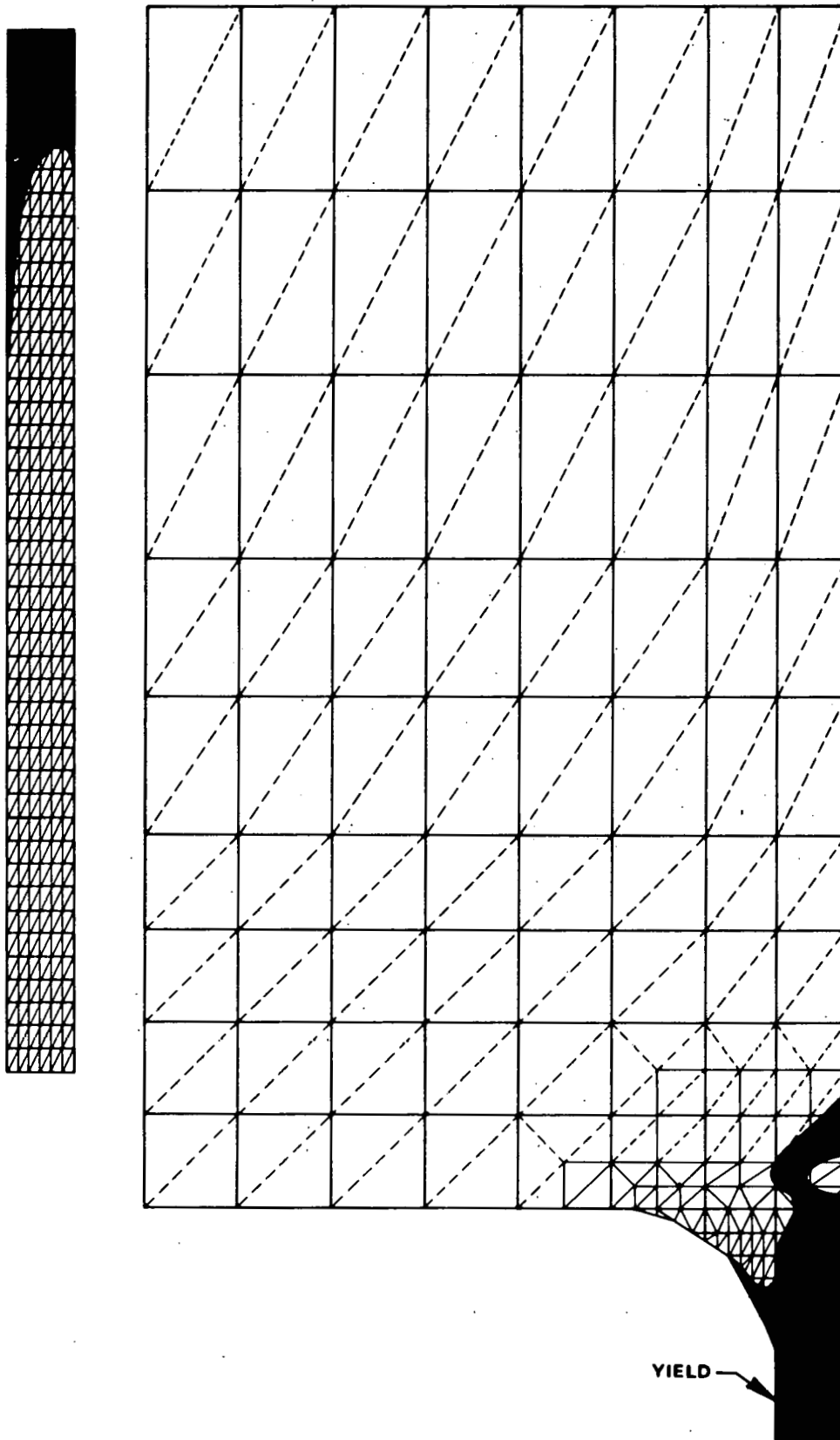


Figure 3B2-15. Yield Region, Startup Transient at  $t = 15$  hours

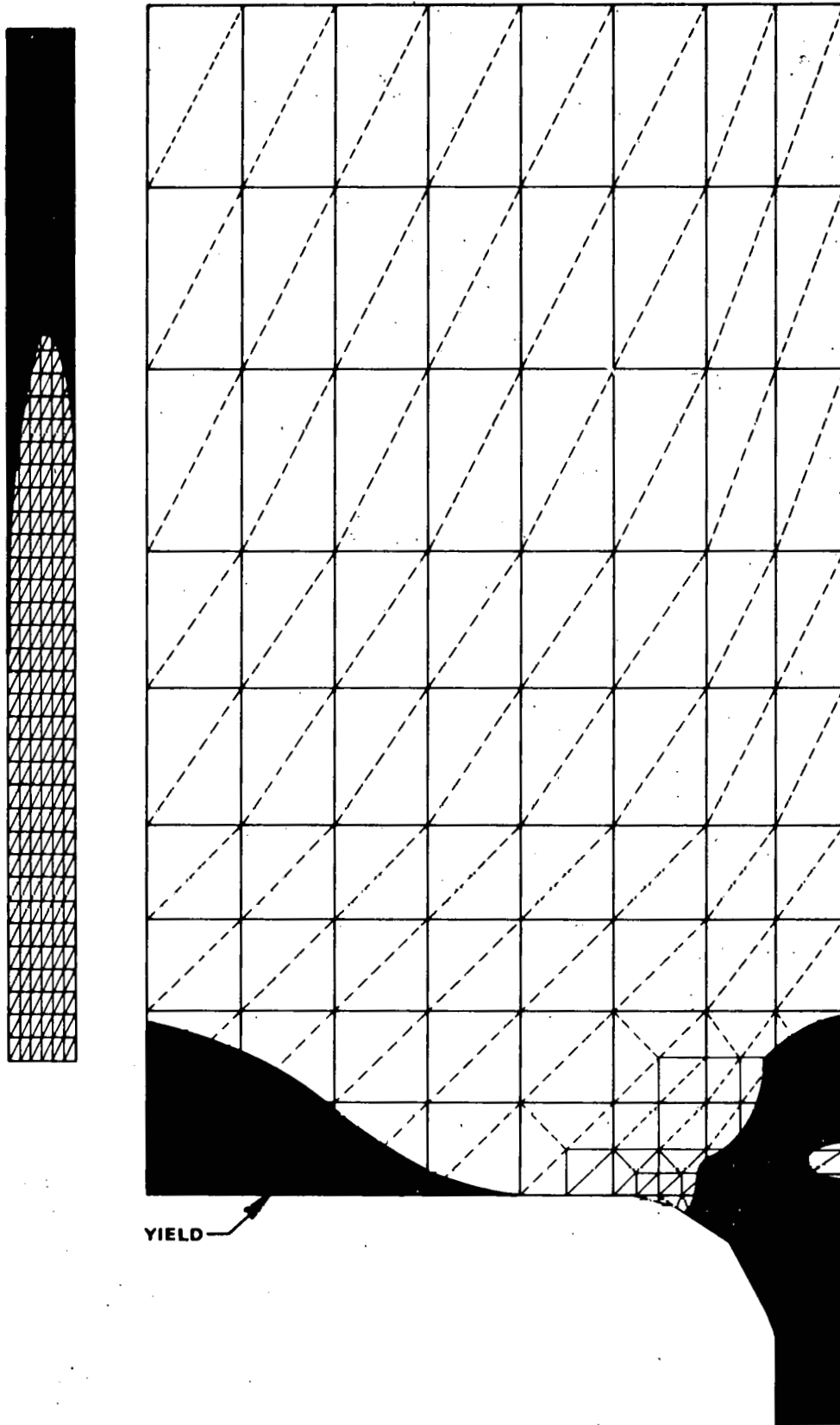


Figure 3B2-16. Yield Regions, Startup Transients at  $t = 40$  hours

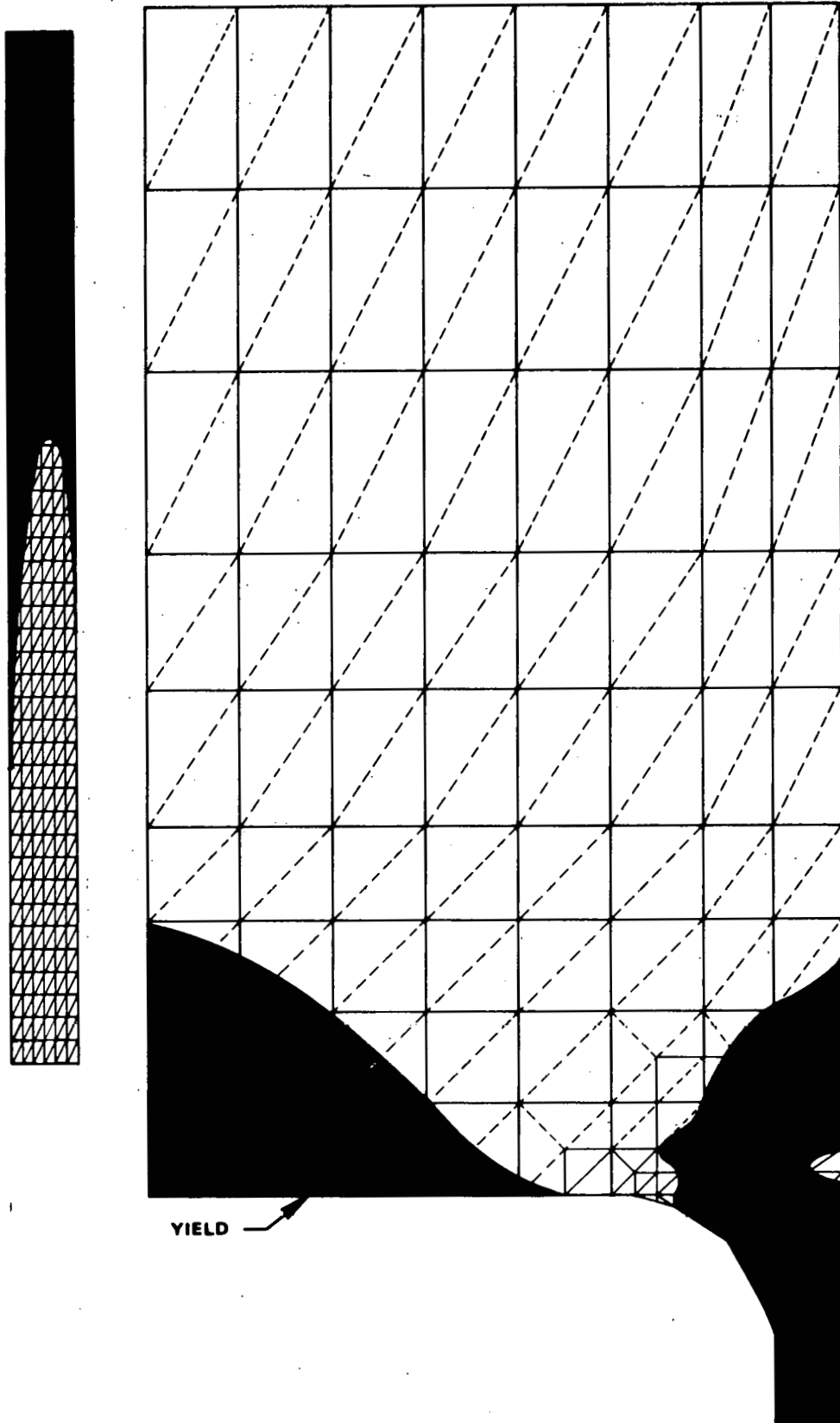


Figure 3B2-17. Yielded Zones, Startup Transient at  $t = 114$  hours (Steady-State after Transient)

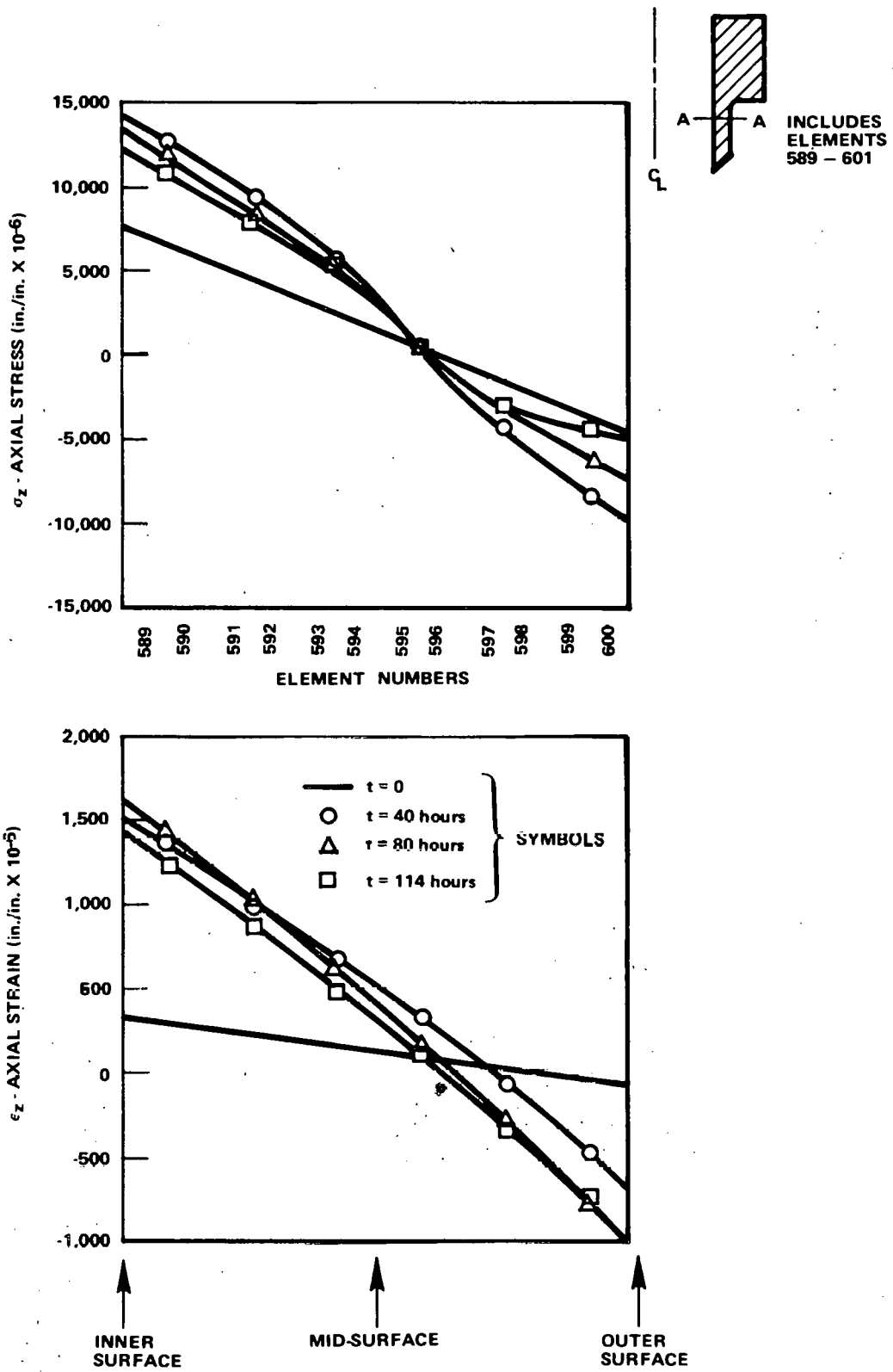


Figure 3B2-18. Stress-Strain History of Cylinder at Section A-A for Heatup Transient (Axial Components)

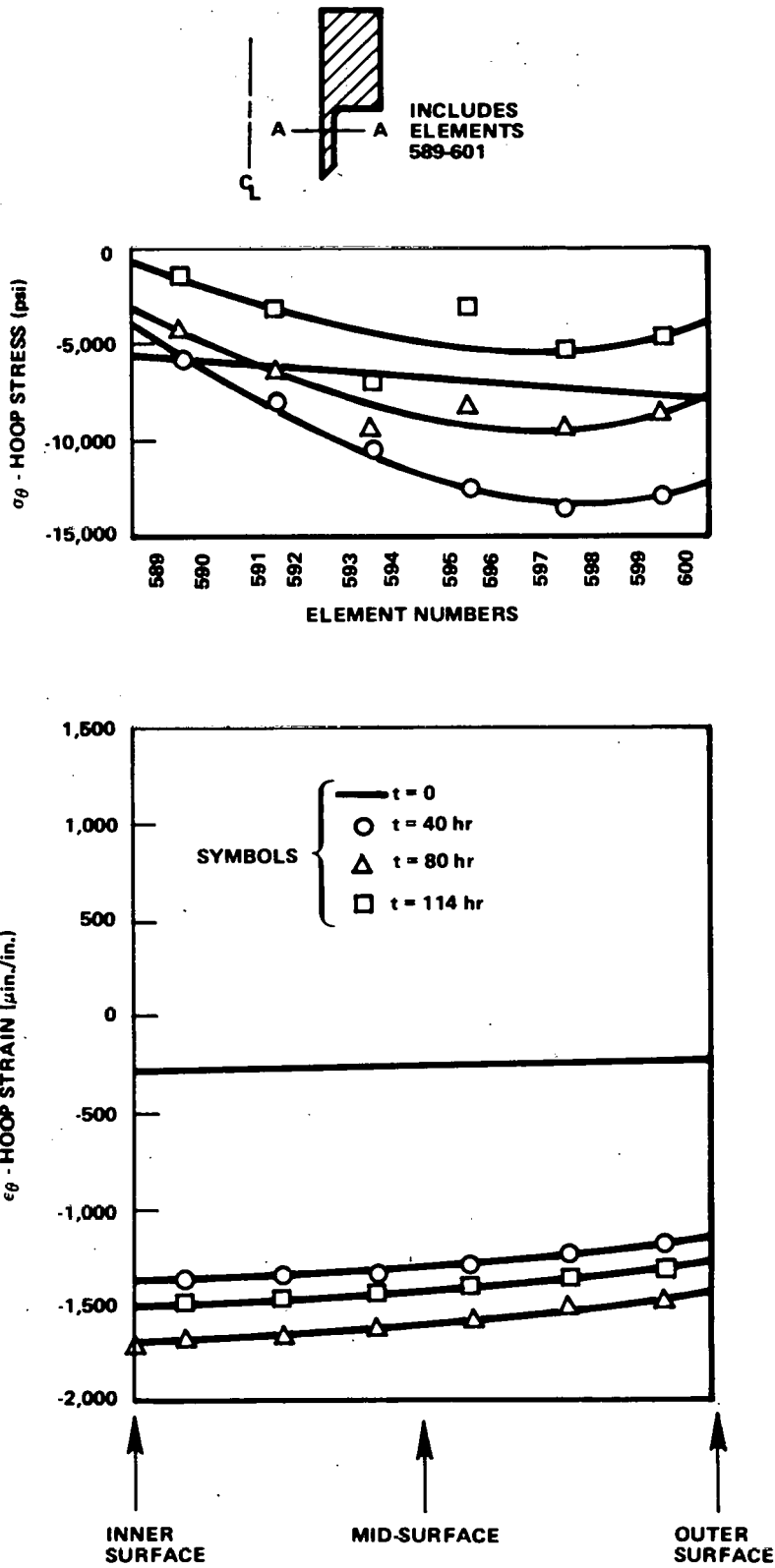


Figure 3B2-19. Stress-Strain History of Cylinder at Section AA for Heatup Transient (Circumferential Component)



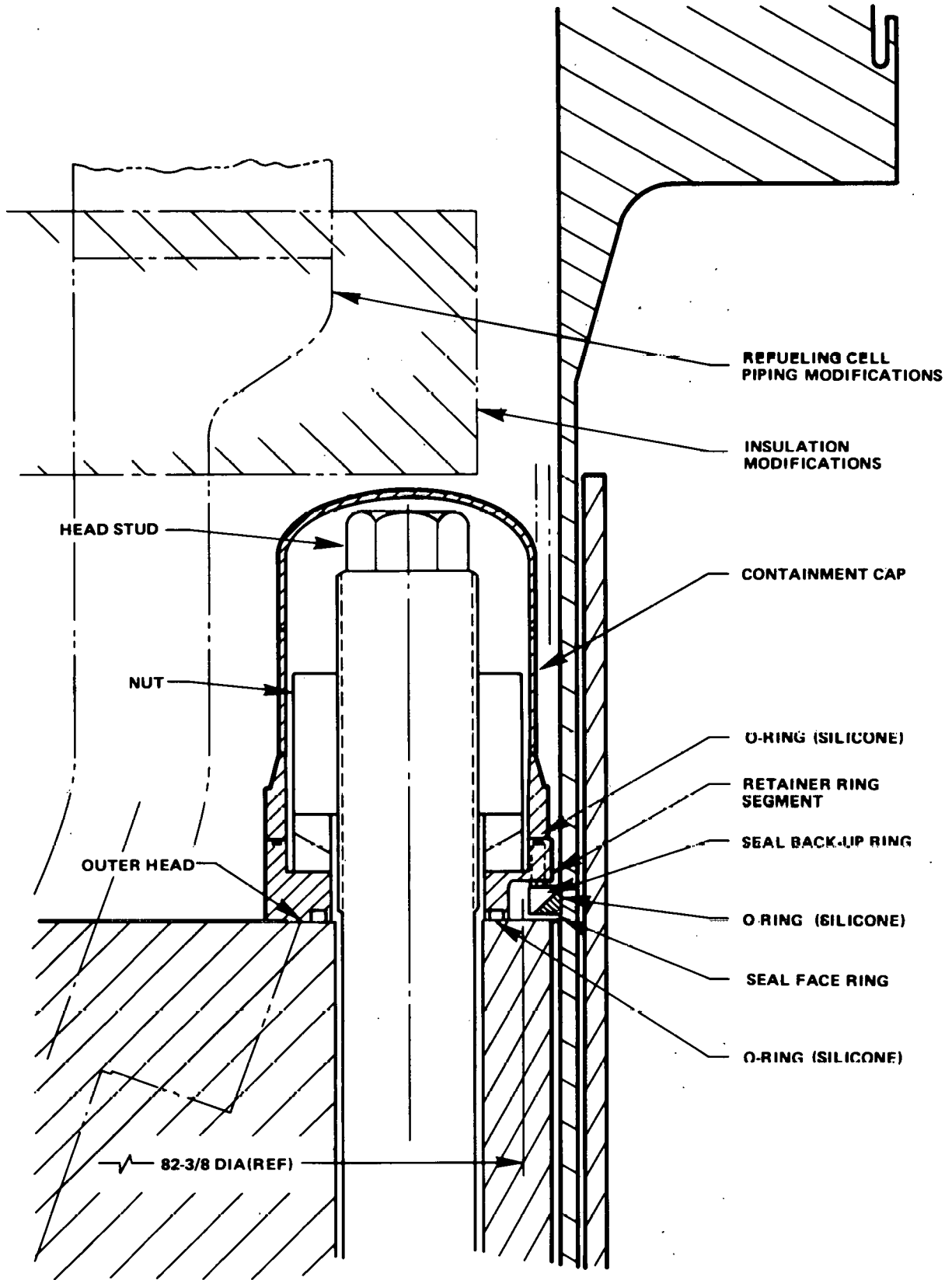


Figure 3B2-20. Existing Back-Up Seal

quid sodium temperature were to be increased to 1000°F, the outer head temperature in the area of the seal would reach 620°F. This is excessive for the existing seal design and material. A new sealing scheme will be required. The new sealing mechanism therefore, must be able to withstand outer head temperatures of 621°F and temperatures of 300°F in the region of the vessel support flange. The outer head rotates  $\pm 0.5^\circ$  during temperature changes, so any new seal will have to comply without being over stressed. Provision must also be made for in-service inspection of the studs.

Designs

Two alternate schemes which could be employed to replace the existing seal for elevated temperature operation are:

1. An elastomer seal located in a cooler area and with inflatable tubes to provide sealing contact pressure (Figure 3B2-21).
2. An all metal membrane with a bellows to provide flexibility during thermal cycling (Figure 3B2-22).

Both options would seal to the head with a nickel coated "C" seal and be held down by belleville washers and the existing studs (Figure 3B2-23). Either design will work but the inflatable tube design offers more advantages such as: no welding during installation, can accept large radial differences, and the existing stud tensioner may be used. The bellows concept should not be dropped but carried on as a backup.

In either design the subassembled parts would be brought into the refueling cell via the "man access assembly". This assembly can be removed from the wall without too much difficulty. A new seal should be on hand in case the existing one is damaged during removal. The existing backup seal (Figure 3B2-20) will have to be removed and the surface of the outer head inward of the studs polished for a new seal. The instrumented fuel assemblies (Figure 3B2-21) connections and the cover gas fill line will have to be disconnected to allow the new sealing scheme to be placed over the outer head. In the case of the bellows design, the existing cable clips on the inner surface of the vessel wall (Figure 3B2-21) will have to be removed and relocated to the top of the vessel flange. Final leak checking could be done by injecting helium gas into the cover gas and "sniffing" with a helium leak detector.

*Inflatable Tube Seal (Figure 3B2-21)*

This design utilizes inflatable tubes behind elastomer rings to provide a constant sealing pressure. The base plate and seal shell will be brought into the refueling cell as a single unit. The base plate will seal to the polished area of the outer head with a metallic seal, like a "C" seal. The sealing force will be provided by belleville washers under the existing spherical washers. They are to insure sealing loads over thermal excursions where the studs would normally be unloaded. The cover plate and the seal retainer are in segments to allow for access to the studs for in-service inspections. The seal retainer segments will be positioned via standoffs between the studs. The cover plate segments and cover gasket seal provide sealing between the segments and around the standoff screws. Inflatable tubes act as "air bags". They will be pressurized by an argon source with an adequate ballast tank to provide constant pressure. The actual sealing will be done by the two elastomer rings, which are located far enough from the thermally hot areas so as not to lose their properties.

*Metal Bellows Seal (Figure 3B2-22)*

This design would be installed as a complete subassembly. The base ring seals to the outer head with a metal seal, as above. The bellows upper skirt section is then welded to the vessel inner wall. The existing containment caps would be used to seal the studs after being reworked to accommodate metal seals. A new stud tensioner design is necessary to clear the bellows.

**3.2.2(2).3 Conclusion**

Of the two designs, the inflatable tube shows more promise. As a structure it is easier to calculate and predict stresses, the inflatable tubes can provide for large radial differences and it is not permanently attached (welded) to the vessel. The bellows design should not be totally dropped but kept as a backup design.

Either scheme will work. They both require about the same installation effort and will cost about the same. The inflatable tube design is preferred, but the bellows is a close second. They both offer advantages and disadvantages.

*Inflatable Tube Seal*

Advantages:

- No welding during assembly
- Tubes and seals easily replaced

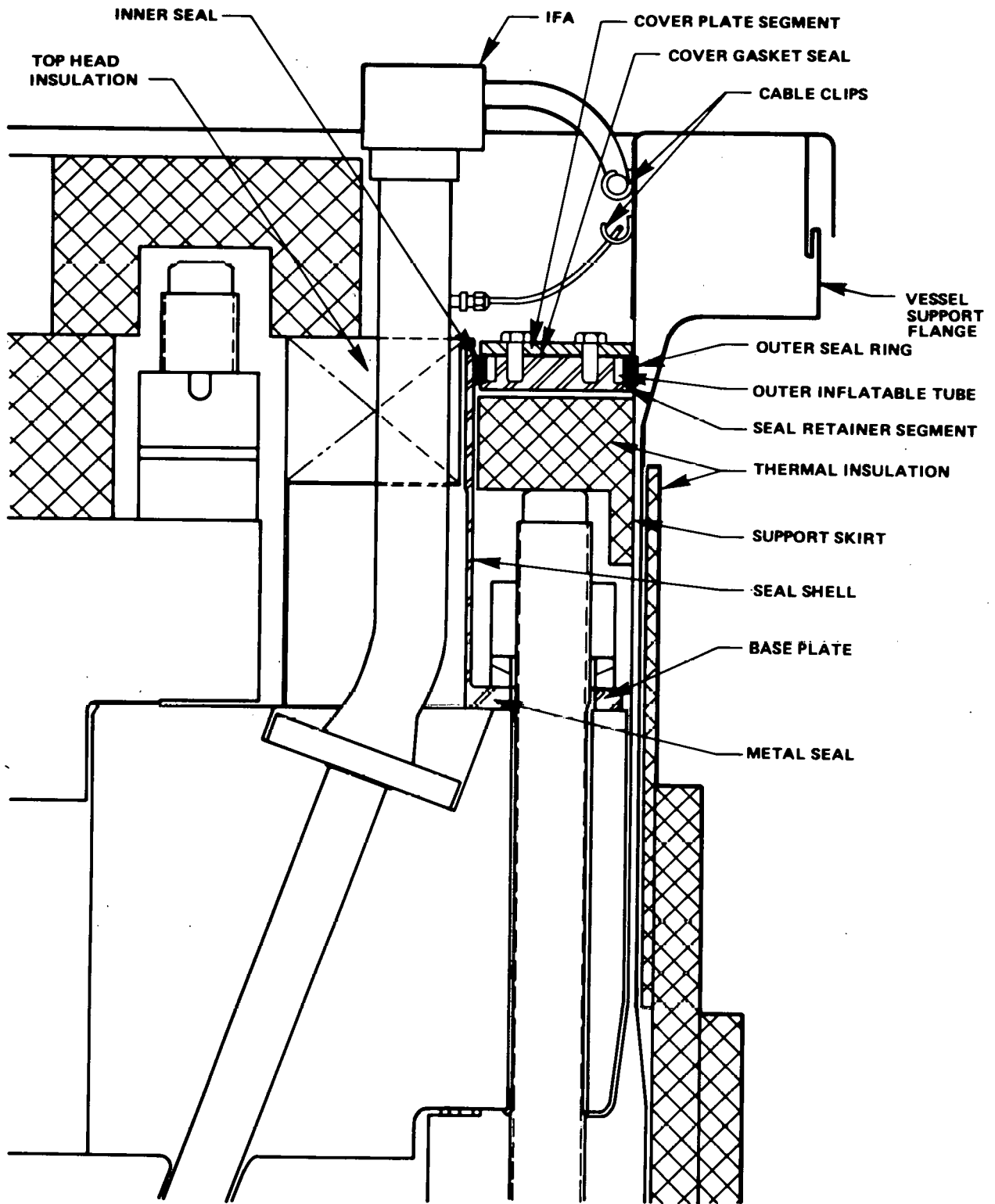


Figure 3B2-21. Inflatable-Tube Seal

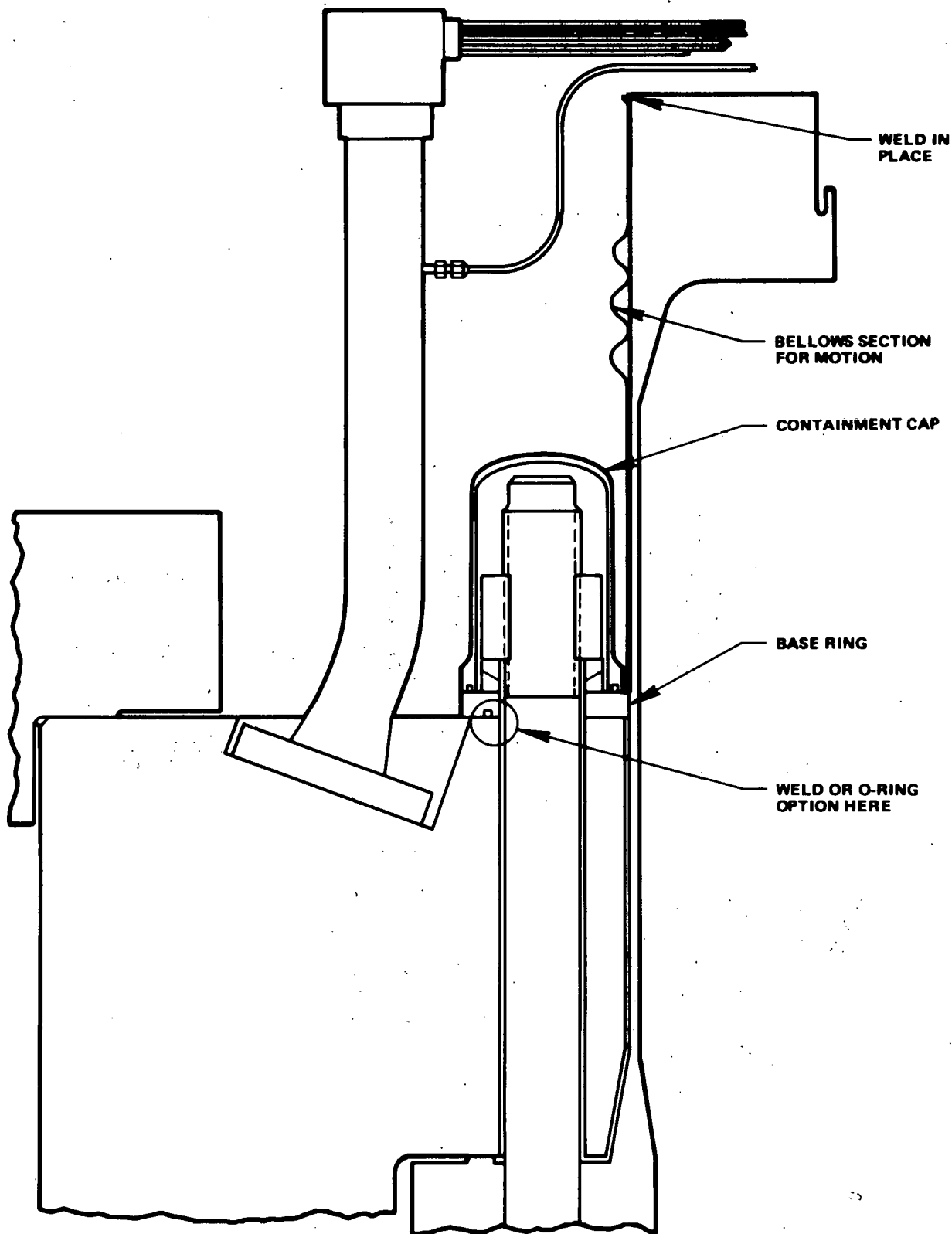


Figure 3B2-22. Metal Bellows Seal

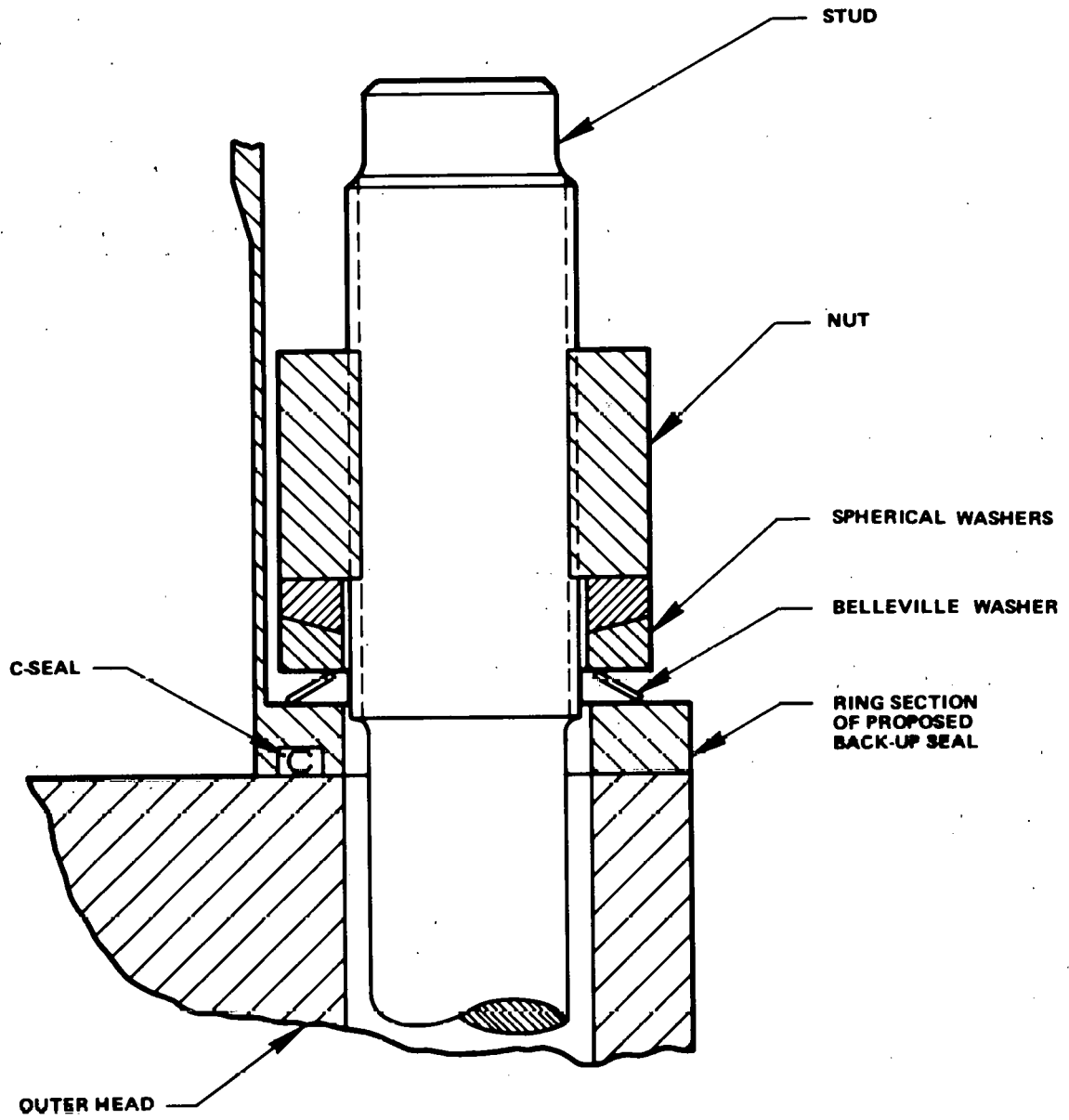


Figure 3B2-23. Belleville Washer Location

Can accept large radial differences  
 Uses existing stud tensioner  
 Stresses easily predicted

Disadvantages:

Entire seal must be broken for stud in-service inspection  
 Requires a new thermal insulation

*Metal Bellows Seal*

Advantages:

All metal, no elastomer  
 Main seals not broken for in-service inspection  
 Uses existing insulation

Disadvantages:

Requires welding at installation  
 Stresses hard to predict  
 Requires a new stud tensioner

**3.2.2(3) Task 3B2 - Reactor - Part 3**

**3.2.2(3).1 Discussion**

During elevated temperature operation, as well as lower temperature operation, the highest stressed region of the reactor vessel is the flange to vessel junction. The primary cause of these high stresses is flange rotation due to thermal gradients. The present stress levels are well within the stress requirements of the new ASME Code and will probably remain adequate should the reactor temperature be increased to 1000°F. As a back-off position, for the remote possibility if the stress levels prove excessive, the sodium level can be lowered. Lowering the sodium level 6 to 8 inches would move the thermal gradient sufficiently far from the flange and reduce its rotation.

The sodium level is controlled by an overflow standpipe, a flattened vertical pipe in the reactor which connects with the primary drain tank. The excess sodium in the vessel pours over the open top and out through this pipe. To lower the level, the standpipe will have to be altered. The best way to do this is to cut a 4 inch diameter hole in the front face of the pipe. The hole would be located so as to control the sodium level at a new lower depth. Should the desire arise to operate the reactor at the original depth again, it would be a simple matter to close the hole with a set of plates through-bolted on both sides of the hole.

The equipment proposed for this operation consists of an argon gas driven drill motor (Figure 3B2-24), a specially designed cutter with a chip capturing boot, a chip vacuuming system, and a backup catch basin for chips. The operating procedure further safeguards against the possibility of dropping chips. If it should ever prove necessary to lower the sodium level, this is the most practical way to do it.

**3.2.2(3).2 Drilling Equipment**

The most straight forward way to produce a hole is to simply cut it. Figure 3B2-24 represents a general method for accomplishing this. The power source for cutting is an argon driven "air motor". The scheme shown uses a coil spring to provide the feeding force. Another concept uses an air motor with a positive gear feed. In either case the motor will be mounted on a bracket as shown. The bracket will index and lock on the overflow pipe in the correct location. The argon exhaust will be ducted away so as not to interfere with the chip collection. The cutter itself can be either a hole saw or a disc with one or more flycutters. The latter appears to be the best since it will require a lower feeding force. Both options will require a pilot drill for cutter stabilization. The problem of chip capture is easily overcome by shrouding the cutter with a rubber boot and inserting a rubber skirted pan below the cutting area inside the standpipe. The rubber boot (or boots if a separate one is used for the pilot drill) will mount around the cutter shaft on a teflon bushing and will not turn with respect to the tube. A vacuum hose could be attached to the boot to suck away the chips as they are formed or they could all be vacuumed away during the cleanup after the hole is cut. Both methods should be tested to establish the easiest. As a backup to the boot (or boots) a catch basin would fit around the front of the overflow to catch any chip that might not be picked up with the vacuum.

During the operation the operator will be on a special platform in the reactor (Figure 3B2-25). This operator bucket will be passed through the man access door in sections and assembled in the refueling cell.

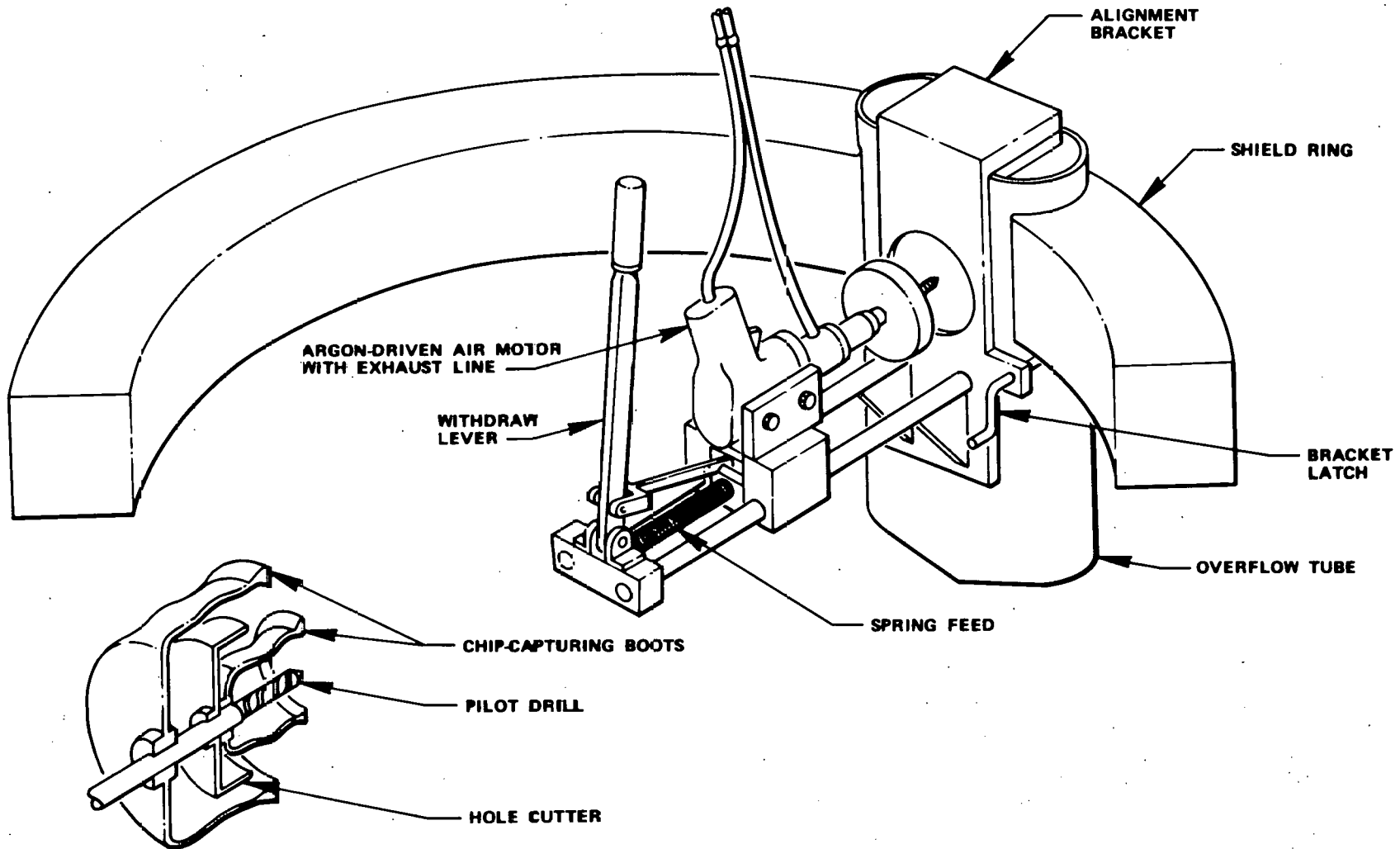


Figure 3B2-24. Hole Drilling Assembly

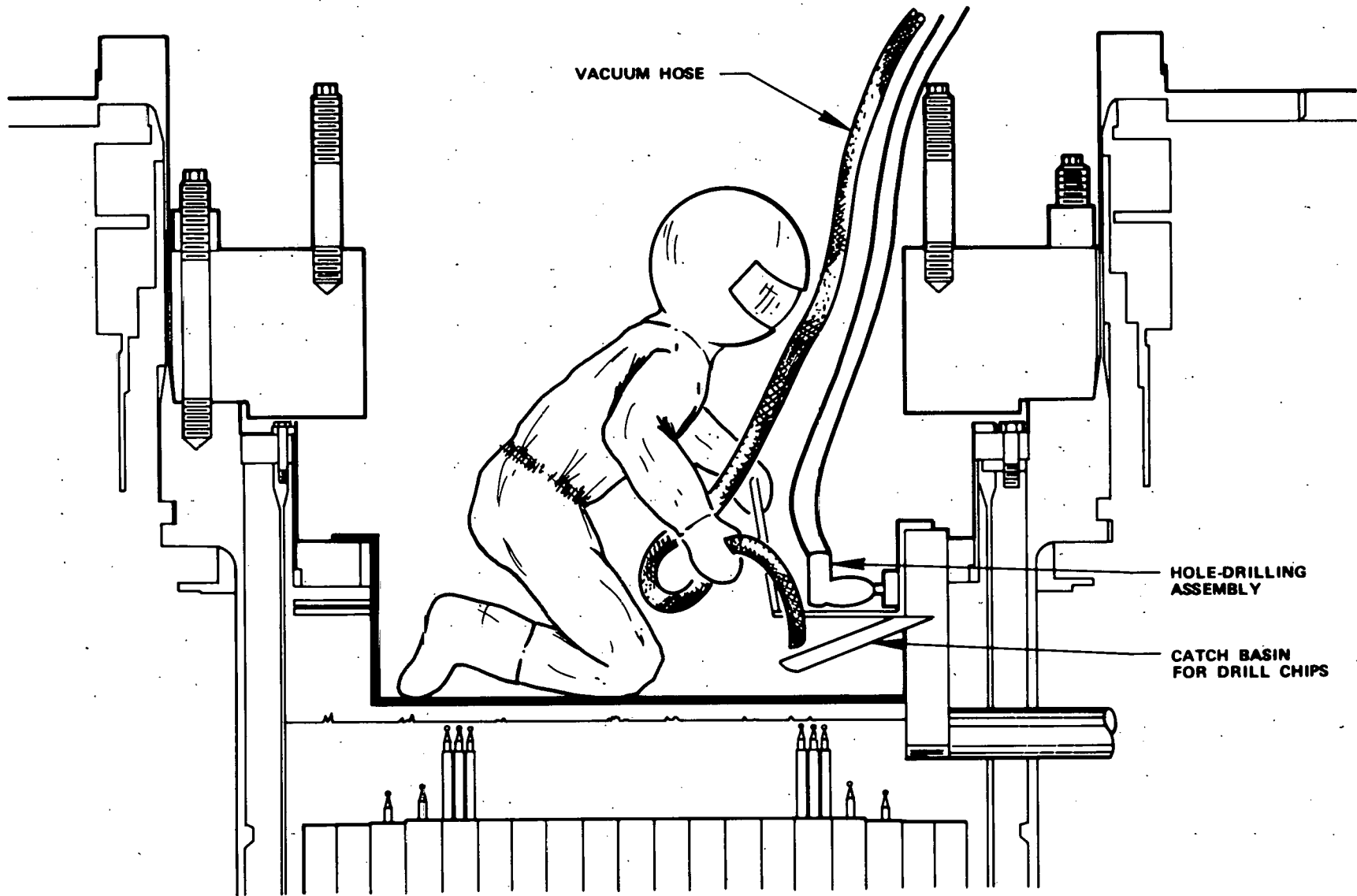


Figure 3B2-25. Hole Drilling Operation



**3.2.2(3).3 Drilling Procedure**

The drilling will have to be done under adverse conditions. The operator will be in a space suit, he will be in tight quarters, and the metal parts will be approximately 300°F. To insure success, the operation will have to be rehearsed a number of times under mocked up conditions.

The proposed procedure is:

1. Remove reactor inner head and lower the sodium to the refueling level.
2. Lower the sodium temperature as low as possible.
3. Install operator bucket (Figure 3B2-25) on shield ring with crane.
4. Operator will now enter the bucket.
5. Place catch basin around and pan inside of the standpipe.
6. Lower hole drilling assembly into place with crane (assembly weighs approximately 100 lbs).
7. Lock assembly to standpipe.
8. Drill.
9. When drilling is done, withdraw cutter and vacuum away remaining chips.
10. Plastic bag cutter assembly to insure against dropping any chips.
11. Remove drilling assembly with crane.
12. Vacuum catch basin and inside pan and remove.
13. Remove bucket.

The entire operation is practical but a dress rehearsal will be required to show if any problem areas exist.

**3.2.2(3).4 Hole Location**

To establish the depth at which to place the hole in the standpipe, the following thinking was used. At present the overflow pours over the edge of the standpipe. The height at the crest was measured at 1/8 inch for a flow of 2 gal/min. The fluid flow characteristics are similar to those of a weir, but with two exceptions:

1. The nappe is not ventilated.
  2. The ratio of the crest height to width is 1/2. For a normal weir it is greater than 1 1/2.
- By the same analogy, sodium spring through an oversized hole is not a true weir either.

The cross sectional area of the existing flow over the standpipe is 3.73 sq in. The area of a 4 inch diameter hole is 12.56 sq in. (4 inches as an optimum size for cutting). If the two flow velocities are equal, the depth of the sodium through the hole would be 1.35 in. Not quite 1/2 way up. The velocity through the hole will be slightly higher due to reduction surface to area of flow. If for example the flow rate were doubled, which is unlikely, the depth through the hole would be 0.82 in., only 0.52 inches lower.

When an actual new depth is established for the sodium, a 4 inch diameter hole located 0.91 inches above the proposed level should maintain the level within 1/4 inch of desired. However, since water can be used to model liquid sodium it would be wise to verify these assumptions by test.

**3.2.2(3).5 Recommendation**

Since this operation and the equipment required are unique only so much can be designed on assumptions, then experiments and tests must be made.

A working model of this hole drilling assembly should be made and tested to establish the optimum cutters, speed and feed. Then it should be evaluated for chip capture and modified as required. Finally, it should be tested under simulated conditions to evaluate operator performance. Only after such rigorous testing can we state that we have a workable design.

**3.2.2A Appendix A Thermal Model of the SEFOR Main Flange and Head**

**3.2.2A.1 Summary**

The thermal model generated by Fukushima<sup>5</sup> has been examined in the light of more recent data.<sup>6</sup> Somewhat different heat transfer coefficients were calculated. The temperature distribution calculated by TIGER-IV<sup>c</sup> using the new coefficients is compared to the data on Figure A-1.

The effective heat transfer coefficients recommended for use at a sodium temperature of 760°F are also shown on the figure.

**3.2.2A.2 Heat Transfer Through the Inner Head**

The inner head (Figure A-2) is a flat steel plate with insulation on top and two steel plates suspended beneath. Heat flows from the sodium, through the argon cover gas space and the inner head assembly, into the refueling cell.

A one-dimensional model of this heat transfer is described in Appendix B. The major uncertainties in applying the model are the emissivities of the sodium surface and of the steel surfaces beneath the head, and the effectiveness of the natural convection heat transfer. Experimental work by the French<sup>7</sup> suggests that all surfaces in contact with the cover gas become coated with sodium and exhibit an emissivity of 0.11. However, Kreith<sup>8</sup> gives the following typical values for shiny surfaces (at 500° F):

Polished Aluminum	0.05	Polished Iron	0.08
Polished Brass	0.10	Polished Silver	0.02
Polished Copper	0.05	Polished Zinc	0.03

Good agreement with the inner head temperature measurements<sup>6</sup> can be achieved by assuming that the emissivity of the steel surfaces is 0.10, the emissivity of the sodium surface is 0.02, and that the effectiveness of the natural convection is one-half of that predicted by the French model.

The equivalent heat transfer coefficients between the sodium and the lower surface of the head is shown in Figure Three. The coefficients increase with increasing temperature because of an increasing contribution from radiation heat transfer. The contribution from natural convection actually drops slightly as the Na vapor concentration increases. The coefficient for heat transfer from the top of the head is essentially constant at 0.14 Btu/hr-ft<sup>2</sup>°F. However, a value of 0.2 was found to give better agreement in the two-dimensional TIGER-V model.

**3.2.2A.3 Heat Transfer Through the Outer Head**

The outer head (Figure A-2) is an annular steel member with roughly a rectangular cross-section. It has insulation on top, but no plates suspended beneath. Most of its lower surface and its inner surface are in contact with the cover gas. Part of its upper surface is separated from the insulation by a nitrogen gap. The remaining part is in contact with a flange on the inner head. Its outer surface is separated from the support skirt by a slight argon gap.

A one-dimensional approximation to this very complicated arrangement is described in the appendix. Again, both the radiation and the convection heat transfer are uncertain. Good agreement of the one-dimensional model with the measured temperatures<sup>6</sup> is achieved by assuming low emissivity and assuming that the heat transfer by convection is reduced to half of the calculation value.

The equivalent heat transfer coefficient between the sodium and both the lower surface and the lower part of the inner surface of the outer head is shown on Figure A-3. The values from the one-dimensional analysis were increased by 64% to give better agreement in the two-dimensional TIGER-V model. The upper part of the inner surface is shielded from thermal radiation and from convection currents by the same steel plates which shield the inner head. Consequently, the coefficients calculated for the inner head are used in this region.

The equivalent heat transfer coefficient between the outer head top surface and the refueling cell is essentially the same as for the inner head.

From the outer surface of the outer head, heat is transferred horizontally across the argon gap, through the support skirt, and through the insulation into the nitrogen cooling gas. Heat flows across the gap by both radiation and conduction. Here the major uncertainties are the width of the gap and the emissivity of the steel surfaces. The measurements<sup>6</sup> show only one value for the outer head temperature at the gap, and two values for the skirt temperature at the gap. If it is assumed that the smaller measured delta-T is associated with a narrow gap, then the heat transfer coefficients are the following:

	Polished Surface ( $\epsilon = 0.15$ )		Weathered Surface ( $\epsilon = 0.85$ )	
	$h_{gap}$	$h_{skirt}$	$h_{gap}$	$h_{skirt}$
Close Gap (0.01 inches)	12.4	0.54	15.8	0.68
Wide Gap (0.06 inches)	2.4	0.73	5.6	1.68

Conduction across the gap dominates. Trial runs of the TIGER-V model indicate that the best agreement results when coefficients of 10.0 and 0.6 Btu/hr ft<sup>2</sup>°F are used for the gap and the outside of the skirt, respectively.

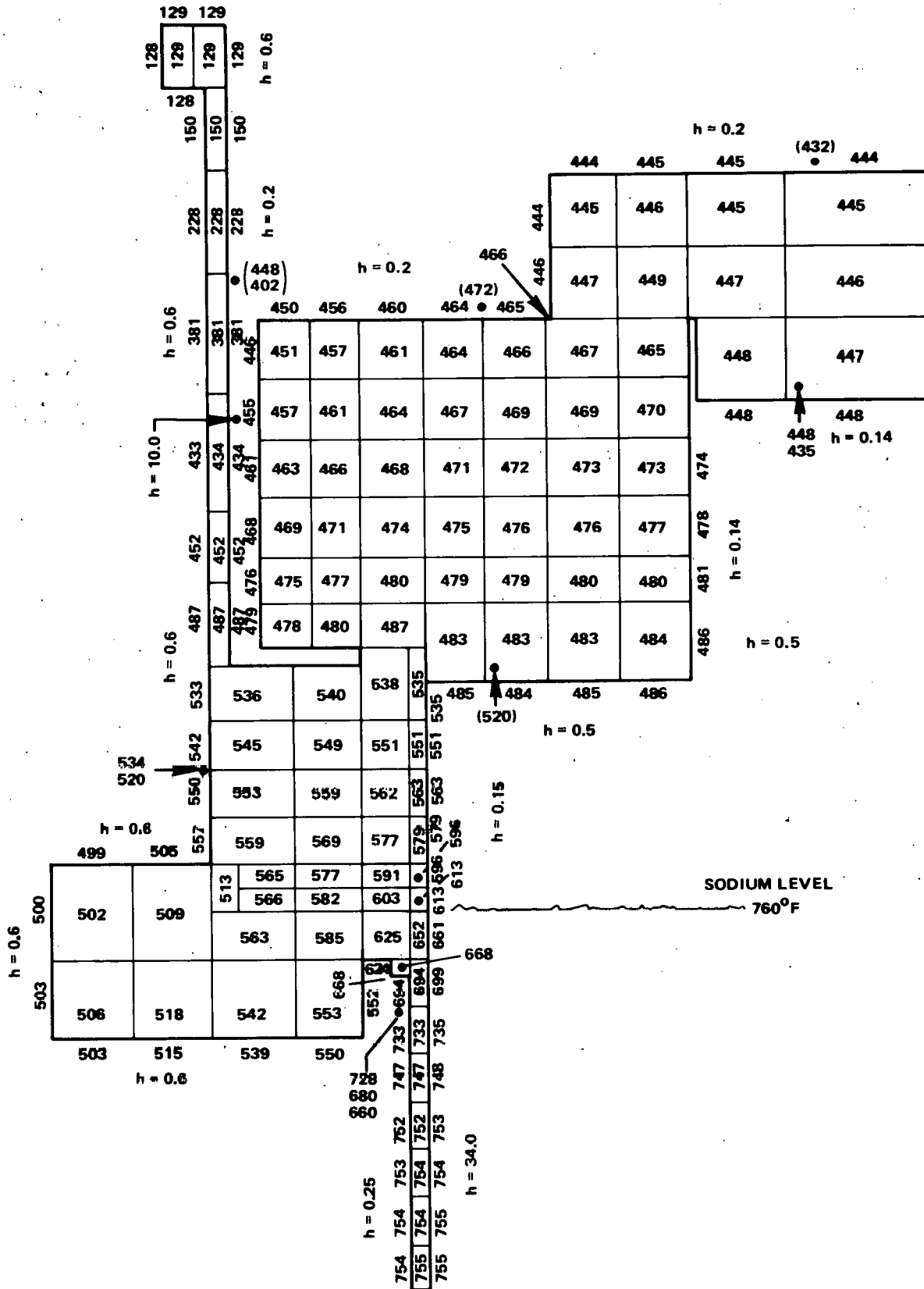


Figure 3B2A-1. Temperature Distribution (1A165) Steady State at 760°F

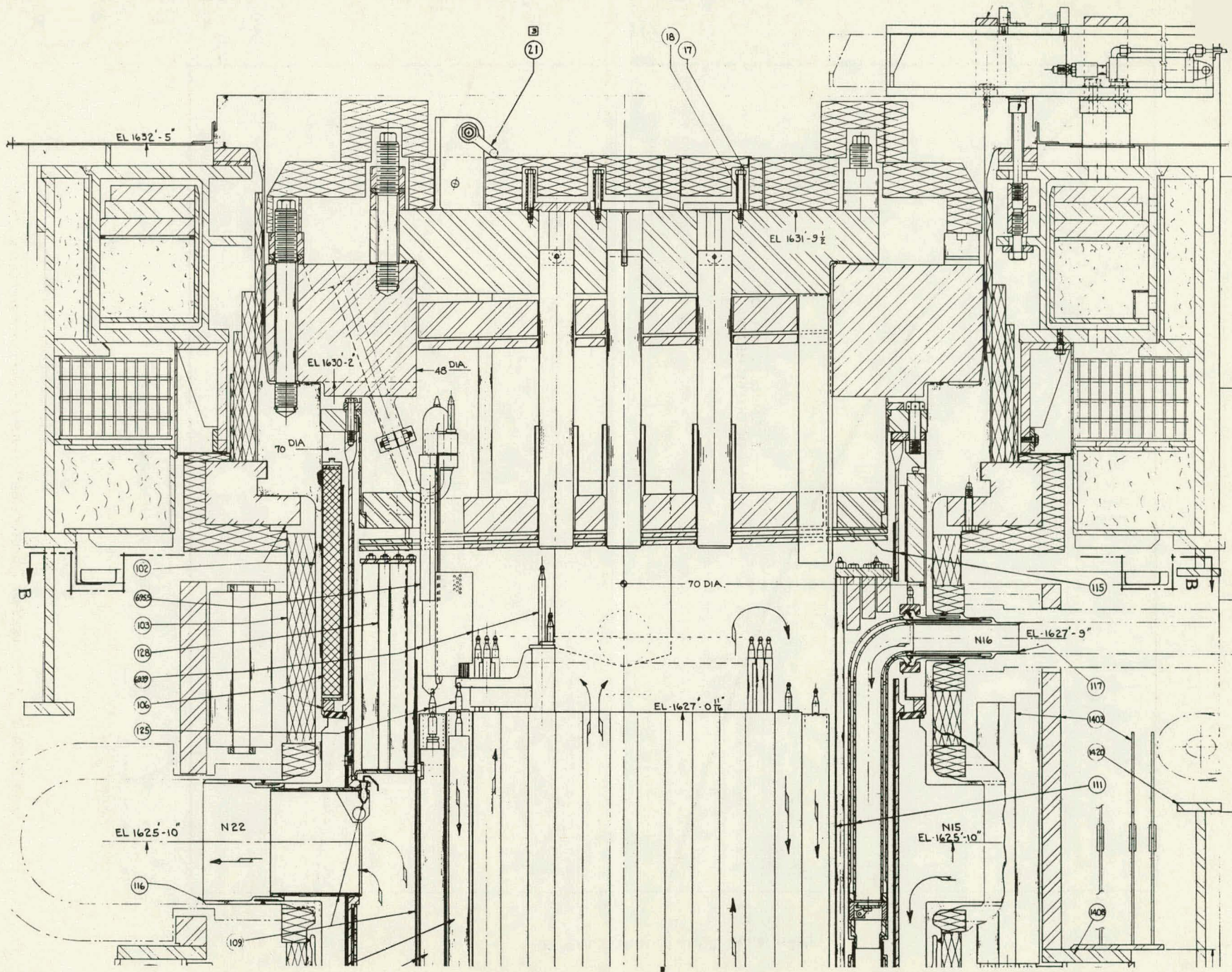


Figure 3B2A-2. SEFOR Vessel

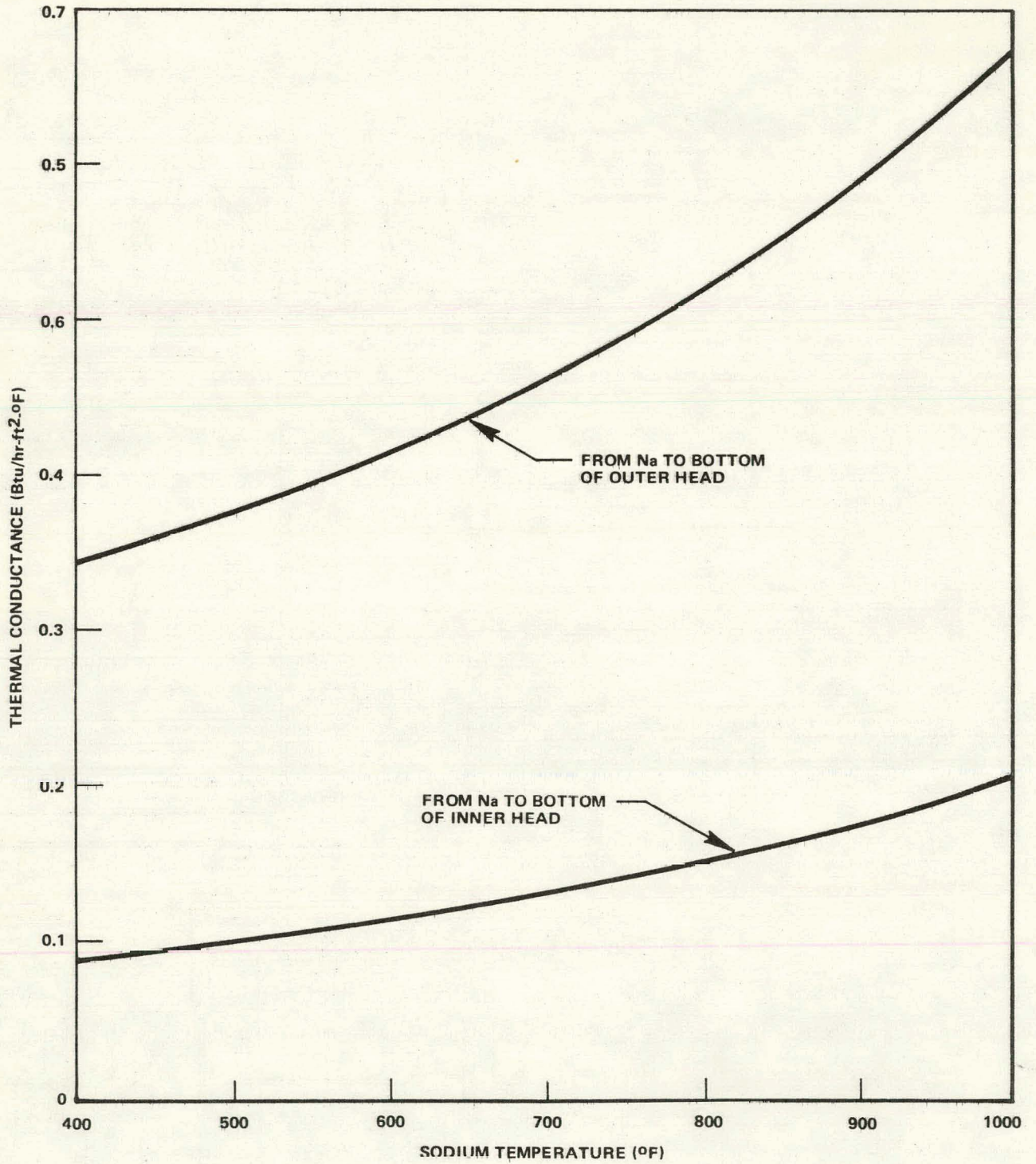


Figure 3B2A-3. Effective Heat Transfer Coefficients for the Inner and Outer Heads

**3.2.2A.4 Heat Transfer Through the Vessel Wall**

The vessel wall (Figure A-2) is made of 3/4-inch thick steel. It is wetted by sodium on the inside and is insulated on the outside. The insulation is cooled by nitrogen gas. However, near the vessel main flange, there is space for the cooling gas to contact the wall directly. In addition, there is a row of tightly paced B<sub>4</sub>C rods arranged against the inside of the vessel wall.

The major uncertainty in predicting the heat transfer in this region is whether the heat flow from the bulk sodium to the wall is better characterized by natural convection or by conduction through the sodium-steel-B<sub>4</sub>C composite. The data<sup>6</sup> shows three different values for the outside wall temperature in this region. Considering the two extreme values results in the following estimates of the heat transfer coefficients:

<u>T<sub>sodium</sub></u>	<u>T<sub>outside</sub></u>	<u>Convection Model</u>		<u>Conduction Model</u>	
		<u>h<sub>inside</sub></u>	<u>h<sub>outside</sub></u>	<u>h<sub>inside</sub></u>	<u>h<sub>outside</sub></u>
750	700	223	8.6	34	2.4
750	655	263	19	34	4.9

Fukushima's analysis<sup>5</sup> shows that an upper limit for the coefficient on the outside is about 10 Btu/hr-ft<sup>2</sup>°F. This indicates that the conduction model is probably closer to reality. Consequently, a value of 34 Btu/hr-ft<sup>2</sup>°F is recommended for the heat transfer coefficient on the inside. Since the outside insulation is the same as that on the head, a value of 0.25 Btu/hr-ft<sup>2</sup>°F is recommended in Appendix B.

**3.2.2A.5 Heat Transfer Through the Vessel Flange**

The vessel main flange (Figure A-2) is a heavy steel ring welded to the vessel wall and to the support skirt. The lower part of its inner surface contacts sodium. The upper part of the inner surface contacts the cover gas. The top of the flange is in contact with the outer head. The upper part of the outer surface is insulated. The lower part of the outer surface and the bottom surface are in contact with a support ring.

On the inner surface, the heat transfer coefficient is the same as for the vessel wall below the sodium level and the same as for the outer head above the sodium level. Heat is transferred by conduction from the lower surface and the lower part of the outer surface.

On the upper part of the outer surface there is insulation in series with a cooling gas film. The insulation has a coefficient of about 0.16 Btu/hr-ft<sup>2</sup>°F<sup>5</sup>. The gas film has a coefficient of about 5.0 Btu/hr-ft<sup>2</sup>°F<sup>5</sup>. Therefore, the equivalent overall coefficient would be 0.155 Btu/hr-ft<sup>2</sup>°F. However, a value of 0.6 Btu/hr-ft<sup>2</sup>°F gives better agreement with the measurements.

**3.2.2B Appendix B Vessel Heat Transfer Calculations**

**3.2.2B.1 Calculation of Heat Transfer Through the Inner and Outer Heads**

A short FORTRAN program was written to calculate the temperature distribution and heat flux through the inner head. The same program was used for the outer head by eliminating the two steel plates (regions 2, 3, 4, and 5) from consideration. The model considers heat transfer in one dimension only. The physical arrangement is shown on Figure B-1. A listing of the program follows the figure.

The following is a description of the program and the calculational assumptions. The input parameters are shown in NAMELIST/TEMP and are described below.

PO	Cover gas pressure, lb/in <sup>2</sup>
ENA	Emissivity of the sodium surface
EST	Emissivity of the steel surfaces
EINS	Emissivity of the insulation surface
ECELL	Emissivity of the inner surfaces of the refueling cell
TNA	Temperature of the sodium, °F
TCFLL	Temperature of the interior of the refueling cell, °F
FCTR	Arbitrary factor for adjusting the calculated heat transfer by natural convection.

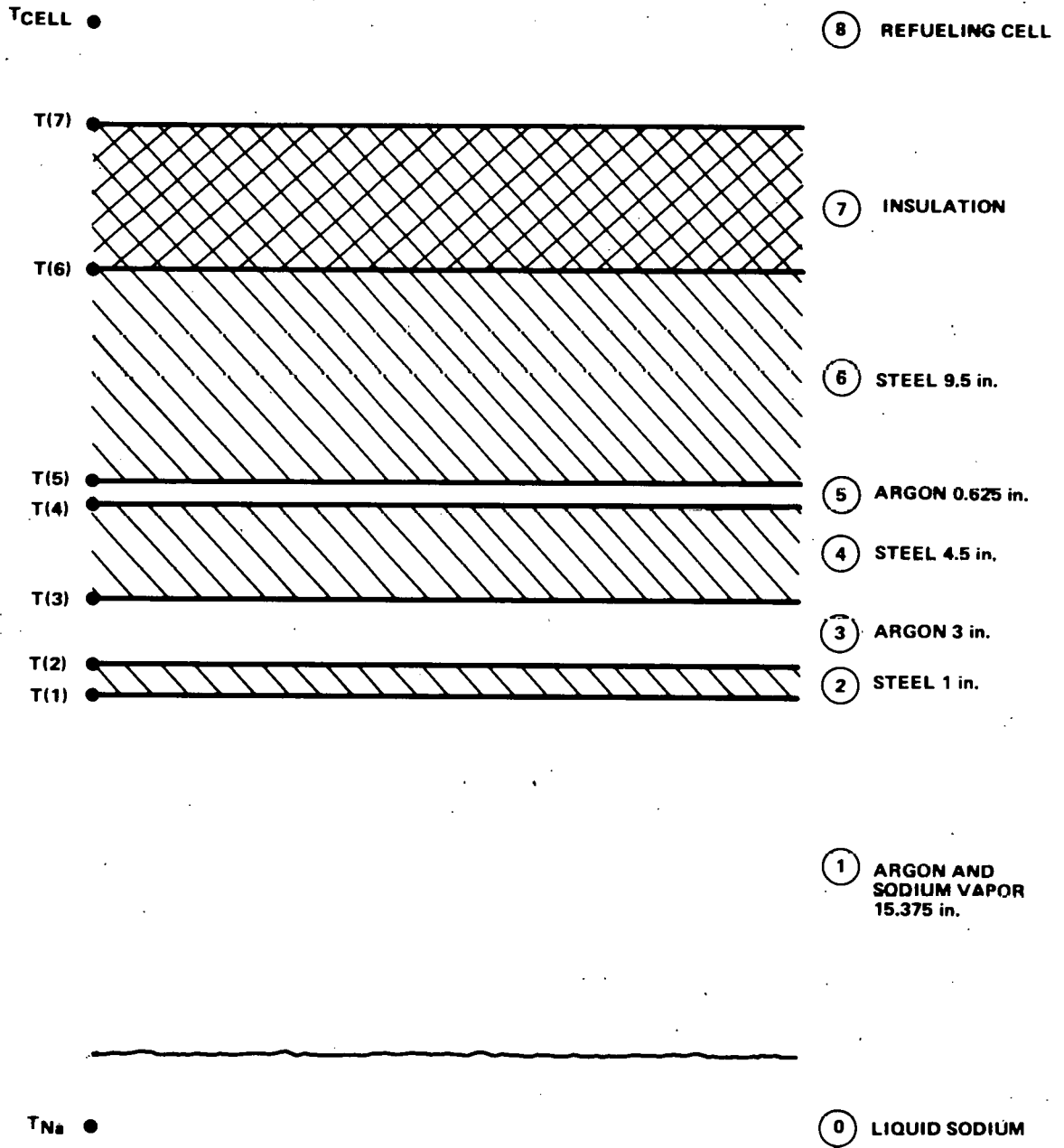


Figure 3B2B-1. One-Dimensional Heat Transfer Model of the SEFOR Inner Head

1234567890123456789012345678901234567890123456789012345678901234567890 C

FORTRAN SYMTAB  
INCODE IBMF

DIMENSION L(9), T(9), D(9), Q(9), QC(9), QK(9), QR(9)  
REAL K, NU, L, L1, LT

NAMELIST /TEMP/ P0, ENA, EST, EINS, ECELL, TNA, TCELL, FCTR  
NAMELIST /INAL/ Q, QC, QK, QR, T

RHOAR(P,T1) = 54.0\*P/(14.7\*(460.0 + T1))

VISCAR(T1) = 0.04816 + 8.909E-5\*T1 - 3.258E-8\*T1\*T1 +  
8.344E-12\*T1\*T1\*T1

CONDAR(T1) = 9.254E-3 + 1.287E-5\*T1 - 2.645E-11\*T1\*T1 +  
1.644E-13\*T1\*T1\*T1

RHONA(P,T1) = 25.0\*P/(14.7\*0.7302\*(460.0 + T1))

PVNA(T1) = 14.7\*(10.0\*\*((6.48 - 10021.0/(460.0 + T1)))/  
((460.0 + T1)\*\*0.5))

CONDST(T1) = 8.45 + 4.25E-3\*T1

EMISV(E1,E2) = 1.0/(1.0/E1 + 1.0/E2 - 1.0)

PRANTL(CP,U,K) = CP\*U/K

GRSHF(R,TA,TB,L1,U) = 4.18E8\*R\*R\*(TA-TB)\*L1\*L1/L1/  
(U\*U\*(0.5\*(TA+TB) + 460.0))

DATA CPAR, CONDNA, VISCNA, CPNA, DH/0.1243, 0.037, 0.04, 0.622,  
4.0/

DATA (L(I), I = 1,8)/1.28, 0.0833, 0.2500, 0.375, 0.052, 0.791,  
0.5, 0.08337

CONTINUE

CALL ZRNLST(INAL)

CALL ZRNLST(TEMP)

READ(5,TEMP)

IF(P0.LT.0.1) STOP

WRITE(6,TEMP)

INITIAL GUESS ON TEMPERATURE DISTRIBUTION (LINEAR)

LT = 0.0

DO 10 I = 1,8

LT = LT + L(I)

GRAD = (TNA - TCELL)/LT

T(1) = TNA - GRAD\*L(1)

D(1) = TNA - T(1)

DO 20 I = 2,7

T(I) = T(I-1) - GRAD\*L(I)

D(I) = T(I-1) - T(I)

T(8) = TCELL

D(8) = T(7) - T(8)

26 CONTINUE

HEAT FLUX THROUGH L(1) DUE TO CONVECTION

TAV = 0.5\*(TNA + T(1))

P = PVNA(TAV)

C = P/P0

CP = CPAR\*(1.0 - C) + CPNA\*C

U = VISCAR(TAV)\*(1.0 - C) + VISCNA\*C



1234567890123456789012345678901234567890123456789012345678901234567890123456789 ;

```

K = CONDAR(TAV)*(1.0 - C) + CONDNA*C
R = RHOAR(P0,TAV)*(1.0 - C) + RHONA(P,TAV)
PR = PRANTL(CP,U,K)
GR = GRSHF(R,TNA,T(1),L(1),U)
NU = 0.0529*(GR*PR)**0.347
H = K*NU/L(1)

```

```

000 HEAT FLUX THROUGH L(1) DUE TO RADIATION

```

```

F = EMISV(ENA,EST)
QR(1) = 1.714E-9*F*((TNA+460.0)**4.0 - (T(1)+460.0)**4.0)
Q(1) = QC(1) + QR(1)

```

```

000 HEAT FLUX THROUGH L(2)

```

```

TAV = 0.5*(T(1) + T(2))
K = CONDST(TAV)
QK(2) = K*(T(1) - T(2))/L(2)
Q(2) = QK(2)

```

```

000 HEAT FLUX THROUGH L(3) DUE TO CONVECTION

```

```

TAV = 0.5*(T(1) + T(2))
R = RHOAR(P0,TAV)
U = VISCAR(TAV)
K = CONDAR(TAV)
GR = GRSHF(R,T(2),T(3),L(3),U)
PR = PRANTL(CPAR,U,K)
NU = 0.0529*(GR*PR)**0.347
QC(3) = 0.0
QK(3) = 0.0
IF(NU,LE.1.0) GO TO 28
H = K*NU/L(3)
QC(3) = H*(T(2) - T(3))*FCTR
GO TO 29

```

```

000 HEAT FLUX THROUGH L(3) DUE TO CONDUCTION

```

```

28 QK(3) = K*(T(2) - T(3))/L(3)

```

```

000 HEAT FLUX THROUGH L(3) BY RADIATION

```

```

29 F = EMISV(FST,EST)
QR(3) = 1.714E-9*F*((T(2)+460.0)**4.0 - (T(3)+460.0)**4.0)
Q(3) = QK(3) + QR(3) + QC(3)

```

```

000 HEAT FLUX THROUGH L(4)

```

```

TAV = 0.5*(T(3) + T(4))
K = CONDST(TAV)
QK(4) = K*(T(3) - T(4))/L(4)
Q(4) = QK(4)

```

```

000 HEAT FLUX THROUGH L(5) BY CONDUCTION

```

```

TAV = 0.5*(T(4) + T(5))
K = CONDAR(TAV)
QK(5) = K*(T(4) - T(5))/L(5)

```

567890123456789012345678901234567890123456789012345678901234567890 CA

000 HEAT FLUX THROUGH L(5) BY RADIATION

$$F = \text{EMISV}(\text{EST}, \text{EST})$$

$$QR(5) = 1.714F - 9 * F * ((T(4) + 460.0) ** 4.0 - (T(5) + 460.0) ** 4.0)$$

$$Q(5) = QK(5) + QR(5)$$

000 HEAT FLUX THROUGH L(6)

$$TAV = 0.5 * (T(5) + T(6))$$

$$K = \text{CONDST}(TAV)$$

$$QK(6) = K * (T(5) - T(6)) / L(6)$$

$$Q(6) = QK(6)$$

000 HEAT FLUX THROUGH L(7)

$$TAV = 0.5 * (T(6) + T(7))$$

$$HINS = 0.136 + 7.0E-5 * TAV$$

$$QK(7) = HINS * (T(6) - T(7))$$

$$Q(7) = QK(7)$$

000 HEAT FLUX THROUGH L(8) BY CONVECTION

$$TAV = 0.5 * (T(7) + TCELL)$$

$$CP = \text{CPAR}$$

$$U = \text{VISCAP}(TAV)$$

$$K = \text{CONDAR}(TAV)$$

$$PR = CP * U / K$$

$$P = 14.7$$

$$R = \text{RHOAR}(P, TAV)$$

$$TA = T(7)$$

$$TB = TCELL$$

$$L1 = 0.9 * DH$$

$$GR = \text{GRSHF}(R, TA, TB, L1, U)$$

$$C1 = 0.54$$

$$C2 = 0.25$$

IF (GR.GT.2.0E7) GO TO 30

$$C1 = 0.14$$

$$C2 = 0.333$$

30 NU = C1 \* ((GR \* PR) \*\* C2)

$$H = K * NU / L1$$

$$QC(8) = H * (T(7) - TCELL)$$

000 HEAT FLUX THROUGH L(8) BY RADIATION

$$F = \text{FMISV}(LINS, ECELL)$$

$$QR(8) = 1.714F - 9 * F * ((T(7) + 460.0) ** 4.0 - (TCELL + 460.0) ** 4.0)$$

$$Q(8) = QC(8) + QR(8)$$

000 AVERAGE HEAT FLUX

$$QAV = 0.0$$

DO 40 I=1,8

40 QAV = QAV + Q(I)

$$QAV = QAV / 8.0$$

$$ERR = 0.0$$

$$DT = 0.0$$

DO 50 I=1,8

$$ERR = ERR + \text{ABS}((QAV - Q(I)) / QAV)$$

$$D(I) = D(I) * QAV / Q(I)$$

1234567890123456789012345678901234567890123456789012345678901234567890 C

```
50 DT = DT + D(I)
   IF(ERR.LE.0.01)GO TO 80
   DO 60 I=1,8
60 D(I) = D(I)*(1.0 + (TNA - TCELL - DT)/DT)
   T(1) = TNA - D(1)
   DO 70 I=2,7
70 T(I) = T(I-1) - D(I)
   GO TO 26
80 CONTINUE
```

```
WRITE(6,6000)
N=0
WRITE(6,6100) N,TNA
DO 2000 N=1,8
WRITE(6,6100) N , T(N) , QK(N) , QC(N) , QR(N) , Q(N)
```

```
2000 CONTINUE
```

```
6000 FORMAT(1H1,10X, 6HREGION,5X,4HMIN.,5X,19HHEAT TRANSFERRED BY,5X,
1 5HTOTAL /
2 1H ,10X, 6H NO ,5X,4HTEMP,5X,19HCOND CONV RAD,5X /
3 1H ,10X, 6H*****,4X,6H*****,4X,19(1H*),4X,6H*****/ / )
6100 FORMAT(1H0,10X, 16,4X,F6.1,3X,F6.1,F7.1,F6.1,F10.1)
GO TO 1
```

```
END
MASS P*,X1SS,10L
SELECT XREF
```

The statement functions follow the NAMELIST and are described below.

RHØAR(P,TI)	Density of argon at pressure P and temperature T1, lb <sub>m</sub> /ft <sup>3</sup>
VISCAR(TI)	Absolute viscosity of argon at temperature T1, lb <sub>m</sub> /hr ft
CØNDAR(TI)	Thermal conductivity of argon at temperature T1, Btu/hr ft °F
RHØNA(P,TI)	Density of sodium vapor <sup>9</sup> at pressure P and temperature T1, lb <sub>m</sub> /ft <sup>3</sup>
PVNA(TI)	Vapor pressure of sodium <sup>9</sup> at temperature T1, lb/in <sup>2</sup>
CØNDST(TI)	Thermal conductivity of steel at temperature T1, Btu/hr ft °F
EMISV(E1,E2)	Gray body radiation factor for two parallel plane, one with emissivity E1 and the other emissivity E2.
PRANTL(CP,U,K)	Prandtl number for a fluid with specific heat CP, viscosity U, and thermal conductivity K.
GRSHF(R,TA,TB,L1,U)	Grashof number for natural convection of a fluid with density R, temperature TB, and viscosity U, from a heated surface of characteristic length L1 and temperature TA.

The single valued variables are contained in the DATA statements and are described below.

CPAR	Specific heat of argon, Btu/lb <sub>m</sub> °F
CØNDNA	Thermal conductivity of sodium vapor <sup>9</sup> , Btu/hr ft °F
VISCNA	Viscosity of sodium vapor <sup>9</sup> , lb <sub>m</sub> °F
CPNA	Specific heat of sodium vapor <sup>9</sup> , Btu/lb <sub>m</sub> °F
DH	Diameter of the inner head, ft
L(I)	Thickness of region I, ft. (Note: a value is input for region eight simply to aid in making the initial guess on temperature distribution).

The heat flux through region one is calculated using the procedure presented in Reference (7). The heat flux due to convection can be arbitrarily reduced to account for deviations of the SEFOR from the experiment in Reference (7). These deviations include friction and heating effects of the guide tubes which pass vertically through the cover gas space.

Heat flows through regions two, four, and six by conduction only.

Heat flows through region three by radiation and convection. The convection correlation from reference (7) is used.

Heat flows through region five by radiation and conduction. Natural convection is assumed to be less effective than conduction because of the narrowness of the gap.

Region seven consists of mirror insulation. The heat transfer coefficients (HINS) for this insulation is assumed to be a linear function of temperature. The data is taken from reference (5).

Heat flows through region eight by convection and radiation. The convection correlation from Reference (8) page 311 for horizontal plates is used.

Figure B-2 shows the calculated temperatures of the two heads versus sodium temperature. Table 3B2B-1 is a typical output from the inner head calculation. The model fits the inner head data quite well. However, it predicts temperatures for the outer head which are too high.

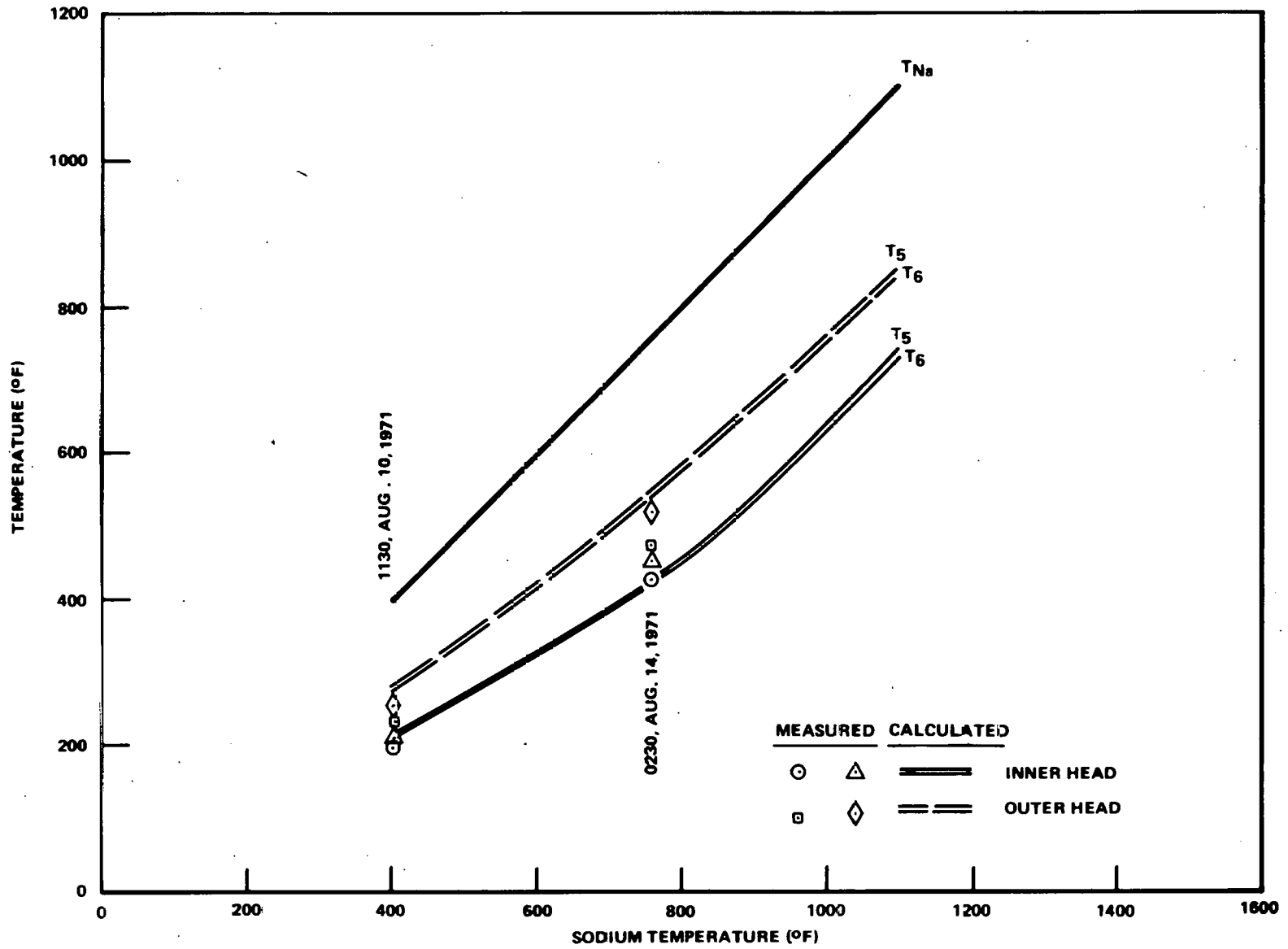


Figure 3B2E-2. Temperature of the SEFOR Head

Table 3B2B-1

INNER HEAD TEMPERATURE DISTRIBUTION

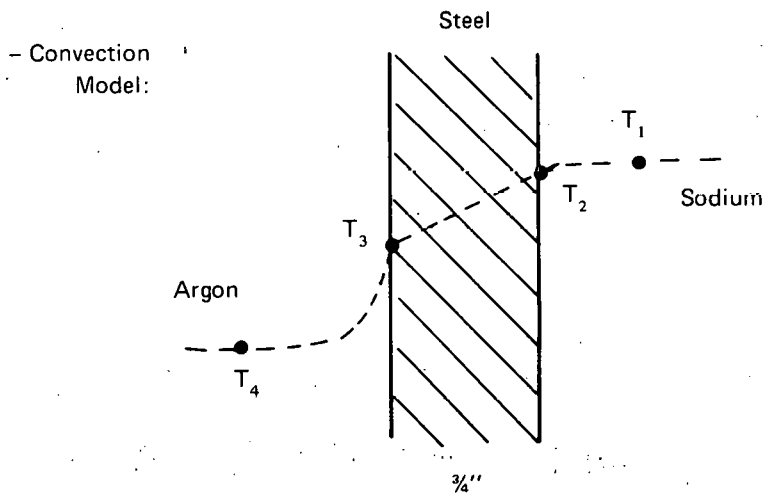
SNUMR = 1A106, ACTIVITY # = 01, REPORT CODE = 06, RECORD COUNT = 00028

NAMELIST	TEMP		
PO	0.14700000F 02	FNA	0.20000000E-01
ECELL	0.90000000E 00	TNA	0.76000000E-03
FST	0.10000000E 00	FINS	0.90000000E 00
TCELL	0.10000000F 03	FCTR	0.50000000E 00

FND NAMELIST TEMP

REGION NO.	MIN. TEMP	HEAT TRANSFERRED BY			TOTAL
		COND	CONV	RAD	
0	760.0				
1	606.3	0.	19.2	26.8	46.0
2	606.0	46.0	0.	0.	46.0
3	511.5	0.	10.0	36.1	46.1
4	509.9	46.0	0.	0.	46.0
5	431.6	23.1	0.	22.8	45.9
6	428.1	46.0	0.	0.	46.0
7	132.6	46.0	0.	0.	46.0
8	100.0	0.	11.0	35.0	46.0

3.2.2B.2 Calculation of Heat Transfer through the Vessel Wall



On the Sodium Side -

$$Nu = 0.508 \left( \frac{Pr}{0.952 + Pr} Gr Pr \right)^{1/4}$$

$$Pr = \frac{C_p \mu}{k}$$

$$C_p = 0.3 \text{ BTU/lb}_m \text{ } ^\circ\text{F}$$

$$\mu = 0.68 \text{ lbm/hr. ft}$$

$$k = 41 \text{ BTU/hr. ft. } ^\circ\text{F}$$

$$Pr = 0.005$$

$$Gr = \frac{gL^3}{\mu^2} P_2 (P_2 - P_1)$$

$$g = 32.2 \times (3600)^2 \text{ ft/hr}^2$$

$$\rho = 59.6 - 7.95 \times 10^{-3} T \text{ lbm/ft}^3$$

$$P_2 = 54 \text{ lbm/ft}^3$$

$$(P_2 - P_1) = 7.95 \times 10^{-3} (T_1 - T_2)$$

$$L = 2 \text{ ft.}$$

$$Gr = 3.9 \times 10^8 (T_1 - T_2)$$

$$Nu = 5.08 (T_1 - T_2)^{1/4}$$

$$h_{1-2} = \frac{K}{L} Nu = 104 (T_1 - T_2)^{1/4}$$

$$\frac{q}{A} = h_{1-2} (T_1 - T_2) = 104 (T_1 - T_2)^{5/4}$$

Through the Steel

$$\frac{q}{A} = \frac{K}{L} (T_2 - T_3)$$

$$K = 12 \text{ BTU/hr. ft. } ^\circ\text{F}$$

$$L = \frac{3}{4} \text{ inch} \div 12 \frac{\text{inches}}{\text{ft.}}$$

$$\frac{q}{A} = 192 (T_2 - T_3)$$

On the Gas Side

$$\frac{q}{A} = h_{3-4} (T_3 - T_4)$$

Data

$$T_1 = 750^\circ\text{F}$$

$$T_4 = 100^\circ\text{F}$$

These five equations can be solved, iteratively, for each of the three measured values of  $T_3$ . An equivalent  $h_{1-2}$  can then be calculated.

$T_3$	$h_{3-4}$	$q/A$	$T_2$	$H_{1-2}$
700	8.6	5160	726.9	223
655	19	10500	710.1	263

- Conduction Model:

On the Sodium Side

$$h_{1-2} = 34 \text{ BTU/hr. ft.}^2\text{°F} \tag{1}$$

$$\frac{q}{A} = 34 (T_1 - T_2) \tag{2}$$

Through the Steel

$$\frac{q}{A} = 192 (T_2 - T_3) \tag{3}$$

On the Gas Side

$$\frac{q}{A} = h_{3-4} (T_3 - T_4) \tag{4}$$

Data

$$T_1 = 750\text{°F} \tag{5}$$

$$T_2 = 100\text{°F}$$

For each of the measured values of  $T_3$ , these five equations can be solved directly:

$$h_{3-4} = 28.8 \left( \frac{750 - T_3}{T_3 - 100} \right)$$

$T_3$	$q/A$	$h_{3-4}$	$T_2$
700	1440	2.4	707.5
655	2730	4.93	669.2



REFERENCES

1. SEFOR FDSAR, Supplement 16, Section IX C.
2. Rally, F. C., "SEFOR Stress Matrix Memo 72-1," G.E. Vessels & Internals Unit, BRD January, 1972.
3. Rashid, Y.R., "CREEP-PLAST; A Two-Dimensional, Finite Element, Elastic Plastic, Creep Analysis Computer Program," to be published.
4. A.P. Bray and R.C. Higbee, "TIGER-V for the Philco 2000 – Specifications, Input Formats, Error Designations," July 27, 1961.
5. T.Y. Fukushima, "SEFOR Support Skirt Thermal Analysis," memo to C. E. Russell, August 25, 1971.
6. G.B. Kruger, memo to Distribution, August 18, 1971.
7. G. Lemercier, X. Elie, and B. Morin, "Heat Transfer Between a Free Level of Liquid Sodium and a Metal Wall, Through an Inert Gas," EURFNR-850, May 1970.
8. F. Kreith, "Principles of Heat Transfer," International Textbook Co., 1958.
9. G.H. Golden and J.V. Tokar, ANL-7323, "Thermophysical Properties of Sodium," May 1967.

### 3.2.3 Task 3B3 Elevated Temperature Operation Driver Fuel Analysis

#### 3.2.3.1 Objective

The objective of this task is to perform thermal, hydraulic, and stress analyses of the present SEFOR fuel rods and assemblies to determine fuel rod performance at elevated coolant outlet temperature operation.

#### 3.2.3.2 Discussion

A steady-state analysis of the present SEFOR fuel using updated criteria, materials properties, and methods was performed. The work includes the nominal peak driver rod (the peak power driver rod on a nominal basis presently in the SEFOR core); the hot rod (the peak nominal driver rod with a 10% decrease in flow and a 6.8% increase in power); and the hot rod in the tolerance extreme position (the hot rod in the maximum physical offset position in its flow cell). The above rods were analyzed for three coolant  $\Delta T$ 's across the core leading to a 1000°F outlet temperature. Inlet temperatures were 800, 850, and 900°F. The analysis was performed at both the core midpoint and core outlet. The results of the driver fuel structural analysis were then extrapolated to the guinea-pig lead rods. The results are preliminary pending the development of a more sophisticated structural stress analysis model. Changes in the as-designed core versus the present core are shown in Table 3B3-1.

Major parameter changes used to update the original design are as follows:

- Lower fuel thermal conductivity
- Lower gap conductance
- Higher yield strength of fuel clad
- Lower peak power hot spot
- Higher fission gas pressure due to improved calculational procedure
- The possibility that the SEFOR fuel is out of specification as regards condensible gases
- Different flow distribution due to improved calculational method
- Different thermally-induced stresses due to improved calculational method
- Different structural criteria.

The fuel temperature calculations were undertaken with the object in mind of determining what probability the peak driver fuel (and guinea-pig lead fuel) has of running, at the present SEFOR operating conditions, at a temperature in excess of 5000°F. The object of the fuel-rod stress calculations was a simplified look at SEFOR fuel-rod stresses and a comparison to the 300 MWe Demonstration Plant structural design stress criteria.\* No attempt was made to evaluate the strain fatigue, thermal ratcheting, or buckling portion of the structural criteria. Only two axial locations on the peak driver fuel rod were examined. These were at the core midplane and core outlet. The following conditions were considered for the structural analysis of the present SEFOR fuel rods:

- Fission gas pressure
- Fuel rod bending due to temperature gradient
- Radial temperature gradient
- Circumferential temperature gradients
- Vibration stress
- Axial temperature gradients
- Fuel-clad mechanical interaction

The following areas were not included in the scope of the task:

- Local spacer loads
- Local thermal stress (from spacer perturbation of the coolant flow)
- End and Segmenting Plug discontinuities
- Transient Conditions

Because the SEFOR fuel is a low burnup fuel, no allowance has been made for irradiation induced swelling or creep. This assumption should be quantitatively evaluated at a later time (it has been superficially checked). In addition, no allowance for corrosion and/or fuel-clad chemical attack has been made. Also no allowance was made for tolerance uncertainty.

The SEFOR lead rods (guinea-pig rods) operate at a 14% higher power rating than the peak driver fuel. The analysis has indicated the highest power guinea-pig rods have a  $\sim 76\%$  probability of exceeding a 5000°F (50% = 5230°F) centerline fuel temperature at a reactor power of 20 MWt. If these guinea-pig rods are removed from their

\* The Demo Plant stresses are not calculated using nominal temperatures but rather using probabilistic cladding temperatures.

Table 3B3-1

CORE CHARACTERISTICS - DRIVER FUEL

	Original Design	Present Fuel Analysis Option 1, 2(a)	Elevated Temperature Operation
Power (MWt)	20	20	20
O.D. Heat Flux (Btu/hr-ft <sup>2</sup> )			
Average	152,000	153,000	153,000
Maximum	280,000	270,000	270,000
Linear Power in Fuel (kW/ft)			
Average	11.3	10.5	10.5
Maximum (without uncertainties)	20.8	18.4	18.4
Specific Power (kw/kg)			
Average	10.5	8.89	8.89
Maximum	19.1	15.65	15.65
Power Density (kw/liter)			
Average	37.7	36.8	36.8
Maximum	69.6	64.7	64.7
Coolant Temperatures (°F)			
Inlet	700	700	*
Average Core Outlet	820	820	1000
Maximum During Transients	1050	1050	**
Fuel Temperature (°F)			
Average	1900	~2100	~2200
Maximum	<5000	<5100	<5100
Coolant Velocity (ft/sec)			
Average	5.4	5.4	***
Maximum	8.3	8.3	***
Power Peak-to-Average Factors			
Radial	1.47	1.43	1.39
Axial	1.24	1.24	1.26
Local	1.01	--	--
Total	1.81	1.76	1.78
Burnup (MWd/Te)			
Peak Local	--	2830	**
Peak Rod	1500	2280	7380

\*Three Values of Inlet Temperature Were Studied (800, 850, and 900°F)

\*\*Not Evaluated

\*\*\*Depends on Inlet Temperature

Table 3B3-1 (Continued)

CORE CHARACTERISTICS - DRIVER FUEL

	Original Design	Present Fuel Analysis Option 1, 2(a)	Elevated Temperature Operation
Peak Internal Gas Pressure (psi)	570	1020	1965
Fluence, Peak Local (nvt)	$2.6 \times 10^{21}$	$4.8 \times 10^{21}$	$15.5 \times 10^{21}$
Pressure Drop (psi)			
Total Reactor	28.9	28.9	***
Core	3.8	3.8	***
Flow Rate ( $10^5$ lb/hr)			
Core Flow	18.67	18.67	***
Leakage	2.82	2.82	***
Total	21.50	21.50	***

\*\*\*Depends on Inlet Temperature

present peripheral locations and placed in the central location at 20 MWt, ~ 25 to 30% of the peak pellet weight would be expected to be  $\geq 5000^\circ\text{F}$  and a centerline temperature of  $5900^\circ\text{F}$  would be obtained.

Preliminary structural calculations on the present nominal peak driver fuel at elevated temperature operation indicate that the SEFOR fuel will slightly exceed (~ 1%) stress criteria specifications at the end of the elevated temperature operation. This is based on 20 MWt operation with conservative values for the material mechanical properties and the assumption that the condensable gases (moisture) is two times the SEFOR fuel specification. The hot rod exceeds the criteria at the end of elevated temperature by ~ 10%, and the hot rod in the tolerance extreme condition exceeds the criteria by 60%. Future work will include a further evaluation of the criteria with respect to the SEFOR fuel rod design.

Due to reassignment of priorities by Program Management, the transient analysis was not completed as part of this task.

3.2.4 Task 3B4 - Physics

3.2.4.1 Objective

The objective of this task is to establish control requirements for SEFOR during elevated temperature operation.

3.2.4.2 Discussion

Operation of SEFOR Core I or Core II at 20 MW with  $1000^\circ\text{F}$  outlet temperatures for extended periods of time imposes some additional requirements on the reflector, shield and core over those imposed by the initial test program. The reflector must compensate for the additional reactivity effects of burnup and higher temperature defect. The shield must be capable of operation at 20 MW for extended time periods with two reflectors down. The core must be capable of sustaining power without refueling for several weeks. None of these requirements is outside the range of the present system.

● Reflector Control System

Control of the SEFOR reactor is provided by ten movable reflector segments. Of the ten, eight are coarse reflectors which must be either full up or full down. Two shim drives are provided for power level adjustments. The shim drives are located  $180^\circ$  apart. The total measured worth of the reflector control

system is 9.7\$. The combined worth of the two shim rods with all the coarse rods up is ~ 2.3\$.

Components of reactivity for which the reflectors must provide compensation in going to power include a shutdown margin (~\$1.00), thermal expansion of the core, and Doppler defect. These reactivity effects are summarized in the table below for the three suggested inlet coolant temperatures of 700, 800, and 900°F. Also shown is the net reactivity available for burnup compensation assuming a shutdown margin of \$1.00 with one stuck reflector element (equivalent to \$1.80 shutdown margin with all reflectors down).

Inlet Coolant Temperature (°F)	Doppler 350° full power	Thermal Expansion 350° to full power	Net available for burnup	Equivalent full power days
700	3.02\$	1.80\$	3.08\$	410
800	3.08\$	1.98\$	2.88\$	380
900	3.11\$	2.16\$	2.63\$	350

If only the two shim rods are used to compensate for burnup a maximum cycle time of 300 days results. From the above discussion this type of operation is well within the available capability of the reflector control system.

The recommendation was made that shim capability (fine positioning control) be added to two additional reflector segments to provide the reactivity required to compensate for burnup and temperature feedback during the elevated temperature operation. This modification is planned as part of the reactor preparation program.

- Primary Shield Design

All fixed components of the SEFOR primary shield have been designed to accommodate 50 MW operation of SEFOR for ten years with a 0.7 load factor. This is equivalent to 25 years at 20 MW with a 0.7 load factor. Operation of the core with the shim rods lowered increases the heat load on the primary shield cooling system by 40%. An additional 10% load due to the increase in outlet temperature is estimated, giving an increase of 50% in the total primary shield cooling requirement over the case with 820°F outlet and all reflectors raised.

The present cooling system for the primary shield was designed to provide adequate cooling for the shield with the reflectors down at 20 MW. Operation with two shim rods withdrawn, therefore, is well within the capabilities of the present system.

- Core Reactivity

Operation of the core at 20 MW for extended periods of time requires that excess reactivity be loaded at the beginning of an operating cycle to compensate for the planned burnup reactivity. This may be accomplished in SEFOR with the present core and fuel design. Available control for burnup compensation limits cycle time.

In SEFOR, one full power day is equivalent to 0.75¢ in reactivity. The present *license* limit on excess reactivity is 0.50\$ at 20 MW which is equivalent to 67 full power days. The current core is loaded to full size, but contains 11 B<sub>4</sub>C rods to limit the excess reactivity to the license limit. Replacing these rods with fuel would add ~7\$ in reactivity which is equivalent to ~930 full power days. With Core II, the excess reactivity available with a full core load of fuel would be ~\$3.50 which is equivalent to ~470 full power days. Each of these full core loadings gives excess reactivity greater than that which is available for burnup compensation in the reflectors. Hence, considering only reactivity effects, the cycle time is not limited by the core loading capabilities.

## 4.0 TASK 4 OPTION IIIA PLUS SELECTED PLANT TESTS

### 4.1 TASK 4A – TEST PROGRAM

#### 4.1.1 Discussion

The Option III test program will provide safety oriented information about fuel rod performance under transient conditions for the FFTF and LMFBR Demonstration Plants. This program will utilize the increased test capabilities associated with the SEFOR booster core and the package loop. The booster core will provide higher linear steady-state operating powers in the central test region. The package loop will provide multi-pin assembly test capability in flowing sodium.

#### 4.1.2 Test Program Preliminary Plan

The test program consists of two generic types of tests: loss-of-flow (LOF) tests, and transient overpower (TOP) tests. The LOF tests will utilize the package loop and be focused toward investigating simulated undercooling accidents initiated from steady-state linear powers which correspond to predicted peak powers in LMFBR Demonstration Plants ( $\sim 15$  kW/ft). The capability for higher steady-state test fuel power will also be utilized in extending the region of experimentation for the TOP capsule tests previously conducted under Option I. Additionally, some of the TOP tests will utilize the multi-pin and flowing coolant capabilities of the package loop.

##### 4.1.2.1 Loss-of-Flow Tests

The objective of the LOF Series of tests is to establish the consequences of undercooling accidents in multi-rod bundles. The information obtained will be extended to hypothetical reactor accidents through computational models which these test data will help to confirm.

The experiments in this series will progress from a single pin test used to qualify the loop and analytical techniques through seven pin tests of specific accident situations and into nineteen pin tests. The number of pins in each test will be selected to provide the most realistic simulation of the accident being investigated within the limitations of a nineteen-pin bundle.

Experiments to investigate the effect of bundle size, burnup, flow decay rate, failed fuel pins, local blockages and combined loss-of-flow/overpower transients are planned. Seven-pin tests will be utilized to reduce both cost and inlet temperature. The larger (nineteen pin) bundles will be used only when test requirements make this desirable.

Current plans require two package loops in each of nine test series with the exception of Series 1 and 3 which require only one package loop each. The number of loops devoted to investigation of each parameter was established to provide adequate coverage of the anticipated events either totally within the series or by comparison with tests in other series. The objectives of each of the nine test series are listed below.

##### SEFOR Series LOF 1 (1 Loop, 1 Pin)

This test will be a calibration experiment and proof test for the package loop. The package loop will contain a single fuel pin to facilitate a rigorous thermal analysis. The results will be compared to previous single pin, flow transient tests in stagnant and flowing coolant capsules.

##### SEFOR Series LOF 2 (2 Loops, 7 Pins)

The two tests in this series will investigate loop operation with 7 pins. Also, following the flow reduction, the reactor SCRAM time will be varied to determine the progression of damage to the fuel bundle.

##### SEFOR Series LOF 3 (1 Loop, 19 Pins)

The objectives of this test are to verify the package loop operation with 19 fuel pins and to evaluate the effect of bundle size (for the same rapid flow reduction) by comparison with tests in Series 1 and 2.

##### SEFOR Series LOF 4 (2 Loops, 19 Pins)

This series will investigate the influence of burnup on the progression of damage resulting from a loss-of-flow accident. The fission gas plenum pressure and cladding mechanical properties will be varied.

**SEFOR Series LOF 5 (2 Loops, 7 or 19 Pins)**

The purpose of this series is to study the effect of flow decay rate. One test in this series will investigate the effect of an intermediate flow decay rate (simulating a pump coast-down, etc.) and the other a very gradual decay rate (e.g. gradual buildup of debris at the inlet or lower blanket). Both of these tests will be compared to the tests in Series 2 or 3 which investigate the very rapid flow reduction accident.

**SEFOR Series LOF 6 (2 Loops, 7 or 19 Pins)**

The tests in this series will investigate the consequences of operating with failed fuel during a loss-of-flow accident. Parameters to be investigated include the operating period following the initial failure which permits sodium entry. The results from this series will be compared to the tests in Transient Overpower Series 2.

**SEFOR Series LOF 7 (2 Loops, 19 Pins)**

The tests in this series will investigate the consequences of a local flow blockage. The mode of failure and the potential for propagation to adjacent pins will be studied.

**SEFOR Series LOF 8 (2 Loops, 7 or 19 Pins)**

The tests in this series will investigate the consequences of a loss-of-flow caused overpower transient accident. These tests will investigate parameters such as timing of the events of a loss-of-flow/overpower transient accident.

**SEFOR Series LOF 9 (2 Loops, 7 or 19 Pins)**

The purpose of this test series is to investigate in more detail the "worst case" of the previous tests. In order to do this, the results of the previous tests will have to be examined and the proper combination of parameters selected.

**4.1.2.2 Transient Overpower Tests**

The objective of this series is to evaluate fuel pin design variables, steady-state operating parameters, and their effect on fuel pin performance under transient overpower conditions. These tests are intended to supplement tests conducted under the Option I program.

Both stagnant coolant capsules (24) and flowing sodium package loops (9) are planned. Such variables as steady-state power levels, total burnup, fuel pin length, axial power profile, and fuel pin configuration (e.g. annular fuel and blanket) will be evaluated with the stagnant coolant capsules. Energy magnitude of the test transients will be varied. Results of these tests will be considered in the design and planning of the package loop (both seven pin and nineteen pin) tests. The package loops add the capability of evaluating flowing sodium and multi-pin configuration effects on fuel pin performance (e.g., failure threshold) under transient overpower conditions.

The above experiments are grouped into six test series; the objectives of each series are listed below.

**SEFOR TOP-5 Series (6 Capsules)**

This series of tests will investigate the effect of fuel pin length and axial power profile upon transient fuel rod performance; since the fuel specimen length will be dictated by the irradiation facility (GETR, up to 36 inches; EBR-II, up to 13.5 inches), the effect of possible differences due to steady-state pre-irradiation (GETR, thermal vs. EBR-II fast) flux will also be evaluated.

**SEFOR TOP-6 Series (6 Capsules)**

The purpose of this series is to investigate the transient performance of pins pre-irradiated at different power levels (i.e., fission gas release rate and distribution). Total burnup will be the same for each fuel specimen.

**SEFOR TOP-7 Series (6 Capsules)**

This series will evaluate effects of total burnup (fission gas inventory) on fuel performance and investigate design variables affecting fuel pin failure threshold. Information gained will supplement results from Series TOP-3 and 4 of Option I.

**SEFOR TOP-8 Series (6 Capsules)**

These tests will evaluate fuel pin performance during possible reactor accident conditions. Simulated transients will be of low energy magnitude. Test conditions will include multiple transients interspersed with steady-state operation. Both zero burnup and intermediate burnup specimens will be tested.

**SEFOR TOP-9 Series (5 Loops)**

This series will evaluate fuel performance in multi-pin (7) configurations and flowing sodium conditions (package loop). Tests will include both zero and intermediate burnup fuel specimens.

**SEFOR TOP-10 Series (4 Loops)**

These tests will be similar to the TOP-4 series but will use a 19-pin package loop. Both zero burnup and pre-irradiated fuel specimen performance will be evaluated.

**4.1.2.3 Design Basis Experiments**

*Test Environmental Requirements*

Both the loss-of-flow and the transient overpower tests should be performed under conditions that provide a practical simulation of the operating environment of a fuel assembly of an LMFBR core. The specific environmental requirements include:

- Prototypic axial and radial power distributions in the fuel test assembly.
- Thermal-hydraulic characteristics of an LMFBR flow channel.
  - Static head of sodium coolant
  - Axial velocity profile of coolant
  - Simulation of radial heat transfer characteristics in fuel region
- LMFBR vapor-condensation potential in the fuel region and above.
- Sufficient cover gas volume to minimize pressurization due to voiding and/or thermal expansion of sodium.
- Prototypic conditions for grid or wire wrap spacers for fuel rods in the test section.

*Steady-State Test Requirements*

In addition to the environmental conditions, the parameters and steady-state test requirements for both the loss-of-flow and the transient overpower tests are as follows:

- Test Section
  - 19 pre-irradiated fuel rods
  - 30 inch active fuel length
  - 80 inch fuel rod length overall
- Steady-State Test Conditions
  - Peak fuel rod power - 15 kW/ft.
  - Inlet temperature  $\sim 700^{\circ}\text{F}$  ( $<800^{\circ}\text{F}$ )
  - Exit temperature  $\sim 1000^{\circ}\text{F}$
  - Sodium coolant velocity in test section - 30 ft/sec (maximum)
  - Duration - up to 5 days at steady-state conditions prior to transient operation

*Design Basis Loss-of-Flow Experiment*

Subsequent to the steady-state operation, the design basis loss-of-flow experiment has the following transient test requirements:

- Transient Test Conditions
  - Rapid flow reduction down to 10% in  $<0.10$  sec. with slower controlled flow reductions also possible.
  - Final flow rate  $<1\%$ .
  - Test termination by delayed reactor scram (5 to 10 seconds).
  - Total molten fuel volume 60 to 80 v/o.
  - Sodium exit temperature up to  $1600^{\circ}\text{F}$  (max).



*Design Basis Transient Overpower Experiment*

Following steady-state operation the design basis overpower experiment has the following transient test requirement.

- Transient Test Conditions
  - Reactivity insertion rates up to  $\sim 10\$/\text{sec}$
  - Total molten fuel volume  $\sim 65\text{-}70\text{ v/o}$

*Test Data Requirements (In-Pile Test Section)*

- Temperature
  - Sodium inlet
  - Sodium exit
  - Test section liner (thermocouple response time  $< 25$  milliseconds)
- Coolant Flow
  - Inlet Flow rate
  - Outlet flow rate
- Coolant Pressure
  - Inlet pressure
  - Exit pressure
- Special Instrumentation
  - Accelerometers
  - Strain gauges
  - Acoustic emission monitoring

*Failure Detection (Auxiliary Loop Instrumentation)*

- Delayed neutron monitors
- Loop cover gas activity monitor

*General Considerations*

The overpower and undercooling tests require simulating as well as possible those conditions that have first order effects upon the transient performance of the fuel rods and subsequent failure phenomena. For both types of tests, steady-state conditions typical of an operating LMFBR must be simulated. However, a fundamental difference exists in the predominant transient conditions affecting the overpower versus the undercooling fuel and coolant behavior.

The transient overpower performance of fuel rods (prior to failure) is primarily affected by the internal power generation, structure and history of the fuel rod and, to a lesser extent, the transient behavior in the coolant and adjacent rods. The ability to simulate these conditions depends upon the reactor capabilities and test fuel parameters. The potential for failure propagation will be influenced, to a large extent, by localized synergistic effects.

On the other hands, the phenomena associated with undercooling transients depend upon conditions throughout a large portion of a fuel assembly. The phenomena that are expected to occur during the loss-of-flow tests include:

- Initial formation and growth of sodium vapor in the channels.
- Subsequent coolant expulsion and re-entry
- Cladding dryout and failure
- Potential fission gas release
- Potential molten fuel-coolant interaction
- Potential failure propagation

Experimental data indicating the axial and radial extent of these phenomena as well as the timing of events are required for developing transient undercooling failure models.

In order to investigate these phenomena under simulated LMFBR conditions, careful consideration must be given to the geometrical and thermal hydraulic requirements for the package loop. The following conditions have been investigated:

- Axial geometrical simulation of fuel assembly and exit channel
- Steady-state axial velocity profile
- Sodium static head and inertia
- Transient radial and axial temperature distributions in a fuel assembly
- Heat capacity effects of assembly liners, coolant and structural material

A Demonstration Plant fuel assembly is compared with the package loop preliminary design in Figure 4A-1. The figure shows that the flow area ratio ( $A/A_0 = \text{local flow area/fuel bundle flow area}$ ) is the same for the Demo Plant fuel assembly and package loop at critical positions along the vertical axis. As a consequence, equal coolant velocities in the respective fuel sections result in comparable axial velocity profiles as shown at the right of Figure 4A-1. These flow area requirements for the package loop design are reasonable and consistent with space constraints for loop instrumentation. The sodium column above the active fuel is comparable, to within six inches, between the Demonstration Plant and the package loop. Thus, a preliminary analysis of the package loop indicates it is possible to simulate the hydraulic characteristics (including the sodium inertia and static head above the core) of a Demonstration Plant fuel assembly.

A model has been developed, using the THTE program, that treats the region (3-1/2 rows of pins) near the channel wall of a 127 pin fuel assembly. Transient computations have been performed for a moderate and a rapid flow coastdown. The flow transients and corresponding radial temperature profiles near the core exit are shown in Figures 4A-2 and 4A-3. The temperature profiles indicate that the coolant temperature near the channel wall increases at a slower rate than in the assembly core because of the large thermal capacity of the liner. This effect is more pronounced for the rapid flow coastdown. For moderate superheats ( $<50^\circ\text{F}$ ), a significant portion of the coolant is below the saturation temperature at incipient boiling. Radial condensation in this region may reduce the vapor slug growth rate and delay coolant voiding in the channel. This effect must be taken into account in the thermal hydraulic design of the package loop.

Figure 4A-4 shows the ratio of liner heat capacity to sodium and steel heat capacity as a function of bundle size (number of pins). Liner wall thickness is a parameter. The figure shows that the ratio for a 219 pin fuel assembly with a 140 mil liner thickness can be simulated by a 19 pin bundle with a 50 mil liner thickness. This gives one indication that it is feasible to simulate the liner heat capacity effect of a demonstration plant fuel assembly by a 19-pin package loop.

Typical transient temperature distributions in the axial direction of a demonstration plant fuel assembly are presented in Figure 4A-5 for a slow and a rapid flow coastdown. For the slow coastdown, the coolant in the plenum region has heated significantly by the time nucleation occurs near the top of the fuel region. By comparison, the coolant in the lower half of the fuel region has a much larger subcooling. Hence, coolant expulsion is expected to proceed predominantly in the upward direction for this flow coastdown.

The temperature distributions for the rapid flow coastdown are significantly different. The distributions suggest voiding will occur near the center of the core and proceed more uniformly in both directions. However, significant subcooling in both upper and lower regions is expected to result in greater axial condensation. This provides two examples of the thermal-hydraulic conditions that can occur in undercooling transients.

For both the overpower and undercooling tests, the transient conditions will be varied throughout this experimental program to investigate the corresponding response of fuel rods and fuel bundles. The different test conditions will result in various combinations of fuel-cladding failure, failure propagation and sodium voiding. Loop instrumentation will be utilized to measure the test conditions and to monitor the progress of these events during the transient by measuring the local pressure, temperature and coolant flow in the system.

The position and number of these sensors will be based on the data requirement of the individual test. For example, provision should be made to monitor sodium exit temperatures of the fuel bundle subchannels for the local flow blockage experiments. The testing program also includes operation of the package loop under conditions designed to produce fuel rod failure. In this case, there is a great experimental incentive to measure the local temperature distribution across a fuel bundle in the peak power region to detect fuel rod failure and failure propagation. The data will be used to characterize the loop conditions during both steady-state and transient undercooling or overpower operation for a subsequent detailed thermal hydraulic analysis.

Significant amounts of molten fuel ( $\sim 80$  v/o) are expected in conjunction with cladding failure during the transient phase of some experiments. The loop test vehicle must provide for containment of this liquid fuel. In addition, molten fuel-coolant interaction (MFCI) is anticipated during some tests. Any pressure pulses resulting from MFCI must also be contained by the loop.

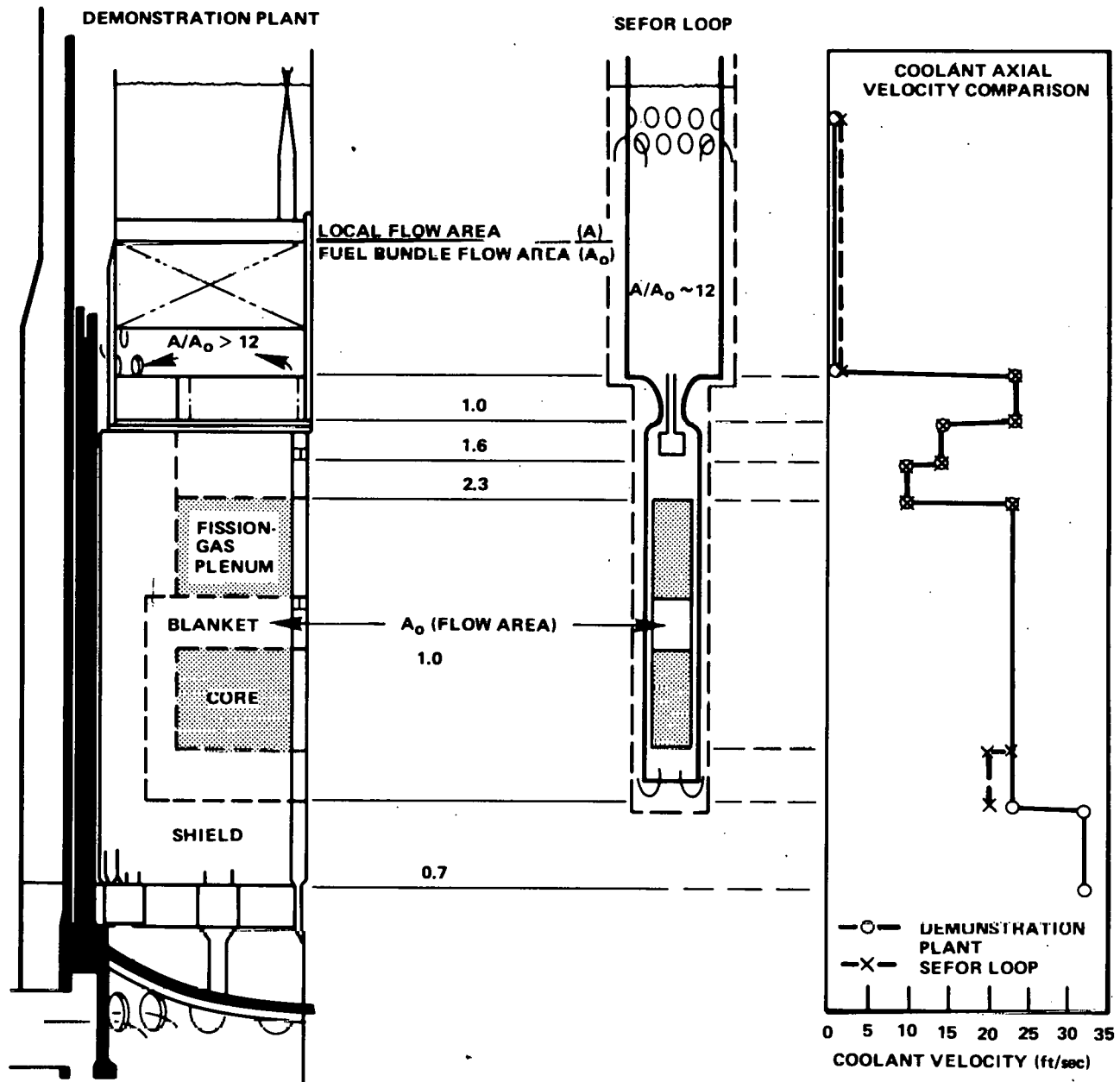


Figure 4A-1. Comparison of Demo Plant and SEFOR Loop Flow Geometries

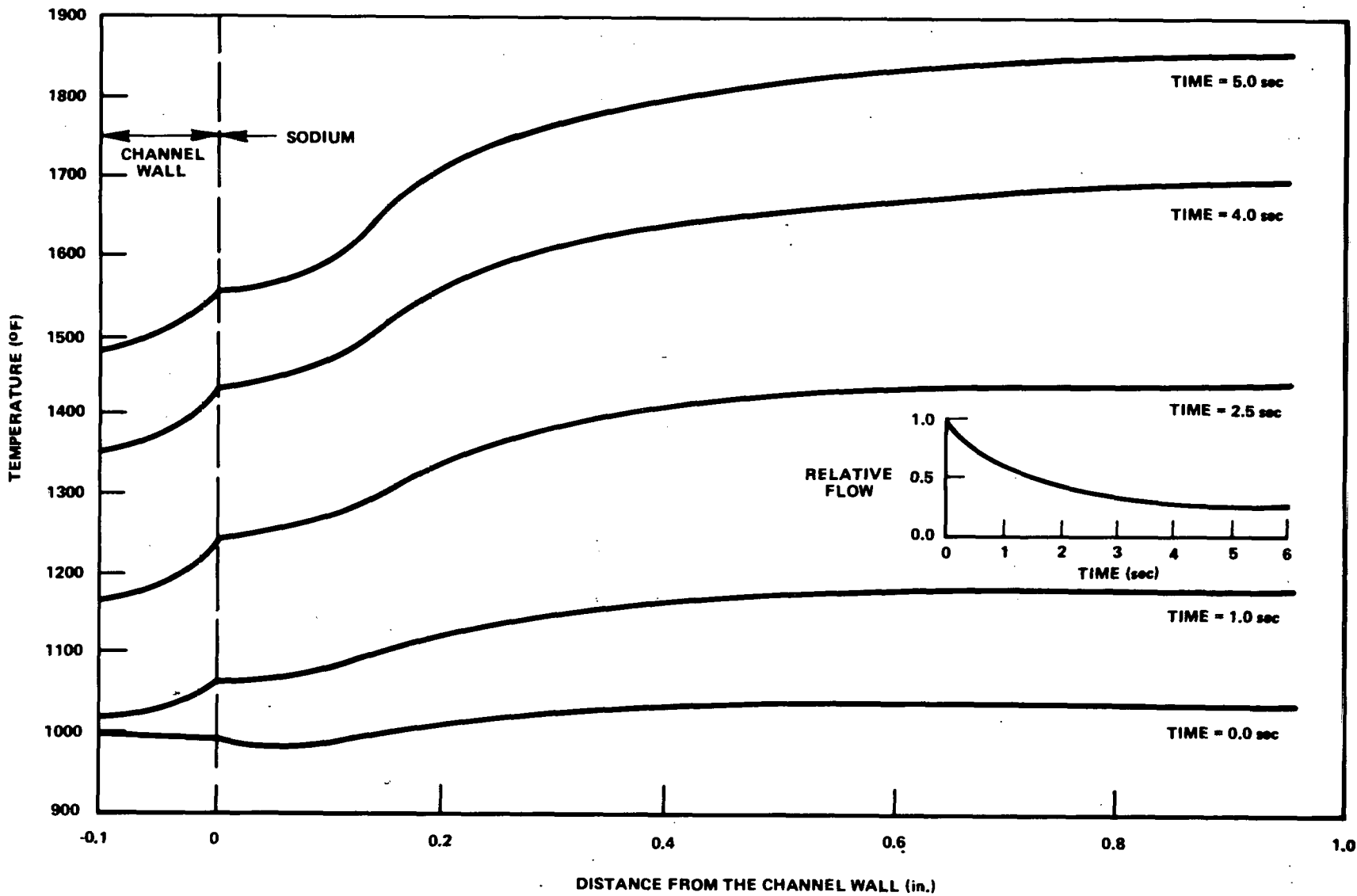


Figure 4A-2. Nominal Flow Coastdown Radial Temperature Distribution at 28.5 inches Above the Active Core Bottom

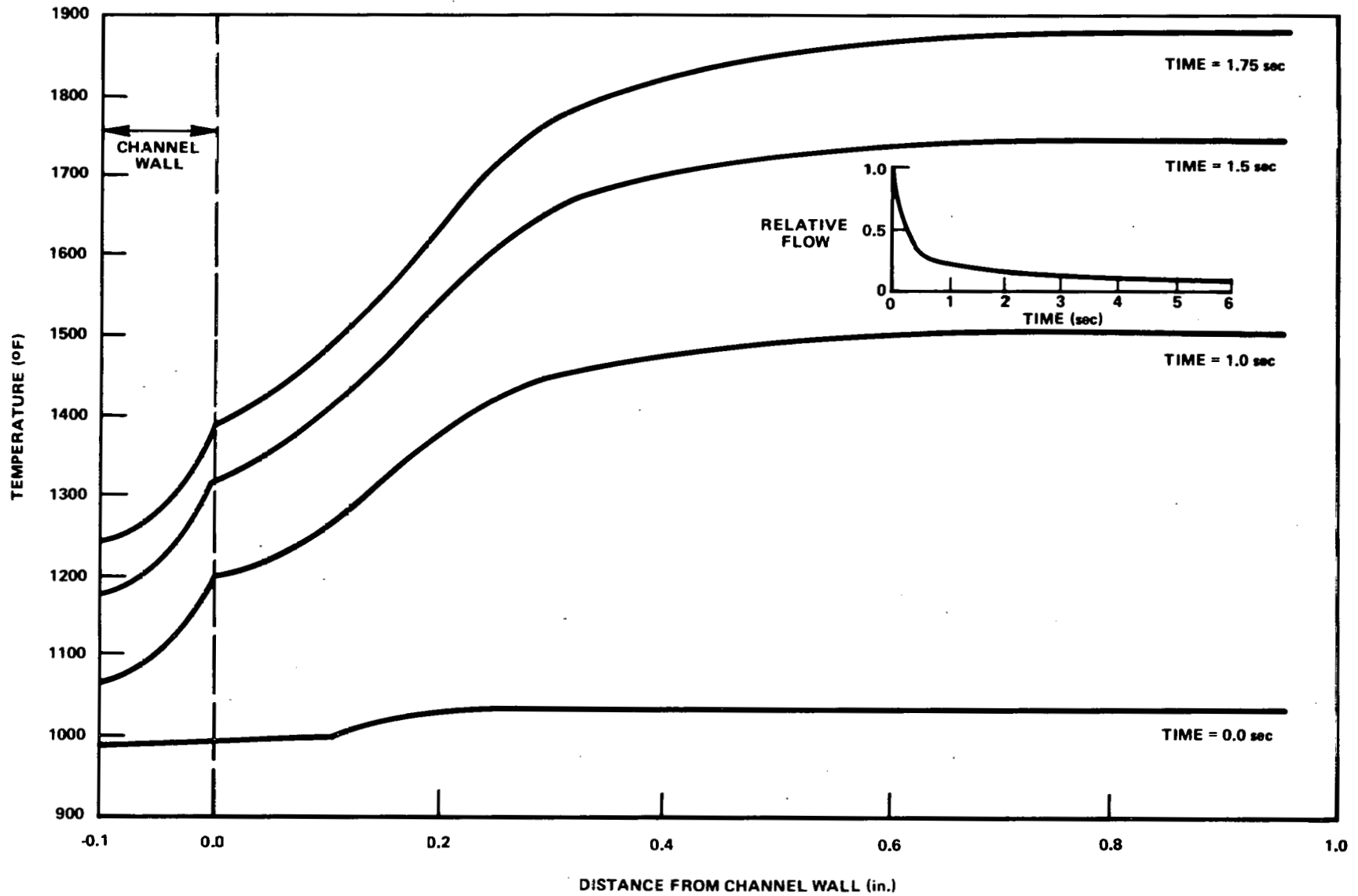


Figure 4A-3. Rapid Flow Coastdown Radial Temperature Distribution at 28.5 inches Above the Active Core Bottom

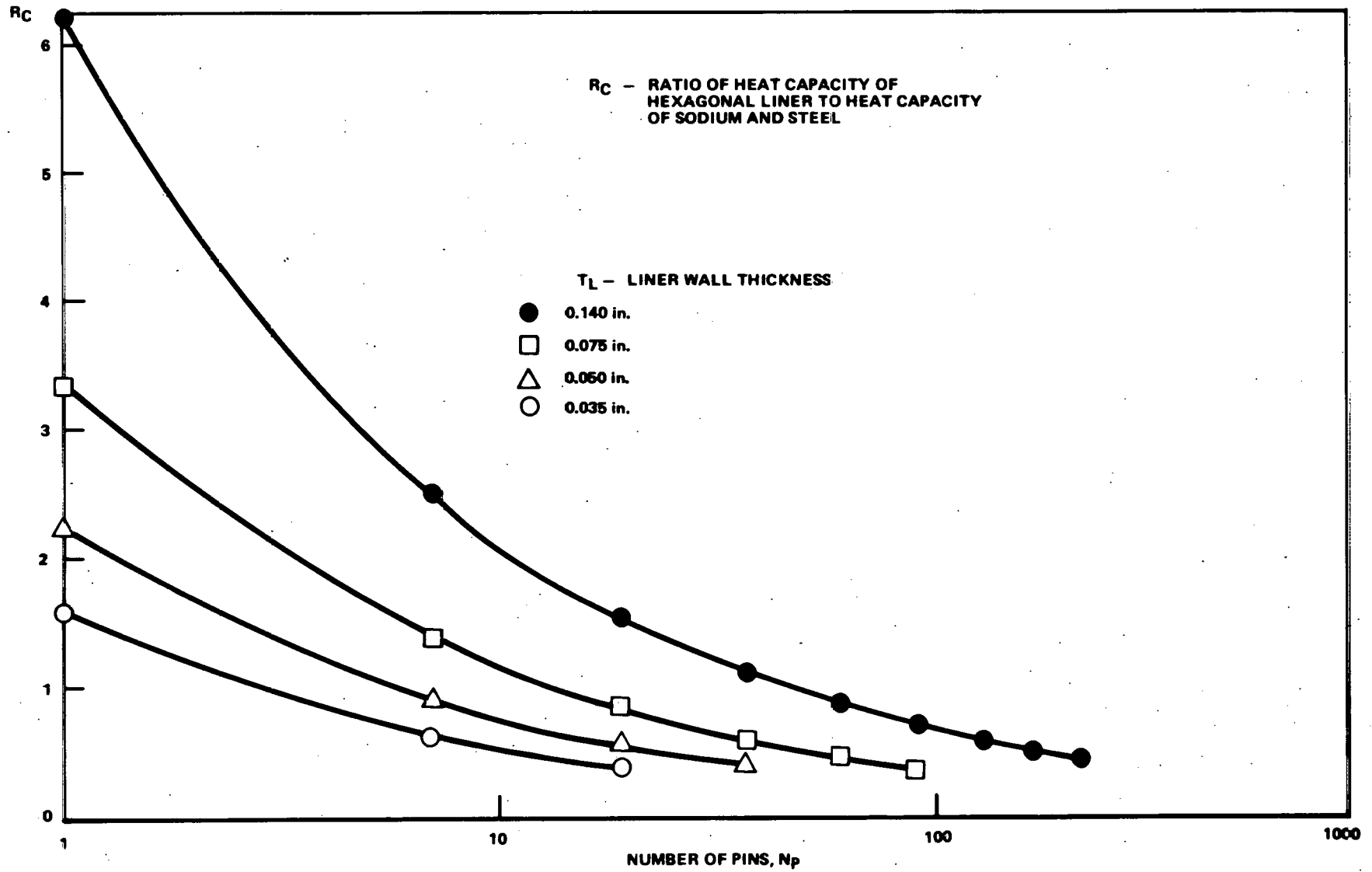


Figure 4A-4. Effect of Liner Heat Capacity with Bundle Size

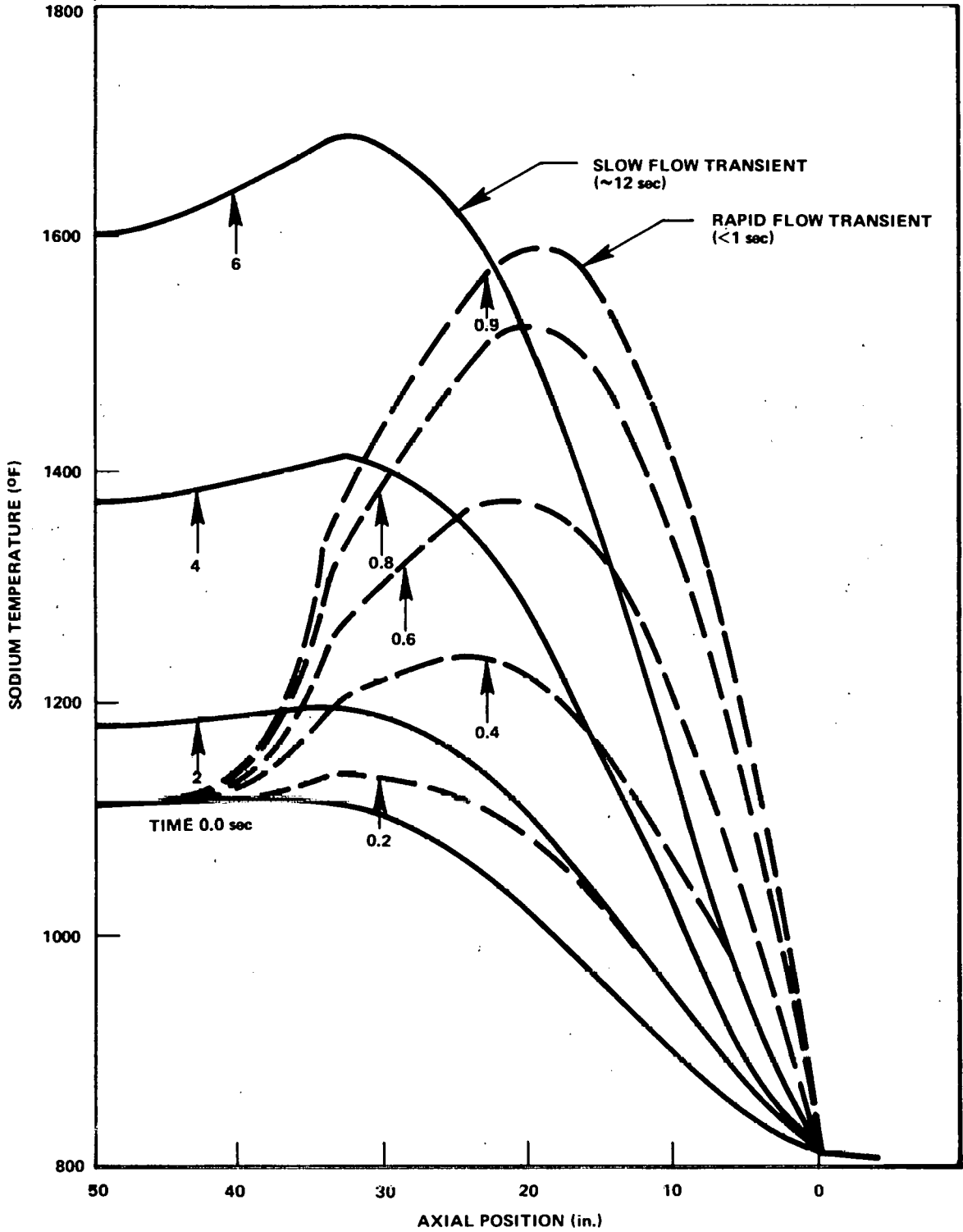


Figure 4A-5. Axial Temperature Profiles for Slow and Rapid Flow Transients

**4.2 Task 4B Option IIIA Development Design**

**4.2.1 Task 4B1 Control Drive System**

**4.2.1.1 Objective**

The objective of this task is to establish the scope design of a head mounted In-Core Control System to provide added control if needed for the Option III-A core configuration.

**4.2.1.2 Accomplishments**

Design requirements for the Control Drive System were established and a design specification prepared and issued.

The following table shows the In-Core Control System parameters.

Number of Drives	3
Type	dual purpose pneumatic actuated
Drive Stroke	36 inch
Drive Speed	15 inch/sec.
Scram Time (to 90% of stroke)	0.75 sec
Control Material	B <sub>4</sub> C
Average Worth	1.25\$

Layout drawings of the as-constructed center head port positions and the fuel channel locations were made to factor into the design as-built information. Three head ports were assigned for the drive position, these include 2 of the outer control drive ports and the sodium sampling port.

Consideration was given to 3 different systems - a shim only system using single purpose drives, a combination of shim (1) and scram drives (2) all being single purpose, and a dual purpose system consisting of three shim scram drives. The dual purpose drive system was selected for its added operating flexibility and lower rod worths.

Pneumatic actuated and mechanically actuated drives were considered. Design layouts were made for each type of drive and dynamic analysis carried out with a major emphasis on initial acceleration, maximum velocity, terminal velocity and elapsed time for scram cycle. The pneumatic actuated drive design was selected primarily for its shorter scram cycle and adjustable characteristics, making it possible to vary the drive pneumatic pressure, etc. to obtain performance which is tailored to the reactor conditions. A scope drawing was prepared for the pneumatic actuated drive system.

The scope design utilizes an in-sodium damper for terminating the scram stroke. Consideration is being given by the reactor vessel design group to lowering the sodium level in the reactor vessel due to stresses in the reactor vessel flange. This lowering of the sodium level would eliminate the in-sodium damper, so study of alternate damping systems was initiated.

A preliminary failure modes and effects analysis for the drive system was completed to establish quality level requirements for the assemblies. A piping and instrumentation diagram for the control drive pneumatic system was completed.

**4.2.2 Task 4B2 - FRED**

**4.2.2.1 Objectives**

The objectives of this task are to evaluate the present FRED design (as described in GEAP-13649) and identify modifications required for operation in the off-center position, including providing added cooling for the FRED Rods.

**4.2.2.2 Accomplishments**

Design emphasis was placed on relocating the FRED with a minimum of modifications. The existing locations for the off-center thru head ports were based on the original SEFOR in-core drive design, which had a pair of control rods positioned near the inner periphery of the hex channel below, with the rest of the channel space planned for fuel rods and a tightener rod. This resulted in non-coaxial alignment of the off-center ports with the hex channels below which formed the core lattice (See Section A-A of Figure Dwg. 264R149). Because the present concentric drywell could not slide into the non-aligned hex channel below, a new drywell design was required. Since a new drywell had to be made, this allowed more design latitude in providing a forced convection cooling system for the FRED B<sub>4</sub>C



rods. Preliminary heat transfer calculations were done which indicated the merit of such a forced convection cooling system. If helium was used as the cooling gas, calculations showed it was possible to operate a 1\$ FRED rod at a reactor power of 20 MW without exceeding at 1600°F FRED rod clad temperature. Combining the Forced Convection Cooling System with the drywell required the consideration of a combination of different factors such as:

- ASME Section III codeability of the drywell
- Drywell geometry vs. heat transfer characteristics and helium flow requirements
- Special material costs and manufacturability.

These factors were considered in arriving at a reference design for the FRED off-center drywell and Forced Convection Cooling System (Figure Dwg. 264R149). The design requirements were defined with the issuance of the FRED System Modification Design Specification. The new drywell design is an ASME Section III Codeable assembly of non-coaxial tubes welded together via special eccentric forgings. Forced convection cooling is provided by a helium supply system and an inner sleeve which diverts the helium flow down around the outside of the FRED Rod and then up around the inside of the drywell. There is an inlet and an outlet port located above the drywell reactor head flange. The small amount of exhaust flow exits into the refueling cell where, studies have shown, it poses no problem.

Other design modifications required are a reduction in the diameter of the positioner screw and nut to allow sufficient drywell wall thickness, a new positioner motor mounting, a new FRED accumulator mounting, a new hex channel without the side rods, and some minor modifications to provide clearance between equipment planned for mounting in adjacent ports.

#### 4.2.3 Task 4B3 - Fuel and Control Assembly Design

##### 4.2.3.1 Objective

The long-term objectives of this task are to establish design and safety criteria and to develop the design of the reactor core for performance of the Option III-A tests. The objectives during Phase A were to establish the criteria, to perform preliminary analyses of the booster fuel and to initiate preliminary design of the control assemblies.

##### 4.2.3.2 Discussion

Design and safety criteria for the SEFOR core for Option III-A testing were established, scope designs involving three alternate cores were developed, preliminary analyses of the booster fuel were performed and preliminary design of control assemblies was initiated. Investigations of booster fuel included thermal-hydraulic performance and analyses of stresses. A conceptual design for the booster and driver fuel was developed.

##### 4.2.3.3 Core Design Criteria

- Structural
  - The criteria for stress or strain are specified in Table 4B3-1.
- Thermal-hydraulic
  - For steady-state and transient operation, the fuel center temperature at the axial peak of the peak fuel rod shall not exceed the solidus temperature of the mixed oxide fuel (for the enrichment used) with a confidence of 95%.
  - The peak hot spot in the cladding shall not exceed 1260°F with a confidence of 95%. Provide capability for initiating power transients from full power without damage to fuel core or systems.
  - Provide adequate cooling for loop in all planned test conditions.
- Physics
  - Provide adequate reactivity control for insertion and removal of loop.
  - Provide adequate reactivity control for insertion and removal of test assembly from loop.
  - Provide adequate reactivity with margin to permit transients from full power.
  - Provide adequate reactivity to compensate for loss due to burnup.
  - Provide adequate reactivity to operate at power without the loop in the core.
  - Provide Doppler coefficient  $(T dk/dT) \geq 0.004$  with uncertainties applied.
  - Reactor control adequate to provide protection to reactor and plant under all planned operations and all possible test fuel relocations and conditions.

- Testing Capability
  - Deliver 2000 peak w/cc to the test fuel within loop at core center, and a peak steady-state linear power of at least 15 kW/ft for loss of flow tests.
  - Test Fuel rod power ratio not to exceed 1.2.
  - Provide simulated LMFBR transients in test fuel within loop from initial prototypical LMFBR conditions.

**4.2.3.4 Safety Criteria**

*General Criteria*

The reactor design shall provide a high degree of stability such that oscillations in local or bulk power can not occur throughout the operating range.

The design shall provide adequate margin to accommodate any cyclic loads on reactor and control components which have the potential for producing fatigue and wear failure.

The core nuclear and coolant flow characteristics, mechanical design features, and safety instrumentation shall:

- (a) reduce to a practical minimum the probability of unplanned positive reactivity additions and/or local and bulk coolant flow reductions that cause an imbalance between the generated power and heat dissipation and
- (b) limit the magnitude and rate of reactivity additions associated with potential mechanical and electrical failures, system malfunctions and operator errors such that consequences of such faults do not lead to a reduction of reliability and life expectancy of the fuel and core structures. The severity of transients considered as credible<sup>1</sup> shall be limited by reducing to a practical minimum the potential for unplanned reactivity additions.

Operating limits<sup>2</sup> shall be established from a conservative interpretation of experimental and analytical information to assure that adequate and defensible margins exist between the planned operating range and any core damage threshold.

A highly reliable fuel design with adequate margins included in specified operating limits shall be provided which minimizes the probability of fuel failure initiating accidents, or core damage occurring as a result of credible accidents.

The nuclear, mechanical, and thermal hydraulic characteristics of the core shall be designed such that the existing engineered safeguards systems and modified control systems shall provide adequate protection for the plant.

**4.2.3.5 Specific Criteria**

- Power Coefficients
  - The net power coefficient of reactivity shall be negative and of such magnitude that the stability of gross and local core power can be assured for steady-state and operational transients throughout the operating range.
  - The prompt power coefficient of reactivity (energy coefficient) shall be negative and of such a magnitude (with margin) that power excursions due to reactivity insertions from credible faults or planned transients can be terminated by normal safety system action without loss of fuel integrity (below the safety limits for the fuel).
  - The prompt power coefficient of reactivity (energy coefficient) shall be negative and of such a magnitude that the calculated energy release (including the effect of sodium void reactivity limits) for all disruptive accidents including core disassembly is within the design bases of the containment system.
  - The Doppler coefficient ( $T dk/dt$ ) is the only prompt negative power coefficient which shall be considered as sufficiently reliable for core disassembly evaluations. The Doppler coefficients used for safety analysis (the "minimum Doppler coefficient") shall be the smallest value calculated anytime during the operating life of the core, and reduced by all uncertainties involved in the calculation. The specific conditions (e.g. sodium-in or sodium-out) existing during the transient shall be used in establishing the "minimum Doppler" for analyzing the transient response of the reactor.

<sup>1</sup> Credible transients will be defined in the conformance review of the design.  
<sup>2</sup> Includes normal operating limits, alarm settings, safety system trip settings, and safety limits.

- Sodium Void Reactivity

The maximum positive reactivity due to voiding in a single fuel assembly (and the interchannel volume around it, if any) anytime during the operating life of the core when combined with hypothesized<sup>3</sup> fuel redistributions in the voided fuel assembly under this condition and including all calculational uncertainties shall be limited. The limit shall be chosen such that normal plant protection system action combined with protection provided by the fuel assembly channels will limit the damage to the extent necessary to assure cooling of all fuel assemblies and permit removal of the damaged assembly.

The maximum positive reactivity (including all calculational uncertainties) due to gross core voiding shall be kept to a practical minimum.

- Other Reactivity Additions

The maximum positive reactivity due to a hypothesized<sup>3</sup> fuel redistribution in a single channel anytime during the operating life of the core, including all calculational uncertainties, shall be limited to a value such that the plant protection system, combined with protection provided by the fuel assembly channel will limit the damage to the extent necessary to assure cooling of all fuel assemblies and permit removal of the damaged assembly.

The maximum reactivity worth of any core component designed to be movable (fuel bundles, control element, etc.) shall be limited such that the power excursion resulting from the hypothesized<sup>3</sup> accidental motion of such a component anytime during the life of the core and including all calculational uncertainties will be terminated by the plant protection system before the core reaches a core damage threshold<sup>4</sup>.

- Core and Rod Power

The core power shall be limited such that the calculated peak fuel temperature in the hot spot fuel rod (including all uncertainties) shall not exceed the solidus temperature for steady power operation at the safety system trip setting.

The energy added to the hot spot fuel rod during a credible<sup>1</sup> transient or planned transient shall be limited such that the fuel does not exceed the fuel safety limit.

- Fuel Clad Structural Integrity and Temperature

The fuel cladding shall maintain its structural integrity during steady-state, credible<sup>1</sup> and planned transient operating conditions that may occur during the life of the core. Steady-state and transient operating temperatures for the cladding shall be limited such that the local hot spot temperatures, including all calculational uncertainties, are below the safety limit for the cladding.

- Thermal Hydraulic

The flow resistance of the core (pressure drop) in conjunction with the main coolant circuit, shall provide reliable shutdown cooling to the core by natural circulation in the primary cooling circuits.

The core inlet region shall be designed such that instantaneous loss of flow in one primary loop (main or auxiliary) does not result in excessive fuel cladding temperatures during the resulting transient and the shutdown cooling period following the transient assuming normal plant protection action occurs.

The sodium flow channels and core structure shall be designed to prevent entrapment of gases.

The flow inlet region to the core shall be designed to restrict passage of foreign material into the fuel channel and limit the magnitude of flow reduction to a fuel channel such that any damage due to local undercooling is limited to the affected channel.

(3) The models used for these analyses will be developed during the conformance review of the design.

(4) By definition, the core damage threshold is above the safety limit. Degradation of the core components could result from power and/or temperature in the range between the safety limit and damage threshold, but no safety problem would exist for operation below the core damage threshold.

● Core Structure

Permanent core structures shall be shielded such that radiation damage does not change material properties to such an extent that their ability to sustain imposed loads is decreased below the design value.

The core structures shall be designed to withstand the specified number of transient loads during their design life. The intent of the structural requirements of the ASME Pressure Vessel Code Section III shall be met for all load-carrying structural members as a minimum requirement for further restrictions on secondary stresses imposed where radiation damage is significant.

● Fuel Movement

The axial position of the fuel shall be positively maintained during power operation. The positive reactivity addition to the core due to failure of the axial position control (from either the initial motion or in returning from a displaced position back to the original position) shall be limited to a value such that the resulting power excursion will be terminated by the plant protection system action before the fuel reaches the fuel damage threshold.<sup>3</sup>

Sufficient hold-down capability shall be provided to positively maintain axial core position under flow conditions corresponding to the maximum flow capability for the primary pumps and for loading conditions such as that resulting from an earthquake or a large power excursion.

The radial support of the fuel in the assembly and the assembly in the core shall assure that any reactivity oscillations due to vibratory motion of the fuel and/or the fuel assembly do not introduce reactivity effects leading to power oscillations.

The magnitude of the reactivity effect associated with the movement of fuel resulting from a failure in the radial support system or fuel assembly structure shall be limited such that the power excursion will be terminated by normal plant protection system action before the fuel reaches the fuel damage threshold.

Core Performance Objectives

Power	23 MWt
Inlet Temperature	700° F
Outlet Temperature	820° F
Peak Linear Power Booster	~11 kW/ft
Burnup in Booster (Peak Local)	50,000 MWd/Te

Core Fuel Requirements

- New fuel to be contained in 0.310" O.D. fuel rods.
- Fuel to be mixed oxide with depleted uranium.
- Pu 239/total Pu ratio to be as high as practicable.

Core Mechanical Design Constraints

- Use existing grid plate and support structure.
- Use existing core restraint system.
- Use existing pump and heat exchange system.
- Subassemblies to use present channel outside dimensions.
- Use present design for nose, latch and orifice scheme (different orifice sizes).
- Use same core height.
- Use four channels for in-core control and FRED.
- Use center position for package loop.
- Use present reflector control system supplemented by in-core control.

Package Loop Requirements

Loop will be cooled by primary coolant.  
 Loop will be loaded through center through-head port into center channel.  
 Loop will contain up to 19 fully enriched UO<sub>2</sub> fuel rods. 0.250" OD, 30"L, 0.015" Clad  
 Loop will be surrounded by ZrHy to increase test fuel power density.  
 Loop structural design will be adequate to contain pressures generated in test.  
 Primary coolant temperature in center channel will be <1050°F during or following tests.  
 Primary coolant inlet will be <700°F.

4.2.3.6 Scope Design

The scope design includes three alternate core designs. The cores consist of the following fuel regions:

Alternate No. 1	
Booster	6 Channels
New Subassemblies	30 Channels
Modified Core I Subassemblies	68 Channels
Off Center FRED	1 Channel
In-Core Control	3 Channels
Alternate No. 2	
Booster	6 Channels
New Subassemblies	98 Channels
Off Center FRED	1 Channel
In-Core Control	3 Channels
Alternate No. 3	
New Subassemblies	69 Channels
Off Center FRED	1 Channel
No Booster	3 Channels

The test region is located in the center channel

The subassembly compositions for the three alternate cores are listed in Table 4B3-2.

Table 4B3-1

**ALLOWABLE STRESS INTENSITY**

Allowable Stress Intensity<sup>(d)</sup> <  $RS_m$

Values of "R" for Various Loading Conditions

Principal Stresses Being Considered		Normal	Upset	Emergency <sup>(c)</sup>	Faulted <sup>(c)</sup>
Primary Membrane	$P_m$ A <sup>(a)</sup>	1.0	1.0	1.1	1.2
	B <sup>(b)</sup>	1.0	1.0	1.1	1.2
$P_m + P_B$ Primary Bending	A	1.5	1.5	1.65	1.80
	B	1.0	1.0	1.10	1.20
$P_m + P_B + Q$ Secondary	A	1.5	1.5	1.65	1.80
	B	N.A.	N.A.	N.A.	N.A.

Notes:

(a) "A" signifies  $\sigma_{yield}$  and  $\sigma_{ultimate}$  criterion

(b) "B" signifies minimum stress to cause rupture criterion

(c) 10% and 20% increases are tentative selections for emergency and faulted conditions

Stress or Strain Criteria

Mode of Loading	Quasi-Brittle (Less than 10% Elongation)	Ductile
Design Stress Intensity $S_m$	0.67 $\sigma_{yield}$	0.90 $\sigma_{yield}$ (when unirradiated and linear transition to brittle point)
	0.33 $\sigma_{ultimate}$	0.50 $\sigma_{ultimate}$
	0.80 of minimum stress to cause rupture	0.80 of minimum stress to cause rupture
Strain	Obtain percent allowable uniaxial strain for a given fluence and temperature. Multiply this value by the fraction for the biaxiality ratio at the point of interest. This is allowable combined plastic strain and thermal creep strain. Elastic strain from irradiation-induced creep and uniform swelling strain are considered to be nondamaging.	
Buckling (Elastic, Elastic-Plastic, or Creep)	$\leq 800^\circ F$	Use Article I-11 of the ASME Boiler and Pressure Vessel Code
	$> 800^\circ F$	Apply the code charts and formulas or use a suitable method of analysis or model testing but use a factor of safety of 2.0 minimum for loads and duration of load

Table 4B3-2

SUBASSEMBLY COMPOSITIONS

Alternate	No. 1	No. 2	No. 3
Booster	60 Fuel Rods 1 SS Rod	60 Fuel Rods 1 SS Rod	—
Inner Drives	36 Fuel Rods 24 BeO Rods 1 SS Rod	36 Fuel Rods 24 BeO Rods 1 SS Rod	36 Fuel Rods 24 BeO Rods 1 SS Rod
Outer Drives	3 x 1" Fuel Rods 3 x 1" SS Rods 1 BeO Tightener Rod	36 Fuel Rods 24 BeO Rods 1 SS Rod	36 Fuel Rods 24 BeO Rods 1 SS Rod
Pu/U+Pu			
Booster	0.50	0.50	—
Inner Drives	0.20	0.16	0.33
Outer Drives	0.20		

New Subassemblies - 61 Rods ~ 0.310 OD, in core rods contain fuel, BeO or stainless steel

4.2.3.7 Nuclear Characteristics of the Booster Fuel

- The peak linear power in the booster is 10 to 11 kW/ft.
- The axial power distribution is shown at 3 radial locations in Figure 4B3-1. Note that the ZrH<sub>1.6</sub> is 30 inches in length and extends downward from the top of the core.
- The radial power distribution at the axial peak is shown in Figure 4B3-2.
- The total power in the booster assembly is 1.2746 x 10<sup>6</sup> watts at a core power of 23 MW.
- The peak and rod averaged burnup in the peak fuel rod could not be calculated because of insufficient information on the fuel cycle. Information can be inferred from Figure 4B3-1, giving the axial power distribution and the power information from the booster assembly for any desired core burnup.
- The peak flux in the booster fuel rod is: Total 1.07 x 10<sup>20</sup> neutrons/cm<sup>2</sup>/full power day  
Peak fluence above 0.1 MeV is 7.44 x 10<sup>19</sup> neutrons/cm<sup>2</sup>/full power day.
- Smear density is 9.54 g/cc. Fuel height is 91.16 cm (36 inches).

The fuel compositions are as follows:

$$Pu/(Pu + U) = 0.50$$

$$Pu-239/(Pu-239 + Pu-240) = 0.9176$$

$$U-238/U-238 + U-235 = 0.9978$$

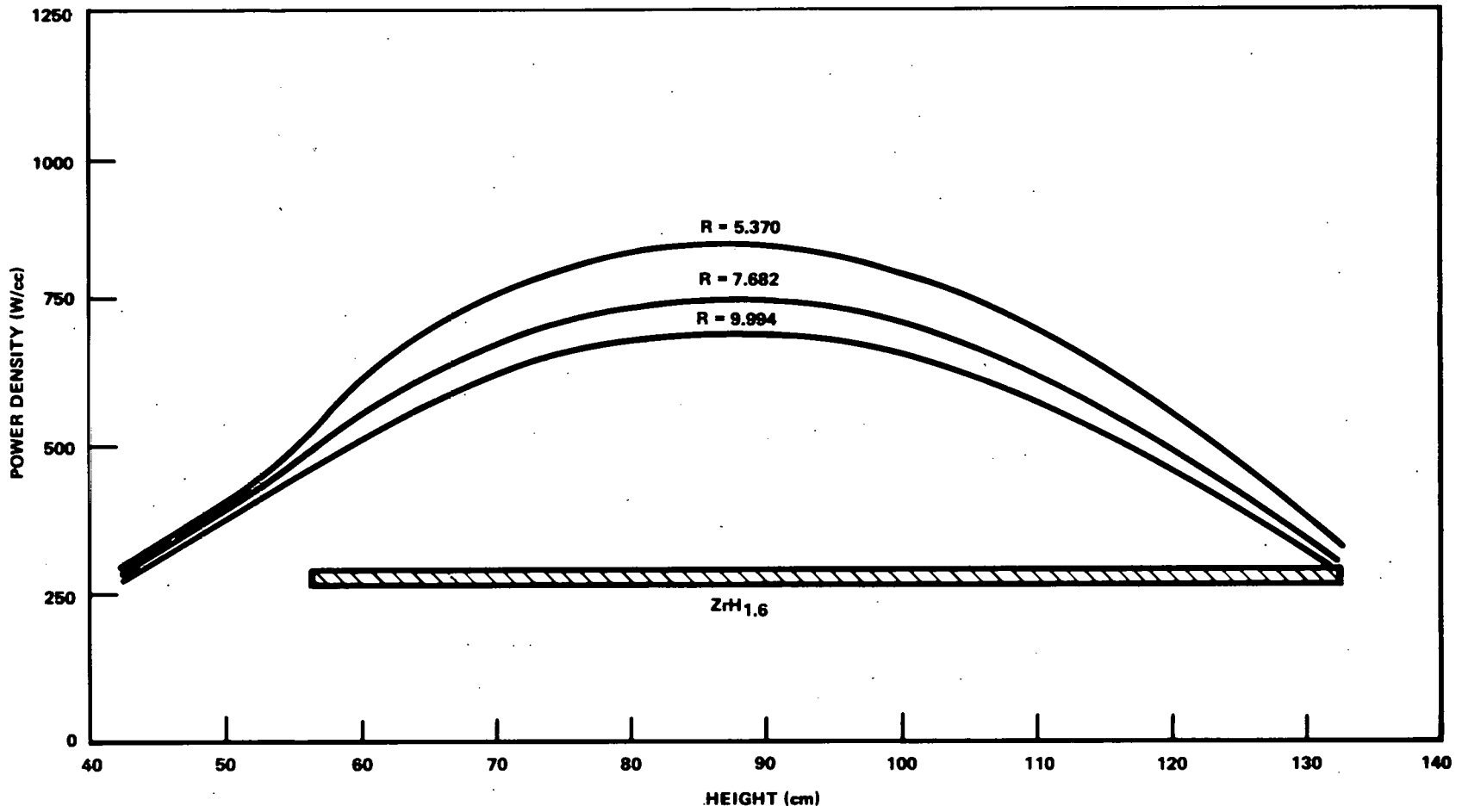


Figure 4B3-1. Axial Power Distribution, In Booster



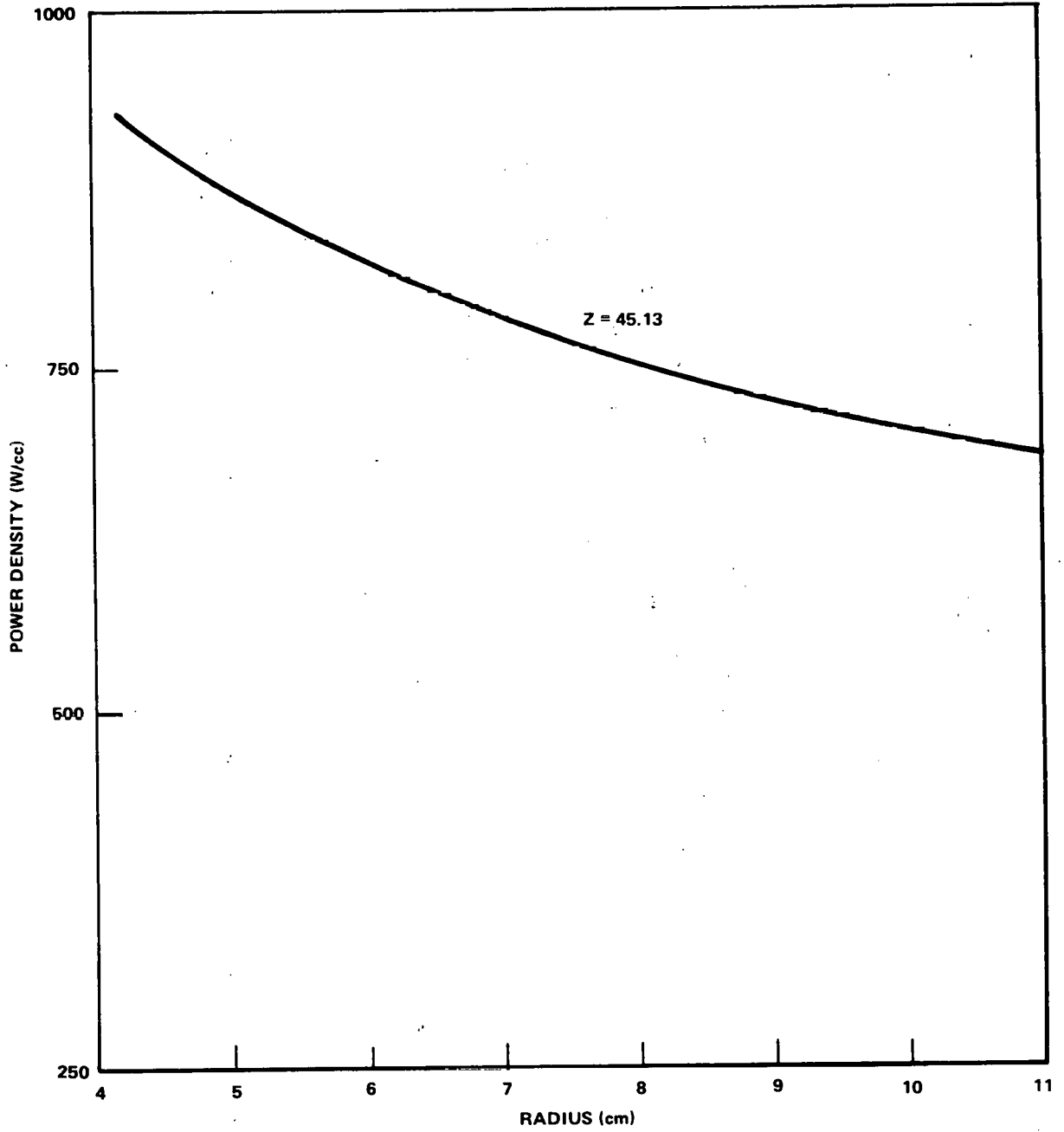


Figure 4B3-2. Relative Power Density versus Axial Peak Location

#### 4.2.3.8 Thermal-Hydraulic Performance of the Booster Fuel

##### *Operating Conditions*

The planned test program for the closed loop in Option III requires that the SEFOR power be increased to 23 MWt and that some or all of the present fuel be replaced by higher powered driver assemblies. The inner six of these assemblies have very high enrichment ( $\sim 50\%$  Pu) to achieve a high flux in the loop. These inner six assemblies are referred to as the "booster fuel." Since the booster assemblies operate under the most severe conditions in the reactor, this analysis has been limited to those assemblies. An analysis was not performed on the whole core, so it was necessary to use the flow rates determined from a previous evaluation (Ref. 1).

The basic characteristics of the booster assembly are summarized in Table 4B3-3. The assembly has a radial power profile at the midplane as shown in Figure 4B3-2 and the axial power profile is shown in Figure 4B3-1. The peak power in the innermost fuel rod in the booster assembly is 11.0 kW/ft and the average power is 7.0 kW/ft. Each booster assembly produces 1275 kW of power.

The present assembly flow distribution in SEFOR is inadequate for Option III. Since the booster assembly produces almost five times as much heat as the present inner assemblies, the present inner assembly flow rate of 6.9 lb/sec would result in a 600°F temperature rise in the booster assembly. The booster assembly also has a higher pressure drop than the present assemblies for the same flow rate. For these reasons, it will be necessary to re-orifice the reactor to greatly increase the flow in the booster assemblies. Since this will increase the reactor pressure drop, it is expected that the leakage flow will increase, resulting in a lower fraction of the total flow available to cool the core. In a preliminary evaluation (Ref. 1), it was felt that 16 lb/sec would be available to cool each booster assembly. This flow was used for this study. Further analysis of the core and the pump are needed to confirm this flow.

##### *Fuel Rod - Channel Clearance*

The cladding temperatures in the booster assembly are quite sensitive to the clearance between the outer row of fuel rods and the channel wall. A study was made to determine what spacing would minimize the cladding temperature using the FULMIX computer code (Ref. 2).

Since the booster assembly must fit into the present SEFOR configuration, the channel outer dimension across flats must remain at the present 3.150 inches. It has been assumed that the present channel wall thickness of 0.060 inches will be adequate for the higher pressure drop and temperature of the booster. This assumption will be verified in later analyses. Since the channel dimensions and rod diameter are fixed for this study, there is a unique rod pitch-to-diameter ratio for each edge spacing. It has been assumed for this study that the fuel rods expand uniformly to fill the channel. Experience with Demo Plant wire-wrapped fuel bundles have confirmed this assumption when the differences between the compacted rod bundle and the channel inside dimensions are not large. However, the rods in these bundles have been fixed only at the lower rod support. The booster fuel is fixed at both the top and bottom, but there is looseness. It is assumed that the rods will behave as if they were only fixed at the bottom.

The booster rod bundle is placed in the channel after the channel is fastened to the reactor lower support plate. This requires that the rod bundle fit easily into the channel without excessive force. This is accomplished by providing clearance in the rod bundle. This clearance is the difference between the inside dimensions of the channel and the outside dimensions of a theoretically tight bundle of unbowed rods. It is assumed for this study that 0.030 inches of clearance is adequate for insertion of the bundle into the channel.

Table 4B3-4 shows the maximum cladding temperatures and maximum temperature gradients across the fuel rod for various fuel rod-channel clearances. These results are based on nominal conditions and cold dimensions. The effect of using hot dimensions is small, but the effect of using worst conditions is not known and would require further studies. Of particular concern is the tolerance in the clearance and the looseness in the top and bottom support of the edge rods that is needed to insert the bundle in the channel. The results might be different if the motion needed for insertion must occur only on the edge rods rather than have the clearance uniformly distributed across the bundle.

Both the maximum temperature and the temperature gradient are minimized when the clearance is in the range of 0.035 - 0.038 inches. The 0.038 inch clearance was selected because the maximum occurs at an edge rod rather than the corner rod as in the 0.035 inch case. For convenience in running the FULMIX code, it was assumed that the channel has sharp corners. Since the actual channel has rounded corners, the FULMIX code uses a larger flow area in the corner. The actual case would have higher temperatures for the corner rods than is shown in Table 4B3-4. Thus, the actual case would favor the larger clearance since the corner rod is not the maximum for clearance above 0.035 inches.

All of the clearance shown in Table 4B3-4, with the exception of the 0.062 inch case, require that the wire along the edge be smaller than the wires on the interior rods. With the 0.062 inch case, all of the fuel rods would have the same wire diameter. This would be a convenience in fabrication. Although the maximum temperature for the full

wire case is only 11°F above the optimum the maximum gradient is tripled. A trade-off study is needed to determine if the optimum clearance is worth the increased fabrication difficulties. For this study, the optimum clearance (0.038 inches) was used. A 0.067 inch wire on interior rods will provide 0.030 inches of clearance in the bundle for this spacing.

#### *Cladding Temperatures of the Peak Rod*

With a 0.038 inch clearance, the maximum cladding temperature occurs at the top of the core for the edge rod located in the middle of the hot side of the booster assembly. The cladding temperatures for this fuel rod have been calculated for both nominal and hot (uncertainties included) conditions with and without the effects of the wire wrap. The results of these calculations are shown in Table 4B3-5. The peak cladding I.D. temperature without the wire wrap effects is 1022°F for nominal conditions. Wire wrap effects will increase this temperature to 1053°F. The peak cladding temperatures with uncertainty factors included are 1079°F without wire wrap effects and 1112°F with wire wrap effects. A detailed analysis of the effects of wire wrap on the cladding temperature was not performed for this study. It was assumed that the effect of the wire wrap on the booster fuel is the same as the effect of a 0.070-inch wire on a 0.250-inch O.D. fuel rod. (These effects have been determined in a previous analysis and are reported in Reference 3.) The decrease in the effect due to a smaller wire diameter is assumed to be counteracted by the increase due to the large rod O.D. The cladding thickness was the same for both cases.

A study of the uncertainty factors for the booster fuel has not been performed. Uncertainty factors that were used for the study of SEFOR operation at elevated temperature (Ref. 4) were used in this study. These factors assume a 10% decrease in flow and a 6.8% increase in power, and are based on the uncertainties in the present core.

The circumferential distributions of the cladding midwall temperature at the core midplane and at the top of the core are shown in Figures 4B3-4 and 4B3-5 respectively. These distributions are for nominal conditions and are inferred from FULMIX results. FULMIX calculates the coolant temperatures for six 60° segments around each fuel rod. These are inadequate to determine the exact circumferential distributions. Since more detailed results were not available, it was necessary to reduce the distribution based on maxima, minima, and points of inflection.

#### *Fuel Temperature of Peak Booster Rod*

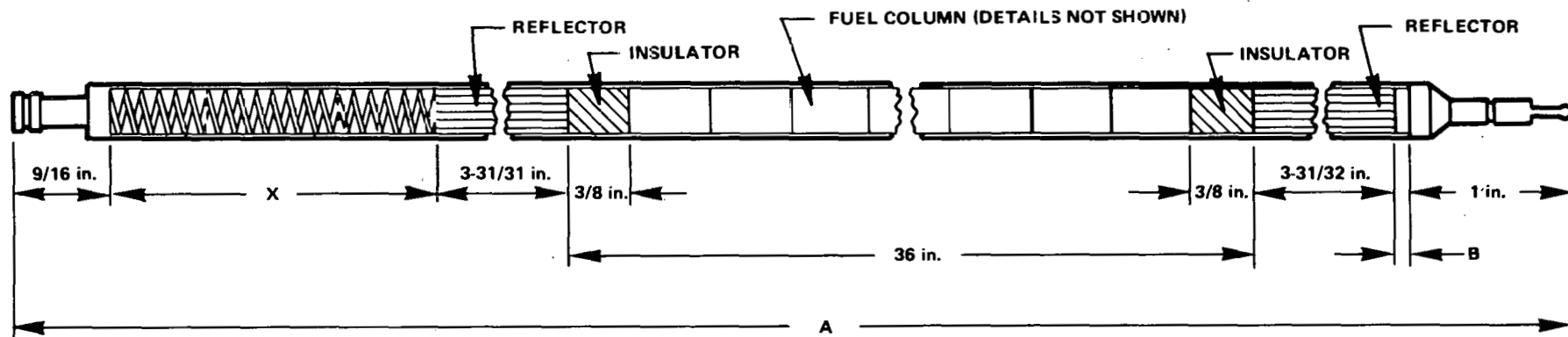
The peak power of the SEFOR booster fuel rod is 11.02 kW/ft. This will yield a peak centerline fuel temperature of ~3500°F. This would leave a design margin (to melting) of ~1500°F on temperature and ~6 kW/ft on linear power. The fuel rod design for this study is shown in Figure 4B3-3.

Table 4B3-3

**BOOSTER ASSEMBLY CHARACTERISTICS  
SEFOR FOLLOW-ON  
CORE POWER: 23 MW**

Rod O.D., in.	0.310
Clad Thickness, in.	0.015
Pellet Diameter, in.	0.274
Fuel Density, % of T.D.	88.5
Pu/ (U + Pu), %	50
Active Fuel Height, in.	36
Insulator Pellet Height, in.	3/8
Reflector Pellet Height, in.	3-31/32
Gas Plenum Height, in.	15
Overall Fuel Rod Length, in.	
Rod P/D	1.23
Number of Rods per Bundle	61
Number of Fuel Rods per Bundle	61
Method of Rod Spacing	Wire Wrap
Wire Wrap Pitch, in.	6
Design Average Burnup, MWd/Te	50,000
Max. Linear Power:	
Average, kW/ft	6.97
Peak, kW/ft	11.02
Fuel Temperature:	
Nominal, °F	~3,500
Peak, °F	~4,000
Max. Clad Temperature:	
Nominal, °F	1,022
Peak, °F	1,112
Coolant Inlet Temperature	700
Coolant Outlet Temperature:	
Nominal, °F	958
Peak, °F	990
Max. Internal Gas Pressure, psi	1,490
Max. Coolant Flow Rate, lb/sec	16
Total Core Pressure Drop, psi	17

254



GEAP-13787

CLADDING o.d. 0.310 in.  
WALL THICKNESS 0.015 in.

**DIMENSION**

**MIN  
(in.)**

**MAX  
(in.)**

A

$45\frac{1}{2} + X$

$47 + X$

B

0

$1\frac{1}{2}$

Figure 4B3-3. Booster Fuel Rod, SEFOR Option III-A

Table 4B3-4

TEMPERATURE EFFECT OF FUEL ROD-CHANNEL CLEARANCE

Clearance In.	Maximum Cladding Temperature**			Maximum Gradient Across Rod*** °F
	Interior Rod °F	Edge Rod °F	Corner Rod °F	
0.015	1031	1058	1078	68
0.025	1023	1035	1047	38
0.033	1017	1019	1025	17
0.035	1017	1018	1020	17
0.038	1018	1019	1015	18
0.040	1019	1020	1014	22
0.045	1025	1022	1011	32
0.062	1031	1025	1009	61

\*No Reduction in wire diameter for edge rods.

\*\*Temperature is averaged over 60° segment.

\*\*\*Gradient is maximum difference between the six adjacent coolant cells around rod. Maximum occurs on corner rod on hot side for small clearances and on edge rod on cold side for large clearances.

Table 4B3-5

PEAK CLADDING TEMPERATURES

	Without Wire Wrap Effects		With Wire Wrap Effects	
	Core Midplane °F	Top of Core °F	Core Midplane °F	Top of Core °F
With Uncertainties				
Coolant	878	1050	878	1050
Clad O.D.	901	1060	998	1100
Clad Midwall	925	1070	1014	1106
Clad I.D.	949	1079	1030	1112
Nominal				
Coolant	850	995	850	995
Clad O.D.	872	1004	963	1042
Clad Midwall	894	1013	966	1047
Clad I.D.	894	1022	970	1053

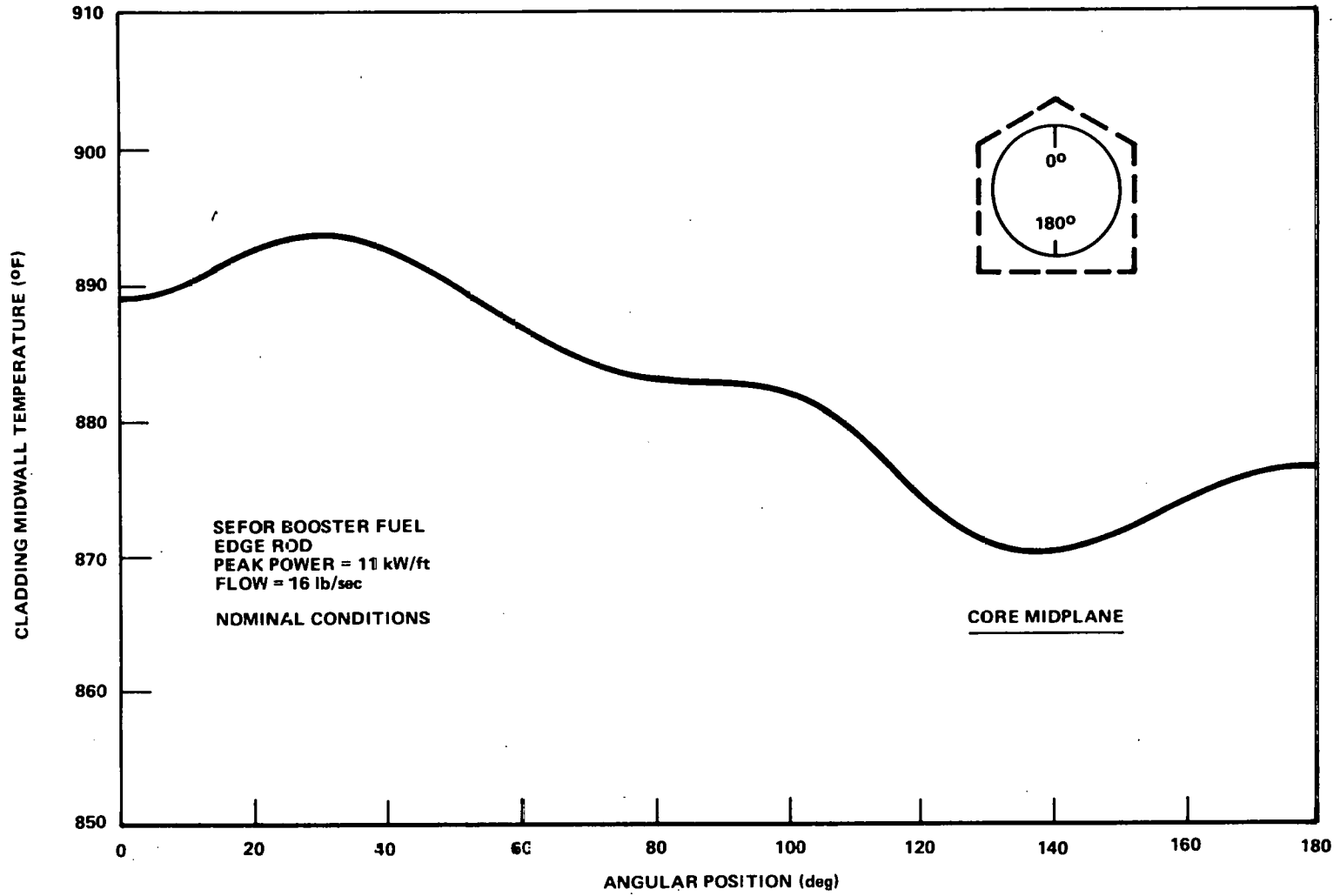


Figure 433-4. Circumferential Distribution of the Midwall Cladding Temperature in the Peak Rod at the Core Midplane

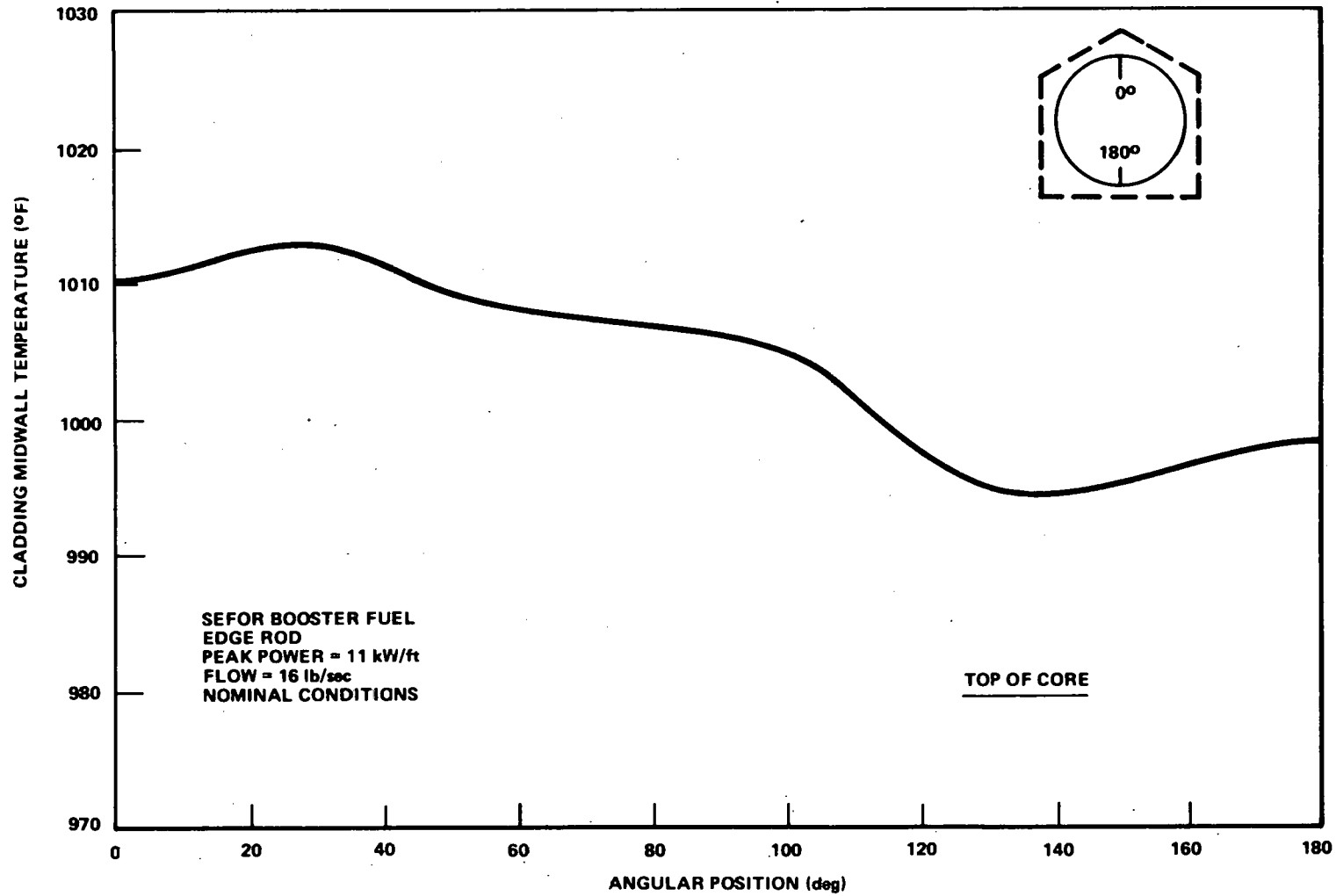


Figure 4B3-5. Circumferential Distribution of the Midwall Cladding Temperature in the Peak Rod at the Top of the Core



**4.2.3.9 Stress Analysis of the Booster Fuel Rod**

Two rod axial locations on the SEFOR peak booster fuel rod were considered for structural analysis. These were the core midplane (peak power region), and the core outlet (peak clad temperature region). These were analyzed for two fuel rod conditions, nominal and hot rod. The temperatures of the clad I.D. and O.D. at these points and for these conditions were calculated in the manner which has been previously discussed. They are shown in Table 4B3-4, Figure 4B3-3 for rod design.

The material properties came from Reference 7 except for the values of yield and ultimate stress which have been updated and are shown in Figure 4B3-9. This came from Reference 6. The SEFOR booster fuel has been designed for a total peak rod cumulative burnup of approximately 50,000 MWd/Te. In this preliminary report, the fuel was analyzed at only one point in time, 50,000 MWd/Te burnup, the end of life state.

The following conditions were considered for the stress study of the present SEFOR fuel rods:

- Fission gas pressure
- Fuel rod bending
- Radial heat flow
- Circumferential gradients
- Vibration
- Axial gradients
- Fuel-clad mechanical interaction

The following areas were not analyzed due to the preliminary nature of this task:

- Local spacer loads
- Local thermal stress (from spacer perturbation of the coolant flow)
- End and segmenting plug structural and/or thermal discontinuities
- Transient conditions

Because of the very preliminary nature of these calculations, no allowance has been made for irradiation induced creep or swelling. However, allowance for corrosion and/or fuel-clad chemical attack has been made.†

The criteria to which these stresses will be compared are shown in Table 4B3-12. They are from Reference

5.

*Fission Gas Pressures and Stresses*

The fission gas pressure at 50,000 MWd/Te burnup has been calculated versus plenum length for the range of temperature between 1,000°F and 1,200°F. The original SEFOR fuel specification on condensible and non-condensable gases has been assumed for the booster fuel. To convert the fission gas pressure into a hoop stress, the following equation is used:

$$\sigma_{\omega}^* = 2\sigma_z^* = \frac{DP}{2t}$$

where

- $\sigma_{\omega}$  = Hoop stress (psi)
- $\sigma_z$  = Axial stress (psi)
- D = Clad I.D. (in.)
- t = Clad thickness (in.)
- P = Fission gas pressure

Given the plenum temperature discussed in the previous section on thermal analysis, (and taking corrosion and chemical attack into account), then the pressures and stresses shown in Table 4B3-6 are predicted at 50,000 MWd/Te burnups.

† Includes effects of fuel-clad chemical attack, sodium corrosion, and an assumed defect of one mil.

\* Subscripts are defined

- $\omega$  = circumferential
- z = axial
- r = radial

*Thermal Stresses in Clad During Normal Operation*

There are three types of thermal stresses in the clad during normal operation: radial temperature gradient stress, local stresses (i.e., the self-equilibrating thermal stress due to a non-linear circumferential gradient), and the bending stress caused by restraint of the local stress. The radial temperature gradient stress is found from

$$\sigma_{\omega} = \sigma_z = \pm \frac{E\alpha \phi t}{2K(1-\mu) 12 \text{ in/ft}}$$

where

- $\sigma_{\omega}$  = Hoop stress (psi)
- $\sigma_z$  = Stress in z direction (psi)
- E = Young's Modulus (psi)
- $\alpha$  = Instantaneous coefficient of linear expansion (in/in<sup>°</sup>F)
- t = Clad thickness (in.)
- $\mu$  = Poisson's Ratio
- $\phi$  = Heat Flux (Btu/hr·ft·°F)
- K = Clad conductivity (Btu/hr·ft·°F)

The nominal peak power is 11.0 kW/ft for the booster fuel, hence  $\phi = 375,000 \text{ Btu/hr}\cdot\text{ft}^2$ ). The clad temperatures vary from 1000 to 1100<sup>°</sup>F for 316 stainless steel annealed.

		<b>1000<sup>°</sup>F</b>	<b>1100<sup>°</sup>F</b>
$\alpha$ (in/in·°F)	=	$11.39 \times 10^{-6}$	$11.61 \times 10^{-6}$
E (psi)	=	$23.0 \times 10^6$	$22.4 \times 10^6$
t (in.)	=	0.015	0.015
K(Btu/hr·ft·°F)	=	15.67	15.87
$\mu$	=	0.305	0.310
$\frac{E\alpha}{24K(1-\mu)}$	=	1.002	0.9895

In order to simplify the calculations, the assumption was made that  $\frac{E\alpha}{24K(1-\mu)} = 0.995$  in the temperature range of interest. Therefore,  $\alpha_{\omega} = \alpha_z = \pm 5596 \text{ psi}$ .

At the core outlet, the value of  $\phi$  is  $\sim 0.4\phi_c$  (Ref 12). Therefore,  $\alpha_{\omega} = \alpha_z = \pm 2560 \text{ psi}$ .

The hot rod was assumed to generate power at 1.0683 times the nominal rod, therefore

$$\alpha_{\omega} = \alpha_z \text{ (mid-core)} = \pm 6916 \text{ psi}$$

$$\alpha_{\omega} = \alpha_z \text{ (end of core)} = \pm 2766 \text{ psi}$$

These stresses are negative on the clad I.D. and positive on the clad O.D. and act in both the longitudinal and circumferential directions.

The local (self-equilibrating thermal stresses) and bending stresses were calculated by the fitting of a Fourier series to the clad mid-thickness temperature distribution to obtain the zero-th and first harmonic of distribution. Subtracting the zero-th harmonic (or average temperature) leaves the temperature distribution associated with the thermal stresses when thermal curvature is suppressed along the full length of the rod by an applied or restraining bending moment. Further subtracting the first harmonic temperature component determines the temperature distribution which causes the self-equilibrating thermal stresses. The results of this analysis are in Table 4B3-7. These stresses occur throughout the clad with the given sign.

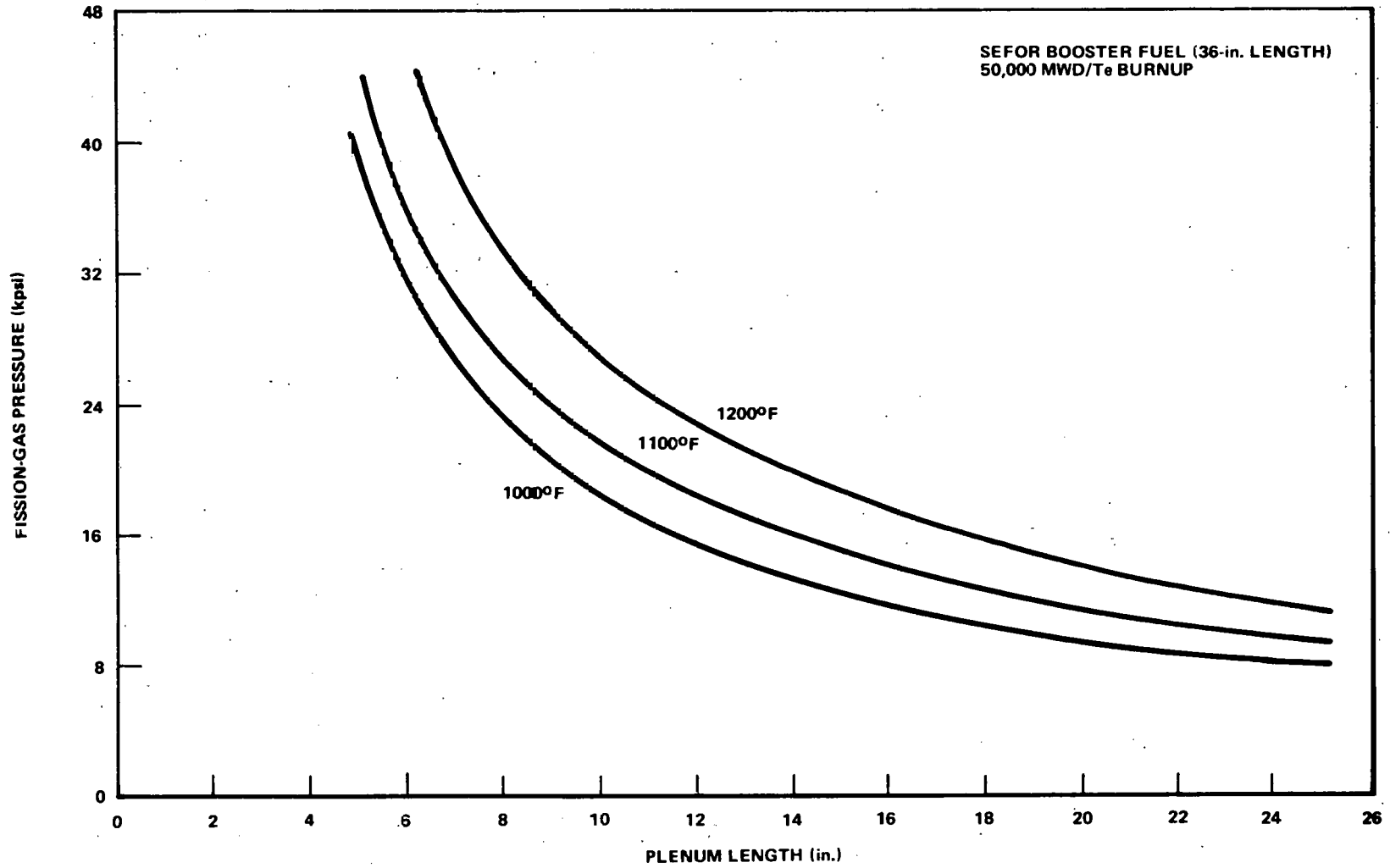


Figure 4B3-6. Fission Gas Pressure versus Plenum Length, 36-inch SEFOR Booster Fuel Rods

Table 4B3-6

**FISSION GAS PRESSURE AND STRESS VS. PLENUM LENGTH  
(50,000 MWd/Te Burnup)**

**Nominal Peak Cladding Temperature  
(1053°F)**

Plenum Length	5	10	15	20
Fission Gas Pressure	4,047	2,023	1,349	1,011
*Circumferential Stress	40,782	20,391	13,594	10,195
*Longitudinal Stress	20,391	10,195	6,797	5,097
†Radial Stress	-4,047	-2,023	-1,349	-1,011

**Hot Spot Peak Cladding Temperature  
(1112°F)**

Plenum Length	5	10	15	20
Fission Gas Pressure	4,479	2,239	1,493	1,119
*Circumferential Stress	48,150	24,075	16,050	12,037
†Longitudinal Stress	24,075	12,037	8,025	6,018
†Radial Stress	-4,479	-2,239	-1,493	-1,119

\*Occur throughout the clad

†Negative of fission gas pressure at clad I.D. and going to zero at the clad O.D.

Table 4B3-7

**LOCAL AND SELF-EQUILIBRATING THERMAL STRESSES†**

	Local Stress	Bending Stress	Local and Bending Stress
Core Midplane			
Max.	1028	2126	3154
Nominal			
Min.	-777	-2403	-3181
Hot Spot*			
Max.	1207	2498	3705
Min.	-912	-2823	-3737
Core Outlet			
Max.	1090	1486	2576
Nominal			
Min.	-436	-2002	-2439
Hot Spot*			
Max.	1280	1746	3026
Min.	-512	-2352	-2865

\*Hot Spot assumes to be 1.10 (flow decrease) x 1.068, (Power Increase = 1.175) greater than nominal.

†These stresses occur throughout the clad with the given sign.

*Vibration*

Vibration of fuel rods is caused by the turbulent fluid motion as it passes through the fuel assembly. This fluid turbulence tends to be damped as the flow proceeds through the assembly. Vibrational loads and stresses were computed using two different parallel flow induced vibration correlations. The two, that of Chen (Ref. 9) and of Reavis (Ref. 8), both indicate negligible stresses ( $\leq 50$  psi) due to fuel rod vibration induced by parallel flow.

*Axial Gradients*

The clad sustains a radial growth due to thermal expansion and irradiation induced swelling, both of which have non-linear axial distributions. At the lower end of the core these expansions tend to reinforce each other while at the upper end of the core the expansions tend to counteract in the axial direction. The result is a non-linear radial deflection of the clad which results in an axial bending stress.

Stress resulting from this distortion is essentially a thermal stress. These stresses have been calculated to be  $\leq 10$  psi and are thus negligible.

*Fuel-Clad Mechanical Interaction*

During the lifetime of the fuel both the clad and fuel swell. The clad swelling is a function of temperature and of fluence to a power while the fuel swelling is assumed to be a linear function of burnup (Ref. 11). The General Electric LMFBR Demonstration Plant Fuel has a peak rod burnup of  $> 100,000$  MWd/Te. The 0.220-inch diameter fuel pellet has a 5 mil diametral gap to prevent fuel-clad mechanical interaction. By comparison, the SEFOR booster pellets are 0.280-inch diameter with a 6-mil diametral gap. Considering the fact that the booster fuel will run at considerably lower fuel rod linear power and has a lower pellet theoretical density, it is likely that the booster fuel rods, like the GE Demo Plant rods, will not suffer fuel-clad mechanical interaction. This assumption should be verified by analysis with a fuel modeling code such as LIFE or BEHAVE.

**4.2.3.10 Combined Stresses**

A summary of individual steady-state stresses is tabulated in Tables 4B3-9, -10, -11. Tables 4B3-9, -10, -11 show the longitudinal, radial, and hoop stresses for the booster fuel rod in the nominal position and the hot rod position for both midcore and core outlet. All fission gas induced stresses (and creep rupture damage fraction) have been calculated using the SEFOR specification limit on entrained gases and moisture in the fuel.

The present design criteria shown in Table 4B3-1 has two material categories, ductile and quasi-brittle. A material is assumed to go from ductile to quasi-brittle when the total elongation of the material decreases to 10% (which is mostly due to irradiation effects). Materials irradiated sufficiently to have total elongation below 10% are termed "quasi-brittle", and those with elongations above this, "ductile". For 316 stainless steel annealed Reference 10 lists  $5.0-8.5 \times 10^{21}$  nvt  $> 0.1$  MeV as the fast fluence needed to reduce total elongation to 10% for temperatures of  $\sim 1100^\circ\text{F}$ . The SEFOR booster fuel peak rod fluence will exceed this amount approximately 1/2 way through its life (i.e.,  $\sim 4,000$  MWd/Te Burnup). Therefore, the peak burnup SEFOR fuel rod (at core midplane) should be considered ductile until the cumulative peak rod burnup surpasses 4000 MWd/Te. The core outlet operates at 0.46 power of the core midplane. Therefore, the upper plenum should remain ductile through operation to approximately 8000 MWd/Te cumulative peak rod burnup. Thus, from Table XIV and the above the following criteria will be used:

Stress Type	Criteria Burnup $> 8000$ MWd/Te
Primary Membrane - $P_M$	$0.67 \sigma_Y, 0.33 \sigma_U$
$P_M + \text{Primary Bending} - P_B$	$1.0 \sigma_Y, 0.5 \sigma_U$
$P_M + P_B + \text{Secondary}$	$1.0 \sigma_Y, 0.5 \sigma_U$

Also to be included with the above primary stresses is the criterion that the stress intensity must be less than 0.8 that stress necessary to cause rupture.

The material properties used with the above criteria come from Reference 6 and are shown in Figure 4B3-8. Figure 4B3-9 is the unirradiated properties from Figure 4B3-8 along with the associated error band. Figure 4B3-10 is the irradiated properties from Figure 4B3-8 having a fluence  $> 4.0 \times 10^{21}$  nvt  $> 0.1$  MeV. The fact that the criteria are to be applied conservatively, and according to standard ASME practice, the lower band (est. to be 95% confidence) is used for each material property. For the unirradiated properties, at 1100°F, 0.9 of the yield strength is 13,500 psi and 0.5 the ultimate strength is 26,500 psi. Therefore, for the ductile category the yield strength is limiting (assuming creep rupture is not). For the irradiated properties 0.67, the yield strength is 22,000 psi and 0.33 the ultimate strength is 17,000 psi. Therefore, the ultimate strength is limiting in the quasi-brittle category (again assuming the creep rupture is not). The 0.8 of the creep rupture stress was calculated for 50,000 MWd/Te for various plenum lengths versus temperature and is shown in Figure 4B3-7.\* From Figure 4B3-7 for the peak temperature of the hot rod case (1112°F) a plenum length of  $\sim 11$ -12 inches is needed to satisfy the creep rupture criteria. Therefore, if the plenum is at least 12 inches long, creep rupture is not limiting at operation out to 50,000 MWd/Te. The present limiting stresses are then:

**Hot Rod Limiting Stress**

**Criteria (psi)  
( $> 8000$  MWd/Te Burnup)**

Stress Type	Core Midplane (1030°F)	Core Outlet (1112°F)
Primary Membrane – P <sub>M</sub>	21,000	17,000
P <sub>M</sub> + Primary Bending – P <sub>M</sub> + P <sub>B</sub>	31,500	25,500
P <sub>M</sub> + P <sub>B</sub> + Secondary Stresses – P <sub>M</sub> + P <sub>B</sub> + S	31,500	25,500

In this analysis all stresses, other than fission gas pressure induced, were thermal in origin and hence secondary. There were no primary bending stresses considered in this analysis. With the present criteria, principal stresses in each direction are combined using the maximum shear theory of failure. This theory is defined by the ASME Code for Nuclear Vessels (Section III) in terms of principal stresses and states that the maximum algebraic difference between principal stresses is the stress intensity. Part I of the criteria deals with primary stresses. The higher temperature, and thus lower stress limits, of the core outlet make the core outlet critical for fission gas pressures. The principal pressure stresses, the combined primary stress intensity and the criterial limits for primary membrane stresses for the hot rod are shown in Table 4B3-8 versus plenum length. Note that with a plenum length of 15 inches, the stress intensity only slightly exceeds the criteria. Considering the fact that at 50,000 MWd/Te burnup the fluence is 15 times that of Figure 4B3-8, an increase in the UTS above that shown in the figure is to be expected. Such an increase will allow a 15-inch plenum design to meet the criteria for a hot rod core.

The second part of the criteria deals with primary membrane plus primary bending stresses. In this analysis, it was assumed that no primary bending stress exists. Therefore, part two does not apply. Part three is primary membrane plus primary bending plus secondary stresses. The stress intensity of the principal stresses involving these types of stresses must be less than the yield stress and/or one half the ultimate stress. The individual stresses from Tables 4B3-9, -10, and -11 (which assume a 15-inch plenum, 50,000 MWd/Te burnup) are combined into principal stresses in Table 4B3-12. Also Table 4B3-12 combines the principal stresses into a maximum stress intensity and compares it to the criteria. The criteria is not exceeded under the conditions examined at any position on the rod.

The conclusions to be drawn from the above steady-state stress analysis are:

- a. Possibly too conservative if the lowest possible value of material mechanical properties are used.
- b. A 15-inch plenum on the booster fuel rods should insure their meeting of all structural criteria at a burnup of 50,000 MWd/Te with the reactor operating at full power (23 MWt).

\* Assumes reactor operates at 23 MW power.

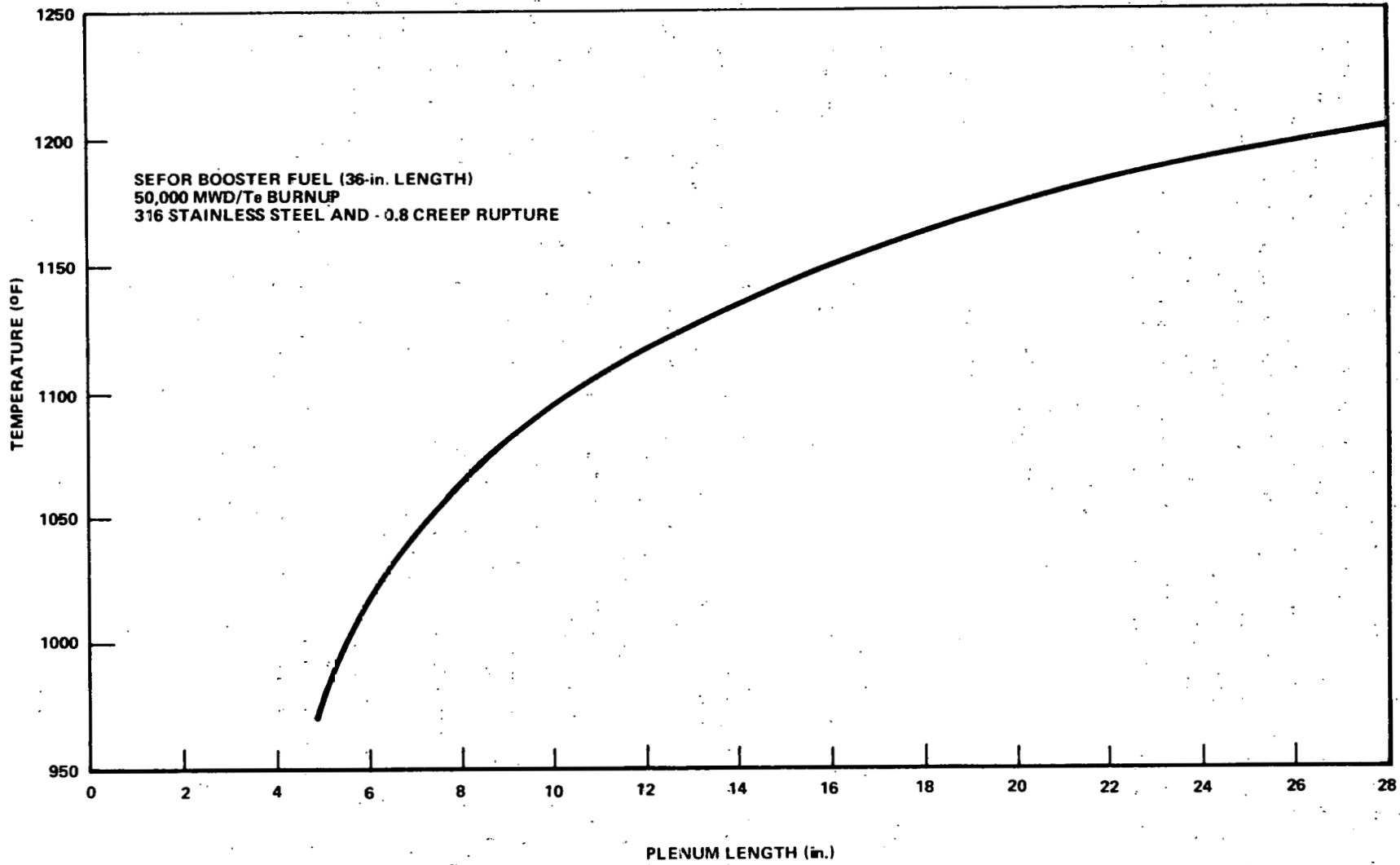


Figure 4B3-7. Plenum Length versus Temperature, 36-inch SEFOR Booster Fuel Rods

Table 4B3-8

PRIMARY MEMBRANE STRESSES  
(HOT SPOT ROD AT CLAD I.D. FOR 50,000 MWd/Te BURNUP)

Stress	Plenum Length (in.)			
	5	10	15	20
Principal Circumferential (psi)	48,150	24,075	16,050	12,037
Principal Longitudinal (psi)	24,075	12,037	8,025	6,018
Principal Radial (psi)	-4,479	-2,239	-1,493	-1,119
Maximum Stress Intensity (psi)	52,629	26,314	17,543	13,156
Limiting Criteria* (psi)	17,000	17,000	17,000	17,000

\*For fluences  $>0.4 \times 10^{22}$

Table 4B3-9

LONGITUDINAL STRESSES (psi)

	Pressure Stress*	Radial Gradient	Local and Bowing Stress**		Principal Stress	
			Max.	Min.	Max.	Min.
Peak Nominal Booster Rod End of Core						
Clad I.D.	6,797	-2,560	2,576	-2,439	6,813	1,798
Clad O.D.	6,797	2,560	2,576	2,439	11,933	6,918
Mid-Core						
Clad I.D.	6,797	-5,596	3,154	-3,181	4,355	-1,980
Clad O.D.	6,797	5,596	3,154	-3,181	15,547	9,212
Hot Spot Booster Rod End of Core						
Clad I.D.	8,025	-2,766	3,026	-2,865	8,285	2,394
Clad O.D.	8,025	2,766	3,026	-2,865	13,817	7,926
Mid-Core						
Clad I.D.	8,025	-6,916	3,705	-3,737	4,814	-2,628
Clad O.D.	8,025	6,916	3,705	-3,737	18,646	11,204

\* Assumes 15-inch plenum, 500,000 MWd/Te Burnup

\*\* Maximum is most positive sum of local and bowing stresses  
Minimum is most negative sum



Table 4B3-10

RADIAL STRESSES

	Pressure Stress*	Radial Gradient	Local and Bowing Stress**		Principal Stress	
			Max.	Min.	Max.	Min.
Peak Nominal Booster Rod						
End of Core						
Clad I.D.	-1,349	0	0	0	-1,349	-1,349
Clad O.D.	0	0	0	0	0	0
Mid-Core						
Clad I.D.	-1,349	0	0	0	-1,349	-1,349
Clad O.D.	0	0	0	0	0	0
Hot Spot Booster Rod						
End of Core						
Clad I.D.	-1,493	0	0	0	-1,493	-1,493
Clad O.D.	0	0	0	0	0	0
Mid-Core						
Clad I.D.	-1,493	0	0	0	-1,493	-1,493
Clad O.D.	0	0	0	0	0	0

\* Assumes 15-inch plenum, 50,000 MWd/Te Burnup

\*\* Maximum is most positive sum of local and bowing stresses  
Minimum is most negative sum

Table 4B3-11

CIRCUMFERENTIAL STRESSES

	Pressure Stress*	Radial Gradient	Local and Bowing Stress**		Principal Stress	
			Max.	Min.	Max.	Min.
Peak Nominal Booster Rod End of Core						
Clad I.D.	13,594	-2,560	0	0	11,034	11,034
Clad O.D.	13,594	2,560	0	0	16,154	16,154
Mid-Core						
Clad I.D.	13,554	-5,596	0	0	7,998	7,998
Clad O.D.	13,554	5,596	0	0	19,190	19,190
Hot Spot Booster Rod End of Core						
Clad I.D.	16,050	-2,766	0	0	13,284	13,284
Clad O.D.	16,050	2,766	0	0	18,816	18,816
Mid-Core						
Clad I.D.	16,050	-6,916	0	0	9,134	9,134
Clad O.D.	16,050	6,916	0	0	22,966	22,966

\* Assumes 15-inch plenum, 50,000 MWd/Te Burnup

\*\* Maximum is most positive sum of local and bowing stresses  
Minimum is most negative sum

Table 4B3-12

PRIMARY MEMBRANE & PRIMARY BENDING & SECONDARY – PRINCIPAL STRESSES\*

	Principal Circumferential Stress	Principal Radial Stress	Principal Longitudinal Stress		Maximum Stress Intensity <sup>†</sup>	Criteria Longitudinal Stress
			Max.	Min.		
<b>Peak Nominal Booster Rod</b>						
<b>End of Core</b>						
Clad I.D.	11,034	-1,349	6,813	1,798	12,383	25,500
Clad O.D.	16,154	0	11,933	6,918	16,154	25,500
<b>Mid-Core</b>						
Clad I.D.	7,998	-1,349	4,355	-1,988	9,978	31,500
Clad O.D.	19,190	0	15,547	9,212	19,190	31,500
<b>Hot Spot Booster Rod</b>						
<b>End of Core</b>						
Clad I.D.	13,284	-1,493	8,285	2,394	14,777	25,500
Clad O.D.	18,816	0	13,817	7,926	18,816	25,500
<b>Mid-Core</b>						
Clad I.D.	9,134	-1,493	4,814	-2,628	11,762	31,500
Clad O.D.	22,966	0	18,646	11,204	22,966	31,500

\* Assumes 15-inch plenum, 50,000 MWd/Te Burnup

<sup>†</sup> Using the algebraic difference between principal stresses,  $\sigma_{Intensity} = \sigma_{Max. Principal} - \sigma_{Min. Principal}$

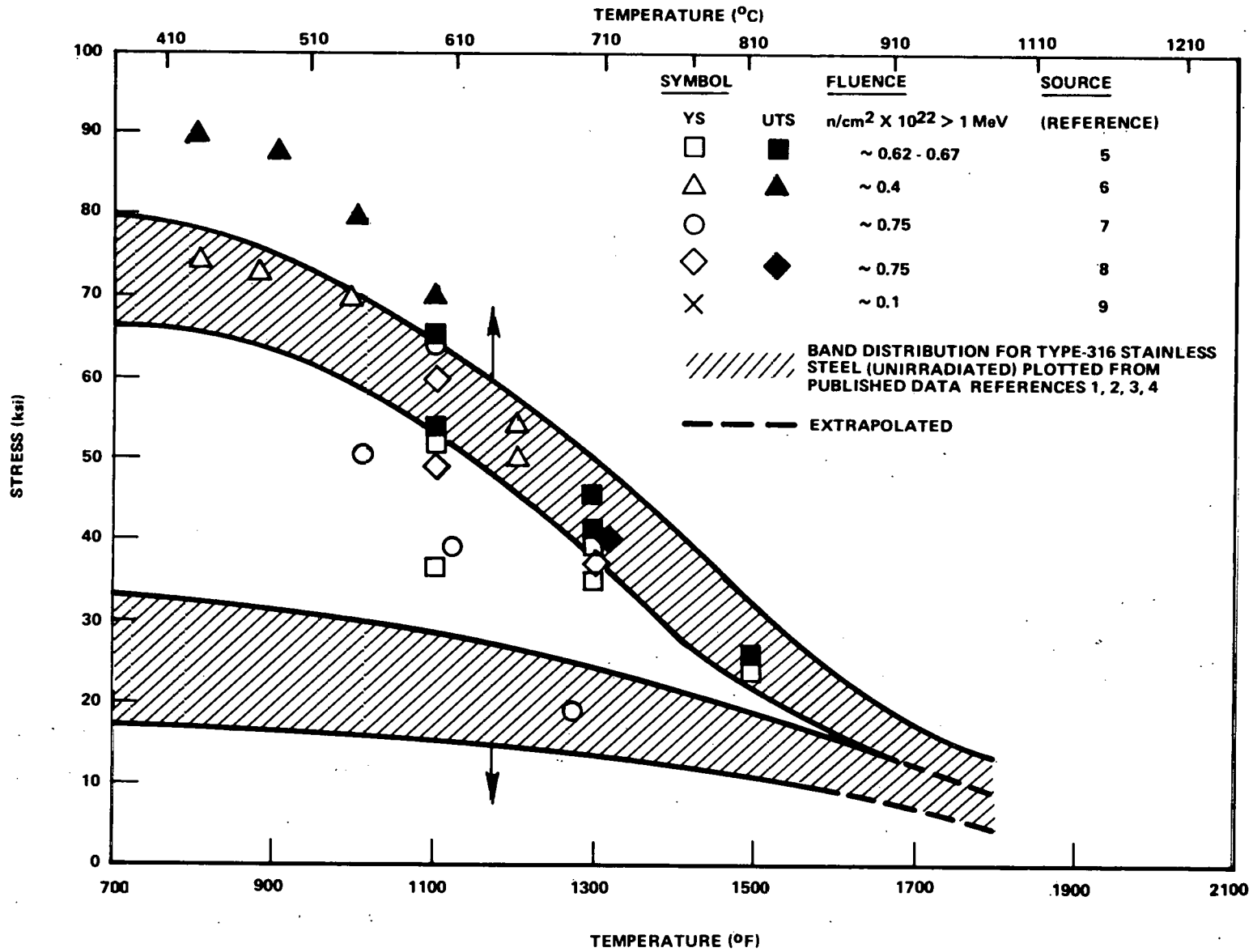


Figure 4B3-8. Effect of Irradiation on UTS and YS of 316 Stainless Steel

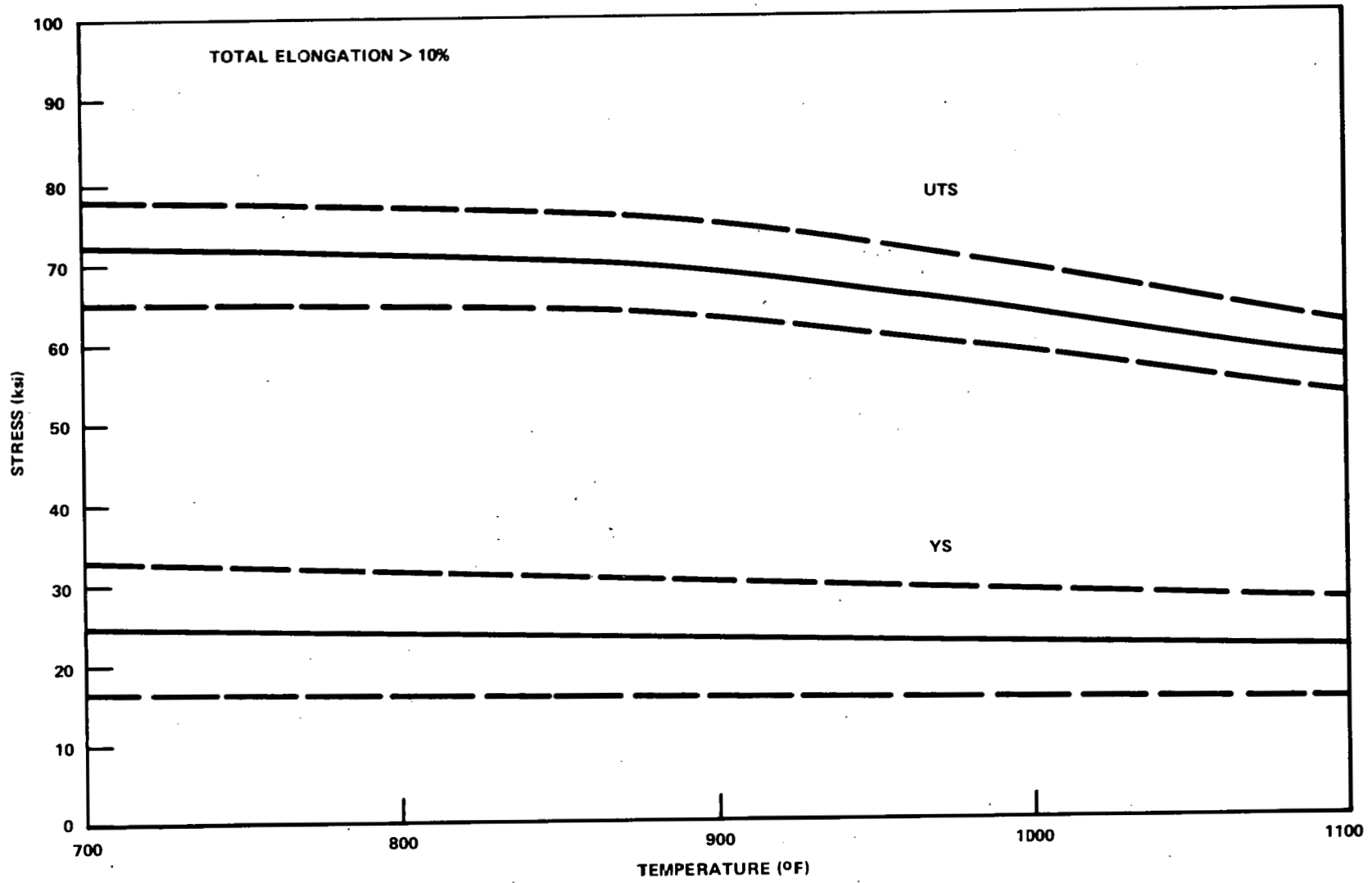


Figure 4B3-9. 316 SS UTS and YS Unirradiated Properties

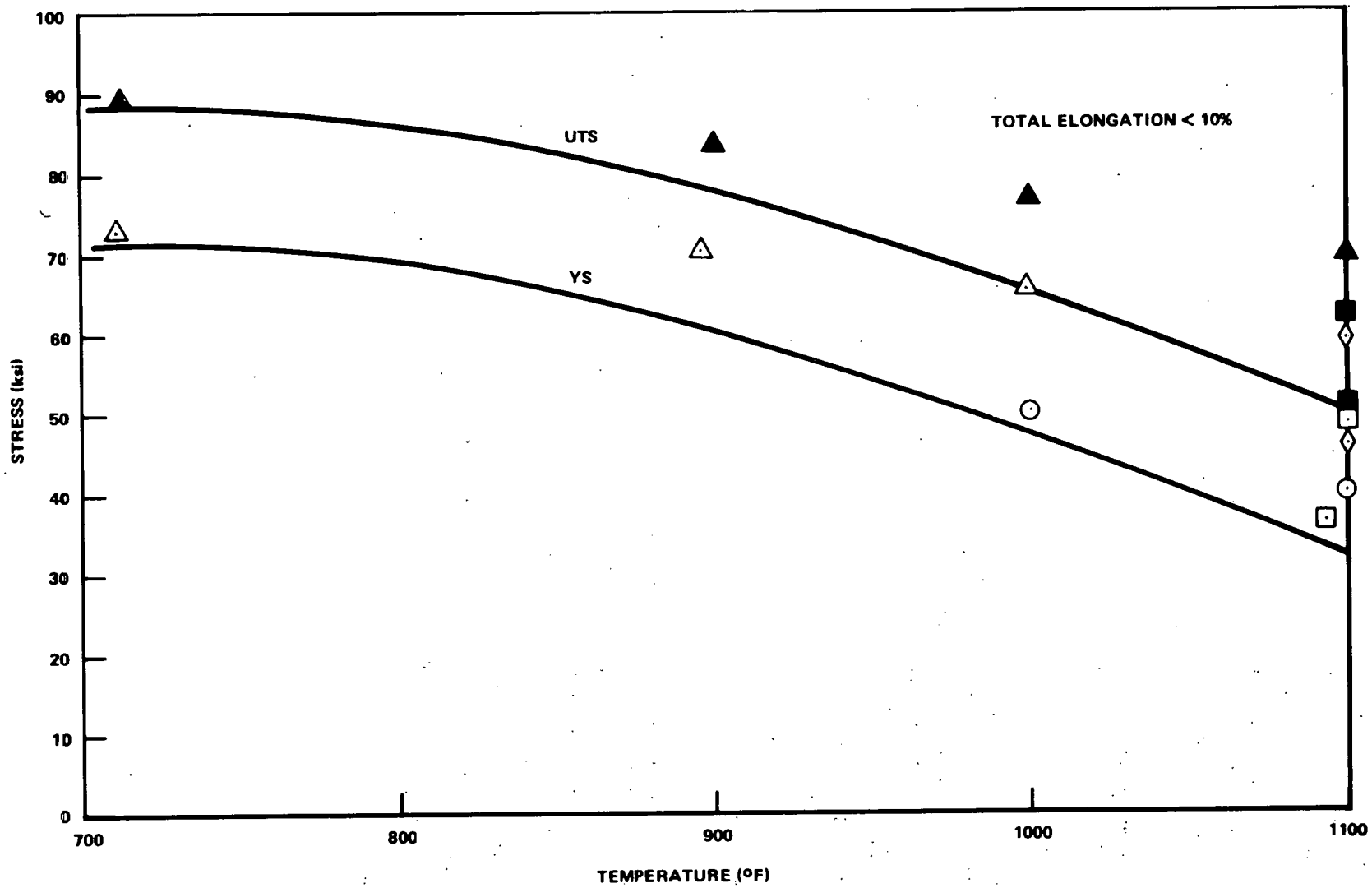


Figure 4B3-10. 316 SS UTS and YS Irradiated Properties, 0.4 to 0.75 X 10<sup>22</sup> nvt 7.1 MeV.

#### 4.2.3.11 Option III-A, Booster and Driver Fuel Assembly Design

A conceptual design for the Option III-A Booster and Driver Fuel has been developed. The basic concept involves inserting the fuel rods and the extension rods as a unit after the channel has been first inserted and then locked to the core plate. The fuel bundle consists of (61) 0.310-inch O.D. fuel rods. Thirteen of these rods act as tie rods which hold the bundle together. An adaptor joins the fuel bundle and the extension rod-tightening rod assembly. In order to minimize the costs of modification and production, several components from the existing design are incorporated into this conceptual proposal. These include (with minor modifications in some cases) the six extension rods, the tightening rod and tightening sleeve, the orifice piece and the channel-bellows seal assembly. A lock which locks the fuel assembly to the channel wall has been incorporated in the design. Preliminary analysis indicates that the increased pressure drop and flow rate through the fuel assembly will result in a net lifting force of approximately 220 lbf. on the assembly – hence, the need for the lock.

##### 4.2.3.11.1 Design Parameters

The conceptual design was developed using the following general parameters:

The existing core plate will be used.

The existing design for the orifice piece and the channel-bellows seal assembly will be used with the following exceptions:

- a. The inside walls of the channel must be clean (no side rods) and locking slots (for the fuel assembly-channel lock) will have to be machined into the sides.
- b. The orifice piece may have to be re-orificed.

All components will be of new manufacture.

A locking device, locking the fuel assembly to the channel is required.

In order to reduce development and manufacturing costs, as much of the existing design as possible should be incorporated into the new design.

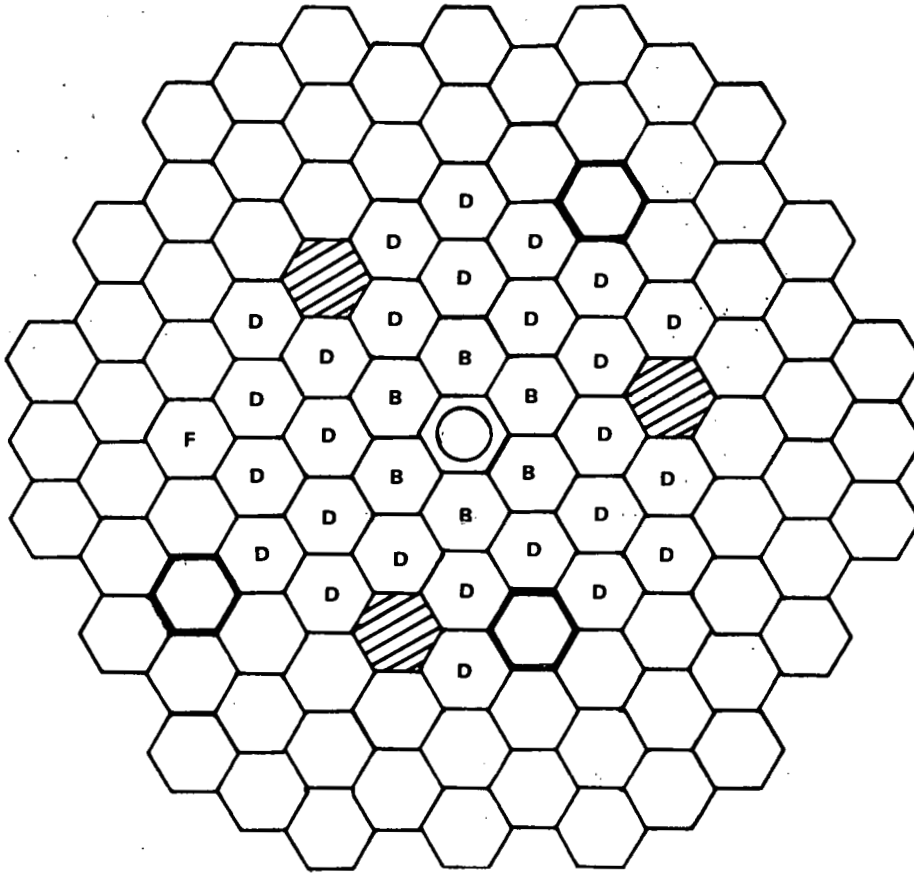
A positive mechanical interlock is needed to insure that the loading of the booster precedes the loading of the inner driver fuel.

##### 4.2.3.11.2 Conceptual Design

###### *Fuel Assembly*

The three core alternates being considered for Option III-A are shown in Figures 4B3-11 and 4B3-12. The fuel assemblies – both booster and driver – are comprised of a 61-rod fuel bundle joined through an adaptor to six upper extension rods and one tightening rod. The fuel bundle-extension rod assembly is loaded as a unit into its channel. The three-step loading sequence is illustrated in Figure 4B3-13. In step one, the channel and bellows-orifice assembly is positioned on the core plate and locked into place. In step two, the fuel assembly is inserted as a unit into the channel and lowered until it comes to rest on the orifice piece. In step three, the tightening rod is lowered four inches to the same height as the surrounding extension rods. This final lowering of the tightening rod accomplishes two things – a mechanical interlock connecting the fuel assembly to the channel is activated, and the extension rods become frictionally restrained between the channel and the tightening rod through spring loading.

An assembly drawing of the proposed fuel assembly is presented in Figure 4B3-14. The assembly will be described starting from the bottom and proceeding upwards. Detailed drawings of the various components appear on the following pages.








-  **BOOSTER**
-  **DRIVER**
-  **FRED**
-  **MOVABLE CONTROL**
-  **FIXED CONTROL**

Figure 4B3-11. Alternate Core Pattern I.



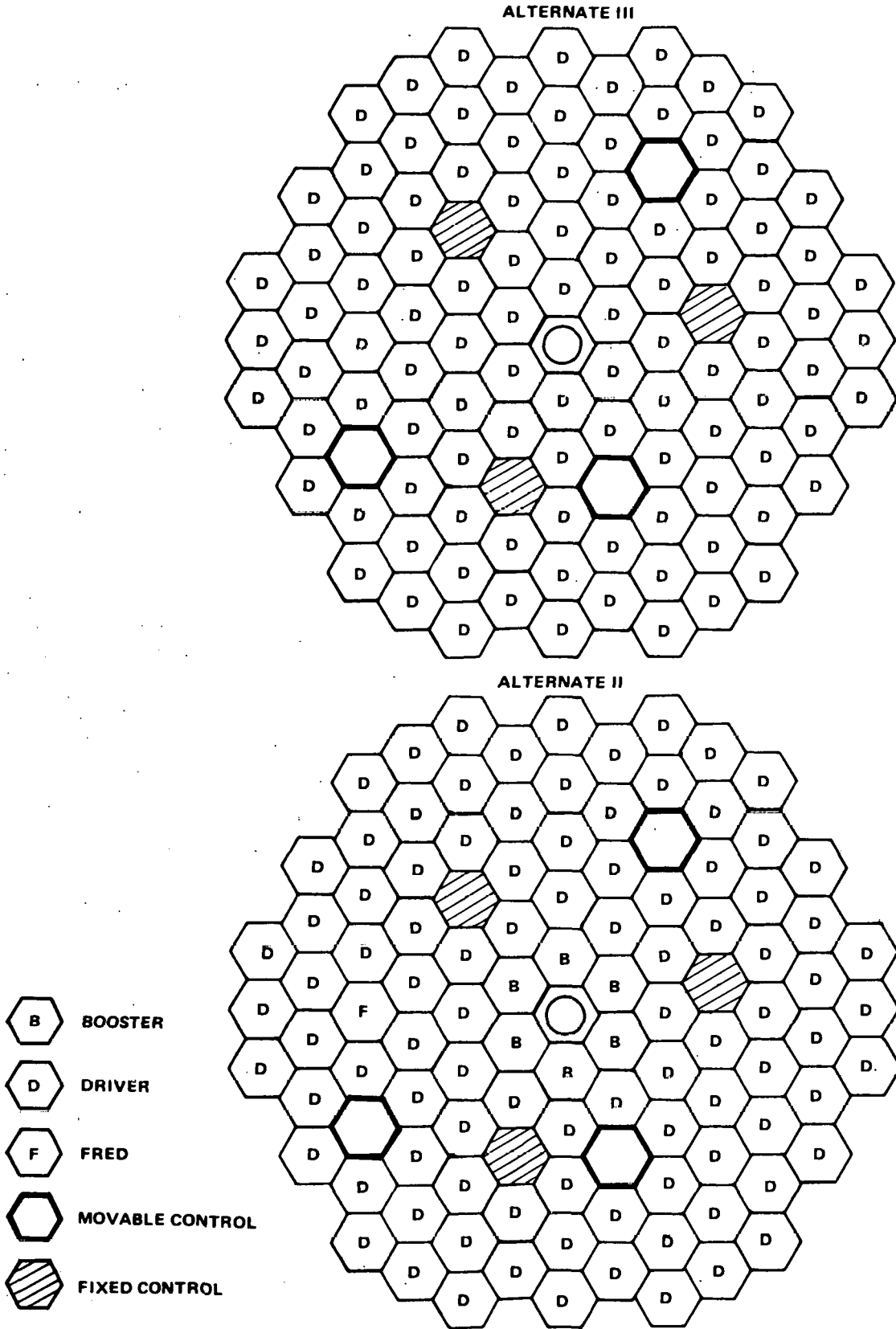


Figure 4B3-12. Alternate Core Patterns II and III

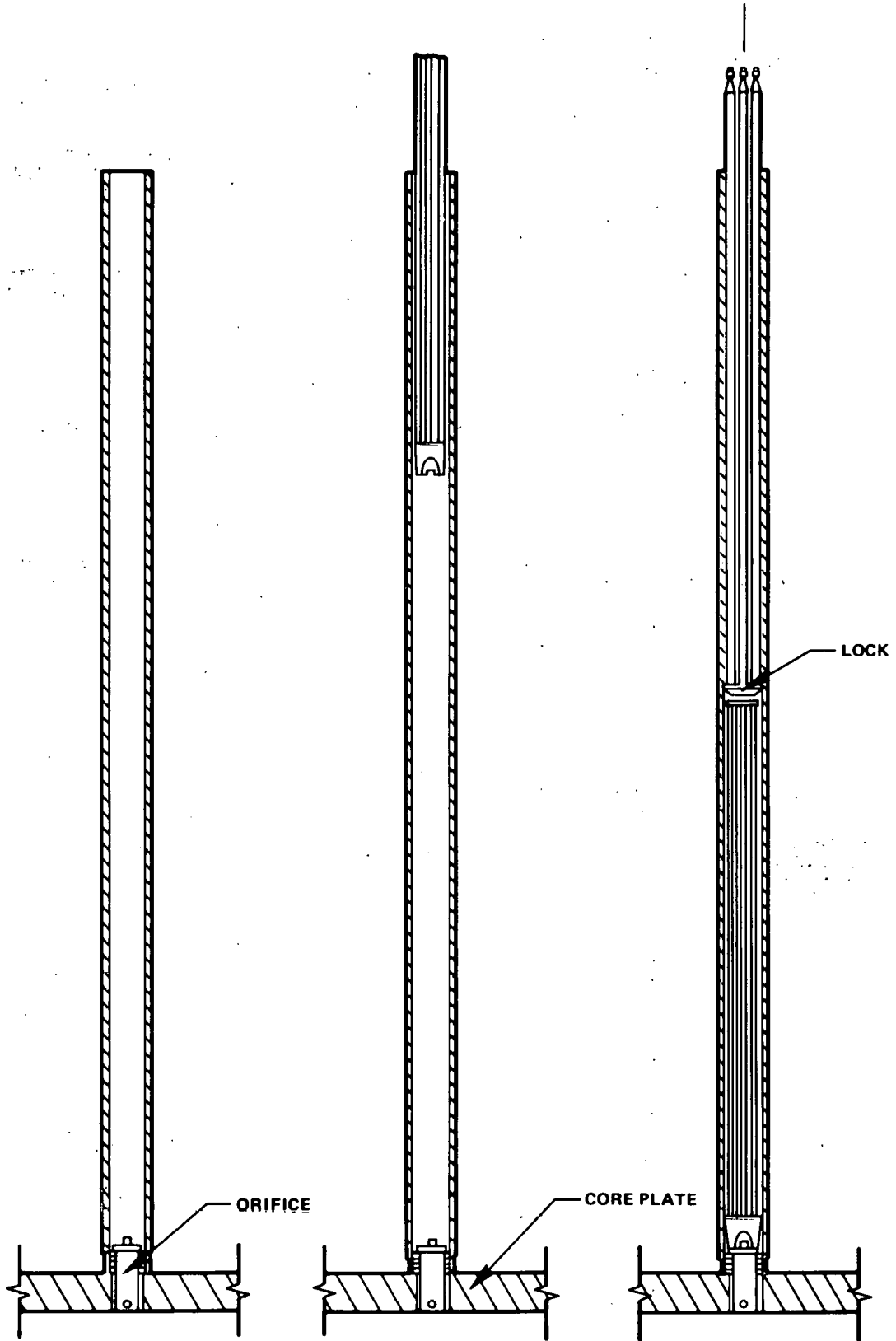


Figure 4B3-13. Fuel Loading Sequence

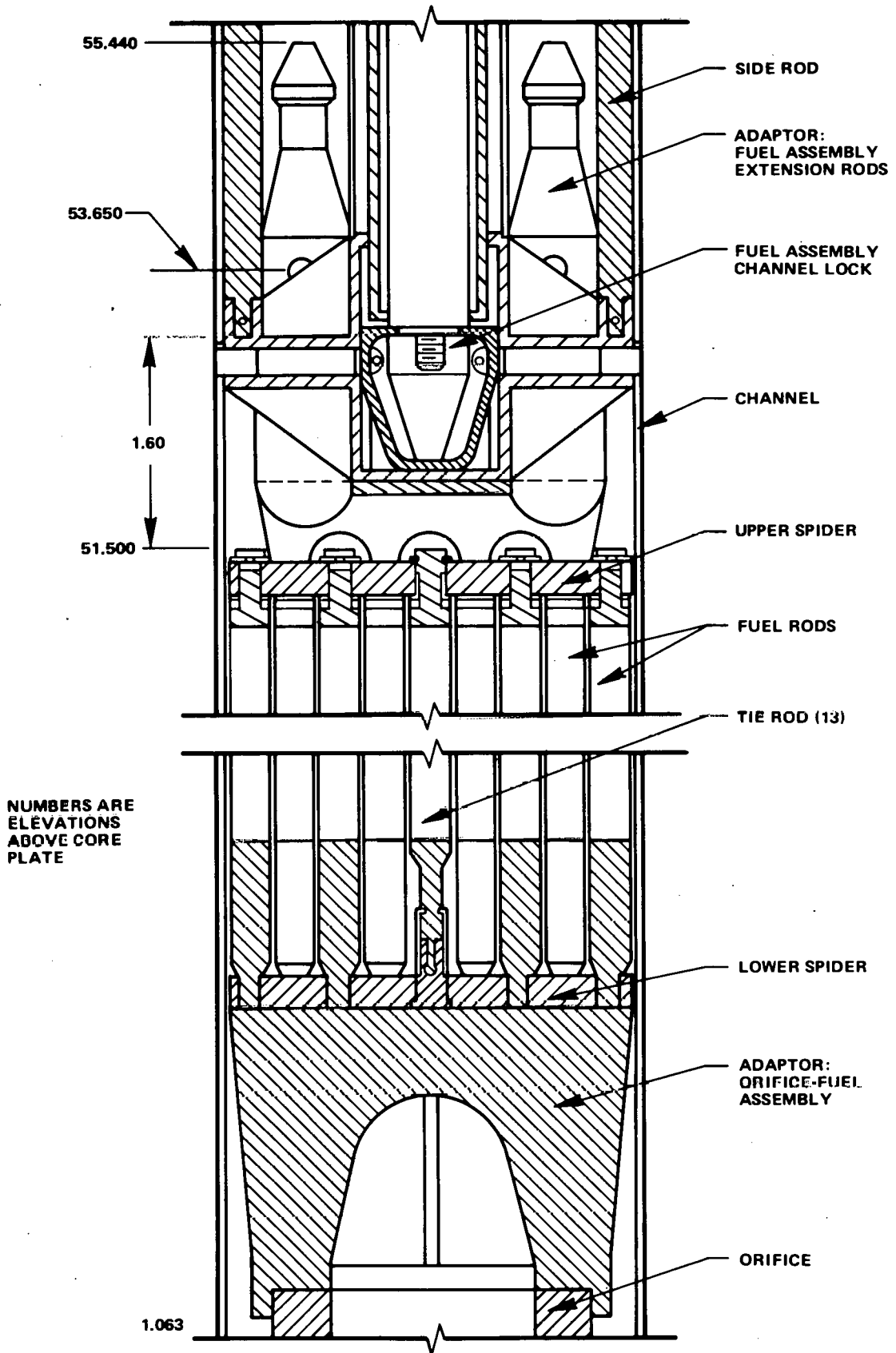
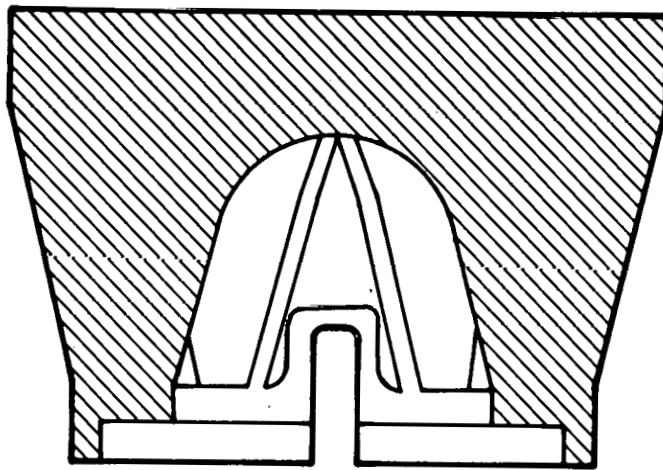
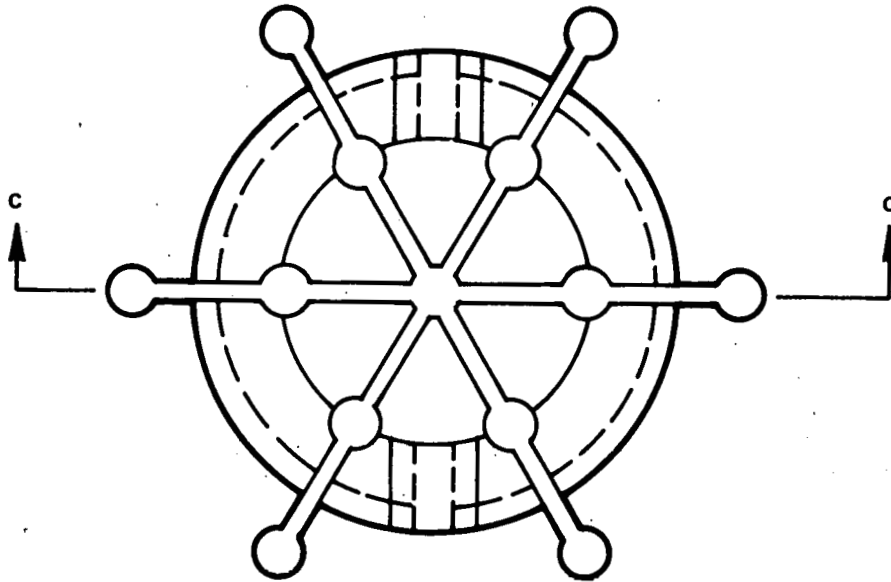
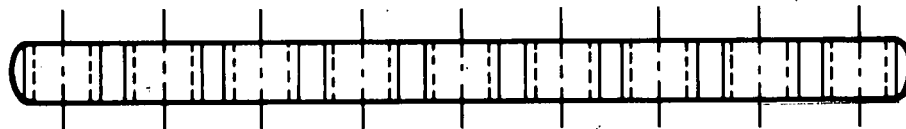
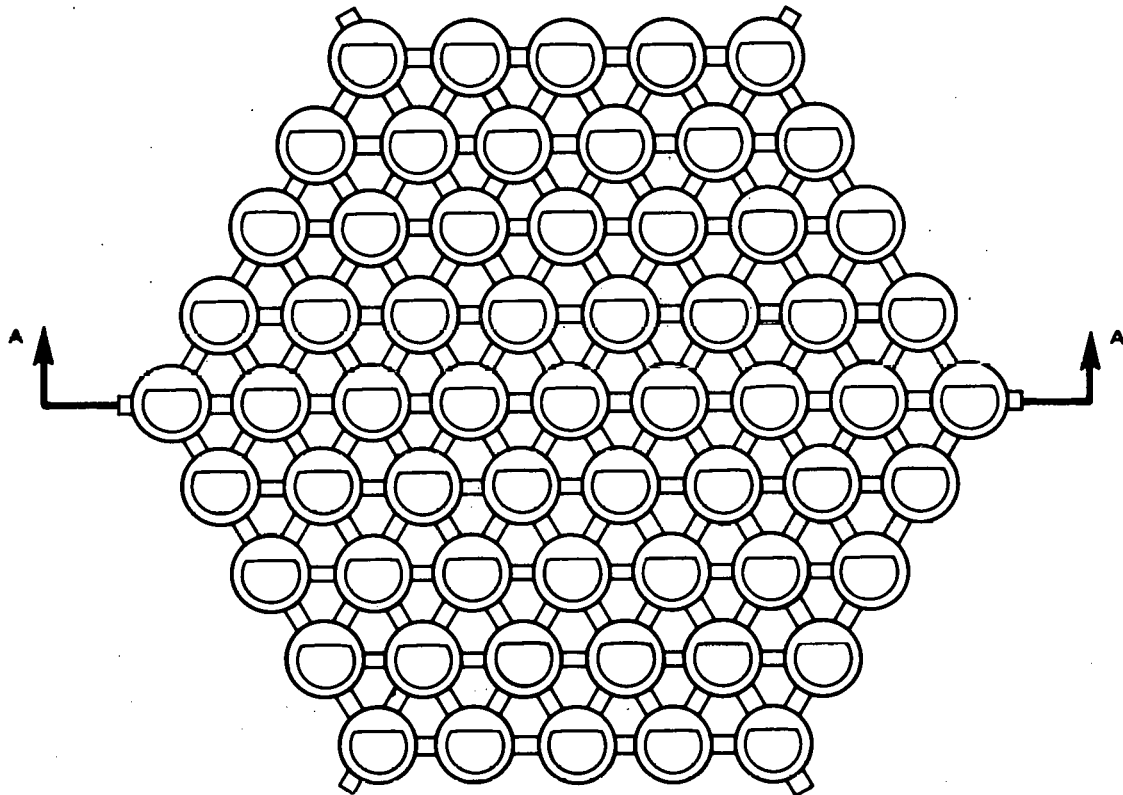


Figure 4B3-14. SEFOR Fuel Assembly Details



SECTION C-C

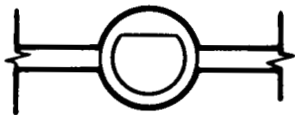
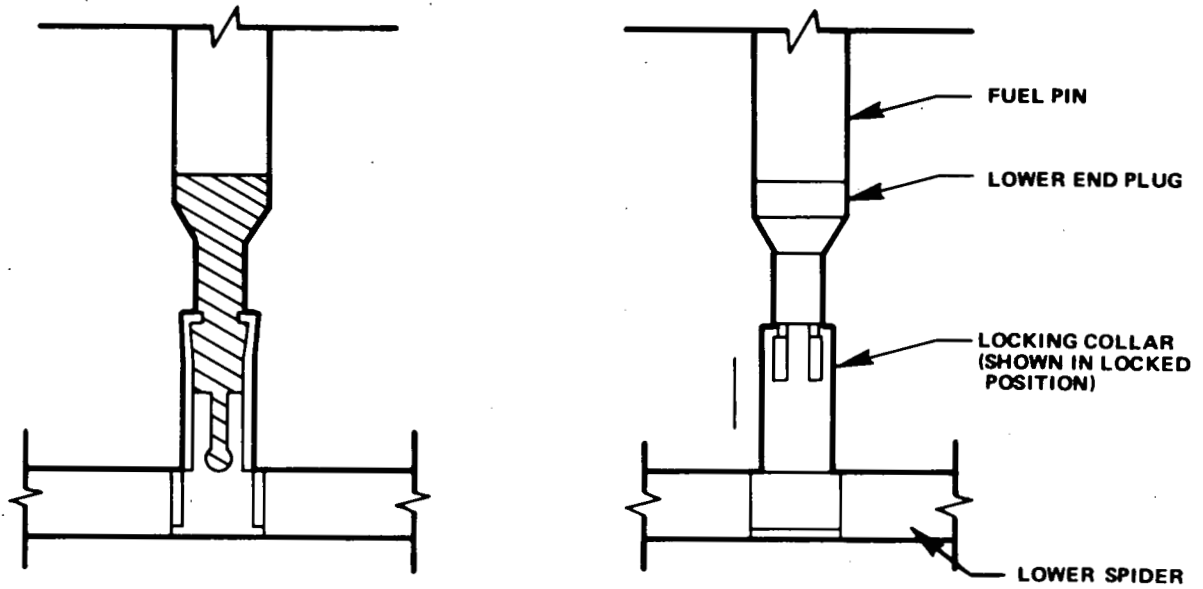
Figure 4B3-15. Fuel Assembly Orifice Adapter



SECTION A-A

**THE UPPER SPIDER IS IDENTICAL EXCEPT  
THE HOLES WHICH RECEIVE THE UPPER  
END PLUGS ARE CIRCULAR, NOT SEMICIRCULAR**

*Figure 4B3-16. Fuel Assembly Spider, Upper and Lower*



BOTTOM VIEW OF SUPPORT HOLE IN LOWER SPIDER

Figure 4B3-17. Aligned, Self-Centering Fuel Pin to Spider Connector

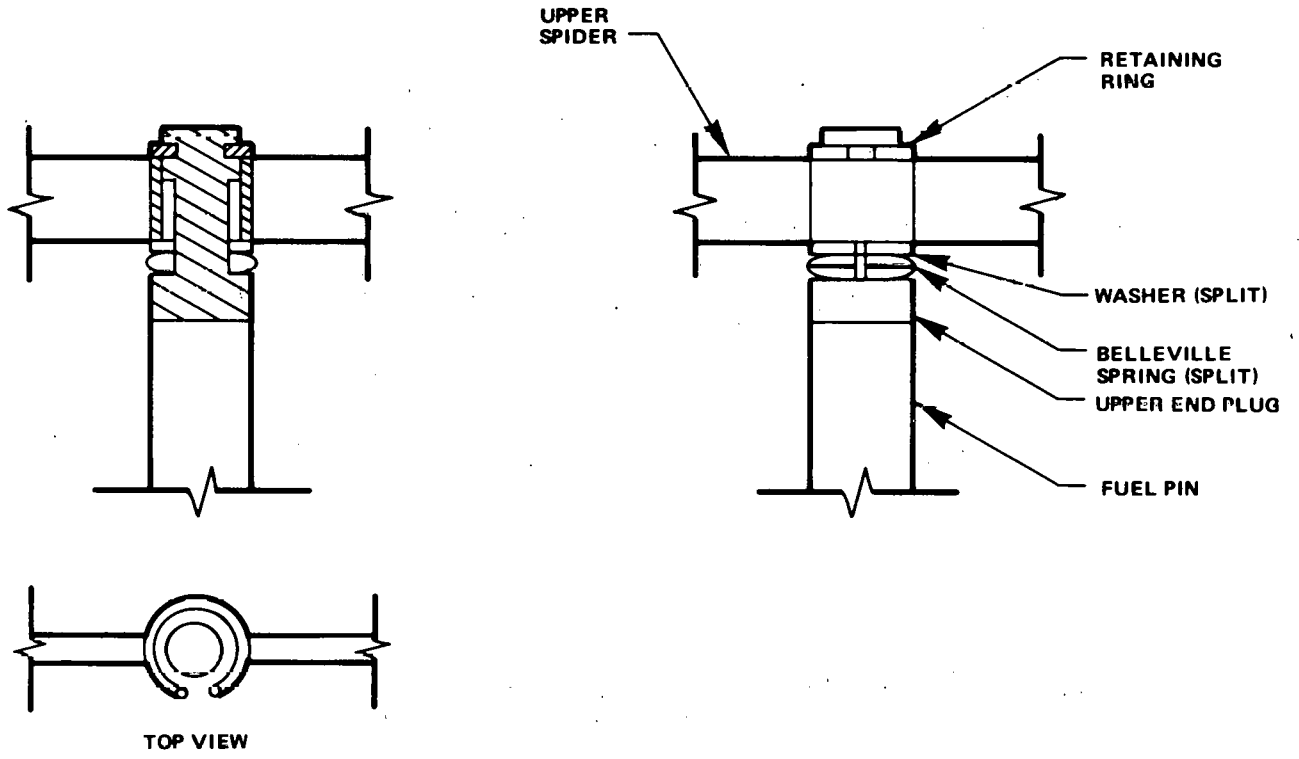


Figure 4B3-18. Self-Centering Fuel Pin Upper Spider

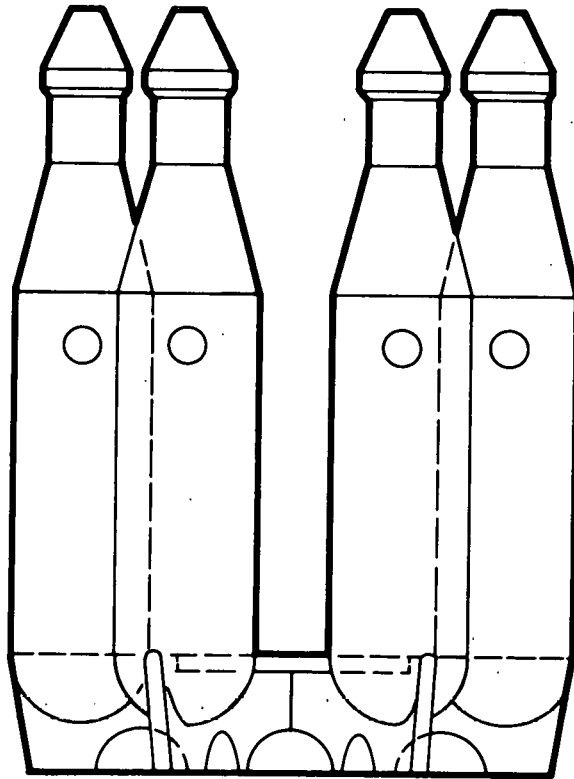
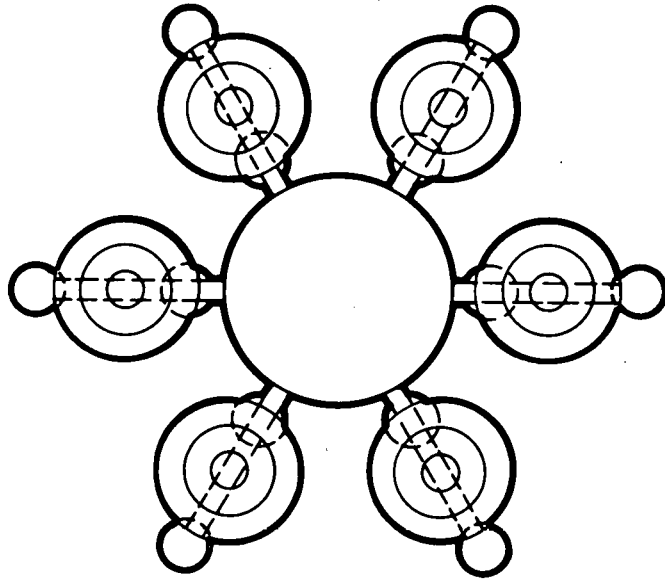
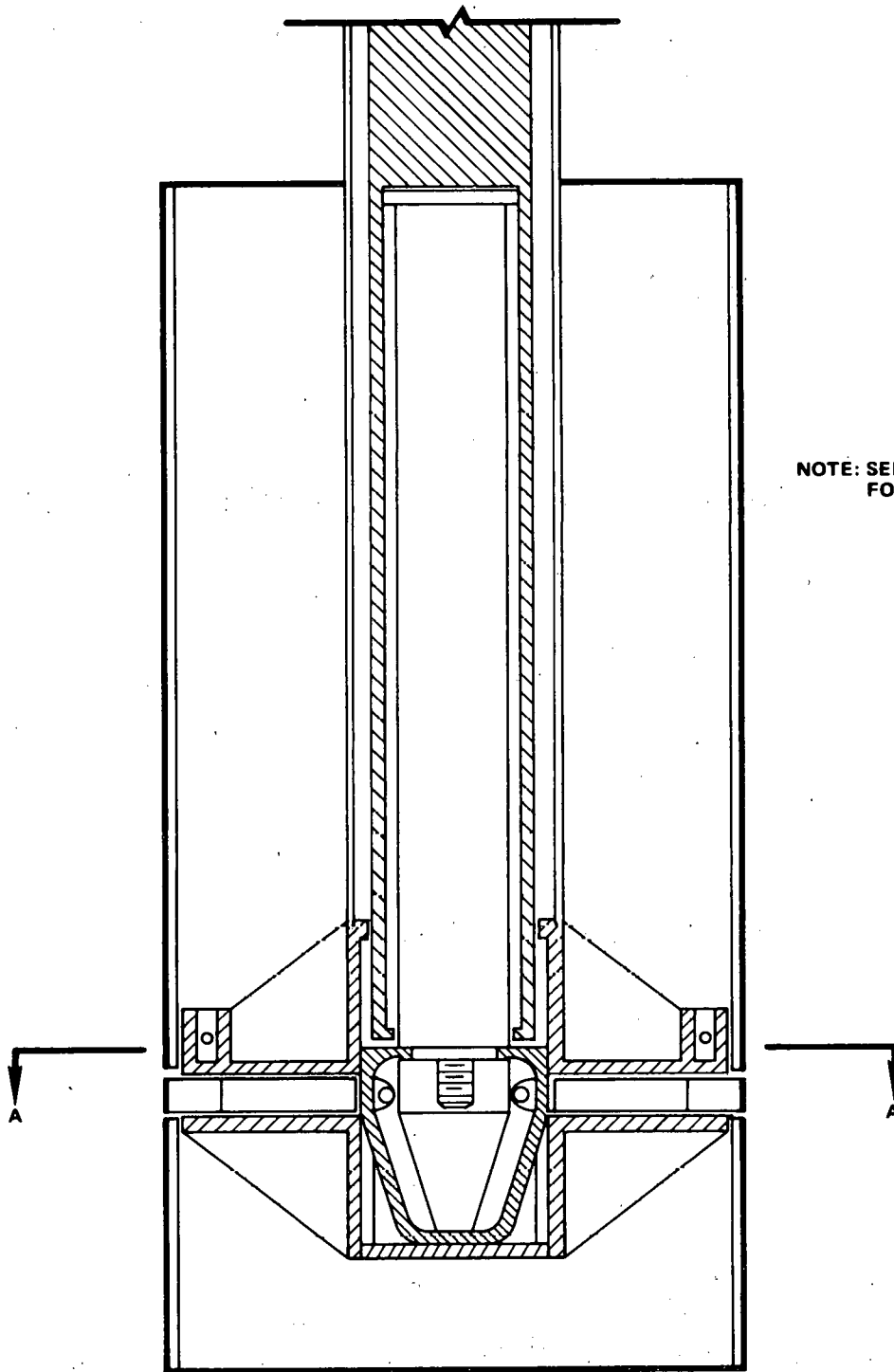


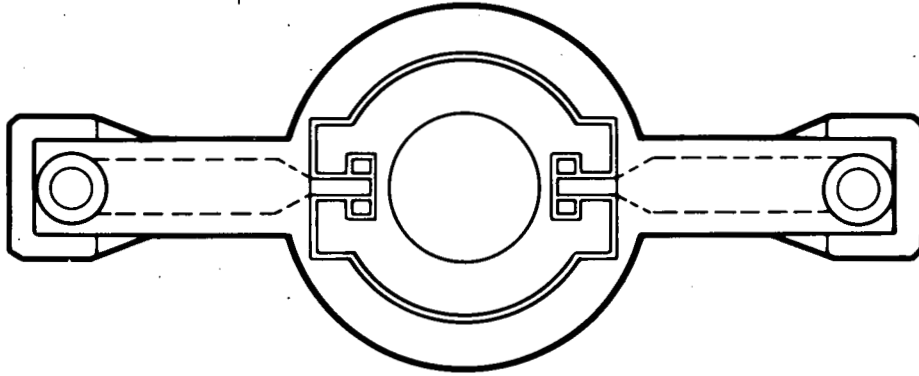
Figure 4B3-19. *Adaptor for Fuel Assemblies Incorporating Extension Rods*





NOTE: SEE FIGURE 4B3-21  
FOR SECTION A-A

Figure 4B3-20. Fuel Assembly Channel Lock



SECTION A-A (FROM FIGURE 4B3-20)

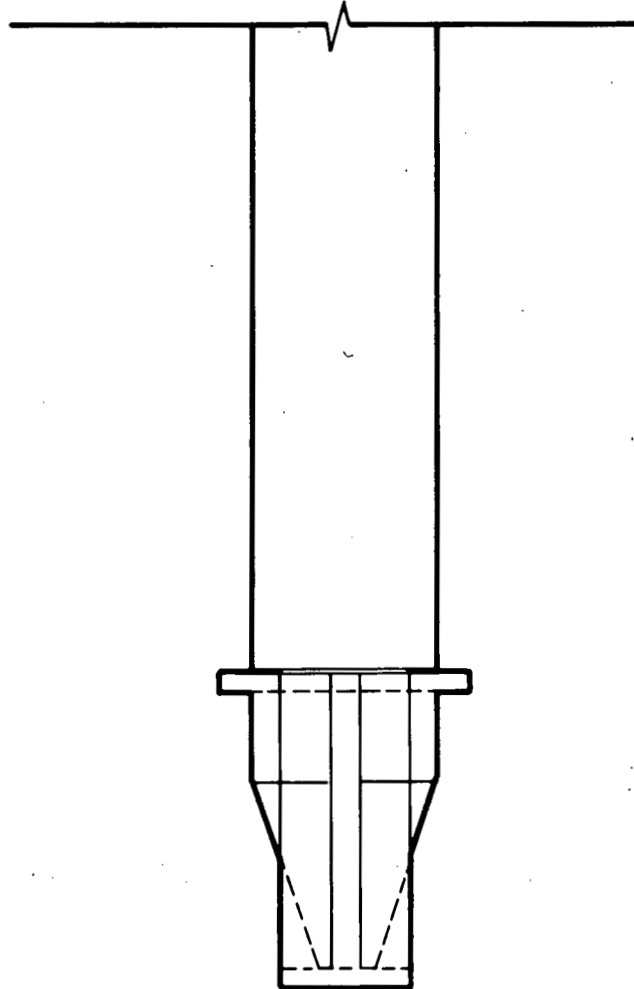


Figure 4B3-21. Lower End of Fuel Assembly Tightening Rod

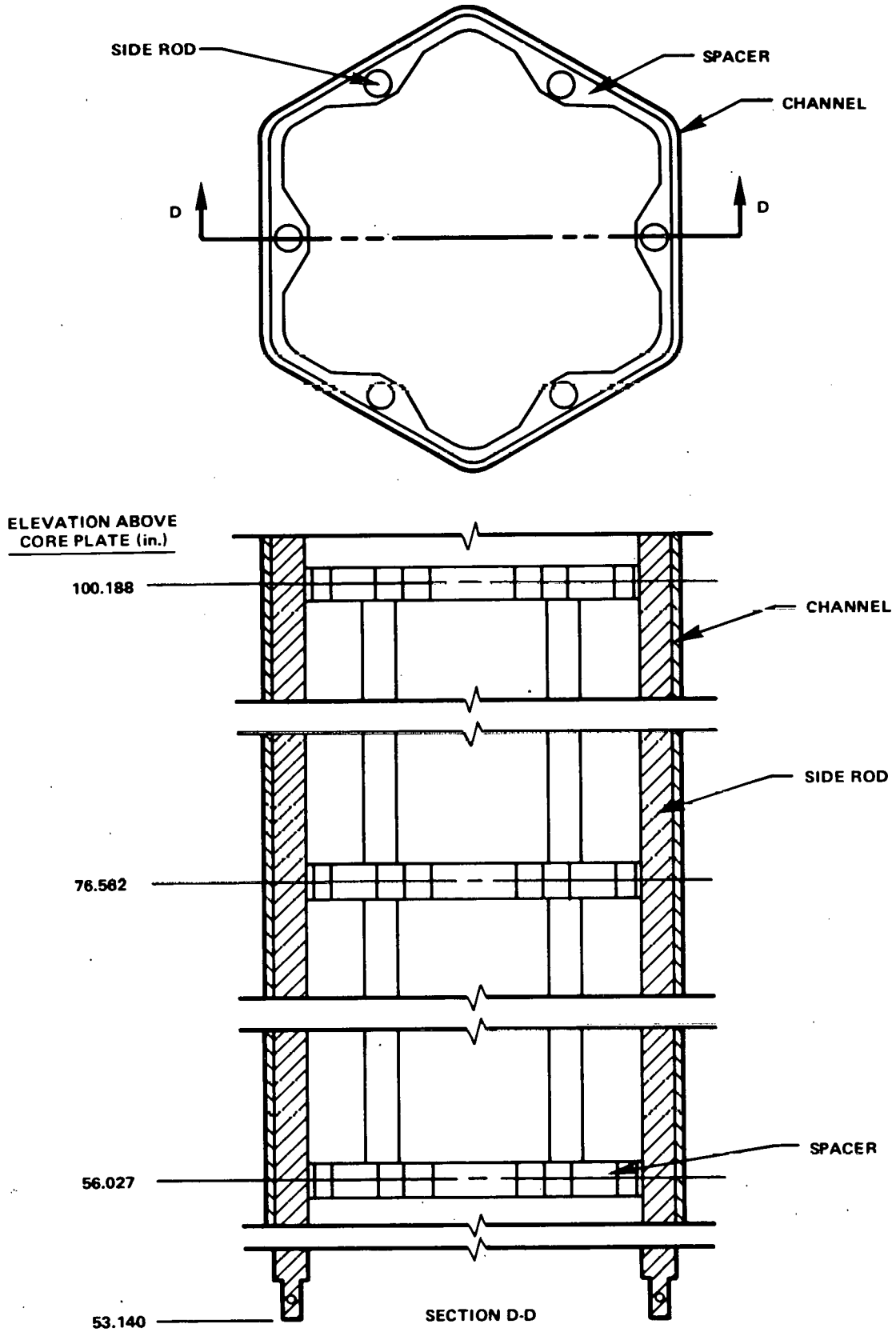


Figure 4B3-22. Extension Rod Spacer Assembly

The orifice piece is the same design as the existing orifice piece with the exception that the orifice itself may have to be changed in order to provide the appropriate flow rate through the fuel assembly.

An adaptor has been designed (Figure 4B3-15) which adapts the orifice piece to the fuel bundle. It would rest directly on the orifice piece, but would not be locked to it. Casting would probably be the most suitable method of manufacturing the adaptor.

A lower spider (Figure 4B3-16) joins the adaptor to the fuel bundles. The spider would have to be cast, and then semi-circular holes which receive the lower end plugs would have to be machined. The receptacles for the lower end plugs of the thirteen tie rods would be inserted into the spider after which the spider would be welded to the adaptor. The semi-circular holes insure that the start angles of the wire wrap remain fixed.

There are two types of lower end plugs, the rod connectors (13) and positioning (no axial restraint) connectors (48). The positioning connectors are simply semi-circular plugs which fit into the semi-circles in the spider. They would be loosely toleranced so that they would center themselves to equalize the forces on the rods from the wire wrapping. The tie rod connectors are illustrated in Figure 4B3-17. They are comprised of three parts - the end plug, a slotted end plug receiver (permanently restrained by the spider), and a locking collar. When the locking collar is in its uppermost position, the end plug is free to be inserted or removed from the receiver. When the collar is lowered, retaining prongs snap into a groove in the lower end plug and the connector assembly is locked into place. The receiver, like the positioning lower end plugs, is also loosely toleranced so that it can center itself to equalize these forces from adjacent wire-wrapped fuel rods on its own fuel rod.

A longitudinal-sectional view of the booster fuel pin is shown in Figure 4B3-3. The axial dimensions of the rod internals are the same as those in the existing design with the exception of the plenum length, "X". This dimension will have to be calculated as it is dependent on expected burnup and linear power.

The upper end plug is illustrated in Figure 4B3-18. It is held in place by a conventional, split retaining ring. The upper spider is identical to the lower spider with the exception of the holes which are circular instead of semi-circular. A split, Belleville spring takes up any axial differential length that may exist between fuel pins. The springs also allow the entire bundle to grow without putting a high compressive load on the fuel pins. Since the upper spider is, in effect, locked to the channel wall, any differential growth between the fuel bundle and the channel could be taken up by one or more Belleville springs incorporated into the design of either the lower or upper adaptors. These springs would enable differential growth to take place without stressing either the channel wall or the fuel assembly. In addition, the locking mechanism would be pre-loaded against the channel wall - thereby preventing fuel shifting due to sloppy or loose tolerances in the locking mechanism.

The upper spider is welded to the fuel assembly-extension rod adaptor (Figure 4B3-19). This adaptor has six fingers or extensions which are the male components of the adaptor-extension rod mating assembly. The mating assembly is the same as that of the existing design. The large circular flat on the adaptor is a platform to which the tightening sleeve is welded. All downward restraining force exerted by the fuel assembly-channel lock is transmitted through this circular flat.

The fuel assembly-channel lock is illustrated in Figures 4B3-20 and 4B3-21. When the fuel assembly is inserted, the tightening rod lowers almost four inches before the lock is engaged. In lowering four inches, the tightening rod forces the existing frictional restraints out against the extension rods. When the tightening rod is lowered the final 5/8 inch, the locking arms are forced outward, and engage the channel.

An extension rod spacer assembly (Figure 4B3-22) is attached (pinned) to the lock assembly. This provides uniform channel-extension rod spacing.

The extension rods and tightening rod are identical to the existing design from the locking assembly on up.

#### *Procedural Interlocks*

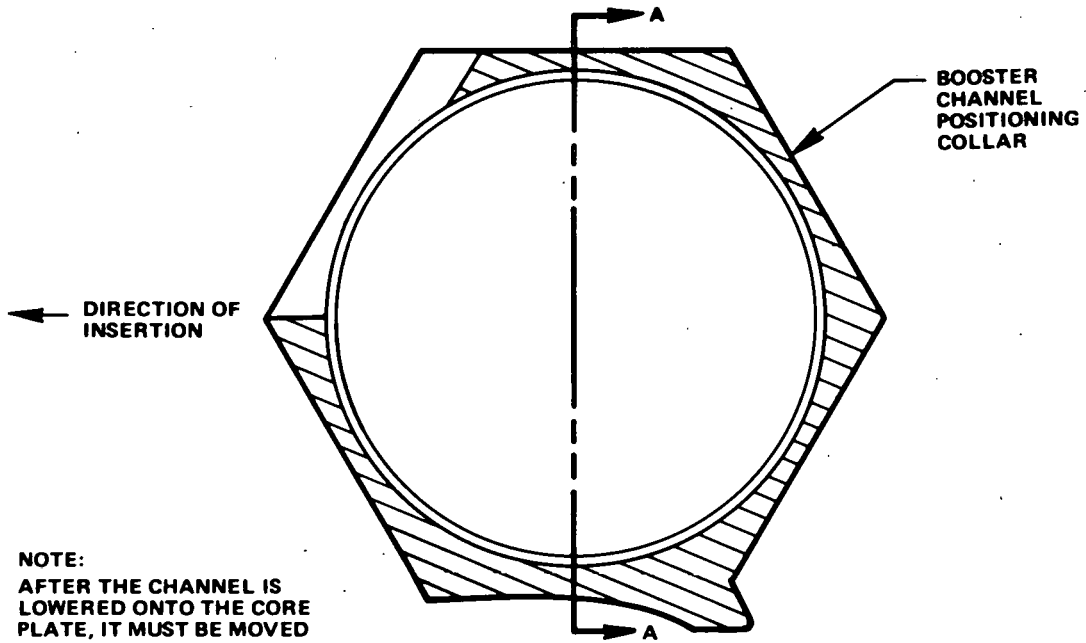
A system of mechanical interlocks has been incorporated into the design to insure that the correct loading sequence is not altered.

The first step in loading the new fuel in the core is to load all the channels. There are two types of channels, booster and driver. Collars have been added to the bellows seal containment ring on all the channels. Figure 4B3-23 illustrates the collar on the booster channel. The male end fits into the female slot on an adjacent booster-channel. The collars on the driver channels are illustrated in Figure 4B3-24. By inspection, the booster collars cannot engage the driver collars, thus the channel locations are fixed.

The lower adaptors (orifice piece to lower spider) are illustrated in Figures 4B3-25 and 4B3-26 for booster fuel and driver fuel, respectively. Spring-loaded flaps on the booster adaptors engage slots in the walls of the driver

channels and prevent insertion. There are no locks on the driver adaptors, and no slots in the booster channel walls. A tool would have to be designed to compress the locks upon insertion into the top of the channel.

Finally a sequence interlock (Figure 4B3-27) has been designed which insures that the booster fuel is loaded first. The interlock is attached to the tightening sleeve of adjacent inner driver fuel. It fits through slots (see Figure 4B3-28 for locations) in the driver and booster channel walls. Once it is in place, the adjacent booster fuel cannot be inserted as the lower adaptor interferes with it. If, on the other hand, if the booster is inserted first (as it should be), the interlock merely passes between the booster extension rods without interference.



NOTE:  
AFTER THE CHANNEL IS LOWERED ONTO THE CORE PLATE, IT MUST BE MOVED HORIZONTALLY UNTIL IT CONTACTS THE ADJACENT BOOSTER CHANNEL

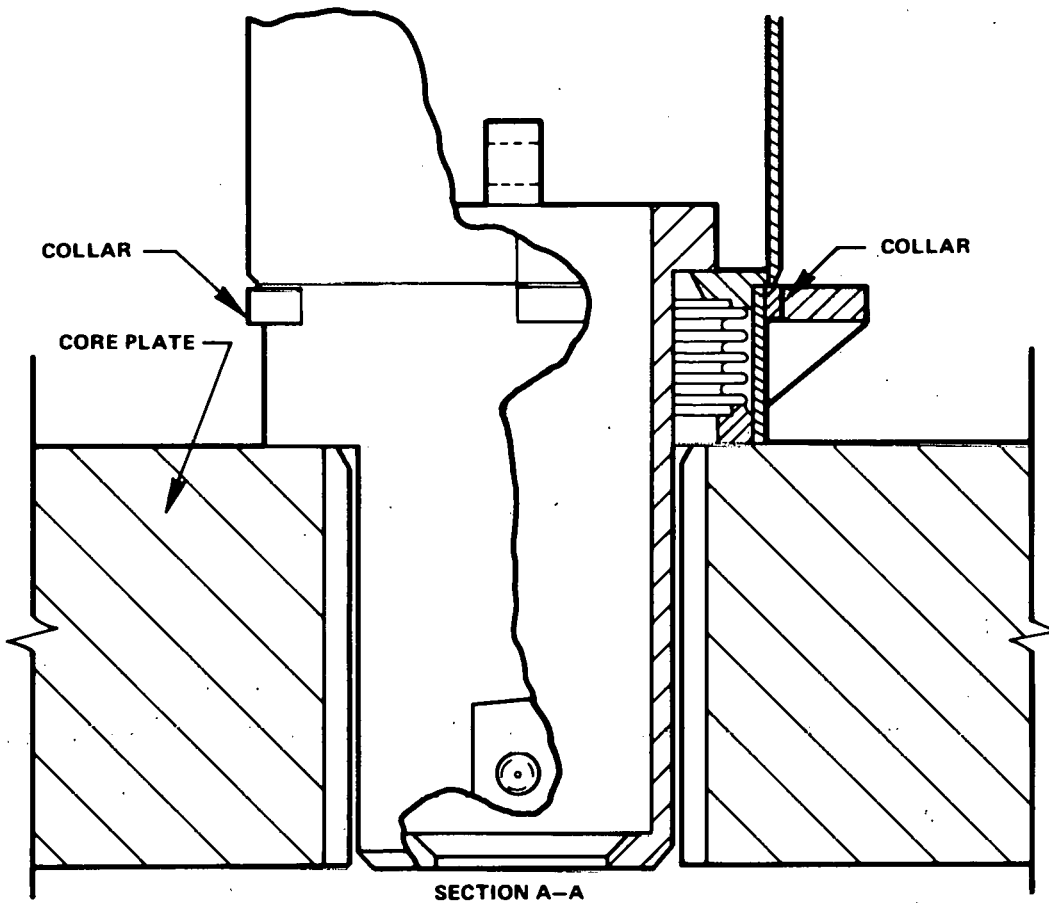


Figure 4B3-23. Booster Channel Positioning Collar

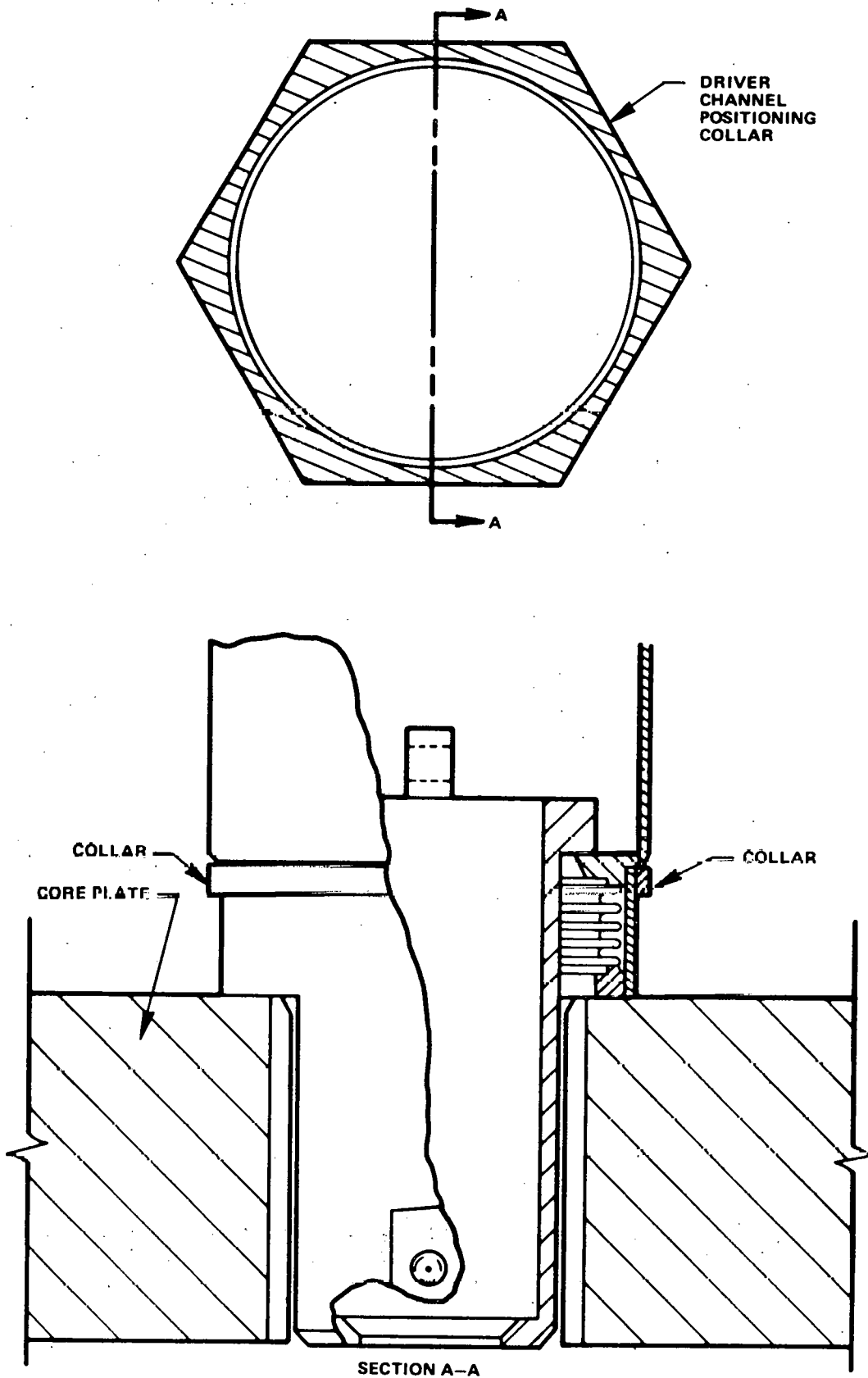


Figure 4B3-24. Driver Channel Positioning Collar

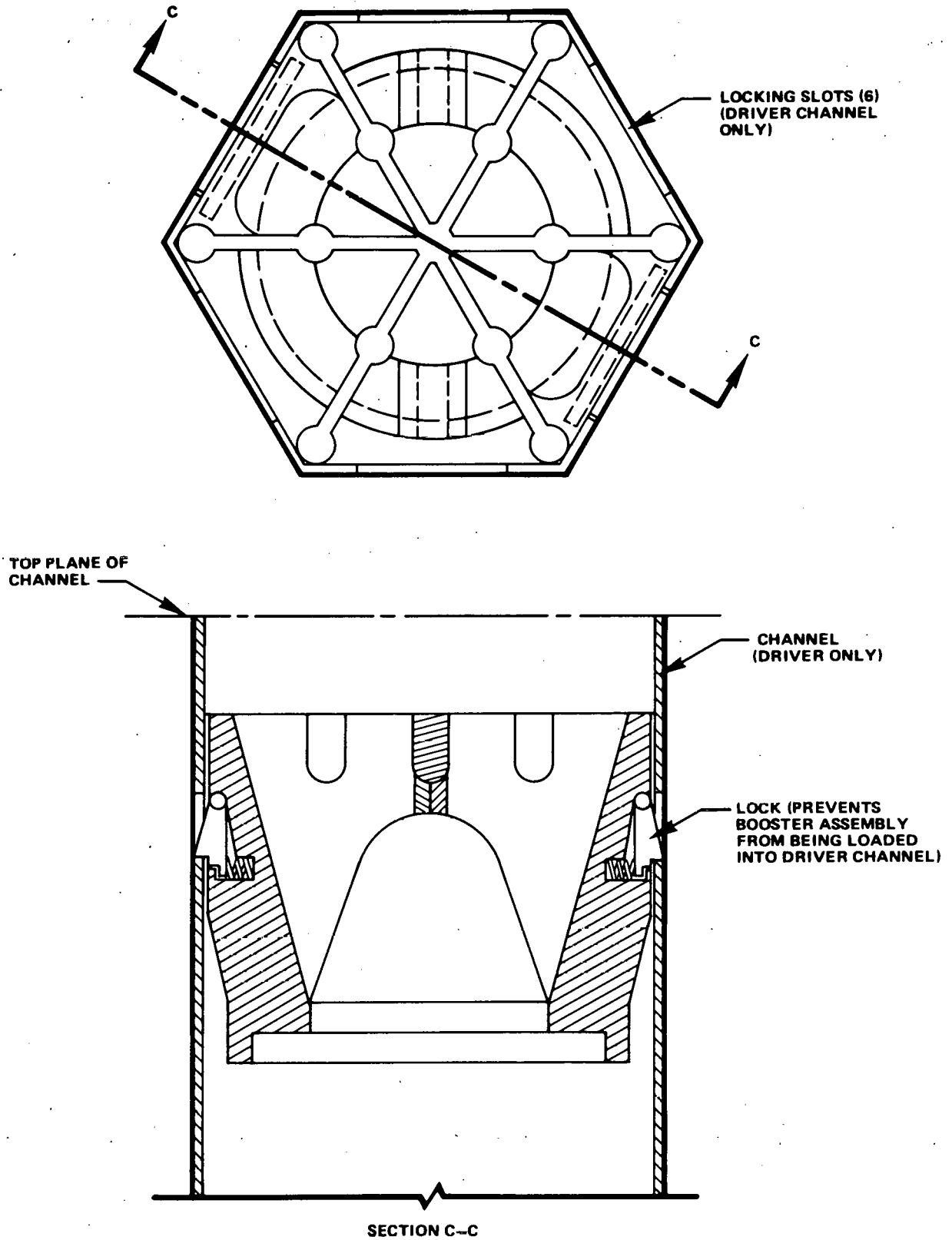
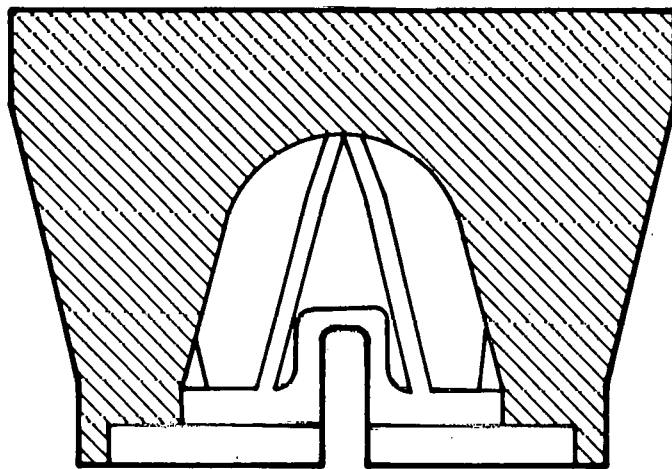
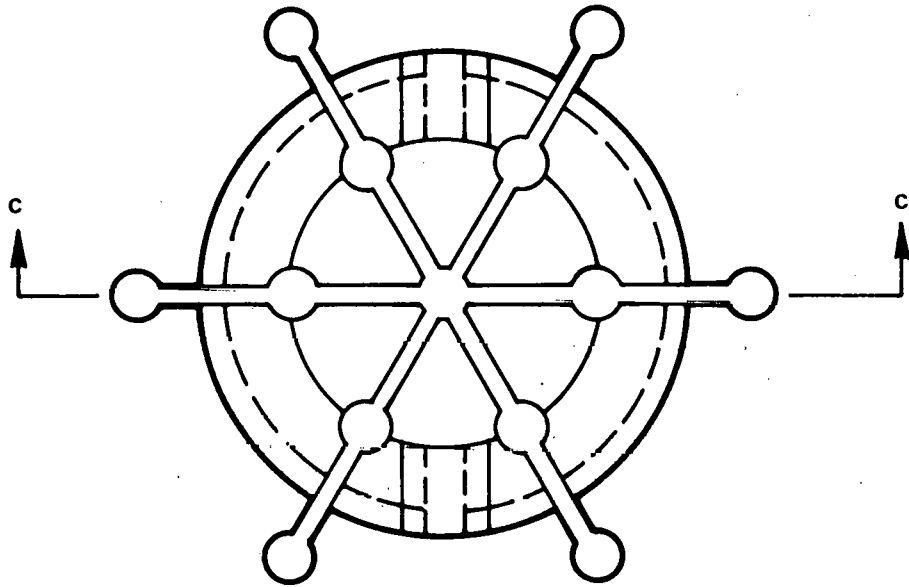


Figure 4B3-25. Booster Fuel Assembly Orifice Adaptor





SECTION C-C

Figure 4B3-26. Driver Fuel Assembly Orifice Adaptor

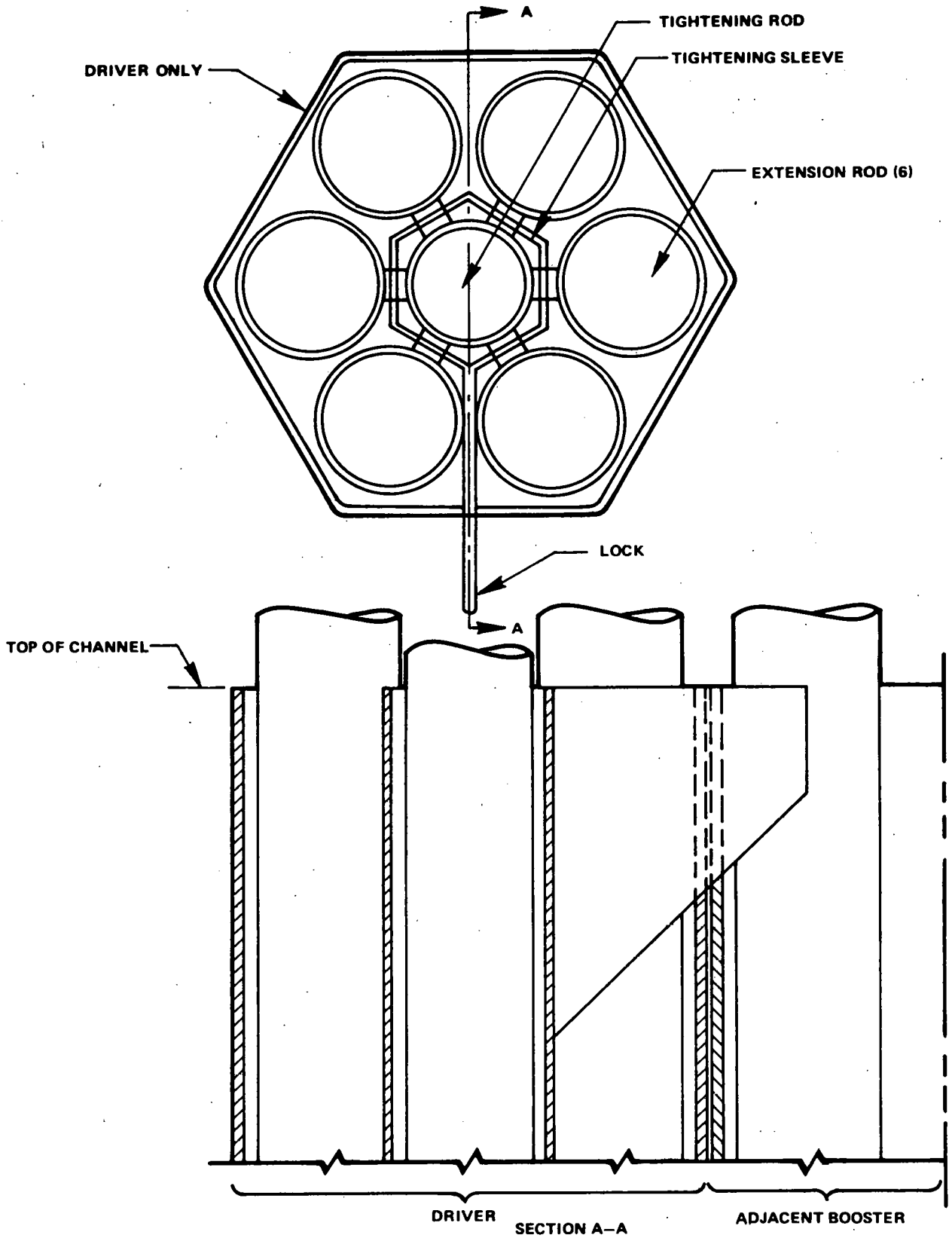


Figure 4B3-27. Loading Sequence Interlock Provisions, Booster-Driver Assemblies

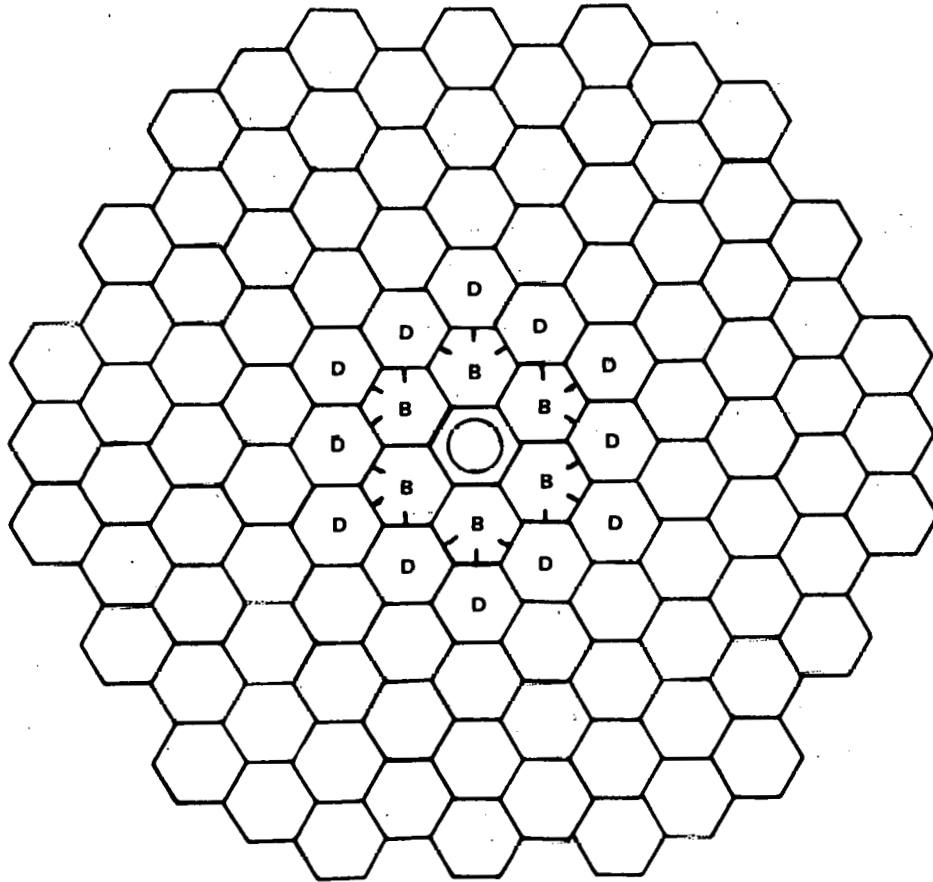


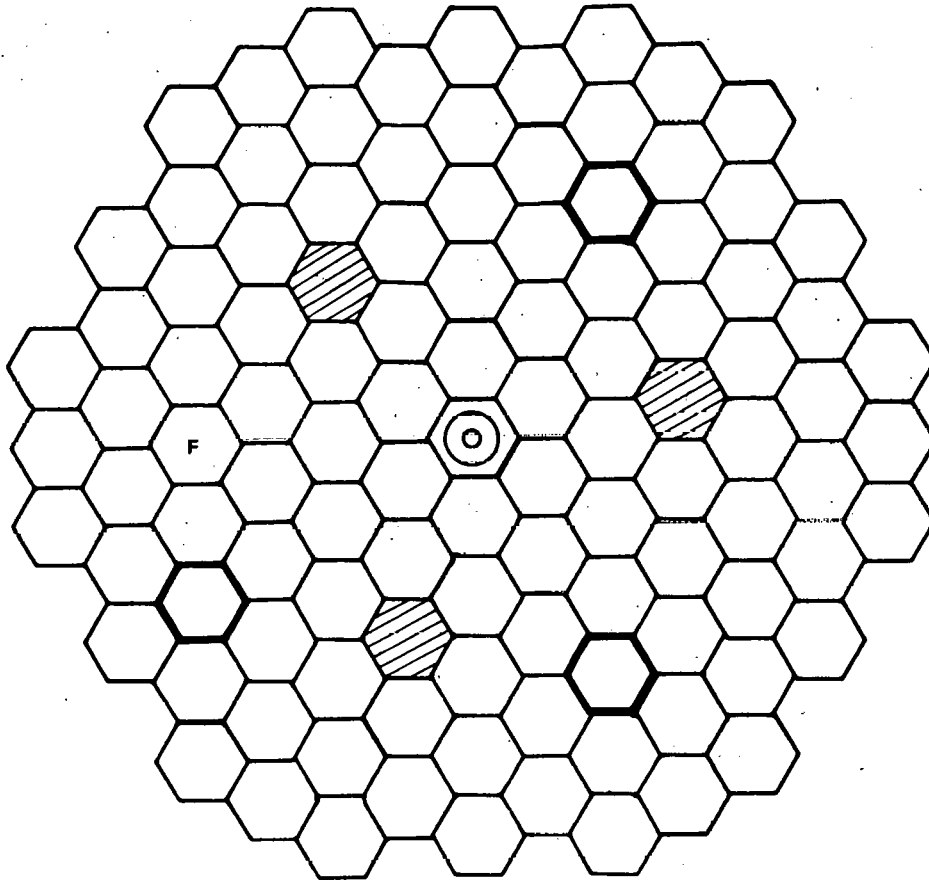
Figure 4B3-28. Locations of Sequence Interlocks

**4.2.3.12 Control Element Design**

The SEFOR control system consists of three movable controls, three fixed controls, and one FRED assembly (Fast Reactor Excursion Device). The movable control is primarily used for the safe shutdown of the reactor. The fixed control is utilized as a fixed poison with the option of replacement with fuel rods if additional reactivity is needed. The FRED device is used to produce transient operation at various rates for the reactor. The location of the control system elements are shown in Figure 4B3-29.

**4.2.3.13 Control Rod Worth**

Physics calculations have been made of the worth of the movable control rod design which has been proposed and is seen in Figure 4B3-30. With 40% B-10 enrichment of  $B_4C$ , the calculated rod worths in the locations of Figure 4B3-29 are \$1.86 and \$1.20 under the outer refueling port and the sodium sampling port, respectively. No conceptual design presently exists for the first control element.






-  **FRED**
-  **MOVABLE CONTROL**
-  **FIXED CONTROL**

Figure 4B3-29. Core Pattern

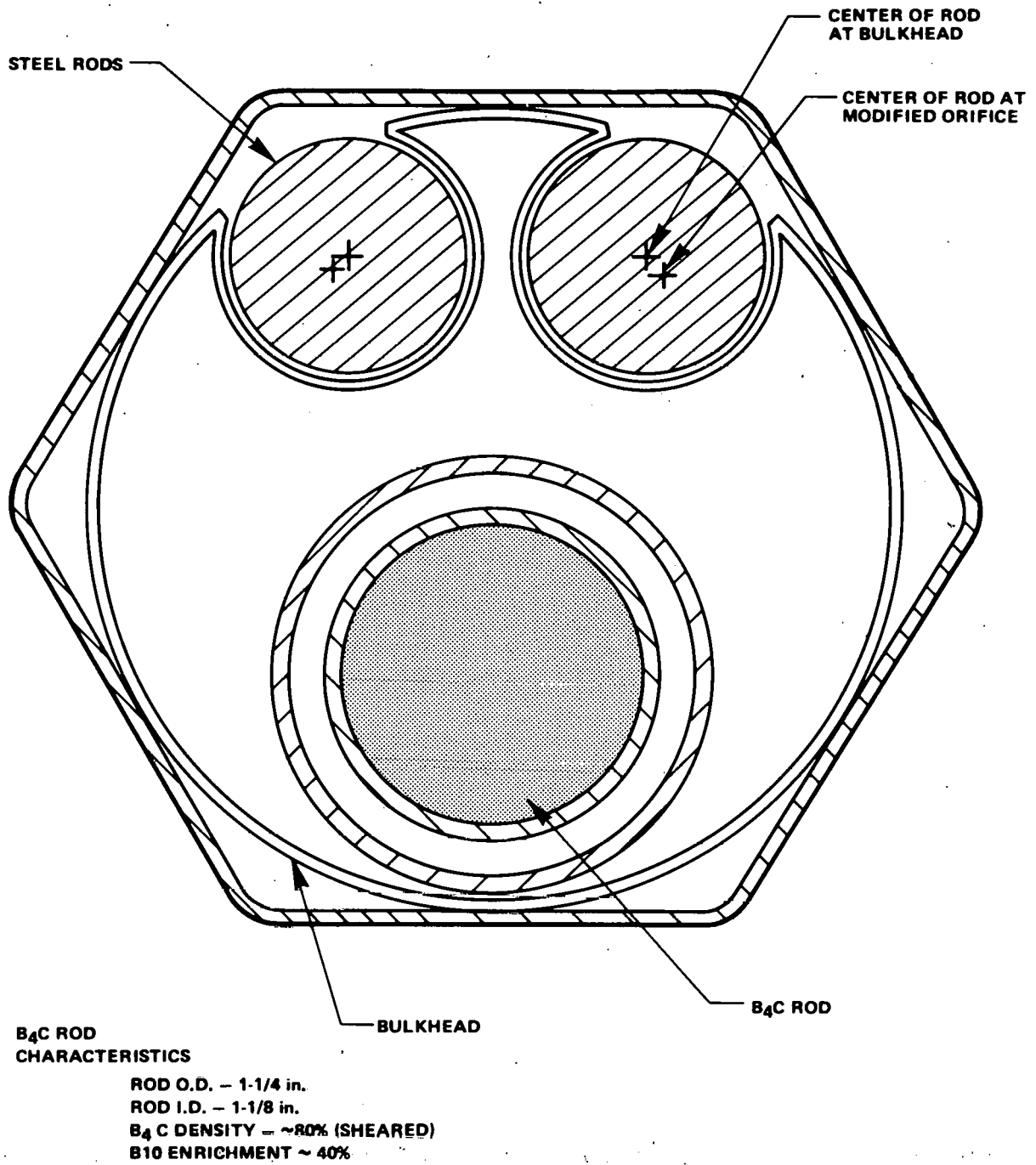


Figure 4B3-30. Movable Control Assembly Cross-Section

## REFERENCES

1. "Engineering Study of the Conversion of SEFOR to a Fast Reactor Test Facility. Task 1: Conceptual Design and Preliminary Evaluation," NEDC-13602, April, 1970.
2. Magee, P.M., "FULMIX-Turbulent Interchange Mixing Code for Fuel Bundle Thermal-Hydraulic Analysis," Core Development Memo 150-13, April 15, 1971.
3. Feerick, B.T., and Magee, P.M., "Calculated Cladding Temperature Distribution for Internal Elements of ESADA Fuel Bundles," December 2, 1969.
4. Feerick, B.T. and Lipps, A.J. "Preliminary Steady-State Analysis of Present SEFOR Core Driver Fuel for Elevated Temperature Operation."
5. Tsui, E.Y.W., et al., "Interim Stress Design Criteria for LMFBR Vessel and Core Structures," GEAP-13719, May, 1971.
6. Rung, P.J., "Radiation Met. Memo 71-3," March, 1971.
7. FFTF, LMFBR Materials Handbook.
8. Reavis, J.R., "Vibrational Correlation for Maximum Fuel Element Displacement in Parallel Turbulent Flow," Nuclear Science Engineering, 38, 63 (1969).
9. Chen, S.S., et al., "Vibration and Stability of Tubes Exposed to Pulsating Parallel Flow," ANS Trans., Biltmore Hotel, Los Angeles, California, June 29-July 2, 1970.
10. Bennet, J.W., "Basis for Establishment and Use of A Strain Criteria for LMFBR Core Components," Memo to Distribution dated May 13, 1971, File BB0901.
11. Stephen, et al., "The Effect of Fuel Density in Fuel-Clad Mechanical Interaction in the Demonstration Plant," Memo of January 25, 1971.
12. Meyer, R.A., et al., "Design and Analysis of SEFOR Core I," GEAP-13598, June, 1970.

#### 4.2.4 Task 4B4 Systems

##### 4.2.4.1 Objective

The objective of this task is to evaluate the capabilities of the SEFOR system/components to operate under Option III Conditions (i.e.: increased reactor power up to 23 MW and new reactor fuel with increased pressure drop).

##### 4.2.4.2 Plant Tests

Tests were conducted in September, 1971 on the SEFOR main and auxiliary air blast coolers (ABC) in conjunction with plant operation at 5, 10, and 15 MW. Outlet air temperatures were measured so that heat balances could be performed on the units. The main ABC tests showed that the air side pressure drop was higher than predicted by the vendor. This effect on Option III-A test operation is discussed below. Overall heat transfer coefficients calculated from heat balance data proved to be exactly as predicted.

Test data on the auxiliary ABC was inconclusive. Due to the large amount of natural circulation cooling, the auxiliary ABC fans had to remain "off" during the 5 and 10 MW tests. Even at 15 MW, cooling requirements were met by one of two fans operating; thus few conclusions could be drawn from this test on the ultimate capacity of the ABC. Earlier tests, however, had shown that the auxiliary cooling system could dissipate 1.3 MW which exceeds Option III emergency cooling requirements.

##### 4.2.4.3 SEFOR Component Evaluation

###### 4.2.4.3.1 Pumps

Under Option III the main primary pump will be called upon to deliver its rated discharge pressure capacity of 38 psi at 5000 gpm. For the initial SEFOR core the system pressure drop was approximately 20 psi. This low pressure drop has been accompanied by reduced voltage and power requirements and lower winding temperatures for the main primary pump. GE-LMGD—Large Motor Generator Department, received the September, 1971 pump performance test data and calculated that the main primary pump is capable of producing the required Option III head/flow condition without exceeding 350°F stator winding temperature.

###### 4.2.4.3.2 Intermediate Heat Exchangers (IHxs)

The overall heat transfer coefficient required to transfer 23 MW of heat in the main IHX is calculated to be about 1200 Btu/he-ft<sup>2</sup>-°F. Heat transfer coefficients of 1300-1400 have been determined from SEFOR test data at rated flow conditions of 5000 gpm and comparable terminal temperatures. The required U's and experimentally determined U's are shown on Figure 4B4-1. It is concluded that there is ample margin in the main IHX for achieving 23 MW.

The auxiliary cooling system (AIHX and AABC) have demonstrated heat removal capability of 1.3 MW in tests preceding SEFOR Follow-On Phase A. This heat removal capability exceeds the 5% heat removal requirements for Option III emergency cooling.

###### 4.2.4.3.3 Air Blast Coolers

In the September, 1971 test the ABC outlet air temperatures were measured by nine thermocouples arranged in a grid pattern about three feet above the coils. There was very little temperature variation at the nine locations. The log mean temperature difference (corrected for a two-pass crossflow exchanger) was calculated from the terminal temperatures. The overall heat transfer coefficient was then calculated using the power (MW) from the sodium heat balance. As shown in Figure 4B4-2, the data from tests at 5, 10, and 15 MW fall on the predicted curve. The predicted curve was based on an air side "h" proportional to velocity to the 0.7 power.

However, the main air blast cooler pressure drop is significantly higher than predicted by the Vendor. As shown on Figure 4B4-3, extrapolating the system pressure drop data points to intersect with the fan static pressure curve at rated speed indicates that the blower is capable of delivering only about 88% of rated air flow. (An additional test at a higher blower speed is needed to reduce the uncertainty in this extrapolation.) This reduced air flow capability means that there will be insufficient main ABC blower capacity to hold the reactor sodium inlet temperature at 700°F during 23 MW operation (even with allowing 1 MW to be dissipated through the auxiliary cooling system). Figure 4B4-4 shows the relationship of reactor inlet temperature as a function of rated ABC air flow for several ambient temperatures. Means of increasing blower capacity are under investigation; other alternates such as reducing reactor power requirements and/or accepting higher reactor inlet temperatures will be considered and compared to the cost of additional blower capacity.



**4.2.4.4 Nitrogen System**

As shown on Figure 4B4-5, the estimated heat load for Option III-A 23 MW operation is 467 tons. This represents about a 10% increase over the present 20 MW operation. The 10% increase is due to the incremental increase in  $\gamma$ -heating of the shielding and reflectors. The recommended increase in capacity to 500 tons at 95°F ambient for the Elevated Temperature Operation will provide ample margin for Option III-A conditions.

**4.2.4.5 Control and Instrumentation**

A functional block diagram was prepared for the 19-pin package loop outlining electrical and instrument requirements. In addition the data, signal conditioning and cabling requirements for tying into the Data Acquisition System were established. Modifications to the Reactor Protection System were determined to be minimal.

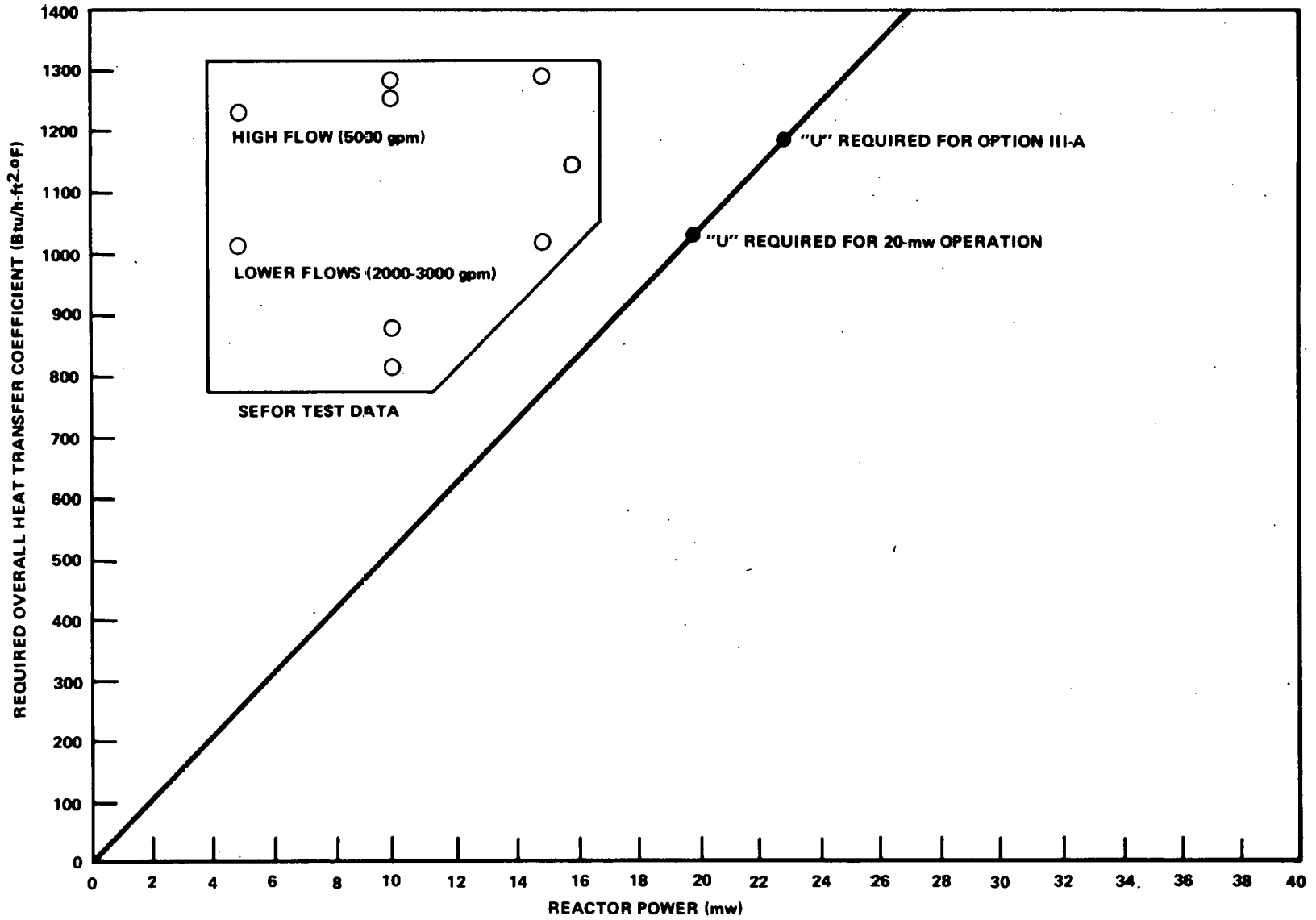


Figure 4B4-1. SEFOR Main IHX Required Overall Heat Transfer Coefficient versus Reactor Power

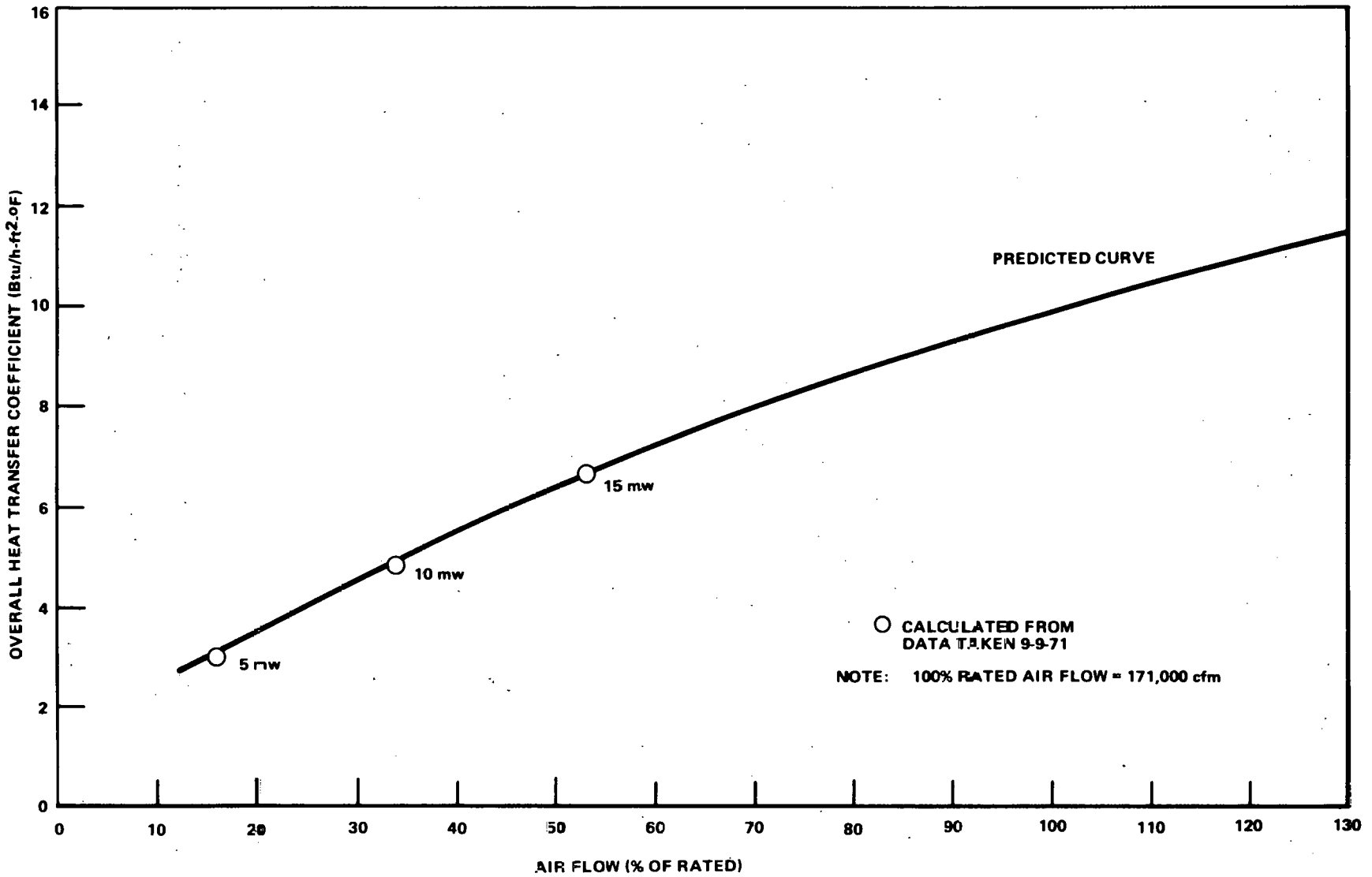


Figure 434-2. Main Air Blast Cooler Overall Heat Transfer Coefficient versus Air Flow

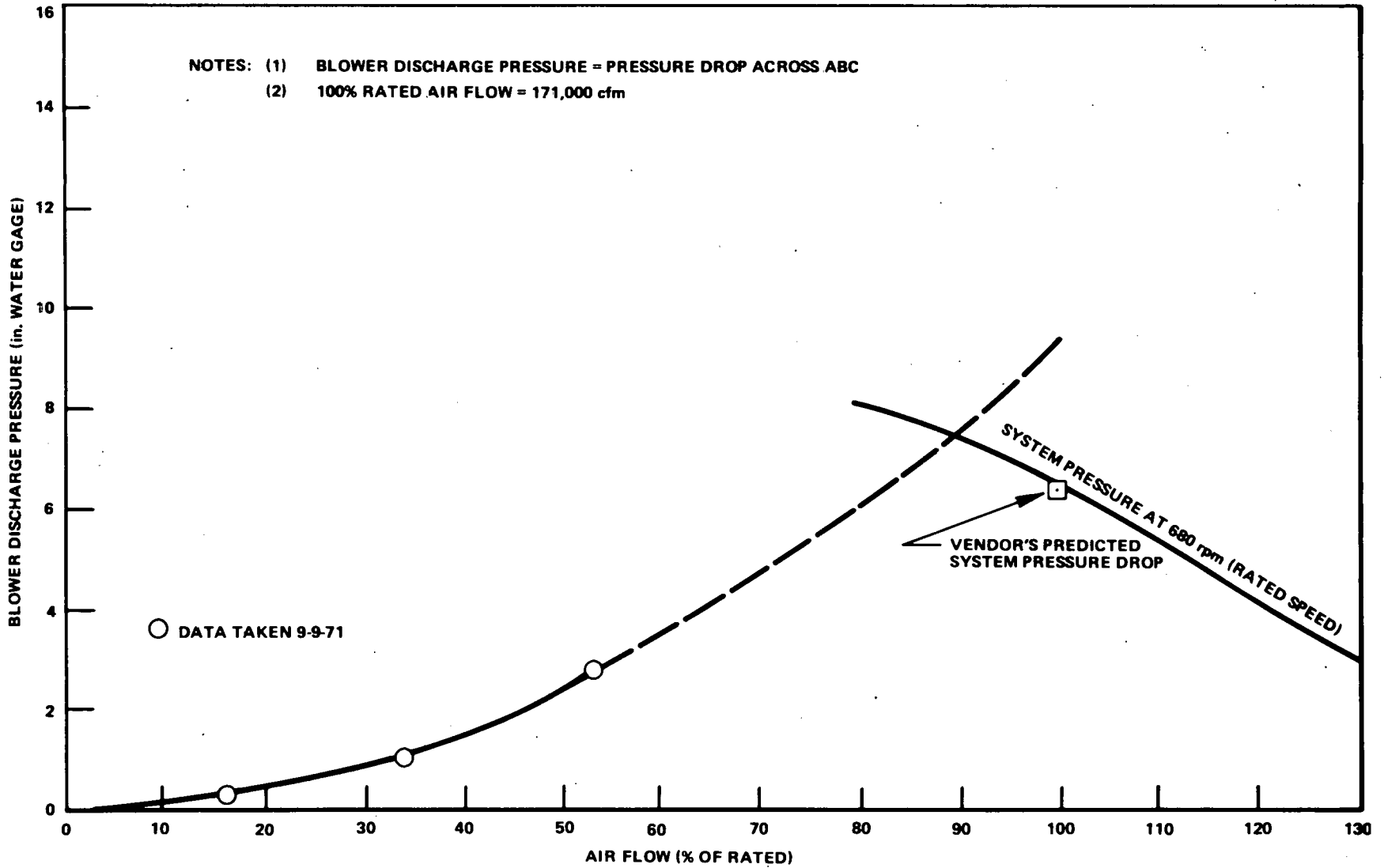


Figure 4B4-3. Main Air Blast Cooler Blower Discharge Pressure versus Air Flow

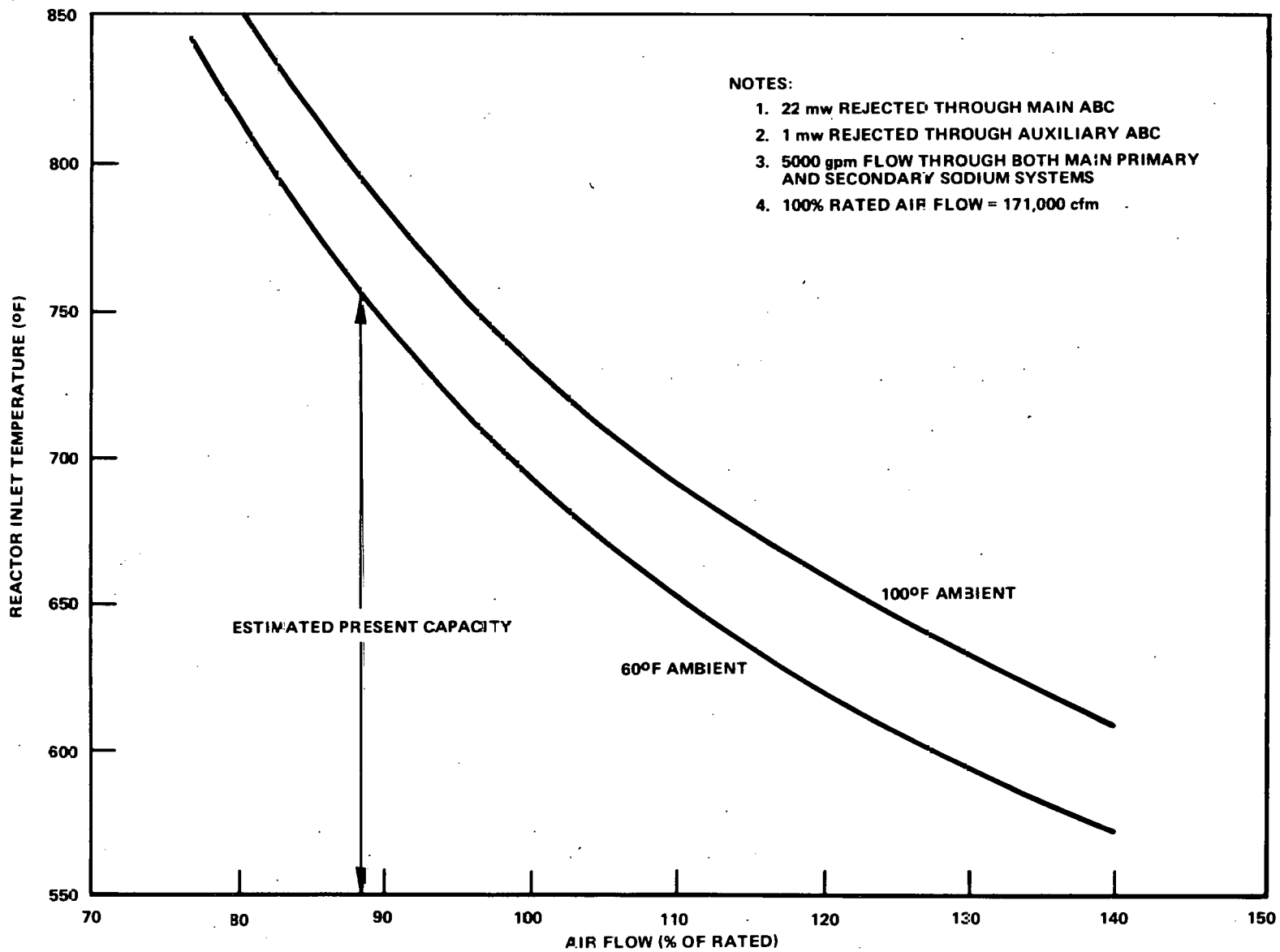


Figure 4B4-4. Reactor Inlet Temperature as a Function of Air Blast Cooler Air Flow, Option III-A, 23 MW Operation

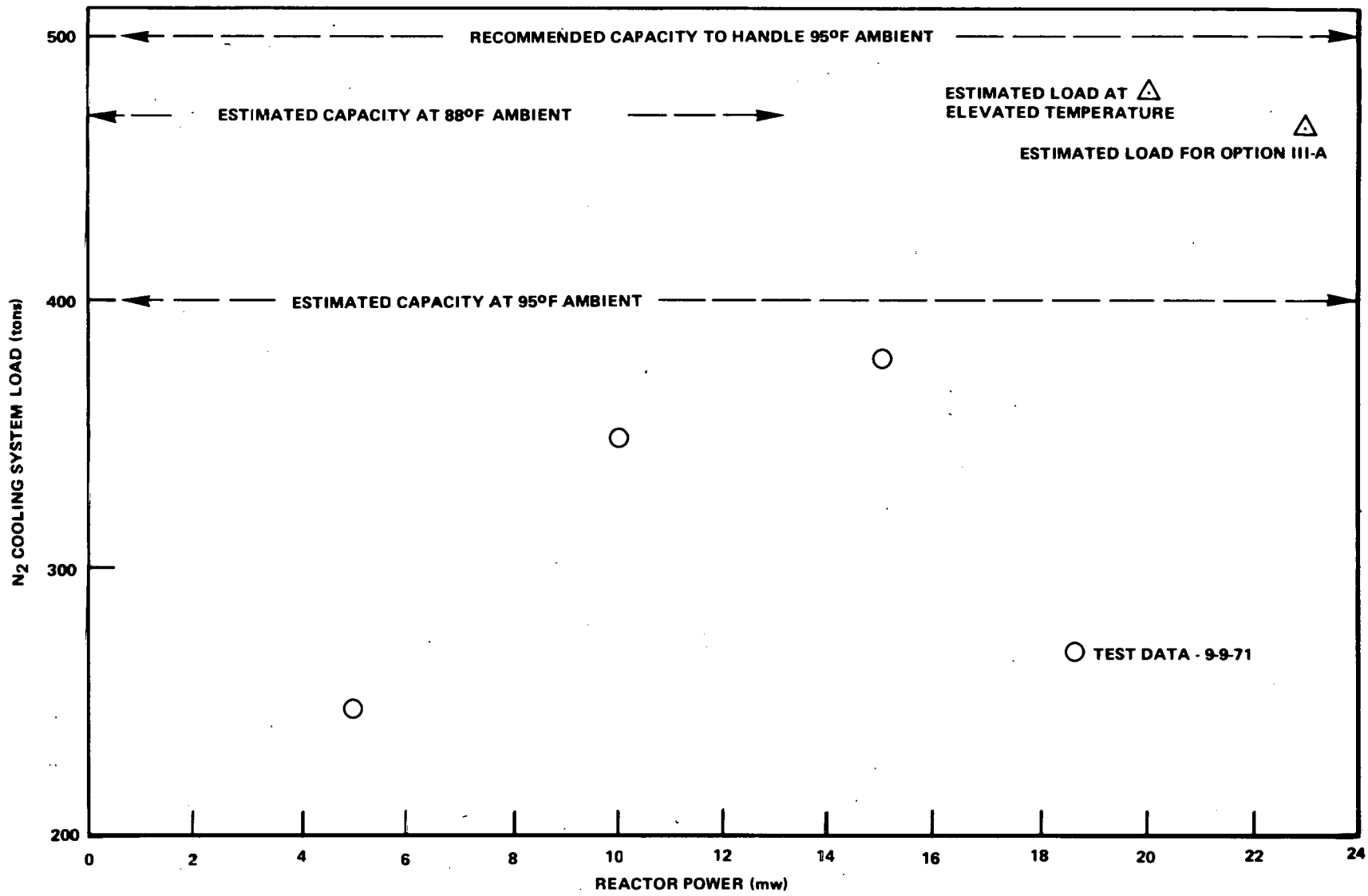


Figure 4B4-5. SEFOR Nitrogen Cooling System Load

**4.2.5 Task 4B5 – Physics**

**4.2.5.1 Objective**

The objective of Phase A nuclear design efforts was to develop core concepts originated in the Task I effort to the point that preliminary specifications for a critical experiment program could be formulated.

**4.2.5.2 Discussion**

The feasibility of performing safety tests in SEFOR without major modifications to the plant was indicated in the Task I scoping study (NEDC-13602). The "booster" core concept was suggested in this prior study as a means of achieving target test conditions with a minimum replacement of existing SEFOR fuel rods. This concept involves the use of a "booster" region in which highly enriched fuel (50% PuO<sub>2</sub>-50% UO<sub>2</sub>) is loaded into the six channels surrounding the center channel in small diameter rods (approximately 0.310-inch O.D.). The resultant increase in flux per reactor megawatt requires that new fuel replace the present fuel with either lower enriched or smaller diameter rods in at least two additional rows of channels; the "inner driver". The flux level in the remaining channels is low enough to permit the use of fuel of the present design; the "outer driver". Several alternate core loadings for the driver regions were outlined in the Task I report. Further evaluation of driver fuel options was done during Phase A so that reference concepts could be selected for the purpose of critical experiment planning.

Initial contacts with Argonne National Laboratory were made during Phase A so that a preliminary program plan could be developed for a mockup critical experiment. A series of working meetings were held at which design requirements were reviewed, preliminary test specifications were outlined and a preliminary test program was developed. Because of FTR work in ZPR-9 (currently scheduled to end in August 1972), the preliminary SEFOR Follow-On critical experiment schedule does not meet the information needs of the core design schedule. Possible remedies for this schedule problem are under study.

Core nuclear design and critical experiment planning activities during Phase A are described in the following. This work is preliminary in nature and is reported here to give an indication of progress and direction rather than final conclusions, however, these changes are expected to be small relative to the differences between the three alternate cores.

**4.2.5.3 Core Design**

**4.2.5.3.1 Requirements**

The principle nuclear design requirement to be met by the follow-on core with respect to testing capability is that it deliver a peak steady-state linear power of at least 15 kW/ft to the test fuel in the reference package loop design for loss-of-flow tests. Rod-to-rod power ratios are not to exceed 1.2. This fuel is fully enriched UO<sub>2</sub> contained in 0.250-inch U.D. rods. The fission density in the test fuel is enhanced through the use of a Zr Hydride annulus surrounding the 19 fuel rods. The steady-state core power is constrained to be no more than 23 MWt so as not to exceed the stretch capacity of the SEFOR heat removal equipment.

A further requirement of the core design is that it be capable of depositing energy to test fuel in transient overpower tests initiated from steady-state power levels. The range of energy deposition to be provided ranges from raising the peak test fuel energy density to LMFBR safety limits in repetitive transients to developing molten fuel-coolant interactions with significant vapor pressures.

The rate of energy deposition is to be controllable within a broad range with a minimum time constant on the order of milliseconds. Test fuel initial conditions are to be representative of an operating LMFBR. For this evaluation the test vehicle was assumed to be the reference package loop concept. The peak driver fuel energy density was constrained to be less than the solidus under all proposed transients.

A nominal 3-foot core height is required to provide capability for testing full length fuel rods under prototypic conditions. The core height was constrained to be no greater than the present core height.

In addition to the requirements on the core nuclear design relative to testing capability and the constraints already mentioned, several additional requirements and constraints affect the nuclear design.

The existing grid plate and core support structure are to be used.

The existing core clamping system is to be used.

Subassemblies will use the present channel outside dimensions

The center core position is to contain the package loop.

The existing movable reflectors are to be used for reactor control, supplemented as required by in-core control.

Four in-core locations, accessible through the head, are to be available for in-core control and the FRED.

Fuel will be mixed oxide (Pu+U)O<sub>2</sub> contained in rods.

#### 4.2.5.3.2 Options

Three alternate core designs are presently being considered for further development. The first is a refinement of the Task I concept with a booster region (6 channels), an inner driver region (30 channels), containing new fuel, and an outer driver (72 channels) in which the present fuel is used. The second alternate includes the booster with all new driver subassemblies. The third alternate is a uniform driver core with no booster region. These alternates are summarized in Table 4B5-1.

These alternates have evolved from the Task I study and scoping studies performed during Phase A to better define the driver fuel. The first alternate is being considered as a means of minimizing the amount of new fuel required. The technical feasibility of this concept depends on the capability of the existing fuel to sustain extended operation. The second alternate evolved from the first because of this feasibility question and to improve the capability of overpower operation. The third alternate, by eliminating the booster region, improves overpower capability, increases the reflector worth and simplifies the design. This alternate evolved from the driver fuel scoping studies done for the booster core. These alternates form the basis for further core design development which will lead to the selection of a reference design in April 1972.

All new fuel in each of these alternates is contained in 0.310-inch O.D. rods. In the booster region the small diameter rods are required to keep the linear power (i.e. fuel center temperature) within acceptable limits. In the driver regions the small diameter rods provide the fuel temperature margin between steady-state operating conditions and fuel center melting required to permit transient overpower testing. Subassembly options are summarized in Table 4B5-2 for the core design alternates. All of the subassemblies containing small diameter rods contain 36 fuel rods, 24 BeO rods and one steel rod. The fuel and BeO rods are uniformly mixed. A cross section of the 61 rod subassembly is shown in Figure 4B5-1. The rods are on a pitch of 1.2 diameters, with a diameter of 0.310 inch to the outside of the clad. All fuel and BeO rods are clad with stainless steel tubing, with a 0.015 inch wall thickness.

The fuel composition varies between the core design alternates. The most important variation is in the Pu/U+Pu atom ratio. This ratio was set at 0.50 for the booster region based on the Task I results and fabrication considerations. The ratio varies for the driver fuel between the alternate designs as required for criticality considerations. A summary of Pu/U+Pu for the alternate core designs is given in Table 4B5-3. Uranium in the booster and driver fuel is depleted uranium. The Pu-239/Pu ratio is 0.92 for the booster region. It is desirable to keep the Pu-239 fraction in the Pu as high as possible to keep the maximum Doppler effect possible in the booster. In the driver the Pu-239/Pu ratio is 0.88 as the AEC indicated that this material is likely to be available.



Table 4B5-1

REFERENCE SCOPE DESIGN

Test Region

Center Channel of SEFOR

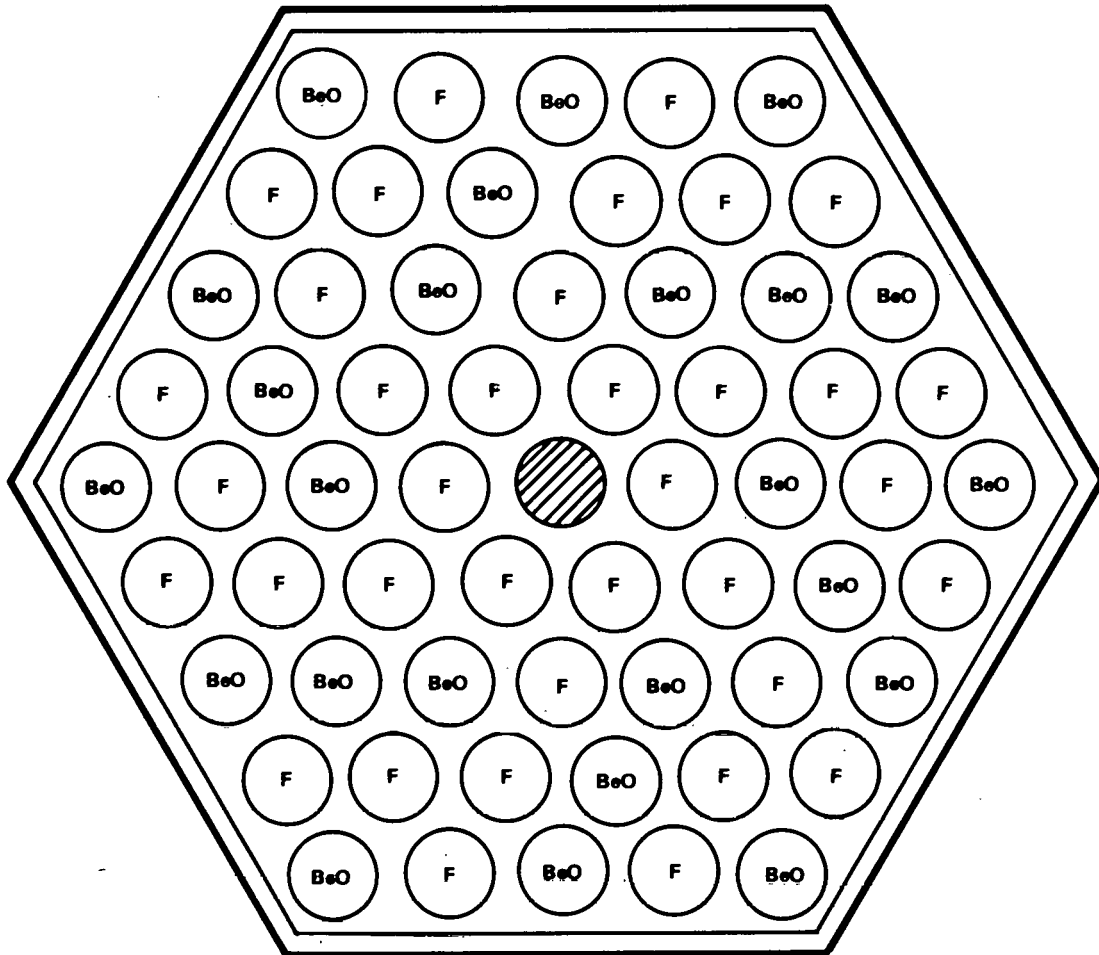
Core Design Alternates

I	Booster	6 Channels
	New Subassemblies	30 Channels
	Modified Core I Subassemblies	68 Channels
	Off-Center FRED	1 Channel
	In-Core Control	3 Channels
II	Booster	6 Channels
	New Subassemblies	98 Channels
	Off Center FRED	1 Channel
	In-Core Control	3 Channels
III	New Subassemblies	69 Channels
	Off Center FRED	1 Channel
	In-Core Control	3 Channels
	No Booster	

Table 4B5-2

SUBASSEMBLY OPTIONS

	I	II	III	
Booster	60 Fuel Rods	60 Fuel Rods	—	
	1 SS Rod	1 SS Rod	—	
Inner Driver	36 Fuel Rods	36 Fuel Rods	36 Fuel Rods	
	24 BeO Rods			24 BeO Rods
	1 SS Rod			1 SS Rod
Outer Driver	3 x 1" Fuel Rods			
	3 x 1" SS Rods			
	1 BeO Tightener Rod			



TENTATIVE ARRANGEMENT OF FUEL, BeO, AND STEEL RODS

Figure 4B5-1. 61-Rod Subassembly Cross-Section

Table 4B5-3

	Pu/U+Pu		
	I	II	III
Booster	0.50	0.50	-
Inner Driver	0.20		
Outer Driver	0.20	0.16	0.31

New Subassemblies - 61 rods ~ 0.310 O.D. In-Core Rods Contain Fuel, BoO or Stainless Steel

4.2.5.3.3 Calculation and Results

Core nuclear design calculations were performed using one and two dimensional multigroup diffusion theory. Cross sections were obtained from ENDF/B-II with revisions in the Pu-239 cross sections to make them equivalent to ENDF/B-III. Processing to obtain multigroup data in 4, 11, and 29 groups was done using the ENDRUN and TDOWN codes. A description of the files and data processing procedure is given in Appendix A.

Parameters of importance to the core nuclear design are given in Table 4B5-4 for the three alternate core designs. The alternates which use the booster concept (I and II) are expected to be quite similar when measured with these parameters. Significant differences appear between the uniform core and the booster core alternates. With respect to the booster concepts the uniform core has a significantly higher reflector worth, a lower peak power density and fuel center temperature, which results in a larger Doppler feedback available from 23 MW before fuel melts, and a lower maximum bundle worth. Ability of the three cores to deliver power to the test fuel is about the same and in each case exceeds the minimum requirement. Improvements in the testing capability appear to be more readily achieved with the uniform core because of the flexibility in the subassembly composition. These results are preliminary and in some cases only estimates. They are subject to change before a reference core is selected, however, these changes are expected to be small relative to the differences between the three alternate cores.

Table 4B5-4

CORE DESIGN PARAMETERS

	I Booster plus present fuel	II Booster plus all new driver	III 73 channel uniform core
Peak Power in Test Fuel (dW/ft)	16.5	16.5	17.0
Dopp'ler (Isothermal T dk/dT)	-.0075	-.0075	-.0075
Reflector Worth (\$)	~5	~6	~9
Test Assembly Worth (\$)	5.50	~5.50	~6.50
Test Fuel Slumping Worth (\$) (Maximum hypothetical)	~.70	~.70	~.80
Sodium Void Reactivity	All Neg.	All Neg.	All Neg.
Peak Core Fuel Power (kW/ft)	10.2 (16.5 in outer driver)	10.2	6.4
Core Fuel Peak Centerline Temperature @ 23 MW (4200°F in outer driver)	~3400°F	~3400°F	~2500°F
Doppler w/instantaneous energy addition, peak core centerline to solidus from 23 MW	~46¢	~46¢	~83¢
Core Bundle Worth (\$) (maximum worth bundle)	~10	~10	~5

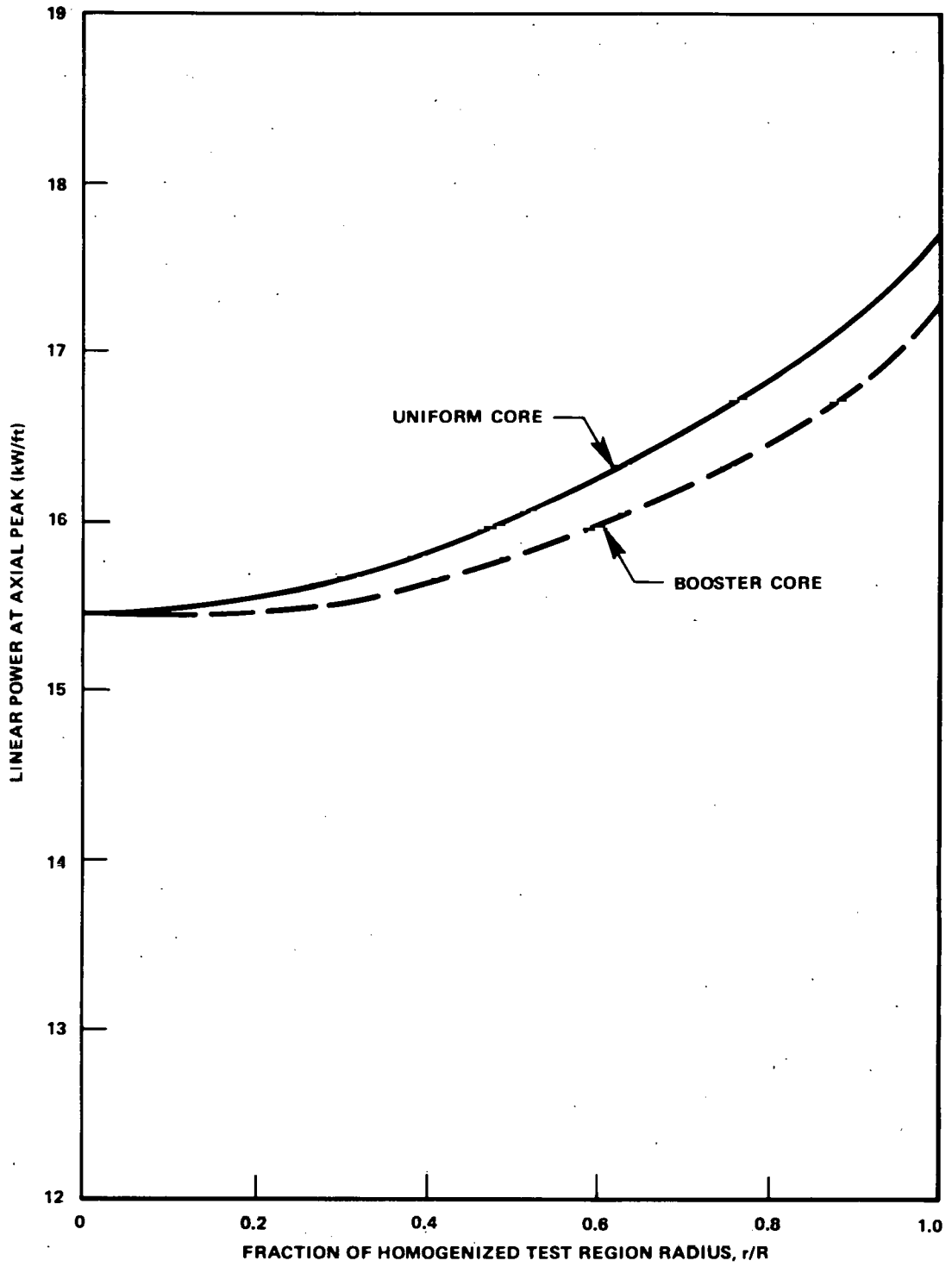


Figure 4B5-2. Radial Power Distribution in Test Fuel Region

**4.2.5.3.4 Test Fuel Linear Power**

Peak test fuel linear powers in Table 4B5-4 were computed using one dimensional (radial) diffusion theory calculation. These values represent the radial average value at the axial peak location, assuming an axial peaking factor of 1.26. In performing the calculations the test fuel is homogenized with the sodium and clad within the region enclosed by the fluted liner. The radial distribution of power within the homogenized region is shown in Figure 4B5-2.

**4.2.5.3.5 Doppler**

The isothermal Doppler coefficients given in Table 4B5-4 were computed using diffusion theory calculations with uniform fuel temperatures of 350°F and 700°F. Only the contribution of U-238 was considered. The Doppler coefficient was computed from

$$A_{Dop} = \frac{\Delta k}{\ln(T_2/T_1)}$$

where

$$\begin{aligned} \Delta k &= k(700^\circ\text{F}) - k(350^\circ\text{F}) \\ T_2 &= (700 + 460)^\circ\text{R} \\ T_1 &= (350 + 460)^\circ\text{R} \end{aligned}$$

Values for  $k(700^\circ\text{F})$  and  $K(350^\circ\text{F})$  were computed.

For the alternate I booster core concept additional Doppler calculations were performed to determine the contribution to the total Doppler from each region. The mismatch in power density between the booster and driver fuel and the large difference in thermal time constant between the small diameter rods and the large diameter rods make this an important consideration in evaluating the transient response of the booster core. The contribution from each region is given below.

Region	Alternate I Contribution to Core Isothermal Doppler
Booster	-0.0010
Inner Driver	-0.0037
Outer Driver	-0.0028

**4.2.5.3.6 Reflector Worth**

The worth of the reflector was estimated using 29 group radial diffusion theory calculations to normalize to the measured Core I value of 9.5\$. The reactivity effect of changing the reflector density by 10% was computed for Core I and for the alternate core designs.

Control requirements for the follow-on core were estimated in the Task I study to total ~6\$, with ~3\$ required for scram. The uniform core would permit these requirements to be met without in-core control. Further evaluation of the control requirements is necessary to substantiate this conclusion.

**4.2.5.3.7 Test Assembly Worth**

The reactivity effect of inserting the reference package loop into the center channel was computed using one-dimensional (radial) diffusion theory for Alternate I. It was estimated that the test assembly worth would be nearly the same for Alternate II and somewhat larger for the uniform core. Additional calculations are required to improve the accuracy of the numbers shown on the table.

**4.2.5.3.8 Test Fuel Slumping Worth**

Estimates of the maximum hypothetical test fuel slumping reactivity were made by first computing the worth of the intact fuel column and normalizing an assumed axial fuel worth curve, then computing the worth of the slumped fuel using the normalized worth distribution. The axial fuel worth distribution was assumed to be proportional to the axial power density distribution which in turn was assumed to be a chopped cosine giving peak to average power ratio of 1.26 ( $P(z) \propto \cos(0.0621z)$ ),  $z$  in inches.

The maximum hypothetical fuel slumping reactivity corresponds to a fuel configuration in which all of the test fuel concentrates around the core midplane, filling all available space inside the Zr Hydride annulus.

Calculations were done for Alternate I. The value of fuel slumping  $\Delta K$  for Alternate II was assumed to be the same as that computed for Alternate I. The increase in fuel slumping worth shown for Alternate III is proportional to the estimated increase in test assembly worth. Further analysis is required to improve the accuracy of this number.

#### 4.2.5.3.9 Sodium Void Reactivity

The reactivity effect of voiding sodium from the core is expected to be negative for all voiding patterns. This expectation is based on the negative void reactivity computed for Core I, the size of the follow-on alternate cores and the presence of BeO in the alternate designs. Calculations will be done to verify this expectation prior to selecting a reference core design.

#### 4.2.5.3.10 Peak Core Fuel Linear Power

The peak core fuel power density was computed using two dimensional diffusion theory with 11 energy groups. Search calculations were specified to give a K of 1.0 with all reflectors up and all in-core control out of the core. For alternate I the fuel rod to steel rod ratio in the outer driver was the search variable. For Alternate II and III the enrichment of the driver fuel was varied. Values given in Table 4B5-4 for the first two alternates are for the booster fuel. The lower value shown for the uniform core is due primarily to the enrichment difference between the booster fuel and the uniform core fuel.

#### 4.2.5.3.11 Core Fuel Peak Centerline Temperature

The peak fuel center temperature was estimated from the calculated peak linear power. It was assumed that the  $\Delta T$  across the fuel is proportional to linear power. A fuel surface temperature of  $1000^{\circ}\text{F}$  was assumed, and the calculation was normalized to give center melting ( $\Delta T = 4000^{\circ}\text{F}$ ) with a linear power of 17 kW/ft.

#### 4.2.5.3.12 Doppler Feedback from 23 MW

The Doppler feedback which would be provided by the core in a rapid transient from 23 MW was calculated using the computed Doppler coefficients. The reactivity given in Table 4B5-4 corresponds to that which would accrue given a rapid energy addition such that the peak core fuel centerline temperature reaches the solidus. The value for Alternate II was assumed to be the same as that computed for Alternate I.

This quantity has both safety and operational significance for the follow-on core. A rough estimate of the magnitude of a rapid reactivity insertion which could be sustained by the core at 23 MW without fuel melting is  $(1 + \Delta k(\text{Dop})/2)$  where  $\Delta k(\text{Dop})$  is the value shown in Table 4B5-4. This assumes that the reactor control system responds to protect the core after the Doppler acts to bring the reactivity below prompt critical.

A tentative conclusion which can be drawn from these numbers is that super-prompt transients can be initiated from near full power for these core design alternates. A final conclusion as to the transient overpower testing capabilities awaits further analysis and safety evaluations.

#### 4.2.5.3.13 Bundle Worth

The reactivity effect of inserting a booster subassembly into the booster region was computed for Alternate I to be 10\$ in the Task I study. It was assumed to be the same for Alternate II in this study. A maximum worth of 5\$ for a uniform driver subassembly was estimated based on the amount of fuel in the subassembly, the amount of fuel in the core, and the calculated worth of a booster subassembly. Further analysis is required to more accurately determine this number.

#### 4.2.5.3.14 Control Rod Worth

Calculations were performed to determine the worth of the in-core control rod design for the Option III-A core. With natural  $\text{B}_4\text{C}$  at 80% theoretical density the calculated rod worth is \$1.01 at the location of the outer refueling port and \$0.65 for the sodium sampling port. With 40% B-10 the calculated rod worths in these locations are \$1.86 and \$1.20. The maximum worth of the reference rod design for the outer refueling port was estimated to be \$3.05 assuming 95% B-10 in  $\text{B}_4\text{C}$  at 80% theoretical density. These results are summarized in Figure 4B5-3. The  $(\rho, \alpha)$  reaction rate is shown in Figure 4B5-4 as a function of boron-10 enrichment.

Analysis was performed using two-dimensional diffusion theory with triangular mesh to obtain a precise description of the rod location in SEFOR. Four neutron energy groups were used in the two-dimensional calculations. Good agreement between four group and 29 group  $\text{B}_4\text{C}$  worth calculations was found using one-dimensional diffusion theory.

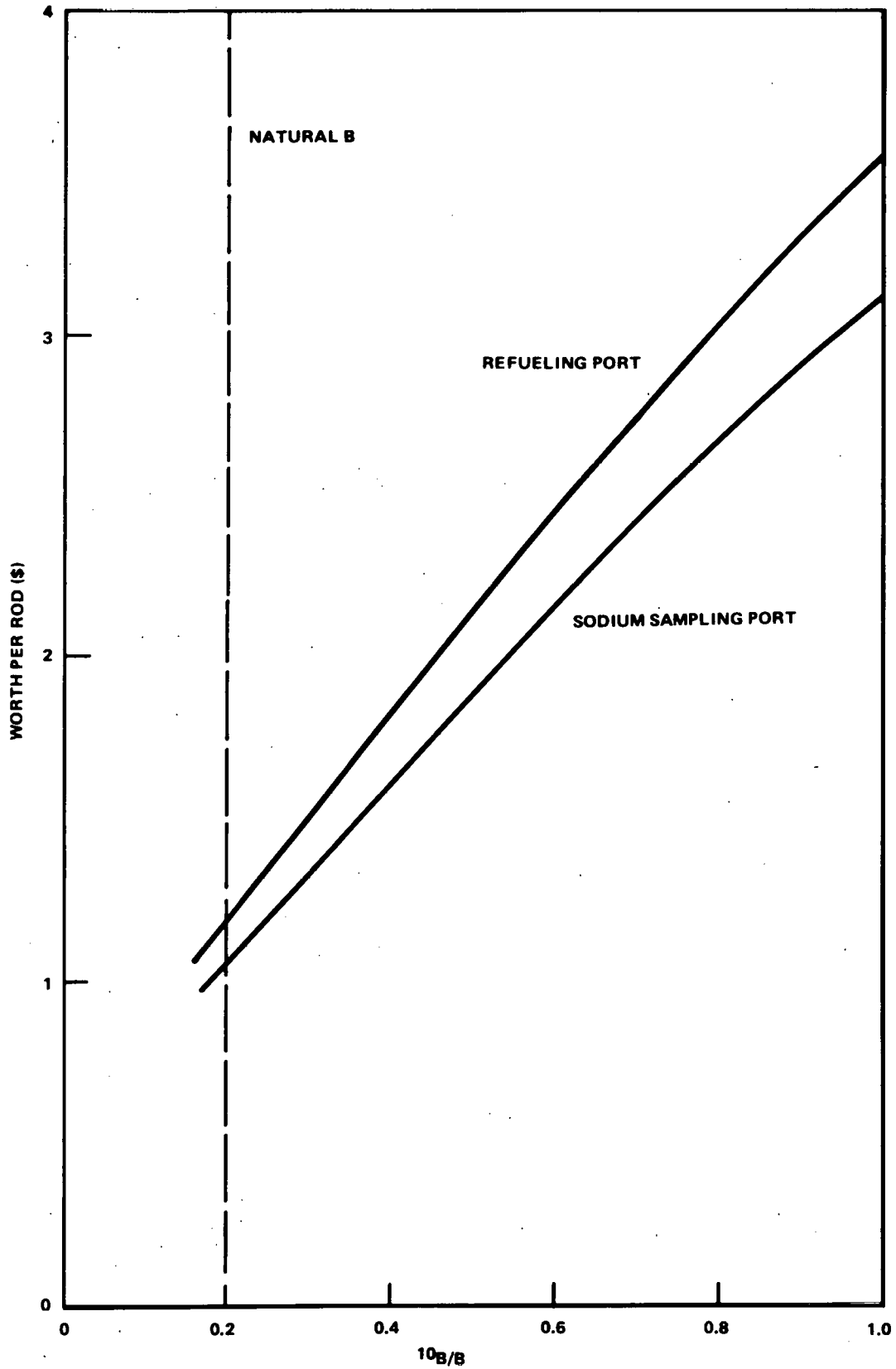


Figure 4B5-3. Absorption Rate in Control Rods,  $(\eta, \alpha)$  versus Boron Enrichment



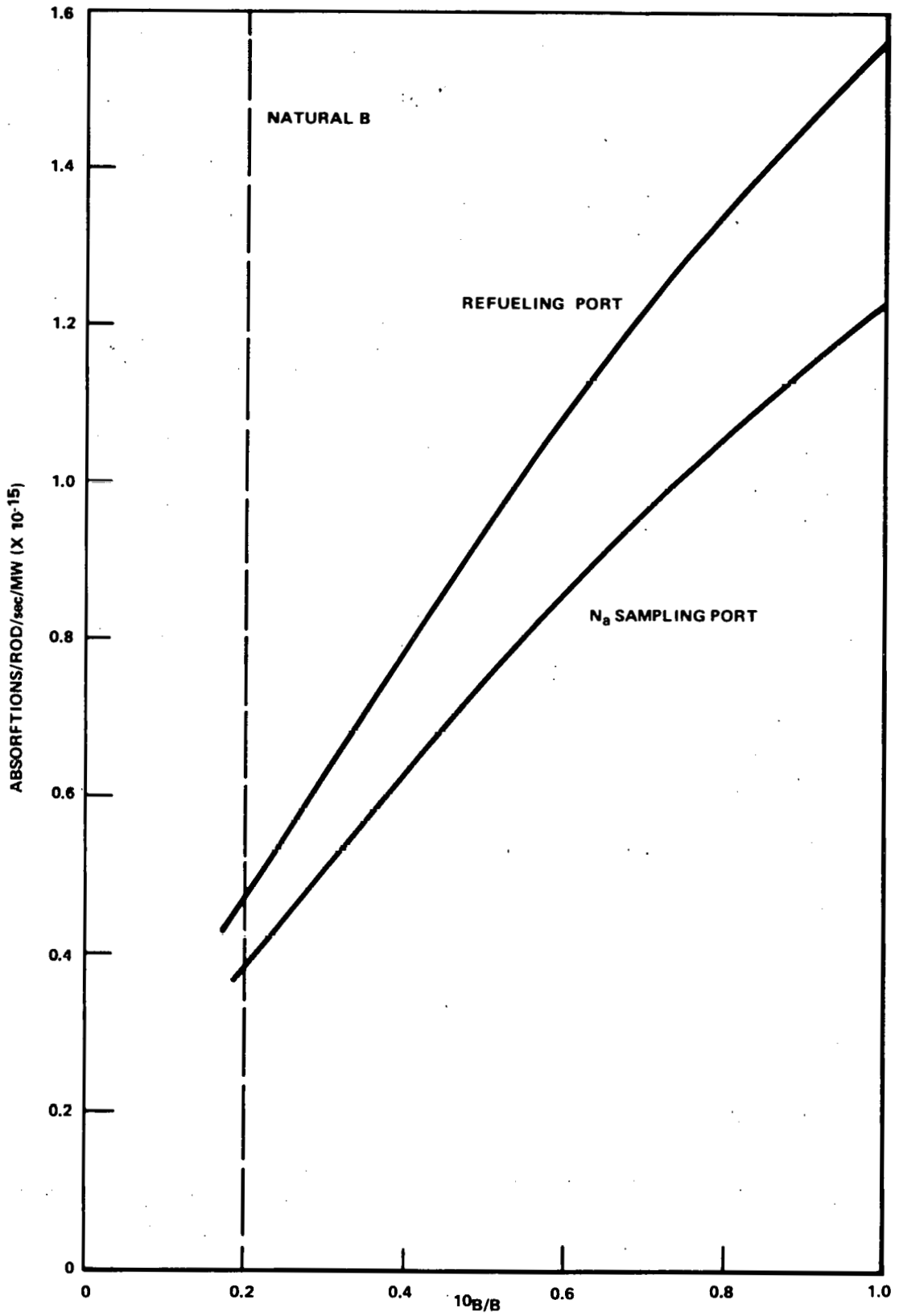


Figure 4B5-4. Control Rod Worth versus Boron Enrichment

**4.2.5.4 Critical Experiments**

The SEFOR Follow-On critical experiments will be performed in the ZPR-9 facility at ANL. A recent meeting with ANL on the critical experiments was held at BRD of GE, Sunnyvale, California on December 7, 1971. At the meeting, GE presented the preliminary specifications of critical experiments and ANL presented the preliminary program plan for the SEFOR Follow-On critical assembly. Based on these presentations, the preliminary test specifications and test program are subsequently described in detail. In addition, the calculations supporting the planning for the critical experiments are also given below.

**4.2.5.5 Preliminary Test Specifications**

**4.2.5.5.1 Scope of Specifications**

The planned engineering mockup critical experiments for the SEFOR Follow-On project are intended to provide physics and engineering data for SEFOR fuel and core design as well as for safety evaluation. A series of critical experiments are to be performed on the mockup using ZPR-9 at ANL. The specifications of the critical experiments are intended to serve as a description of the exact required test data and test sequence. The specifications are comprised of the following sequential tests:

1. Initial Loading to Critical
2. Preliminary Reflector Worth Measurements
3. Reaction Rate Measurements
4. Material Worth Measurements
5. Doppler Measurements
6. Fuel Slumping Test
7. Axial Fuel Expansion Test
8. Sodium Void Experiment
9. Neutron Spectrum Measurements
10. Reflector Worth Measurements
11. Subcritical Measurements

It should be noted that if the design criteria are not met by the measured results at any stage of the critical experiments, an alternate core loading may be specified and the test sequence may be rearranged. In particular, it is planned to review the overall test results following the completion of Doppler measurements. Should it be necessary to specify an alternate core loading, the test items 1 through 5 will be repeated.

**4.2.5.5.2 Responsibilities**

The division of responsibilities between ANL and GE is briefly described as follows:

**GE Responsibilities**

1. Specify material requirements for mockup.
2. Specify critical experiments. The experimental objectives, required data and priorities should be included in the specifications.
3. Calculate experimental results using available GE computer codes prior to critical experiments.
4. Inform ANL for any core design changes.
5. Review and comment on ANL proposed mockup.
6. Assign a GE engineer to ZPR-9 at ANL if necessary. The assigned engineer should coordinate with ZPR-9 personnel for the critical experiments and assist ANL in transmitting experimental data to GE.
7. Analyze test results upon receiving experimental data from ANL.

**ANL Responsibilities**

1. Procure required material for mockup according to GE specifications.
2. Work out mockup details with GE agreement.
3. Perform critical experiments according to GE specifications.
4. Calculate and analyze experimental results.
5. Transmit experimental data to GE.

4.2.5.5.3 Specifications

- Initial Loading to Critical
  - Objective
 

The objective is to determine the minimum critical size (mass) and to determine the ratio of the fuel rods to stainless steel rods in the outer driver region for the full size core.
  - Background
 

The initial loading to critical, which is the first step in the whole series of critical experiments, is carried out in order to establish a critical condition on the mockup in a systematic and safe manner. The minimum critical provides a check on calculations and information for a full size critical. The full size critical is a required test condition for starting experimental measurements.
  - General Procedure
 

The fuel loading is started in the calandria which is located in the center region of the mockup. The standard method of loading fuel from center out is used. Fuel should be added so as to maintain a cylindrical array of fuel. The critical condition will be achieved when the radial reflector is fully inserted in the critical assembly and the nuclear power is zero. The following two critical conditions are requested:

    - Minimum Critical
 

For this critical condition, there will be no stainless steel rods in the outer driver. The fuel rods are to be loaded in the outer driver to reach criticality.
    - Full Size Critical
 

For this critical condition, the outer driver will be loaded with fuel rods and stainless steel rods. The fuel rods and stainless steel rods will be uniformly distributed and the ratio of the fuel rods to stainless steel rods will be adjusted for a full size critical.
  - Priority Assignment
 

Minimum Critical:	Preferred
Full Size Critical:	Required
  
- Preliminary Reflector Worth Measurements
  - Objective
 

The objective is to provide preliminary information on reflector worth for core design evaluation.
  - Background
 

The reflector worth is one of the most important parameters in core design. It is planned to find out at an early stage of the critical experiments, whether the design criteria in reflector worth can be met by the measured results.
  - General Procedure
 

During the initial loading to critical, the fuel is first loaded, and the reflector is then loaded in arcs. The subcritical reactivities are measured using the subcritical monitoring system which employs source multiplication and noise analysis.
  - Priority Assignment
 

Preliminary reflector worth measurements: Required.
  
- Reaction Rate Measurements
  - Objective
 

The objective is to establish a complete mapping of the power distribution throughout the assembly and to determine the fission ratios of U-238, Pu-239, U-235, Pu-240 and Pu-241.
  - Background
 

The reference core has a test fuel region, a booster, an inner driver, and an outer driver. Because of the different fuel compositions in each region and the presence of the  $Zr_{1.6}$  annulus around the test fuel, it is expected that the spatial neutron flux variations in shape as well as in spectrum will not be the same as that in a uniform core. For this reason, foil irradiations at

more locations become necessary. It is of particular interest that the power generation in the test fuel be known in terms of percentage of the total power generation and that the axial peak-to-average factor in the test fuel be determined.

— General Procedure

The thin metallic foils of U-238, U-235, and Pu-239 are used for irradiation traverses. The fission product gamma activities of the irradiated foils are counted in order to find the relative reaction rates. The measured reaction rates from the axial foil irradiation traverses and from the radial foil irradiation traverses are used for a mapping of the power distribution. The fission ratios are obtained using the absolute fission counters. It is planned to change the thickness of the  $ZrH_{1.6}$  annulus from 0.20 inch to 0.15 inch and repeat the reaction rate measurements inside the central subassembly.

— Priority Assignment

Reaction rate measurements with 0.20 inch  $ZrH_{1.6}$ : Required

Reaction rate measurements with 0.15 inch  $ZrH_{1.6}$ : Desired.

● Material Worth Measurements

— Objective

The objective is to measure the reactivity worth of the  $ZrH_{1.6}$  annulus, the worth of the test fuel, the worth of the fuel subassembly in booster region, the worth of the calandria, the worth of the simulated  $B_4C$  control rod at different locations, and the radial and axial small sample reactivity worths.

— Background

The material worth measurements are necessary in order to perform fuel handling and core reactivity adjustment. The  $ZrH_{1.6}$  annulus is a special material in the core and its reactivity effect should be known. The reactivity effect due to removal of the test loop is of interest and can be measured by replacing the calandria with sodium in the mockup.

— General Procedure

The techniques in measuring reactivity include control rod compensation, inverse kinetics, source multiplication, etc. The reactivity changes are measured for the following conditions:

19 test fuel pins are replaced with sodium  $ZrH_{1.6}$  annulus is replaced with sodium

$ZrH_{1.6}$  annulus is replaced with sodium

Calandria is replaced with sodium

Fuel subassembly measurement in booster region, inner driver, outer driver

$B_4C$  control rod measurement at 3 different radial positions

Axial and radial small sample reactivity traverses.

— Priority Assignment

All measurements are required.

● Doppler Measurements

— Objective

The objective is to provide the magnitude of the SEFOR Doppler coefficient which is required information for safety evaluation.

— Background

The reference core has a test fuel region, a booster, an inner driver, and an outer driver. Because of the different fuel compositions in each region and the presence of the  $ZrH_{1.6}$  annulus around the test fuel, the spatial Doppler coefficient variations are expected to be larger than that in a uniform core. The calculated results for the reference core are given below:

Region	Radius, cm	Sample	Doppler Coefficient $\frac{dk}{dT} / \text{kg}$
Booster I	4.214162→ 6.525983	U-238	$-2.46 \times 10^{-5} \frac{\Delta k}{k} / \text{kg}$
Booster II	6.525983→ 8.837804	U-238	$-1.43 \times 10^{-5} \frac{\Delta k}{k} / \text{kg}$
Booster III	8.837804→ 11.149625	U-238	$-1.11 \times 10^{-5} \frac{\Delta k}{k} / \text{kg}$
Inner Driver	11.149625→ 25.633749	U-238	$-0.97 \times 10^{-5} \frac{\Delta k}{k} / \text{kg}$
Outer Driver	25.633749→ 43.997146	U-238	$-0.41 \times 10^{-5} \frac{\Delta k}{k} / \text{kg}$

- General Procedure  
A Doppler-oscillator drawer, running through both reactor halves, is used for the Doppler measurements. A calibrated Servo-controlled autorod is used to measure the reactivity worth of the Doppler sample relative to the reference. It is planned to measure the U-238 Doppler effect in the booster, the inner driver, and the outer driver.
- Priority Assignment  
U-238 Doppler sample measurements: Required

- Fuel Slumping Test

- Objective  
The objective is to measure the reactivity effect due to a 19-pin fuel slumping in the test fuel region.
- Background  
The hypothetical fuel slumping accident is that the melting fuel moves symmetrically from both ends of the core toward the midplane and the slumped fuel region contains no steel or sodium, permitting the slumping reactivity worth to be the maximum value.
- General Procedure  
In principle, the fuel slumping test is to be performed by placing the total amount of the test fuel in the midplane region inside the  $ZrH_{1.6}$  annulus and measuring the reactivity change.
- Priority Assignment  
Fuel Slumping Test: Required

- Axial Fuel Expansion Test

- Objective  
The objective is to measure the reactivity effect due to axial fuel expansion in different regions.
- Background  
The two segment fuel rods, which have no significant expansion effect, are loaded in the outer driver. However, the fuel in the other regions has no provisions to reduce the axial expansion effect, and hence the reactivity effect due to axial expansion needs to be measured.
- General Procedure  
It is planned to measure the fuel expansion reactivity effect in the test fuel region, the booster, and the inner driver. The expansion is to be simulated by inserting the spacers (empty cans) into the fuel drawers.
- Priority Assignment  
Axial fuel expansion test: Desired

- Sodium Void Experiment

- Objective  
The objective is to determine the reactivity worth of the sodium voiding at different locations.
- Background  
Loss-of-flow tests in the package loop are planned for SEFOR and are intended to lead to localized overheating and voiding of the test fuel region. The reactivity effect from sodium voiding is of interest.
- General Procedure  
The reactivity changes are to be measured for the following cases:  
(1) The sodium cans in the upper half of the test fuel region are replaced with empty cans.  
(2) The sodium cans in the whole test fuel region are replaced with empty cans.  
In addition, the axial and radial void sample reactivity traverses in the core are to be made.
- Priority Assignment  
Sodium Void Experiment: Required.

- Neutron Spectrum Measurements

- Objective  
The objective is to measure the neutron spectra in the mockup.
- Background  
The inaccuracy in the calculated spectra may cause a discrepancy between the experimental results and the calculated results. It is important that the various sources of systematic errors in the calculational techniques and in the measurements be known.
- General Procedure  
The proton-recoil technique is employed in neutron spectrum measurements. This technique involves using proton-recoil proportional counters. An alternate method in neutron spectrum measurements is to employ the time of flight technique. It is planned to measure the neutron spectra at the midplane of the booster, the midplane of the inner driver and the midplane of the outer driver.
- Priority Assignment  
Neutron spectrum measurements: Preferred.

- Reflector Worth Measurements

- Objective  
The objective is to measure the reactivity worth of a 36° segment radial reflector, the reactivity worth of a 90° segment radial reflector, and the reactivity worth of the whole radial reflector.
- Background  
The radial reflector provides the means of reactor scram and the means of reactivity control in the SEFOR core. The results of the reflector worth measurements are required for SEFOR core design.
- General Procedure  
The techniques in measuring reactivity include rod drop, source multiplication, noise analysis etc. The radial reflector is initially fully inserted. Next, a 324° segment and then a 270° segment are allowed to remain in place and later only a 72° segment is left in place and finally the radial reflector is completely removed. An additional worth measurement of the 288° segment is to be performed after increasing the thickness of the B<sub>4</sub>C shield to the design value.
- Priority Assignment  
Worth measurement of 36° segment reflector: Required.  
Worth measurement of 90° segment reflector: Required.  
Worth measurement of 288° segment reflector: Required.  
Worth measurement of whole radial reflector: Required.

- Subcritical Measurement

- Objective  
The objective is to measure  $\beta/\lambda$  and shutdown margin.

- Background  
The subcritical measurement employs the source multiplication and noise analysis. The measurement of  $\beta/\lambda$  is necessary for dealing with the reactor dynamics and the measurement of shutdown margin is necessary for reactor operation from the safety point of view.
- General Procedure  
During the reflector worth measurements, the subcritical monitor system is in place. The noise analysis is used to measure  $\beta/\lambda$  and can be used to normalize the subcritical monitor reactivity measurement using source multiplication technique. After the reflector is completely removed, insert all three in-core control rods for additional reactivity measurement using source multiplication technique. Finally, replace the calandria with sodium and make the last reactivity measurement.
- Priority Assignment  
Subcritical measurement: Desired.

#### 4.2.5.6 Preliminary Test Program

##### 4.2.5.6.1 Scope of the Preliminary Test Program

The present planning for critical experiments is based on the SEFOR Follow-On Option 3A core which is composed of test region, booster, inner driver, and outer driver. Based on the preliminary specifications, the preliminary test program describes the measurements, techniques, equipment, and time estimation for the specified tests.

##### 4.2.5.6.2 Test Program

- Initial Loading to Critical

After the completion of the present FTR program in ZPR-9, the following steps will be performed:

- (1) Unload FTR fuel, radial shield and B<sub>4</sub>C control zones
- (2) Perform annual checkout of facility
- (3) Remove back drawers and clean matrix tubes
- (4) Align matrix
- (5) Load back drawers and preload core drawers
- (6) Decontaminate cell, prepare for fuel loading and install safety and control rods
- (7) Approach to critical
- (8) Achieve critical
- (9) Calibrate safety rods and measure temperature coefficients.

The initial fuel loading to critical begins with a preloaded core (drawers loaded with all materials except fuel), and then, fuel is added from center out. A number of fission chambers and BF<sub>3</sub> proportional counters are located in and around the assembly for recording the count rates. The count rates are recorded after each loading step, and a plot of inverse count rate versus mass of fuel should yield a curve which extrapolates to the critical mass as the critical mass is approached. It is noted that consideration is given to loading first the fuel and then the reflector in arcs in order to have the preliminary reflector worth measurements. The criticality can be achieved by adjusting fuel after the reflector is fully inserted. The estimated time for the initial loading to critical is 92 work days.

- Preliminary Reflector Worth Measurements

During the initial loading to critical, the subcritical monitoring system is in place. After the fuel is loaded, a measurement is made using the subcritical monitoring system. Subsequent measurements are made in a similar manner when the 180° segment reflector, 270° segment reflector and finally the whole radial reflector are installed. During the preliminary reflector worth measurements, the fuel may be reduced or the safety rods may be used if the loaded fuel is over estimated. The criticality is achieved by adjusting fuel after the completion of the preliminary reflector worth measurements. It is noted that the subcritical monitoring system employs both noise technique and source multiplication technique. The estimated time for the preliminary reflector worth measurement is 14 work days. However, the time required for the measurements is included in the initial loading time.

- Reaction Rate Measurements

An accurate mapping of the power distribution in the test fuel is desirable. It is necessary that the thin metallic foils of U-235 and U-238 be placed along three fuel pins at different radii. The power distribution inside the fuel pins should also be measured. The axial and radial foil irradiation traverses in the booster, inner driver, and outer driver cover the periphery of the core and the boundaries between regions. The foils of U-238, U-235, and Pu-239 are used for irradiation traverses in each region. The radial traverses at Z = 0, 6, 12, and 17.5 inches with one more detailed axial traverse in each region are planned.\* The absolute fission ratios among Pu-239, Pu-240, Pu-241, U-238 and U-235 are obtained using Kirn type gas flow fission counters. The absolute fission ratios are measured at one location and are used to normalize the foil fission traverses. It is planned to change the thickness of the ZrH<sub>1.6</sub> annulus from 0.20 inch to 0.15 inch and repeat the reaction rate measurement inside the central subassembly. The estimated time for the reaction rate measurements is 26 work days.

\*Z is taken as the axial dimension in the critical assembly and Z=0 is located at the axial midplane of the assembly.



- **Material Worth Measurements**

The following are the replacement type measurements:

- (1) 19 test fuel pins are replaced with sodium
- (2)  $ZrH_{1.6}$  annulus is replaced with sodium
- (3) Calandria is replaced with sodium
- (4) Fuel subassembly measurements in booster region, inner driver and outer driver.
- (5)  $B_4C$  control rod measurements at three different radial positions.

The replacement type measurement involves determining a reference critical position and measuring a subcritical condition. The subcriticality is determined both from the rod drop using an inverse kinetics code and from a noise technique.

The following materials are used for small-sample reactivity measurements:

Pu-239, U-238, SS, Na,  $PuO_2$  (11.5% Pu-240)

U-235, Boron,  $B_4C$ , Ta, Mo,  $U-238O_2$

The radial worth traverse is measured at  $Z=0$  using the radial Pneumatic Sample Changer. The axial worth traverse is measured in the booster region, inner driver and outer driver using the modified Pneumatic Sample Changer. The estimated time for the material worth measurement is 72 work days.

- **Doppler Measurements**

The standard Doppler equipment modified for off-center measurements is used. The 12-inch long by 1/2-inch diameter Doppler element is employed, although it may be necessary to go to the 1-inch diameter element if the signal is too small in some locations. The Doppler reactivity is measured using the calibrated autorod and the accuracy is generally very good.

The  $U-238O_2$  Doppler measurements are made in the following locations:

- (1) Center of booster at  $Z=0$  midplane of core, and 12 inches.
- (2) Center of partially sodium-voided booster at  $Z=0$ .
- (3) Center of inner driver at  $Z=0$ .
- (4) Center of outer driver at  $Z=0$  and 12 inches.
- (5) In the outer driver near the radial reflector boundary at  $Z=0$ .

The estimated time for the Doppler measurements is 58 work days.

- **Fuel Slumping Test**

For simulating the fuel slumping accident reactivity effect, the enriched fuel pellets are removed from the test fuel calandria and placed in a special container at the midplane. Meanwhile, the calandria is filled with sodium and moved axially away from  $Z=0$ . The reactivity associated with both pellet and calandria movement is measured using a calibrated control rod or the standard subcritical measurement technique.

It is planned to oscillate a small U-235 sample through one of the test fuel calandria pin holes. This involves development of a new piece of equipment. When the reactivity effect for each material is known, the reactivity change due to any fuel slumping can be calculated. The estimated time for the fuel slumping test is 38 work days.

- **Axial Fuel Expansion Test**

The axial worth measurements give the fuel expansion data. The small spacers between the pellets in the test fuel-region may be used to simulate the expansion. The reactivity change can be measured using either a calibrated control rod or the subcritical measurement technique. The estimated time for the axial fuel expansion test is 10 work days.

- **Sodium Void Experiment**

The sodium voiding of the test fuel region is of primary interest. The reactivity changes are measured with a calibrated control rod for the sodium-voided test fuel calandria. The radial and axial small sample sodium

worth measurements provide the sodium worth values for each region. In addition, a replacement type sodium-void measurement is planned in the booster region to supplement the small sample sodium worth data. The estimated time for the sodium void experiment is 16 work days.

- Neutron Spectrum Measurements

Regional neutron spectrum measurements are planned. Measurements are to be made using the proton recoil counters in the booster, inner driver and outer driver regions at Z=0. The energy range covered by these counters is about 1 KeV to 2 MeV. The estimated time for the neutron spectrum measurements is 18 work days.

- Reflector Worth Measurements

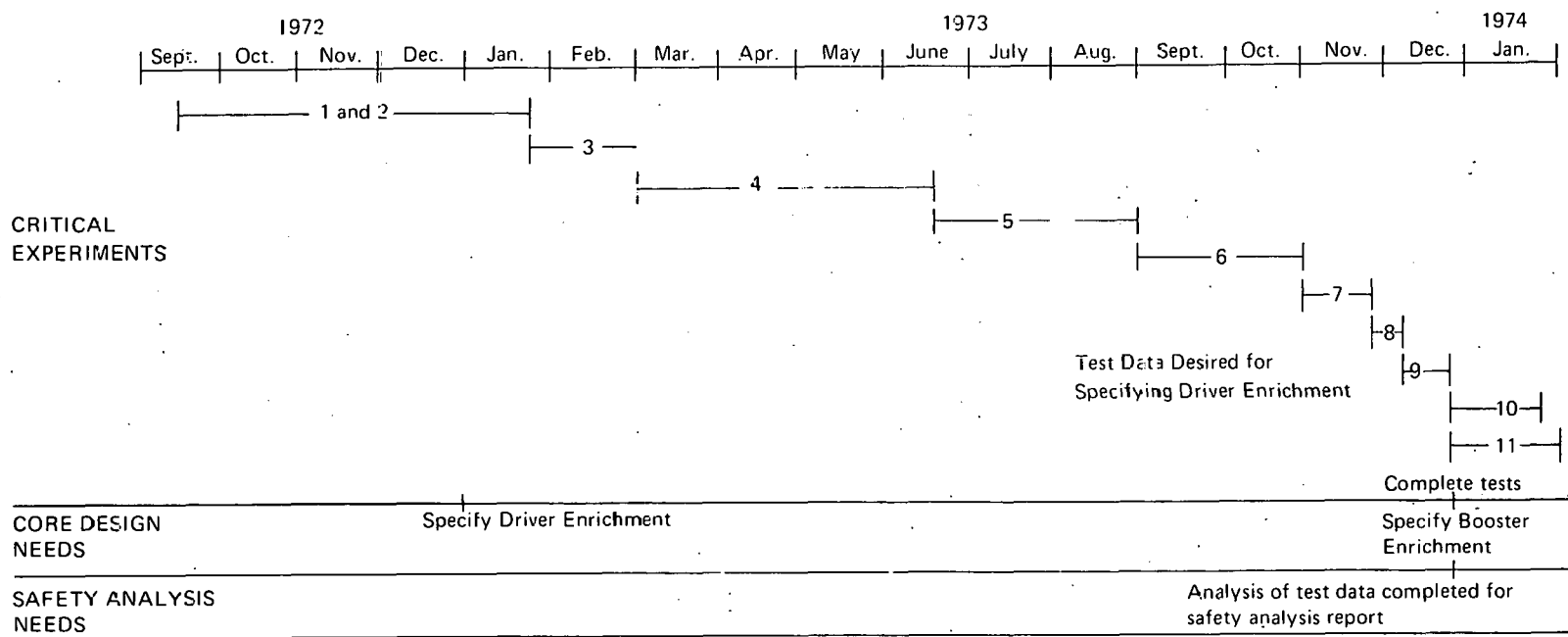
The techniques in measuring reactivity include rod drop, source multiplication, noise analysis etc. The radial reflector is initially fully inserted. Next, a 324° segment and then a 270° segment are allowed to remain in place and later only a 72° segment is left in place and finally the radial reflector is completely removed. An additional worth measurement of the 288° segment is to be performed after increasing the thickness of the B<sub>4</sub>C shield to the design value. The estimated time for the reflector worth measurements is 18 work days.

- Subcritical Measurement

During the reflector worth measurements, the subcritical monitor system is in place. The noise analysis is used to measure  $\beta/\lambda$  and can be used to normalize the subcritical monitor reactivity measurement using source multiplication technique. Insert all three in-core control rods after the reflector is completely removed for the additional reactivity measurement using source multiplication technique. Finally, replace the calandria with sodium and make the last reactivity measurement. The estimated time for the subcritical measurement is 22 work days.

#### 4.2.5.6.3 ZPR-9 Schedule

The present FTR program is scheduled to end by August 1, 1972, but additional experiments requested by FTR will probably extend to mid-September 1972. Attached is a chart schedule based on the estimated experimental time. The schedule requirements of the critical experiments, the core design needs and the safety analysis needs are shown. The preliminary plan for the critical experiments does not meet the needs of the core design and licensing. Changes required to accommodate the experimental tests to the core design and safety analysis needs are under study by GE and ANL.



- 1 - Unload FTR core, prepare facility for loading, annual checkout, loading to critical, safety rod calibration and temperature coefficient measurement.
- 2 - Preliminary reflector worth measurements
- 3 - Reaction rate measurements
- 4 - Material worth measurement
- 5 - Doppler measurements

- 6 - Fuel slumping test
- 7 - Axial fuel expansion test
- 8 - Sodium void experiment
- 9 - Neutron spectrum measurements
- 10 - Reflector worth measurements
- 11 - Subcritical measurements

#### 4.2.5.7 Calculations

##### 4.2.5.7.1 Introduction

During the planning for critical experiments in the past, there were the following problems:

- (1) Shortage of  $B_4C$  for the radial shield mockup.
- (2) Excess stainless steel in the booster region due to required canning, cladding and structure on the critical assembly.
- (3) Unavailability of SS-316 stainless steel for mockup

Calculations were done in order to investigate the effects on the core characteristics due to these problems.

##### 4.2.5.7.2 Thickness Reduction of $B_4C$ Shield

ANL had indicated that there was not enough  $B_4C$  for the radial shield mockup. An investigation of reactivity effects on the reflector worth measurement due to the thickness reduction of  $B_4C$  shield was conducted. Diffusion theory calculations using one-dimensional code were performed to estimate the reflector worth for five different  $B_4C$  thicknesses and the results are given in Table 4B5-5. It can be seen that there is no significant reactivity effect ( $\sim 1\%$ ) on the reflector worth measurement for a  $B_4C$  thickness reduction from the SEFOR design value to one quarter of the design value.

##### 4.2.5.7.3 Excess Stainless Steel

The stainless steel in the booster region on the critical assembly was expected to be too high by 22% due to required canning, cladding and structure. The excess steel may affect the neutron energy spectrum and  $k_{eff}$ . Diffusion

Table 4B5-5

REFLECTOR WORTH FOR DIFFERENT B<sub>4</sub>C THICKNESSES

Thickness of B <sub>4</sub> C Shield	Corrected Reflector Worth \$
100%*	7.27
75%	7.29
50%	7.31
25%	7.33
0%	7.75

\*100% is defined as the SEFOR design thickness (13.481 cm).

theory calculations using a one-dimensional code were performed to determine the Doppler coefficient change due to 30% excess steel in the booster region and the results are given in Table 4B5-6. It can be seen that the Doppler Coefficient ( $T dk/dT$ ) of the booster region is  $-1.17 \times 10^{-4} \delta k/k$  for the 30% excess steel case and  $-1.14 \times 10^{-3} \delta k/k$  for the normal case. There is approximately a 3% effect on the Doppler coefficient for the 30% excess steel. In addition, the 30% excess steel causes an increase of 0.0011 in  $k_{eff}$ . More calculations were performed to determine the power generation distribution in the core both for the 30% excess steel case and the normal case, and the results are given in Table 4B5-7. It appears that there is no significant difference in power generation distribution between the two cases.

Table 4B5-6

DOPPLER COEFFICIENT OF BOOSTER REGION

Temperature Change	Excess Steel in Booster	$k_{eff}$ Change	Doppler Coefficient $(T \frac{dk}{dT})$
350°F → 700°F	None	1.03617100 → 1.03604694	$1.147 \times 10^{-3}$
700°F → 1120°F	None	1.03604694 → 1.03568178	$1.140 \times 10^{-3}$
350°F → 700°F	30%	1.03759906 → 1.03715979	$1.178 \times 10^{-3}$
700°F → 1120°F	30%	1.03715979 → 1.03678432	$1.171 \times 10^{-3}$

6

**4.2.5.7.4 Unavailability of SS-316**

Since there was no SS-316 available at ANL, it was planned to replace SS-316 with SS-304 for the SEFOR mockup. Diffusion theory calculations using one-dimensional code in 11 groups were performed to compare the neutron energy spectra for the normal case with that for the replacement case. The calculated results are given in Table 4B5-8. It appears that there is no significant difference in spectra between the two cases. The difference in  $k_{eff}$  is 0.00242.

Table 4B5-7

**POWER GENERATION**

Excess S.S.	Test Fuel	Booster	Inner Driver	Outer Driver
None	2.55%	28.22%	28.74%	40.49%
30%	2.61%	28.56%	28.81%	40.00%

Table 4B5-8

SPECTRA COMPARISON

Energy Group	1	2	3	4	5	6	7	8	9	10	11	Remarks
Energy Range	2.23MeV ↓ 6.06MeV	820keV ↓ 2.23MeV	302keV ↓ 820keV	111keV ↓ 302keV	40.5keV ↓ 111keV	15keV ↓ 40.5keV	5.5keV ↓ 5.5keV	2.01keV ↓ 5.5keV	750eV ↓ 2.01keV	101.5eV ↓ 750eV	0.25eV ↓ 101.5eV	
Spectrum (%) Case I	8.8241	17.2726	22.4416	20.6864	12.8169	8.1399	4.5992	1.5568	2.1972	1.2065	0.2588	$k_{eff}=1.03888$
Spectrum (%) Case II	8.8152	17.2474	22.4215	20.6739	12.8139	8.1910	4.5880	1.5622	2.2148	1.2120	0.2600	$k_{eff}=1.04130$

Case I: Normal Case

Case II: SS316 are replaced with SS304

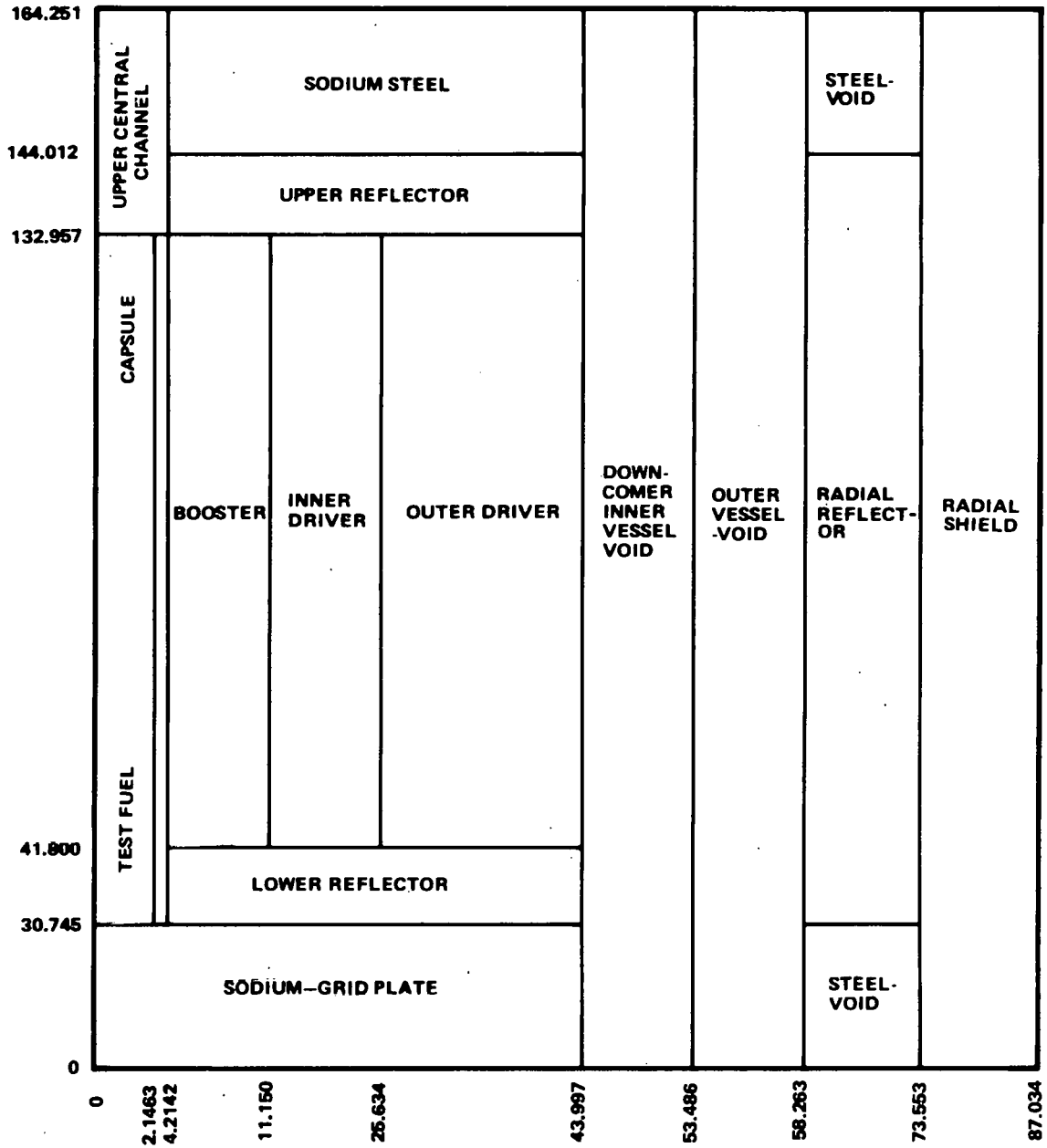


Figure 4B5-5. SEFOR Reference Core Geometry, SEFOR Follow-On, Option III



4.2.5.8 Cross-Section File Generation

Two 29-group cross-section libraries for the SEFOR Follow-On nuclear analysis have been generated, one in MUG\* and one in SNLIB\* format. U-238 and Pu-240 cross sections are given for 350, 700, and 1400°F in capsule and driver regions and for 350, 700, and 1120°F in the booster. The reactor configuration is shown in Figure 4B5-5 and a listing of available materials by region is given in Table 4B5-9 for MUG format and Table 4B5-10 for SNLIB. Tape assignments will be available in the near future.

Cross sections of all materials except zirconium were obtained through TDOWN from the GMUG2\*\* library. Zirconium cross sections and inelastic scattering matrix, given in Table 4B5-11 were calculated from BAS04\*\*\* 60-group values. Compositions used to obtain self-shielded cross sections are summarized in Table 4B5-12.

Corrections to the elastic removal cross sections in the core and driver regions and the vessel and shroud were made using one-dimensional diffusion calculations on the SEFOR Follow-On Option 3 reference core. Elastic removal cross sections for the axial reflector materials were corrected using fluxes computed for the radial reflector. Corrections to the elastic removal cross sections for the upper shield and grid plate materials were made using fluxes computed for the vessel and shroud.

SEFOR FOLLOW-ON

CROSS SECTION GROUP STRUCTURE

29Gp.	$\Delta u$	$\sim E_g$	11 Gp.	$\Delta u$	$\sim E_g$	4 Gp.	$\Delta u$	$\sim E_g$										
1	0.5	6.06 MeV	}	1	1.5	2.23 MeV	}	1	2.5	820 keV								
2	0.5	3.68		2	1.0	820 keV		}	2	2.0	111 keV							
3	0.5	2.23		3	1.0	302			}									
4	0.5	1.36		4	1.0	111												
5	0.5	820 keV		5	1.0	40.5	}		}	}	}							
6	0.5	495		6	1.0	15		}				}	}	}				
7	0.5	302		7	1.0	5.5									}	}	}	}
8	0.5	182		8	1.0	2.01	}	}	}	}								
9	0.5	111		9	1.0	750 eV					}	}	}	}				
10	0.5	67		10	2.0	101.5	}	}	}	}								
11	0.5	40.5		}	}	}					}	}	}	}	}			
12	0.5	24.5	}				}	}	}	}						}	}	}
13	0.5	15																
14	0.5	9.1	}				}	}	}	}						}	}	}
15	0.5	5.5																
16	0.5	3.25	}				}	}	}	}						}	}	}
17	0.5	2.01																
18	0.5	1.21	}				}	}	}	}						}	}	}
19	0.5	750 eV																
20	0.5	455	}				}	}	}	}						}	}	}
21	0.5	276																
22	0.5	168	}	}	}	}	}	}	}	}								
23	0.5	101.5									}	}	}	}	}	}	}	}
24	0.5	61.5	}	}	}	}	}	}	}	}								
25	0.5	37.2									}	}	}	}	}	}	}	}
26	0.5	22.6	}	}	}	}	}	}	}	}								
27	1.5	5.0									11	6.0	0.250	}	}	}	}	}
28	1.5	1.11	}	}	}	}	}	}	}	}								
29	1.5	0.250																

\*Cross section file formats presently in use by BRD.  
 \*\*The G.E. Library of self-shielded cross sections based on YENDF/B II data, revised.  
 \*\*\*A G.E. file for LMFBR calculations.

Table 4B5-9

## MATERIALS AVAILABLE ON MUG FILE

File Name: SF029

Number of Groups: 29

Inelastic Downscattering to Group 29

Maximum Number of Downscatter Groups - 15

Materials	Test Fuel	Capsule	Booster	Inner Driver	Outer Driver	Vessel & Shroud	Radial Reflector	Radial Shield	Axial Reflector	Grid Plate	Axial Shield
Cr	1	51	101	151	201	251	301	351	451	501	551
Fe	2	52	102	152	202	252	302	352	452	502	552
Ni	3	53	103	153	203	253	303	353	453	503	553
Na	4	54	104	154	204	254			454	504	554
Oxygen	5		105	155	205				455		
Be				156	206				456		
B-10					207			357		507	
C					208			358		508	
Mo				159	209						
A1						260	310	360			
U-235	11		111	161	211				461		
U-238	12*		112**	162*	212*				462		
Pu-239			113	163	213						
Pu-240			114**	164*	214*						
Be(n,2n)				915	920				945		
U-238(n,2n)	900		900	900	900				900		
H		999									
Zr		40									

\*Cross sections for these materials are given at 350°F. Cross sections at 700° and 1400°F are available by adding 10 and 20 respectively to the 350° material numbers.

\*\*Same as above reference except additional temperatures are 700 and 1120°F.

Table 4B5-10

MATERIALS AVAILABLE ON SNLIB FILE

File Name: SF029  
 Number of Groups: 29  
 Position of IHT: 5  
 Number of Materials: 97

Materials	Test Fuel	Capsule	Booster	Inner Driver	Outer Driver	Vessel & Shroud	Radial Reflector	Radial Shield	Axial Reflector	Grid Plate	Axial Shield
Cr	124	224	324	424	524	624	724	824	924	1024	1124
Fe	126	226	326	426	526	626	726	826	926	1026	1126
Ni	128	228	328	428	528	628	728	828	928	1028	1128
Na	111	211	311	411	511	611			911	1011	1111
O	108		308	408	508				908		
Be				404	504				904		
B-10					505			805		1005	
C					506			806		1006	
Mo				442	542						
A1						613	713	813			
U-235	150		350	450	550				950		
U-238	180*		380*	480*	580*				980		
Pu-239			390	490	590						
Pu-240			300**	400 <sup>±</sup>	500*						
Be(n,2n)				414	514				914		
U-238(n,2n)	185		183	183	183				183		
H	1***										
Zr		4C									

\*Cross sections for these materials are given at 350°F. Cross sections at 700° and 1400°F are available by adding 1 and 2 respectively to the 350° material numbers.

\*\*Same as above reference except additional temperatures are 700° and 1120°.

\*\*\*This material number represents the transport corrected cross sections. P0 and P1 cross sections for hydrogen may be obtained by using material numbers 2 and 3 respectively.

Table 4B5-11

ZIRCONIUM CROSS SECTIONS

Group	Transport	Capture	Elas	Inelas
1	1.0460	0.18000	0.01845	4.4953
2	1.0460	0.18000	0.01845	4.4953
3	2.0190	0.10000	0.08232	2.2519
4	2.8750	0.01400	0.12348	1.3000
5	4.5810	0.01400	0.19482	0.3300
6	6.1800	0.01400	0.26620	0.0
7	7.2320	0.01400	0.30900	0.0
8	7.8100	0.01400	0.33580	0.0
9	8.2750	0.01400	1.7810	0.0
10	8.3544	0.01400	1.8010	0.0
11	8.9200	0.01400	1.9230	0.0
12	8.0340	0.01400	1.7300	0.0
13	8.4760	0.01400	1.0938	0.0
14	7.4370	0.0190	0.9630	0.0
15	8.725	0.0	1.1298	0.0
16	7.346	0.2300-3	0.9504	0.0
17	7.446	0.6800-3	1.6050	0.0
18	6.4351	0.5960-3	0.5944	0.0
19	6.1556	0.8620-3	0.5690	0.0
20	6.1560	0.1126-2	0.5690	0.0
21	6.1560	0.1443-2	0.5690	0.0
22	6.1568	0.1898-2	0.3276	0.0
23	6.1570	0.2438-2	0.2650	0.0
24	6.1578	0.3148-2	0.2650	0.0
25	6.1604	0.5285-2	0.1247	0.0
26	6.1610	0.5800-2	0.08833	0.0
27	6.1646	0.9866-2	0.08833	0.0
28	6.1748	0.2031-1	0.08833	0.0
29	7.3316	0.9962-1	0.03551	0.0

ZIRCONIUM INELASTIC SCATTERING MATRIX (I>I+J)

J (I+..)	I=1	I=2	I=3	I=4	I=5	I=6
1	0.3166	0.3166	0.78539	0.36126	0.0	0.0
2	0.3166	0.5104	0.83904	0.48287	0.13572	
3	0.5104	0.5085	0.37895	0.27910	0.93080-1	
4	0.5085	0.3548	0.14368	0.11254	0.49010-1	
5	0.3548	0.1949	0.88340-1	0.4375-1	0.39060-1	
6	0.1949	0.9183-1	0.1320-1	0.1577-1	0.995-2	
7	0.9183-1	0.3931-1	0.3300-2	0.3900-2	0.220-2	
8	3.931-2	0.1587-1	0.0	0.8100-3	0.180-2	
9	1.587-2	0.6175-2		0.0	0.0	
10	0.6175-2	0.2351-2		0.0		

Table 4B5-11 (Continued)

J (I+..)	I=1	I=2	I=3	I=4	I=5	I=6
11	2.3510-3	0.8796-3		0.0		
12	0.8796-3	0.27999-3		0.0		
13	2.7999-4	0.0		0.0		
14	0.0					
15						
16						
17						
18						
19						
20						
21						
22						
23						
24						
25						
26						
27						
28						
29						
30						
31						
32						
33						
34						

Table 4B5-12

## COMPOSITIONS USED TO OBTAIN SELF-SHIELDED CROSS SECTIONS

	Material	Density (atom/b-cm)
Test Fuel	O	1.3863-2
	Na	6.8598-3
	Cr	2.3025-3
	Fe	8.4830-3
	Ni	1.3330-3
	U-235	6.4465-3
	U-238	4.8520-4
Capsule	H	1.15639-2
	Na	1.45567-2
	Cr	3.01692-3
	Fe	1.11149-3
	Ni	1.74658-3
Booster	O	1.7030-2
	Na	1.0734-2
	Cr	2.0917-3
	Fe	7.7064-3
	Ni	1.2110-3
	U-235	2.5500-5
	U-238	4.2321-3
	Pu-239	3.9170-3
Pu-240	3.4060-4	
Inner and Outer Drivers	Be	3.7768-3
	O	1.5841-2
	Na	6.8099-3
	Cr	6.4207-3
	Fe	2.2629-2
	Ni	3.7745-3
	Mo	2.0170-4
	U-235	1.0560-5
	U-238	4.7926-3
	Pu-239	1.1276-3
	Pu-240	1.0137-4
	Outer driver also contains 1.0-10 atom/b-cm of B-10 and carbon.	
Vessel and Shroud	Na	9.5714-3
	Al	4.1870-3
	Cr	4.4078-3
	Fe	1.4550-2
	Ni	2.9746-3

Table 485-12 (Continued)

	Material	Density (atom/b-cm)
Radial Reflector	Cr	5.4730-3
	Fe	2.0163-3
	Ni	7.4002-2
	Al	2.1517-3
Radial Shield	Cr	1.9430-3
	Fe	7.1585-3
	Ni	1.1249-3
	Al	7.8350-3
	B-10	2.8350-3
	C	1.7809-2
Axial Reflector	U-235	7.4304-5
	U-238	5.5930-6
	Cr	3.7678 3
	Fe	1.3882-2
	Ni	4.0829-2
	O	4.8450-4
	Be	3.2471-4
	Na	6.3937-3
Grid Plate	Cr	3.9508-3
	Fe	1.4556-2
	Ni	2.2873-3
	Na	1.5723-2
	B 10	3.6350-4
	C	2.2832-3
Axial Shield	Cr	5.2623-3
	Fe	1.9300-2
	Ni	3.0466-3
	Na	1.2583-3

## 4.2.6 Task 4B6 - Package

### 4.2.6.1 Objective

The long-term objective of this task is to generate a design for the package loop within which transient safety tests involving overpower and undercooling of test fuel pins and bundles will be conducted during the Option III-A tests. The objectives during Phase A is to complete the conceptual design studies.

### 4.2.6.2 Conceptual Design Studies

Conceptual design studies have been completed for the package Loop.

An outline drawing of the package loop is shown on Figure 4B6-1. The package loop will be installed in the SEFOR vessel in a vertical position suspended from the upper flange. The portion of the loop above the flange which includes the electromagnetic pump and instrumentation connection will extend above the reactor vessel into the refueling cell atmosphere. The portion of the loop below the flange extends downward into the reactor core so that the 30-inch long test fuel region is centered in the reactor core. The loop overall length is 18 feet with a diameter of 2-3/4 inches over the lower portion. The pump stator which is the outer portion of the EM pump is removable and will not be installed during shipping and handling hence the maximum diameter of the loop to be handled will be a 6-1/4-inch flange.

Figure 4B6-2 shows a more detailed assembly drawing of the loop. The path of sodium flow around the loop is indicated by the arrows. The test region of the package loop has the capability to test fuel bundles containing up to 19 fuel pins 1/4 inch in diameter any or all of which may contain pre-irradiated fuel. The test fuel pins have an overall length of approximately 77 inches made up of a 30-inch long fuel zone, an axial blanket of 1/2 inch length below the fuel and 15 inches length above the fuel, and a 30-inch long fission gas plenum in which is located the spring hold down system for the fuel and blanket pellets. The lower end of the fuel pins will terminate in an end fitting which is attached to spacer bars which support the fuel pin assembly. Spiral wire wrap will be used to space and stabilize the fuel pins within the fuel bundle. The package loop design provides a cylinder of zirconium hydride surrounding the 30-inch length of fuel to enhance the test fuel fission cross section. Section D-D of Figure 4B6-2 shows a cross section of the test region of the package loop which includes the 19 fuel rods surrounded by a fluted liner which simulates the effect of another ring of fuel pins, making the test region more typical of a larger array of fuel pins. An inert gas-filled space surrounding the fluted liner is provided for insulation between the inlet flow and the test region.

Sodium flow through the test region will be monitored by two electromagnetic flowmeters one located upstream and one downstream of the test fuel region. Pressure within the package loop test region will be monitored by one or more pressure transducers located just above the fuel pins in the outlet flow from the test region.

The major items of instrumentation on the package loop will be a number of thermocouples distributed over the outer surface of the fluted flow tube which surrounds the test fuel bundle. Approximately 12 thermocouples will be located in the 30-inch fuel region with others located in specific areas of the loop such as flowmeters and pump. One of the most important features of the package loop design is the capability to perform sudden loss-of-flow experiments. Loss-of-flow to the test region is created by a pressure actuated bellows type valve which moves a stopper into an orifice closing off flow to the fuel bundle. Details of the loss-of-flow mechanism are shown on Figure 4B6-2. As shown, flow blockage to the test bundle is complete, however, the design can be modified by the addition of a tube from the orifice to the fuel bundle which would block flow to any desired portion of the test bundle. An 1/8-inch O.D. tube is used to conduct the argon gas which actuates the bellows to close the valve.

All loop instrumentation which includes thermocouples, flowmeters and pressure transducers is combined as a part of a central support tube. Including all instrumentation in one package has advantages such as allowing manufacture on the instrument package to proceed in parallel with the loop manufacture and providing a convenient package loop. A conceptual design for the instrumentation package for the loop is shown in Figure 4B6-3. Figure 4B6-4 shows a sequence of steps that might be followed in assembly of a package loop with pre-irradiated fuel. In this concept the test fuel bundle is remotely inserted through the lower end of the instrumentation package which requires the lower flowmeter and thermocouples to be temporarily moved aside during fuel bundle insertion. Next, the flow separator tube to which the thermocouples are attached is installed over the lower end of the instrument package. Finally, the outer closure tube is installed over the flow separator tube and one closure weld is made.

The loop design and method of assembly that has been described thus far would apply regardless of where the loop will be fabricated. Two alternate facilities have been considered in some detail for the assembly, inspection, sodium filling, and loading into a cask for shipment to the SEFOR site as well as the completion of a post-test examination program. The two assembly sites that have been considered are the RML facility at Valleritos, California



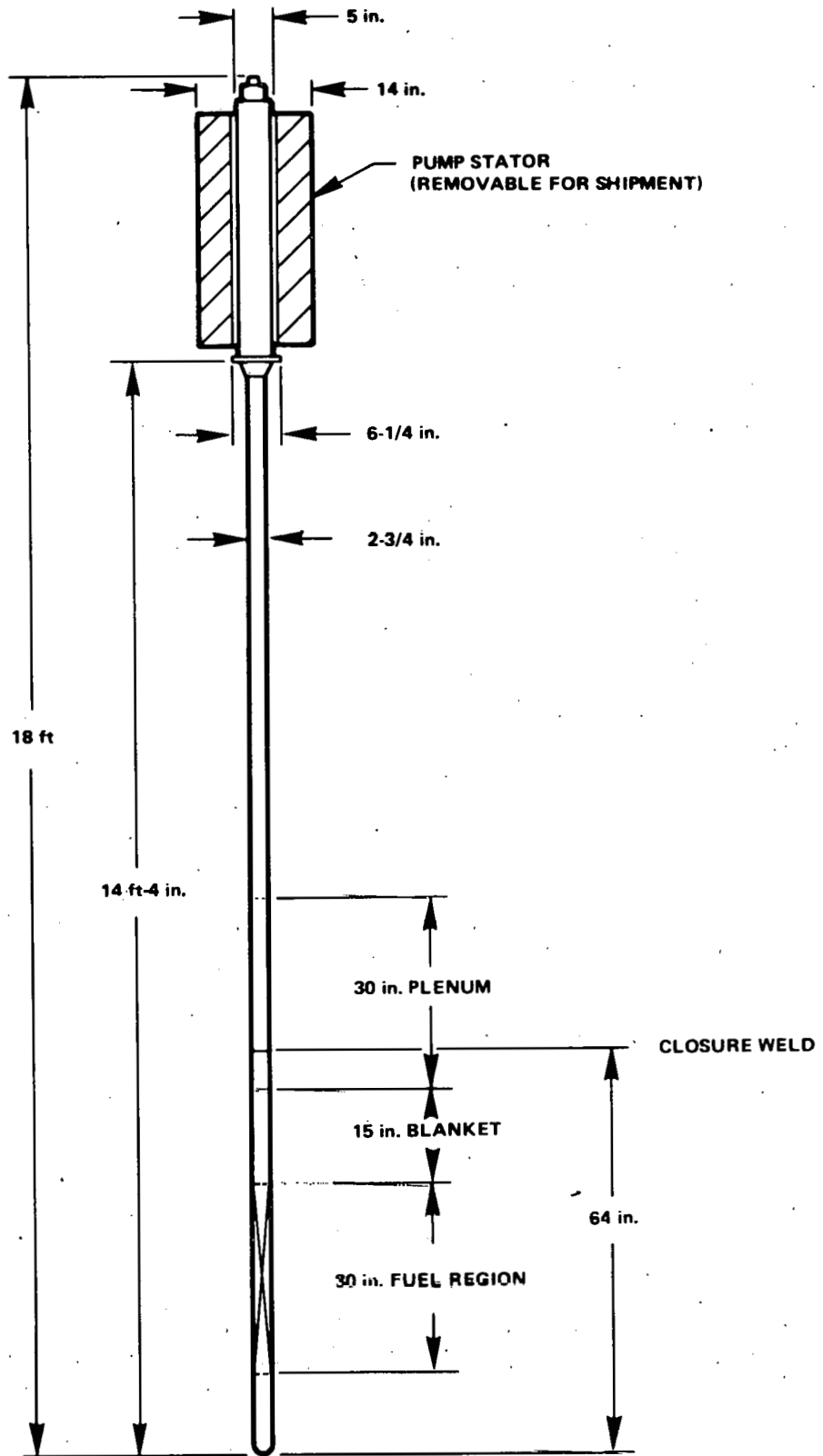
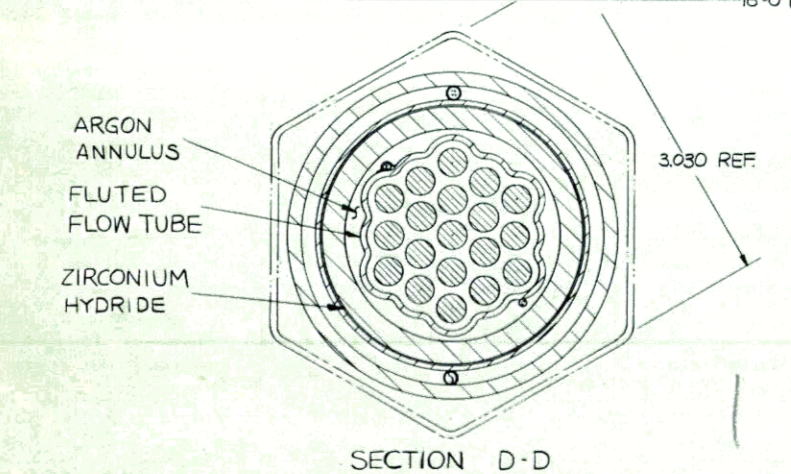
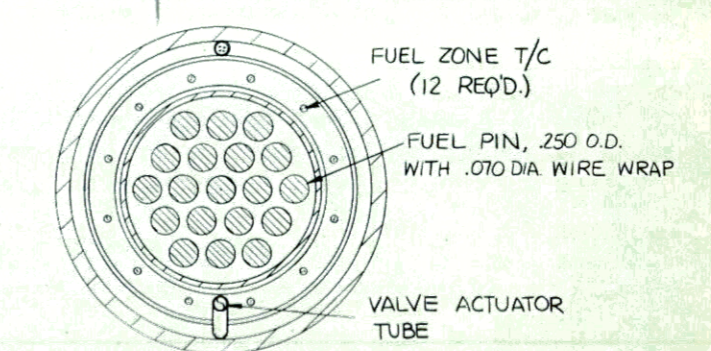
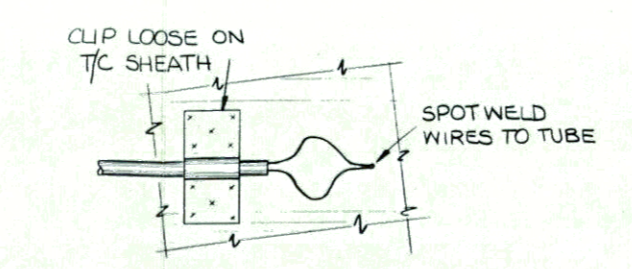
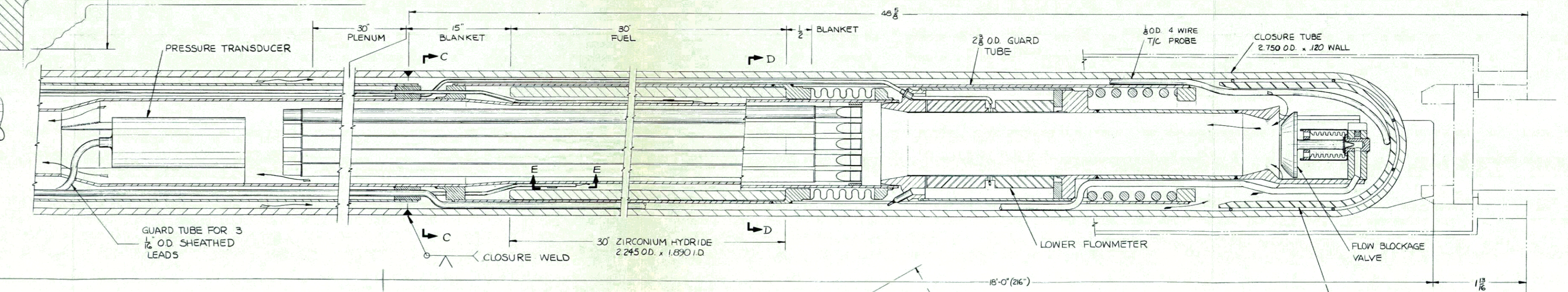
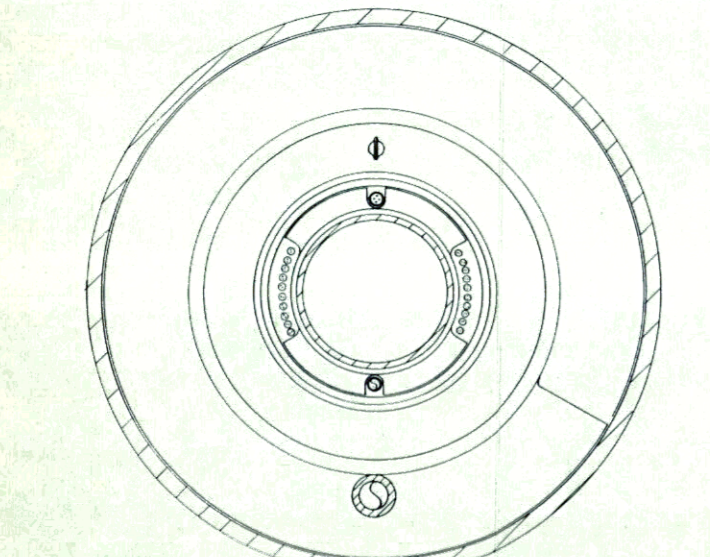
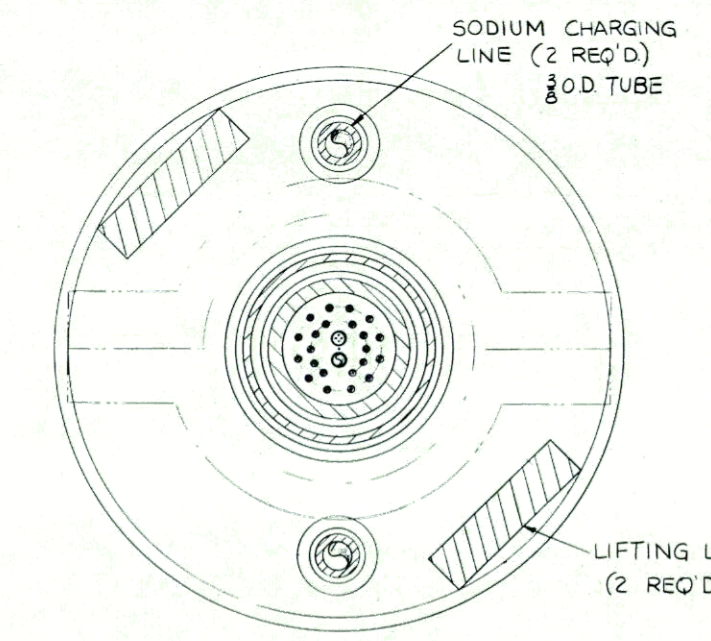
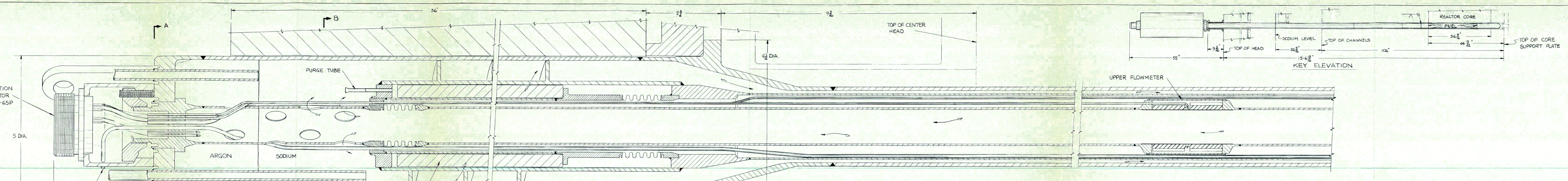


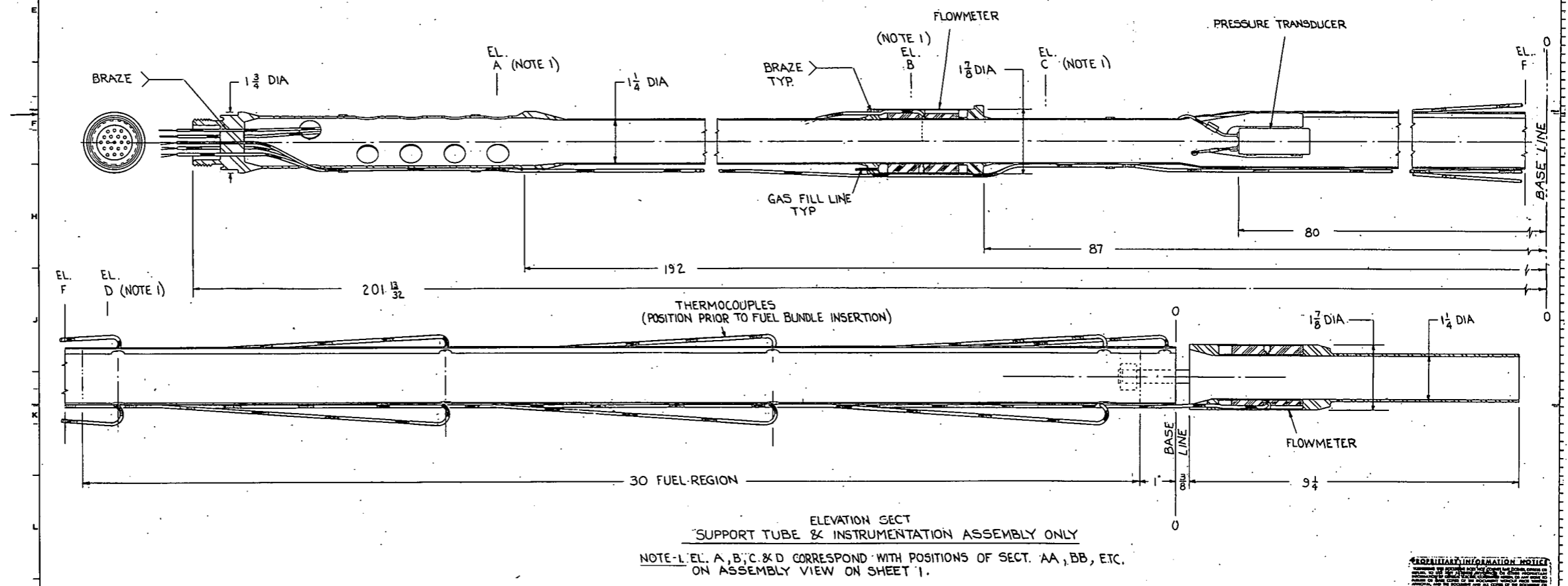
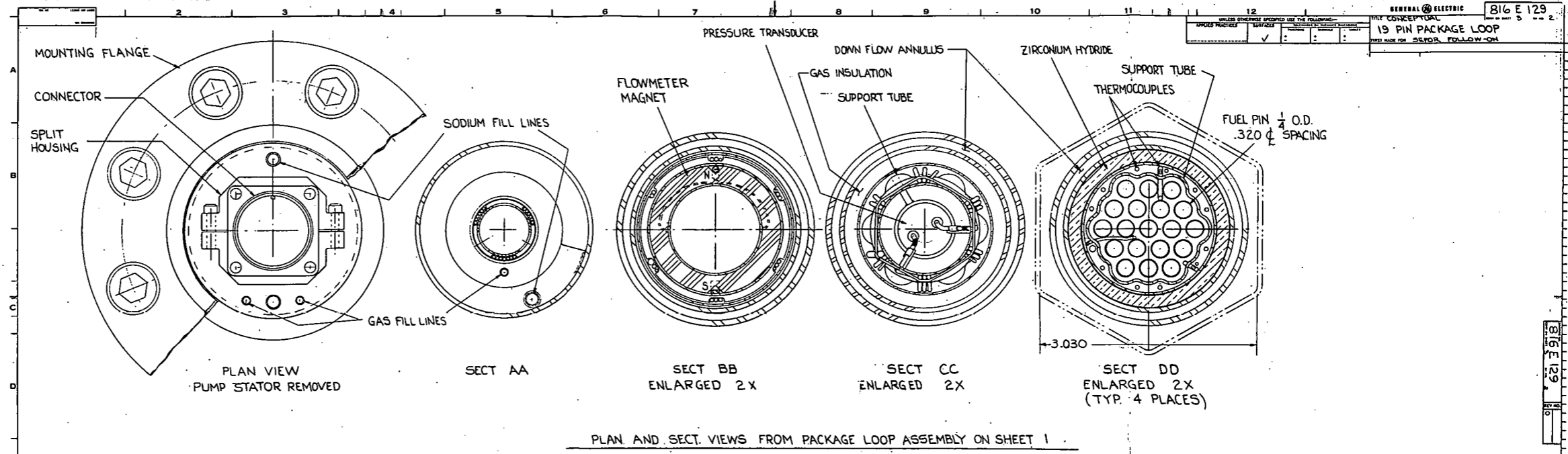
Figure 4B6-1. Package Loop Outline



264R148

264R148

264R148



PRELIMINARY INFORMATION NOTICE  
 This drawing is preliminary and is subject to change without notice. It is not to be used for manufacturing or construction purposes. It is for information only.

DATE	BY	CHKD	BRNO	816 E 129
10-1-77	...	...	...	...

Figure 4B6-3. Package Loop Support Tube and Instrumentation Assembly Drawing  
 341A/341B

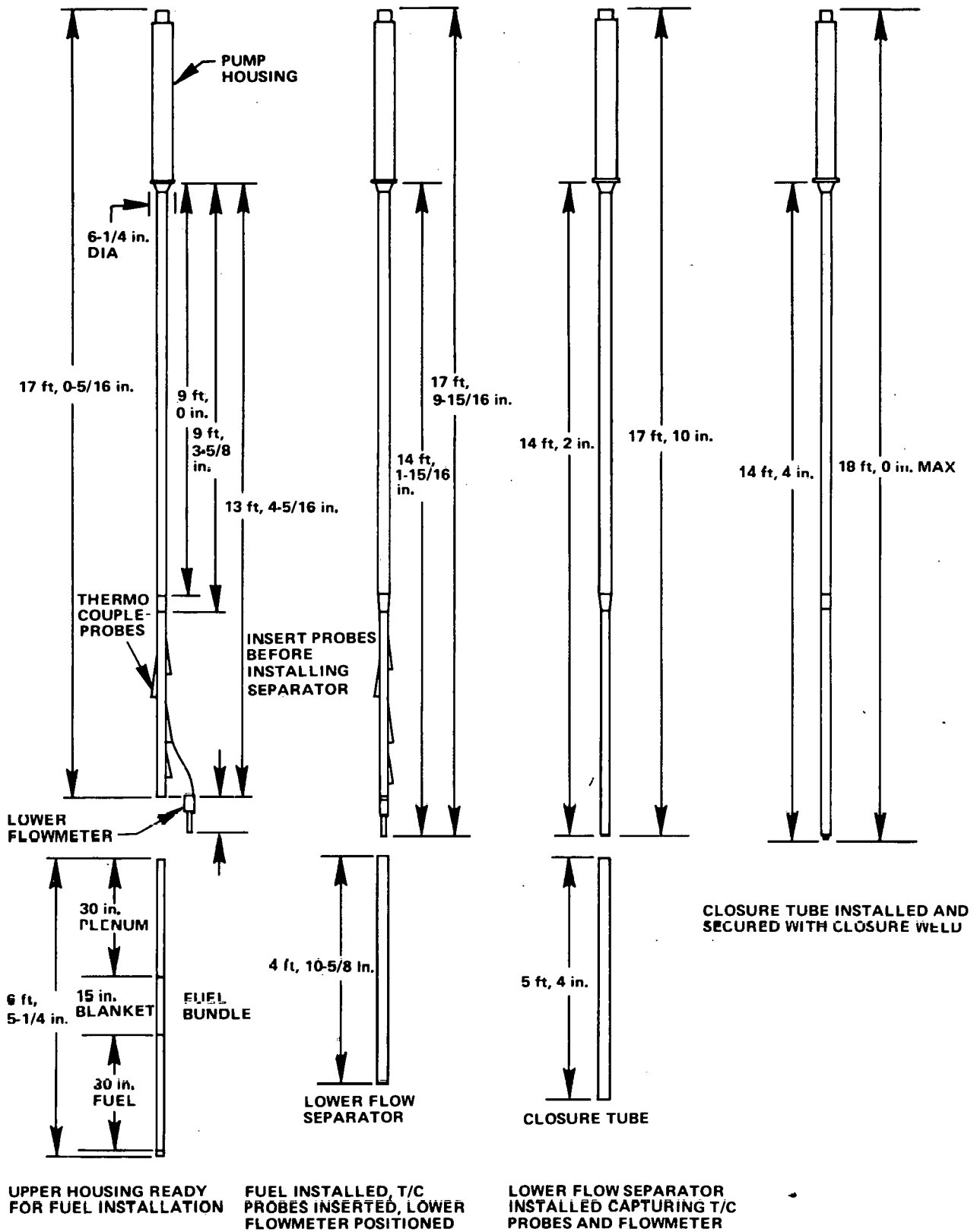


Figure 4B6-4. Package Loop Assembly Sequence Drawing

and the Hot Fuel Examination Facility (HFEF) of the NRTS in Idaho. In summary, with respect to both facilities considered, all operations required for the de-encapsulation of fuel, remote assembly of the loop, sodium filling, and post-test examination of the proposed SEFOR loop are feasible. Modifications would be required at RML to permit entrance and exit of the assembled loop. The HFEF on the other hand is specifically designed to handle loops larger than the proposed SEFOR package loop with a possible advantage of sharing of costs of special purpose equipment among SEFOR, FEFPL, TREAT, and PBF.

Work has been completed on the development of a calculational model of the SEFOR package loop which can be used to perform heat transfer analysis to determine steady-state operating temperatures and transient temperatures for several test cases.

Also, heat transfer calculations are to be performed for several special situations including heat load with the loop in an air atmosphere and furnace melting of the sodium in full loop. The 19-inch pin package loop has been modeled on the General Electric Company's computer program Transient Heat Transfer Version D. Preliminary calculations that have been completed to date include calculation of a steady-state test section inlet temperature of 790°F for a total fuel power of 575 kW and an assumed reactor inlet temperature of 708°F. Preliminary transient calculations have been completed for a slow-flow coastdown and a rapid-flow coastdown which indicate that sodium boiling will be initiated in the test fuel at about 6 seconds and 2.25 seconds respectively after initiation of flow coastdown. The package loop model is reasonably well behaved and will be the basis for future calculations.

#### **4.2.7 Task 4B7 Fuel Handling and Shipping**

##### **4.2.7.1 Objective**

The objective of this task is to perform an integration function among the related component design efforts to the Option III-A Tests, including liaison with the cask designer.

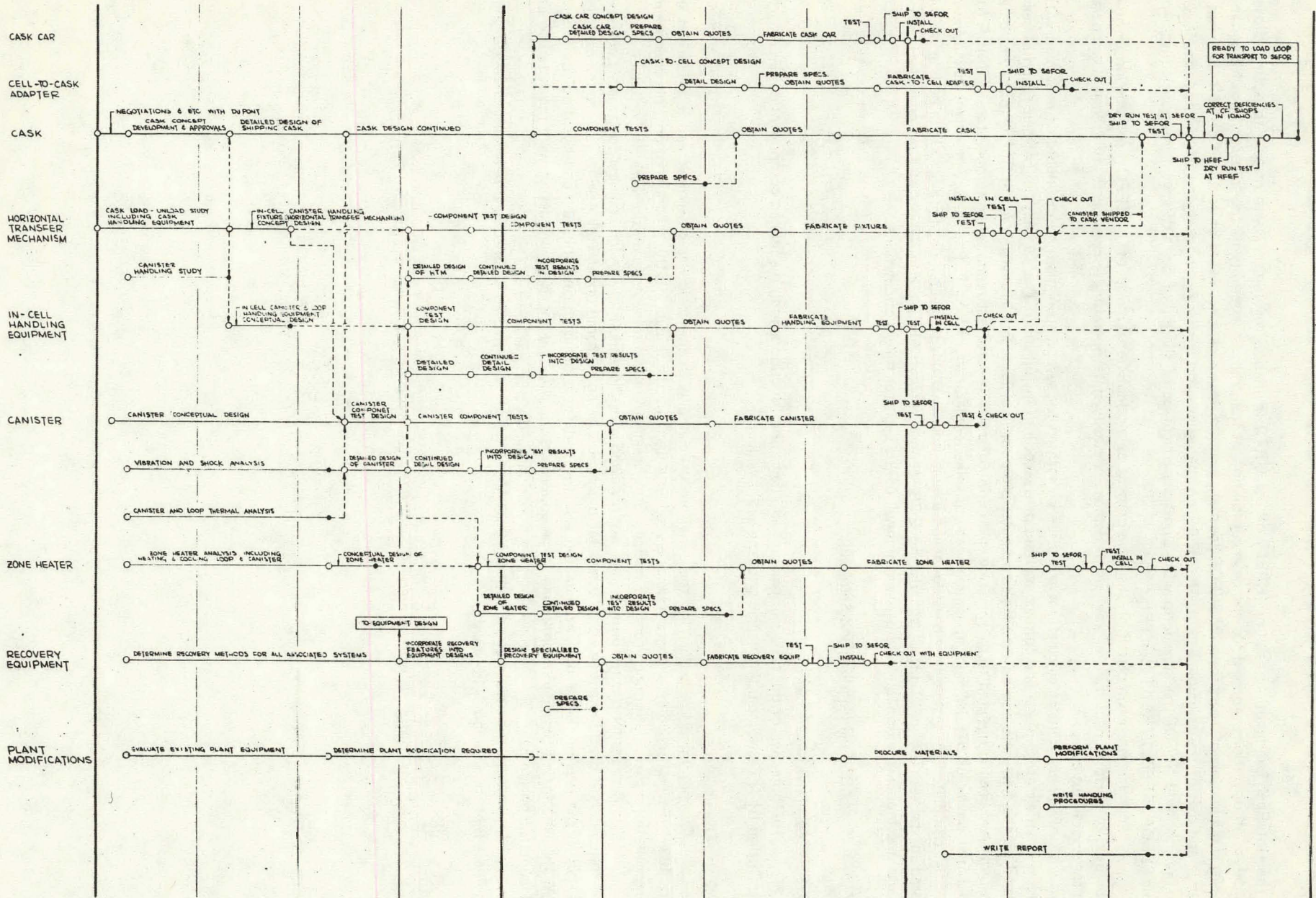
##### **4.2.7.2 Discussions**

The preliminary schedule for the activities associated with this task was developed and is presented in Figure 4B7-1. Several schedule changes were analyzed to determine the impact on the schedule of possible changes in activity duration. It was determined that the shipping cask design and procurement are on the Task 4B7 critical path.

The package loop conceptual design was reviewed with the responsible design engineer for possible changes to the shipping and handling activities. A computer program is being prepared under Task 4B6 to analyze the package operation in the reactor. Since this program can also be used for analysis during shipping and handling equipment design, the anticipated boundary conditions to be applied during shipping and handling design were requested to be included in the program.

Liaison has been maintained with the cask Vendor (E. I. duPont) to assure the timely start of cask design when Phase B of the program is initiated.

**SEFOR FOLLOW-ON**  
**OPTION III TASK 4-B7 FUEL HANDLING AND SHIPPING**



344

GEAP-13787

Figure 4B7-1. SEFOR Fuel Handling and Shipping Equipment Development Plan

## 5.0 TASK 5 - SAFETY AND LICENSING

### 5.1 Objective

The objectives of this task are to:

- Perform safety analyses and prepare a preliminary plan to obtain license and technical specification changes for Option I Plus Selected Plant Tests
- Perform safety analyses and prepare a preliminary plan to obtain license and technical specification changes for Elevated Temperature Operation
- Prepare scoping work plans for safety analysis and licensing efforts related to the Option III-A experiments and plant tests

### 5.2 Safety Analysis, Option I Plus Selected Plant Tests

The analysis in support of the Technical Specification changes required for operation of the reactor with fuel capsule is essentially complete. A draft of the submittal is almost complete and ready for management review. Submittal to the DRL is planned for early January. The following work was performed to provide the necessary information for the proposed technical specification change.

A preliminary set of Design Safety Criteria was developed. These criteria cover the design of the capsule, insertion into the reactor and its potential effects on the reactor. The criteria will be used to judge the acceptability of proposed experiment and capsule designs.

A review was made of the proposed capsule design and variations on the basic design were investigated to determine the capability of the various designs to absorb the energy from potential fuel-coolant interactions inside the capsule. A capsule design which is surrounded by zirconium hydride in the fuel channel, but does not contain zirconium hydride was chosen from these investigations. Calculations of the capacity of the capsule to absorb energy indicate that the current design can contain with margin the energy expected from hypothesized molten fuel coolant interaction.

The potential effects of molten fuel coolant interactions were studied using the ANL-MFCI computer code. A range of input assumptions believed to be conservative were used. Pressures were calculated which result from mixing molten fuel with sodium over a region of the capsule from 1/2 inch to 1-1/2 inch long at various elevations in the capsule. It was assumed that heat transfer persisted until a large fraction of the sodium in the reaction zone was vaporized. The calculated pressures were less than the capacity of the capsule and provide supporting evidence of the acceptability of the containment barrier in the capsule.

Thermal analysis of the consequence of fuel debris within the capsule supports the conclusion that molten debris will not come in contact with the capsule outer barrier. Internal barriers and sodium coolant will provide the necessary protection.

A number of transients were analyzed to determine the possible range of experiments under the Option I program. Evaluations of the reactor performance were coupled with evaluations of the response of the test capsule. These evaluations include FRED transients and transients involving both STOP (Short Term Overpower) and FRED operation. The results of these evaluations have been used as the bases for the initial submittal to DRL for Option I and will be used to provide a base for evaluating potential STOP/FRED operation.

Thermal analysis of the driver fuel for a representative transient discussed in the previous paragraph was analyzed. The thermal analysis for the nominal dimension geometry and adverse geometry were performed.

The stress levels and consequent allowable number of fatigue cycles for STOP/FRED operation were estimated for an arbitrary 25 percent power peaking and 30 percent peak to minimum power skewing in the driver fuel rods adjacent to a capsule located in the center of the reactor. These values appear to be an envelope of the probable magnitude of the peaking and skewing resulting from the use of  $ZrH_{1.6}$  around the capsule.

Analysis of the effect of power peaking in the core fuel indicates that the row of fuel surrounding the test channel will have to be replaced with steel rods and the reactor steady-state power limited to 16 MWt when the test assembly is in the center channel. This procedure will keep the core fuel from experiencing central melting and will make the stresses caused by thermal gradients acceptable.

One-dimensional diffusion theory calculations were performed to provide estimates of various reactivity effects required for the safety evaluation and licensing of transient overpower tests in SEFOR during Option I.<sup>1</sup> For the purpose of obtaining fuel slumping worths and adjusting for the difference in height between the active fuel and the

proposed test fuel, it was assumed that the material worth per gram was proportional to the square of the SEFOR axial power density distribution. For this analysis a chopped cosine power distribution was assumed which gave an axial peak to average power ratio of 1.26.

For the purpose of obtaining reactivity estimates for a "worst" case for licensing, the TOP-1A capsule<sup>2</sup> was assumed to be located in the center channel of SEFOR with Zr hydride sufficient to contain three capsules (as planned for future TOP tests). This innovation was discussed prior to the analysis<sup>3</sup>.

The results of the calculations are summarized below.

	Reactivity (\$)
1. Replace Na by $ZrH_{1.6}$ in center channel.	1.89
2. Insert test capsule into $ZrH_{1.6}$ annulus.	0.26
3. Slump top and bottom 1/2 of test fuel into center 1/3.*	0.066
4. Slump half of top and bottom 1/3 of test fuel into center 1/3.	0.033

\*Corresponds to test fuel filling available space inside heat sink.

### 5.3 Safety Analysis, Elevated Temperature Operation

Work was also performed to support the Technical Specification change that will be necessary for elevated temperature operation.

A crossflow SEFOR main IHX model was developed and the equations programmed in flexible form for model checkout. Transient results for 8 to 36-node crossflow IHX models were compared to transient response of a 224-node SEFOR crossflow main IHX mode. Counterflow IHX models having up to 16 axial segments were also compared with the detailed 224-node crossflow IHX mode. Some of the simpler IHX models studied provided good agreement with the results of the detailed model for the transient analyzed. The overall system analysis requires the use of a simplified model for the IHX.

Revised models of the main IHX and air blast cooler were added to the SEFOR thermal hydraulic transient system code. Selected system thermal transients were analyzed using the revised transient code.

A report was written describing the main IHX and air blast cooler models that were added to the SEFOR thermal hydraulic transient system code and selected flow oscillations studied using the code. The revised code was used to continue SEFOR elevated temperature thermal transient analysis.

### 5.4 Safety Analysis, Option III-A Tests

Preliminary information gathering was done in preparation to performing a state-of-the-art DBA assessment of the Option III-A core. An important part of this effort is a review of experimental data on fuel dynamics during overpower transients. A more realistic description of fuel dynamics is considered to be important in reducing the magnitude of calculated energy release in core disassembly excursions.

Preliminary safety criteria for the Option III-A core and the closed loop have been developed.



REFERENCES:

- 1) Memo, K. W. Cook to D. D. Freeman, "Reactivity Effects of SEFOR F. O. Capsule," December 8, 1971.
- 2) Memo, T. Hikido to Distribution, "SEFOR capsule TOP-1A Design," December 9, 1971.
- 3) Telecons with N. W. Brown and K. W. Cook.

## 6.0 TASK 6 - QUALITY ASSURANCE PLAN

### 6.1 Objective

The objective of this task is to complete a preliminary Quality Assurance Program Plan.

### 6.2 Preliminary SEFOR Follow-On Quality Assurance Program Plan

A preliminary plan for SEFOR Follow-On quality assurance activities is presented in the Quality Assurance Project Plan for Development Programs. This plan provides the general quality assurance criteria applicable to the development activities of SEFOR Follow-On.

The plan has been developed to meet BRD business requirements and to comply with USAEC quality assurance standards, and describes those activities of participating organizations which are related to quality throughout the entire scope of the development program. It includes the responsibilities of management and planning, equipment design and development, procurement, fabrication, assembly, experiment performance, and post experimental examination and reporting.

The requirements of this plan will be applied to SEFOR Follow-On quality assurance-related activities via the media of Quality Control Instructions (QCI). QCI's will be prepared to provide detailed implementation guidance for the general criteria specified in the Plan.

The plan is transcribed in full in the following eleven sections, 6.1 through 6.11.

## 6.1 INTRODUCTION

### 6.1.1 Objectives and Scope of BRD Development Programs

The Breeder Reactor Department (BRD) of the General Electric Company conducts development programs whose objectives are the advancement of engineering and technology related to liquid metal fast breeder reactors (LMFBR).

These programs are composed of a number of tasks, which include performance experiments (both in-pile and out-of-pile) and analytical work requiring the development and use of analytical methods.

Included in the individual scopes of these various development programs are major components of the LMFBR, e.g., fuels, materials, steam generators, heat exchangers, instrumentation, safety technology, shielding, refueling techniques and equipment, sodium technology, pumps, radwaste systems, core development, and other equipment/components.

### 6.1.2 Quality Assurance of BRD Development Programs

The inherently evolutionary nature of development programs dictates that the constituent tasks be changing, resulting in redirection of the task structures and implementation of the work scopes as new knowledge and progress occurs. These circumstances require that quality assurance programs for development activities be more flexible than quality assurance programs for the more routine and predictable projects such as reactor equipment manufacturing or site construction and installation.

Consequently, quality assurance activities relating to development programs are designed to allow for unknown variables to a greater degree than the more routine programs. This intent is accomplished by providing quality assurance programs which establish restraints within reasonable limits; allow an adequate degree of judgment by technical and quality assurance personnel; and are designed to be readily adaptable to changing program requirements. Although these criteria are applicable to all quality assurance programs, the degree and direction of emphasis will differentiate the development quality assurance program from classic manufacturing quality assurance programs.

By necessity, therefore, quality assurance programs for development are variable; however, the goal is unchanging to provide confidence in the accuracy and adequacy of data and conclusions.

### 6.1.3 Quality Assurance Program Plan

This Quality Assurance Plan for Development Programs provides a description of the guidelines, restraints, and activities which are employed to obtain the desired quality of development program implementation and products.

Because of the differences between various development programs, this plan contains general quality requirements applicable to all programs. Specific quality requirements for individual development programs are derived from these general requirements and presented in other appropriate documents, which depend upon the complexity

and extent of the development program. For complex programs, additional quality planning documents are generally necessary and, for small and less complex programs, quality sections in other documents (such as design specifications) will generally suffice.

This plan is primarily a description of the responsibilities and activities of the BRD Engineering and Quality Assurance organizations required to assure the quality of Development Programs. Since a major objective of quality assurance programs is the systematic procedural control of quality-related activities, functions which are normally controlled by formal procedures are identified, and areas are described which will require further procedural definition, depending on the individual development program.

#### 6.1.4 Definitions

*Quality Assurance* — comprises the collective planned and systematic activities and events with their associated responsibilities, effort, equipment, procedures, and management that provide an organization with the means to meet its product quality objectives.

*Quality Control* — comprises those functions of quality assurance related to controlling and achieving the physical characteristics of products to predetermined engineering requirements.

*Product* — includes any material, part, assembly, and product, software package, system, or saleable service developed, manufactured, or processed by BRD for sale or lease to an external customer, or for an interdepartmental transfer to another Company component.

*Product Quality* — means the composite of the product's intrinsic and attributed characteristics and levels of excellence.

*Quality Characteristic* — is an element of product quality, such as configuration, functional performance, reliability, durability, maintainability, or safety. Intrinsic quality characteristics are those which are in the product by virtue of its design configuration, composition, physical properties and construction. Attributed quality characteristics are those assigned to the product by the user whether or not they are intrinsic in the product.

*Quality Level* — is a quantitative or qualitative measure of a product characteristic in absolute physical units or as compared to a quality standard or other reference.

*Quality Record* — is documentation that provides evidence that product characteristics were controlled, inspected, or tested.

*Failure* — is the inability of an item to perform within specified limits.

*Incident* — is an unusual or unplanned occurrence affecting the performance, reliability or safety of a reactor or test facility, or personnel safety, which requires or may require special evaluation, and corrective or preventive action.

*Item* — is any level of unit assembly, including system, subsystem, subassembly, component, part or material.

*Nonconformance* — is a characteristic of an item that does not conform to a specified requirement.

*Quality Objective Evidence* — comprises any recorded fact or facts pertaining to the quality of an item, process, or service based on observation, measurement or test that can be verified.

*Repair* — is the process of restoring a nonconforming item characteristic to an acceptable condition, although it does not then conform to a specified requirement.

*Rework* — is the process by which a nonconforming item is made to conform to specified requirements.

## 6.2 MANAGEMENT AND PLANNING

### 6.2.1 Department and Project/Program Management

The General Manager of BRD has reporting to him section level managers who are responsible for design and development areas of specialization. The section level manager positions include:

- Advance Engineering
- Design Engineering
- Development Engineering
- Plutonium Fuel Development
- Program Management

Reporting to each section level manager are subsection level managers who are responsible for specific design and development work specialties. Project/Program tasks responsibilities are assigned to the applicable subsection level manager. Figure 6-1 is a partial organization chart of BRD showing the General Manager and the section level and subsection level managers who have responsibilities under development programs.

#### 6.2.1.1 Objectives

The overall objective of BRD management is to plan, organize, and integrate all development program activities of BRD into the successful design and development of a fast sodium metal reactor demonstration plant. Project/Program tasks are performed to gather analytical and experimental data in support of the design and development effort.

#### 6.2.1.2 Organization Description

The General Manager of BRD has the overall responsibility for implementation of development programs. Major contributors to the project organization and their spheres of activities include:

##### *Program Administrative Management*

- The Manager of the Program Management Section has been assigned by the General Manager of BRD the responsibility and authority to provide the overall planning, scheduling, funding, cost control, integration, and coordination of BRD programs. He is responsible for establishing from all BRD components, as required, project organizations to implement BRD programs.
- The Manager of Development and Test Programs reports to the Manager of the Program Management Section and has responsibility for program management of all development and test programs within BRD.
- Program Managers are assigned the responsibility for individual development program management and report to the Manager of Development and Test Programs

##### *Program Functional Management*

- The Manager of the Development Engineering Section has been assigned by the General Manager of BRD the responsibility and authority to provide engineering, development, and testing support, as required, to development projects.
- The Manager of the Design Engineering Section has been assigned by the General Manager of BRD the responsibility and authority to identify design needs, execute design, and to provide safety, quality assurance and documentation support, as required, to development projects.
- The Manager of the Advance Engineering Section has been assigned by the General Manager of BRD the responsibility and authority to perform engineering and testing, as required by development projects.
- The Manager of the Plutonium Fuels Development Section has been assigned by the General Manager of BRD the responsibility and authority to develop fuel fabrication processes and to provide mixed oxide fuel and fast reactor fuel assemblies for reactor development testing.
- The Managers of the various Subsections in the Development, Design, and Advance Engineering Sections have responsibility for the technical and administrative management of the specific development program tasks assigned to them. Among their responsibilities, special emphasis is placed on intra-department integration of the tasks.

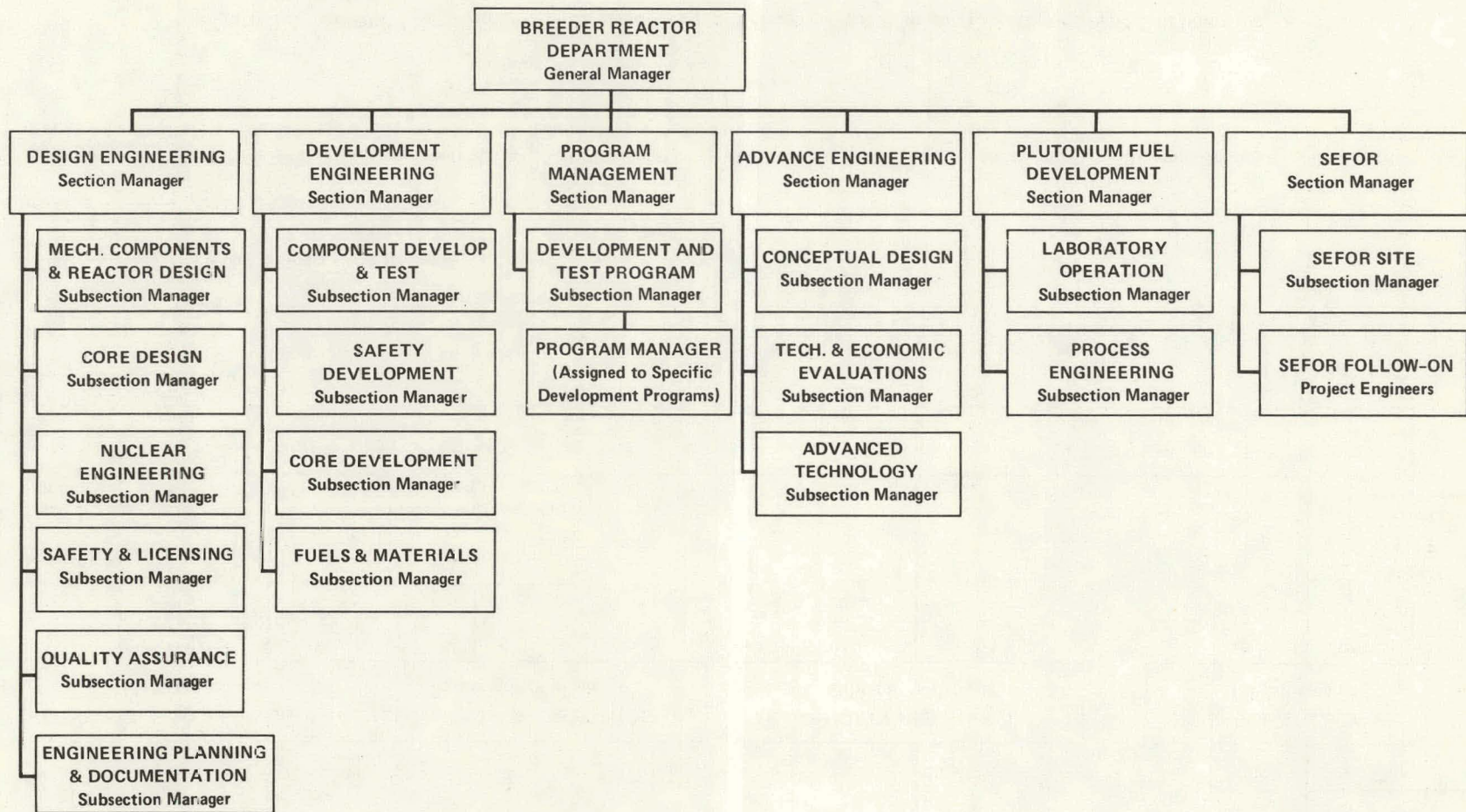
#### 6.2.2 Task Management

##### 6.2.2.1 Objectives

Task management objectives are to successfully accomplish each assigned task on schedule, for the budgeted cost and to obtain the required analytical and experimental data.

##### 6.2.2.2 Organization

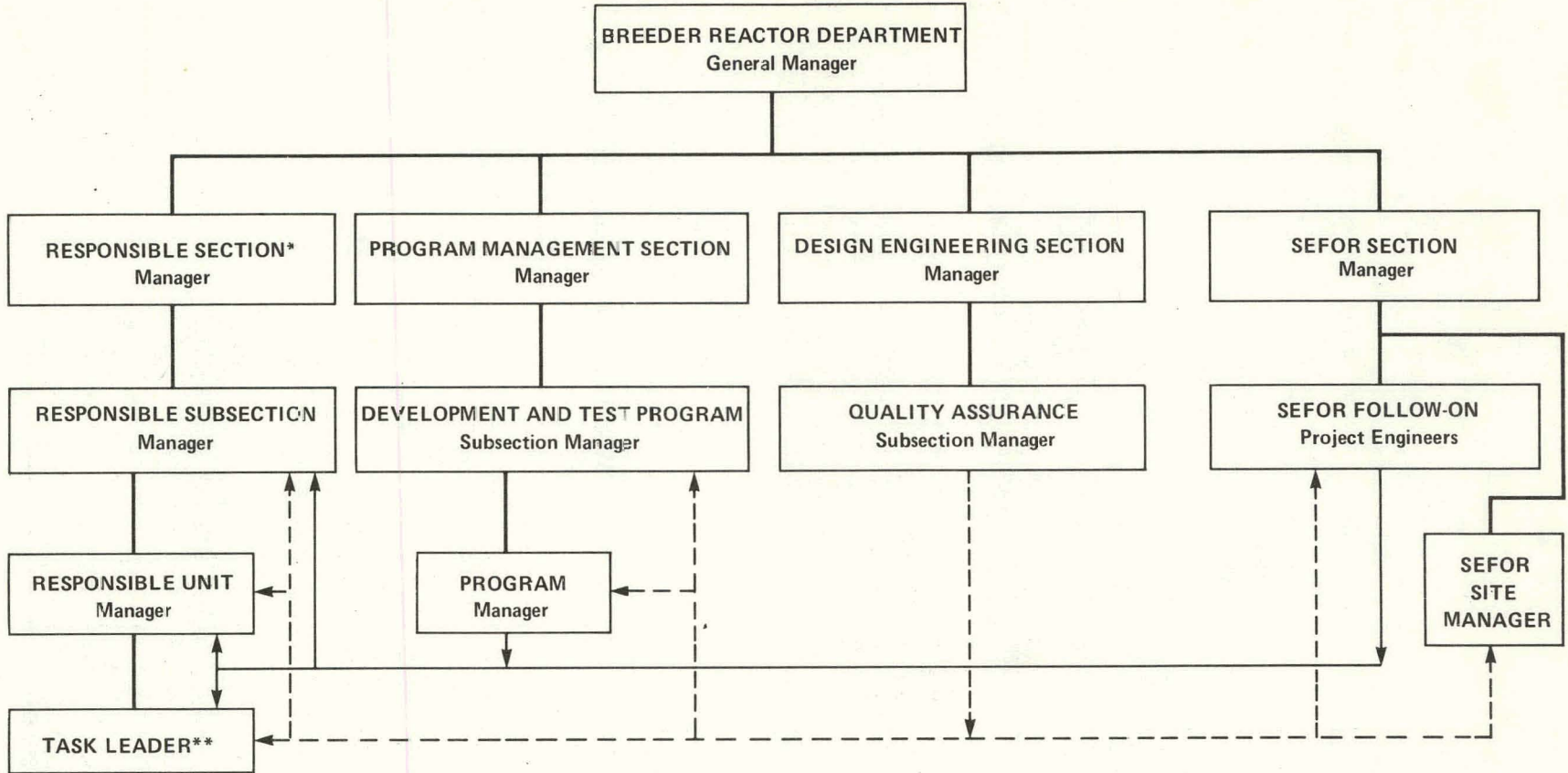
The organization structure for a typical task is shown in Figure 6-2 and is described below.



351

GEAP-13787

Figure 6-1. General Electric Breeder Reactor Department Partial Organization Chart



- Direct Reporting
- Project Guidance and Counsel
- - - - - Quality Assurance Interfaces

\*May be one of: SEFOR Facility, Design Engineering, Development Engineering, Advance Engineering, or Plutonium Fuel Development Sections  
 \*\*May also be the Responsible Subsection Manager or the Responsible Unit Manager

Figure 6-2. General Electric Breeder Reactor Department Development Program Task Management Relationships

### 6.2.2.2.1 Specific Task Assignments

The following procedure is utilized to define the specific components and individuals which participate in a given development task, in accordance with their organizational charter responsibilities:

- (1) The Program Manager identifies for each task a *Responsible Component* which is charged with meeting work scope/schedule/cost milestones for the task. This assignment is approved by the Manager of Development and Test Programs and Responsible Section Manager.
- (2) The Program Manager identifies for each task one or more *Reviewing Components* to monitor and review task activities. (Generally, the responsible and reviewing components are counterparts from the various Engineering Sections.) The assignment of the reviewing component is approved by the Manager of Development and Test Programs and the Reviewing Section Manager.
- (3) The Responsible Subsection Manager appoints a Task Leader.
  - A Task Leader reporting to the responsible Subsection Manager (or Unit Manager) is designated for each development program task. The Task Leaders have responsibility for detailed implementation of the tasks.
  - A Responsible Engineer is assigned to the Task Leader, when appropriate, to assist the Task Leader in the technical liaison with responsible performing components.
- (4) During the conduct of task activities the responsible component may subcontract work (by mutually agreed upon Job Orders) to other components -- referred to in this plan as *Performing Components*. Both the responsible and reviewing components may be performing components on certain items of work scope.

The specific responsibilities of the Program Manager, Task Leader, and Responsible, Reviewing and Performing Components are further defined in the subsequent discussion.

### 6.2.2.2.2 Management and Control of Task Activities

A systematic approach to the management of task activities has been adopted to structure the work and facilitate planning, measurement, control, integration and quality assurance activities. This management "system" entails a further definition of responsibilities, including technical documentation and review/approval requirements for various task activities. The system, described below, will be periodically reviewed and updated to meet changing requirements of development programs.

Table I summarizes the key features of the management system in a general form applicable to all development tasks. The left side of Table 6-1 lists the various activities and milestone documents for each of the program phases. Table 6-1A lists Experimental Activities and Table 6-1B lists Analytical Activities. Tasks may encompass activities in each area. Review/approval responsibilities of Program Management; Responsible, Performing and Reviewing Components; and Quality Assurance are listed for each work control/milestone document in Table I. The intended contents of the work control/milestone documents and their use in planning, measurement, control, integration and quality assurance activities are discussed below.

### 6.2.2.3 Planning

Design and development programs have generally the same phases to be accomplished; however, the activities vary depending upon the objectives of each program or task.

The following will define some of the typical activities/documents prepared during each phase.

#### 6.2.2.3.1 Planning Phase - Experimental Activities

- (1) *The Task Design Requirements* for each task will be documented prior to preparation of task planning documentation for each contracting period. These design requirements, which cover the work on a given task for a single contracting period, may be abstracted from a more comprehensive set of product design requirements which is created and maintained on a functional basis. This ensures coordination of the overall design requirements with all of the development programs at BRD disposal.
- (2) *The Task Planning Documentation* will reference the Task Design Requirements and define the task work scope, schedule and cost estimate agreed to by the Responsible and Reviewing Components for the contract period. The cost estimate will reflect spending both by subtask and by performing component. Resolution of component participation in task activities is therefore determined prior to the initiation of work.
- (3) The Form 189 proposal and contract are developed from the task planning documents to establish the work scope and funding for the contract period.
- (4) *The Experimental Proposal* is intended to provide an overview of an experiment prior to the commitment of significant resources. A typical outline for the experimental proposal is:

Table 6-1A

TYPICAL ACTIVITIES AND DOCUMENTATION REVIEW & APPROVAL REQUIREMENTS FOR DEVELOPMENT PROGRAMS

NOTES:

A - Approval

D - Distribution or Attendance for Information and Optional Review/Comment

R - Mandatory Review/Comment Prior to Release

Experimental Activities

Planning Phase

Task Design Requirements  
Task Planning Documentation Form 189 and Contract  
Experimental Proposal

Experiment Development Phase

Design Basis Specification  
Experiment Quality Plan

Design Phase

Design Specifications and Drawings  
Fabrication and Procurement Specifications and Drawings  
Design Reviews

Fabrication Phase

Manufacturing, Process, Assembly, Inspection and QC Plans

Test and Operation Phase

Operation and Test Procedure  
Examination Procedure

Data Analysis

Data Analysis Plan

Reporting

Task Reviews  
Quarterly Reports  
Internal Memos and Reports  
Topical Reports

	Program Management			Responsible* Component				Performing** Component			Reviewing Component		QA	BRD
	Program Manager	Manager of Development and Test Program	Section Manager	Responsible Engineer	Task Leader	Responsible Unit Manager	Responsible Subsection Manager	Responsible Section Manager	Responsible Engineer	Responsible Unit Manager	Responsible Subsection Manager	Responsible Subsection Manager	Responsible Section Manager	BRD QA Subsection Manager
Task Design Requirements				R	R	A						A		
Task Planning Documentation Form 189 and Contract	A	R	A	R	R	A						A	R	
Experimental Proposal	R			R	R	R	A	D	R	R	D	R	A	A
Design Basis Specification	D			R	R	R	A	D	R	R	A	R		A
Experiment Quality Plan				R	R	A			R	A				A
Design Specifications and Drawings				R	R	R	A		R	R	A	R		A
Fabrication and Procurement Specifications and Drawings				R	R	A			R	A				A
Design Reviews				D	D	D	D		D	D	D	D		D
Manufacturing, Process, Assembly, Inspection and QC Plans				R		R			R	A				A
Operation and Test Procedure	D			R	R	A	D		R	A		A		A
Examination Procedure	D			R	R	A	D		R	A		R		R
Data Analysis Plan	D			R	R	A	D		R	A		D		D
Task Reviews	D				D	D	D					D		
Quarterly Reports	A				R	R	R	A				R	R	D
Internal Memos and Reports	D				D	D	D	D				D	D	D
Topical Reports	A			R	R	R	R	A				R	D	D

\*Prime responsibility for performing or initiating will be determined during the Planning Phase

\*\*Entries for Performing Components apply only to those documents created or utilized by the Performing Components



Table 6-1B

TYPICAL ACTIVITIES AND DOCUMENTATION REVIEW AND APPROVAL REQUIREMENTS FOR DEVELOPMENT PROGRAMS

NOTES:

A - Approval

D - Distribution or Attendance for Information and Optional Review/Comment

R - Mandatory Review/Comment Prior to Release

Analytical Activities

Planning Phase

Task Design Requirements  
Task Planning Documentation Form 189 and Contract  
Analytical Methods Proposal

Design Phase

Engineering Analysis Specification  
Computer Program Specification

Test and Operation Phase

Program Evaluation Plan

Data Analysis

Analytical Studies Plan

Reporting

Task Reviews  
Quarterly Reports  
Internal Memos and Reports  
Topical Reports

	Program Management			Responsible* Component				Performing** Component			Reviewing Component		QA	BRD
	Program Manager	Manager of Development and Test Programs	Section Manager	Responsible Engineer	Task Leader	Responsible Unit Manager	Responsible Subsection Manager	Responsible Section Manager	Responsible Engineer	Responsible Unit Manager	Responsible Subsection Manager	Responsible Subsection Manager	Responsible Section Manager	BRD QA Subsection Manager
Task Design Requirements				R	R	A						A		
Task Planning Documentation Form 189 and Contract	A	R	A	R	R	A						A	R	
Analytical Methods Proposal	R			R	R	R	A	D	R	R	A	R	A	A
Engineering Analysis Specification				R	R	R	A	D	R	R	A	R		
Computer Program Specification				R	R	A	D		R	A	D	R	A	
Program Evaluation Plan				R	R	A	D		R	A	D	R	A	
Analytical Studies Plan				R	R	A	D		R	A	D	R		
Task Reviews					D	D	D					D		
Quarterly Reports					R	R	R	A				R	D	D
Internal Memos and Reports					D	D	D	D				D	D	
Topical Reports				R	R	R	R	A				R	D	D

\*Prime responsibility for performing or initiating will be determined during the Planning Phase

\*\* Entries for Performing Components apply only to those documents created or utilized by the Performing Components

- Objectives
- Justification and Relation to Design Requirements
- Experimental Hardware
- Test Procedure
- Post-Test Examination
- Data Analysis
- Expected Results (Technical Content, Format)
- Experimental Work Plan

The Experimental Work Plan will define the elements of work to be accomplished, documents prepared, reviewed and issued and items to be procured. The Experimental Work Plan may also be a separate document from the Experimental Proposal. In this case, review and approval authorities are the same as the Experimental Proposal.

#### 6.2.2.3.2 Experiment Development Phase

- (1) *The Design Basis Specification* provides classification information and a description of critical features of a proposed experiment in sufficient detail to permit the required design work to be performed by others.
- (2) *Experiment Quality Plans* document the specific quality assurance and quality control activities and procedures required of performing organizations and the quality level of effort.

#### 6.2.2.3.3 Design Phase

- (1) *Design Specifications and Drawings* provide detail, design description and requirements for hardware performance, inspection and test.
- (2) *The Fabrication and Procurement Specifications and Drawings* include the detailed information and instructions required for fabrication and special quality requirements for control of an experiment. These documents comprise the subject matter for *Design Reviews*.
- (3) *Design Reviews* are scheduled by the responsible component with QA and the performing and reviewing components. The progress of design activities is investigated, and the adequacy of the design approach is determined.

#### 6.2.2.3.4 Fabrication Phase

- (1) *Manufacture, Process and Assembly Plans* define the sequence of manufacture and how to accomplish each step.
- (2) *Inspection Procedures and QC Plans* define what characteristics are to be inspected and how inspection is to be accomplished.

#### 6.2.2.3.5 Test and Operation Phase

- (1) *The Operation and Test Procedure* includes the plan for operation and test of an experiment and special quality requirements for control, including data acquisition requirements.
- (2) *The Examination Procedure* documents the procedures to be followed and data to be obtained during post-test examination of experimental hardware.

#### 6.2.2.3.6 Data Analysis

- (1) *The Data Analysis Plan* defines the manner in which the data from an experiment will be processed and presented for engineering application.

#### 6.2.2.3.7 Reporting

- (1) *Task Reviews* will be scheduled on at least a semiannual basis to provide reviewing components and other interested parties information and an opportunity to contribute and influence task activities. These reviews will be scheduled by the Program Manager, with the Task Leader responsible for the formal agenda. Minutes will be recorded, and the Task Leader will respond to major comments and suggestions.
- (2) *Quarterly Reports* will be prepared to provide a periodic statement of task progress, and a summary of significant results and conclusions.
- (3) *Internal Memos and Reports* are the formal correspondence and progress reports which keep the participants informed of task activities.

- (4) *Topical Reports* are the formal summations of task activities and experiment results at milestones during the tasks and at the completion of a task.

**6.2.2.3.8 Planning Phase – Analytical Activities**

- (1) *The Task Design Requirements, Task Planning Documentation and Form 189* are defined under the planning phase for Experimental Activities.
- (2) *The Analytical Methods Proposal* (analogous to the experimental proposal) is intended to provide an overview of a computational methods development effort to interested parties, prior to commitment of significant resources. The typical outline for this document is:
- Objectives
  - Justification and Relation to Design Requirements
  - Scope of the Proposed Analysis
  - Physical Phenomena to be Modelled and Approach
  - Computer Program Structure and Logic
  - Program Checkout and Evaluation

**6.2.2.3.9 Design Phase**

- (1) *The Engineering Analysis Specification* is a detailed documentation of the assumptions, equations, data, etc. comprising the technical basis of the program. Justification of key elements in the approach will be provided.
- (2) *The Computer Programming Specification* is a detailed documentation of the input/output provisions, subroutine structure, computational logic, etc., for a digital computer program. The information in the engineering analysis specification and computer programming specification are in sufficient detail to permit a knowledgeable engineer or computer programmer to actually create the program, and to permit users to understand and evaluate the program.

**6.2.2.3.10 Test and Operation Phase**

- (1) *The Program Evaluation Plan* documents the procedures, tests, etc. which will be followed to verify that the program meets the engineering specification. In addition, this plan describes the calibrations, comparisons with experimental data, etc. which will be performed to establish or assess the accuracy of the technical approach embodied in the program.

**6.2.2.3.11 Data Analysis**

- (1) *The Analytical Studies Plan* documents the computational tools, input data, cases to be studied, etc. in advance of performing significant analytical studies with existing codes.

**6.2.2.3.12 Reporting**

- (1) *Reporting* is the same as described under Experimental Activities.

**6.2.2.4 Documentation**

Some of the documents referred to in Table 6-1 will not be applicable to specific experiments and analyses, and in some instances it may be convenient to group several of the documents together. (For example, an analytical proposal might be sufficiently detailed as to meet the requirements of the engineering analysis specification, computer programming specification and program evaluation plan.) Documentation will be maintained throughout each development task to adequately document what was accomplished, when it was accomplished, and the individual responsible for the work.

**6.2.3 Management of Development Programs Quality Assurance**

**6.2.3.1 BRD Quality Organization**

The BRD Quality Organization is composed of the BRD Quality Assurance Subsection (BRD QA) and Quality Control representatives assigned to remote BRD satellite components. These QC representatives receive technical direction and assistance from BRD QA to ensure a coordinated, standard Quality Assurance Program and the integration of BRD Quality Organization activities.

Organizationally, the Manager of the Quality Assurance Subsection reports directly to the Manager of the Design Engineering Section. Functionally, the Manager of Quality Assurance is responsible for the coordination and integration of quality-related activities of BRD as a whole without regard to organization lines. In the discharge of this responsibility, the Manager of Quality Assurance has direct access to the General Manager of BRD, and is accountable to him for reporting the quality status and quality performance of development programs.

The BRD QA Subsection is composed of three Units: Quality Engineering, Quality Systems, and Quality Surveillance, whose managers report directly to the Manager of Quality Assurance. These Units are staffed with engineers of selected disciplines to provide the expertise required to meet the varied technical demands of the development programs.

Figure 6-3 depicts the organizational structure of BRD QA and its reporting relationships to higher management. In addition, the most important functional activities of BRD QA are listed under the responsible units.

### 6.2.3.2 BRD Quality Organization Responsibilities and Authorities

#### 6.2.3.2.1 Responsibility

BRD QA is responsible for planning the developing the structure which provides assurance that development programs comply with requirements established by governing criteria. This structure is a quality assurance program which consists of guidance and methods for the controlled and systematic implementation of development programs by responsible functional personnel to predetermined requirements.

BRD QA is not directly responsible for performing development program work, but is responsible for measuring quality program implementation by means of surveillance, inspection, and audit, and for documenting and reporting to higher management the quality status and quality performance of these programs.

The broad functional responsibilities of BRD QA are to ensure that:

- Technical management of development programs is identified, with responsibilities and authorities defined.
- Coordination and integration of development activities between participating organizations is accomplished.
- Adequate planning of development programs is performed by the responsible personnel.
- Systematic procedural methods are available to govern the sequence of events for development programs.
- Procedural methods comply with contract and quality assurance regulatory requirements.
- Program activities are performed in accordance with the governing procedures.
- Equipment and materials obtained for development program use comply with predetermined engineering and quality standards.
- Fabrication of items for development experiments is in accordance with predetermined engineering and quality standards.
- Performance of experimental and analytical tasks is in accordance with previously approved plans and procedures.
- Quality records and objective quality evidence are acquired and maintained to verify the quality of development programs.

QC representatives assigned to BRD satellite components are responsible for inspection planning, surveillance and audit, quality records, and quality status reporting of development program work performed by the components. The QC representatives are responsible for complying with quality policies established by BRD QA and implementing the requirements of the Quality Assurance Program for Development Programs.

#### 6.2.3.2.2 Authority

BRD QA has been delegated by the General Manager of BRD the authority to establish methods to measure the quality status and quality performance of development programs, and to prevent or correct conditions detrimental to quality. This authority is exercised by the following methods:

- Issue of instructions and procedures for guidance of BRD personnel in performance of quality-related activities.
- Review and approval of applicable procedures and instructions governing the administrative conduct of development programs.
- Review and approval of technical specifications and drawings and purchasing documents for the procurement or fabrication of materials and equipment.

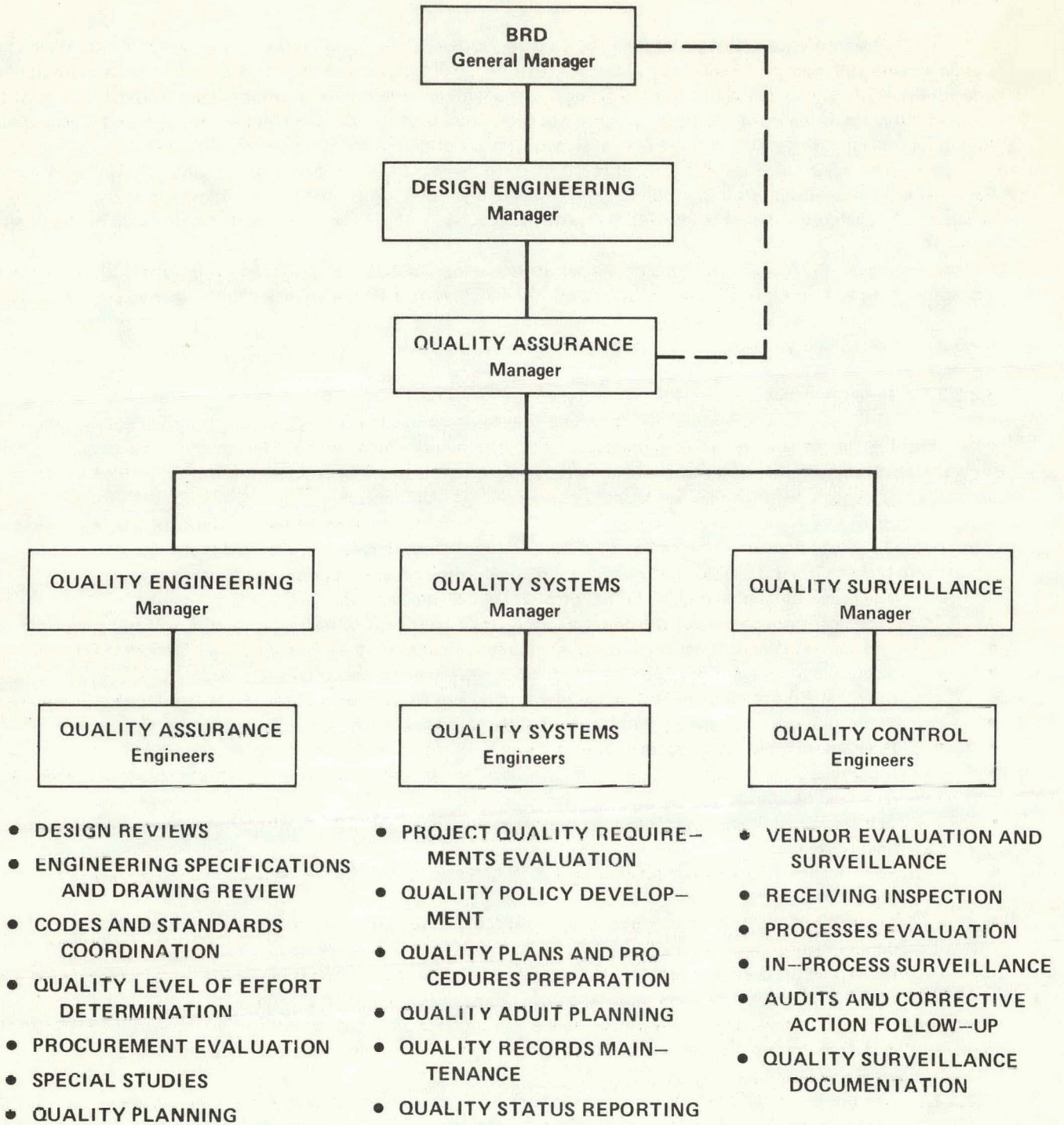


Figure 6-3. BRD Quality Assurance Organization

- Quality Assurance release of materials and fabrication items at predetermined points during surveillance of development activities.
  - Audit of development program activities and establishment of corrective action requirements.
- QC representatives assigned to BRD satellite components have the authority to prevent or correct conditions detrimental to quality in accordance with quality policy and technical direction from BRD QA.

### 6.2.3.3 Planning

#### 6.2.3.3.1 BRD QA Planning

Systematic BRD QA planning activities are performed prior to initiation of development programs to identify required BRD Quality Organization participation and define the quality objectives. Planning activities are continuous throughout a development program to determine and meet quality goals for each phase of the program.

Planning activities are performed to determine and establish the methods for assuring that development programs are implemented in a manner to meet product quality objectives and contractual requirements.

Activities which are performed as part of the overall quality planning include:

- Review of proposals, contracts, and work scopes to identify BRD business and customer quality requirements.
- Preparation of quality policy, plans, instructions, and procedures to define quality responsibilities and quality/project/functional interfaces.
- Review of engineering documents to verify compliance to requirements of engineering, quality assurance, safety, codes and standards, and other applicable specifications.
- Participation in design reviews to assure that the quality of design is adequate to meet program objectives; that items can be manufactured to meet engineering requirements; that inspection and test criteria are established; and that inspection and test methods are available.
- Determination that adequate management review of development programs is accomplished in order to ensure sufficient management attention and dissemination of information to affected personnel.

Additional quality planning activities for hardware and experimental Tasks are discussed under specific headings later in this Plan.

Quality planning activities applicable to analytical Tasks which have no specific hardware content are concerned primarily with verifying that adequate project and functional planning is performed for the accomplishment of those Tasks; that the Tasks are performed in accordance with the planning; the proper control is exercised for data, records, and other documentation; and that the Tasks' end products (reports, software, etc.) are properly reviewed, approved, and disseminated.

#### 6.2.3.3.2 Designation of Quality Effort

During preliminary planning, the level of quality assurance/quality control effort for material, components, and systems is determined by classification of products, based on the importance and significant nature of their use. Classification and assignment of quality levels is determined as described in applicable procedures and instructions. Product classifications and quality levels are designated in appropriate specifications and other engineering documentation.

#### 6.2.3.4 Documentation

Quality-related activities are documented as governed by applicable policies and instructions.

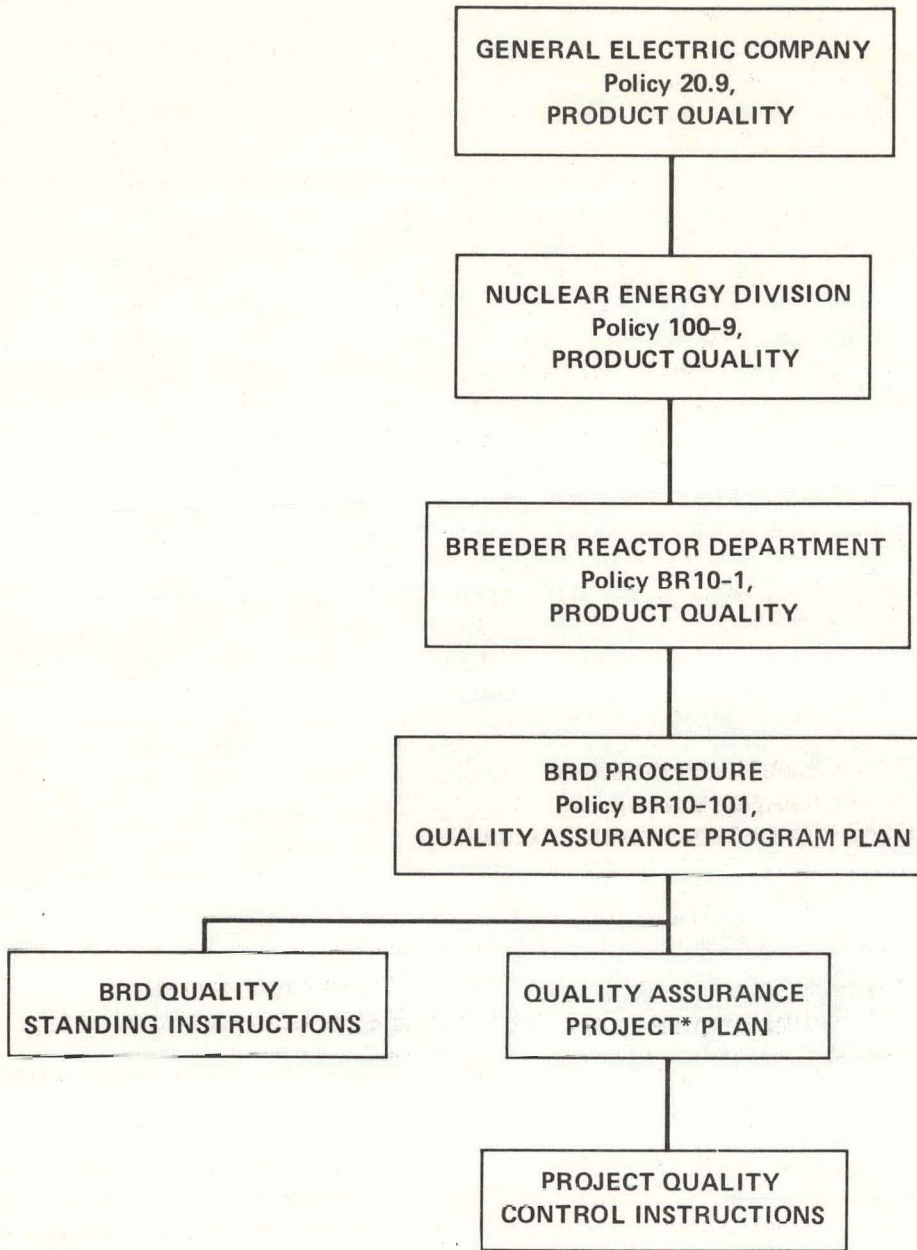
Documents used for recording and transmitting information related to the implementation of the Quality Assurance Program comprise the quality reporting system, which records and methods, practices, activities and tests that affect the quality of the various Tasks.

The quality reporting system includes records that supply adequate information of a documentary nature to verify the performance of the specified Task in accordance with applicable drawings and specifications. These records are readily retrievable and easily identified with the activity they document and verify.

#### 6.2.3.4.1 Policy and Procedures

The BRD Quality System is developed from three policy documents covering Product Quality (See Figure 6-4):

- Company Policy 20.9



\* EXAMPLES: DEVELOPMENT PROJECTS, FUEL PROJECTS, PLANT DESIGN AND CONSTRUCTION PROJECTS

Figure 6-4. Typical BRD Quality System Documentation

- Division Policy 100-9
- BRD Policy BR10-1

This policy is implemented through a series of lower tier program and planning documents:

- BRD Procedure BR10-101, Quality Assurance Program Plan, establishes the broad major quality assurance concepts applicable to all BRD functions and describes the integration of BRD quality assurance activities.
- Quality Standing Instructions (QSI) are prepared and distributed to interpret requirements established by BR10-101, Quality Assurance Program Plan. These QSI's provide detailed guidance for implementation of the Plan's quality requirements by all BRD personnel.
- Quality Assurance Project Plans apply the general quality requirements of BR10-101 to specific projects. Project Plans include additional quality requirements, which may be contractually imposed.
- Quality Control Instructions (QCI) are prepared to interpret quality requirements of Project Plans and provide specific instructions to affected personnel.

#### 6.2.3.4.2 Quality Record

Quality records acquired during the progress of development programs are maintained in central quality files for the period of time required by contract, regulations, or BRD business policy (whichever is the longest period). The record system permits retrieval by project and by subject.

Quality records include (but are not limited to):

- Inspection reports
- Item release records
- Nonconforming item records
- Audit reports
- Vendor certifications
- Vendor surveys
- Document review records
- Quality-related correspondence
- Corrective action records
- Quality activity records
- Quality status reports
- Management review records

#### 6.2.3.4.3 Quality Status Reports

The status of the quality of BRD products and activities is reported regularly to upper management and appropriate personnel through a formal BRD QA reporting system.

The reporting system comprises annual, monthly, and special reports. BRD QA activities, interfaces, problems, potential problems, problem solutions, and other accomplishments (related to the quality of BRD products and services) are contained in these various reports.

Dissemination of reports to customers and outside agencies is governed by contract requirements and regulations.

#### 6.2.3.4.4 Management Reviews

Periodic reviews of development programs are performed by high level BRD management. Management reviews encompass the status and progress of significant aspects of development programs. Reviews are governed by formal procedures and are documented. BRD QA maintains formal records of these reviews.

#### 6.2.3.5 Training and Indoctrination

Training and indoctrination of BRD personnel is accomplished in order to assure that activities affecting quality of development programs are performed by qualified personnel. Training and indoctrination requirements apply to personnel of projects, functional, and quality organizations.

Training and indoctrination methods include: information seminars, formal training courses, on-the-job training programs, technical consultations, distribution of information publications, guidance procedures and instructions, management reviews, and internal communications and reports.

Various BRD components are responsible for implementing separate divisions of the overall BRD training and indoctrination program. BRD quality organizations are responsible for advancing quality awareness and acceptance



of quality concepts. In addition, BRD quality organizations participate with other BRD components in operator training and qualification for special fabrication processes (e.g., welding, brazing, coating, plating, etc.), and nondestructive testing (e.g., radiography, penetrant, magnetic particle, helium leak check, etc.)

### 6.3 DESIGN AND DEVELOPMENT

#### 6.3.1 Scope

The Quality Assurance Program is directed toward achieving proper control of design and development activities without placing unnecessary burdensome restraints and demands upon engineers. The intent of BRD QA participation in the program is to aid the design & development functions through the following activities:

- Participation in task and experiment planning by identification of quality requirements and interfaces.
- Participation in the establishment of standards and procedures for preparation of design and development documentation.
- Design and document reviews to determine the adequacy of:
  - a) Quality of design
  - b) Safety considerations
  - c) Quality requirements
  - d) Codes and Standards identification
- Performance of audits to maintain level of conformance to instructions and assure proper records.
- Coordination and feedback of information to engineers, management and interfacing organizations.
- Establishing and obtaining corrective action.

#### 6.3.2 Task Planning

Task planning is performed by the responsible subsection manager, unit managers, task leader or responsible engineer. The planning establishes, as a minimum, the activities to be accomplished, the items or processes to be developed, the individuals/organizations responsible, and the schedule.

BRD QA activities (i.e. design and document reviews, procedure requirements, surveillance requirements, etc.) are identified, as applicable, and BRD QA reviews and approves task planning.

#### 6.3.3 Design Definition and Control

Activities of responsible engineering and quality personnel are planned to provide assurance that the design basis and applicable regulatory requirements are correctly defined by design and engineering documentation developed for the task.

Design definition and control activities include:

- Classification of items with respect to function, and relative importance to the project.
- Criteria stating requirements to be satisfied by the design.
- Application of Federal, State, and Industry codes, standards, and practices, or preparation of new or supplemental codes and standards, if required.
- Performance of engineering studies to establish adequacy of design criteria.
- Selection of parts, materials, and processes on the basis of prior qualification for the intended services, or on the basis of development and qualification testing.
- Preparation of design description documents to serve as a common technical basis for project activities.
- Preparation of specifications, drawings, and instructions to define detailed design, procurement, fabrication, installation, test, operation, and maintenance requirements.
- Identification methods to assure control and traceability of materials and associated documentation.
- Criteria stating requirements for the quantitative and qualitative verification and acceptance of work processes.
- Control of interfaces between participating design organizations to establish coordination of design activities.

#### 6.3.4 Document Review and Control

##### 6.3.4.1 Document Reviews

In accordance with engineering planning procedures and instructions, significant engineering documentation

and its revisions undergo a systematic review and evaluation by qualified independent review sources prior to issuance. Engineering document reviews are accomplished with the intent of verifying completeness and adequacy with respect to design criteria, design practices, codes and standards, quality requirements and intended application.

**6.3.4.2 Document Control**

Design drawings, specifications and other significant documents are issued and revised only after required reviews and approvals as defined in engineering planning procedures and instructions.

Revisions are in accordance with the proper authorizing documents which require the same organizational review and approvals as the original document. Revision and date are identified on the applicable document.

**6.3.5 Design Review**

Design reviews are performed by technically qualified engineers and managers of interfacing functions, including BRD QA. Design reviews are programmed and the results documented. Design reviews are conducted to provide assurance that studies, calculations, and analyses involving nuclear effects, electrical, mechanical, thermal, hydraulic, safety, reliability, maintainability, codes and standards, and quality requirements are complete and correct.

**6.3.6 Codes and Standards**

Applicable AEC, ASTM, USASI, ASME and other recognized codes and standards are employed by BRD for development programs. Should required codes and standards not exist for application to experimental tasks, BRD develops new or supplementary standards and procedures where possible.

**6.4 PROCUREMENT**

**6.4.1 Scope**

Two categories of vendors participate in BRD development programs: (1) other NED components, and (2) outside companies. Except for methods of funding and contract award, the vendor-customer relationships are essentially the same for both categories of vendors. The major objectives for BRD relationships with vendors are to ensure that:

- Procurement documents adequately define the item or service contracted to facilitate satisfactory manufacture, inspection, test, and acceptance.
- The vendor has the capability to provide the sub-contracted items or services, as is evidenced by past performance or in-depth survey.
- There is agreement between BRD and the vendor on the administrative, technical, quality, cost, and schedule terms of the contract.
- The vendor performs in accordance with contract terms.
- Resolution of vendor-customer differences is accomplished.

**6.4.2 Quality Assurance Functions**

The procurement of materials, equipment, and services for BRD development programs is accomplished in an orderly, planned, sequential manner to provide assurance that procured items conform to predetermined engineering requirements and that there is objective evidence of their quality. The BRD Quality Organization performs the following activities to ensure the quality of procured items:

- Review of procurement documents
- Evaluation and participation in selection of procurement sources
- Audit of configuration control
- Source surveillance and inspection
- Receiving inspection, or audit or receiving inspection functions
- Surveillance and audit of control of received items

The stringency of the requirements levied on vendors is determined by the established product classification and need for quality level of effort. The most rigorous requirements apply to procurement of engineered items which affect nuclear safety, with decreasing degrees of stringency down to the least rigid, which is procurement of standard off-the-shelf items which do not affect nuclear safety.

Quality instructions, procedures, and other related documentation prepared or approved by the BRD Quality Organization provide requirements for the control of manufacture, fabrication, and assembly by vendors.

#### 6.4.3 Procurement Document Control

Procurement documents for significant development program items and changes to these documents are routed through BRD QA or the responsible quality control organization for review and approval prior to final processing by the procurement function. Procurement documents consist of Job Orders (if the vendor is a GE component) or Material Request (if the vendor is an outside company), procurement specifications and drawings, and other related documents required to provide instructions to suppliers.

Quality review of procurement documents provide assurance that:

- Applicable regulatory requirements, design bases, or other engineering and quality requirements are adequately included or referenced in these documents.
- Procurement documents receive technical review by qualified personnel of appropriate engineering disciplines to assure adequacy of the engineering requirements.
- Procurement documents receive quality assurance review to assure adequacy of engineering and quality requirements specified by the originator.
- Special quality requirements are included in the procurement document package, e.g., requirements for inspection, quality records, vendor audit, etc.
- Changes to procurements receive similar review and approval as the original procurement.
- Vendors establish quality assurance programs consistent with this Plan, and exercise similar procurement controls over their suppliers.

#### 6.4.4 Vendor Evaluation and Selection

Vendor evaluation and selection is the joint responsibility of the BRD Quality Organization, responsible engineering representatives, and procurement functions, and is accomplished by one or more of the following methods:

- Selection of vendors from an approved vendor list.
- Evaluation of vendor performance history records of similar BRD procurements.
- Performance of vendor capability surveys.

When BRD performs facility surveys to determine vendor capability, the facility review team is normally composed of representatives from the responsible engineering function, the procurement function, and quality. These surveys provide sufficient data to evaluate the vendor's ability to design, fabricate and supply materials and equipment of an acceptable quality.

#### 6.4.5 Configuration Control

The currentness and adequacy of drawings and specifications, as they relate to procurement documents and contracts, is controlled by BRD procedures and instructions which specify the methods by which document changes are initiated, reviewed, approved, distributed, and implemented.

Applicable drawings and specifications are revised to reflect the as-built configuration of items when received. Procurement documents and contracts routinely require BRD suppliers to provide as-built information in order that revision of BRD drawings and specifications may be performed by the responsible BRD function.

#### 6.4.6 Source Surveillance and Inspection

Surveillance and inspection of vendor fabrication and assembly activities is performed by the BRD Quality Organization or a team composed of engineering and quality representatives, depending upon the relative importance and complexity of the procurement. Source surveillance and inspection is performed to evaluate the quality of items produced and the effectiveness of the vendor's quality assurance program, and to provide assurance of compliance by the vendor with BRD quality and engineering requirements. Source surveillance and inspection requirements and activities are defined in procedures and instructions prepared or approved by BRD QA.

Provisions for access to vendor facilities is established in procurement documents and supplier contracts when required.

#### 6.4.7 Receiving Inspection

Procured items undergo a planned and comprehensive receiving inspection upon receipt by a component assigned to perform inspection or by the BRD Quality Organization. The receiving inspection functions of each assigned organization are performed in accordance with established inspection procedures and standards which have been prepared by the responsible organization and approved by the BRD Quality Organization.

Receiving inspection for development program articles is performed to verify compliance with the quality requirements as they are defined in purchase specifications and applicable drawings.

Sampling inspection is used if the required receiving inspection test criteria prescribes destructive testing. Sampling is also used when the items are in sufficient quantity and/or are lacking in any significant application.

Purchased materials which do not comply with designated requirements are identified as nonconforming, segregated, and documented in accordance with applicable procedures and instructions by each organization pending further disposition.

**6.4.8 Control of Received Items**

Procedures and instructions for the identification, control, handling, preservation, and storage of received items are prepared and implemented by participating organizations. These procedures are subject to review and approval by the BRD quality Organization.

Records and identification of materials are maintained to provide assurance of traceability to the origin of data and materials.

Provisions for shelf-life control, handling, and utilization are established and implemented for materials subject to deterioration with age or environment.

The BRD Quality Organization performs surveillance and audit or received item control by responsible organizations.

**6.5 FABRICATION AND ASSEMBLY**

**6.5.1 Scope**

Experimental equipment used in development programs is fabricated by either BRD components or vendors. The BRD Quality Organization performs surveillance and audit of the fabrication activities of these manufacturing organizations to ensure and verify compliance with engineering requirements.

**6.5.2 Quality Assurance Functions**

To assure the quality of fabricated items, the BRD Quality Organization plans and implements surveillance and audit activities, consisting of:

- Review of plans, procedures, specifications, and drawings related to fabrication.
  - Identification of characteristics to be inspected and inspection methods.
  - Preparation of surveillance and audit plans and procedures.
  - Inspection, verification, and audit (according to planning) of fabrication, assembly, test, special processes, and material handling and control.
  - Documentation of quality activities to provide objective evidence of the quality of fabricated items.
- If items are fabricated by vendors, the BRD Quality Organization also performs:
- Review and approval of vendor quality assurance programs.
  - Vendor capability surveys.
  - Source inspection.
  - Vendor quality program audit.

**6.5.3 Material Identification and Control**

The BRD Quality Organization performs surveillance and audit to assure that materials, parts, and assemblies are identified as required in specifications and drawings and in accordance with established procedures during the phases of fabrication, processing, assembly, and handling operations in order to prevent use of unauthorized or defective materials.

Identification is required on items or on records traceable to the item through the use of serial numbers, part numbers, heat numbers material certifications, stamping practices, tagging, or travel cards, as appropriate.

**6.5.4 Control of Processes**

The BRD Quality Organization performs surveillance and audit to assure that manufacturing organizations provide the degree of process control required to obtain the desired quality. Special fabrication and assembly and nondestructive examination processes are controlled in accordance with established qualified procedures and instructions and performed by trained and certified personnel.

**6.5.5 Manufacturing Planning**

The BRD Quality Organization performs surveillance and audit to assure that components performing fabrication and assembly prepare and utilize formal detailed instructions for manufacturing activities, and prepare detailed fabrication and assembly plans. Typical contents of these fabrication and assembly plans are:

- A block diagram flow chart and/or step-by-step instructions for the total sequence of fabrication, assembly, inspection, and test experiment.
- Step-by-step signature of operator/technician to verify that the task was performed as specified.
- Signature of quality control personnel at steps or holdpoints which require verification.
- Reference to an applicable special or general procedure at steps where the complete instruction cannot be entered in the space available.
- Signature of responsible management, engineering, or quality control personnel at critical steps or holdpoints in the sequence to certify adequacy of previous work before proceeding. Engineering and/or quality release signatures are required at these holdpoints.
- Recording of specified data at each step where required.
- Specification of inspection procedure and job title of quality control personnel at steps where verification is required.

The fabrication and assembly plan is prepared by functional personnel and approved by the BRD Quality Organization to provide assurance that both fabrication and quality control requirements are adequately covered. Corrections and revisions to the plan are made in accordance with formal change control procedures.

**6.5.6 Fabrication and Assembly Documentation**

The BRD Quality Organization performs surveillance and audit of manufacturing organizations to assure that fabrication and assembly activities are adequately documented. Data and records which are typical of those required to verify the quality of processes and products are:

- Process Control Records
- Receiving Inspection Reports
- Material Certifications (physical and chemical)
- Non-conformance/Discrepancy Reports
- Process Inspection Reports (radiographic, leak check, dye penetrants, etc.)
- Proof Test Reports
- Inspection Data
- As-built Drawings and Engineering Change Notices

**6.5.7 Handling, Storage, Preservation and Shipping**

The BRD Quality Organization performs surveillance and audit to assure that implementation of the handling, storage, shipping, cleaning, and preservation of material and equipment by manufacturing organizations complies with the following requirements:

- Materials and equipment are not damaged or allowed to deteriorate during these activities.
- Special environmental requirements are specified and provided when stipulated.
- Shipping is in accordance with Federal, State, and local regulatory requirements.
- Prescribed documentation, including quality control release for shipment, accompanies shipments when required.
- Protection is provided during all phases of fabrication and installation to prevent damage to parts, components, and equipment.
- Marking, labeling, packaging and packing is controlled procedurally.
- Applicable assembly, inspection and test operations are completed prior to shipping.
- Applicable records that accompany material or part to provide objective quality evidence displays completed inspection verification.

**6.6 INSPECTION AND TEST**

**6.6.1 Scope**

Materials and equipment required for development experiments undergo planned inspection and test activities from receipt through processing to final acceptance.

The objective of inspection and test activities is the assurance that components, systems, and processes essential to development program performance are controlled and tested in conformance with contract requirements and applicable codes, standards, specifications, and drawings. Of equal importance is the requirement for quality objective evidence by means of quality data and records of these activities.

#### 6.6.2 Configuration Control

The BRD Quality Organization verifies that the hardware corresponds to applicable drawings and specifications, and that as-built data is disseminated to responsible functions for revision of applicable drawings and specifications.

Hardware deviations are recorded and reported as nonconforming items and processed according to the relevant BRD and/or participating organization's procedures, policies and instructions. Any resulting requirements for changes to applicable specifications and drawings are reflected in as-built revisions.

#### 6.6.3 Process Control

Organizations participating in fabrication activities perform processes of major significance in accordance with planned and qualified procedures and methods as required by the applicable codes, standards, specifications, or other contractual requirements.

Personnel responsible for the performance or verification of processes requiring special skills are trained, tested, and certified in order to provide assurance of the quality of items subject to these processes.

The quality organizations of BRD and other participants verify the quality of process control activities via the media of inspection and audit of procedures, implementation, and records.

#### 6.6.4 Shop Inspection and Test

The inspection functions (quality control functions) of the participating fabrication shops are applied to procurement, receiving, fabrication and testing. Inspections are the direct responsibility of the shops, and the BRD Quality Organization performs review and approval of shop plans and procedures, monitoring and surveillance of shop functions, examination of shop reporting systems and records, and an effective system of audits.

Shop inspection and test activities comply with the following general requirements:

- Final verification of the performance of quality-related activities is accomplished by personnel other than those who perform the activities.
- Quality is controlled by either inspection or process control, or a combination of both.
- Inspection activities are performed in accordance with documented inspection plans, procedures, and instructions.
- Inspections are performed on procured and fabricated items prior to their installation into a component or system.
- The quality status of items or material inspected is identified by records and/or material identification.
- Each characteristic inspected is traceable by documentation and/or item identification to an individual or function responsible for its accomplishment.
- Test activities are performed in accordance with approved test plans and procedures.
- Inspection and test activities are performed by trained and qualified personnel.
- Adequate data and records of inspection and test activities are acquired and maintained.

### 6.7 EXPERIMENT PERFORMANCE

#### 6.7.1 Scope

Development program experiments involving material and equipment include tests performed (both in pile and out-of-pile) by BRD components, other NED components, other companies, or national laboratories, dependent upon the experimental objectives and the test facilities required.

Test plans are provided by the Responsible BRD Component. Test procedures and instructions to implement test plans are initiated by Performing Components. Engineers from the Responsible Component monitor and/or participate in test performed by engineers of the performing organization.

The BRD Quality Organization or other responsible quality organizations perform surveillance and audit to ensure that development program experiments are performed in accordance with approved test plans, procedures, and instructions.

**6.7.2 Quality Assurance Functions**

The BRD Quality Organization reviews the plans, procedures, and instructions for experiment performance to verify the adequacy and thoroughness of the responsible and performing organizations' planning, and to determine surveillance and audit requirements.

Surveillance and audit are planned and performed by the BRD Quality Organization to ensure that experiments are performed in accordance with approved procedures by qualified personnel, and that data is properly acquired and documented by the performing organization. These activities of the BRD Quality Organization are documented and recorded on appropriate quality forms in accordance with quality instructions.

The degree of BRD quality surveillance and audit of an experiment is governed by the complexity and significance of the experiment, and by which organization is designated to perform the experiment. These factors determine the following alternatives:

- BRD quality review and approval of quality program plans submitted by the responsible organization prior to performing experiment, but waiver of BRD quality surveillance and audit if the responsible organization is qualified by past performance and has demonstrated adequate quality practices.

- BRD quality surveillance and audit of experiment tests, and review of quality planning and test planning.

The objective of the BRD Quality Organization is to ensure that adequate planning of experiments is performed by the responsible BRD organization; implementation of experiments is accomplished in accordance with approved procedures by the performing organization; appropriate data and records are acquired by the performing organization; and there is adequate coordination and integration between all responsible functions.

**6.8 POST EXPERIMENTAL EXAMINATIONS**

**6.8.1 Scope**

Post experimental examination of development program material and equipment is performed by BRD components, other NED components, other companies, or national laboratories, as determined by equipment and facility requirements.

Examination procedures developed by the Responsible Component and performing organization provide the basis for post experimental examinations.

The BRD Quality Organization or other responsible quality organizations perform surveillance and audit of post experimental examinations of materials and equipment to provide assurance of pre-planned, systematic evaluation of experiments. The purpose is to ensure the credibility of development data, resulting in an accurate definition of experiment products and validation of the process or experiment for future adaptations.

**6.8.2 Quality Assurance Functions**

The BRD Quality Organization reviews the procedures and instructions for post experimental examinations to verify the adequacy and thoroughness of the responsible performing organizations' planning, and to determine surveillance and audit requirements.

Surveillance and audit is planned and performed by the BRD Quality Organization to ensure that examinations are conducted in accordance with approved procedures by qualified personnel, and that data is properly acquired and documented by the performing organization. These activities of the BRD Quality Organization are documented and recorded on appropriate quality forms in accordance with quality instructions.

**6.8.3 Experiment Records**

Records and data of experimental work are documented by performing organizations in order that the information may be used in reporting the results and significance of the experiment.

Typical information recorded for development experiments include:

- Description of experiment, test or research work
- Environmental conditions
- Special characteristics to be investigated
- Parameters being measured
- Failure observations and failure reports
- Total accumulated operating time as well as operating time occurring after significant changes in experiment conditions

- Discrepancies noted during experiment or test involving relevant specifications or requirements
- Records of repair/maintenance
- Records of unusual, unexpected or questionable occurrences involving the equipment
- Records of modification to experiment/test equipment
- Identity of personnel performing work
- References to supporting information or documentation

**6.8.4 Final Report**

A final report is prepared by the responsible organization upon completion of the experiment, test or research effort. This report contains complete, documented information describing the performance and results of the subject experiment, test or research. BRD QA verifies the completion and distribution of the final report.

**6.9 CALIBRATION CONTROL**

**6.9.1 Scope**

The selection, acquisition, calibration, maintenance, and control of tools, gages, and other inspection, measuring, and test devices used in activities affecting the quality of development programs are performed in accordance with formal, documented systems. These systems govern the use of inspection equipment by BRD components performing development program activities. Vendors are required to maintain calibration control systems which are equivalent to systems used by BRD. The BRD Quality Organization performs surveillance and audit of the calibration control programs of BRD components and vendors.

**6.9.2 Calibration Program**

Tools, gages, and other inspection, measuring, and testing devices, which are used to acquire experimental data or monitor manufacturing operations during design and development activities are included in a calibration control program which meets the following requirements:

- Frequency of calibration is determined on the basis of type, purpose, usage rate, maintenance cycle, and degree of accuracy of the equipment.
- Measuring and test equipment is calibrated to written procedures with the use of standards traceable to national standards.
- Calibrated equipment is identified in a manner which shows calibration date and date of next calibration.
- The calibration program includes adequate provisions for calibration history, calibration due-date control, control of out-of-service equipment, maintenance history, removal from service of discrepant equipment, and environmental control of metrology facilities.
- Equipment requiring calibration is properly stored, issued handled, and transported.
- Equipment that is damaged, overdue for calibration, or has had unauthorized adjustments is formally documented and withdrawn from service.
- Equipment that is discovered out of control is removed from use and any measurements obtained with such equipment is validated with equipment that is within calibration period.

**6.10 NONCONFORMANCES, FAILURES, AND INCIDENTS**

**6.10.1 Scope**

The BRD Quality Organization performs surveillance and audit of BRD development program activities to ensure that material and equipment which do not conform to engineering specifications, drawings, or other established requirements are identified and documented as nonconforming, segregated to the extent feasible, and held for further review and disposition. BRD QA also performs surveillance and audit of vendors to ensure that vendor quality programs provide a similar and adequate degree of nonconformance control.

BRD implements formal established procedural methods to process failures or incidents, which result from nonconformances of other causes. BRD QA participates in and coordinates the activities or BRD teams assigned to investigate and correct such events.



### 6.10.2 Nonconformance Control System

The BRD nonconformance control system is governed by procedures and instructions which establish the following minimum requirements:

- The acceptance or rejection of nonconforming items is based on criteria established in applicable specifications and drawings.
- A nonconformance report form is used to document nonconformances and indicate the status of the discrepant item.
- A controlled area is provided to segregate discrepant materials or items pending disposition when feasible.
- Nonconformances, which are designated as minor, are reworked to standard, approved rework processes as determined by the responsible supervisor and quality representative.
- A Material Review Board is convened to designate the disposition of the materials or items found to have major nonconformances.
- The system for handling nonconforming materials and items includes a method for notifying affected organizations of the status of nonconformances.
- The system for controlling nonconformances includes provisions for establishing corrective action to prevent recurrence of discrepancies.

Vendor nonconformance control systems are required to meet the above criteria.

Reporting of nonconformances, their disposition, and resultant corrective action to customers is governed by specific contractual terms.

### 6.10.3 Failures and Incidents

Failures or incidents may result from nonconformances or other causes. If failures or incidents occur, BRD places a high degree of emphasis on documentation, investigation, determination of corrective and preventive action, notification of affected personnel, and reporting to customers.

BRD QA and other BRD quality organizations are responsible for initiating and coordinating investigations of reported failures and incidents. BRD procedures require immediate notification of BRD QA by all BRD personnel when actual or potential failures or incidents are discovered.

High level review and investigation boards are formed of management and technical personnel from the Department as a whole, with BRD QA as coordinator, to perform in-depth analysis of such occurrences and to establish preventive and corrective action. The General Manager of BRD is kept fully informed during the investigation sequence.

Summation reports of findings and corrective and preventive action are disseminated internally to affected BRD personnel, and externally to customers as required by contract or Government regulations.

## 6.11 QUALITY ASSURANCE AUDITS

### 6.11.1 Scope

Audits of development program activities are performed by the BRD Quality Organization to determine adherence to the Quality Assurance Program and to measure its effectiveness. Selected activities of all phases of development programs, from inception to completion, are evaluated to a documented audit program plan which is in accordance with relevant BRD management policies, directives, and specific project requirements. The audit program includes both BRD components and vendors.

In addition to audits by BRD, vendors are required to establish internal audit programs which are equivalent to the BRD audit program.

### 6.11.2 Evaluation of Quality Assurance Program

Measurement of the Quality Assurance Program is accomplished by means of BRD QA audits which evaluate the quality assurance methods, procedures, and instructions for the control and verification of task performance. These audits are generally concerned with management systems (e.g., documentation control, change control, nonconforming material control, vendor quality assurance program, etc.) of the BRD Quality Organization, BRD technical organizations, and vendors.

### 6.11.3 Process Audits

Process audits are performed, where required, to evaluate and assess the performance of work, including fabricating, assembling, cleaning, inspecting, testing, repairing, modifying, etc. These audits are performed to determine

compliance with engineering requirements by participating manufacturing organizations, which include BRD components and vendors.

**6.11.4 Reporting and Corrective Action**

Audit reports of findings and evaluations are prepared by BRD QA and distributed to affected personnel and appropriate management for review and action. Requests for corrective action are a part of audit reports.

The audit system provides for reaudits and follow-up of corrective action requests, and is designed to establish methods which assure that corrective action is accomplished to prevent recurrence of discrepancies.

Audit reports or audit program summaries are distributed to customers as specifically defined by contractual terms.

CONTRIBUTORS  
PHASE A FINAL REPORT

Task 1—Program Management

J. O. Arterburn  
G. B. Kruger  
R. E. Shavdahl  
B. V. Brown  
W. J. Clabaugh

Task 2A—Driver Fuel Performance

C. F. Barrett  
B. T. Feerick  
A. J. Lipps, Jr.

Task 2B—Transient Experiments on Encapsulated Fuel

H. C. Pfefferlen  
T. Hikido  
G. R. Thomas  
R. T. Fernandez  
R. C. Nelson

Task 2C1—Subcriticality Monitor

H. S. Bailey

Task 2C2—Shielding Tests

M. L. Weiss

Task 2C3—Doppler Tests

D. D. Freeman

Task 2C4—Oscillator Tests

G. R. Pflasterer

Task 3A1—Systems Behavior

J. T. Cochran

Task 3A2—Vented Fuel

W. E. Baily  
D. A. Cantley  
C. N. Spalaris  
R. M. Pifferetti  
M. L. Weiss

Task 3A3—Coolant Chemistry

J. S. Armijo  
R. W. Lockhart

Task 3A4—Core Clamping

P. M. Magee  
H. J. Snyder, Jr.

Task 3A5—Core Fuel Assembly Instrumentation

D. P. Hines

Task 3A6—Boiling Detection

L. R. Boyd  
P. W. Swartz

Task 3A7—Failed Equipment Detection

L. R. Boyd  
P. W. Swartz

Task 3A8—DAS

L. R. Boyd  
P. W. Swartz

Task 3A9—Pu Capture Ratio

No Work Performed on This Task

Task 3A10—Level Indicator

D. A. Greene  
J. M. Haar  
R. V. Myers  
L. E. Pohl  
P. W. Swartz  
R. W. Lockhart

Task 3A11—Leak Detector

D. A. Greene  
J. M. Haar  
R. V. Myers  
L. E. Pohl  
P. W. Swartz  
R. W. Lockhart

Task 3A12—Cold Trap

D. A. Greene  
J. M. Haar  
R. V. Myers  
L. E. Pohl  
P. W. Swartz  
R. W. Lockhart

Task 3A13—Vapor Trap

D. A. Greene  
J. M. Haar  
R. V. Myers  
L. E. Pohl  
P. W. Swartz  
R. W. Lockhart

Task 3A14—Refueling Cell Equipment

J. T. Cochran  
L. J. Nemeth

Task 3A15—Refueling Cell Hoist and Grapple

J. T. Cochran  
L. J. Nemeth

Task 3B1—Systems

J. C. Whipple  
J. M. Day  
J. C. Lee  
W. R. Gee, Jr.

Task 3B2—Reactor

F. G. Rally  
J. W. Pyron  
N. E. Hackford  
W. H. Whitling  
W. A. Brummond

Task 3B3—Fuel

B. T. Feerick  
A. J. Lipps, Jr.  
T. L. Gregory

Task 3B4—Physics

D. D. Freeman  
Y. S. Lu

Task 4A—Test Program

H. C. Pfefferlen  
T. Hikido  
G. R. Thomas  
R. T. Fernandez  
R. C. Nelson

Task 4B1—Control Drive

E. R. McKeehan  
W. J. Margetanski  
F. E. Funk  
W. R. Graham

Task 4B2—FRED

E. R. McKeehan  
W. J. Margetanski  
F. E. Funk  
W. R. Graham

Task 4B3—Fuel Control Assembly Design

F. E. Gelhaus  
P. M. Magee  
A. L. Grantz  
T. L. Gregory

Task 4B4—Systems

J. C. Whipple  
J. M. Day  
J. C. Lee  
W. R. Gee, Jr.

Task 4B5—Physics

G. R. Pflasterer  
D. D. Freeman  
Y. S. Lu

Task 4B6—Package Loop Design

N. P. Hansen

Task 4B7—Fuel Handling and Shipping

A. L. Bashford

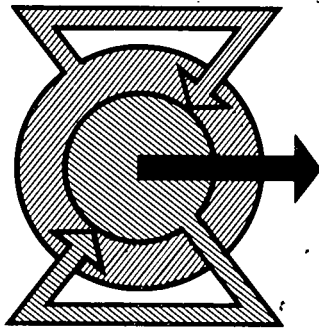
Task 5—Safety and License

K. Hikido  
N. W. Brown  
R. K. Stitt

Task 6—Quality Assurance

H. J. Stock  
T. O. Bryan, Jr.  
C. R. McMillan  
L. C. Lawrence

**BREEDER REACTOR DEPARTMENT**  
SUNNYVALE, CALIFORNIA 94086



Expanding the World's Energy Reserves

**GENERAL**  **ELECTRIC**